Wayne E. Hall

Data of Geochemistry

Sixth Edition

Chapter L. Phase-Equilibrium Relations of the Common Rock-Forming Oxides Except Water

---

GEOLOGICAL SURVEY PROFESSIONAL PAPER 440-L

Data of Geochemistry

Sixth Edition

George W. Morey

MICHAEL FLEISCHER, *Technical Editor*

Chapter L. Phase-Equilibrium Relations of the Common Rock-Forming Oxides Except Water

By GEORGE W. MOREY

GEOLOGICAL SURVEY PROFESSIONAL PAPER 440-L

A discussion of the melting relations of the common rock-forming oxides and the binary, ternary, quaternary, and quinary systems formed by them

UNITED STATES GOVERNMENT PRINTING OFFICE, WASHINGTON : 1964

UNITED STATES DEPARTMENT OF THE INTERIOR

STEWART L. UDALL, *Secretary*

GEOLOGICAL SURVEY

Thomas B. Nolan, *Director*

For sale by the Superintendent of Documents, U.S. Government Printing Office
Washington, D.C. 20402

DATA OF GEOCHEMISTRY, SIXTH EDITION

Michael Fleischer, *Technical Editor*

The first edition of the Data of Geochemistry, by F. W. Clarke, was published in 1908 as U.S. Geological Survey Bulletin 330. Later editions, also by Clarke, were published in 1911, 1916, 1920, and 1924 as Bulletins 491, 616, 695 and 770. This, the sixth edition, has been written by several scientists in the Geological Survey and in other institutions in the United States and abroad, each preparing a chapter on his special field. The current edition is being published in individual chapters, titles of which are listed below. Chapters already published are indicated by boldface.

CONTENTS

ILLUSTRATIONS

TABLES

PHASE-EQUILIBRIUM RELATIONS OF THE COMMON ROCK-FORMING OXIDES EXCEPT WATER

By GEORGE W. MOREY

ABSTRACT

A major concern of geology is to explain the characteristic association of certain minerals in well-known rock types and the relation of these minerals to each other. In considering the genesis of the minerals it is necessary to know the melting and crystallization relations of the various oxides which make up the greater proportion of the earth's crust. The available information about the melting points and phase-equilibrium relations of these nine oxides (Na_2O, K_2O, MgO, CaO, FeO, Al_2O_3, Fe_2O_3, SiO_2, and TiO_2) are summarized in this chapter, and a discussion is given of various types of phase-equilibrium diagrams, which are illustrated by examples.

INTRODUCTION

A major concern of geology is to explain the characteristic association of certain minerals in well-known rock types and the relation of these rocks to each other. Some rocks are of sedimentary origin, formed by the weathering of more primitive rocks and the subsequent consolidation of the sediments. Other rocks, the metamorphic rocks, are formed by the alteration by heat or pressure either of such sediments or of the primary igneous rocks, which are formed by the cooling and crystallization of a rock magma. In considering the genesis of the minerals of which the many igneous rock types are composed, it is necessary to know the melting and crystallization relations of the various oxides which make up the greater proportion of the earth's crust. It was shown by Clarke and Washington (1922) that 10 oxides make up 99 percent of the earth's crust. One of these is water, which is excluded from consideration in this chapter. The other nine oxides and their percentages are: Na_2O 3.84, K_2O 3.13, MgO 3.49, CaO 5.08, FeO 3.80, Al_2O_3 15.34, Fe_2O_3 3.08, SiO_2 59.12, TiO_2 1.05. The available information about the melting points and phase-equilibrium relations of these nine oxides is summarized in this chapter. The oxides are considered in the order of the periodic system, except that FeO is placed after MgO and CaO, and Fe_2O_3 after Al_2O_3.

The consideration of the melting phenomena in mixtures involves a discussion of the often complex phase-equilibrium relations, and the further consideration of the changes in these relations at temperatures below that at which a liquid can be formed is often pertinent to geologic phenomena. One hundred and forty phase-equilibrium diagrams, which represent the relation between composition and temperature, with reference to the melting and crystallizing process, and subsequent changes in the nature of the solid phases, have been assembled. They offer a means of expressing in graphic and compact form a large amount of information which is vital to our understanding of the processes of magmatic differentiation. To those conversant with such diagrams the information thus available is apparent at a glance, but much thought and study and actual use of these diagrams is necessary to attain such a degree of competence. Much of the discussion is based on purely geometrical relations, which arise in part from the methods used in expressing composition by means of geometrical figures; but in larger part from the thermodynamic relations underlying the study of heterogeneous equilibrium.

The usual expression of the phase rule,

$$P+F=C+2,$$

in which P is the number of phases, F the number of degrees of freedom, and C the number of components, is an incidental qualitative consequence of the equations (Gibbs, 1906) between those quantities which connect the thermodynamic stability of the different phases with their composition. These equations may be applied analytically, or, as is commonly done, graphically. It is from a consideration of the fundamental equations, or of the surface of thermodynamic stability derived from them, that the various theorems are derived that govern the application of geometric laws to the chemical relationships expressed in phase-equilibrium diagrams. In the following pages many examples illustrating special points in phase-equilibrium theory are considered in detail.

The derivation of these theorems is out of place here. They are covered in some detail in well-known textbooks. One elementary text is Findlay (1951); more advanced ones are Ricci (1951); Darken and Gurry (1953), and Zernicke (1955). The several volumes of Bakhuis Roozeboom (1901–13) remain unsurpassed. The treatise by Korzhinskii (1959) specially pertains to the physiocochemical basis of paragenesis. The volume "Phase Diagrams for Ceramists," by Levin and others (1956) contains an excellent discussion of elementary principles as well as an extensive collection of phase-equilibrium diagrams. The review papers by Schairer (1957a), Roedder (1959), and Stewart (1960) give excellent surveys of phase-equilibrium relations in silicate systems. The classic book by Bowen (1956) on the "Evolution of the Igneous Rocks" is a necessity for the comprehension of the process of magmatic differentiation.

The phase-equilibrium diagrams are arranged in the following sections: The component oxides, binary systems, ternary systems, quaternary systems, quinary systems, and petrogeny's residua system. In the introduction to each section is a short discussion of pertinent phase-equilibrium theory, with references to systems which illustrate the points in question. These systems are discussed in considerable detail. As far as possible the references include all work up to January 1, 1961. Compositions are in weight percent unless otherwise specified.

THE COMPONENT OXIDES

In the introduction are listed the nine oxides which form the components of the systems discussed below. K_2O is not known in pure form, and little is known about Na_2O except that its melting point is 917°C (Brewer and Margrave, 1955); neither of these oxides is known in nature. Al_2O_3, SiO_2, FeO, Fe_2O_3, and TiO_2 require individual discussion. FeO and Fe_2O_3 are discussed in the section on the binary system FeO–Fe_2O_3. Pertinent information about melting points and inversion of oxides is assembled in table 1.

TABLE 1.—*Phase transformations of oxides*

Oxide	Transformation	Temperature (°C)	Reference
MgO	Melting	2800	Kanolt, 1914.
CaO	Melting	2572	Kanolt, 1914.
CaO	Inversion	420	Sosman, Hostetter, and Merwin, 1915.
Al_2O_3	Melting	2040	Bunting, 1931.
TiO_2	Melting	1825	Bunting, 1933.

SILICA

Silica (silicon dioxide, SiO_2), is noteworthy for the number of its polymorphous crystalline forms, and for the sluggishness with which many of the forms, when unstable, change over into the form stable under the conditions of the experiment. The interrelations of these various forms were but vaguely understood until the work of Fenner (1913), which is a classic of the literature of silica. It forms the basis of the exhaustive discussion by Sosman (1927). The best known crystalline modifications of silica are listed in table 2, and shown graphically in figure 1.

TABLE 2.—*Modes of silica*

[From R. B. Sosman, unpublished data, 1957]

	Temperature range (°C)	Stability	Pressure (atmospheres)
Crystalline:			
Quartz, low	−273–573	Stable	1
Quartz, high	573–867	do	1
Tridymite S–I	−273–64	Metastable	1
Tridymite S–II	64–117	do	1
Tridymite S–III	117–163	do	1
Tridymite S–IV	163–210	do	1
Tridymite S–V	210–475	do	1
Tridymite S–VI	745–867	do	1
	867–1470	Stable	
Tridymite M–I	−273–117	Metastable	1
Tridymite M–II	117–163	do	1
Tridymite M–III	>163	do	1
Cristobalite, low	−273–267	do	1
Cristobalite, high	267–1470	do	1
	1470–1713	Stable	1
Coesite	ca. 200–1700	do	ca. 21–40
Keatite	Monotropic?		1
Silica W	Monotropic?		1
Amorphous:			
Liquid silica	>1723	Stable	1
Vitreous silica	−273–1723	Metastable	1
Supra-piezo-vitreous silica		do	ca. 35 up
Compacted vitreous silica		do	ca. 100 up
Silica M	Indefinite	[1]	

[1] Produced from all other phases by high-speed neutrons.

The stable form at ordinary temperature is low quartz,[1] the commonest of minerals. When low quartz is heated to 573°C it changes into high quartz. This inversion is an example of a kind of inversion called by Sosman the "high-low" type, which is characterized by proceeding promptly and rapidly throughout the crystal, whether from higher or lower temperature. The principal features of the high-low quartz inversion are (1) a gradual increase in the rate of change of all properties with increasing temperature, beginning 50°C or more before the inversion is reached; Day, Sosman, and Hostetter (1914) found that the volume increased more and more rapidly as the temperature approached the inversion temperature; (2) an absence of a similar preliminary effect on the high-temperature side of the inversion point, and a small rate of change in properties above the inversion point; and (3) a change in symmetry, and an abrupt change in nearly all the physical properties at the inversion point.

The speed of the inversion is great, and there is little superheating or undercooling. Several observers have found the inversion to take place at a higher tempera-

[1] This is often called β-quartz, sometimes α-quartz. To avoid this confusion, Sosman (1927) introduced the terms "high quartz" and "low quartz" to designate the high- and low-temperature forms. He also extended this system, which is generally adopted, to the other crystalline forms of silica.

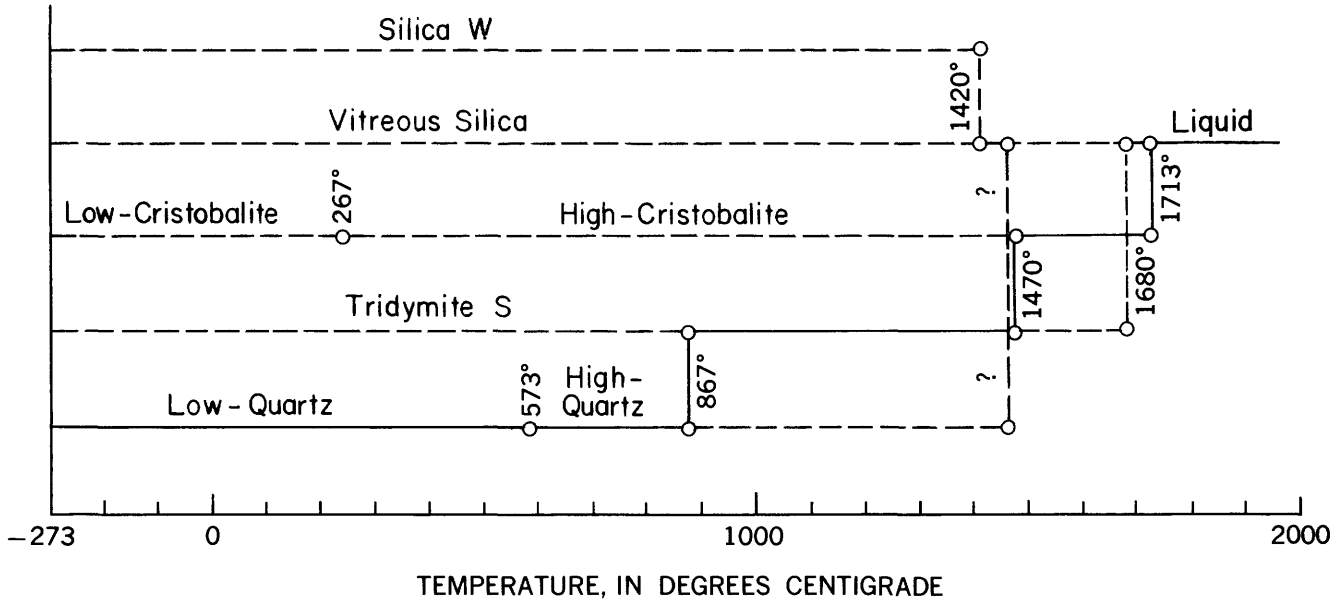

FIGURE 1.—Graphic representation of the relations among the forms of silica, as revised by R. B. Sosman (unpublished data, 1957).

ture on heating, a lower temperature on cooling. Bates and Phelps (1927), who worked with blocks of quartz, found that at the beginning of the inversion reached with increasing temperature there was a slight drop in temperature. They give 573.3°C for the low-high inversion, 572.4°C for the high-low inversion. Gibson (1928b) found that the inversion was accompanied by a little superheating or undercooling, and that the true temperature of equilibrium between the high and low forms of quartz is at 572.3°±0.2°C. Before a block of low-quartz changes to the high variety, it superheats so much that its temperature never falls to the equilibrium value. If the inversion is considered to take place adiabatically, the apparent heat capacity of low quartz, about 573°C was calculated to be 4±1 cal per gram per degree, a value more than 10 times that of low quartz at 550°C, or of high quartz at 600°C.

Keith and Tuttle (1952), using a highly sensitive differential thermal method, found that quartz, instead of being invariably pure SiO_2 as previously believed, often contains material in solid solution which affects the high-low inversion. Synthetic quartz grown in the presence of germanium was found to have an inversion break 40°C above the normal range, and quartz grown in the presence of lithium and aluminum had the inversion temperature lowered as much as 120°C. Schreyer and Schairer (1960) found that when glasses in the system MgO–Al_2O_3–SiO_2 of composition between SiO_2 and $MgO \cdot Al_2O_3$ were crystallized, solid solutions were obtained which were isostructural with high quartz. Members of the series having SiO_2 content less than 73 percent could be quenched to room temperature as high quartz, but an inversion takes place on cooling more siliceous mixtures. These solid solutions are similar to the phases called "silica O" by Roy (1959).

Gibson (1928a) studied the increase in the inversion temperature of quartz resulting from hydrostatic pressures up to 2,640 bars, and Yoder (1950) extended the study to 10,000 bars. The quartz used by Yoder had an inversion temperature at atmospheric pressure of 572.3°±0.2°C, which was raised to 815°C by 10,000 bars pressure. The experimental results are represented by the equation

$$\Delta T = -1.6 + 2.871 \times 10^{-2} p - 4.284 \times 10^{-7} p^2$$

in which ΔT represents the increase in inversion temperature produced by a pressure of p bars, and the P-T curve is shown in figure 2.

High quartz is the stable form of silica from 573° to 867°C, at which temperature high tridymite becomes stable (Kracek, 1939). The transition is sluggish, and quartz can be overheated for long periods without change. When a transition takes place in the absence of fluxes, cristobalite is almost invariably formed, and Sosman (1927) states that the direct transformation of quartz to tridymite by heat alone has not been definitely proved. Fenner (1913) accelerated the transitions by fluxes, of which sodium tungstate was most frequently used, and obtained some conversion to tridymite at 875°C in 24 hours; at 1000°C the conversion was complete within 118 hours, and at 1300°C in 3 hours.

Mosesman and Pitzer (1941) calculated from the thermodynamic properties of high quartz and tridy-

mite that the transition temperature of quartz to tridymite would be raised by pressure. Tuttle and Bowen (1958) determined the transition curve up to 1,000 atm and Kennedy and others (1962) determined it up to the quadruple point gas+liquid+quartz+tridymite in the binary system H_2O–SiO_2, at 1160°C, 1,500 atm. Their results are represented by a straight-line equation,

$$t=867+0.195p,$$

in which t=temperature in degrees centigrade and p is the pressure in atmospheres.

The change of high quartz to cristobalite is the usual one when quartz is heated without a flux, but the amount of inversion becomes appreciable only above 1000°C. Day and Shepherd (1906) found the transformation to be largely complete after 6 days at 1160°C; Fenner found only a small percentage transformed at 1250°C after 108 hours, two-thirds transformed after 90 hours at 1300°C, 85 percent after 4 hours at 1500°C, and the transformation was practically complete after one hour at 1570°C. The metastable inversion temperature at which quartz and cristobalite would be in equilibrium (the metastable invariant point quartz+cristobalite+vapor) is difficult to determine directly; Sosman (1927) estimates it to be below 1250°C.

The metastable melting of quartz has been observed. The metastable melting point is probably below 1470°C, according to Sosman (1927). The rate of melting is slow and in this temperature range may be equalled or exceeded by the rate of crystallization of the liquid into cristobalite; above 1500°C melting is more rapid than crystallization, and glass is obtained on cooling. Various samples of quartz differ greatly in their readiness to melt or to invert to cristobalite.

The formation of quartz directly from other forms of silica without the aid of flux is practically unknown. Below 867°C quartz is the stable crystalline form, but there is no record of either cristobalite or tridymite changing over into the stable quartz without the aid of a flux, and the transformation with such aid requires special treatment. The occurrence of tridymite and cristobalite as low-temperature minerals is pertinent. The forms of tridymite and their relationship were an outstanding puzzle which has been solved by the work of Hill and Roy (1958 a, b); indeed, Flörke (1955) questioned the existence of tridymite as a phase. Hill and Roy found that there is one form of tridymite, which they designated by tridymite S (for stable) which is stable in the range they studied, 870° to 1300°C. This presumably is the form found by Kracek (1939) at the transition point of high quartz and remains the stable form up to 1470°C, when it inverts to cristobalite. Tridymite S probably is characterized by a 20-H stacking. Tridymite M (for metastable) resembles tridymite S, but is metastable at all temperatures. Most laboratory samples of tridymite contain S mixed with M. Tridymite M can be prepared from any form of silica in a few days in the range of 870° to 1200°C either hydrothermally or by fusion with sodium tungstate, and with increasing length of run S always grows at the expense of M. The distinction between these phases is made by means of the X-ray powder diffraction patterns. A third powder pattern, which cannot be wholly ascribed to poor crystallinity of phase M, is obtained in the earliest stages of the conversion of some materials to tridymite. It has been termed tridymite U, for unstable.

These forms of tridymite show a series of displacive transitions, easily detected by differential thermal analysis. These are summarized in the following scheme:

$$\text{Trid-M-I} \overset{113°C}{\rightleftarrows} \text{Trid-M-II} \overset{152°C}{\rightleftarrows} \text{Trid-M-III}$$

$$\text{Trid-S-I} \overset{64°C}{\rightleftarrows} \text{Trid-S-II} \overset{113°C}{\rightleftarrows} \text{Trid-S-III} \overset{138°C}{\rightleftarrows} \text{Trid-S-IV}$$

and correspond to heat effects previously ascribed as caused by inversions of tridymite II to III to IV to V.

The inversion temperature of quartz to tridymite is raised by pressure. Mosesman and Pitzer (1941) predicted that such would be the case from thermodynamic considerations and that the quartz-tridymite curve would terminate at a triple point quartz+tridymite +cristobalite. Tuttle and Bowen (1958) found the inversion temperature to be raised to 1040°C by 103 bars, and Kennedy and others (1962) realized the triple point quartz+tridymite+cristobalite at 1470°C, 400 bars.

Above 1470°C, tridymite becomes unstable with respect to cristobalite, but the transition takes place so slowly that it is possible to heat tridymite to its metastable melting point, which Ferguson and Merwin (1918) found to be 1670°±10°C. The rate of melting is small as compared with the melting of metals and ordinary salts. Cristobalite is a primary phase in many of the silicate systems which have been studied in the Geophysical Laboratory of the Carnegie Institution of Washington, and in these systems its appearance is sometimes erratic. Not infrequently cristobalite will appear within the field of tridymite, and sometimes long heating is necessary to transform it into stable tridymite.

Cristobalite is the stable form of silica from 1470°C to the melting point, 1713°C.[2] It has a high-low in-

[2] Most of the temperatures in this section are given in the Geophysical Laboratory Scale of 1912. This is essentially the same as the International Celsius scale of 1948 up to 1550°C, slightly lower above 1550°C. The melting point of pure silica as cristobalite is 1713°C on the Geophysical Laboratory Scale of 1912, 1723°C on the International Scale of 1948. This subject is thoroughly discussed by Sosman (1952).

version which differs from others of high-low type in that its temperature appears to be greatly affected by the previous thermal history, and even by the source of the cristobalite. Fenner (1913) found cristobalite made from amorphous silica to have a higher inversion temperature than cristobalite made from quartz, even though both samples were made at the same temperature. Hill and Roy (1958b) found that the temperature of the α-β inversion depends on the structure of the starting material and on the temperature and length of the heat treatment. There is no specific order characteristic of a particular temperature. The completely ordered 3-C stacking is the most stable cristobalite throughout the temperature range, and in it the α-β inversion is at 267°±2°C. All disordered cristobalites will tend toward the 3-C cristobalite with time.

Ordinarily the high form of cristobalite cannot be cooled to room temperatures without inverting, but when small cristobalite crystals are embedded in glass they may remain isotropic, presumably because of failure to invert. This was mentioned by Andersen (1919) and later discussed by Greig (1932), who offered additional evidence that the inversion from the high to the low form had failed to take place. The reason probably is that the matrix of adhering glass imposes a mechanical restraint which prevents the change. Levine and Ott (1932) showed that some opals contain high cristobalite, an observation confirmed by E. Posnjak (cited by Greig, 1932) and here again the failure to convert is probably caused by the mechanical restraint of the matrix in which the crystals are embedded.

The stable melting point of crystalline silica is the melting point of high cristobalite, since any of the other forms should invert to high cristobalite before melting, if equilibrium were reached, and will so invert if not too rapidly heated. Finely powdered cristobalite may be expected to melt completely to a liquid if held at 1715° to 1720°C for about 10 to 15 minutes. The value of the present melting temperature of cristobalite rests on two sets of experiments. The first was by Ferguson and Merwin (1918), who found 1710°±10°C. Later Greig (1927a) redetermined this as 1713°±5°C. He found that his purest cristobalite melted practically completely in 30 minutes at 1713°C and that it was largely crystalline, but contained some glass, after 30 minutes at 1710°C. He also cited evidence to show that the small amount of glass appearing at lower temperatures is accounted for by the impurities invariably present in quartz.

Natural silica glass, called lechatelierite, is never pure SiO_2. It is sometimes formed by lightning striking sand, when it is known as a fulgurite, and it is sometimes found as inclusions in volcanic rock. The silica glass found in Meteor Crater, in Arizona, and in the Libyan desert (Cohen, 1959) probably was formed by the impact of a meteor on sandstone.

Crystallization of dry silica glass below 870°C has never been observed; crystallization with the aid of "mineralizers" usually results first in the formation of tridymite, which is later transformed into quartz. Fenner's (1913) experiments showed this sequence, and other examples are cited by Sosman (1927). Quartz, however, can be crystallized directly from alkali silicate melts in which it is the primary phase, a crystallization first effected by Morey and Bowen (1924). It is easily formed by hydrothermal crystallization, and quartz is noteworthy for the ease with which it can be obtained in excellent crystals by heating appropriate mixtures with water under pressure. Morey and Ingerson (1937) gave a critical bibliography of hydrothermal reactions, including the formation of quartz and other forms of silica, and this subject is discussed in Chapter M of this publication series.

Quartz, tridymite, and cristobalite may be termed the classical forms of silica, in contrast to three new forms recently prepared. One of these is coesite, first prepared by Coes (1953) and named by Sosman (1954). Coesite is a high-pressure phase with a density of 2.93, and the change in the inversion temperature of quartz to coesite with pressure has been studied by MacDonald (1956) and by Boyd and England (1959), whose curve is reproduced as figure 2. Coesite has recently been found in nature. Chao, Shoemaker, and Madsen (1960) found it with the glass formed by impact in Coconino Sandstone (Permian) in Meteor Crater, in Arizona. Pecora (1960) discussed this occurrence, and also mentioned the finding of coesite by Chao in a specimen of "suevite" (pumiceous tufflike material) collected by Shoemaker near the rim of the Rieskessel in Bavaria, Germany. A third natural occurrence of coesite was discovered from Waber, near Al Hadida in Arabia (Chao, Fahey, and Littler, 1961). Coesite also has been found in the Teapot Ess Crater at the Nevada test site, formed by the explosion of a 1.2 kiloton atomic device (Chao, Fahey, and Littler, oral communications, 1961).

An even denser modification of SiO_2 was synthesized by Stishov and Popova (1961) at a reported pressure in excess of 160 kilobars, at temperatures of 1200° to 1400°C. This occurs in coesite-bearing sandstone at Meteor Crater, in Arizona, and has been named stishovite (Chao and others, 1962). Stishovite is tetragonal with an X-ray powder pattern very similar to that of rutile, suggesting that it is isostructural with rutile, with silicon in sixfold coordination. The unit-cell dimensions (natural material) are a=4.179 A,

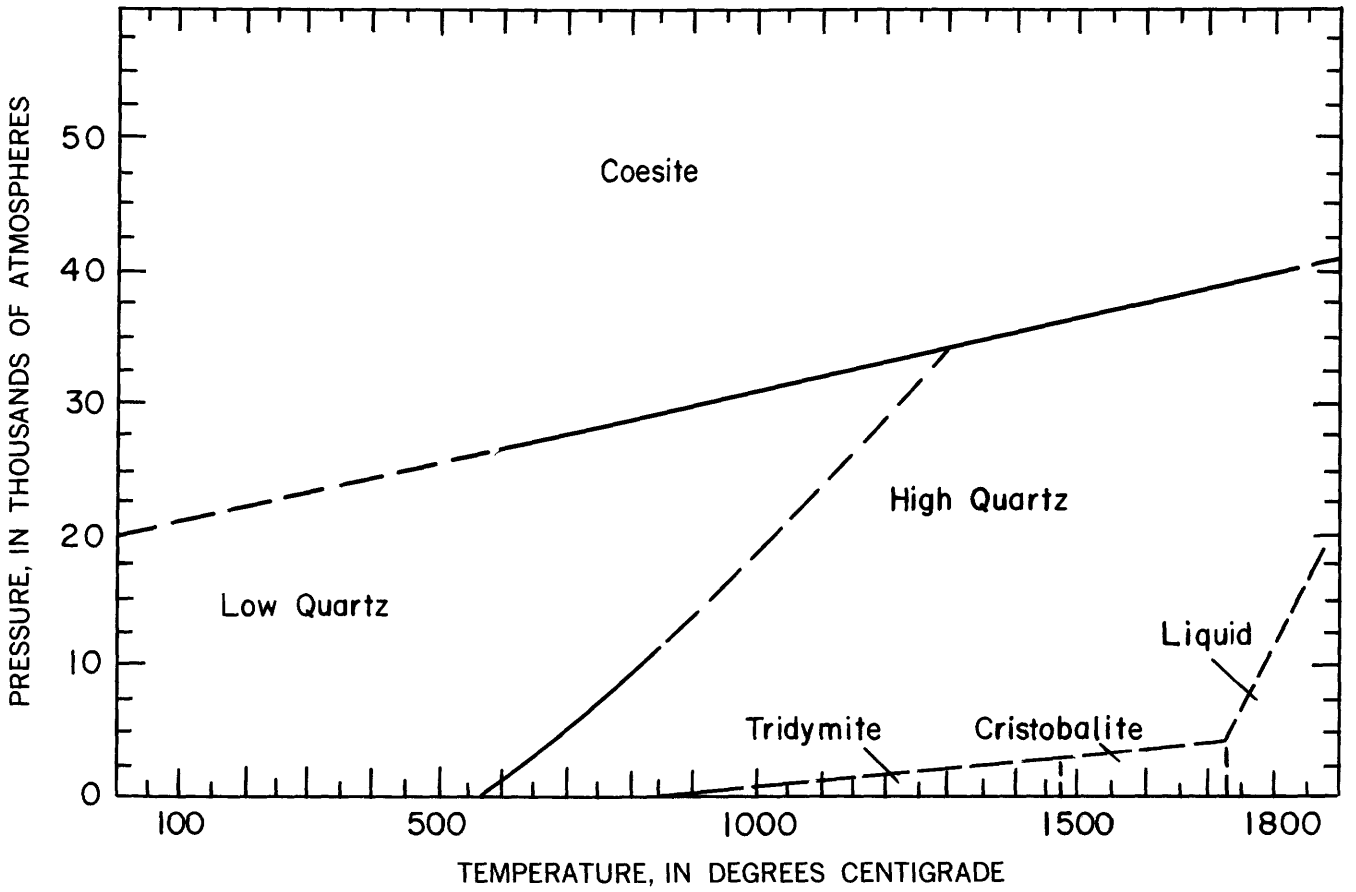

FIGURE 2.—Pressure-temperature curves for several inversions between forms of silica. Modified from Boyd and England (1959).

c=2.665 A, the calculated specific gravity is 4.28, and measured specific gravity (synthetic material) 4.35. The higher index of refraction is 1.826, the lower is 1.799, both ±0.002 (synthetic material). The synthetic material consisted of fibrous aggregates and acicular and rarely elongate tabular crystals of maximum size 0.5 mm. The natural crystals are of submicron size. Stishovite is less readily attacked by hydrofluoric acid than coesite, but is readily dissolved by alkaline solutions and by melts.

Another newly discovered form of silica is keatite, produced hydrothermally by Keat (1954) from amorphous precipitated silica in the presence of a small amount of alkali at temperatures from 380° to 585°C, and water pressures of 500 to 18,000 psi. This form has also been called silica K. Shropshire, Keat, and Vaughan (1959) found it to be tetragonal and determined its structure. A third new form, silica W, was discovered by Weiss and Weiss (1954) on cooling gaseous SiO. Silica W is formed as microcrystalline fibers composed of chains of SiO_4 tetrahedra joined at edges instead of at corners as in the usual silica structure. It has a density of 1.98, the lightest known phase of silica.

There also appear to be different forms of vitreous silica. Bridgman (1939) showed that at 31 to 33 kilobars the compressibility of vitreous silica shows a sharp reversible change. When it is subjected to pressures of above 100 kilobars, there is a permanent change in density of about 18 percent, up to 2.61, which is almost the density of quartz (2.651 at 0°C and atmospheric pressure).

ALUMINUM OXIDE

Aluminum oxide, Al_2O_3, occurs as the mineral corundum, or α-alumina. Corundum appears to be the stable form at all temperatures. Kanolt (1914) found a melting point of 2050°C; Geller and Yavorsky (1945) found 2015°±15°C and state that a more accurate determination necessitates the prevention of contamination of the alumina by vapors of other elements in the furnace atmosphere. The boiling point is 2250°C (Ruff and Schmidt, 1921). A second form, metastable γ-alumina, discovered by Hansen and Brownmiller (1928), is formed when a hydrated aluminum oxide is heated at 550°–950°C. Heating a hydrated alumina at a lower temperature apparently gives amorphous

alumina (Edwards and Tosterud, 1933) and heating to a higher temperature gives corundum.

Several other forms of aluminum oxide have been described but their existence has not been fully established. Beta-alumina, described by Rankin and Merwin (1916) apparently is an aluminate, the sodium form of which has the formula $Na_2O \cdot 11Al_2O_3$ (Ridgeway, Klein, and O'Leary, 1936; Bragg, Gottfried, and West, 1931; Beevers and Ross, 1937). The literature of this subject has been critically discussed by Schairer and Bowen (1955), who found β-alumina to be unstable with respect to corundum in their silicate melts.

The decomposition of $Al_2O_3 \cdot 3H_2O$ (gibbsite) or $Al_2O_3 \cdot H_2O$ (boehmite), leads to metastable aluminas, three of which have been described; namely, γ-alumina, δ-alumina, and θ-alumina: of these, γ-alumina has an undersaturated cubic spinel structure, δ-alumina a tetragonal structure, and θ-alumina is isomorphous with β-Ga_2O_3 (Ervin, 1952; Saalfeld, 1958; Rooksby and Rooymans, 1961).

TITANIUM OXIDE

Titanium oxide, TiO_2, is found in nature as the minerals rutile, anatase, and brookite, of which rutile appears to be the stable form, the other two, monotropic. Bunting (1933) found the melting point to be 1825°±20°C. Several observers have studied the conversion of anatase and brookite to rutile. Schroder (1928) found that the expansion curve of anatase has a sharp break at 642°±3°C, resulting from an inversion from the holohedral low-temperature form to a probably tetragonal high-temperature form. He found the monotropic inversion of anatase to rutile to take place readily at 915°C; that of brookite to rutile to be detectable at 650°C. Bunting (1933) found that anatase and brookite change to rutile in the presence of a flux at much lower temperatures than found by Schroder, and concluded that if there is a temperature at which rutile is at equilibrium with either anatase or brookite it must be below 400°C.

BINARY SYSTEMS

In this section are given the binary systems formed by the nine oxides listed in the Introduction, with the combinations arranged in the order of that listing, which is essentially the order of the periodic table. The simplest type of system is that in which no compounds are formed, there is no solid solution, and a simple binary eutectic is formed. Nine of the following systems meet these requirements, but examples illustrating many of the possible complications in phase-equilibrium relations are explained in detail. The system CaO–SiO_2 shows the following: simple eutectics; compounds—like $CaO \cdot SiO_2$—with congruent melting points; a compound, $3CaO \cdot 2SiO_2$, that has an incongruent melting point; a compound, $2CaO \cdot SiO_2$, that shows reactions in the solid state; and reactions in which two liquid layers are formed. The system Na_2O–CaO–SiO_2 has examples of both congruently and incongruently melting compounds. Several simple binary systems are discussed in connection with the ternary system Na_2O–Al_2O_3–SiO_2. The binary system Na_2O–$Al_2O_3 \cdot 6SiO_2$ (albite)–$CaO \cdot Al_2O_3 \cdot 2SiO_2$ (anorthite) is an example of a system showing complete solid solution with the melting point rising from one component to another. The system $2CaO \cdot SiO_2$ (calcium orthosilicate)–$2FeO \cdot SiO_2$ (fayalite) is a more complicated solid-solution system and $CaO \cdot SiO_2$–$FeO \cdot SiO_2$ is an illustration of a binary join which is only in part binary.

Na_2O–Al_2O_3

No reliable phase-equilibrium data exist for the system Na_2O–Al_2O_3, chiefly because of the high temperature and the change in composition of mixtures resulting from volatilization of sodium oxide. Schairer and Bowen (1956) estimated the melting point of $Na_2O \cdot Al_2O_3$ to be 1850°±30°C. Matignon (1923) estimated its melting point as 1650°C but Brownmiller and Bogue (1932) and Kammermeyer and Peck (1933), who determined optical properties and X-ray pattern, found the melting point to be above 1700°C. The substance known as "β-alumina" is an alkali or alkaline earth aluminate.

Na_2O–SiO_2

The binary system Na_2O–SiO_2 is basic to the study of the sodium feldspars and feldspathoids and also of glass and other ceramic products. The original phase equilibrium was by Morey and Bowen (1924) who worked on that part of the system between $Na_2O \cdot SiO_2$ and SiO_2. Kracek (1930) extended the study to the sodium orthosilicate composition, $2Na_2O \cdot SiO_2$. Bowen and Schairer (1929b) and Bowen, Schairer, and Willems (1930) in studies on the system Na_2SiO_3–Fe_2O_3–SiO_2, obtained additional data. Two crystalline compounds: sodium metasilicate, $Na_2O \cdot SiO_2$, first described by Niggli (1913), and sodium disilicate (Morey, 1914), each melts congruently, but sodium orthosilicate, $2Na_2O \cdot SiO_2$, melts incongruently with formation of crystalline Na_2O and liquid. Sodium disilicate has several polymorphic forms described by Morey, Kracek, and England (1953). There are rapid reversible transformations at 707° and 678°C.

The phase-equilibrium diagram is figure 3, and the invariant points are given in table 3. With the exception of compositions near the disilicate-quartz eutectic, there

695-382 O—64——2

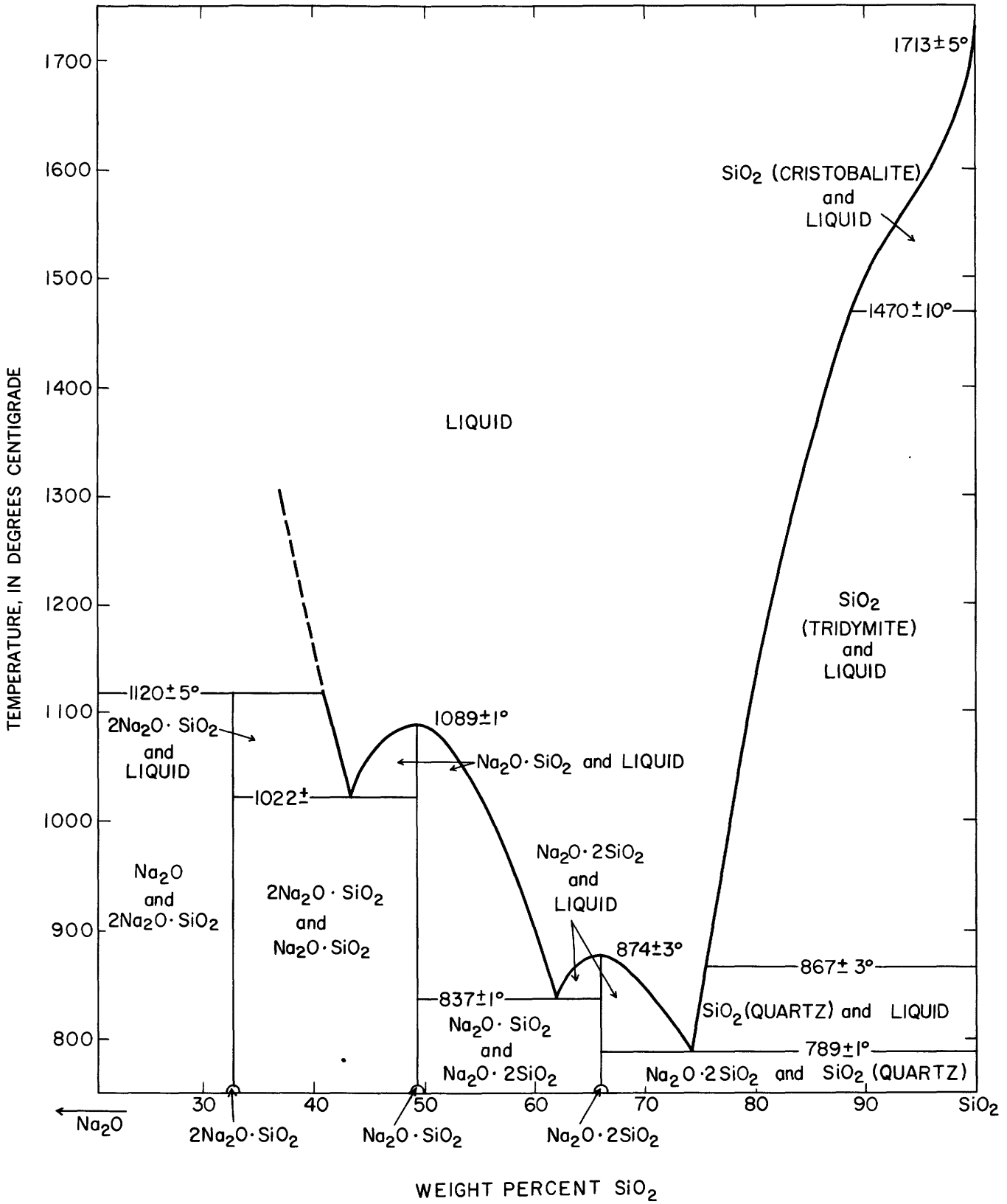

FIGURE 3.—The binary system Na_2O–SiO_2. Based on Morey and Bowen (1924) and Kracek (1930).

TABLE 3.—*Invariant points in the system* Na_2O–SiO_2

Phase reaction	Temperature (°C)	Composition of liquid (percent by weight)	
		Na_2O	SiO_2
$2Na_2O \cdot SiO_2 \rightleftharpoons Na_2O + L$	1120	59. 3	40. 7
$2Na_2O \cdot SiO_2 + Na_2O \cdot SiO_2 \rightleftharpoons L$	1022	56. 9	43. 1
$Na_2O \cdot SiO_2 \rightleftharpoons L$	1089	50. 79	49. 21
$Na_2O \cdot SiO_2 + Na_2O \cdot 2SiO_2 \rightleftharpoons L$	837	37. 9	62. 1
$Na_2O \cdot 2SiO_2 \rightleftharpoons L$	874	34. 04	65. 96
$Na_2O \cdot 2SiO_2 + SiO_2$ (quartz) $\rightleftharpoons L$	789	25. 8	74. 2

is little difficulty in reaching equilibrium in this system. Sodium metasilicate can be studied either by the quenching method or by the heating-curve method (Morey, 1923). It crystallizes so readily that melts of 25 g. or more cannot be cooled as glass, but always crystallize. On the other hand, it undercools to such an extent that the cooling curve method is not reliable. The $Na_2O \cdot 2SiO_2$–quartz eutectic shows the remarkable melting point lowering of 924°C from the melting point of SiO_2, resulting from the addition of 25.8 percent of Na_2O. The forms $3Na_2O \cdot 2SiO_2$, described by D'Ans and Loeffler (1930), and $Na_2O \cdot 3SiO_2$, described by Budnikov and Mateev (1956), do not exist.

Na_2O–TiO_2

Washburn and Bunting (1934) found the congruent melting point of $Na_2O \cdot TiO_2$ to be 1030°C, of $Na_2O \cdot 2TiO_2$ 985° C, and of $Na_2O \cdot 3TiO_2$, 1128°C.

K_2O–Al_2O_3

Brownmiller (1935) found that the compound $K_2O \cdot Al_2O_3$ melts above 1650°C and that "β-alumina," an alkali aluminate, is formed from mixtures richer in alumina.

K_2O–SiO_2

The phase-equilibrium relations in the system K_2O–SiO_2 were first inferred from the study of the ternary system H_2O–K_2SiO_3–SiO_2 by Morey and Fenner (1917), who found the hydrate, $K_2O \cdot 4SiO_2 \cdot H_2O$, but did not prepare the anhydrous tetrasilicate itself. The compound $K_2O \cdot 2SiO_2$ was first prepared by Morey (1914). The results of the study of the the system $K_2O \cdot SiO_2$–SiO_2 by Kracek, Bowen, and Morey (1929, 1939) are shown in figure 4 and the invariant points are given in table 4. Evidence that no orthosilicate exists was given by Morey and Fenner, but it was not conclusive and more study is needed. Potassium metasilicate, $K_2O \cdot SiO_2$, melts at 976°C and crystallizes readily. The melt retains CO_2 tenaciously and is hygroscopic. When melted in an atmosphere of steam, water is taken up, the melting point is lowered, and on cooling, the melt crystallizes with evolution of steam, giving an excellent second boiling point. Potassium disilicate, $K_2O \cdot 2SiO_2$, melts at 1045°C, crystallizes readily, and has an enantiotropic inversion at 594°C. Potassium tetrasilicate, $K_2O \cdot 4SiO_2$, melts at 770°C, has a reversible inversion at 594°C, and is very difficult to crystallize. Potassium silicate glasses richer in SiO_2 than the disilicate are more difficult to crystallize than the corresponding sodium silicate glasses, and both glass and crystals are very hygroscopic.

TABLE 4.—*Invariant points in the system* K_2O–SiO_2

Phase reaction	Temperature (°C)	Composition of liquid (percent by weight)	
		K_2O	SiO_2
$K_2O \cdot SiO_2 \rightleftharpoons L$	976	61. 07	38. 93
$K_2O \cdot SiO_2 + K_2O \cdot 2SiO_2 \rightleftharpoons L$	780	54. 5	45. 5
$K_2O \cdot 2SiO_2 \rightleftharpoons L$	1045	43. 95	56. 05
$K_2O \cdot 2SiO_2 + K_2O \cdot 4SiO_2 \rightleftharpoons L$	742	32. 4	67. 6
$K_2O \cdot 4SiO_2 \rightleftharpoons L$	770	28. 17	71. 83
$K_2O \cdot 4SiO_2 + SiO_2$ (quartz) $\rightleftharpoons L$	769	27. 5	72. 5

MgO–CaO

Rankin and Merwin (1916) from extrapolation of the MgO–CaO boundary in the ternary system MgO–CaO–Al_2O_3 estimated that the binary eutectic between these two oxides is at 67 percent CaO and 2300° ± 50°C. There is no compound formation.

MgO–FeO

FeO is metastable in air at ordinary temperatures and the invariant point $Fe + Fe_3O_4 \rightleftharpoons FeO$ at $P_{O_2} = 0.21$ atm is at 570°C (Ralston, 1929, p. 96). FeO melts incongruently with separation of metallic iron and a liquid containing oxygen in excess of the ferrous ratio (Bowen and Schairer, 1932), and forms with MgO a complete series of solid solutions, the magnesiowüstites (Bowen and Schairer, 1935) which have not been studied beyond ascertaining that the melting temperature rises rapidly as MgO is added to FeO, soon reaching a value above the melting point of iron.

MgO–Al_2O_3

Rankin and Merwin (1916) concluded that spinel, $MgO \cdot Al_2O_3$, which melts congruently at 2135° ± 20°C forms with α–Al_2O_3 a nearly complete series of solid solutions. Satisfactory melting temperatures could not be obtained except for spinel; its eutectic with MgO, 2030° ± 20°C and 55 percent Al_2O_3; and its eutectic with Al_2O_3, 1925° ± 40°C, and 98 percent Al_2O_3.

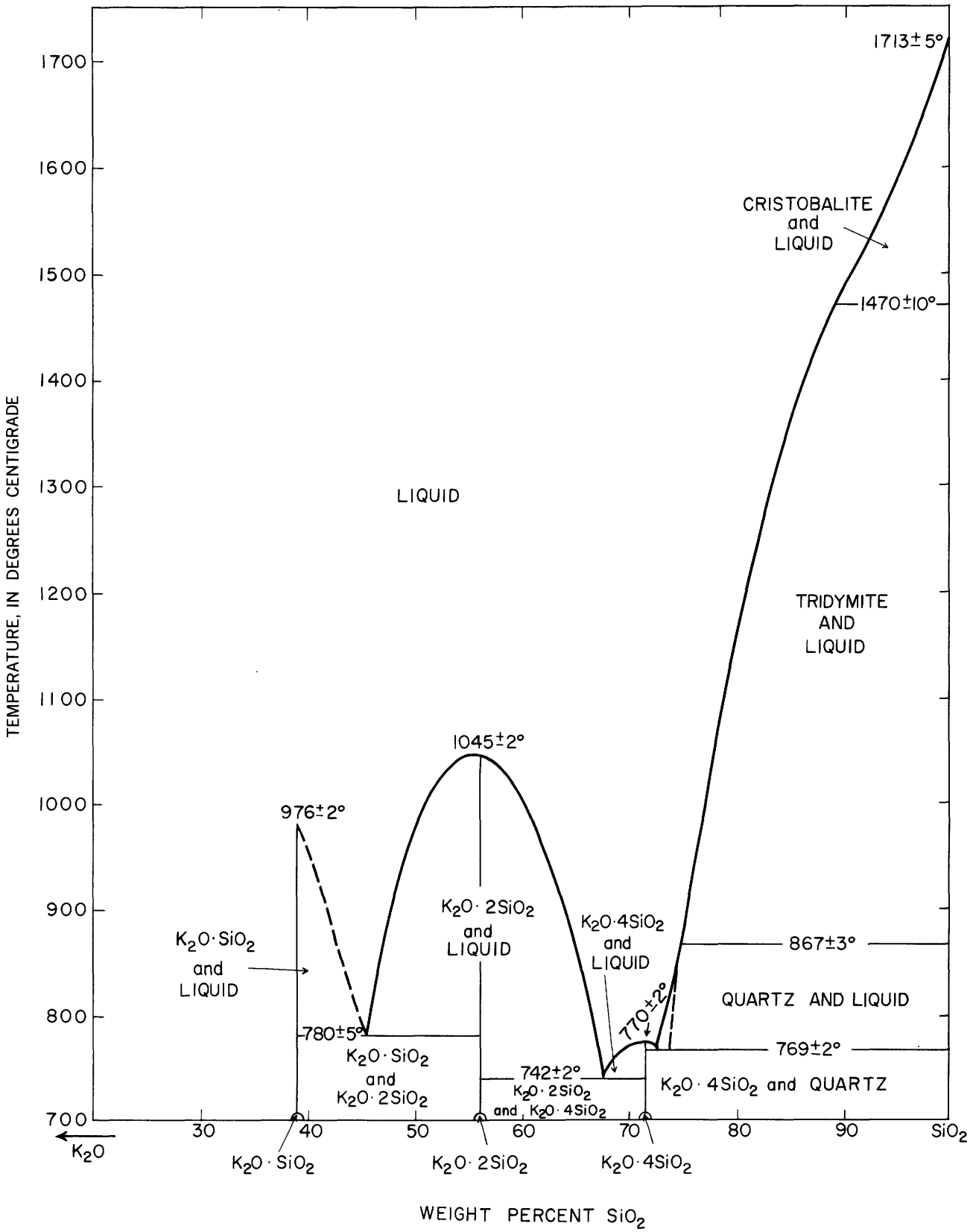

FIGURE 4.—The binary system K_2O-SiO_2. Modified from Kracek, Bowen, and Morey (1929, 1939).

MgO–Fe_2O_3

Roberts and Merwin (1931) found that the compound $MgO \cdot Fe_2O_3$ takes limited quantities of either MgO or Fe_2O_3 into solid solution. On heating in air it loses some oxygen, and the resulting solid solution in the system MgO–FeO–Fe_2O_3 begins to melt at about 1725° ± 25°C.

MgO–SiO_2

The system MgO–SiO_2 shows the relations between the pyroxenes and the olivines, in that the pyroxene enstatite, $MgO \cdot SiO_2$, melts incongruently with formation of the olivine, forsterite, $2MgO \cdot SiO_2$, and more silicious liquid. The phase-equilibrium diagram is figure 5, and the invariant points are given in table 5. The basic study was by Bowen and Andersen (1914), and the region of liquid immiscibility was discovered by Greig (1927a). MgO melts at 2800°C and forms a eutectic with magnesium orthosilicate (forsterite). The chemistry of the magnesium metasilicates is complex and was not clearly understood until Schairer (1954) summarized the older work and clarified the relations among the various forms. $MgO \cdot SiO_2$ melts incongruently at 1557°C to forsterite and a more silicious liquid, and becomes completely liquid on the forsterite liquidus curve. The form found in nature, orthorhombic enstatite, inverts at atmospheric pressure on heating to 1125° ± 25°C to a form now known as protoenstatite, which is the stable form at the incongruent melting point. Atlas (1952) placed this inversion at 985°C in the presence of alkali fluoride and carbonate fluxes. Foster (1951) concluded that while protoenstatite (sometimes called mesoenstatite) is the stable form at elevated temperatures, it inverts at a reasonably rapid rate during cooling to clinoenstatite, which bears a relation to protoenstatite similar to that which low cristobalite bears to high cristobalite. Schairer (1954) found that a sample of protoenstatite was completely changed in two years at room temperature to clinoenstatite.

TABLE 5.—*Invariant points in the system* MgO–SiO_2

Phase reaction	Temperature (°C)	Composition of liquid (percent by weight)	
		MgO	SiO_2
$MgO + 2MgO \cdot SiO_2 \rightleftharpoons L$	1850	62.0	38.0
$2MgO \cdot SiO_2 \rightleftharpoons L$	1890	57.3	42.7
$MgO \cdot SiO_2 \rightleftharpoons 2MgO \cdot SiO_2 + L$	1557	39.2	60.8
$MgO \cdot SiO_2 + SiO_2$ (cristobalite) $\rightleftharpoons L$	1543	35.2	64.8
SiO_2 (cristobalite) + $L_2 \rightleftharpoons L_1$	L_1 1695	30.5	69.5
	L_2 1695	.8	99.2

Boyd and England (1960, 1961a) studied the effects of pressure up to 30,000 atm on the melting of enstatite, and found that the incongruent melting of enstatite is eliminated by application of pressure at least as low as 15,000 atm and probably as low as 6,000 atm. Also, protoenstatite, is replaced at high pressure by orthoenstatite. At pressures present in the upper mantle, and probably in the lower parts of the continental crust, orthoenstatite is stable up to the liquidus and melts congruently.

There is a eutectic between protoenstatite and cristobalite at 1543°C, after which the liquidus curve of cristobalite rises to the invariant point, at which a second liquid layer, rich in silica, is formed. Greig (1927a) also found that the addition of 3 percent of Na_2O or 5 percent of Al_2O_3 was sufficient to cause the two layers to become miscible, and showed that the immiscibility could not be significant in petrology.

MgO–TiO_2

The system MgO–TiO_2 was studied by von Wartenberg and Prophet (1932) and by Coughanour and DeProsse (1953). Coughanour and DeProsse report that three compounds are formed, each of which melts congruently: $2MgO \cdot TiO_2$ at 1732°C, $MgO \cdot TiO_2$ at 1630°C, and $MgO \cdot 2TiO_2$ at 1652°C. The MgO–$2MgO \cdot TiO_2$ eutectic is at 1707°C and 35.9 percent TiO_2; the $2MgO \cdot TiO_2$–$MgO \cdot TiO_2$ eutectic at 1583°C and 60.9 percent TiO_2; the $MgO \cdot 2TiO_2$ at 1592°C and 70.8 percent TiO_2; and the $MgO \cdot 2TiO_2$–$2TiO_2$ eutectic at 1606°C and 91.2 percent TiO_2. No evidence of solid solution was obtained.

CaO–Al_2O_3

The original study of the system CaO–Al_2O_3 was by Rankin and Wright (1915) and it has been further studied by several authors. The phase-equilibrium diagram is figure 6, and the invariant points are given in table 6. Several compounds are formed in this system. $3CaO \cdot Al_2O_3$ melts incongruently at 1535°C with formation of CaO and a liquid richer in Al_2O_3. Rankin and Wright found a eutectic between $3CaO \cdot Al_2O_3$ and $12CaO \cdot 7Al_2O$ at 1395°C and 50 percent by weight of Al_2O_3.

Rankin and Wright reported a stable and an unstable form of $5CaO \cdot 3Al_2O_3$ which contain 52.17 percent Al_2O_3. Büssem and Eitel (1936) determined the structure of the stable form, and on the basis of density measurements gave the compound the revised formula $12CaO \cdot 7Al_2O_3$, which contains 51.46 percent Al_2O_3.

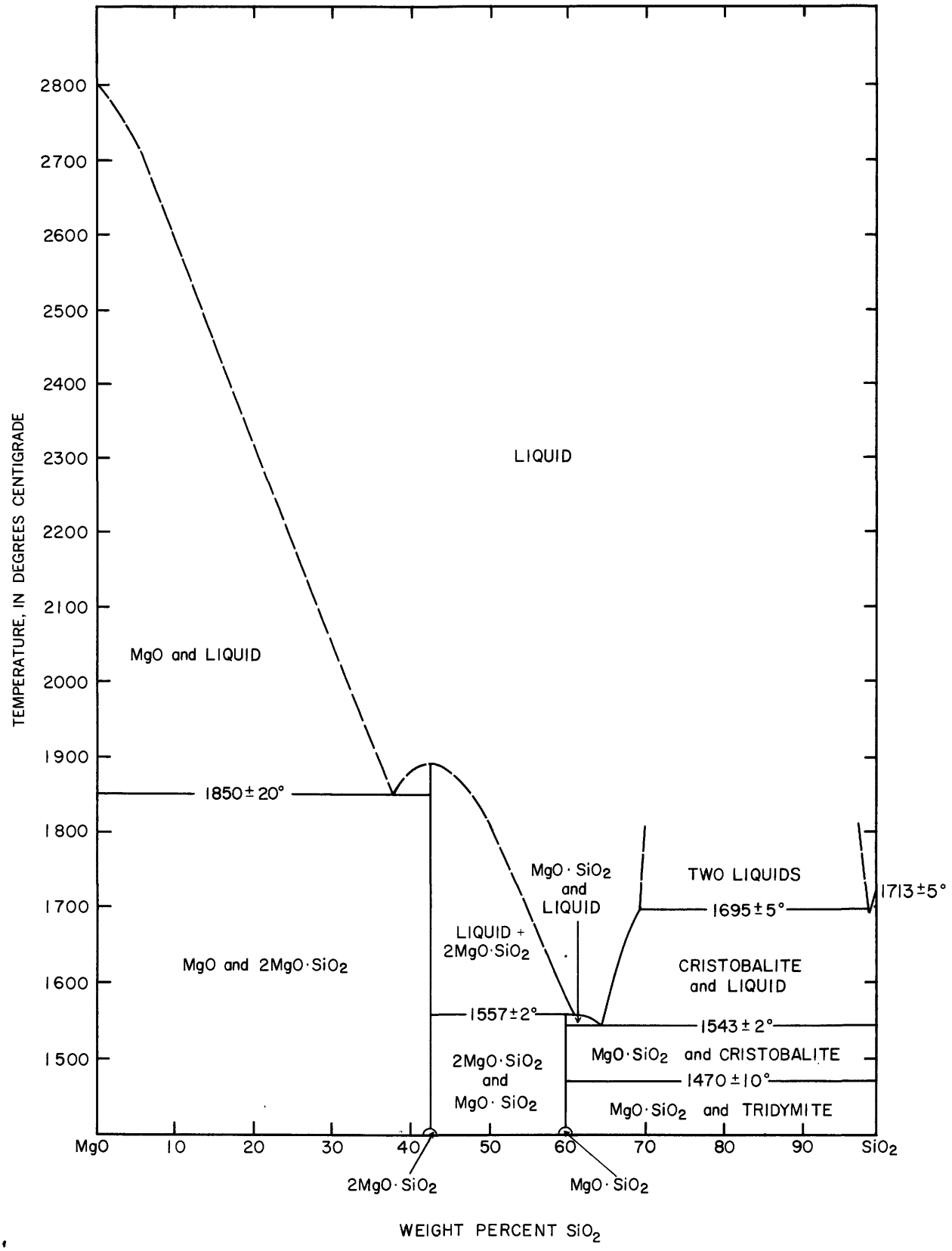

FIGURE 5.—The binary system MgO-SiO_2. Based on Bowen and Andersen (1914) and Greig (1927a).

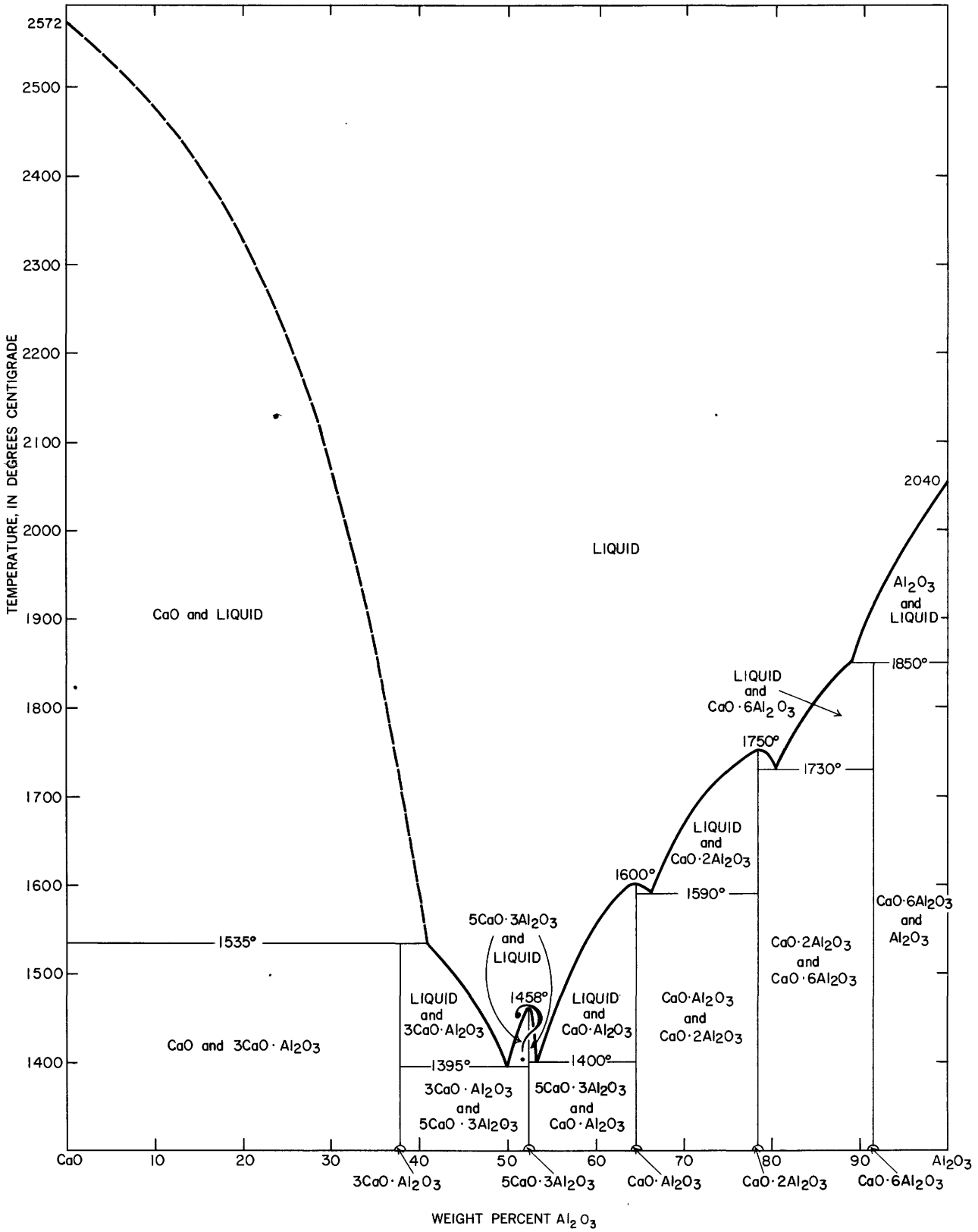

FIGURE 6.—The binary system $CaO-Al_2O_3$. Based on Rankin and Wright (1915) and Goldsmith (1948).

The melting point of this compound is uncertain. It has been given as 1455°C, but Nurse (1962) states that the melting point of the latter can be as low as 1391°C; the higher value which have been obtained by the quenching method are explained by the amazingly rapid growth of this compound during quenching and by the effect of furnace atmosphere. Unless special precautions are taken the normal furnace atmosphere contains enough water to influence the melting curve. In drier atmospheres the field of stability of $12CaO \cdot 7Al_2O_3$ narrows and although it has not been observed to disappear it seems probable that it may do so in the complete absence of water. At 1000 degrees centigrade $12CaO \cdot 7Al_2O_3$ can take up just over one percent of water.

The temperature 1391°C is lower than the eutectic given by Rankin and Wright between $3CaO \cdot Al_2O_3$ and $5CaO \cdot Al_2O_3$ and also than that between $5CaO \cdot 3Al_2O_3$ and $CaO \cdot Al_2O_3$ (1400°C). In figure 6, the original diagram of Rankin and Wright is reproduced, but a question mark has been superimposed to indicate the uncertainty in this region. $12CaO \cdot 7Al_2O_3$ is one of the few compounds in which the index of refraction of the crystalline compound is lower than that of the glass of the same composition. The existence of the unstable form of $5CaO \cdot 3Al_2O_3$ has been confirmed and its structure established (Aruja, 1959). $CaO \cdot Al_2O_3$, one of the main constitutents of high-alumina cement, melts congruently at 1600°C. It forms a eutectic with $CaO \cdot 2Al_2O_3$ at 1590°C, 66.5 percent Al_2O_3. The compound identified by Rankin and Wright as $3CaO \cdot 5Al_2O_3$ has been shown by Goldsmith (1948) to be $CaO \cdot 2Al_2O_3$, which Filonenko and Lavrov (1953) found to melt congruently at 1750°C. They also found a compound $CaO \cdot 6Al_2O_3$, which melts incongruently at 1850°C with formation of corundum and a liquid containing 89 percent Al_2O_3, and which forms a eutectic with $CaO \cdot 2Al_2O_3$ at 1730°C and 80.5 percent Al_2O_3.

TABLE 6.—*Invariant points in the system* $CaO–Al_2O_3$

Phase reaction	Temperature (°C)	Composition of liquid (percent by weight)	
		CaO	Al_2O_3
$3CaO \cdot Al_2O_3 \rightleftharpoons CaO + L$	1535	59	41
$3CaO \cdot Al_2O_3 + 12CaO \cdot 7Al_2O_3 \rightleftharpoons L$	1395	50	50
$12CaO \cdot 7Al_2O_3 \rightleftharpoons L$	1458	48. 54	51. 46
$12CaO \cdot 7Al_2O_3 + CaO \cdot Al_2O_3 \rightleftharpoons L$	1400	47	53
$CaO \cdot Al_2O_3 \rightleftharpoons L$	1600	35. 49	64. 51
$CaO \cdot Al_2O_3 + CaO \cdot 2Al_2O_3 \rightleftharpoons L$	1590	33. 5	66. 5
$CaO \cdot 2Al_2O_3 \rightleftharpoons L$	1750	21. 54	78. 46
$CaO \cdot 2Al_2O_3 + CaO \cdot 6Al_2O_3 \rightleftharpoons L$	1730	19. 5	80. 5
$CaO \cdot 6Al_2O_3 \rightleftharpoons Al_2O_3 + L$	1850	11	89

$CaO–Fe_2O_3$

A preliminary report on the system $CaO–Fe_2O_3$ was published by Sosman and Merwin (1916), and further work was done by Swayze (1946). Phillips and Muan (1958) studied the system by the quenching method in air (P_{O_2}=0.21 atm) and in oxygen at 1 atm pressure. The system is actually ternary, with components Ca, Fe, and O, but in the upper part of figure 7 it is shown projected on the join $CaO–Fe_2O_3$.

Projections are made by straight lines pointing to the O-corner of the composition triangle, called reaction lines. By reaction with the atmosphere during equilibration, O_2 is added or subtracted from the condensed phases with a proportional change in the ratio of Fe_2O_3 to FeO in the mixture. The compositions of all crystalline phases except magnetite are represented by points close to the join $CaO–Fe_2O_3$, and the compositions of the magnetites are represented by points close to the join $FeO–Fe_2O_3$ and slightly on the Fe_2O_3 side of the $FeO \cdot Fe_2O_3$ composition. The lower part of figure 7 shows these relations, and also the compositions of liquids at the liquidus temperature in air. In oxygen at 1 atm pressure the ratios of Fe_2O_3 to FeO are slightly different, and the amount of change from P_{O_2}=0.21 atm to P_{O_2}= 1 atm for some invariant points is given in table 7. A noticeable feature of the system in the subsolidus relations is the decomposition of $CaO \cdot 2Fe_2O_3$ to $CaO \cdot Fe_2O_3$ and Fe_2O_3 below 1155°C in air, 1172°C in oxygen at 1 atm pressure.

TABLE 7.—*Invariant points in the system* $CaO–Fe_2O_3$

[*ss*, solid solution]

Phase reaction	Temperature (°C)	Composition of liquid (percent by weight)		
		CaO	FeO	Fe_2O_3
$CaO + 2CaO \cdot Fe_2O_3 \rightleftharpoons L$	1438	42. 0	------	58. 0
$2CaO \cdot Fe_2O_3 \rightleftharpoons L$	1449	41. 5	------	58. 5
$CaO \cdot Fe_2O_3 \rightleftharpoons 2CaO \cdot Fe_2O_3 + L$	1216	29. 0	1. 0	75. 0
$CaO \cdot Fe_2O_3 + Ca_2O \cdot 2Fe_2O_3 \rightleftharpoons L$	[1] 1206	21. 5	1. 5	77. 0
$CaO \cdot Fe_2O_3 + Ca_2O \cdot 2Fe_2O_3 \rightleftharpoons L$	1205	20. 0	2. 0	78. 0
$CaO \cdot Fe_2O_3 + Fe_2O_3 \rightleftharpoons CaO \cdot 2Fe_2O_3$	1155	------	------	-----
Do	[1] 1172	------	------	-----
$CaO \cdot 2Fe_2O_3 \rightleftharpoons L + Fe_2O_3 ss$	[1] 1228	20. 0	2. 0	78. 0
$CaO \cdot 2Fe_2O_3 \rightleftharpoons L + Fe_2O_3 ss$	1226	19. 0	2. 5	78. 5
$Fe_3O_4 ss \rightleftharpoons L + Fe_2O_3 ss$	[1] 1430	10. 5	8. 0	81. 5
$Fe_3O_4 ss \rightleftharpoons L + Fe_2O_3 ss$	1358	13. 0	7. 0	80. 0

[1] P_{O_2}=1 atm. At all other temperatures listed, P_{O_2}=0.21 atm.

The compound $2CaO \cdot Fe_2O_3$ melts congruently at 1449°C in air and forms a eutectic with CaO at 1438°C and 58 percent Fe_2O_3. The compound $CaO \cdot Fe_2O_3$ melts incongruently at 1216°C with formation of $2CaO \cdot Fe_2O_3$ and a liquid containing excess Fe_2O_3 and some FeO. There is a eutectic between $CaO \cdot Fe_2O_3$ and $CaO \cdot 2Fe_2O_3$ at 1206°C at 1 atm oxygen pressure, at 1205°C in air (P_{O_2}=0.21 atm). $CaO \cdot 2Fe_2O_3$ melts incongruently with formation of a hematite solid solu-

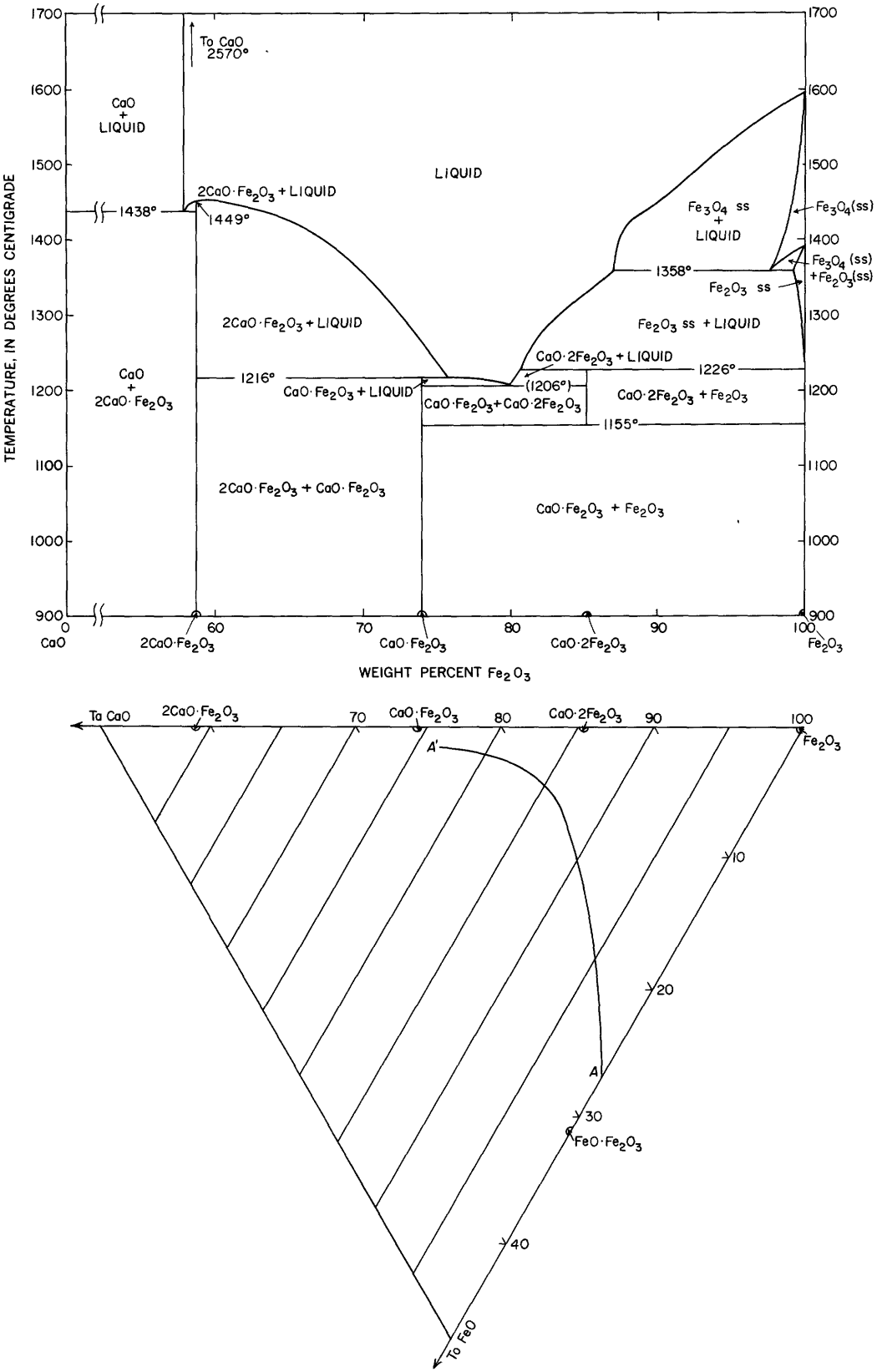

FIGURE 7.—The system $CaO-Fe_2O_3$ in air. The system is actually ternary, since the ratio of Fe_2O_3 to FeO in the liquid changes, as is shown by the line $A'A$ in the lower part of the figure, which is a portion of the system $CaO-FeO-Fe_2O_3$. The upper part of the system is a projection onto the side $CaO-Fe_2O_3$. *ss*, solid solution. Based on Phillips and Muan (1958).

tion at 1228°C at 1 atm oxygen pressure, 1226°C in air. The hematite solid solution decomposes to a magnetite solid solution at 1430°C in 1 atm oxygen pressure, 1358°C in air.

CaO–SiO_2

The system CaO–SiO_2 is of fundamental importance both to geology and to the portland cement industry. The basic work, which was by Day and Shepherd (1906) and Day, Shepherd, and Wright (1906), was the first binary oxide system to be worked out in the Geophysical Laboratory of the Carnegie Institution of Washington. Rankin and Wright (1915), in their study of the ternary system CaO–Al_2O_3–SiO_2, added further details, and Greig (1927a) discovered the region of immiscibility in mixtures high in silica. Much additional work bearing on this system has been summarized by Bogue (1955), by Lea and Desch (1956), and by Welch and Gutt (1959). The phase-equilibrium diagram is figure 8, and the invariant points are given in table 8.

The compound α-$CaO \cdot SiO_2$ (pseudowollastonite) melts congruently—that is, to a liquid of its own composition—at 1544°C. On cooling to 1125°C (Osborn and Schairer, 1941), α-$CaO \cdot SiO_2$ inverts to β-$CaO \cdot SiO_2$, wollastonite, which becomes the stable phase at lower temperatures. The inversion does not take place readily and usually is over-stepped in either direction. Bowen, Schairer, and Posnjak (1933b) showed that there is no solid solution near the composition $CaO \cdot SiO_2$.

TABLE 8.—*Invariant points in the system* CaO-SiO_2

Phase reaction	Temperature (°C)	Composition of liquid (percent by weight)	
		CaO	SiO_2
$3CaO \cdot SiO_2 \rightleftharpoons CaO + L$	2070	71. 5	28. 5
$3CaO \cdot SiO_2 \rightleftharpoons CaO + \alpha$-$2CaO \cdot SiO_2$	1250	76. 75	32. 25
$3CaO \cdot SiO_2 + \alpha$-$2CaO \cdot SiO_2 \rightleftharpoons L$	2050	69. 5	30. 5
α-$2CaO \cdot SiO_2 \rightleftharpoons L$	2130	65. 11	34. 89
α-$2CaO \cdot SiO_2 \rightleftharpoons \beta$-$2CaO \cdot SiO_2$	1420	No liquid	
β-$2CaO \cdot SiO_2 \rightleftharpoons \gamma$-$2CaO \cdot SiO_2$	675	No liquid	
$3CaO \cdot 2SiO_2 \rightleftharpoons \alpha$-$2CaO \cdot SiO_2 + L$	1464	55. 5	44. 5
$3CaO \cdot 2SiO_2 + \alpha$-$CaO \cdot SiO_2 \rightleftharpoons L$	1455	54. 5	45. 5
$CaO \cdot SiO_2 \rightleftharpoons L$	1544	48. 27	51. 73
α-$CaO \cdot SiO_2 \rightleftharpoons \beta$-$CaO \cdot SiO_2$	1125	No liquid	
α-$CaO \cdot SiO_2 + SiO_2$(tridymite) $\rightleftharpoons L$	1436	36. 1	63. 9
SiO_2 (cristobalite) $+ L_1 \rightleftharpoons L_2$	L_1 1698	27. 5	72. 5
	L_2 1698	. 6	99. 4

If a mixture containing 55 percent SiO_2 is cooled from the completely molten condition, it will not begin to crystallize until the liquidus curve of α-$CaO \cdot SiO_2$ is reached at 1522°C. When the melt has cooled to 1500°C the liquid will contain 60 percent SiO_2. Since $CaO \cdot SiO_2$ contains 51.73 percent SiO_2, the mixture at this point will contain crystalline α-$CaO \cdot SiO_2$ and liquid in the proportions to give a total SiO_2 content of 55 percent or in the proportions to give the center of mass at 55 percent SiO_2. These proportions will be $(55-51.73) \div (60-51.73)$ or 40 percent $CaO \cdot SiO_2$ and $(60-55) \div (60-51.73)$ or 60 percent liquid. This same center-of-mass principle holds true in all problems of the relative proportions of phases in systems of any number of components. When the temperature has fallen to 1470°C, the liquid contains 62 percent of SiO_2, and the mixture consists of 68 percent of $CaO \cdot SiO_2$ and 32 percent of liquid. The eutectic temperatures is 1436°C and the liquid contains 63.9 percent SiO_2. Just before tridymite begins to crystallize at the eutectic, the mixture contains 73.1 percent $CaO \cdot SiO_2$, 26.9 percent of a liquid containing 36.1 percent CaO, 63.9 percent SiO_2. When crystallization is complete at the eutectic, the mixture contains 93 percent of α-$CaO \cdot SiO_2$ (pseudowollastonite) and 7 percent of SiO_2 (tridymite). The eutectic point is an invariant point, since there are three phases, liquid, α-$CaO \cdot SiO_2$, and tridymite, coexisting at a constant pressure and temperature. This eutectic with SiO_2 is the lowest temperature invariant point in this system, as in most silicate systems.

If the original mixture contains more CaO than corresponds to $CaO \cdot SiO_2$, the liquidus curve falls to the eutectic at 1455°C and 45.5 percent SiO_2, where it solidifies to a mixture of $3CaO \cdot 2SiO_2$ (rankinite) and α-$CaO \cdot SiO_2$. When pure $3CaO \cdot 2SiO_2$ is heated, it remains unchanged until 1464°C (Osborn, 1943) is reached, when it begins to melt. The system remains at 1464°C until the reaction $3CaO \cdot 2SiO_2 = L + 2CaO \cdot SiO_2$ is complete, and the liquid contains 44.5 percent SiO_2. This is an example of what is called incongruent melting in which one of the solids melts to form a liquid and another solid, and the composition of the melting solid is between the liquid and the new solid formed by the phase reactions. The invariant point at which reaction takes place is called an incongruent melting point, a reaction point (Bowen, 1922), or sometimes a peritectic point. When a melt of composition $3CaO \cdot 2SiO_2$ is cooled from the liquid condition, $2CaO \cdot SiO_2$ begins to crystallize at about 1700°C. As cooling continues the liquid becomes enriched in SiO_2, until at 1464°C the reverse reactions take place and crystalline $3CaO \cdot 2SiO_2$ is formed until all the $2CaO \cdot SiO_2$ and liquid are used.

The compounds $2CaO \cdot SiO_2$ melts at 2130°C. It is known in several forms (Bredig, 1950). The high-temperature form, α-$2CaO \cdot SiO_2$, inverts to an orthorhombic form (Bredig, 1945) at 1438°C, which Tilley

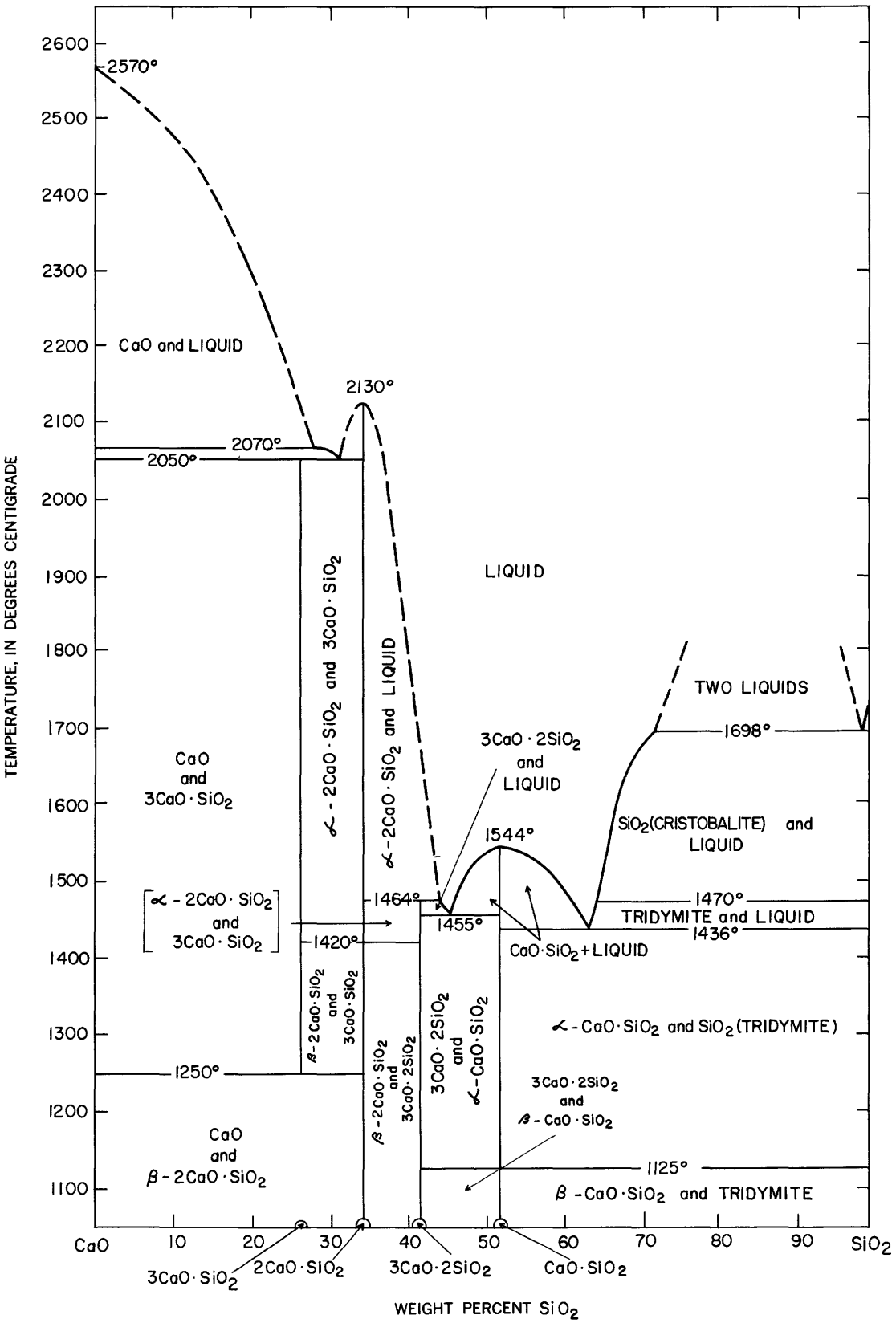

FIGURE 8.—The binary system CaO–SiO_2. Based on Rankin and Wright (1915), Greig (1927a), and Welch and Gutt (1959).

and Vincent (1948) found as a mineral and named bredigite. The inversion temperature is greatly lowered in complex systems. The orthorhombic form inverts at 650°C to the γ-form with an increase in volume of about 10 percent and a resulting "dusting" to a fine powder. When the α-form is undercooled to 675°C, it changes to a monotropic form which corresponds to the mineral larnite. It was called the β-form by Rankin and Wright (1915).

Tricalcium silicate, $3CaO \cdot SiO_2$, is the most CaO-rich compound in the binary system, CaO–SiO_2. It is of great industrial importance as a constituent of portland cement, called "alite" by Tornebohm (1897). It was formerly considered to decompose at 1900°C, but Welch and Gutt (1959) found that it melts incongruently at 2070°C, with formation of liquid and CaO. Hence, it has a short composition range of stability in contact with melt, as shown in figure 8. A mixture of the composition $3CaO \cdot SiO_2$ on cooling first separates CaO at about 2110°C, and on cooling to the reaction point $CaO + L = 3CaO \cdot SiO_2$ at 2070°C, the CaO reacts with liquid to form $3CaO \cdot SiO_2$. There are metastable inversions at 923° and 980°C (Nurse, 1960). Finally, if the compound is cooled to 1250°C it decomposes into CaO and $2CaO \cdot SiO_2$. This also is an invariant point in a condensed system, at which the phase reaction is $3CaO \cdot SiO_2 = CaO + 2CaO \cdot SiO_2$.

An important phenomenon is shown in mixtures rich in silica, namely, the formation of two immiscible liquid phases (Greig, 1927a). The stable phases immediately below the eutectic temperature, 1436°C, in any mixture containing more SiO_2 than $CaO \cdot SiO_2$ is a mixture of $CaO \cdot SiO_2$ and SiO_2, as tridymite. If the mixture contains more than the eutectic composition, 63.9 percent SiO_2, at the eutectic temperature all the $CaO \cdot SiO_2$ melts, leaving tridymite. On further heating the tridymite inverts to cristobalite at 1470°C. If the mixture contains between 72.5 and 99.4 percent of SiO_2, at 1698°C the liquid separates into two immiscible liquids. This is an invariant point, since there are two liquid phases and a solid phase, cristobalite, coexisting at a constant pressure greater than the vapor pressure of any of the melts.

It is evident from the phase-equilibrium diagram that $CaO \cdot SiO_2$ is the only solid phase which can exist in equilibrium with SiO_2. $3CaO \cdot 2SiO_2$ or $2CaO \cdot SiO_2$ are incompatible with SiO_2, and their fields are not adjacent to the field of silica.

CaO–TiO_2

The system CaO–TiO_2 has been studied by von Wartenburg, Reusch and Saran (1937), Coughanour, Roth, and DeProsse (1954), and DeVries, Roy, and Osborn (1954b). The latest revision is by Roth (1958), whose phase-equilibrium diagram is shown in figure 9. Data on the invariant points in the system are given in table 9. The compound $CaO \cdot TiO_2$ which corresponds to the mineral perovskite, melts congruently at 1915°C, and has a eutectic with TiO_2 at 1475°C. The compound $4CaO \cdot 3TiO_2$ melts incongruently at 1755°C with formation of a CaO-richer liquid and $3CaO \cdot TiO_2$ which melts incongruently at 1740°C. The eutectic CaO–$3CaO \cdot 2TiO_2$ is at 1725°C.

TABLE 9.—*Invariant points of the system* CaO–TiO_2

Phase reaction	Temperature (°C)	Composition of liquid (percent by weight)	
		CaO	TiO_2
$CaO + 3CaO \cdot 2TiO_2 \rightleftharpoons L$	1725	61	39
$3CaO \cdot 2TiO_2 \rightleftharpoons 4CaO \cdot 3TiO_2 + L$	1740	54	46
$4CaO \cdot 3TiO_2 \rightleftharpoons CaO \cdot TiO_2 + L$	1755	53	47
$CaO \cdot TiO_2 \rightleftharpoons L$	1915	41. 24	58. 56
$CaO \cdot TiO_2 + TiO_2 \rightleftharpoons L$	1475	17	83

FeO–Al_2O_3

The system FeO–Al_2O_3 was studied by M'Intosh, Rait, and Hay (1937), who found compounds provisionally identified as $3FeO \cdot Al_2O_3$ and $FeO \cdot Al_2O_3$. However, Schairer and Yagi (1952) point out that these investigations took no cognizance of the equilibrium between ferrous oxide melts and metallic iron, and conclude that no reliable data in this system are available.

FeO–Fe_2O_3

$FeO–F_2O_3$ is part of the system iron–oxygen, and the relation between the compositions of the iron oxide phases and the pressure of oxygen must be considered at every temperature. This is true in all systems in which an oxide of iron is a component. The work by Darken and Gurry (1945, 1945) presents a study of these relationships at temperatures both below and above those at which liquid oxide is formed, and include the results of Greig, Posnjak, Merwin, and Sosman (1935). Figure 10 gives their temperature-composition phase-equilibrium diagram at a total pressure of 1 atm; significant data for the lettered points are given in table 10. Low oxygen pressures are given in this table by the ratio P_{CO_2}/P_{CO}, from which may be calculated [3] the partial pressure of oxygen. Addition of oxygen to

[3] The free energy of the reaction $CO + \frac{1}{2}\ O_2 \rightleftharpoons CO_2$ calculated from the free energy changes for the reaction C (graphite) $+ O_2\ (g) \rightleftharpoons CO_2\ (g)$ and C (graphite) $+ \frac{1}{2}\ O_2\ (g) \rightleftharpoons CO\ (g)$ is given by Coughlin (1954) as $\Delta F° = -67500 + 20.71\ T$ from which the pressure of oxygen at any temperature can be calculated.

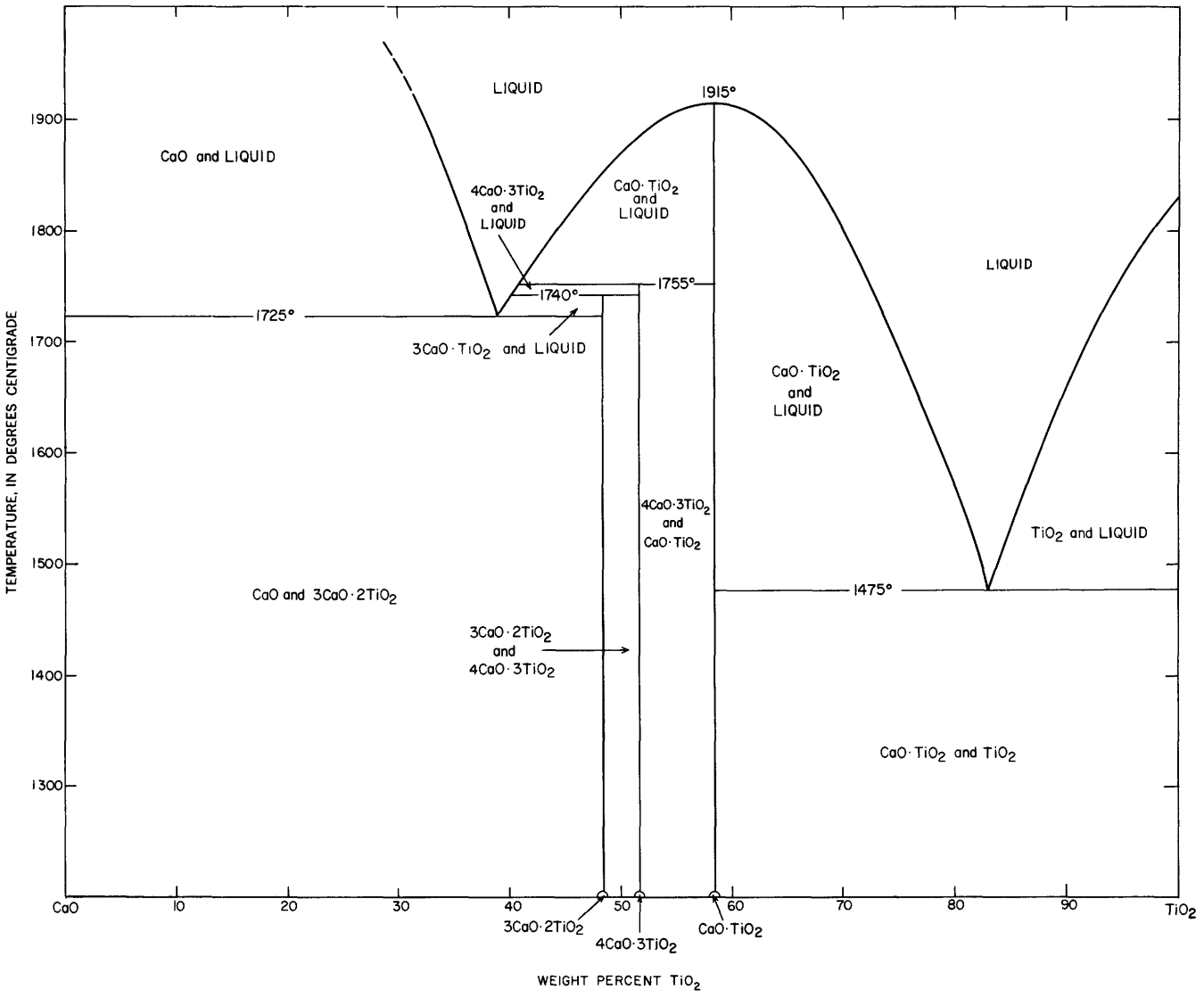

FIGURE 9.—The binary system CaO–TiO_2. Modified from Roth (1958).

iron lowers its melting point from 1535°C to *B* at 1524°C, when a second liquid layer of composition *C* appears. With increase in temperature the two layers probably approach each other in composition as indicated. On further increase in oxygen content, the melting point curve is lowered from *C* to *N*, at which invariant point wüstite of composition near FeO appears. At invariant point *I* magnetite becomes the solid phase, and melts congruently at point *V*, after which the melting curve falls to a eutectic at which the solid phases are a magnetite solid solution of composition *Y* and a hematite solid solution of composition *Z*. Where the line of $P_{O_2}=1$ atm, a magnetite of composition *R* is in equilibrium with iron-oxide liquid of composition R^1.

Below the temperature of *Q* (560°C), FeO (wüstite) is not a stable phase, and at oxygen pressures less than about 10^{-24} atm metallic iron and Fe_3O_4 are the stable phases; at slightly greater oxygen pressures the stable phase pair is Fe_3O_4 and Fe_2O_3; and at higher pressures only Fe_2O_3. Above 560°C a field of wüstite solid solutions separates the fields of iron + wüstite and wüstite + magnetite. Most of the diagram of figure 10 corresponds to a partial pressure of oxygen less than that in air—that is, 0.21 atm.

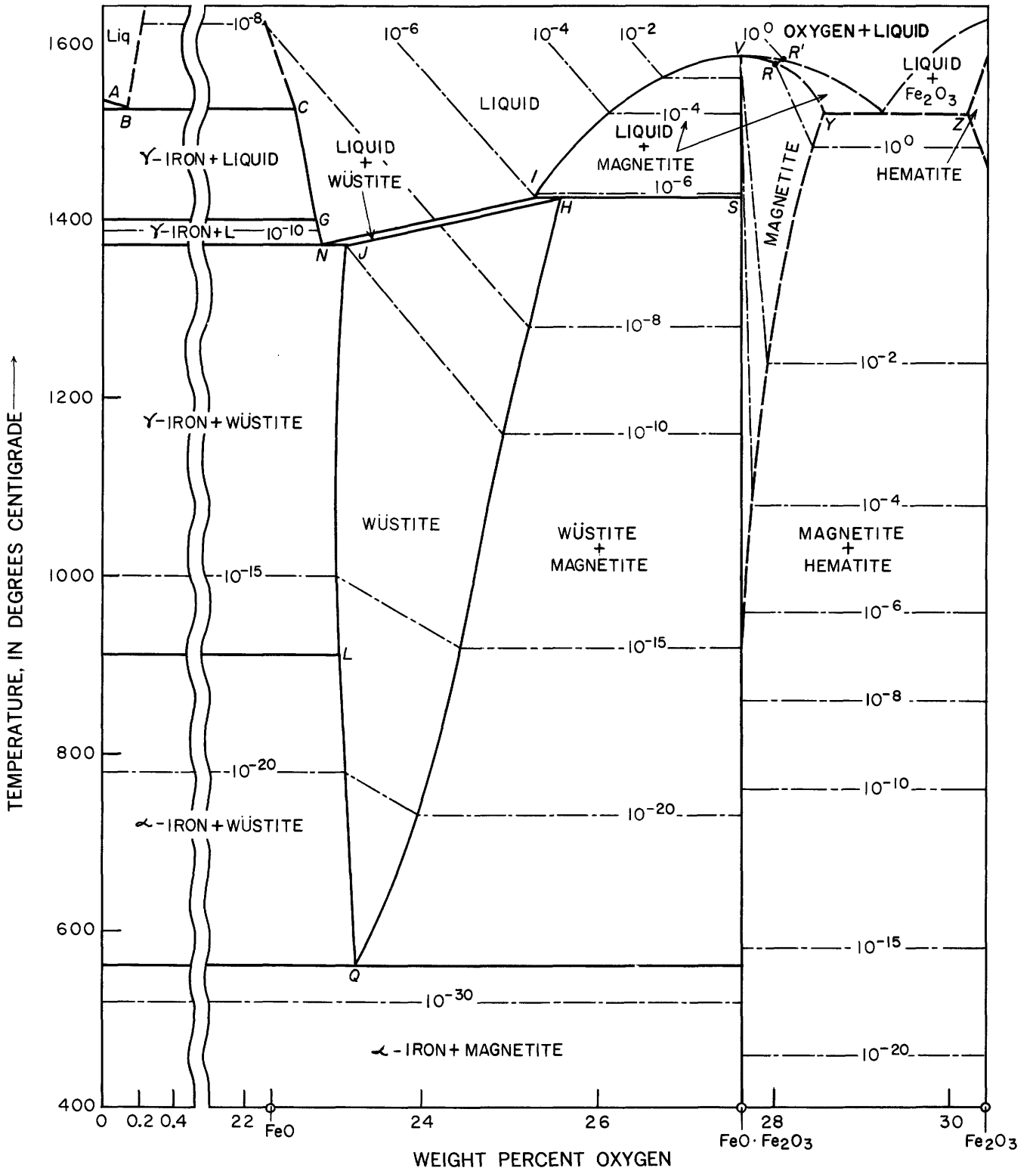

FIGURE 10.—The system iron-oxygen. Heavy solid lines are boundary curves and light dashed lines are O_2 isobars. Modified from Muan (1958a) and from Darken and Gurry (1945, 1946).

TABLE 10.—*Significant points of the system iron–oxygen*

[Reprinted from Darken and Gurry, 1945, 1946]

Invariant point on fig. 10	Temperature (°C)	O (percent)	P_{CO_2}/P_{CO}	P_{O_2}(atm)
A	1535	0		
B	1524	0. 16	0. 209	
C	1524	22. 60	. 209	
G	1400	22. 84	. 263	
H	1424	25. 60	16. 2	
I	1424	25. 31	16. 2	
J	1371	23. 16	. 282	
L	911	23. 10	. 447	
N	1371	22. 91	. 282	
Q	560	23. 26	1. 05	
R	1583	28. 30		1
R'	1583	28. 07		1
S	1424	27. 64	16. 2	
V	1597	27. 64		. 0575
Y	1457	28. 36		1
Z	1457	30. 04		1

Figure 11 shows the fields of iron and its oxides in a *P–T* diagram in which the pressure of oxygen is represented by $P_{O_2}=P_{H_2O}/P_{H_2}$.[4] At temperatures below 1070°C, Fe_2O_3 is the stable phase in the equilibrium with water vapor. Bozorth (1927) found that the protective layer formed on iron by steam at 713°C was built up of layers of FeO, Fe_3O_4, and Fe_2O_3, of thickness 10^{-2}, 2×10^{-4}, and 2×10^{-5} cm, respectively.

FeO–SiO_2

The system FeO–SiO_2 cannot be studied accurately as a binary system because the liquids are never purely ferrous, but Bowen and Schairer (1932) made a close approximation by working in iron crucibles in an atmosphere of oxygen-free nitrogen, obtained by passing the nitrogen through ammoniacal copper solution and then over hot copper gauze. They analyzed the resulting mixtures for the Fe_2O_3 content, with results shown in the upper curve of figure 12. The approach to a binary system is very close except at the iron-rich end, and the melts in their actual behavior are sensibly binary. Bowen and Schairer "without serious misrepresentation and with enormous gain in the utility of the diagram" drew the binary diagram of figure 12 by calculating all iron in each mixture to FeO and plotting the results accordingly. The point given as the melting point of FeO, 1380°C, is the invariant point Fe + liquid=FeO in the binary system, Fe–O, and the liquid contains 11.56 percent Fe_2O_3. From this point the liquidus falls, with FeO (wüstite) as solid phase, to the eutectic with $2FeO\cdot SiO_2$ (fayalite), at 1177°C. Pure fayalite melts congruently with separation of about 0.75 percent of metallic iron, but a mixture having nearly the composition of theoretical fayalite melts at 1205°C about as sharply as the purest silicate compounds in spite of its containing 2.25 percent Fe_2O_3.

From the melting point of fayalite, the melting-point curve falls with increasing FeO to a eutectic with FeO (wüstite) at 1177°C, and with increasing SiO_2 content to a eutectic with tridymite at 1176°C. From this point the liquids curve rises until a region of liquid immiscibility is reached. Greig (1927b) found that at 1689°±10°C the FeO-rich layer in equilibrium with cristobalite contains 42 percent FeO, the SiO_2-rich layer, 3 percent FeO.

Bernal (1936) suggested that common olivine might invert to a spinel-type structure at high pressure, and Ringwood (1958) prepared a spinel form of $2FeO\cdot SiO_2$ at 35 to 40 kilobars pressure and 600°C. Boyd and England (1960) confirmed Ringwood's result and obtained a point on the *P-T* curve at 60 kilobars and 1500°C.

FeO–TiO_2

Grieve and White (1939) found that each of the two ferrous titanates, $2FeO\cdot TiO_2$ (ulvöspinel), and $FeO\cdot TiO_2$ (ilmenite), melted congruently at about 1470°C. $2FeO\cdot TiO_2$ has a eutectic with FeO at 1380°C, 5 percent TiO_2, and with $FeO\cdot TiO_2$ at 1320°C and 42 percent TiO_2. The $FeO\cdot TiO_2$–TiO_2 eutectic is at 1330°C, 68 percent TiO_2.

Al_2O_3–SiO_2

The binary system Al_2O_3–SiO_2 is fundamental to the most widely used refractories and to the clay-working industries in general. The original study of this system was by Shepherd, Rankin, and Wright (1909), but they did not recognize the existence of $3Al_2O_3\cdot 2SiO_2$ (mullite), which was discovered by Bowen and Greig (1924). The present Al_2O_3–SiO_2 diagram (figure 13) is by Aramaki and Roy (1959), who found that mullite melts congruently at 1850°C, and has a eutectic with Al_2O_3 at 1840°C and 78 percent by weight Al_2O_3. Toropov and Galakhov (1951) and Budnikov, Tresvyatskii, and Kushnakovskii (1953) had previously found that mullite melts congruently, as indicated in the diagram. There is an area of solid solution of Al_2O_3 in mullite.

[4] The free energy of the reaction $H_2+\frac{1}{2}O_2=H_2O(g)$ is given by Coughlin (1954) as $\Delta F^\circ=-58{,}850+13.12\ T$ from which the pressure of oxygen at any temperature can be calculated. (See also Eugster, 1959.)

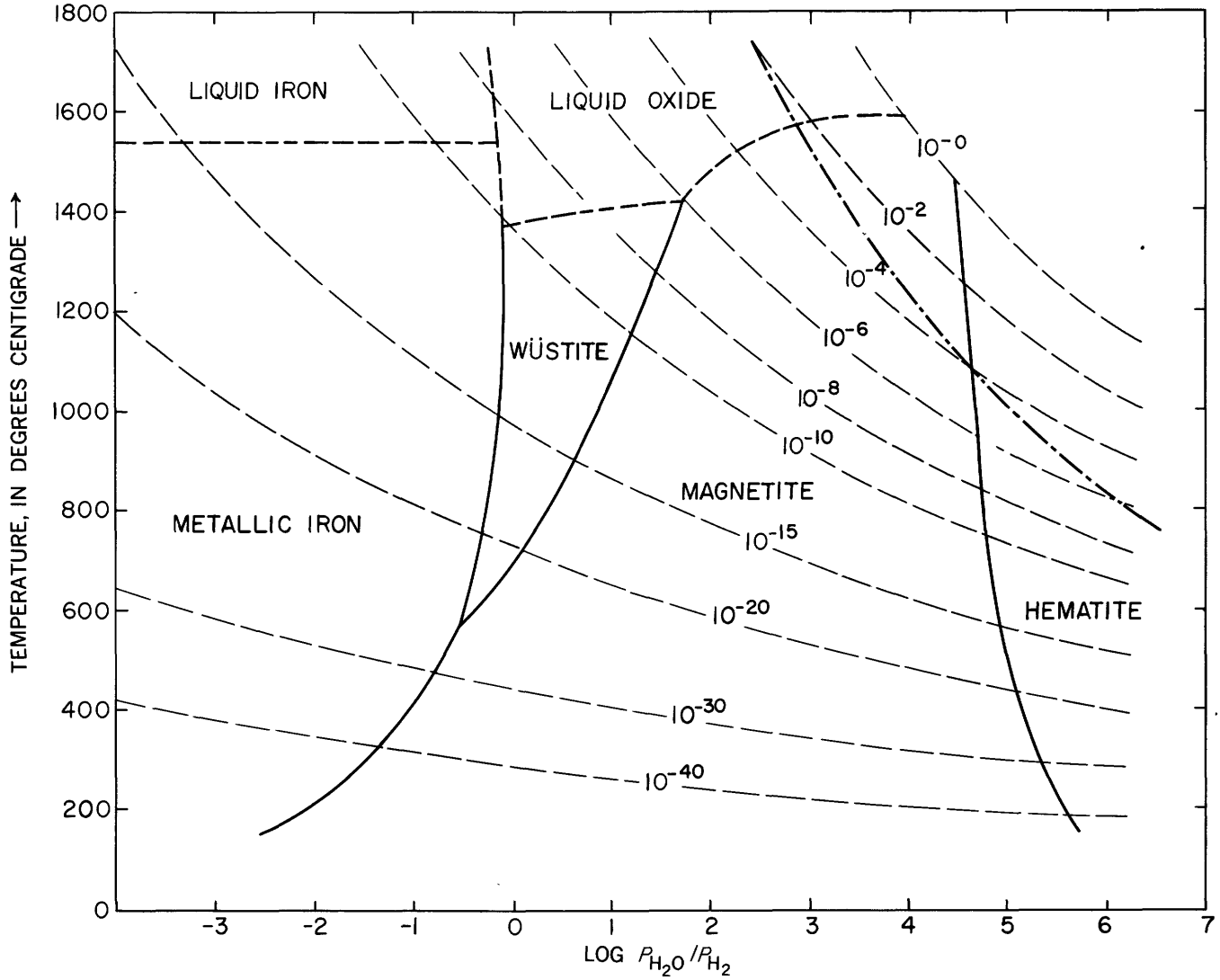

FIGURE 11.—The stability fields of iron and its oxides in which the pressure of oxygen is given by $P_{O_2}=P_{H_2O}/P_{H_2}$. Heavy solid lines are boundary curves between phase areas. Light dot-dash lines are oxygen isobars which may be correlated with the isobars of figure 10. The heavy long-short dash line equilibrium ratios P_{H_2O}/P_{H_2} of pure water vapor as a function of temperature at a total pressure of 1 atm. Modified from Muan (1958a).

The relations among the three minerals sillimanite, kyanite, and andalusite, each of which has the composition $Al_2O_3 \cdot SiO_2$, are not clear. Greig (1926) found that each of them decomposes on heating into mullite and silica, probably in the form of cristobalite, or into mullite and a siliceous liquid. For none of them was the decomposition reversible, nor was there a definite temperature of decomposition but rather a rate of decomposition increasing with the temperature. Kyanite apparently began to change at the lowest temperature, sillimanite at the highest. Kyanite appeared unaltered except for loss of color on heating 48 hours at 1000°C, but some decomposition had taken place. Morey and Ingerson (1941) obtained sillimanite in experiments with superheated steam at high pressure, and Roy (1954) and Roy and Roy (1955) synthesized andalusite. They found no definite stability range, but andalusite formed in the temperature range 450° to 700°C with H_2O pressures of 10,000 to 30,000 psi. Robertson, Birch, and MacDonald (1955) mention in an abstract that they have found a tentative boundary between the sillimanite and kyanite fields, but give no details. Griggs and Kennedy (1956) give a P-T curve for the change of sillimanite to kyanite, which goes to higher temperatures and pressures from about 700°C and 15,000 psi., where it intersects the dissociation curve of

pyrophyllite, ($Al_2O_3 \cdot 4SiO_2 \cdot H_2O$). At a quintuple point are pyrophyllite, quartz, H_2O, sillimanite, and kyanite. Clark, Robertson, and Birch (1957) found points on the curve of equilibrium between sillimanite and kyanite at 18,200 bars at 1000°C and 21,000 bars at 1300°C, with kyanite being the high-pressure phase. In their report they give a tentative phase diagram showing the relationship among the phases kyanite, sillimanite, andalusite, and (mullite+quartz), which is reproduced as figure 14. Clark (1960) determined the kyanite-sillimanite curve more precisely. The agreement was within 1 kilobar in the range from 1000° to 1300°C. The slope of the P-T curve between 1000° and 1500°C is 13.1 bars per degree. The minerals in this system are among the best refractories known. They are extraordinarily reluctant to take part in chemical reaction, and forms persist for long periods outside of their regions of stability.

Al_2O_3–TiO_2

The system Al_2O_3–TiO_2 has been studied by von Wartenberg and Reusch (1932) and by Bunting (1933); $Al_2O_3 \cdot TiO_2$ melts congruently at about 1860°C; the eutectic with Al_2O_3 is at 1850°C and 38 percent TiO_2; that with TiO_2 at 1715°C and 85 percent TiO_2.

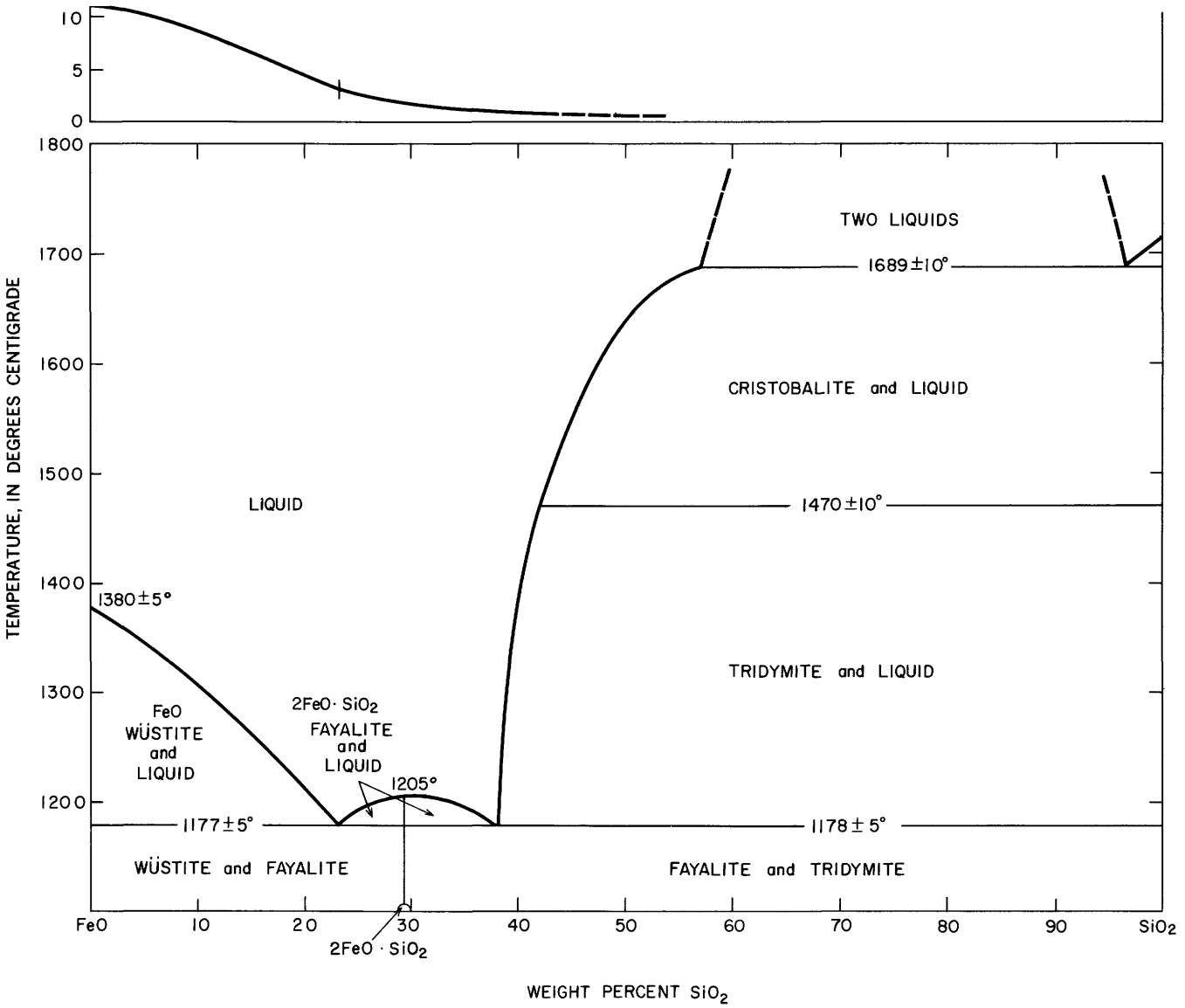

FIGURE 12.—The system FeO–SiO_2. Modified from Bowen and Schairer (1932).

695-382 O - 64 - 3

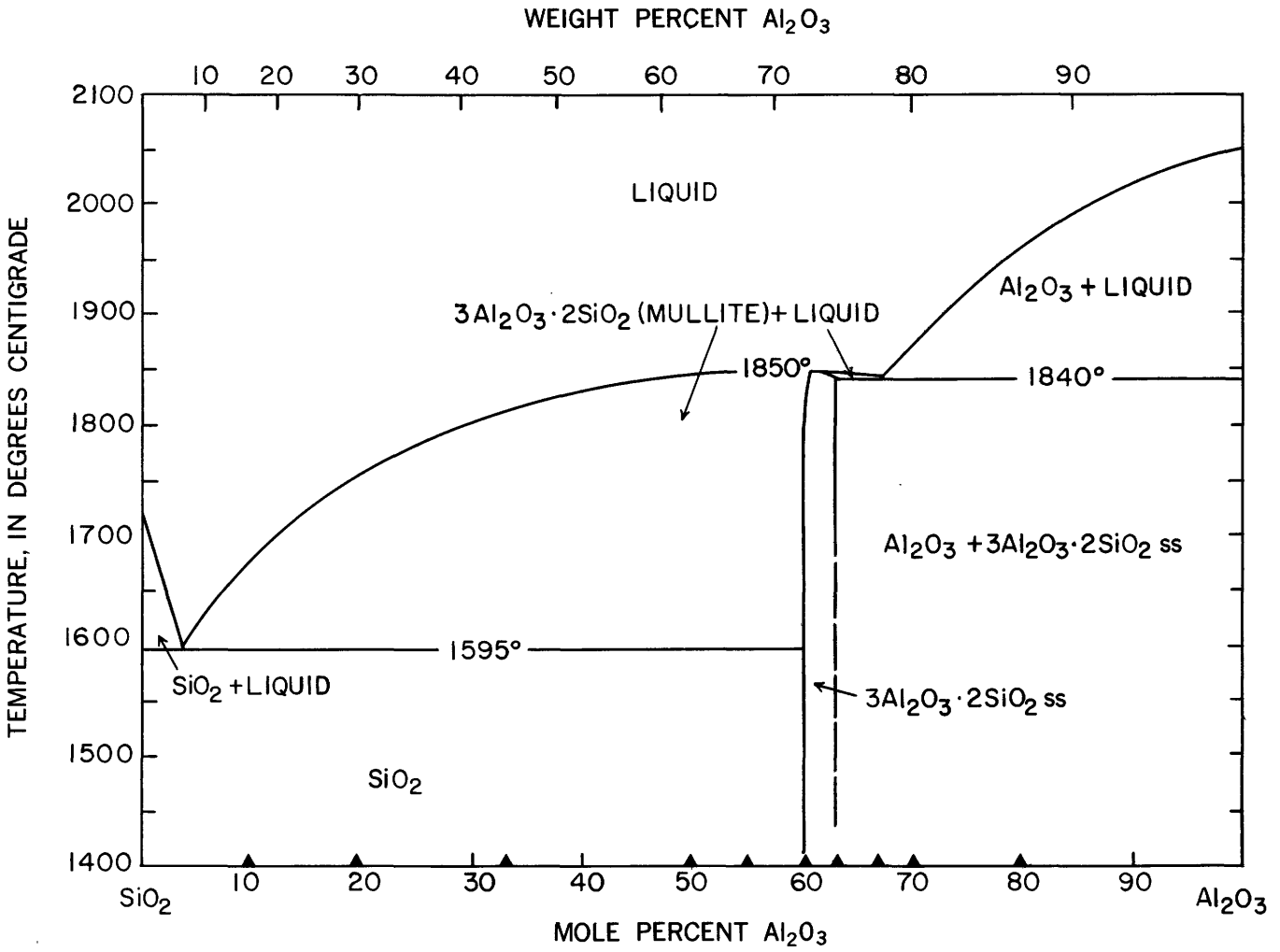

FIGURE 13.—The system Al_2O_3–SiO_2. *ss*, Solid solution. Modified from Aramaki and Roy (1959).

Fe_2O_3–Al_2O_3

Muan and Gee (1956) and Muan (1958b) studied the system Fe_2O_3–Al_2O_3 by the quenching method in air (Po_2=0.21 atm) and in oxygen at 1 atm. The system Fe_2O_3–Al_2O_3 can be considered as binary until Fe_2O_3 starts to dissociate to oxygen and FeO, when a spinel phase is formed. The results are shown in figure 15; the diagram at 1 atm oxygen pressure is a little different. The phase $Fe_2O_3 \cdot Al_2O_3$ (hercynite) is unstable relative to hematite solid solution plus corundum solid solution below 1318°C (Muan, 1958b). The system becomes ternary, neglecting the possible appearance of a metallic iron. As in all systems containing iron oxide, the partial pressure of oxygen must be considered.

Fe_2O_3–SiO_2

Bowen, Schairer, and Willems (1930) inferred from the curve of the tridymite-hematite boundary in the system Na_2O–Fe_2O_3–SiO_2 that no compound exists in this binary system, and that there is almost complete immiscibility between Fe_2O_3 and SiO_2 in the liquid state.

Fe_2O_3–TiO_2

The system Fe_2O_3–TiO_2 was studied by MacChesney and Muan (1959a) in air by the quenching method. The results are shown in figure 16. There is extensive solid solution, and the crystalline phases have compositions approximately represented by parts of the joins $FeO \cdot Fe_2O_3$–$2FeO \cdot TiO_2$, Fe_2O_3–$FeO \cdot TiO_2$, and $Fe_2O_3 \cdot TiO_2$ (pseudobrookite)–$Fe_2O_3 \cdot 2TiO_2$. The most notable feature of the subsolidus relations is the marked influence of TiO_2 on the equilibrium decomposition temperature of the sesquioxide (α-Fe_2O_3) structure of hematite to the spinel structure of magnetite. This decomposition temperature in air rises from 1390°C for the pure iron oxide end member to a maximum of 1524°C as TiO_2 is added.

SiO_2–TiO_2

The system SiO_2–TiO_2 was studied by DeVries, Roy, and Osborn (1954a) who critically reviewed the results of earlier observers. The melting point curve falls from the melting point of SiO_2, 1713°C, to a eutectic with rutile, TiO_2, and cristobalite at 1556°±4°C, 10.5 percent TiO_2. The curve then rises rapidly until at 1780°±10°C, two liquid layers of composition 19 percent TiO_2 and 93 percent TiO_2 are formed in equilibrium with rutile. On further increase in temperature, the TiO_2-rich liquid rises to the melting point of TiO_2 at 1830°C.

TERNARY SYSTEMS

The ternary systems formed by the nines oxides under consideration are given in this section. The combinations of the oxides are arranged in the order of their enumeration in the Introduction. At an invariant point in a ternary condensed system four phases coexist, and at most of the invariant points considered three solids coexist with a liquid. When the composition of the liquid lies within the triangle formed by the compositions of the three solid phases the liquid is a eutectic, and the phase reaction is of the type $S_1+S_2+S_3=L$. When the composition of the liquid is outside of the

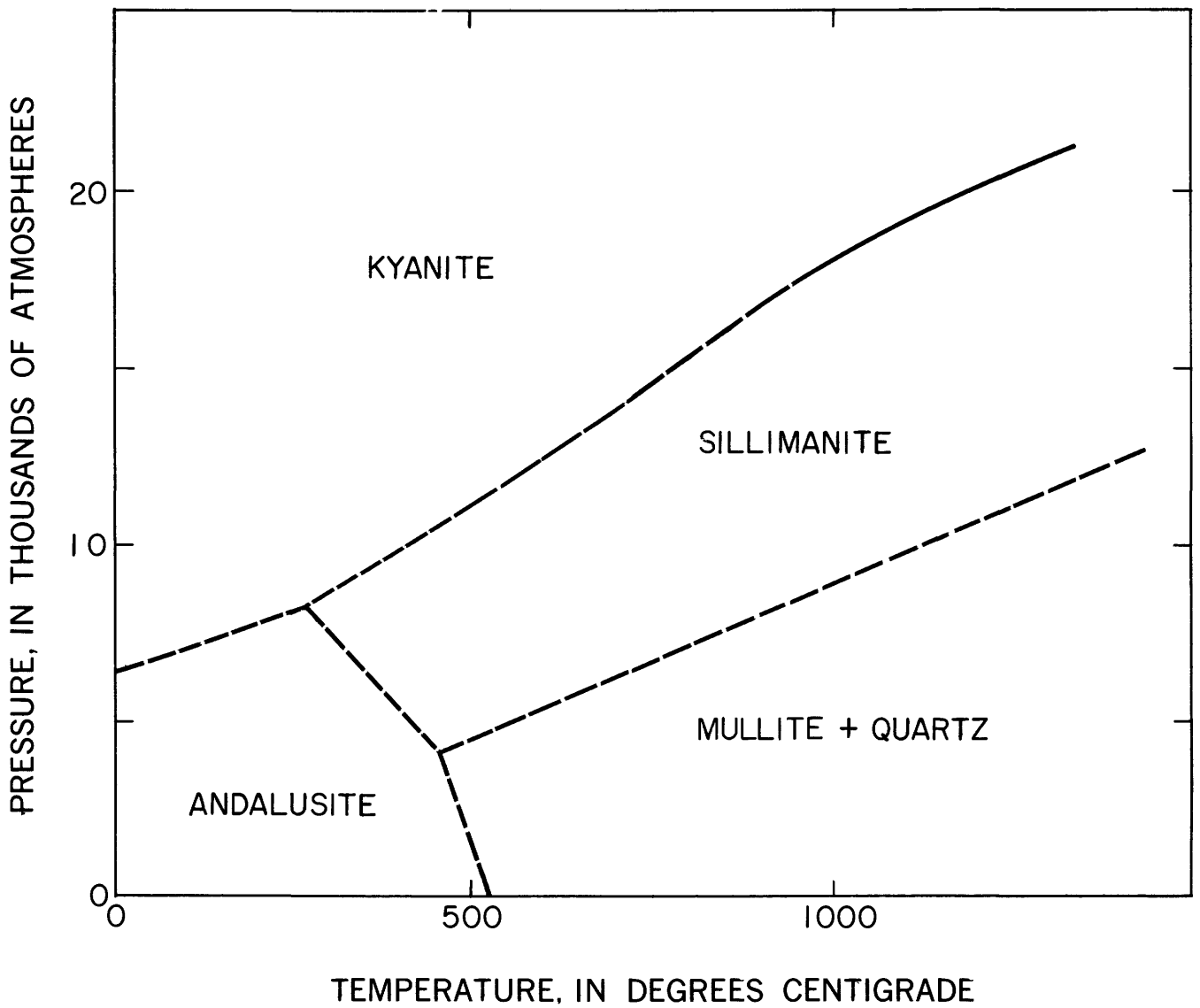

FIGURE 14.—Tentative phase diagram of the composition Al_2O_3·SiO_2. Phase boundaries indicated by short dashes are not experimentally determined and no quantitative significance should be attached to them; longer dashes are an extrapolation of the kyanite-sillimanite equilibrium curve. Modified from Clark, Robertson, and Birch (1957).

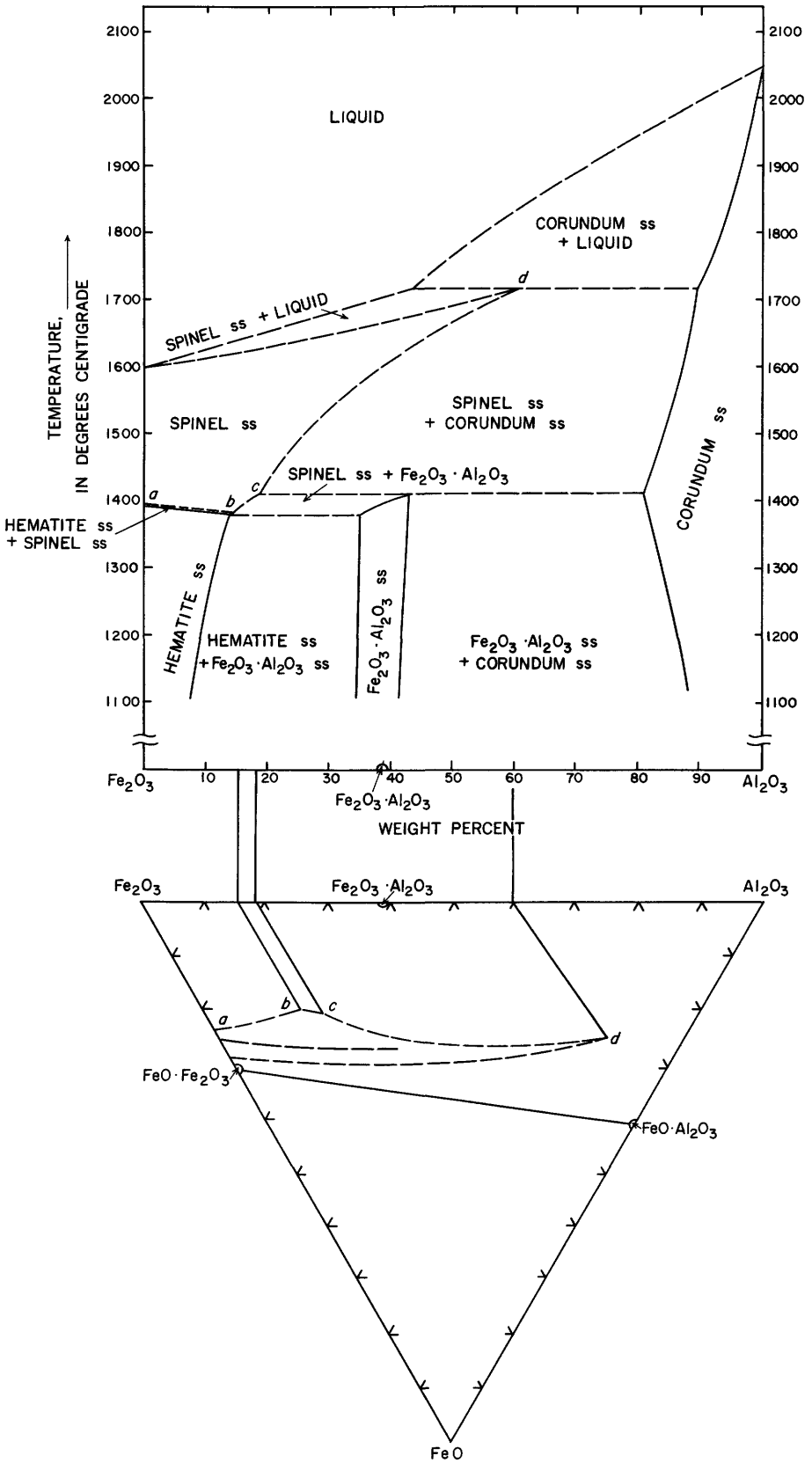

FIGURE 15.—Phase equilibria in the system iron oxide–alumina in air (P_{O_2}=0.21 atm). The upper half of the figure has the appearance of a binary system and is obtained by projecting all compositions onto the join Fe_2O_3–Al_2O_3 along the oxygen reaction line originating in the oxygen corner of the triangle representing the system Fe–Al–O. The phase boundaries are solid lines where the system is binary, dashed lines where the solid phase, spinel, has a composition not on the join Fe_2O_3–Al_2O_3. *ss*, solid solution. Modified from Muan and Gee (1956).

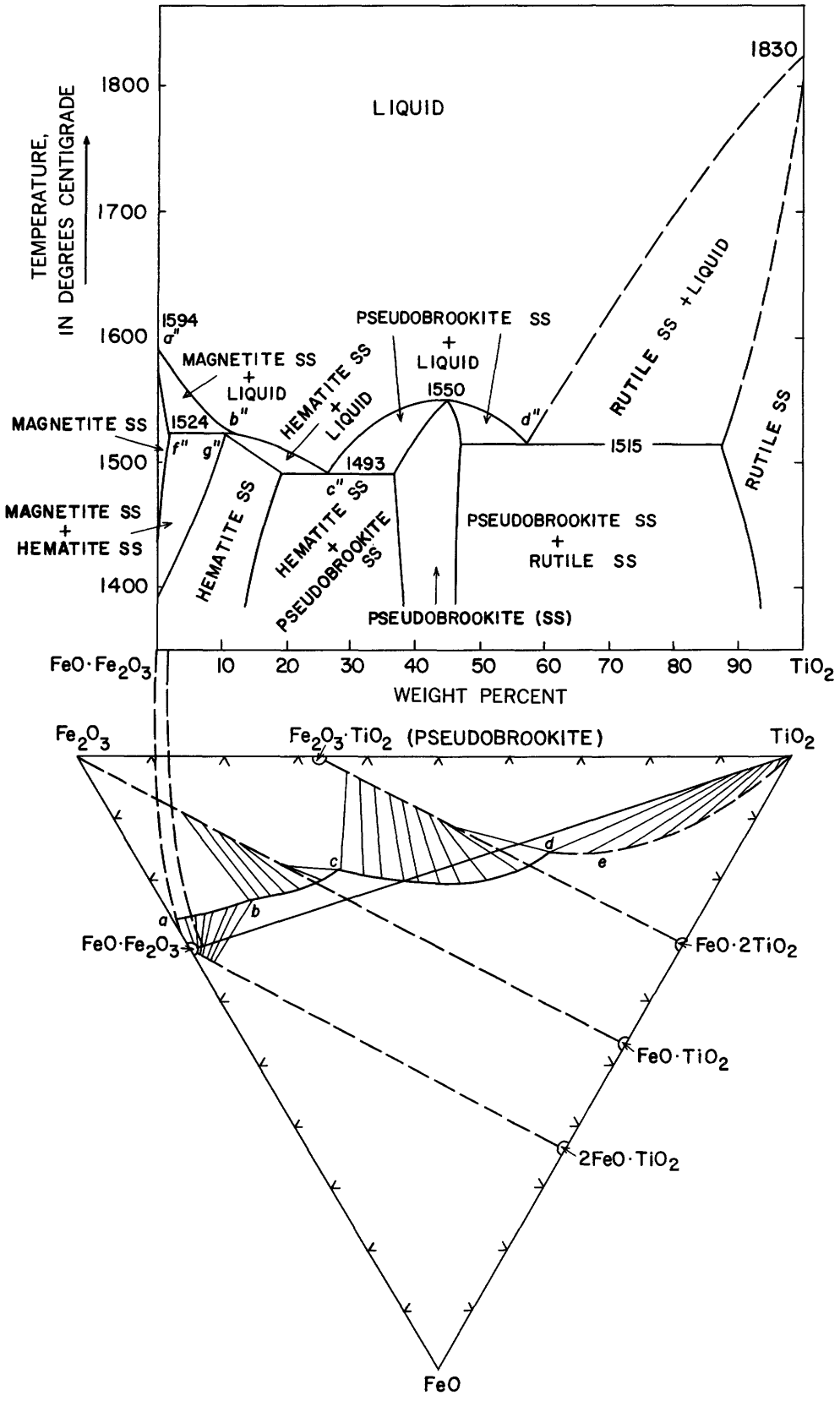

FIGURE 16.—Phase relations in the system iron oxide-TiO_2 in air. The upper half of the figure has the appearance of a binary system and is obtained by projecting all compositions along oxygen reaction lines originating in the oxygen corner of the triangle representing the system Fe-Ti-O. The curve *abcde* represents the composition of liquids along the liquidus surface in air; line *fg* gives the composition of the solid solution at 1524° C. (*ss*, solid solution.) Modified from MacChesney and Muan (1959).

triangle formed by the solid phases, the phase reaction is of the type $S_1+S_2=S_3+L$, and the invariant point is called a reaction point. At temperatures below the invariant point, the univariant assemblies may be $S_1+S_2+S_3$ or S_1+S_2+L; above the invariant point, S_1+S_3+L or S_2+S_3+L. When the composition of one of the solids, say S_3, is within the composition triangle S_1-S_2-L, below the invariant point the univariant assemblies may be $S_1+S_2+S_3$, S_1+S_3+L, or S_2+S_3+L, but above the invariant point the only stable assembly of phases is S_1+S_2+L. In this case the invariant point is a maximum temperature for phase S_3. When the composition of two reacting solids and the coexisting liquid lie on a straight line, that line is one of maximum temperature in the ternary system, and the phase reactions are those of a binary system, with either congruent or incongruent melting. When a solid melts to a liquid of its own composition, that congruent melting point is a maximum on the surface of equilibrium between that solid and liquids in the ternary system.

Some examples of phase relations in ternary systems are discussed in detail. The system Na_2O–K_2O–SiO_2 contains an example of a eutectic and of a reaction point. The phase relations in the ternary system Na_2O–Al_2O_3–SiO_2 are discussed in terms of binary systems within the ternary system and of the boundaries of the several fields. The crystallization paths in the system Na_2O–CaO–SiO_2 are considered. The determination of three-phase boundaries is discussed in connection with the system $Na_2O\cdot Al_2O_3\cdot 6SiO_2$ (albite)–$CaO\cdot MgO\cdot 2SiO_2$ (diopside)–$CaO\cdot Al_2O_3\cdot 2SiO_2$ (anorthite). There is an extended discussion of subliquidus relations in the system CaO–FeO–SiO_2.

Na_2O–K_2O–SiO_2

The part of the system Na_2O–K_2O–SiO_2 within the limits $Na_2O\cdot SiO_2$ (sodium metasilicate)–$K_2O\cdot SiO_2$ (potassium metasilicate)–SiO_2 (fig. 17 and table 11)

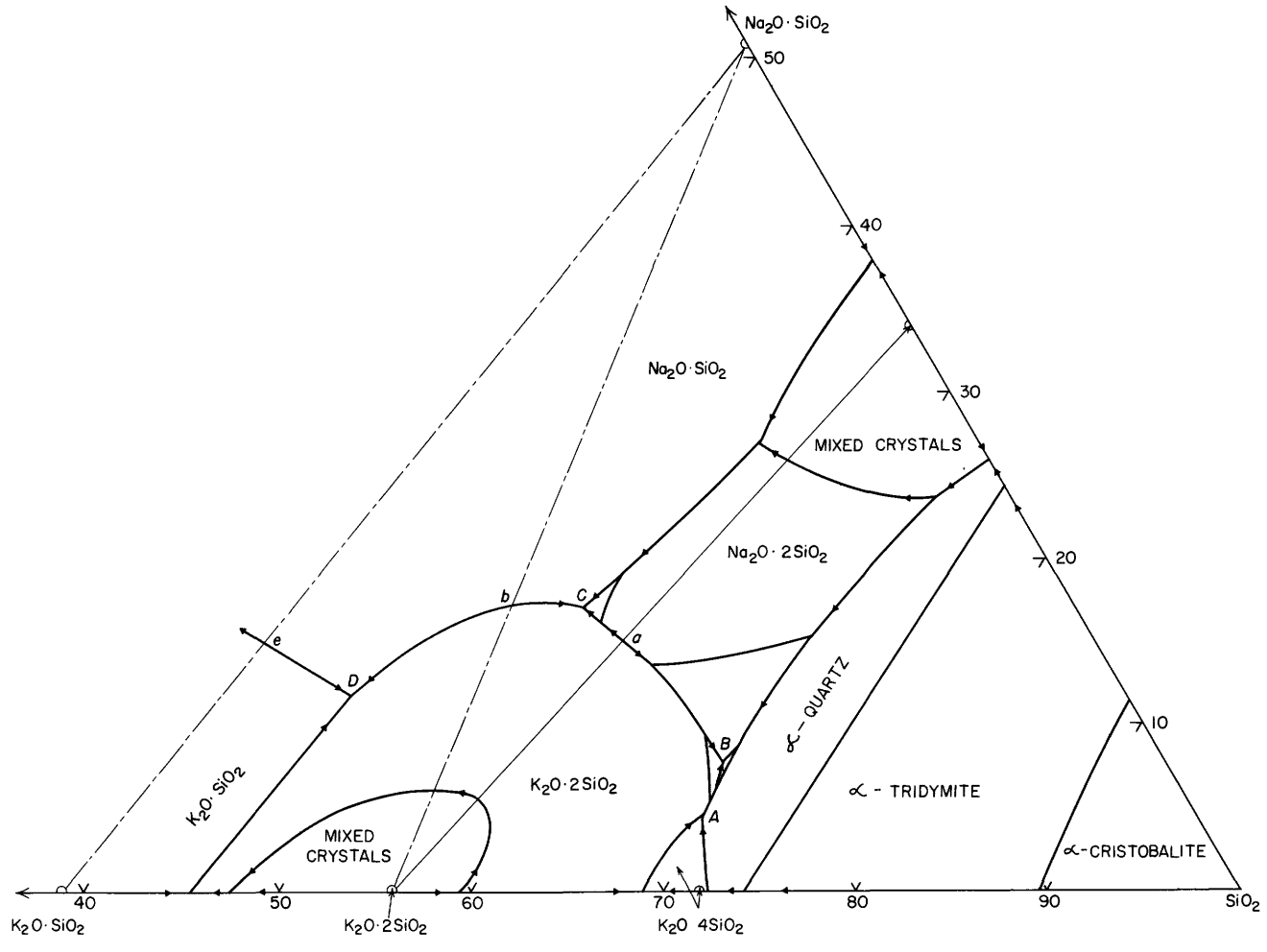

FIGURE 17.—The ternary system K_2O·SiO_2–Na_2O·SiO_2–SiO_2. Modified from Kracek (1932).

TABLE 11.—*Invariant points in the system* K_2O-SiO_2–Na_2O-SiO_2–SiO_2

Invariant point on fig. 17	Phase reaction	Temperature (°C)	Composition of liquid (percent by weight)		
			Na_2O	K_2O	SiO_2
A	$K_2O{\cdot}4SiO_2 \rightleftharpoons K_2O{\cdot}2SiO_2 + SiO_2$ (quartz) $+ L$	640	4. 5	25. 7	69. 8
B	$Na_2O{\cdot}2SiO_2 + K_2O{\cdot}2SiO_2 + SiO_2$ (quartz) $\rightleftharpoons L$	540	8	23	69
a	$Na_2O{\cdot}2SiO_2 + K_2O{\cdot}2SiO_2 \rightleftharpoons L$	705	15. 0	24. 5	60. 5
C	$Na_2O{\cdot}2SiO_2 + K_2O{\cdot}2SiO_2 + Na_2O{\cdot}SiO_2 \rightleftharpoons L$	655	17. 2	25. 4	57. 4
b	$Na_2O{\cdot}SiO_2 + K_2O{\cdot}2SiO_2 \rightleftharpoons L$	680	17. 6	28. 7	53. 7
D	$Na_2O{\cdot}SiO_2 + K_2O{\cdot}SiO_2 + K_2O{\cdot}2SiO_2 \rightleftharpoons L$	645	11. 7	40. 1	48. 2
e	$Na_2O{\cdot}SiO_2 + K_2O{\cdot}SiO_2 \rightleftharpoons L$	745	15	43	42

was studied by Kracek (1932). No ternary compounds are formed, and simple binary systems are formed by $Na_2O{\cdot}SiO_2$–$K_2O{\cdot}SiO_2$, by $Na_2O{\cdot}SiO_2$–$K_2O{\cdot}2SiO_2$, and by $Na_2O{\cdot}2SiO_2$–$K_2O{\cdot}2SiO_2$. Both $Na_2O{\cdot}2SiO_2$ and $K_2O{\cdot}2SiO_2$ take into solid solution limited amounts of Na_2O, K_2O, or SiO_2, depending on the composition of the liquid from which they crystallize. The field of $K_2O{\cdot}4SiO_2$ occupies but a small portion of the ternary diagram, and is terminated at the reaction point *A*, where the phase reaction

$$K_2O{\cdot}4SiO_2 = L + K_2O{\cdot}2SiO_2 + SiO_2 \text{ (quartz)}$$

takes place. The phase assemblages

$(L + K_2O{\cdot}2SiO_2 + K_2O{\cdot}4SiO_2)$ and $(L + K_2O{\cdot}4SiO_2 + SiO_2)$ go to higher temperatures at the side $K_2O{\cdot}SiO_2$–SiO_2; the assemblage

$$(L + K_2O{\cdot}2SiO_2 + SiO_2)$$

goes to the lower temperature and ends at the ternary eutectic *B*, where the phase reaction is

$$Na_2O{\cdot}2SiO_2 + K_2O{\cdot}2SiO_2 + SiO_2 = L$$

and the liquid is inside the triangle formed by three solid phases. A second eutectic is at *D* where the phase reaction is $Na_2O{\cdot}SiO_2 + K_2O{\cdot}SiO_2 + K_2O{\cdot}2SiO_2 = L$. $K_2O{\cdot}4SiO_2$ also exists in two polymorphic modifications with an inversion at 592°C at a pressure of 1 atm (Goranson and Kracek, 1932), which is below the lowest liquidus temperature; hence the low temperature modification $K_2O{\cdot}4SiO_2$ II does not reach the liquidus.

Mixtures containing less SiO_2 than the disilicate join are not hard to crystallize, but those near the ternary eutectic and reaction points cannot be crystallized dry and hydrothermal crystallization must be resorted to. At the eutectic with $Na_2{\cdot}2SiO_2$, $K_2O{\cdot}2SiO_2$, and quartz, 10 days heating was not sufficient to ensure equilibrium. Many of the mixtures are extremely hygroscopic.

Na_2O–MgO–SiO_2

Preliminary studies of the system Na_2O–MgO–SiO_2 were published by Schairer, Yoder, and Keene (1953, 1954) who found the phase diagrams published by Botvinkin and Popova (1937), and Manuilova (1937) to be seriously in error. The preliminary phase-equilibrium diagram by Schairer, Yoder, and Keene is figure 18, and on it are given the temperature of the invariant points. The compositions have not been published.

Na_2O–CaO–Al_2O_3

A part of the system Na_2O–CaO–Al_2O_3 low in Na_2O was studied by Brownmiller and Bogue (1932) (figure 19 and table 12). Two ternary compounds are formed: $Na_2O{\cdot}8CaO{\cdot}3Al_2O_3$, which melts incongruently at 1508°C with separation of crystalline CaO, and $2Na_2O{\cdot}3CaO{\cdot}5Al_2O_3$, which does not dissociate or melt up to 1630°C. No melting was observed on the join $2Na_2O{\cdot}3CaO{\cdot}5Al_2O_3$–$Na_2O{\cdot}Al_2O_3$ up to 1630°C, but from the correlation of all the data obtained a complete series of solid solutions was inferred. There is no solid solution with the ternary compound and $CaO{\cdot}2Al_2O_3$, $CaO{\cdot}Al_2O_3$, or $5CaO{\cdot}3Al_2O_3$, but a series of binary eutectics, at points *a*, *d*, and *h*, and the ternary eutectics *B* and *F*. The point *q* is the eutectic between CaO and $Na_2O{\cdot}Al_2O_3$. Point *J* is a reaction point at which liquid is formed. Point *r* is the binary eutectic between $Na_2O{\cdot}8CaO{\cdot}3Al_2O_3$ and $2Na_2O{\cdot}3CaO{\cdot}5Al_2O_3$, and in the region above the line *r*-$2Na_2O{\cdot}3CaO{\cdot}5Al_2O_3$ the solid phase is one of the solid solution series $2Na_2O{\cdot}3CaO{\cdot}5Al_2O_3$–$Na_2O{\cdot}Al_2O_3$. The area *IJMP* is the field in which $Na_2O{\cdot}8CaO{\cdot}3Al_2O_3$ is the primary phase. Compositions richer in CaO than the line *qPM* have CaO as primary phase. At *P* the phases are CaO,

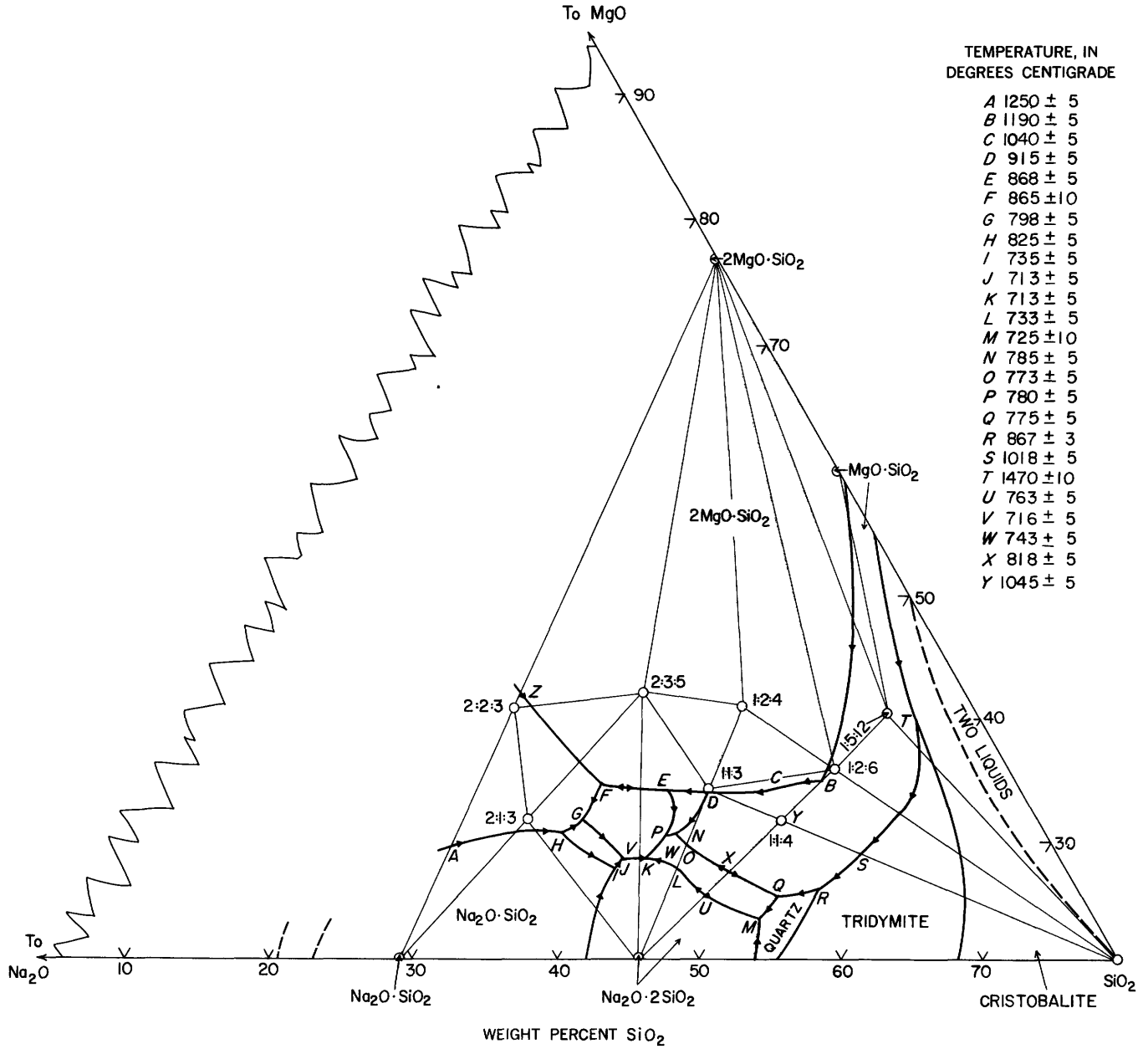

FIGURE 18.—The ternary system Na_2O–MgO–SiO_2. Modified from Schairer, Yoder, and Keene (1954).

TABLE 12.—*Invariant points in the system* Na_2O–CaO–Al_2O_3

Invariant point on fig. 19	Phase reactions	Temperature (° C)	Composition of liquid (percent by weight)		
			Na_2O	CaO	Al_2O_3
a	$CaO{\cdot}2Al_2O_3+2Na_2O{\cdot}3CaO{\cdot}5Al_2O_3 \rightleftharpoons L$	1550	8. 6	21. 3	70. 1
B	$CaO{\cdot}Al_2O_3+2Na_2O{\cdot}3CaO{\cdot}5Al_2O_3+CaO{\cdot}2Al_2O_3 \rightleftharpoons L$	1465	6	27. 5	66. 5
d	$CaO{\cdot}Al_2O_3+2Na_2O{\cdot}3CaO{\cdot}5Al_2O_3 \rightleftharpoons L$	1515	5. 4	30. 2	64. 3
F	$5CaO{\cdot}3Al_2O_3+2Na_2O{\cdot}3CaO{\cdot}5Al_2O_3+CaO{\cdot}Al_2O_3 \rightleftharpoons L$	1430	4. 0	38. 0	58. 0
h	$5CaO{\cdot}3Al_2O_3+2Na_2O{\cdot}3CaO{\cdot}5Al_2O_3 \rightleftharpoons L$	1450	4. 3	40. 4	55. 3
I	$5CaO{\cdot}3Al_2O_3+Na_2O{\cdot}8CaO{\cdot}3Al_2O_3+2Na_2O{\cdot}3CaO{\cdot}5Al_2O_3 \rightleftharpoons L$	1420	5. 0	46. 0	49. 0
J	$5CaO{\cdot}3Al_2O_3+Na_2O{\cdot}8CaO{\cdot}3Al_2O_3 \rightleftharpoons 3CaO{\cdot}Al_2O_3+L$	1423	4. 5	46. 5	49. 0
q	$CaO+Na_2O{\cdot}Al_2O_3 \rightleftharpoons L$	1565	30	20	50
r	$Na_2O{\cdot}8CaO{\cdot}3Al_2O_3+2Na_2O{\cdot}3CaO{\cdot}5Al_2O_3 \rightleftharpoons L$	1462	10. 2	43. 7	46. 1
P	$Na_2O{\cdot}8CaO{\cdot}3Al_2O_3 \rightleftharpoons (Na_2O{\cdot}Al_2O_3{-}2Na_2O{\cdot}3CaO{\cdot}5Al_2O_3)ss+L$	1475	13. 0	42. 5	44. 5
M	$3CaO{\cdot}Al_2O_3+Na_2O{\cdot}8CaO{\cdot}3Al_2O_3 \rightleftharpoons CaO+L$	1490	6. 0	50. 0	44. 0

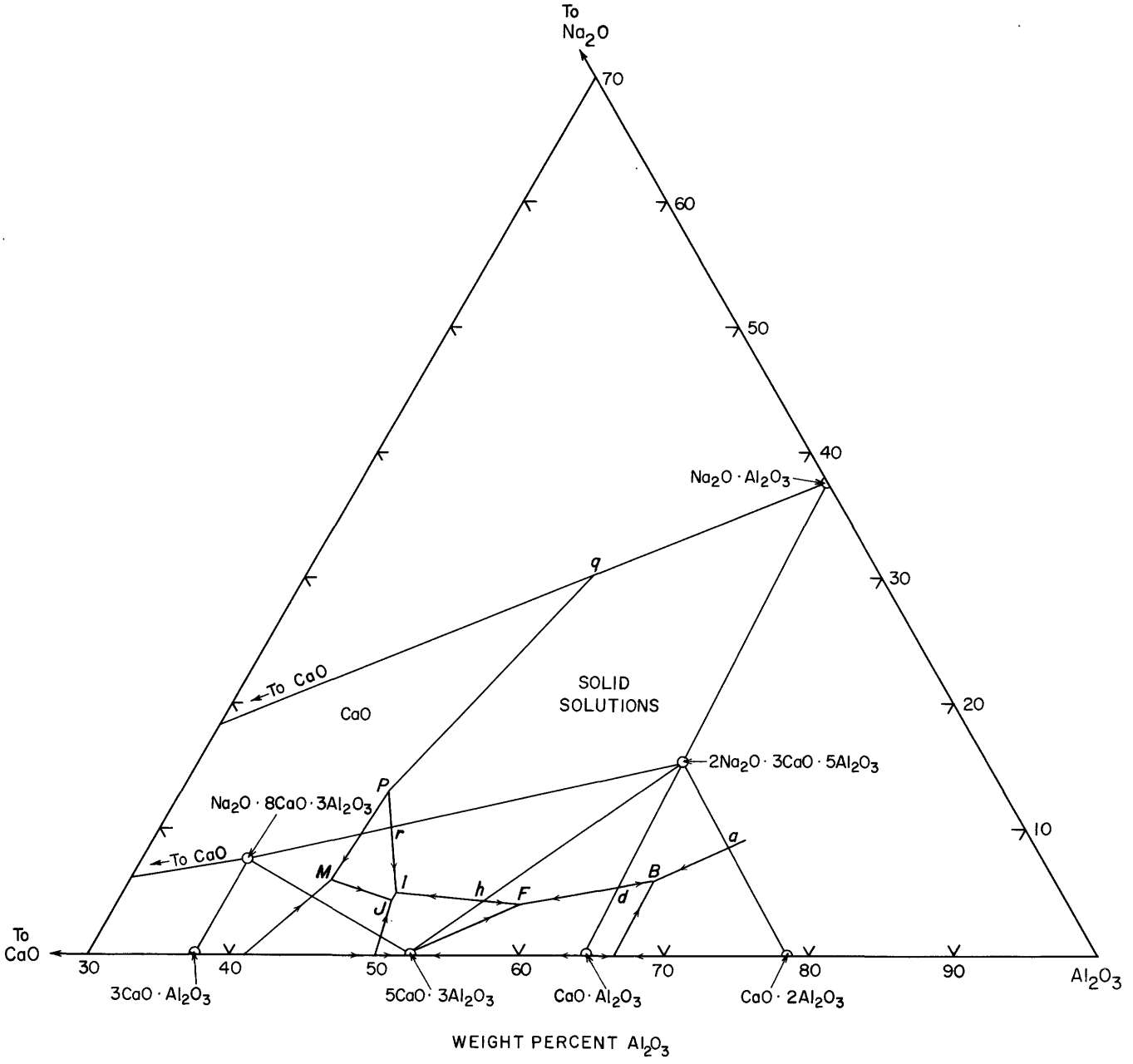

FIGURE 19.—The ternary system Na_2O–CaO–Al_2O_3. Modified from Brownmiller and Bogue (1932).

$Na_2O \cdot 8CaO \cdot 3Al_2O_3$, a solid solution of the $Na_2O \cdot Al_2O_3$–$2Na_2O \cdot 3CaO \cdot 5Al_2O_3$ series, and liquid, but since the solid solution is on the straight line $Na_2O \cdot 8CaO \cdot 3Al_2O_3$–*P* the CaO does not enter into the reaction.

Na_2O–CaO–SiO_2

Morey and Bowen (1925) and Morey (1930a) made the first studies of the system Na_2O–CaO–SiO_2 which included only that portion of the system richer in SiO_2 than the join $Na_2O \cdot SiO_2$–$CaO \cdot SiO_2$. Segnit (1953) extended the study to higher Na_2O contents, where the difficulties caused by the volatilization of Na_2O became serious. Both sets of results are included in figure 20, and the data of the invariant points are in table 13.

The region around the field of the compound $Na_2O \cdot 3CaO \cdot 6SiO_2$ (devitrite) (Morey and Bowen, 1931) is of special interest in glass technology, because

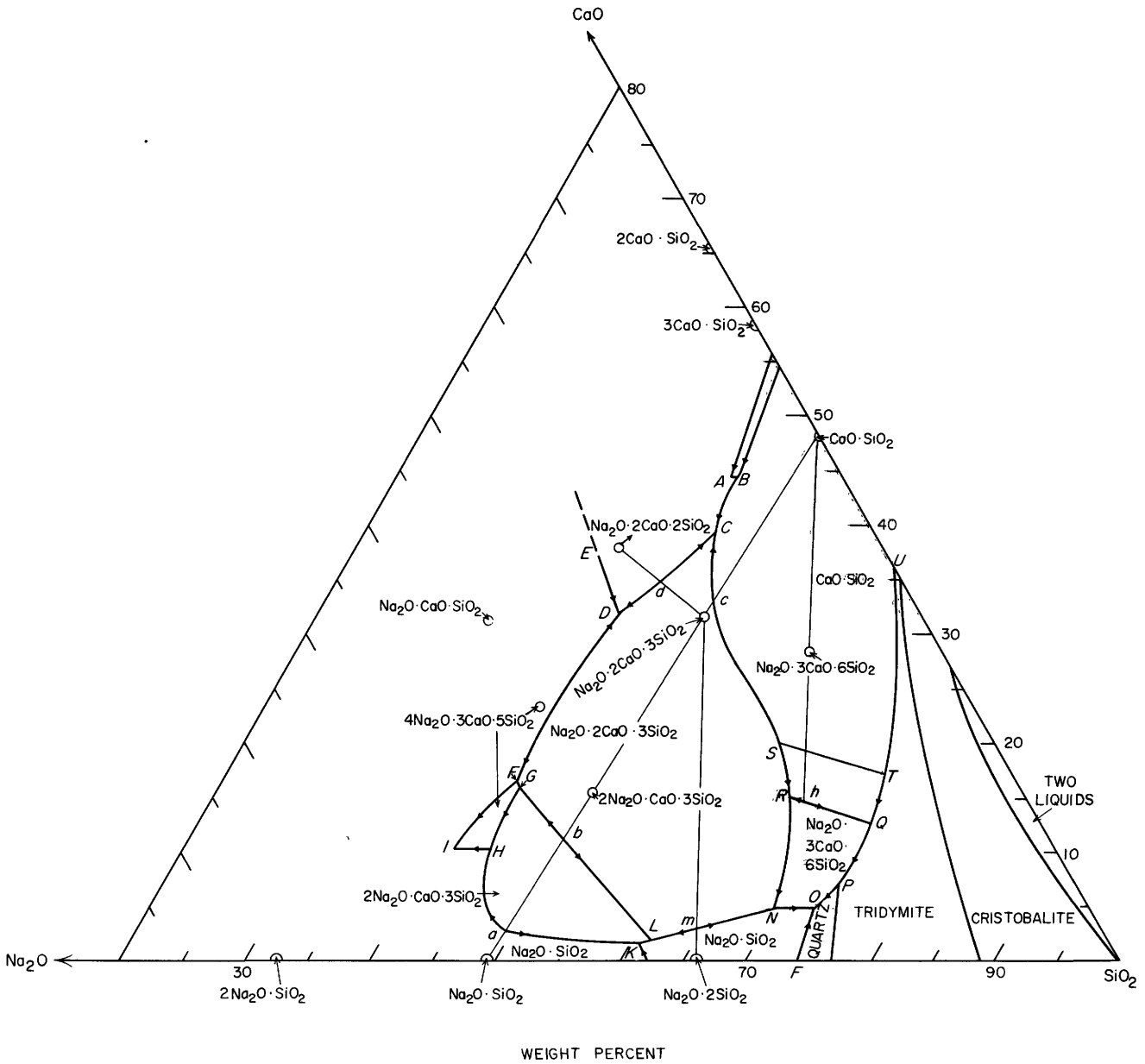

FIGURE 20.—The ternary system Na_2O–CaO–SiO_2. Based on Morey and Bowen (1925) and Segnit (1953).

the primary crystalline phase formed upon devitrification in most commercial glassware is this compound. The region of two liquid layers was discovered by Greig (1927a), and it is noteworthy that addition of less than 2 percent of Na_2O suffices to cause the two immiscible liquids in the binary system CaO–SiO_2 to become completely miscible. The compound devitrite is an extreme example of incongruent melting and a mixture of its composition has a liquidus of 1325°C in the field of $CaO \cdot SiO_2$. The pure compound when heated decomposes at 1060°C into $CaO \cdot SiO_2$ and a liquid containing 15 percent CaO, and its field of primary stability is *NRQPO* in figure 20. It extends down to the ternary eutectic at point *O*, where the liquidus temperature is 725°C. Liquids of this composition, and in the field of devitrite and the immediately adjacent fields of quartz and tridymite, are so viscous at their liquidus temperature that it is difficult to crystallize them. This is the region of most commercial glassware.

TABLE 13.—*Invariant points in the system* Na_2O–CaO–SiO_2

Invariant point on fig. 20	Phase reaction	Temperature (°C)	Composition of liquid (percent by weight)		
			Na_2O	CaO	SiO_2
P	SiO_2 (quartz)$\rightleftharpoons SiO_2$ (tridymite)	867	18. 8	7	74. 2
Q	$Na_2O{\cdot}3CaO{\cdot}6SiO_2+SiO_2\rightleftharpoons CaO{\cdot}SiO_2+L$	1030	13. 6	12. 7	73. 7
O	$Na_2O{\cdot}2SiO_2+Na_2O{\cdot}3CaO{\cdot}6SiO_2+SiO_2\rightleftharpoons L$	725	21. 9	5. 0	73. 1
N	$Na_2O{\cdot}2SiO_2+Na_2O{\cdot}3CaO{\cdot}6SiO_2\rightleftharpoons Na_2O{\cdot}2CaO{\cdot}3SiO_2+L$	760	25. 0	5. 0	70. 0
h	$Na_2O{\cdot}3CaO{\cdot}6SiO_2\rightleftharpoons CaO{\cdot}SiO_2+L$	1060	17. 6	15. 0	67. 4
R	$Na_2O{\cdot}2CaO{\cdot}3SiO_2+Na_2O{\cdot}3CaO{\cdot}6SiO_2\rightleftharpoons CaO{\cdot}SiO_2+L$	1060	18. 8	15. 1	66. 1
m	$Na_2O{\cdot}2SiO_2+Na_2O{\cdot}2CaO{\cdot}3SiO_2\rightleftharpoons L$	862	32. 5	3. 0	64. 5
L	$Na_2O{\cdot}2SiO_2+2Na_2O{\cdot}CaO{\cdot}3SiO_2\rightleftharpoons Na_2O{\cdot}2CaO{\cdot}3SiO_2+L$	827	36. 6	2. 0	61. 4
K	$Na_2O{\cdot}SiO_2+2Na_2O{\cdot}CaO{\cdot}3SiO_2+Na_2O{\cdot}2SiO_2\rightleftharpoons L$	821	37. 5	1. 8	60. 7
c	$Na_2O{\cdot}2CaO{\cdot}3SiO_2+CaO{\cdot}SiO_2\rightleftharpoons L$	1282	16. 1	33. 0	50. 9
	$Na_2O{\cdot}2CaO{\cdot}3SiO_2\rightleftharpoons L$	1284	17. 49	31. 65	60. 86
b	$2Na_2O{\cdot}CaO{\cdot}3SiO_2\rightleftharpoons Na_2O{\cdot}2CaO{\cdot}3SiO_2+L$	1141	38. 7	11. 5	50. 2
a	$Na_2O{\cdot}SiO_2+2Na_2O{\cdot}CaO{\cdot}3SiO_2\rightleftharpoons L$	1060	47. 6	3	49. 4
C	$Na_2O{\cdot}2CaO{\cdot}3SiO_2+CaO{\cdot}SiO_2+Na_2O{\cdot}2CaO{\cdot}2SiO_2\rightleftharpoons L$	1255	12. 5	39. 5	48. 0
B	$3CaO{\cdot}2SiO_2+CaO{\cdot}SiO_2+Na_2O{\cdot}2CaO{\cdot}2SiO_2\rightleftharpoons L$	1270	8. 2	44. 5	47. 3
A	$2CaO{\cdot}SiO_2+3CaO{\cdot}2SiO_2+Na_2O{\cdot}2CaO{\cdot}2SiO_2\rightleftharpoons L$	1280	8. 8	44. 5	46. 7
H	$Na_2O{\cdot}SiO_2+4Na_2O{\cdot}3CaO{\cdot}5SiO_2\rightleftharpoons 2Na_2O{\cdot}CaO{\cdot}3SiO_2+L$	990	45. 0	10. 5	44. 5
D	$Na_2O{\cdot}2CaO{\cdot}3SiO_2+Na_2O{\cdot}CaO{\cdot}SiO_2+Na_2O{\cdot}2CaO{\cdot}2SiO_2\rightleftharpoons L$	1260	24. 0	32. 0	44. 0
G	$4Na_2O{\cdot}3CaO{\cdot}5SiO_2+2Na_2O{\cdot}CaO{\cdot}3SiO_2\rightleftharpoons Na_2O{\cdot}2CaO{\cdot}3SiO_2+L$	1120	40. 0	16. 0	44. 0
F	$4Na_2O{\cdot}3CaO{\cdot}5SiO_2\rightleftharpoons Na_2O{\cdot}2CaO{\cdot}3SiO_2+Na_2O{\cdot}CaO{\cdot}SiO_2+L$	1130	39. 8	16. 7	43. 5
I	$Na_2O{\cdot}SiO_2+Na_2O{\cdot}CaO{\cdot}SiO_2\rightleftharpoons 4Na_2O{\cdot}3CaO{\cdot}5SiO_2+L$	950	48. 0	10. 5	41. 5
	$Na_2O{\cdot}2CaO{\cdot}2SiO_2\rightleftharpoons L$	1450	21. 06	39. 11	40. 83
E	$2CaO{\cdot}SiO_2+Na_2O{\cdot}CaO{\cdot}SiO_2+Na_2O{\cdot}2CaO{\cdot}2SiO_2\rightleftharpoons L$	1440	23. 0	37. 6	39. 4

The join $Na_2O{\cdot}SiO_2$–$CaO{\cdot}SiO_2$ is a binary system (fig. 21) in the ternary system in which there are two metasilicate compounds. $2Na_2O{\cdot}CaO{\cdot}3SiO_2$ melts incongruently at 1141°C with formation of

$$Na_2O{\cdot}2CaO{\cdot}3SiO_2$$

which melts congruently at 1284°C. The eutectic

$$Na_2O{\cdot}SiO_2+2Na_2O{\cdot}CaO{\cdot}3SiO_2=L$$

is at 1060°C, 3 percent CaO, and the eutectic

$$Na_2O{\cdot}2CaO{\cdot}3SiO_2+CaO{\cdot}SiO_2=L$$

is at 1282°C, 33 percent CaO.

$Na_2O{\cdot}2CaO{\cdot}3SiO_2$ has a large field of stability, *LGFDCRN* (fig. 20). It forms a binary system with $Na_2O{\cdot}2SiO_2$, with a eutectic at *m*, and also with $Na_2O{\cdot}2CaO{\cdot}2SiO_2$, with a eutectic at *d*. This compound crystallizes readily throughout its field, but when melted it can be quenched to glass.

The course of crystallization of any mixture in the ternary diagram can be deduced from figure 20, in which the boundary curves are drawn, as well as the lines joining the compositions of the various solid phases. Consider first a mixture in the area $Na_2O{\cdot}SiO_2$–*bLK*. Any composition within this area deposits $Na_2O{\cdot}SiO_2$ as primary phase, and the residual liquid follows a crystallization path lying on the straight line joining the liquid composition with that of $Na_2O{\cdot}SiO_2$ until either the boundary *bL* or *KL* is reached. Here either $2Na_2O{\cdot}CaO{\cdot}3SiO_2$ or $Na_2O{\cdot}2SiO_2$, respectively, appear, and the liquid follows the boundary curve down to the ternary eutectic, where it solidifies completely to a mixture of $Na_2O{\cdot}SiO_2$, $2Na_2O{\cdot}CaO{\cdot}3SiO_2$, and $Na_2O{\cdot}2SiO_2$, in proportions such that the original composition corresponds to the center of gravity of the masses of the three solids.

A composition within the area *abLK* follows an equally simple course, depositing first

$$2Na_2O{\cdot}CaO{\cdot}3SiO_2;$$

then the liquid composition follows the straight line through the point $2Na_2O{\cdot}CaO{\cdot}3SiO_2$ and the original composition, until it meets a boundary curve. This is of $Na_2O{\cdot}SiO_2$, except for mixtures lying in the triangle *bLK*, where $Na_2O{\cdot}2SiO_2$ is the second phase to separate. For all these compositions, the mixture solidifies completely at the ternary eutectic *K*.

Crystallization of mixtures lying within the region where $Na_2O{\cdot}2CaO{\cdot}3SiO_2$ is the primary phase is usually a less simple matter. Consider first a composition within the triangle

$$Na_2O{\cdot}SiO_2\text{–}Na_2O{\cdot}2SiO_2\text{–}2Na_2O{\cdot}CaO{\cdot}3SiO_2$$

bounded by the curve *bL* and the straight line joining *L* with $Na_2O{\cdot}2CaO{\cdot}3SiO_2$. The primary phase is $Na_2O{\cdot}2CaO{\cdot}3SiO_2$; the liquid follows a crystallization

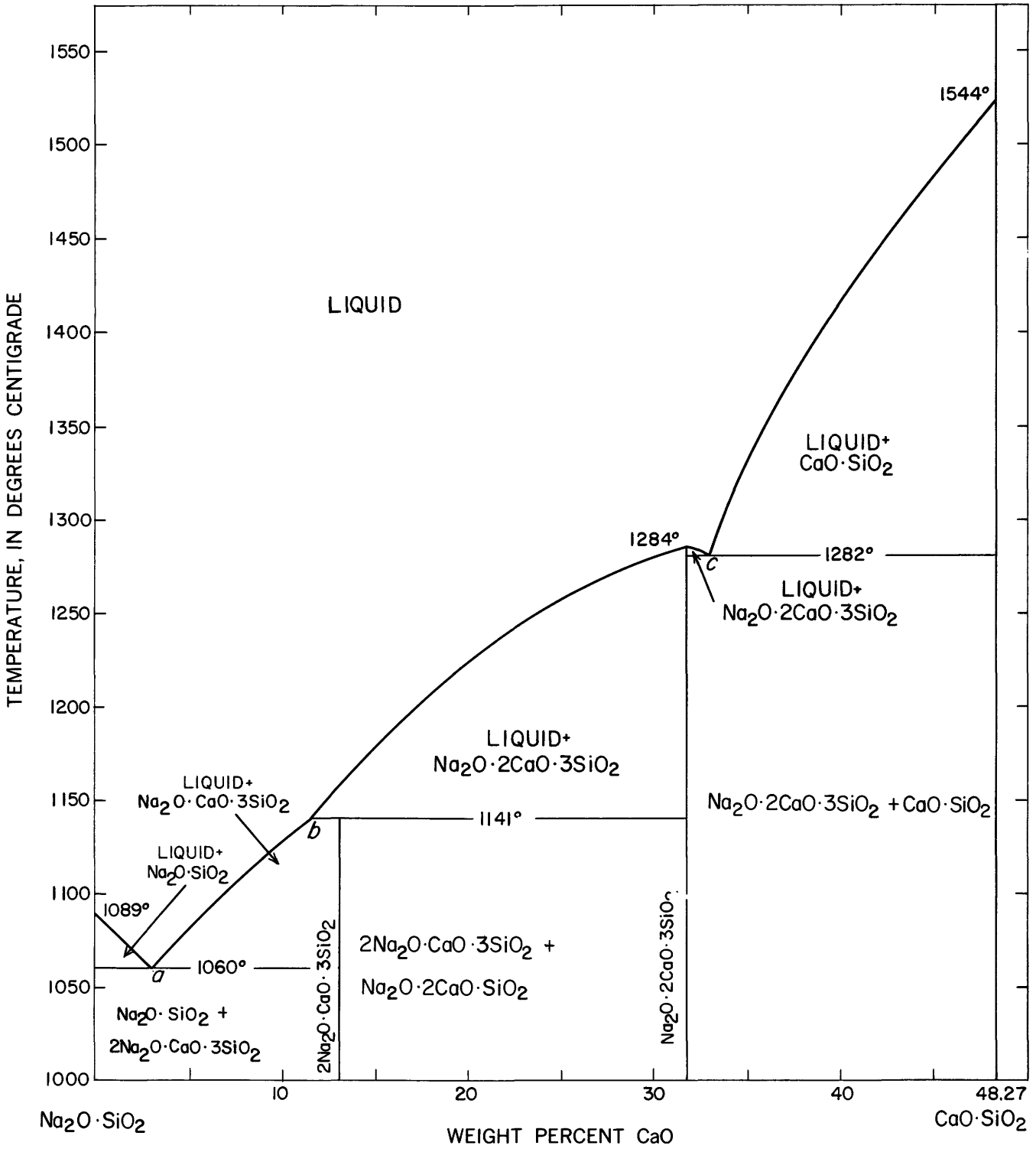

FIGURE 21.—The binary system $Na_2O \cdot SiO_2$–$CaO \cdot SiO_2$. Modified from Morey and Bowen (1925).

path passing through the composition of the primary phase and of the original mixture, until this path cuts the boundary curve bL. At this intersection $2Na_2O \cdot CaO \cdot 3SiO_2$ crystallizes; the liquid then follows the boundary curve, the reaction

$$Na_2O \cdot 2CaO \cdot 3SiO_2 + \text{liquid} = 2Na_2O \cdot CaO \cdot 3SiO_2$$

takes place, and the proportion of the former compound decreases, while that of the latter increases, until at L, where $Na_2O \cdot 2SiO_2$ appears, the compound

$$Na_2O \cdot 2CaO \cdot 3SiO_2$$

has been decomposed entirely. The liquid then follows the boundary curve, LK, finally solidifying completely at the ternary eutectic, K, to a mixture of $Na_2O \cdot SiO_2 \cdot Na_2O \cdot 2SiO_2$ and $2Na_2O \cdot CaO \cdot 3SiO_2$. If the composition lies within the same triangle, but to the right of the join $L - Na_2O \cdot 2CaO \cdot 3SiO_2$, the end products will be the same, but the secondary phase will be $Na_2O \cdot 2SiO_2$, on the boundary mL; at L, reaction takes place resulting in the formation of $2Na_2O \cdot CaO \cdot 3SiO_2$ and the disappearance of

$Na_2O \cdot 2CaO \cdot 3SiO_2$.

Any mixture in the triangle $Na_2O \cdot 2CaO \cdot 3SiO_2$–$2Na_2O \cdot CaO \cdot 3SiO_2$–$Na_2O \cdot 2SiO_2$ will solidify completely to a mixture of the above phases and $Na_2O \cdot 2SiO_2$, but the crystallization path will differ according to the side of the line L–$Na_2O \cdot 2CaO \cdot 3SiO_2$ on which the original composition lies. If the point representing the composition of the glass is to the left of the above line, the secondary phase is

$$2Na_2O \cdot CaO \cdot 3SiO_2$$

and the liquid follows the boundary, bL, until the point L, is reached. Here the reaction

$$L + Na_2O \cdot 2CaO \cdot 3SiO_2 = 2Na_2O \cdot CaO \cdot 3SiO_2 + Na_2O \cdot 2SiO_2$$

takes place until the mixture has solidified completely. If the original mixture lies to the right of the line L–$Na_2O \cdot 2CaO \cdot 3SiO_2$, the same three phases separate, and at L the liquid of composition L reacts with the primary phase to form

$$Na_2O \cdot 2SiO_2 \text{ and } 2Na_2O \cdot CaO \cdot 3SiO_2.$$

Mixtures whose compositions lie within the field of $Na_2O \cdot 2CaO \cdot 3SiO_2$, also in the triangle $Na_2O \cdot 2SiO_2$–$Na_2O \cdot 2CaO \cdot 3SiO_2$–$Na_2O \cdot 3CaO \cdot 6SiO_2$ have a simple crystallization sequence, namely, initial separation of $Na_2O \cdot 2CaO \cdot 3SiO_2$, crystallization of $Na_2O \cdot 2SiO_2$ on the boundary mN, and final solidification at N as the result of a reaction

$$Na_2O \cdot 2CaO \cdot SiO_2 + \text{liquid } N = Na_2O \cdot 2SiO_2 + Na_2O \cdot 3CaO \cdot 6SiO_2.$$

This invariant point is thus a minimum temperature for $Na_2O \cdot 2CaO \cdot 3SiO_2$ and both boundary curves Nm and NR go to higher temperatures. At m there is a maximum temperature on the curve, NmL, and any mixture exactly on the join

$$Na_2O \cdot 2SiO_2 – Na_2O \cdot 2CaO \cdot 3SiO_2$$

will crystallize completely at m to a mixture of these two phases; m is the eutectic in the binary system $Na_2O \cdot 2SiO_2$–$Na_2O \cdot 2CaO \cdot 3SiO_2$.

Mixtures in the above field, but lying between the boundaries mN and NRS, and the tie line $Na_2O \cdot 2SiO_2$–$Na_2O \cdot 3CaO \cdot 6SiO_2$ run a less simple course. If the composition is to the left of the tie line

$$N – Na_2O \cdot 2CaO \cdot 3SiO_2,$$

the second phase to separate is again $Na_2O \cdot 2SiO_2$; if to the right of this line, $Na_2O \cdot 3CaO \cdot 6SiO_2$; but on either side the primary phase,

$$Na_2O \cdot 2CaO \cdot 3SiO_2,$$

must disappear at the reaction point N, as it is not possible for a mixture having the composition under discussion to solidify completely to a mixture of three phases whose composition triangle does not include the original mixture. All these mixtures must solidify as conglomerates of quartz, $Na_2O \cdot 2SiO_2$, and $Na_2O \cdot 3CaO \cdot 6SiO_2$ and at the reaction point, N, all the $Na_2O \cdot 2CaO \cdot 3SiO_2$ will be consumed. The liquid will then follow the boundary curve NO, until at O quartz appears, and the mixture will solidify completely. This is, of course, the sequence when equilibrium is attained, in the mixtures under discussion and in all mixtures whose crystallization gives rise to a liquid near the ternary eutectic, O, in composition, the attainment of equilibrium is an extremely slow process; one which cannot be carried out satisfactorily under the most favorable conditions except in experiments extending over weeks of time.

Glasses in which pseudowollastonite is the primary phase may follow several different crystallization paths depending on the composition, but all the reactions are complicated. Mixtures within the triangle

$$Na_2O \cdot 2CaO \cdot 3SiO_2 – Na_2O \cdot 3CaO \cdot 6SiO_2 – CaO \cdot SiO_2$$

will solidify ultimately as a conglomerate of these three phases, but the path followed is not a simple one.

Initial crystallization of pseudowollastonite is followed by a secondary appearance of $Na_2O \cdot 2CaO \cdot 3SiO_2$, along the boundary curve, *CSR*, entirely outside of the triangle under consideration. The liquid follows this curve until the invariant point, *S*, is reached, at which temperature the pseudowollastonite is inverted to wollastonite. At the still lower temperature invariant point *R*, the reaction $CaO \cdot SiO_2$ + liquid *R* =

$$Na_2O \cdot 2CaO \cdot 3SiO_2 + Na_2O \cdot 3CaO \cdot 6SiO_2$$

takes place, going on until the liquid is entirely consumed. If the initial composition of the mixture is within the triangle $CaO \cdot SiO_2$–SiO_2–$Na_2O \cdot 3CaO \cdot 6SiO_2$ but in the pseudowollastonite field, the result will be similar, except that the second phase to separate is tridymite, on the boundary *UTQP*, and reaction takes place at point *Q*, $CaO \cdot SiO_2$ + liquid *Q* =

$$Na_2O \cdot 3CaO \cdot 6SiO_2,$$

the same type of reaction as that taking place at the invariant point, *N*, but with the compound $Na_2O \cdot 2CaO \cdot 3SiO_2$ replaced by SiO_2.

All mixtures lying within the triangle

$$Na_2O \cdot 2SiO_2 – Na_2O \cdot 3CaO \cdot 6SiO_2 – SiO_2$$

will solidify completely as these crystalline compounds at the ternary eutectic point, *O*, if equilibrium is attained. The only effect of change in composition is to change the crystallization path by which these phases are formed. If the mixture lies within the area to the left of the $CaO \cdot SiO_2$–$Na_2O \cdot 3CaO \cdot 6SiO_2$ join, but within the wollastonite or pseudowollastonite fields, crystallization will result either in intersection of the boundary curve *NRSC*, with consequent separation of $Na_2O \cdot 2CaO \cdot 3SiO_2$, which must later disappear at the reaction point *N*; or the boundary curve, *RQ*, is intersected by the crystallization path; $Na_2O \cdot 3CaO \cdot 6SiO_2$ is formed directly, followed by the crystallization of $Na_2O \cdot 2SiO_2$ along the boundary *NO*, followed by complete solidification at *O*. If the mixture lies to the right of the $CaO \cdot SiO_2$–$Na_2O \cdot 3CaO \cdot 6SiO_2$ join, the initial separation of wollastonite will in all cases be followed by reaction at the line *RQ*, with formation of

$$Na_2O \cdot 3CaO \cdot 6SiO_2$$

and disappearance of $CaO \cdot SiO_2$. Depending on the composition, the next phase to separate will be

$$Na_2O \cdot 2SiO_2$$

or tridymite, or quartz; in all separations the liquid runs down to the ternary eutectic at *O*, where crystallization becomes complete.

Crystallization paths in the various silica fields all run down from SiO_2 to the boundary between the fields of $CaO \cdot SiO_2$ or $Na_2O \cdot 3CaO \cdot SiO_2$ (*UTQPO*) or $Na_2O \cdot 2SiO_2$ (*FO*).

In the former case pseudowollastonite, wollastonite, or $Na_2O \cdot 3CaO \cdot 6SiO_2$ is the second phase to separate, the liquid traces the path *UTQP*, solidifying at *O* to a mixture of $Na_2O \cdot 3CaO \cdot 6SiO_2$, quartz, and $Na_2O \cdot 2SiO_2$. The same final mixture of crystalline phases will result if the crystallization paths cuts the boundary *FO*; in this case $Na_2O \cdot 2SiO_2$ is the second phase to crystallize, and $Na_2O \cdot 3CaO \cdot 6SiO_2$ first appears at the ternary eutectic.

In the region richer in Na_2O, Segnit (1953) found two new compounds. $Na_2O \cdot 2CaO \cdot 2SiO_2$ melts congruently, at about 1450°C, and its field is bounded by those of $Na_2O \cdot CaO \cdot SiO_2$, $2CaO \cdot SiO_2$, $3CaO \cdot 2SiO_2$, $CaO \cdot SiO_2$, and $Na_2O \cdot 2CaO \cdot 3SiO_2$. The compound

$$4Na_2O \cdot 3CaO \cdot 5SiO_2$$

melts incongruently and has a small field, *IFGH*. The compound $Na_2O \cdot CaO \cdot SiO_2$, found by Morey and Bowen (1925), occurs in the region studied by Segnit. The structure of this compound was worked out by Wyckoff and Morey (1926). The compounds $2Na_2O \cdot 8CaO \cdot 5SiO_2$ and $2Na_2O \cdot 4CaO \cdot 3SiO_2$ mentioned by Toropov and Arakelyan (1950) probably do not exist.

Na_2O–FeO–SiO_2

Carter and Ibrahim (1952) studied the system Na_2O–FeO–SiO_2, in part by the use of a "high-temperature microscope" and in part by the quenching method. The only ternary compound, $Na_2O \cdot FeO \cdot SiO_2$, melts incongruently at 976°C, to FeO (wüstite) and liquid, and becomes completely liquid at 985°C. The phase-equilibrium diagram is figure 22 and the data for the invariant points are given in table 14. Schairer, Yoder, and Kean (1954) made a reconnaissance of this system and indicated that several compounds might be formed. Ostrovskii (1956), in addition to

$$Na_2O \cdot FeO \cdot SiO_2,$$

found the compound $4Na_2O \cdot 6FeO \cdot 15SiO_2$(?) with a congruent melting point at 750° to 800°C.

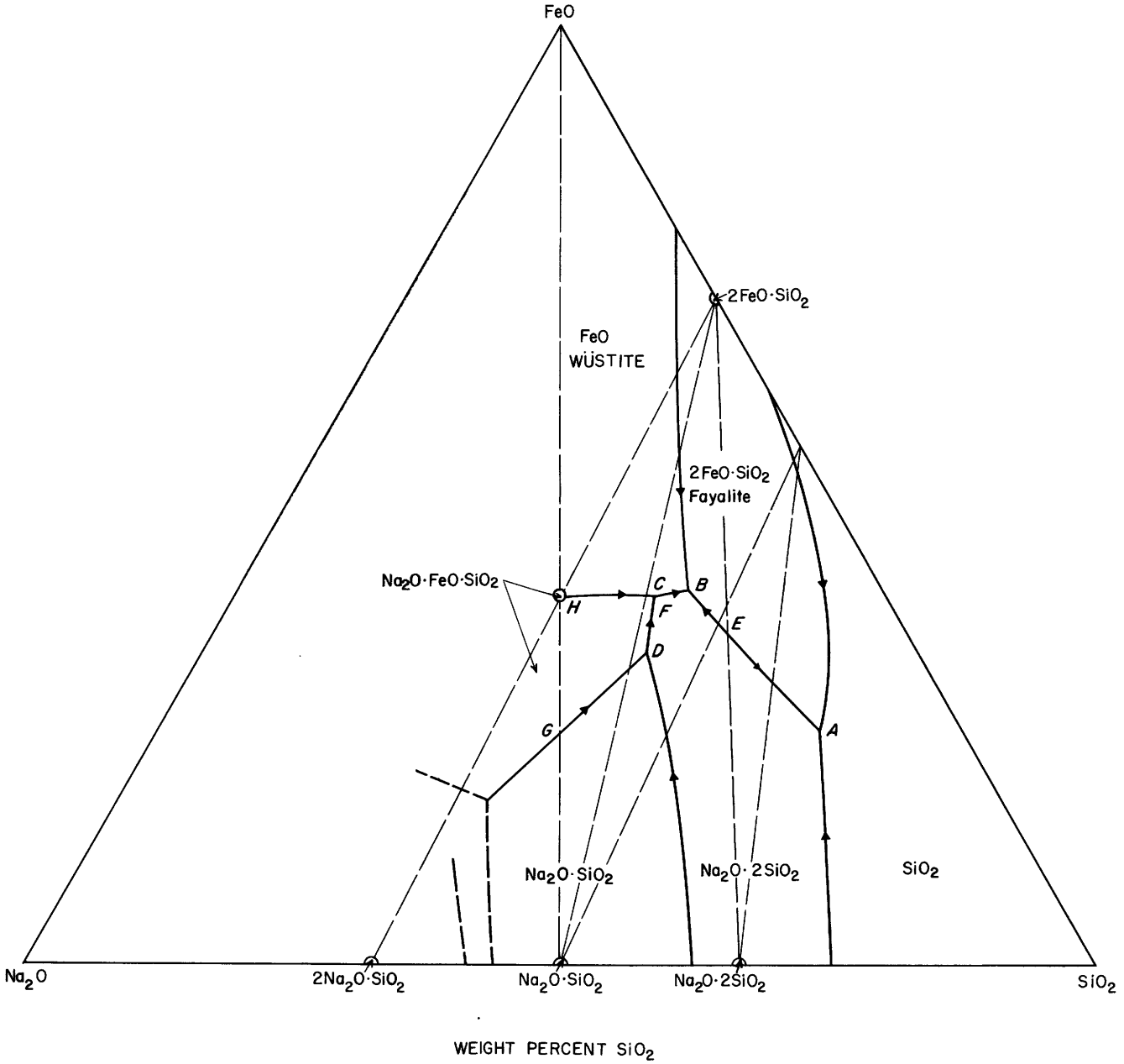

FIGURE 22.—The ternary system Na_2O–FeO–SiO_2. Modified from Carter and Ibrahim (1952).

Table 14.—*Invariant points in the system* Na_2O–FeO–SiO_2

Invariant point on fig. 22	Phase reaction	Temperature (° C)	Composition of liquid (percent by weight)		
			Na_2O	FeO	SiO_2
A	$2FeO·SiO_2 + Na_2O·2SiO_2 + SiO_2 \rightleftharpoons L$	<500	[1]	[1]	[1]
B	$FeO + Na_2O·2SiO_2 + 2FeO·SiO_2 \rightleftharpoons L$	667	18.5	33.5	46
C	$FeO + Na_2O·FeO·SiO_2 + Na_2O·SiO_2 \rightleftharpoons L$	703	23	35.5	41.5
D	$Na_2O·FeO·SiO_2 + Na_2O·2SiO_2 \rightleftharpoons Na_2O·SiO_2 + L$	724	[1] 26.5	[1] 29.5	[1] 44
E	$2FeO·SiO_2 + Na_2O·2SiO_2 \rightleftharpoons L$	675	18	33.5	48.5
F	$FeO + Na_2O·2SiO_2 \rightleftharpoons L$	±720	22	36	42
G	$Na_2O·FeO·SiO_2 + Na_2O·SiO_2 \rightleftharpoons L$	934	40.5	19.5	40
H	$FeO + Na_2O·FeO·SiO_2 \rightleftharpoons L$	976	32	36.5	31.5

[1] Only approximately determined.

Na_2O–Al_2O_3–SiO_2

Portions of the system Na_2O–Al_2O_3–SiO_2 were studied by Bowen and Greig (1925), Tilley (1933), Greig and Barth (1938), and Spivak (1944). The complete diagram was published by Schairer and Bowen (in preliminary form, in 1947; in complete form, in 1956). The revision of the side Al_2O_3–SiO_2 is by Aramaki and Roy (1959). The final diagram is figure 23 and the invariant points are given in table 15. In general, the quenching method was used in the study of this system. The compositions on and near the line albite-silica and compositions in the fields of mullite or of corundum with liquidus temperatures below about 1400°C were very viscous and required periods of weeks or months at temperatures about 75°C below the liquidus to grow enough tiny crystals for the quenching studies. The crystallization of pure albite, $Na_2O \cdot Al_2O_3 \cdot 6SiO_2$, which melts congruently at 1118°C, is possible at atmospheric pressure only by following in detail the procedure described by Schairer and Bowen (1956), but Boyd and England (1961b) found that it crystallizes readily at high pressures. Albite glass can be crystallized com-

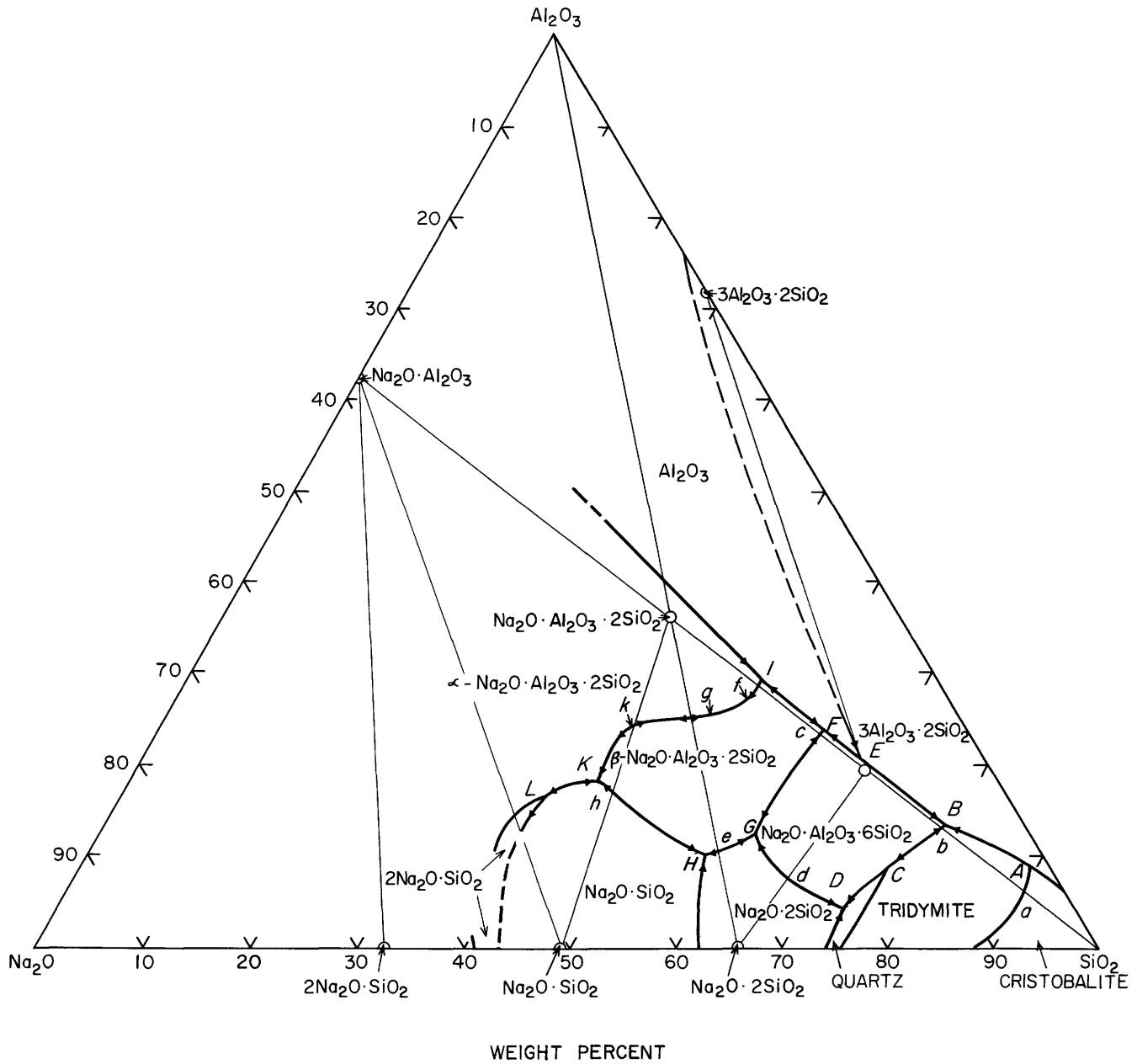

FIGURE 23.—The ternary system Na_2O–Al_2O_3–SiO_2. Based on Schairer and Bowen (1956) and Aramaki and Roy (1959).

pletely at 1100°C in 8 hr at 25,000 atm; a year would be insufficient to crystallize it completely at this temperature at atmospheric pressure. X-ray studies of synthetic albites (MacKenzie, 1957) revealed a wide variation in lattice parameters of the crystals, depending on the conditions of crystallization. The results suggest that for each temperature there is a stable crystalline form of $Na_2O \cdot Al_2O_3 \cdot 6SiO_2$, which is intermediate between high-temperature albite, which is stable only above 1000°C, and low-temperature albite, which is stable only below about 450°C. McConnell and McKie (1960) discussed the kinetics of the ordering process in MacKenzie's experiments and concluded that there is a "smeared" polymorphic transformation—that is, a transformation in which continuity can be associated with the stable coexistence of two or more structural modifications, in this case high- and low-temperature albite—over a range of temperatures.

The compound $Na_2O \cdot Al_2O_3 \cdot 2SiO_2$ exists in four polymorphic forms discussed in detail by Smith and Tuttle (1957). The form stable at the melting point, high-carnegieite (cubic), is stable down to 1250°C where it transforms into a high-nepheline (orthorhombic) form. At a temperature near 900°C, high-nepheline inverts to low-nepheline (hexagonal) which is stable down to room temperatures. The transformation of high-carnegieite into high-nepheline is sluggish and high-carnegieite may be obtained by quenching in the stability field of nepheline, but at 690°C it undergoes a displacive inversion into low-carnegieite, of low symmetry.

The phase equilibrium relations in the ternary system Na_2O–Al_2O_3–SiO_2 may be made clearer by discussing some binary systems in the ternary system. One of these is the binary system $Na_2O \cdot SiO_2$ (sodium metasilicate) – $Na_2O \cdot Al_2O_3 \cdot 2SiO_2$ (nepheline, carnegieite) studied by Tilley (1933) (fig. 24). There is a binary eutectic at 902°C (Spivak, 1944) and 46.75 percent $Na_2O \cdot Al_2O_3 \cdot 2SiO_2$, at which the solid phases are $Na_2O \cdot SiO_2$ and nepheline, neither of which shows solid solution. The inversion temperature of pure

$$Na_2O \cdot Al_2O_3 \cdot 2SiO_2$$

from nepheline to carnegieite is at 1248°C (Bowen, 1912) but carnegieite takes $Na_2O \cdot SiO_2$ into solid solution, thus lowering the inversion temperature from 1248° to 1163°C (curve *CE*). This is in accordance with the general rule (Morey, 1936) that when the high-temperature form takes more of the other material into solid solution the inversion temperature is lowered. When a mixture of crystalline sodium metasilicate and 85 percent nepheline is heated, at 902°C liquid begins to form and the temperature remains constant until all the $Na_2O \cdot SiO_2$ is melted. On further heating, the liquid of the mixture of liquid and nepheline increases in content of $Na_2O \cdot Al_2O_3 \cdot 2SiO_2$ until at 1163°C the liquid has the composition of point *B* of

TABLE 15.—*Invariant points in the system* Na_2O–Al_2O_3–SiO_2

Invariant point on fig. 23	Phase reaction	Temperature (°C)	Composition of liquid (percent by weight)		
			Na_2O	Al_2O_3	SiO_2
a	SiO_2 (tridymite) $\rightleftharpoons SiO_2$ (cristobalite)	1470	3.7	6.1	90.2
A	SiO_2 (tridymite) $\rightleftharpoons SiO_2$ (cristobalite)	1470	2	9	89
B	$SiO_2 + 3Al_2O_3 \cdot 2SiO_2 + Na_2O \cdot Al_2O_3 \cdot 6SiO_2 \rightleftharpoons L$	1050	7.8	13.5	77.7
b	$SiO_2 + Na_2O \cdot Al_2O_3 \cdot 6SiO_2 \rightleftharpoons L$	1062	8.1	13.3	78.6
C	SiO_2 (quartz) $\rightleftharpoons SiO_2$ (tridymite)	867	15	9	76
D	$Na_2O \cdot 2SiO_2 + SiO_2 + Na_2O \cdot Al_2O_3 \cdot 6SiO_2 \rightleftharpoons L$	740	21.5	4.7	73.8
E	$Na_2O \cdot Al_2O_3 \cdot 6SiO_2 + 3Al_2O_3 \cdot 2SiO_2 \rightleftharpoons Al_2O_3 + L$	1104	11.2	20.0	68.8
	$Na_2O \cdot Al_2O_3 \cdot 6SiO_2 \rightleftharpoons L$	1118	11.82	19.44	68.73
d	$Na_2O \cdot 2SiO_2 + Na_2O \cdot Al_2O_3 \cdot 6SiO_2 \rightleftharpoons L$ (Di 62, Ab 38)	767	25.6	7.4	67
c	$Na_2O \cdot Al_2O_3 \cdot 2SiO_2 + Na_2O \cdot Al_2O_3 \cdot 6SiO_2 \rightleftharpoons L$ (Ne24, Ab76)	1068	14.2	23.4	62.4
F	$Na_2O \cdot Al_2O_3 \cdot 2SiO_2 + Na_2O \cdot Al_2O_3 \cdot 6SiO_2 + Al_2O_3 \rightleftharpoons L$	1063	13.8	23.8	62.4
G	$Na_2O \cdot 2SiO_2 + Na_2O \cdot Al_2O_3 \cdot 2SiO_2 + Na_2O \cdot Al_2O_3 \cdot 6SiO_3 \rightleftharpoons L$	732	26.0	12.5	61.5
e	$Na_2O \cdot 2SiO_2 + Na_2O \cdot Al_2O_3 \cdot 2SiO_2 \rightleftharpoons L$ (Di 71, Ne 29)	768	30.5	10.4	59.1
H	$Na_2O \cdot SiO_2 + Na_2O \cdot 2SiO_2 + Na_2O \cdot Al_2O_3 \cdot 2SiO_2 \rightleftharpoons L$	760	32.0	10.1	57.9
f	$Na_2O \cdot Al_2O_3 \cdot 2SiO_2$ (nepheline) $\rightleftharpoons Na_2O \cdot Al_2O_3 \cdot 2SiO_2$ (carnegieite) $+ 3Al_2O_3 \cdot 2SiO_2$	1280	17.5	28.8	53.7
I	$Na_2O \cdot Al_2O_3 \cdot 2SiO_2$ (nepheline) $\rightleftharpoons Na_2O \cdot Al_2O_3 \cdot 2SiO_2$ (carnegieite) $+ 3Al_2O_3 \cdot 2SiO_2$	1270	17.0	29.5	53.5
g	$Na_2O \cdot Al_2O_3 \cdot 2SiO_2$ (nepheline) $\rightleftharpoons Na_2O \cdot Al_2O_3 \cdot 2SiO_2$ (carnegieite)	1248	25.3	25.6	49.1
h	$Na_2O \cdot SiO_2 + Na_2O \cdot Al_2O_3 \cdot 2SiO_2 \rightleftharpoons L$ (Na_2SiO_3 53, Ne 47)	900	37.2	16.9	45.9
k	$Na_2O \cdot Al_2O_3 \cdot 2SiO_2$ (nepheline) $\rightleftharpoons Na_2O \cdot Al_2O_3 \cdot 2SiO_2$ (carnegieite)	1163	30.8	24.8	44.4
K	$Na_2O \cdot Al_2O_3 \cdot 2SiO_2$ (nepheline) $\rightleftharpoons Na_2O \cdot Al_2O_3 \cdot 2SiO_2$ (carnegieite)	915	37.4	18.7	43.9
	$Na_2O \cdot Al_2O_3 \cdot 2SiO_2$ (carnegieite) $\rightleftharpoons L$	1526	21.82	35.89	42.29
L	$2Na_2O \cdot SiO_2 ss(?) + Na_2O \cdot Al_2O_3 \cdot 2SiO_2 ss \rightleftharpoons Na_2O \cdot SiO_2 + L$	955	44.0	16.5	39.5

695-382 O - 64 - 4

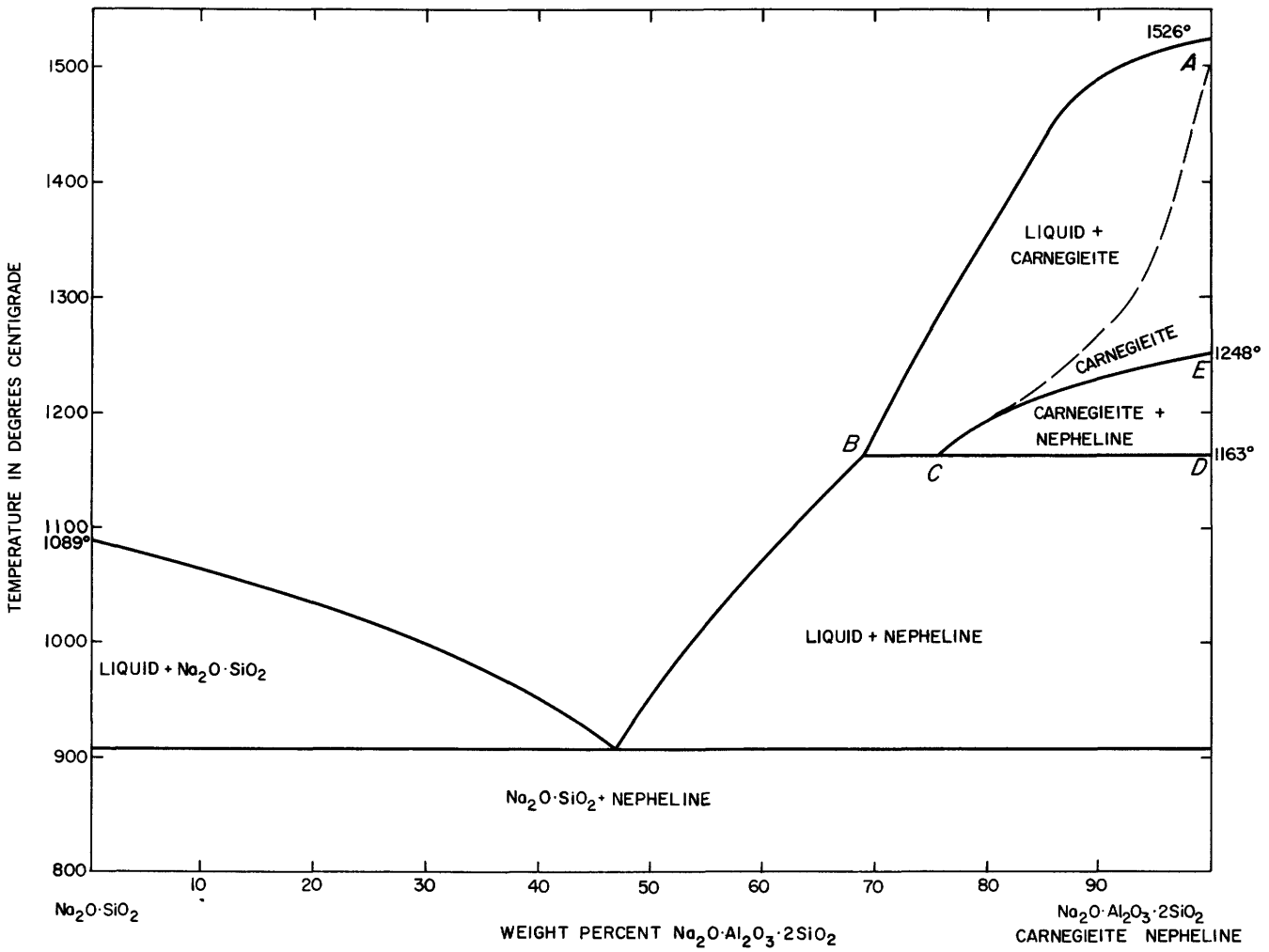

FIGURE 24.—The binary system $Na_2O \cdot SiO_2$ (sodium metasilicate)—$Na_2O \cdot Al_2O_3 \cdot 2SiO_2$ (carnegieite, nepheline). Modified from Tilley (1933).

figure 24. On further heating, the liquid disappears and the composition passes into a region of nepheline plus carnegieite containing $Na_2O \cdot SiO_2$ in solid solution. On crossing the curve *CE*, all the nepheline disappears, and the mixture passes into a divariant region in which carnegieite solid solution is the only phase present, and liquid is not formed until the broken curve *CA* is reached. If the original mixture of $Na_2O \cdot SiO_2$ and nepheline had had a gross composition between *B* and *C*, at 1163°C all the nepheline would have disappeared, and the phases present would have been a liquid of composition on the line *BA* and a carnegieite solid solution on the line *CA*.

Another binary system is $Na_2O \cdot Al_2O_3 \cdot 6SiO_2$ (albite)–silica. This has a eutectic at 1062°C and 31.5 percent SiO_2, and shows the tridymite-cristobalite inversion at 1470°C. All glasses (liquids) in the system albite-silica are extremely viscous, and periods of many months to a year at temperatures about 75° below liquidus temperatures melts were required to obtain any crystallization in these. The system $Na_2O \cdot 2SiO_2$ (sodium disilicate)–$Na_2O \cdot Al_2O_3 \cdot 6SiO_2$ (albite) also is of the simple eutectic type, with a eutectic at 767°C and 38 percent albite. The system

$$Na_2O \cdot SiO_2\text{–}Na_2O \cdot Al_2O_3 \cdot 6SiO_2$$

is not a binary system because the tie line crosses the fields of $Na_2O \cdot 2SiO_2$ and $Na_2O \cdot Al_2O_3 \cdot 6SiO_2$. These are incompatible phases.

$Na_2O \cdot Al_2O_3 \cdot 6SiO_2$ (albite) $- Al_2O_3$ (corundum) also is a simple system with the binary eutectic at 1108°C, 1.5 percent corundum. Preparations in this system required many months for equilibrium to be reached. $Na_2O \cdot Al_2O_3 \cdot 2SiO_2$ (carnegieite) $- Al_2O_3$ also is a binary system with a eutectic at 1475°C, 7 percent Al_2O_3. Owing to the presence of β-Al_2O_3 in all the crystallized glasses of these compositions, it was

difficult to locate the eutectic temperature precisely. The binary system $Na_2O \cdot Al_2O_3 \cdot 2SiO_2$ (carnegieite)–$Na_2O \cdot Al_2O_3$ probably shows a complete series of solid solutions, but the study was difficult because of loss of Na_2O by volatilization.

Tilley (1933) also studied the binary system $Na_2O \cdot 2SiO_2$ (sodium disilicate)–$Na_2O \cdot Al_2O_3 \cdot 2SiO_2$ (nepheline, carnegieite) (fig. 25). In this case there is no solid solution and the nepheline-carnegieite inversion is at 1248°C.

The binary system $Na_2O \cdot Al_2O_3 \cdot 2SiO_2$ (nepheline, carnegieite)–$Na_2O \cdot Al_2O_3 \cdot 6SiO_2$ (albite) was studied by Greig and Barth (1938) (fig. 26). Both nepheline and carnegieite take some albite into solid solution. The inversion temperature of nepheline is raised to 1280°C, and there is a narrow strip of coexistence of nepheline and carnegieite solid solutions. A mixture containing about 5 percent albite on heating passes from a field of nepheline solid solution to a carnegieite solid solution, then into a field of carnegieite plus liquid; a mixture containing 40 percent albite at low temperatures is in the field of nepheline solid solution plus albite; at 1068°C the albite melts and the field of nepheline solid solution plus albite is entered, and at 1080°C the nepheline changes to carnegieite. The binary eutectic is at 1068°C and 76 percent albite. Experimentally, however, it was not possible to crystallize tridymite in any of the preparations, and cristobalite crystals persisted in the tridymite field.

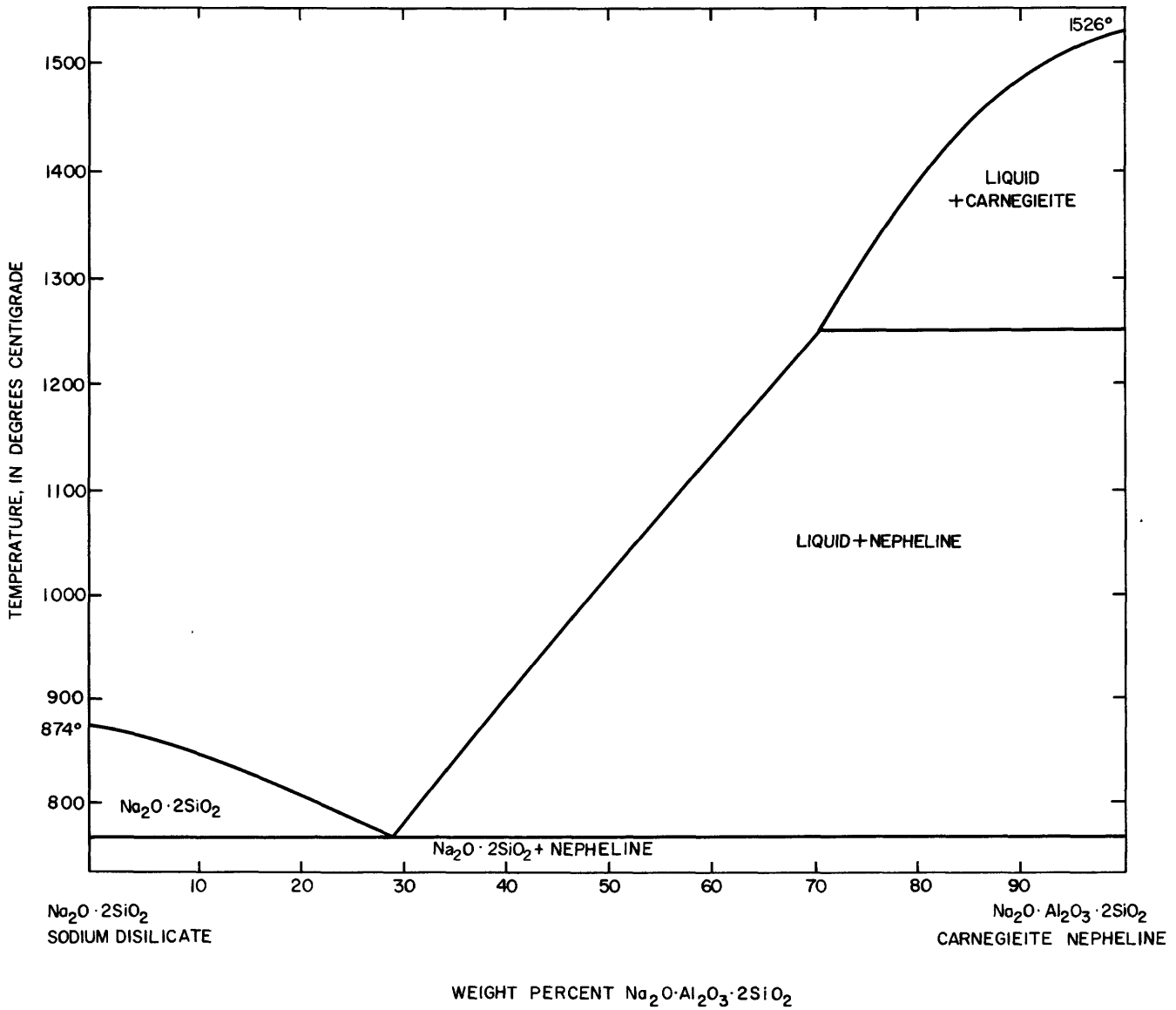

FIGURE 25.—The binary system $Na_2O \cdot 2SiO_2$ (sodium disilicate)–$Na_2O \cdot Al_2O_3 \cdot 2SiO_2$ (carnegieite, nepheline). Modified from Tilley (1933).

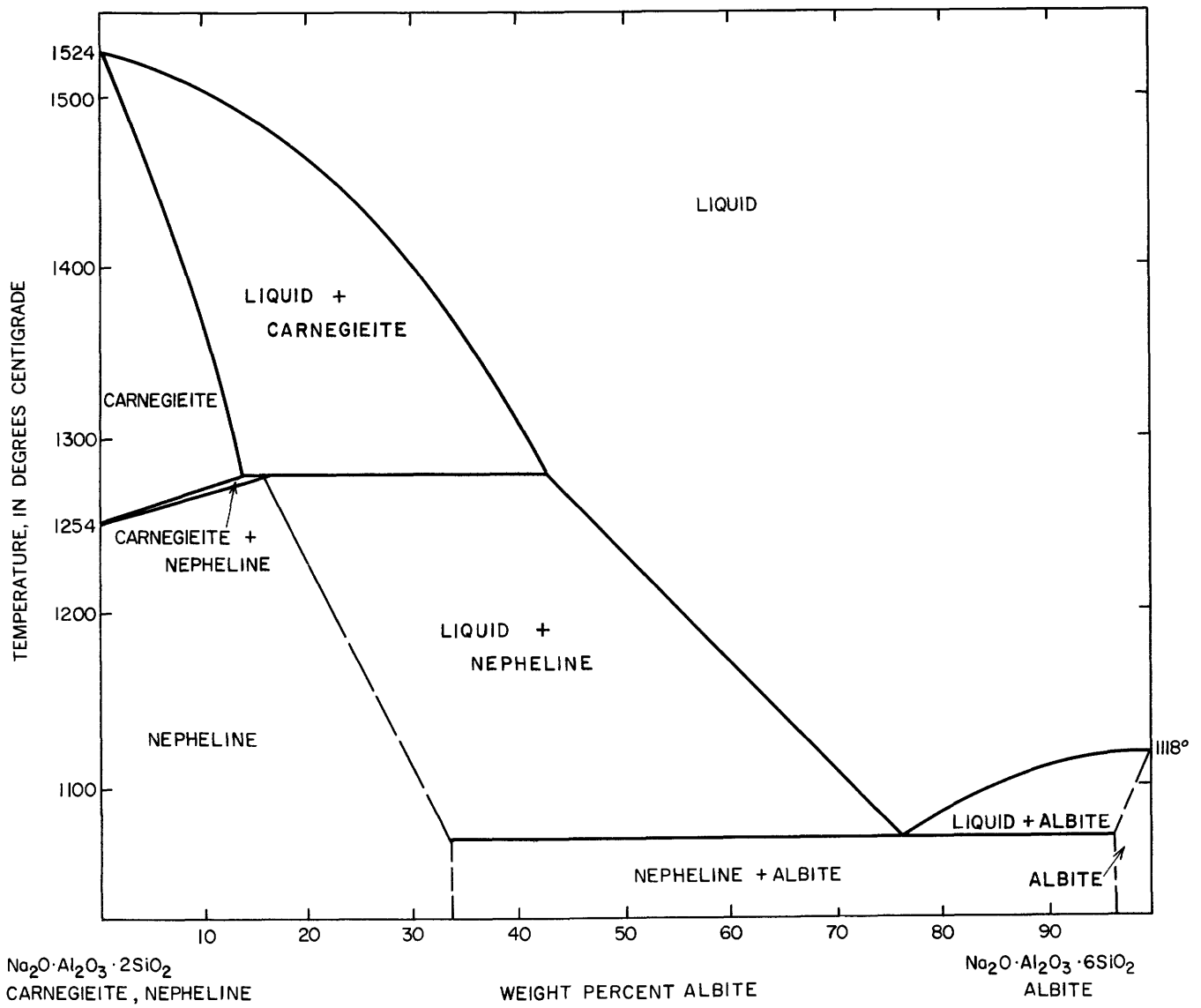

FIGURE 26.—The binary system $Na_2O \cdot Al_2O_3 \cdot 2SiO_2$ (carnegieite, nepheline)–$Na_2O \cdot Al_2O_3 \cdot 6SiO_2$ (albite). Modified from Greig and Barth (1938).

The boundaries of the several fields of figures 24 to 26 need some discussion. The boundary between the fields of cristobalite and tridymite is one of constant temperature, 1470°C, because there is no solid solution in either silica phase, and the same is true of the boundary between quartz and tridymite. The field of albite is bounded by the field of tridymite (*BbC*), with a maximum at *b;* quartz, (*CD*); $Na_2O \cdot 2SiO_2$ (*DdG*), with a maximum at *d*, the eutectic in the binary system $Na_2O \cdot 2SiO_2$–$Na_2O \cdot Al_2O_3 \cdot 6SiO_2$; β-$Na_2O \cdot Al_2O_3 \cdot 2SiO_2$ (*GcF*), with a maximum at *c*; Al_2O_3 (*FE*); and $3Al_2O_3 \cdot 2SiO_2$ (*EB*). The field of $3Al_2O_3 \cdot 2SiO_2$, mullite, is bounded by the side Al_2O_3–SiO_2, the fields of cristobalite, tridymite (*AB*), $Na_2O \cdot Al_2O_3 \cdot 6SiO_2$ (*BE*), and Al_2O_3. Temperature falls from the Al_2O_3–$3Al_2O_3 \cdot 2SiO_2$ eutectic (1840°C) to **E**, where the phase reaction is

$$Na_2O \cdot Al_2O_3 \cdot 6SiO_2 + 3Al_2O_3 \cdot 2SiO_2 = L + Al_2O_3,$$

then to *B*, the eutectic

$$Na_2O \cdot Al_2O_3 \cdot 6SiO_2 + 3Al_2O_3 \cdot 2SiO_2 + SiO_2 = L,$$

at 1050°C. The field of β-$Na_2O \cdot Al_2O_3 \cdot 2SiO_2$ is bound by the field of albite (*FcG*), with a maximum at *c*; $Na_2O \cdot SiO_2$ (*GeH*), with a maximum at *e*; $Na_2O \cdot SiO_2$ (*HhK*) with a maximum at *h*; and $2Na_2O \cdot Al_2O_3 \cdot 2SiO_2$ (*KkgfI*), with maxima at *k* in the binary system $Na_2O \cdot SiO_2$–$Na_2O \cdot Al_2O_3 \cdot 2SiO_2$, at *g* in the binary system $Na_2O \cdot 2SiO_2$–$Na_2O \cdot Al_2O_3 \cdot 2SiO_2$, and at *f*, 1280°C. The point *I*, 1270°C, is the ternary eutectic

liquid + carnegieite + nepheline + corundum. The fields of $Na_2O \cdot 2SiO_2$ and $Na_2O \cdot SiO_2$ have already been bounded except for the boundary between $Na_2O \cdot 2SiO_2$ and quartz, from the eutectic D to the side $Na_2O \cdot SiO_2$; the boundary between the fields of $Na_2O \cdot SiO_2$ and $Na_2O \cdot 2SiO_2$, from the eutectic H to the side; and the boundary between the fields of $Na_2O \cdot SiO_2$ and $2Na_2O \cdot SiO_2$, from L to the side. The field of $2Na_2O \cdot SiO_2$ has not been outlined, nor that of Na_2O, because of extreme experimental difficulties. At the invariant point L, the solid phases are $Na_2O \cdot SiO_2$, probably free from solid solution, a carnegieite solid solution of unknown composition, and a third phase, which may be a sodium orthosilicate solid solution of unknown composition, but the composition of the two solid solutions must be such as to make point L be a reaction point, not a eutectic. Compositions in this high-sodium region were extremely hygroscopic; they attacked the platinum crucibles to give deep-orange colored melts, and "smoked" at their melting temperatures owing to the volatilization of Na_2O.

Pablo-Galan and Foster (1959) studied mixtures low in silica, in which the so-called β-alumina, $Na_2O \cdot 11Al_2O_3$, is the primary phase. They consider β-alumina to be a stable compound, with a field of stability extending well into the phase-equilibrium diagram, at least down to the 1600°C isotherm.

Work at high pressures has extended our knowledge of compounds in this system. Boyd and England (1956) found that nepheline in the range from 10,000 to 35,000 atm decomposed into two new and unknown phases, one of which had optical properties close to those of jadeite and was evidently a pyroxene. Birch and LeComte (1960) found that the melting point of albite is raised by pressure. Measurements were made up to 22,000 atm, and the results are represented by the relation, $t = 1115 + 0.011\ P$, in which t is °C and P is the pressure in bars. At higher pressures albite is decomposed with formation of jadeite and quartz. This reaction is represented by the relation

$$P = 6000\ (\pm 500) + 20\ (\pm 2)\ t.$$

The stability of jadeite had previously been discussed by Yoder (1950), Yoder and Weir (1951), Kracek, Neuvonen, and Burley (1951), and Adams (1953).

Na_2O–Fe_2O_3–SiO_2

Study of the system Na_2O–Fe_2O_3–SiO_2 by Bowen and Schairer (1929b) and by Bowen, Schairer, and Willems (1930) was restricted to the region

$$Na_2O \cdot SiO_2 – Fe_2O_3 – SiO_2.$$

The results are summarized in figure 27 and table 16. The iron content of the liquids is given in terms of Fe_2O_3, but they always contained a small amount of ferrous iron, ranging up to 1.09 percent FeO for a liquid in the acmite field containing 16.64 percent Na_2O, 48.36 percent SiO_2. The course of the tridymite-hematite boundary makes it improbable that any binary compound exists between Fe_2O_3 and SiO_2 and makes it probable that there is almost complete immiscibility between Fe_2O_3 and SiO_2 in the liquid state. The ternary compound $Na_2O \cdot Fe_2O_3 \cdot 4SiO_2$ (acmite) melts incongruently at 990°C, with separation of hematite, and the liquidus for this composition is at 1275°C. A second compound, $5Na_2O \cdot Fe_2O_3 \cdot 8SiO_2$, melts congruently at 838°C. A third compound, $6Na_2O \cdot 4Fe_2O_3 \cdot 5SiO_2$, with a composition outside of the restricted composition triangle Na_2SiO_3–SiO_2–Fe_2O_3 melts congruently at 1091°C. Indications were obtained of a compound $2Na_2O \cdot Fe_2O_3 \cdot SiO_2$, but this was not followed further. Because of the incongruent melting of acmite, and the large area in the composition triangle occupied by the hematite field, some unusual courses of crystallization were found in mixtures rich in acmite. In some mixtures hematite crystallizes out at an early stage, is completely resorbed by reaction with liquid at intermediate stages, and again crystallizes out at a late stage.

K_2O–MgO–SiO_2

The system K_2O–MgO–SiO_2 was studied by Roedder (1951a) with results shown in figure 28 and table 17. Four ternary compounds are formed. $K_2O \cdot MgO \cdot SiO_2$ melts congruently at 1650°C to a thin liquid, has a large field of stability in the ternary diagram and forms binary eutectics with MgO, $K_2O \cdot MgO \cdot 3SiO_2$, $K_2O \cdot 2SiO_2$, and $K_2O \cdot SiO_2$. $K_2O \cdot MgO \cdot 3SiO_2$ melts congruently at 1134°C, and forms binary eutectics with $K_2O \cdot MgO \cdot SiO_2$, $K_2O \cdot MgO \cdot 5SiO_2$, $K_2O \cdot 2SiO_2$, and $2MgO \cdot SiO_2$. $K_2O \cdot MgO \cdot 5SiO_2$ melts congruently at 1089°C but to a viscous liquid. It forms binary eutectics with $K_2O \cdot MgO \cdot 3SiO_2$, $2MgO \cdot SiO_2$, SiO_2 and $K_2O \cdot 4SiO_2$. The compound $K_2O \cdot 5MgO \cdot 12SiO_2$ melts incongruently and has a small field of stability on the liquidus surfaces. The pure crystals begin to melt at 1174°C to form $MgO \cdot SiO_2$ and liquid of composition T. Above 1174°C, $MgO \cdot SiO_2$ goes into solution, but at 1398°C the line

$$MgO \cdot SiO_2 – K_2O \cdot 5MgO \cdot 12SiO_2 – T$$

crosses the boundary between the fields of $MgO \cdot SiO_2$ and $2MgO \cdot SiO_2$, and $MgO \cdot SiO_2$ decomposes with formation of $2MgO \cdot SiO_2$ and a liquid on the boundary curve. At 1453°C this reaction is complete, the liquid

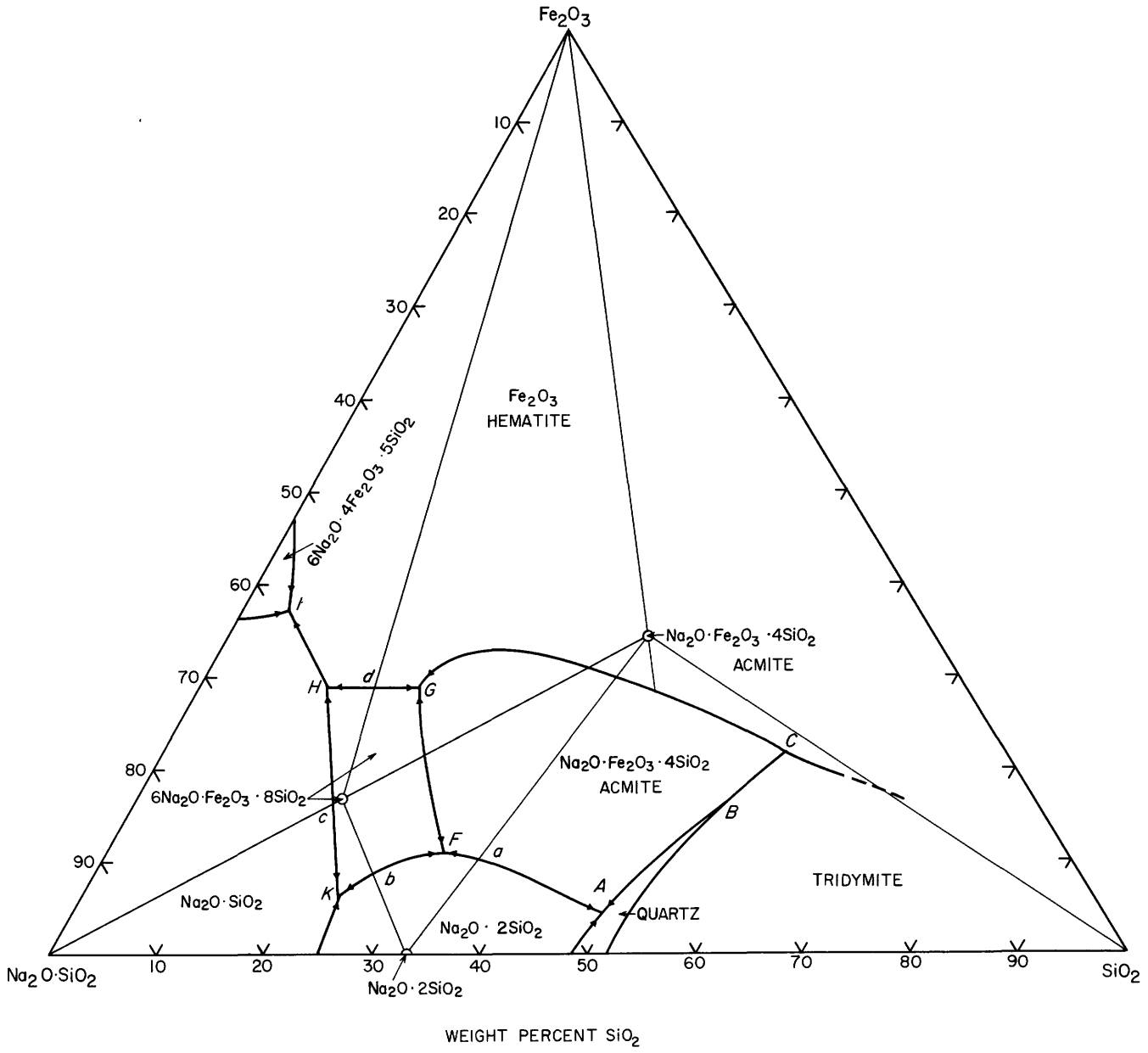

FIGURE 27.—The ternary system Na_2O-SiO_2–Fe_2O_3–SiO_2. Modified from Bowen, Schairer, and Willems (1930).

TABLE 16.—*Invariant points in the system* Na_2O–Fe_2O_3–SiO_2

Invariant point on fig. 27	Phase reaction	Temperature (° C)	Composition of liquid (percent by weight)				
			$Na_2O \cdot SiO_2$	SiO_2	Fe_2O_3	Na_2O	SiO_2
A	SiO_2 (quartz) + $Na_2O \cdot 2SiO_2$ + $Na_2O \cdot Fe_2O_3 \cdot 4SiO_2 \rightleftharpoons L$	760	46. 6	49. 2	4. 2	23. 7	72. 1
B	SiO_2 (quartz) $\rightleftharpoons SiO_2$ (tridymite)	867	31. 0	54. 2	14. 8	15. 7	69. 5
C	$Na_2O \cdot Fe_2O_3 \cdot 4SiO_2$ + SiO_2 (tridymite) $\rightleftharpoons Fe_2O_3 + L$	955	20. 5	57. 8	21. 7	10. 4	67. 9
a	$Na_2O \cdot 2SiO_2 + Na_2O \cdot Fe_2O_3 \cdot 4SiO_2 \rightleftharpoons L$	810	54. 0	35. 0	10. 2	27. 8	62
F	$Na_2O \cdot 2SiO_2 + Na_2O \cdot Fe_2O_3 \cdot 4SiO_2 + 5Na_2O \cdot Fe_2O_3 \cdot 8SiO_2 \rightleftharpoons L$	800	59. 8	31. 2	11. 0	29. 4	59. 6
b	$Na_2O \cdot 2SiO_2 + 5Na_2O \cdot Fe_2O_3 \cdot 8SiO_2 \rightleftharpoons L$	818	65. 5	25. 6	8. 9	33. 3	57. 8
	$5Na_2O \cdot Fe_2O_3 \cdot 8SiO_2 \rightleftharpoons L$	838	64. 2	19. 0	16. 8	32. 6	50. 6
c	$Na_2O \cdot SiO_2 + 5Na_2O \cdot Fe_2O_3 \cdot 8SiO_2 \rightleftharpoons L$	837	65. 3	18. 4	16. 3	33. 2	50. 5
G	$5Na_2O \cdot Fe_2O_3 \cdot 8SiO_2 + Na_2O \cdot Fe_2O_3 \cdot 4SiO_2 + Fe_2O_3 \rightleftharpoons L$	809	50. 7	20. 5	28. 8	25. 8	45. 4
d	$5Na_2O \cdot Fe_2O_3 \cdot 8SiO_2 + Fe_2O_3 \rightleftharpoons L$	816	55. 0	16. 2	28. 8	27. 9	43. 3
H	$Na_2O \cdot SiO_2 + Fe_2O_3 + 5Na_2O \cdot Fe_2O_3 \cdot 8SiO_2 \rightleftharpoons L$	815	59. 2	11. 9	28. 9	30. 1	41. 1
I	$Na_2O \cdot SiO_2 + Fe_2O_3 \rightleftharpoons 6Na_2O \cdot 4Fe_2O_3 \cdot 5SiO_2 + L$	845	58. 6	4. 4	37. 0	29. 8	33. 2
K	$Na_2O \cdot SiO_2 + Na_2O \cdot 2SiO_2 + 5Na_2O \cdot Fe_2O_3 \cdot 8SiO_2 \rightleftharpoons L$	816	70. 1	23. 9	6. 0	35. 6	58. 4

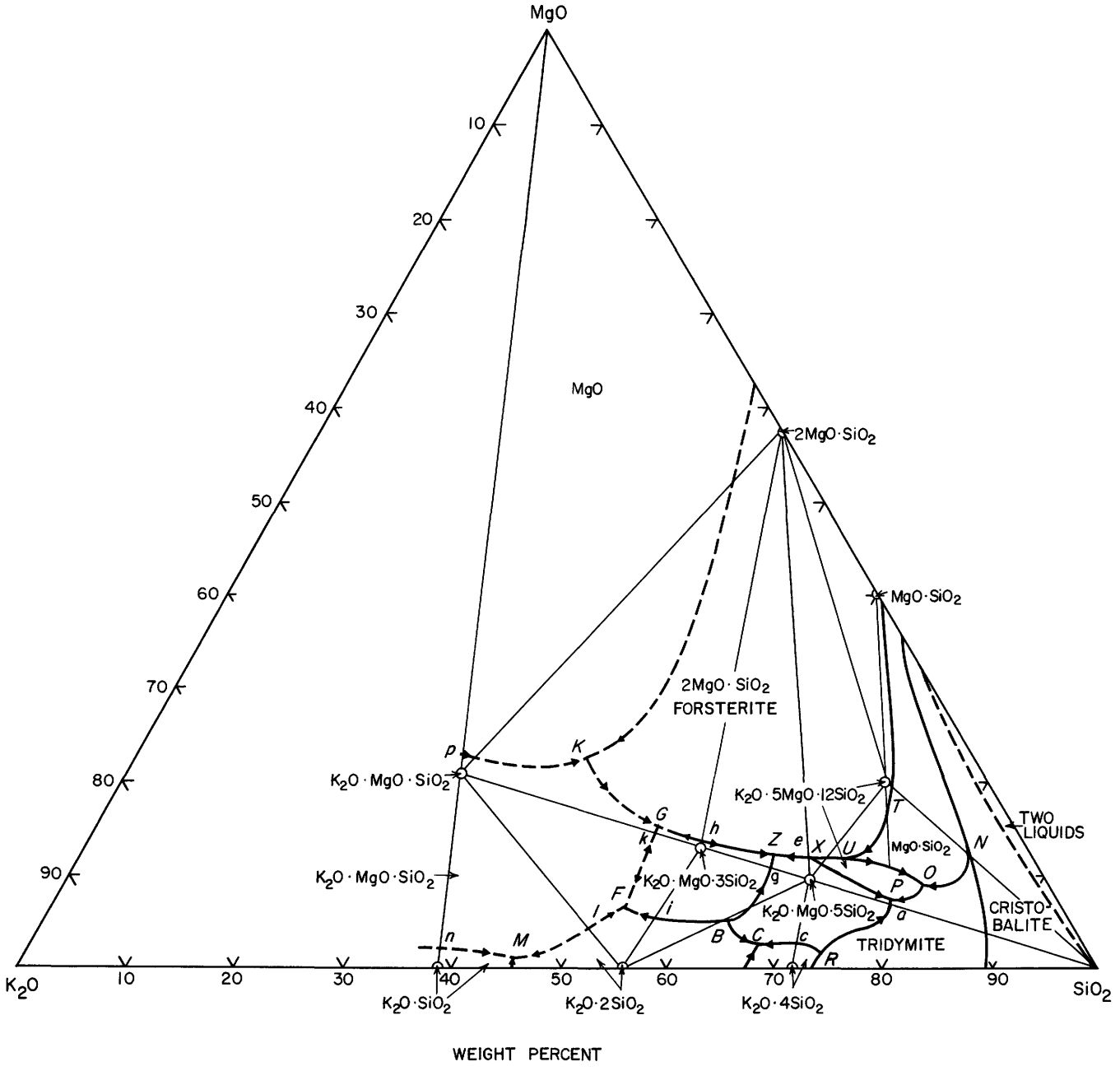

FIGURE 28.—The system K_2O–MgO–SiO_2. Modified from Roedder (1951a).

composition leaves the boundary curve, and melting is complete at 1467°C. A large part of the phase-equilibrium diagram is taken up by the fields of MgO, $2MgO \cdot SiO_2$, and $MgO \cdot SiO_2$. Mixtures high in K_2O, including $K_2O \cdot SiO_2$, $K_2O \cdot MgO \cdot SiO_2$, and more K_2O-rich mixtures, are practically impossible to work with because of hygroscopicity, the difficulty of expelling CO_2, and the volatility of K_2O.

TABLE 17.—*Invariant points in the system* K_2O–MgO–SiO_2

Invariant point on fig. 28	Phase reaction	Temperature (° C)	Composition of liquid (percent by weight)		
			K_2O	MgO	SiO_2
N	SiO_2 (tridymite)$\rightleftharpoons SiO_2$ (cristobalite)	1470			
O	$K_2O{\cdot}5MgO{\cdot}12SiO_2 + SiO_2 \rightleftharpoons MgO{\cdot}SiO_2 + L$	1165	11. 6	8. 8	79. 6
P	$K_2O{\cdot}MgO{\cdot}5SiO_2 + K_2O{\cdot}5MgO{\cdot}12SiO_2 + SiO_2 \rightleftharpoons L$	963	15. 1	7. 2	77. 7
a	$K_2O{\cdot}MgO{\cdot}5SiO_2 + SiO_2$ (tridymite)$\rightleftharpoons L$	987	15. 5	6. 7	77. 8
b	$K_2O{\cdot}5MgO{\cdot}12SiO_2 \rightleftharpoons MgO{\cdot}SiO_2 + L$	1174	13. 5	10. 5	76. 0
R	$K_2O{\cdot}4SiO_2 + K_2O{\cdot}MgO{\cdot}5SiO_2 + SiO_2$ (tridymite) [1]$\rightleftharpoons L$	715	24. 5	2. 0	73. 5
U	$K_2O{\cdot}5MgO{\cdot}12SiO_2 + 2MgO{\cdot}SiO_2 \rightleftharpoons MgO{\cdot}SiO_2 + L$	1155	16. 4	11. 5	72. 1
c	$K_2O{\cdot}4SiO_2 + K_2O{\cdot}MgO{\cdot}5SiO_2 \rightleftharpoons L$	730	26. 5	2. 4	71. 1
	$K_2O{\cdot}MgO{\cdot}5SiO_2 \rightleftharpoons L$	1089	21. 7	9. 3	69. 0
X	$K_2O{\cdot}MgO{\cdot}5SiO_2 + K_2O{\cdot}5MgO{\cdot}12SiO_2 + 2MgO{\cdot}SiO_2 \rightleftharpoons L$	1042	20. 2	11. 8	68. 0
e	$2MgO{\cdot}SiO_2 + K_2O{\cdot}MgO{\cdot}5SiO_2 \rightleftharpoons L$	1053	20. 5	11. 8	67. 7
C	$K_2O{\cdot}4SiO_2 + K_2O{\cdot}2SiO_2 + K_2O{\cdot}MgO{\cdot}5SiO_2 \rightleftharpoons L$	685	30. 0	2. 5	67. 5
g	$K_2O{\cdot}MgO{\cdot}3SiO_2 + K_2O{\cdot}MgO{\cdot}5SiO_2 \rightleftharpoons L$	1030	24. 8	10. 7	64. 5
Z	$2MgO{\cdot}SiO_2 + K_2O{\cdot}MgO{\cdot}5SiO_2 + K_2O{\cdot}MgO{\cdot}3SiO_2 \rightleftharpoons L$	1013	23. 9	12. 0	64. 1
B	$K_2O{\cdot}2SiO_2 + K_2O{\cdot}MgO{\cdot}5SiO_2 \rightleftharpoons K_2O{\cdot}MgO{\cdot}3SiO_2 + L$	795	31. 6	4. 8	63. 6
	$K_2O{\cdot}MgO{\cdot}3SiO_2 \rightleftharpoons L$	1134	29. 9	12. 8	57. 3
T	$K_2O{\cdot}5MgO{\cdot}12SiO_2 \rightleftharpoons MgO{\cdot}SiO_2 + L$	1174	13. 5	10. 5	76. 0
h	$2MgO{\cdot}SiO_2 + K_2O{\cdot}MgO{\cdot}3SiO_2 \rightleftharpoons L$	1131	29. 5	13. 5	57. 0
i	$K_2O{\cdot}2SiO_2 + K_2O{\cdot}MgO{\cdot}3SiO_2 \rightleftharpoons L$	933	38. 3	5. 2	56. 5
F	$K_2O{\cdot}2SiO_2 + K_2O{\cdot}MgO{\cdot}SiO_2 + K_2O{\cdot}MgO{\cdot}3SiO_2 \rightleftharpoons L$	905	40. 5	6. 0	53. 5
k	$K_2O{\cdot}MgO{\cdot}SiO_2 + K_2O{\cdot}MgO{\cdot}3SiO_2 \rightleftharpoons L$	1110	33. 0	14. 0	53. 0
G	$K_2O{\cdot}MgO{\cdot}SiO_2 + 2MgO{\cdot}SiO_2 + K_2O{\cdot}MgO{\cdot}3SiO_2 \rightleftharpoons L$	1105	33. 0	15. 0	52. 0
l	$K_2O{\cdot}2SiO_2 + K_2O{\cdot}MgO{\cdot}SiO_2 \rightleftharpoons L$	910	44. 8	4. 2	51. 0
M	$K_2O{\cdot}SiO_2 + K_2O{\cdot}MgO{\cdot}SiO_2 + K_2O{\cdot}2SiO_2 \rightleftharpoons L$	720	54. 2	. 5	45. 3
K	$2MgO{\cdot}SiO_2 + K_2O{\cdot}MgO{\cdot}SiO_2 \rightleftharpoons MgO + L$	1350	36	22	42
	$K_2O{\cdot}MgO{\cdot}SiO_2 \rightleftharpoons L$	1650	18. 4	20. 7	30. 9
n	$K_2O{\cdot}SiO_2 + K_2O{\cdot}MgO{\cdot}SiO_2 \rightleftharpoons L$	±950	60. 1	1. 7	38. 2
p	$K_2O{\cdot}MgO{\cdot}SiO_2 + MgO \rightleftharpoons L$	>1650			

[1] Tridymite is metastable.

K_2O–CaO–Al_2O_3

The system K_2O–CaO–Al_2O_3 was studied by Brownmiller (1935) with special reference to the effect of small amounts of K_2O on portland cement. No ternary compound was found in the region investigated, and the field of $K_2O{\cdot}Al_2O_3$ is adjacent to those of CaO, $3CaO{\cdot}Al_2O_3$, $5CaO{\cdot}3Al_2O_3$, and $CaO{\cdot}Al_2O_3$. The compound $5CaO{\cdot}3Al_2O_3$ takes as much as 2 percent of K_2O into solid solution. The phase-equilibrium diagram is shown in figure 29, and the invariant points are given in table 18.

K_2O–CaO–SiO_2

The system K_2O–CaO–SiO_2, shown in figure 30 and table 19, was worked out by Morey, Kracek, and Bowen (1930). There are five ternary compounds, the most siliceous of which is $K_2O{\cdot}2CaO{\cdot}9SiO_2$. This compound is very difficult to crystallize in the dry way, and its fusion relations were worked out with the aid of hydrothermal crystallization. Its field, *EFGHIbCa*, is far removed from its composition. The pure compound melts incongruently at 1052°C with formation of α-$K_2O{\cdot}3CaO{\cdot}6SiO_2$, and a liquid of composition K_2O 12.6 percent, CaO 15.0 percent, SiO_2 72.4 percent. On further heating, the $K_2O{\cdot}3CaO{\cdot}6SiO_2$ decomposes into $CaO{\cdot}SiO_2$ (wollastonite) and the liquid composition is K_2O 13.2 percent, CaO 11.8 percent, SiO_2 75.0 percent. The composition $K_2O{\cdot}2CaO{\cdot}9SiO_2$ melts completely at 1198°C. A second compound,

$$K_2O{\cdot}3CaO{\cdot}6SiO_2,$$

the K_2O analog of devitrite ($Na_2O_3{\cdot}3CaO{\cdot}6SiO_2$), also melts incongruently, and exists in a high temperature, or β-form, and a low temperature, or α-form, with

TABLE 18.—*Invariant points in the system* K_2O–CaO–Al_2O_3

Invariant point on fig. 29	Phase reaction	Temperature (°C)	Composition of liquid (percent by weight)		
			K_2O	CaO	Al_2O_3
A	$3CaO{\cdot}Al_2O_3 + K_2O{\cdot}Al_2O_3 \rightleftharpoons CaO + L$	1475	6. 5	48. 8	44. 7
B	$3CaO{\cdot}Al_2O_3 + K_2O{\cdot}Al_2O_3 + 5CaO{\cdot}3Al_2O_3 \rightleftharpoons L$	1425	4. 8	48. 0	47. 2
C	$5CaO{\cdot}3Al_2O_3 + CaO{\cdot}Al_2O_3 + K_2O{\cdot}Al_2O_3 \rightleftharpoons L$	1430	5. 0	39. 0	56. 0

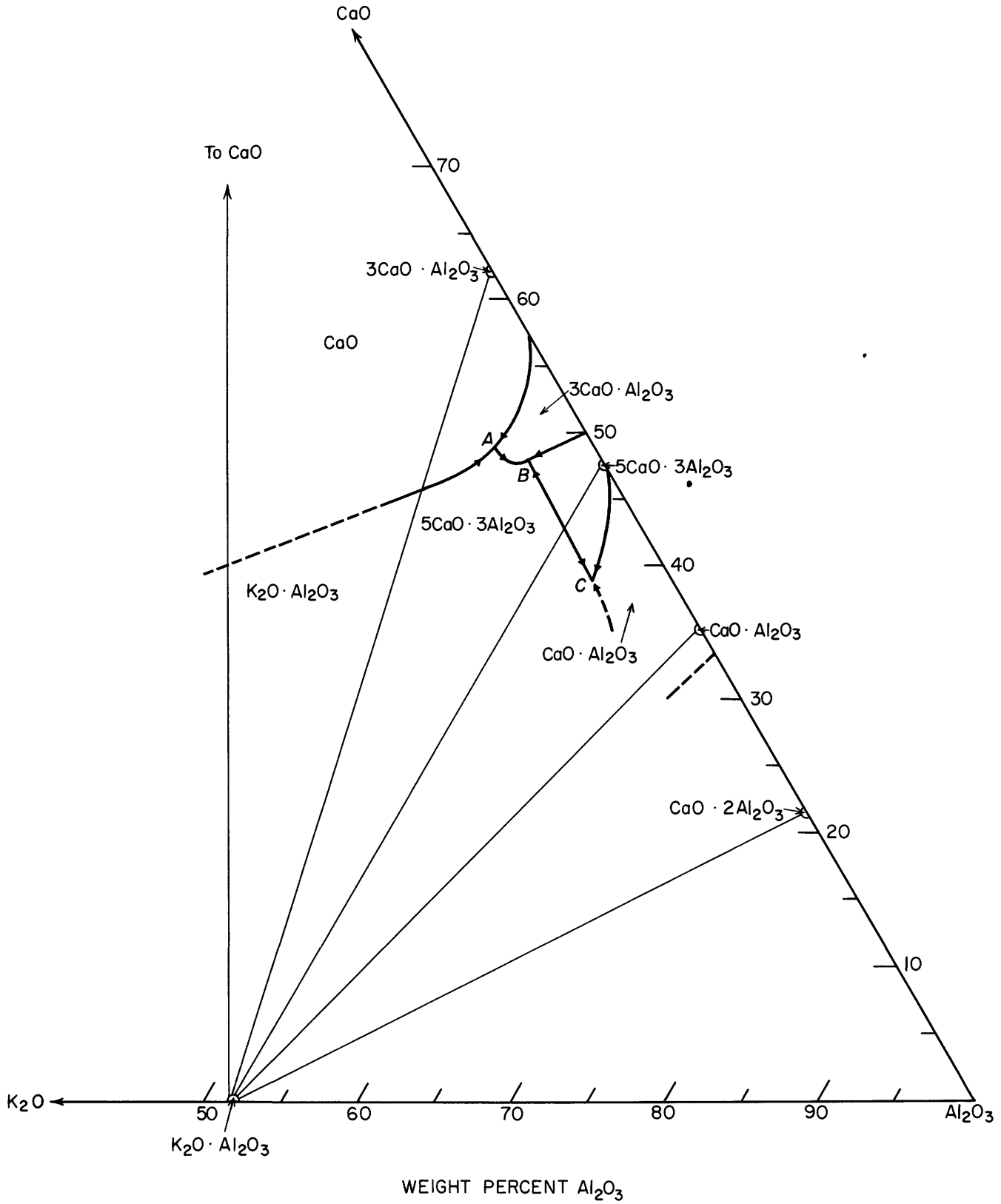

FIGURE 29.—The system K_2O-CaO-Al_2O_3. Modified from Brownmiller (1935).

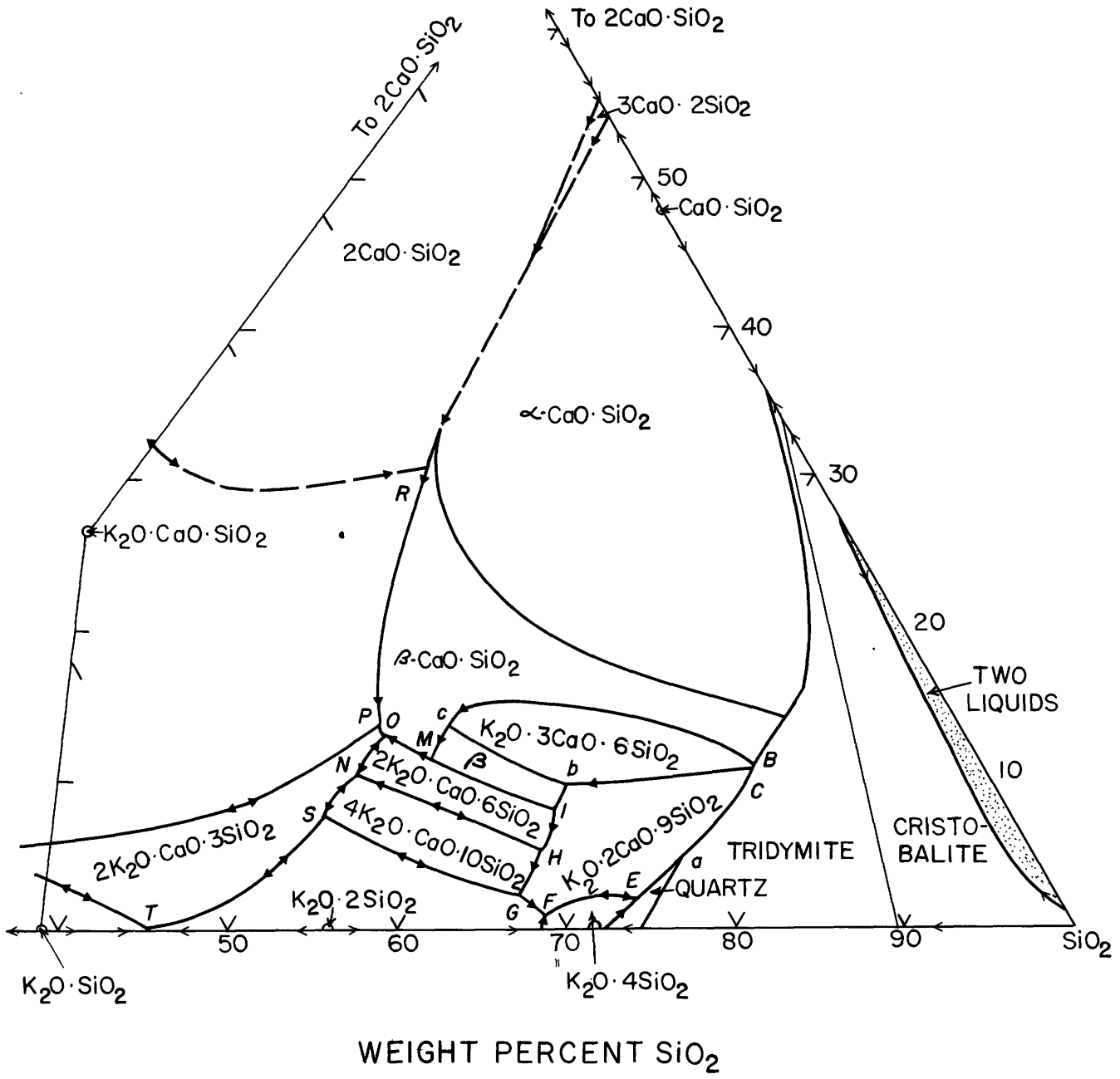

FIGURE 30.—The system K_2O–CaO–SiO_2. Modified from Morey, Kracek, and Bowen (1930, 1931).

an inversion temperature of approximately 1000°C. The α-form melts incongruently at 1120°C with formation of $CaO \cdot SiO_2$ (wollastonite) and a liquid of composition, K_2O 14.5 percent, CaO 16.5 percent, SiO_2 69.0 percent. There are two disilicate compounds:

$$4K_2O \cdot CaO \cdot 10SiO_2,$$

which melts congruently at 946°C, and

$$2K_2O \cdot CaO \cdot 6SiO_2,$$

which melts congruently at 959°C. These disilicate compounds have no analogs in the Na_2O system. There is also one ternary metasilicate compound,

$$2K_2O \cdot CaO \cdot 3SiO_2,$$

which melts incongruently with formation of the orthosilicate, $K_2O \cdot CaO \cdot SiO_2$. The probably congruent melting point of this compound is approximately 1630°C, but accurate work with mixtures high in K_2C

TABLE 19.—*Invariant points in the system* K_2O–CaO–SiO_2

Invariant point on fig. 30	Phase reaction	Temperature (°C)	Composition of liquid (percent by weight		
			K_2O	CaO	SiO_2
B	α–$K_2O{\cdot}3CaO{\cdot}6SiO_2 + SiO_2 \rightleftharpoons \beta$–$CaO{\cdot}SiO_2 + L$	1080	13.3	10.8	75.9
C	$K_2O{\cdot}2CaO{\cdot}9SiO_2 \rightleftharpoons K_2O{\cdot}3CaO{\cdot}6SiO_2 + SiO_2 + L$	1050	13.8	10.5	75.7
a	SiO_2 (α-quartz) $\rightleftharpoons SiO_2$ (tridymite)	867	20.1	5.2	74.7
E	$K_2O{\cdot}2CaO{\cdot}9SiO_2 + K_2O{\cdot}4SiO_2 + SiO_2 \rightleftharpoons L$	720	25.1	1.9	73.0
F	$K_2O{\cdot}2SiO_2 + K_2O{\cdot}2CaO{\cdot}9SiO_2 + K_2O{\cdot}4SiO_2 \rightleftharpoons L$	720	30.8	.9	68.3
G	$K_2O{\cdot}2SiO_2 + K_2O{\cdot}2CaO{\cdot}9SiO_2 \rightleftharpoons 4K_2O{\cdot}CaO{\cdot}10SiO_2 + L$	740	31.6	2.3	66.1
H	$4K_2O{\cdot}CaO{\cdot}10SiO_2 + K_2O{\cdot}2CaO{\cdot}9SiO_2 \rightleftharpoons 2K_2O{\cdot}CaO{\cdot}6SiO_2 + L$	825	28.8	5.3	65.9
I	$2K_2O{\cdot}CaO{\cdot}6SiO_2 + K_2O{\cdot}2CaO{\cdot}9SiO_2 \rightleftharpoons \beta$–$K_2O{\cdot}3CaO{\cdot}6SiO_2 + L$	910	26.6	7.8	65.6
b	β–$K_2O{\cdot}3CaO{\cdot}6SiO_2 \rightleftharpoons \alpha$–$K_2O{\cdot}3CaO{\cdot}6SiO_2$	1000	23.6	11.0	65.4
	$2K_2O{\cdot}CaO{\cdot}6SiO_2 \rightleftharpoons L$	959	31.1	9.3	59.6
	$4K_2O{\cdot}CaO{\cdot}10SiO_2 \rightleftharpoons L$	946	36.5	5.4	58.1
c	β–$K_2O{\cdot}3CaO{\cdot}6SiO_2 \rightleftharpoons \alpha$–$K_2O{\cdot}3CaO{\cdot}SiO_2$	1000	31.1	13.4	56.5
M	$2K_2O{\cdot}CaO{\cdot}6SiO_2 + \beta$–$CaO{\cdot}SiO_2 \rightleftharpoons \beta$–$K_2O{\cdot}3CaO{\cdot}6SiO_2 + L$	930	32.3	11.3	56.4
N	$2K_2O{\cdot}CaO{\cdot}3SiO_2 + 4K_2O{\cdot}CaO{\cdot}10SiO_2 + 2K_2O{\cdot}CaO{\cdot}6SiO_2 \rightleftharpoons L$	890	37.2	10.2	52.6
O	$2K_2O{\cdot}CaO{\cdot}3SiO_2 + 2K_2O{\cdot}CaO{\cdot}6SiO_2 + \beta$–$CaO{\cdot}SiO_2 \rightleftharpoons L$	800	34.2	13.0	52.8
P	$2K_2O{\cdot}CaO{\cdot}3SiO_2 + \beta$–$CaO{\cdot}SiO_2 \rightleftharpoons K_2O{\cdot}CaO{\cdot}SiO_2 + L$	830	34.1	13.7	52.2
R	$K_2O{\cdot}CaO{\cdot}SiO_2 + \beta$–$CaO{\cdot}SiO_2 \rightleftharpoons 2CaO{\cdot}SiO_2 + L$	1180	22.5	31.0	46.5
S	$2K_2O{\cdot}CaO{\cdot}3SiO_2 + K_2O{\cdot}2SiO_2 + 4K_2O{\cdot}CaO{\cdot}10SiO_2 \rightleftharpoons L$	895	40.5	7.7	51.8
T	$K_2O{\cdot}SiO_2 + 2K_2O{\cdot}CaO{\cdot}3SiO_2 + K_2O{\cdot}2SiO_2 \rightleftharpoons L$	770	54.7	.2	45.1
	$K_2O{\cdot}CaO{\cdot}SiO_2 + K_2O{\cdot}23CaO{\cdot}12SiO_2 + L$	1598	41.2	29.7	29.1
	$K_2O{\cdot}CaO{\cdot}SiO_2 \rightleftharpoons L$	1630	44.8	26.7	28.5

is difficult because of their hygroscopicity and the volatilization of K_2O. The K_2O glasses are more viscous than the corresponding Na_2O glasses, and mixtures high in SiO_2 are more difficult to crystallize.

Taylor (1941) studied mixtures along the join $K_2O{\cdot}CaO{\cdot}SiO_2$ and $2CaO{\cdot}SiO_2$, and found the compound $K_2O{\cdot}23CaO{\cdot}12SiO_2$, not shown on figure 30, which has a eutectic with $K_2O{\cdot}CaO{\cdot}SiO_2$ at 1598°C.

K_2O–FeO–SiO_2

Roedder (1952) made a reconnaissance of liquidus relations in the partial system $K_2O{\cdot}2SiO_2$–FeO–SiO_2, with results shown in figure 31. The experiments were made in a nitrogen atmosphere, and iron foil was used for wrapping the quenching charges. Two new ternary compounds were formed: $K_2O{\cdot}FeO{\cdot}3SiO_2$, which melts congruently at about 900°±10°C, and $K_2O{\cdot}FeO{\cdot}5SiO_2$, which also melts congruently at about 900°±10°C. A small region of liquid immiscibility may exist, possibly caused by the presence of some Fe_2O_3.

K_2O–Al_2O_3–SiO_2

The system K_2O–Al_2O_3–SiO_2 was studied by Schairer and Bowen (1955) and their results are given in figure 32 and table 20. The ternary diagram has been modified in harmony with the congruent melting of mullite (Aramaki and Roy, 1959). The compound $K_2O{\cdot}Al_2O_3{\cdot}6SiO_2$, corresponding to the pure potassium feldspar, which occurs as adularia, orthoclase, sanidine, or microcline, melts incongruently at 1150°C (Morey and Bowen, 1922) with formation of $K_2O{\cdot}Al_2O_3{\cdot}4SiO_2$ (leucite) and a more siliceous melt (point *e*, fig. 32). Mixtures on the line leucite–SiO_2, with liquidus temperatures below 1250°C, are practically impossible to crystallize by themselves, and are so viscous that even at temperatures near the liquidus the powdered glasses fail to flow together and barely frit in periods of several days or weeks; the isotherms crossing this line are extrapolated from mixtures nearer the side K_2O–SiO_2. The compound $K_2O{\cdot}Al_2O_3{\cdot}2SiO_2$ melts congruently probably near or above 1750°C; the point, however, has not been determined accurately.

Five polymorphs of $K_2O{\cdot}Al_2O_3{\cdot}2SiO_2$ exist (Smith and Tuttle, 1957). Below 850°C, kalsilite (hexagonal) is the stable phase. Near 1000°C, synthetic kaliophilite (hexagonal) has been obtained but the remainder of the laboratory syntheses from 900°C to the liquidus have yielded orthorhombic $K_2O{\cdot}Al_2O_3{\cdot}2SiO_2$. The synthetic kaliophilite is not identical with natural kaliophilite (hexagonal) but there is a remarkable similarity between their X-ray powder patterns. A second form of natural kaliophilite—anomalous natural kaliophilite—is also known.

Bowen (1917) found an enantiotropic inversion from a hexagonal to an orthorhombic form at about 1540°C, and Tuttle and Smith (1953), in a preliminary report, found that hexagonal kalsilite is stable at atmospheric pressure up to 840°C, when an orthorhombic form appears. The compound $K_2O{\cdot}Al_2O_3{\cdot}SiO_2$ probably exists with a melting point well above 1700°C. The reactions along the boundary curves *URSP* offer

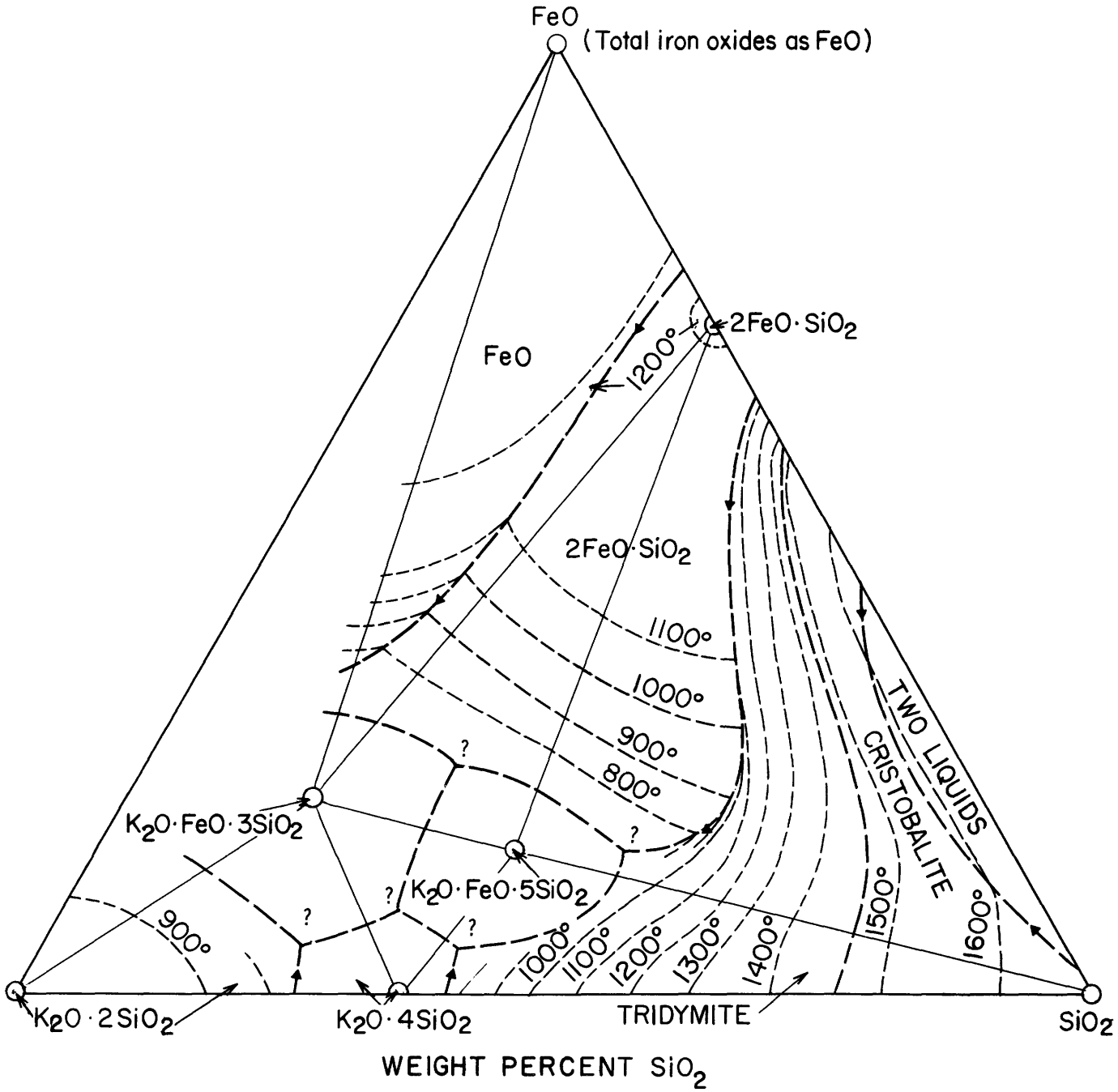

FIGURE 31.—The system K_2O–FeO–SiO_2. Modified from Roedder (1952). Isotherms are in degrees centigrade.

no special difficulties except those resulting from the hygroscopicity of the mixtures and the loss of K_2O by volatilization.

K_2O–Fe_2O_3–SiO_2

Faust (1936) studied crystallization along the join $K_2O \cdot 6SiO_2$–Fe_2O_3 which is not a binary system but an arbitrary line through the ternary systems. A mixture of the composition K_2O, $6SiO_2$ (79.3 percent SiO_2) has a liquidus of 1133°C, and tridymite is the primary phase (Kracek, Bowen, and Morey, 1929). On addition of Fe_2O_3, the melting point is lowered and the mixture crosses the tridymite field until the boundary of the

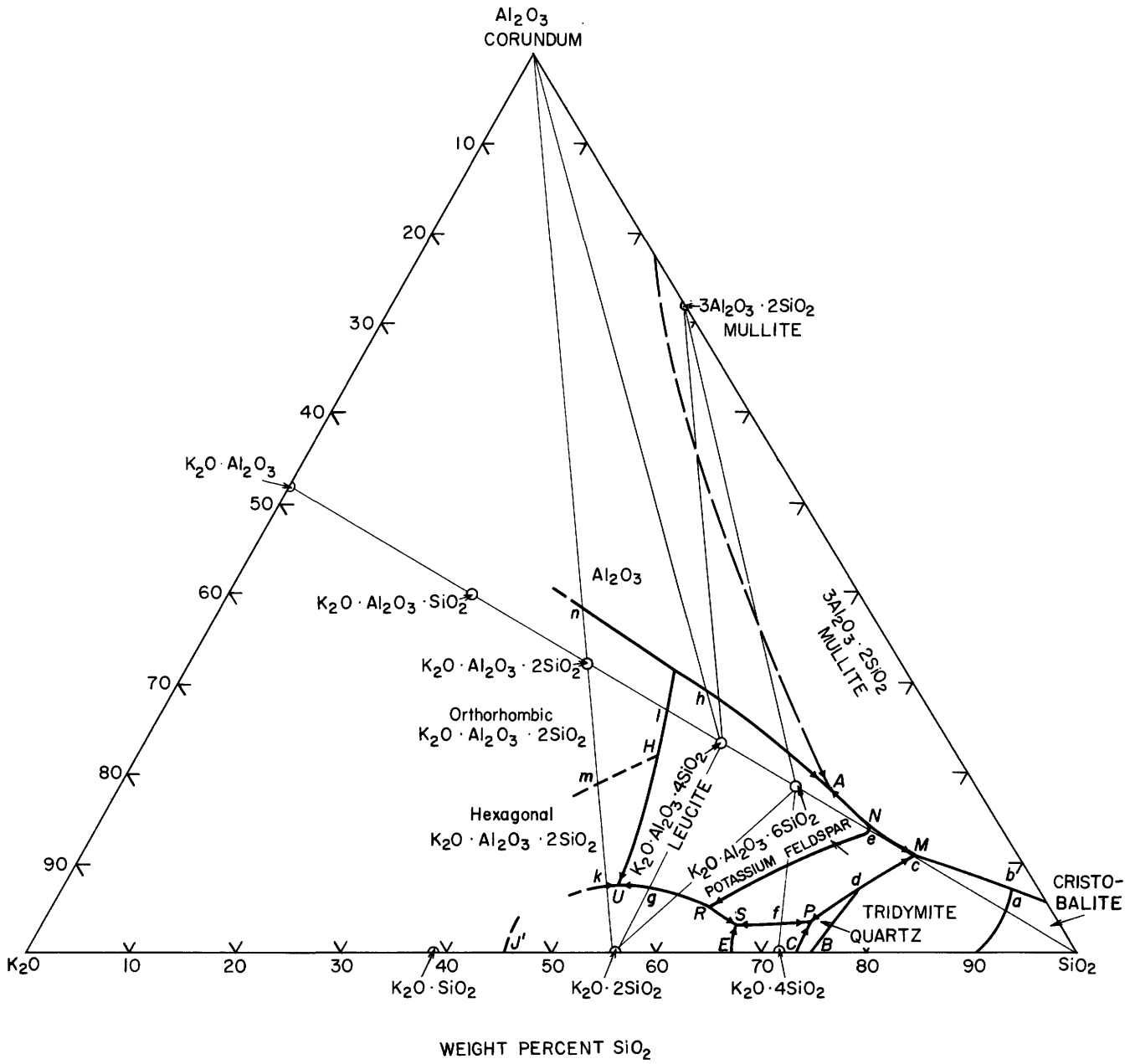

FIGURE 32.—The system K_2O–Al_2O_3–SiO_2. Modified from Schairer and Bowen (1955).

$K_2O \cdot Fe_2O_3 \cdot 6SiO_2$ field is reached at 13.5 percent Fe_2O_3 and 725°C. These mixtures could only be crystallized hydrothermally and metastable tridymite appeared in the quartz field. The next field is that of the analog of orthoclase, $K_2O \cdot Fe_2O_3 \cdot 6SiO_2$, which is difficult to crystallize and probably melts incongruently at 21 percent Fe_2O_3 and 921°C with formation of an iron analogue of leucite, $K_2O \cdot FeO \cdot 4SiO_2$, the composition of which is not on this join. It is the primary phase from 21 to 24.75 percent Fe_2O_3 and 1050°C, where Fe_2O_3 (hematite), appears. The curve was not studied beyond 1265°C because of the increasing rate of dissociation of Fe_2O_3. Faust and Peck (1938) measured the index of refraction of some glasses in this system.

TABLE 20.—*Invariant points in the system* K_2O–Al_2O_3–SiO_2

Invariant point on fig. 32	Phase reaction	Temperature (°C)	Composition of liquid (percent by weight)		
			K_2O	Al_2O_3	SiO_2
a	SiO_2 (tridymite) $\rightleftharpoons SiO_2$ (cristobalite)	1470	4. 3	4. 7	91
b	SiO_2 (tridymite) $\rightleftharpoons SiO_2$ (cristobalite)	1470	2. 4	7. 3	90. 3
M	$K_2O \cdot Al_2O_3 \cdot 6SiO_2 + SiO_2 + 3Al_2O_3 \cdot 2SiO_2 \rightleftarrows L$	985	9. 5	10. 9	79. 6
c	$K_2O \cdot Al_2O_3 \cdot 6SiO_2 + SiO_2 \rightleftarrows L$	990	9. 8	10. 7	79. 5
d	SiO_2 (quartz) $\rightleftharpoons SiO_2$ (tridymite)	867	17. 0	6. 8	76. 2
P	$K_2O \cdot 4SiO_2 + SiO_2 + K_2O \cdot Al_2O_3 \cdot 6SiO_2 \rightleftharpoons L$	710	22. 8	3. 7	73. 5
N	$K_2O \cdot Al_2O_3 \cdot 6SiO_2 + 3Al_2O_3 \cdot 2SiO_2 \rightleftharpoons K_2O \cdot Al_2O_3 \cdot 4SiO_2 + L$	1140	12. 2	13. 7	74. 1
e	$K_2O \cdot Al_2O_3 \cdot 6SiO_2 \rightleftharpoons K_2O \cdot Al_2O_3 \cdot 4SiO_2 + L$	1150	12. 5	13. 5	74. 0
f	$K_2O \cdot 4SiO_2 + K_2O \cdot Al_2O_3 \cdot 6SiO_2 \rightleftharpoons L$	725	26. 1	3. 3	70. 6
A	$K_2O \cdot Al_2O_3 \cdot 4SiO_2 + 3Al_2O_3 \cdot 2SiO_2 \rightleftharpoons Al_2O_3 + L$	1315	13. 9	18. 5	67. 6
S	$K_2O \cdot 2SiO_2 + K_2O \cdot 4SiO_2 + K_2O \cdot Al_2O_3 \cdot 6SiO_2 \rightleftharpoons L$	695	30. 4	3. 2	66. 4
R	$K_2O \cdot 2SiO_2 + K_2O \cdot Al_2O_3 \cdot 6SiO_2 \rightleftharpoons K_2O \cdot Al_2O_3 \cdot 4SiO_2 + L$	810	32. 1	5. 3	62. 6
g	$K_2O \cdot 2SiO_2 + K_2O \cdot Al_2O_3 \cdot 4SiO_2 \rightleftharpoons L$	918	36. 9	7. 4	55. 7
	$K_2O \cdot Al_2O_3 \cdot 4SiO_2 \rightleftharpoons L$	1686	21. 59	23. 36	55. 05
h	$K_2O \cdot Al_2O_3 \cdot 4SiO_2 + Al_2O_3 \rightleftharpoons L$	1588	19. 9	29. 3	50. 8
U	$K_2O \cdot 2SiO_2 + K_2O \cdot Al_2O_3 \cdot 4SiO_2 + K_2O \cdot Al_2O_3 \cdot 2SiO_2 \rightleftharpoons L$	905	39. 3	7. 8	52. 9
k	$K_2O \cdot 2SiO_2 + K_2O \cdot Al_2O_3 \cdot 2SiO_2 \rightleftharpoons L$	923	40. 6	7. 7	51. 7
H	$K_2O \cdot Al_2O_3 \cdot 4SiO_2$ (hexagonal) $\rightleftharpoons K_2O \cdot Al_2O_3 \cdot 4SiO_2$ (orthorhombic)	1540	28. 5	22. 0	49. 5
l	$K_2O \cdot Al_2O_3 \cdot 2SiO_2 + K_2O \cdot Al_2O_3 \cdot 4SiO_2 \rightleftharpoons L$	1615	24. 8	27. 0	48. 2
	$K_2O \cdot Al_2O_3 \cdot 2SiO_2 + K_2O \cdot Al_2O_3 \cdot 4SiO_2 + Al_2O_3 \rightleftharpoons L$	1553	22. 1	31. 3	46. 6
m	$K_2O \cdot Al_2O_3 \cdot 4SiO_2$ (hexagonal) $\rightleftharpoons K_2O \cdot Al_2O_3 \cdot 4SiO_2$ (orthorhombic)	1540	35. 6	19. 0	45. 4
n	$K_2O \cdot Al_2O_3 \cdot 2SiO_2 + Al_2O_3 \rightleftharpoons L$	1680	27. 4	37. 7	34. 9

MgO–CaO–Al_2O_3

Rankin and Merwin (1916) found that no ternary compounds were formed in the system

MgO–CaO–Al_2O_3,

and the fields are those of the components and the four calcium aluminates. The invariant points, all near the side of CaO–Al_2O_3, are given in table 21. The melting surfaces for MgO, MgO·Al_2O_3, and CaO rise steeply from the invariant points, but the glasses could be obtained by quenching in the low-temperature region. The system CaO–Al_2O_3 has been revised since the publication of this work.

TABLE 21.—*Invariant points in the system* MgO–CaO–Al_2O_3

Phase reaction	Temperature (°C)	Composition (percent by weight)		
		MgO	CaO	Al_2O_3
$MgO + 3CaO \cdot Al_2O_3 \rightleftharpoons CaO + L$	1450±5	6. 2	51. 5	43. 3
$MgO + 5CaO \cdot 3Al_2O_3 \rightleftharpoons L$	1345±5	6. 3	46. 0	47. 7
$MgO + CaO \cdot Al_2O_3 + 5CaO \cdot 3Al_2O_3 \rightleftharpoons L$	1345±5	6. 7	41. 5	51. 8
$MgO + CaO \cdot Al_2O_3 \rightleftharpoons MgO \cdot Al_2O_3 + L$	1370±5	6. 9	40. 7	52. 4
$MgO \cdot Al_2O_3 + CaO \cdot Al_2O_3 \rightleftharpoons CaO \cdot 2Al_2O_3 + L$	1550±5	3. 5	33. 3	63. 2

MgO–CaO–Fe_2O_3

The system MgO–CaO–Fe_2O_3 was studied by Hay and White (1940) and by Rait (1949). There is no evidence of a ternary compound, and the phase diagram is divided into sections by the joins MgO–2CaO·Fe_2O_3, MgO·Fe_2O_3–2CaO·Fe_2O_3, and MgO·Fe_2O_3–CaO·Fe_2O_3. The effect of the partial pressure of oxygen was not considered.

MgO–CaO–SiO_2

The system MgO–CaO–SiO_2 has been studied by Allen and White (1909), who worked on the relation of diopside to magnesium and calcium metasilicate; by Bowen (1914), who worked on the partial system diopside–forsterite–silica; and by Ferguson and Merwin (1919b), who completed the system. Revisions of the phase-equilibrium diagram were made by Bowen, Schairer, and Posnjak (1933b), Schairer and Bowen (1942), Osborn (1942, 1943), and Ricker and Osborn (1954). The revised diagram is figure 33, modified from Ricker and Osborn, and the invariant points are in table 22.

There are four ternary compounds in this system. CaO·MgO·$2SiO_2$, the mineral diopside, melts congru-

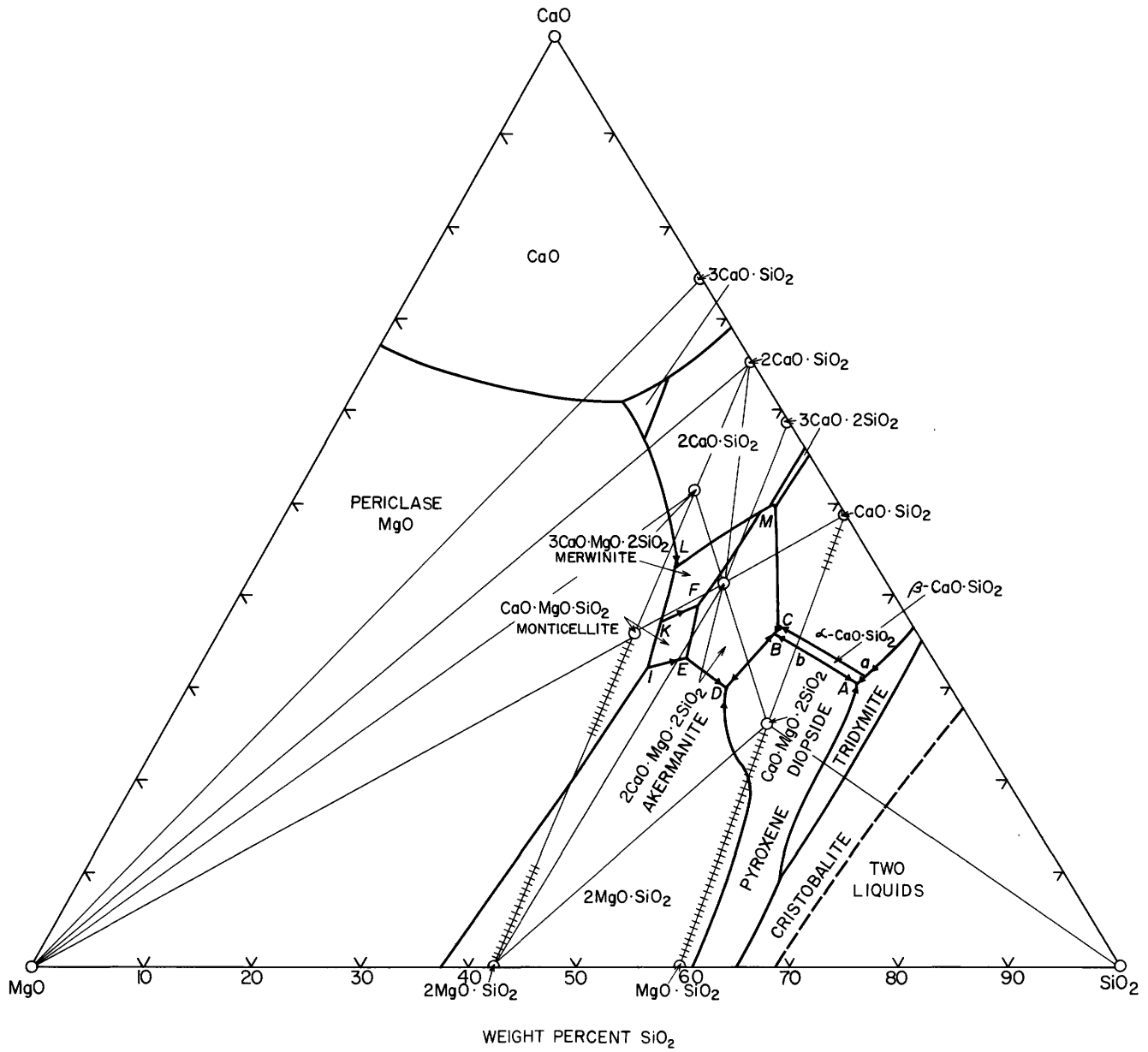

FIGURE 33.—The system MgO–CaO–SiO_2. Modified from Ricker and Osborn (1954).

ently at 1391.5°C and does not take any of its components into solid solution. Yoder (1952a) found that the increase in melting point with pressure can be represented by the expression

$$t_m = 1391.5 + 0.01297\ P$$

when t_m is the melting temperature in °C, and P is the pressure in bars. Boyd and England (1958) extended the melting-point curve to 32,000 bars and 1740°C. The slope of the melting curve decreases with pressure; in the range 20,000 to 30,000 bars the average slope is 10.3°C per 1,000 bars.

Wollastonite (β-$CaO \cdot SiO_2$) takes into solid solution as much as 21 percent diopside, but little or no diopside enters into solid solutions in α-$CaO \cdot SiO_2$ (pseudowollastonite). The inversion temperature of wollastonite is raised by this solid solution from 1125 to 1368°C, so that it has a field on the liquidus surface of the ternary system.

The phase-equilibrium diagrams of the binary system $CaO \cdot SiO_2$–$CaO \cdot MgO \cdot 2SiO_2$ is figure 34. The inversion temperatures of β-$CaO \cdot SiO_2$ (wollastonite) to α-$CaO \cdot SiO_2$ (pseudowollastonite) is raised by solid solution of diopside from 1125°C (point E') to 1368°C

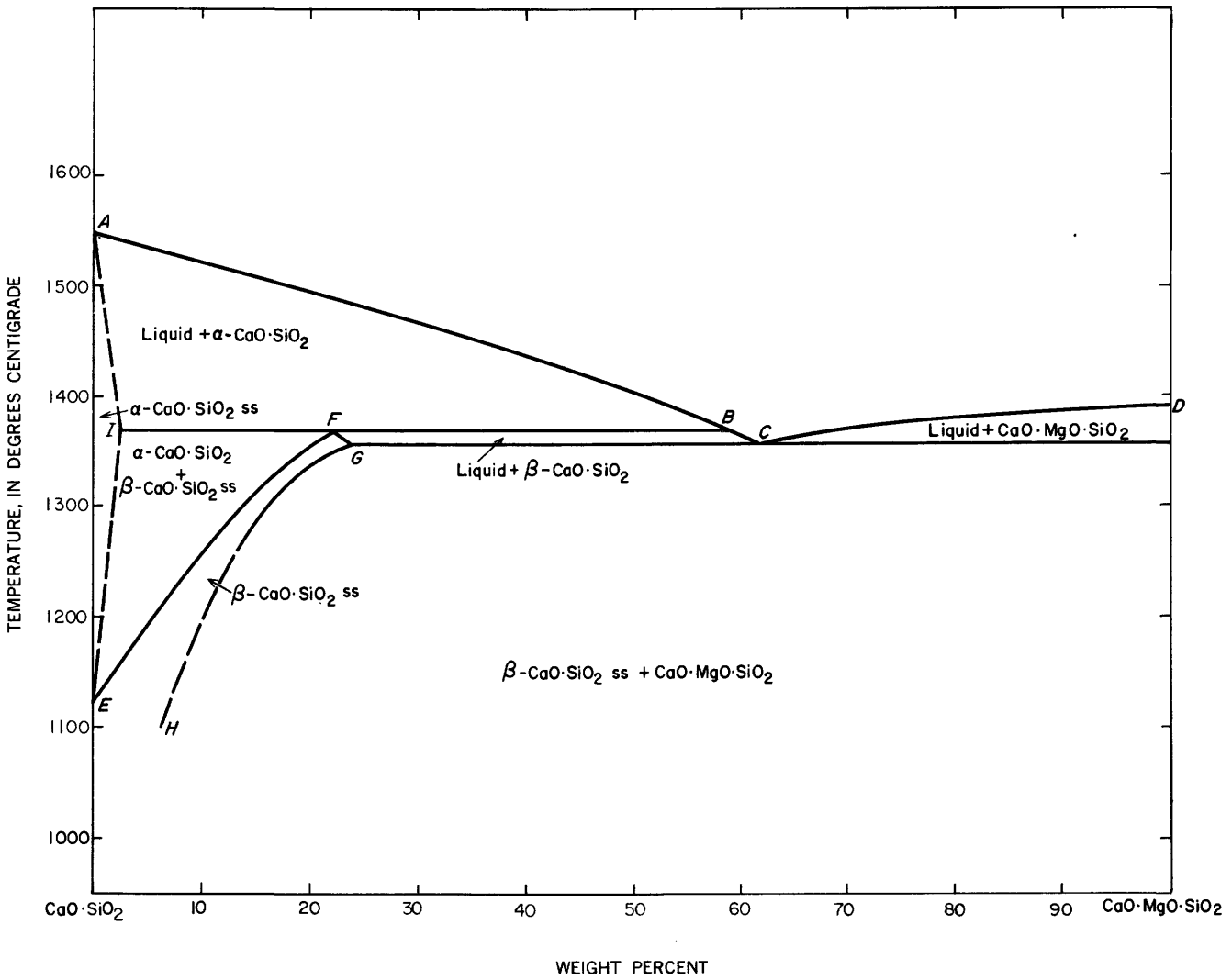

FIGURE 34.—The binary system $CaO \cdot SiO_2$ (wollastonite)–$CaO \cdot MgO \cdot 2SiO_2$ (diopside). Modified from Ricker and Osborn (1954).

TABLE 22.—*Invariant points in the system* MgO–CaO–SiO_2

Invariant point on fig. 33	Phase reaction	Temperature (°C)	Composition of liquid (percent by weight)		
			MgO	CaO	SiO_2
a	β-$CaO \cdot SiO_2 ss + SiO_2 \rightleftharpoons \alpha$-$CaO \cdot SiO_2 + L$	1336	7. 2	31. 3	61. 5
A	β-$CaO \cdot SiO_2 ss + SiO_2 + CaO \cdot MgO \cdot 2SiO_2 \rightleftharpoons L$	1320	8. 0	30. 6	61. 4
	$CaO \cdot MgO \cdot 2SiO_2 \rightleftharpoons L$	1391. 5	18. 62	25. 9	55. 48
b	β-$CaO \cdot SiO_2 ss + CaO \cdot MgO \cdot 2SiO_2 \rightleftharpoons L$	1358	11. 5	34. 4	54. 1
c	β-$CaO \cdot SiO_2 ss \rightleftharpoons \alpha$-$CaO \cdot SiO_2 + L$	1368	10. 8	35. 3	53. 9
B	β-$CaO \cdot SiO_2 ss + CaO \cdot MgO \cdot 2SiO_2 + 2CaO \cdot MgO \cdot 2SiO_2 \rightleftharpoons L$	1350	12. 6	36	51. 4
C	α-$CaO \cdot SiO_2 + 2CaO \cdot MgO \cdot 2SiO_2 \rightleftharpoons \beta$-$CaO \cdot SiO_2 ss + L$	1360	12. 3	36. 7	51
D	$2CaO \cdot MgO \cdot 2SiO_2 + CaO \cdot MgO \cdot 2SiO_2 + 2MgO \cdot SiO_2 \rightleftharpoons L$	1357	20. 2	29. 8	50
E	$2CaO \cdot MgO \cdot 2SiO_2 + 2MgO \cdot SiO_2 \rightleftharpoons CaO \cdot MgO \cdot SiO_2 + L$	1430	22. 3	33. 3	44. 4
	$2CaO \cdot MgO \cdot 2SiO_2 \rightleftharpoons L$	1454	14. 79	41. 14	44. 07
F	$2CaO \cdot MgO \cdot 2SiO_2 + CaO \cdot MgO \cdot SiO_2 \rightleftharpoons 3CaO \cdot MgO \cdot 2SiO_2 + L$	1436	18. 3	39	42. 7
I	$CaO \cdot MgO \cdot SiO_2 + 2MgO \cdot SiO_2 \rightleftharpoons MgO + L$	1502	26. 4	32. 1	41. 5
K	$3CaO \cdot MgO \cdot 32SiO_2 + CaO \cdot MgO \cdot SiO_2 \rightleftharpoons MgO + L$	1490	22. 3	37. 3	40. 3
L	$3CaO \cdot MgO \cdot 2SiO_2 \rightleftharpoons MgO + 2CaO \cdot SiO_2 + L$	1575	18. 2	43. 0	38. 8
M	$2CaO \cdot SiO_2 + 2CaO \cdot MgO \cdot 2SiO_2 \rightleftharpoons 3CaO \cdot MgO \cdot 2SiO_2 + L$	1400	6. 8	49. 5	43. 7

at F, where the diopside content of the wollastonite is 21 percent. The point B (1368°C, 58 percent diopside) is a binary reaction point at which liquid B is in equilibrium with α-$CaO \cdot SiO_2$ and β-$CaO \cdot SiO_2$ solid solutions. The solubility of diopside in pseudowollastonite, if any, is less than 5 percent. Liquids along the line BC are in equilibrium with wollastonite solid solutions along the line FG. The eutectic is at 1358°C and 62 percent diopside, and the solid phases are a wollastonite solid solution G containing 22 percent diopside and pure diopside.

When a mixture containing 10 percent diopside, originally in the region β-$CaO \cdot SiO_2$ solid solution + diopside, in being heated meets the curve HG, the diopside goes into solid solution and a divariant region of wollastonite solid solution is entered. When the curve EF is met, some α-$CaO \cdot SiO_2$ separates, and further heating the mixture causes a region of α-$CaO \cdot SiO_2$ and β-$CaO \cdot SiO_2$ solid solutions until the line IFB is reached, when the β-$CaO \cdot SiO_2$ solid solutions disappear and liquid B is formed. There is no eutectic melting. If the original composition contained more diopside than point G, say 30 percent, the wollastonite solid solution would on heating increase in diopside content until 1358°C when eutectic melting would begin, with formation of liquid C in equilibrium with crystals G. Temperature would remain constant at 1358°C until diopside was melted. When the field of solid solution and liquid would be entered, the solid solutions would change composition along the line GF, the liquid along the line BC.

The compound $2CaO \cdot MgO \cdot 2SiO_2$, which corresponds to the mineral akermanite, melts congruently at 1454°C, and forms a binary eutectic with pseudowollastonite at 1402°C. There probably is no solid solution in this binary system. The compound

$$3CaO \cdot MgO \cdot 2SiO_2$$

is the mineral merwinite and was first identified by Larsen and Foshag (1921). Later Phemister, Nurse, and Bannister (1942) identified it as a frequent constituent of blast-furnace slags. Its field in the ternary system was determined by Osborn (1943), who found it to melt incongruently at 1575°C with formation of liquid, $2CaO \cdot SiO_2$, and MgO. The composition of the compound $CaO \cdot MgO \cdot SiO_2$, corresponding to the mineral monticellite, lies within the field of MgO (periclase). Attempts to prepare the pure compound did not succeed: a glass of that composition crystallized to $2CaO \cdot SiO_2$ and monticellite solid solution. The phase-equilibrium diagram of figure 33 shows a field of the binary compound $3CaO \cdot SiO_2$. This compound decomposes before its melting point in the binary system CaO–SiO_2 but Ricker and Osborn (1954) found that the liquidus surface in the ternary systems has a region of temperature low enough for $3CaO \cdot SiO_2$ to be stable.

MgO–CaO–TiO_2

Solid-state reactions in the system MgO–CaO–TiO_2 were studied by Coughanour, Roth, Marzullo, and Sennett (1955) by heating mixtures usually below the liquidus surface, but a mixture of molecular ratio $MgO : CaO : TiO_2$ of 4:1:9 had melted at 1500°C, of 3:2:6 at 1550°C, of 4:1:4 at 1590°C, and of 4:1:2 at 1672°C. No ternary compounds were found, and little or no solid solution, with the probable exception of the areas adjacent to $3CaO \cdot 2TiO_2$. The samples were studied by X-ray diffraction and by petrographic methods.

MgO–FeO–SiO_2

The system MgO–FeO–SiO_2 was studied by Bowen and Schairer (1935) by heating the mixtures in iron crucibles in a stream of nitrogen, and the equilibrium melts were analyzed for ferrous and ferric iron. The ferric iron increased in amount from almost zero with low FeO content to a maximum of more than 2 percent near the composition of Fe_2SiO_4. The phase-equlibrium diagram of the system, shown in figure 35, is dominated by several fields, one of which, $BCED$, is the area of two liquid layers. There is a field of pyroxene solid solutions containing $MgO \cdot SiO_2$ and $FeO \cdot SiO_2$. This metasilicate line, shown in figure 35, is complicated and only in part binary, owing first to the incongruent melting of $MgO \cdot SiO_2$, so that the first phase to separate along this line is an orthosilicate, $2MgO \cdot SiO_2$, and, second, to the field of tridymite spreading over the other end of the metasilicate line. The pyroxenes are monoclinic at the liquidus, but are orthorhombic at lower temperatures, and the inversion temperature ranges from 1140°C at the $MgO \cdot SiO_2$ end of the series, to approximately 995°C at the extreme iron-rich member. There is a field occupied by the olivines, a complete series of solid solutions between $2MgO \cdot SiO_2$ and $2FeO \cdot SiO_2$, and a large field occupied by the magnesiowüstites, a complete series of solid solutions between MgO and FeO. The invariant points are listed in table 23.

MgO–Al_2O_3–SiO_2

The original study of the system MgO–Al_2O_3–SiO_2 was by Rankin and Merwin (1918). They found only one ternary compound, $2MgO \cdot 2Al_2O_3 \cdot 5SiO_2$, corresponding to the mineral cordierite, which melts incongruently at 1460°C with formation of mullite and liquid. When a glass of the composition of cordierite is quickly cooled, it forms the mineral indialite (Miyashiro and

695-382 O - 64 - 5

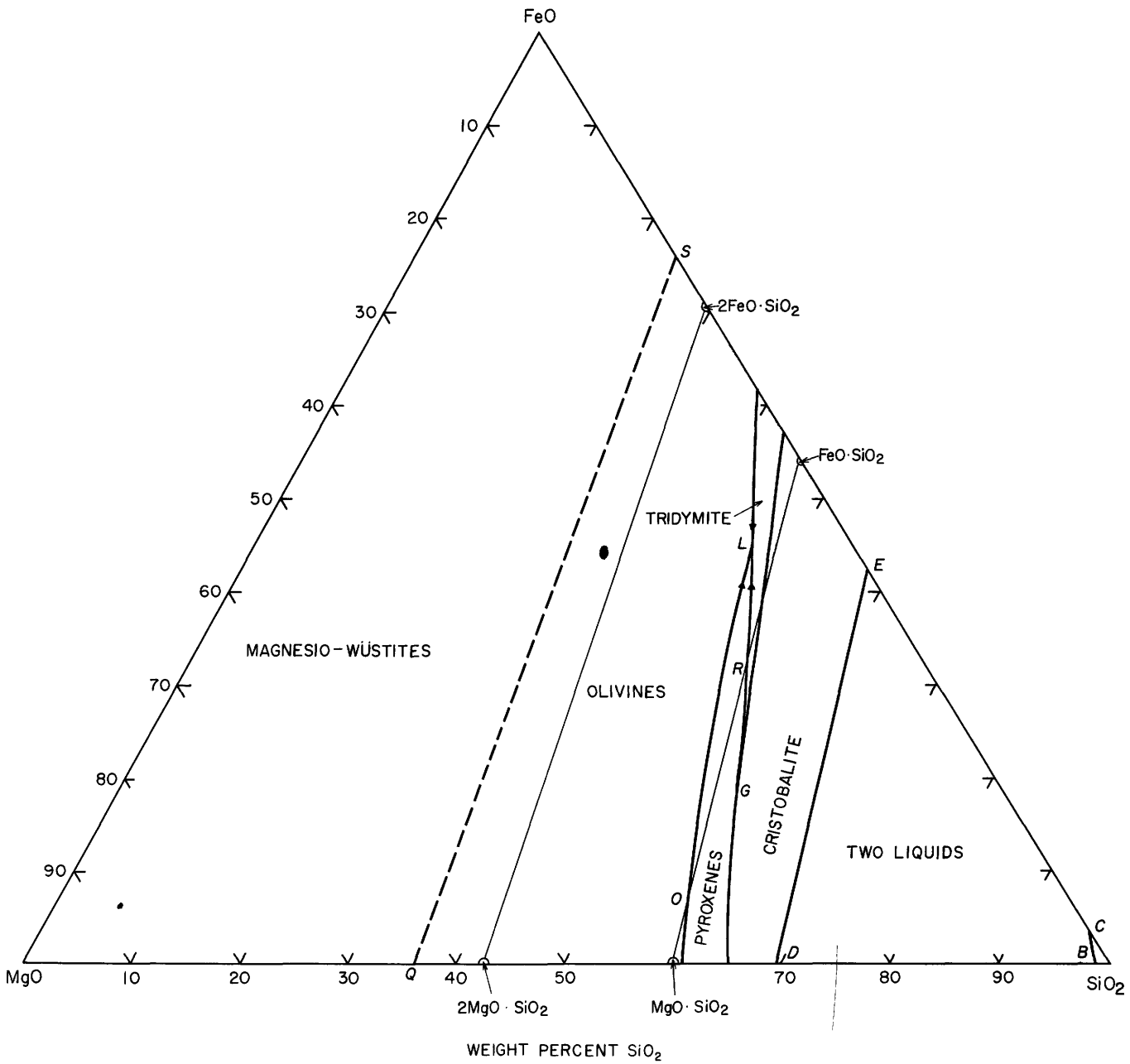

FIGURE 35.—The system MgO–FeO–SiO_2. Modified from Bowen and Schairer (1935).

TABLE 23.—*Invariant points in the system* MgO–FeO–SiO_2

Invariant Point on fig. 35	Phase reactions	Temperature (°C)	Composition of liquid (percent by weight)		
			MgO	FeO	SiO_2
G	SiO_2 (tridymite)$\rightleftarrows SiO_2$ (cristobalite)	1470	23. 5	20	56. 5
L	SiO_2+olivine (Mg_2SiO_4 32, Fe_2SiO_4 68)+clinopyroxene ($MgSiO_3$ 38, $FeSiO_3$ 62)$\rightleftarrows L$.	1305	9	46	45

Iiyama, 1954). Schreyer and Schairer (1959) found that there is no solid solution of MgO, Al_2O_3, or SiO_2 in cordierite, although indialite formed from a glass containing excess SiO_2 at low temperatures may contain excess SiO_2 in metastable solid solution. Yoder (1952) also believed that solid solution in cordierite is doubtful. Cordierite exists in three polymorphic forms, a high temperature or α-form, obtained by crystallization above about 950°C, a stable low temperature or β-form, obtained by hydrothermal crystallization, and an unstable μ-form, obtained by crystallizing the glass at about 850°C (Yoder, 1952c; Karkhanavala and Hummel, 1953). Foster (1950) deduced that a compound $4MgO \cdot 5Al_2O_3 \cdot 2SiO_2$ corresponding in properties with the mineral sapphirine, should have a field of stability in the ternary system, and Keith and Schairer (1952) found such a field, which is shown in their phase-equilibrium diagram (figure 36). The small sapphirine field is the area *NWX;* the reaction points are included in table 24. Aramaki and Roy (1959) revised the side Al_2O_3–SiO_2.

Pyrope, the garnet of the composition

$$3MgO \cdot Al_2O_3 \cdot 3SiO_2$$

is also in this system. It is not stable at the liquidus, but on heating decomposes to a mixture of $2MgO \cdot SiO_2$, $MgO \cdot Al_2O_3$, and $2MgO \cdot 2Al_2O_3 \cdot 5SiO_2$. It is, however, stable at increased pressures, and Boyd and England (1959) gave a preliminary diagram of the stability field of pyrope (fig. 37).

At pressures above 23,000 atm and temperatures above 1200°C, pyrope forms rapidly from glass or from mixtures of anhydrous crystalline phases of its composition. Below 1100°C reactions involving pyrope become sluggish, and curve *A* of figure 37 has not been extended to lower temperatures. The reactions were accelerated by the presence of H_2O. The phases stable for the pyrope composition below curve *A* are not the same as those stable at atmosphere pressure—cordierite+forsterite+spinel. At the pressures indicated for the run below *A*, cordierite is unstable, and the stable assemblage for the pyrope composition is aluminous enstatite+sapphirine, and possibly sillimanite, but it is possible that the sillimanite may enter into solid solution in the sapphirine. The melting of pyrope must be incongruent at the lower temperature end of curve *B*. Curve *C* represents the approximate position of one of the melting curves of the assemblage enstatite+sapphirine (+sillimanite?), and probably is the solidus curve determined by the melting of enstatite in this assemblage. The invariant point at the intersection of curves *A*, *B*, and *C* is at 1510°C and 21,600 atm.

Boyd and England (1960) found evidence of the formation of a spinel-type structure in some runs on the join $2MgO \cdot SiO_2$–$2FeO \cdot SiO_2$ at approximately 75,000 atm and 1300°C. The mixture, 10 percent $2MgO \cdot SiO_2$–90 percent $2FeO \cdot SiO_2$, crystallized to a mixture of spinel and olivine.

Mixtures richer than 10 percent $2MgO$–SiO_2 yielded only olivine, and higher pressure would be necessary to convert it to the spinel structure. Boyd and England also found that when mixtures on the join $MgSiO_3$–Al_2O_3 were crystallized at 1400°C and 18,200 atm pressure, only a solid solution of Al_2O_3 in enstatite, from 0 to 14 percent Al_2O_3, was formed; between 14 and 22 percent Al_2O_3, sapphirine appeared but the composition of the enstatite continued to change; for compositions containing more than 22 percent Al_2O_3, sillimanite also is formed and the composition of the enstatite is invariant.

MgO–FeO–Fe_2O_3

Roberts and Merwin (1931) studied the melting relations in the system MgO–FeO–Fe_2O_3 in air, hence at a partial pressure of oxygen of approximately 0.21 atm. Two series of solid solutions are formed. One of these extends from MgO toward $MgO \cdot Fe_2O_3$ and FeO to a liquid boundary curve at this oxygen pressure and 1770°±20°C where the coexisting solid contains 73 percent Fe_2O_3. The second solid solution extends, with increasing temperature, from $MgO \cdot Fe_2O_3$ toward the iron oxide boundary, which it reaches at 1380°±5°C.

Paladino (1960) studied the system in the solid state at 1000°, 1100°, 1200°, and 1300°C, and at oxygen pressures of 1.0, 0.21 (air), and 0.01 atm. He found that the spinel field is at a higher MgO content than the join Fe_3O_4–$MgFe_2O_4$ near $MgFe_2O_4$, and a mixture of the composition $Mg_2Fe_2O_4$ contains Fe_2O_3 and a spinel richer in MgO under all the experimental conditions chosen.

CaO–FeO–Fe_2O_3

Gurry and Darken (1950) determined the compositions of some mixtures equilibrated in oxygen at 0.2 atm and 1 atm oxygen pressure and in CO_2 at 1 atm pressure and constructed a tentative diagram for the equilibrium at 1600°C.

CaO–FeO–SiO_2

The system CaO–FeO–SiO_2 is of importance not only in geology because of the insight it gives on the relationship between the pyroxenes and olivines, but also in metallurgy because of the insight it gives on the action of iron-bearing slags on silica refractories. Bowen, Schairer, and Posnjak (1933a) published a

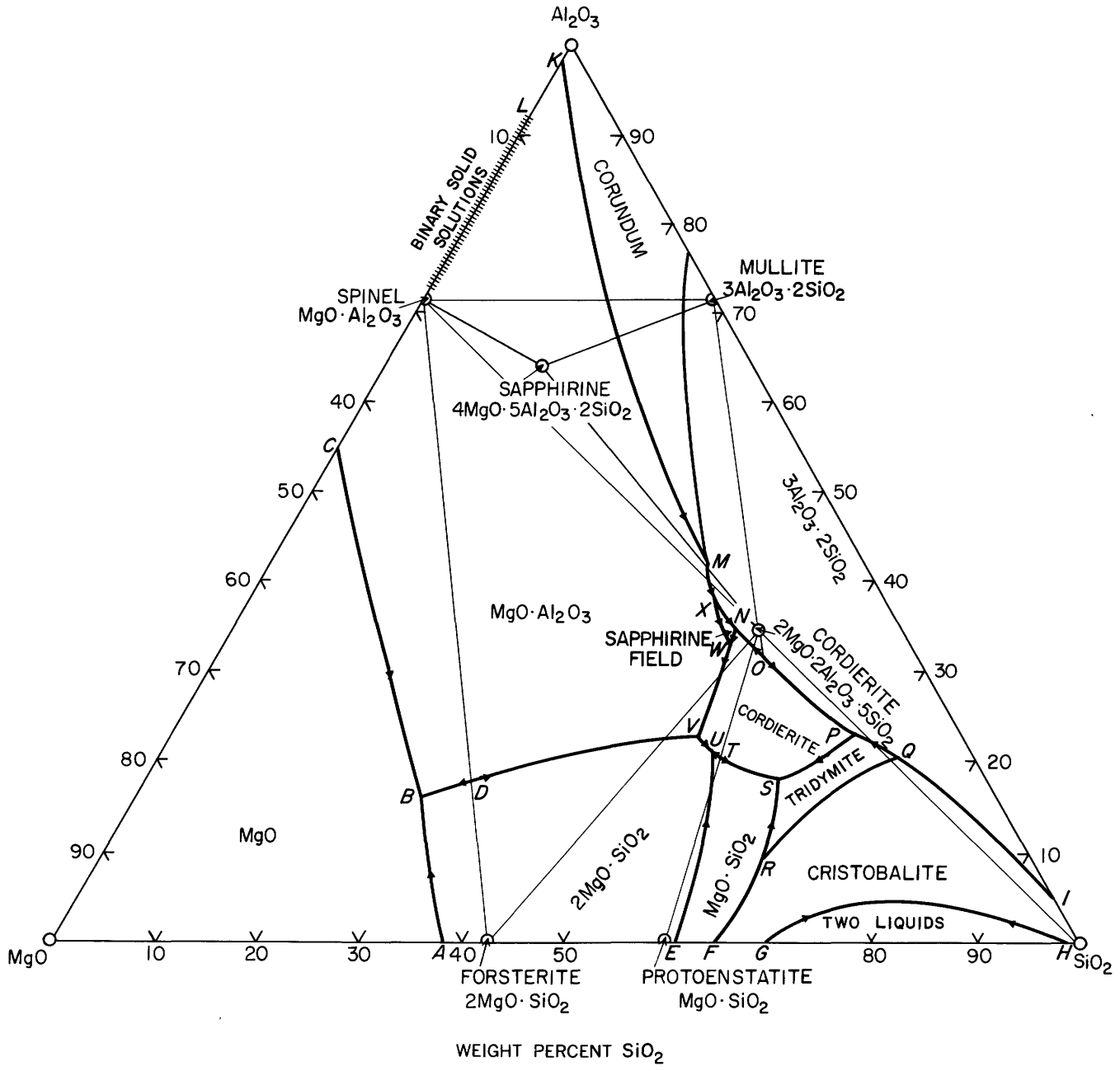

FIGURE 36.—The system MgO–Al_2O_3–SiO_2. Modified from Keith and Schairer (1952).

TABLE 24.—*Invariant points in the system* MgO–Al_2O_3–SiO_2

Invariant point on fig. 36	Phase reactions	Temperature (°C)	Composition of liquid (percent by weight)		
			MgO	Al_2O_3	SiO_2
S	$MgO \cdot SiO_2 + 2MgO \cdot 2Al_2O_3 \cdot 5SiO_2 + SiO_2 \rightleftharpoons L$	1355	20. 50	17. 50	62. 06
P	$3Al_2O_3 \cdot 2SiO_2 + SiO_2 \rightleftharpoons 2MgO \cdot 2Al_2O_3 \cdot 5SiO_2 + L$	1440	9. 25	22. 5	68. 25
V	$2MgO \cdot SiO_2 + 2MgO \cdot 2Al_2O_3 \cdot 5SiO_2 \rightleftharpoons MgO \cdot Al_2O_3 + L$	1370	25. 7	22. 8	51. 5
U	$MgO \cdot SiO_2 + 2MgO \cdot SiO_2 + 2MgO \cdot 2Al_2O_3 \cdot 5SiO_2 \rightleftharpoons L$	1360	25. 0	21. 0	54
B	$MgO + MgO \cdot Al_2O_3 + 2MgO \cdot SiO_2 \rightleftharpoons L$	1700	56. 0	16. 0	28. 0
M	$MgO \cdot Al_2O_3 + 3Al_2O_3 \cdot 2SiO_2 \rightleftharpoons Al_2O_3 + L$	1575	15. 2	42. 0	42. 8
W	$MgO \cdot Al_2O_3 + 2MgO \cdot 2Al_2O_3 \cdot 5SiO_2 \rightleftharpoons 4MgO \cdot 5Al_2O_3 \cdot 2SiO_2 \rightleftharpoons L$	1453	17. 4	33. 5	49. 1
N	$2MgO \cdot 2Al_2O_3 \cdot 5SiO_2 + 4MgO \cdot 5Al_2O_3 \cdot 2SiO_2 \rightleftharpoons 3Al_2O_3 \cdot 2SiO_2 + L$	1460	16. 3	34. 4	49. 3
X	$4MgO \cdot 5Al_2O_3 \cdot 2SiO_2 \rightleftharpoons MgO \cdot Al_2O_3 + 3Al_2O_3 \cdot 2SiO_2 + L$	1482	16. 9	36. 8	46. 3
T	$MgO \cdot SiO_2 + 2MgO \cdot 2Al_2O_3 \cdot 5SiO_2 \rightleftharpoons L$	1365	----------	----------	----------

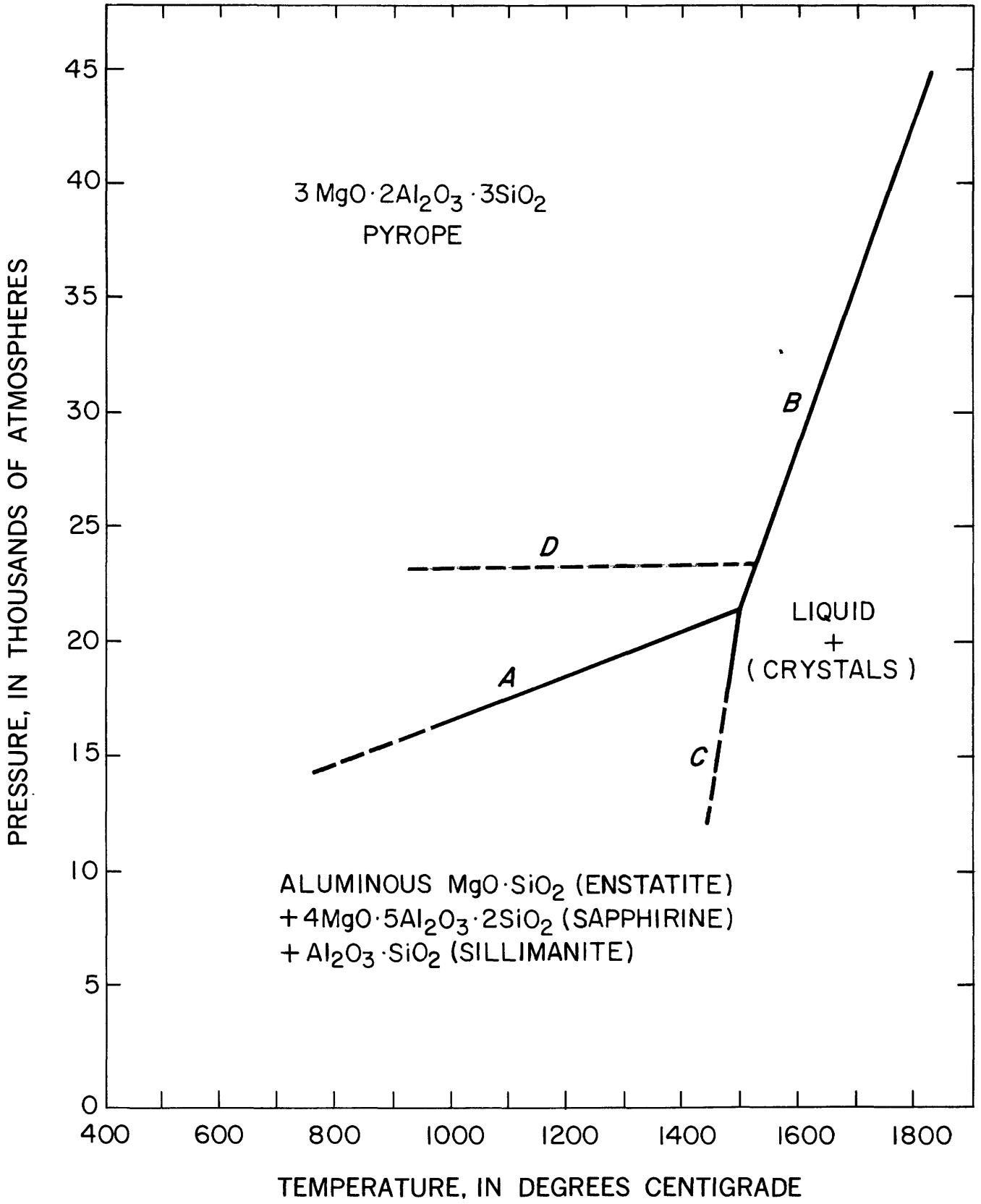

FIGURE 37.—The stability field of $3MgO \cdot Al_2O_3 \cdot 3SiO_2$ (pyrope). Modified from Boyd and England (1959).

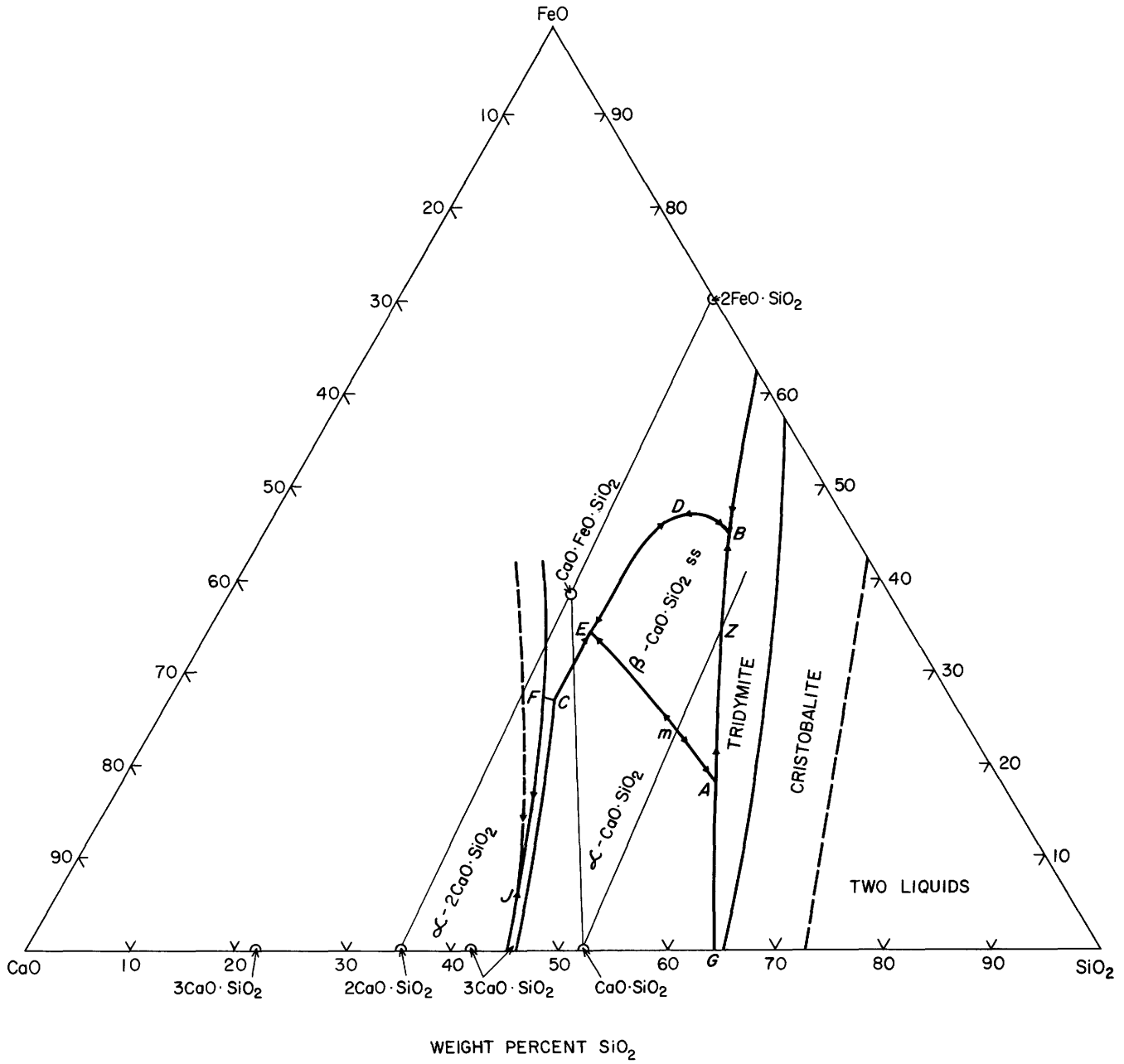

FIGURE 38.—The system CaO–FeO–SiO_2. Modified from Bowen, Schairer, and Posnjak (1933b). *ss*, solid solution.

study of the olivine solid solutions, and also (1933b) published a comprehensive study of the system, with a discussion of its applications and of the literature. The system actually has oxygen as a component, and even though the final melts were made in an iron crucible in an atmosphere of nitrogen, some Fe_2O_3 was present in all melts; small in amount in the high-silica part of the ternary diagram, more than 1 percent along the iron-rich part of the metasilicate join, and more than 2 percent on the orthosilicate join near $2FeO \cdot SiO_2$. The phase-equilibrium diagram is figure 38, and the invariant points are listed in table 25. The silica-rich part of the phase-equilibrium diagram is occupied by a region of two liquid layers and the fields of cristobalite and tridymite.

The phase-equilibrium diagram of the binary system $2CaO \cdot SiO_2$ (calcium orthosilicate)–$2FeO \cdot SiO_2$ (fayalite), determined by Bowen, Schairer and Posnjak (1933a) is given in figure 39. The results are expressed as a binary system by calculating all iron oxide as FeO, although some Fe_2O_3 was always present. The amount of Fe_2O_3 is indicated in the upper part of the diagram.

TABLE 25.—*Invariant points in the system* $CaO–FeO–SiO_2$

Invariant point on fig. 38	Phase reactions	Temperature (°C)	Composition of liquid (percent by weight)		
			CaO	FeO	SiO_2
A	$SiO_2+\beta$–$CaO·SiO_2$ss (93$CaSiO_3$)$\rightleftharpoons\alpha$–$CaO·SiO_2+L$	1272	26. 5	18. 5	55
M	β–$CaO·SiO_2$ss (91$CaSiO_3$)$\rightleftharpoons\alpha$–$CaO·SiO_2+L$	1285	27. 8	23. 2	49
B	$SiO_2+\beta$–$CaO·SiO_2$ss (28 $CaSiO_3$)+olivine (4Ca_2SiO_4, 96Fe_2SiO_4ss) $\rightleftharpoons L$.	1105	11. 5	45. 5	43
E	α–$CaO·SiO_2$+olivine (43Ca_2SiO_4, 57Fe_2SiO_4ss)$\rightleftharpoons\beta$–$CaO·SiO_2$ss (97$CaSiO_3$)+*L*.	1193	30	34	36
C	α–$CaO·SiO_2$+olivine (58Ca_2SiO_4, 42Fe_2SiO_4ss)$\rightleftharpoons 3CaO·2SiO_2+L$	1120	36	27	37
F	$3CaO·2SiO_2$+olivine (59Ca_2SiO_4, 41Fe_2SiO_4ss)$\rightleftharpoons 2CaO·SiO_2+L$	1227	37	28	35
D	β–$CaO·SiO_2$ss (50$CaSiO_3$)+olivine (20Ca_2SiO_4, 80Fe_2SiO_4ss)$\rightleftharpoons L$	1093	17	46	37
	$CaO·FeO·SiO_2\rightleftharpoons L$	1208	29. 83	38. 22	31. 95
J	α–$CaO·SiO_2+\beta$–$2CaO·SiO_2\rightleftharpoons 3CaO·2SiO_2+L$	1420?	50	8	42

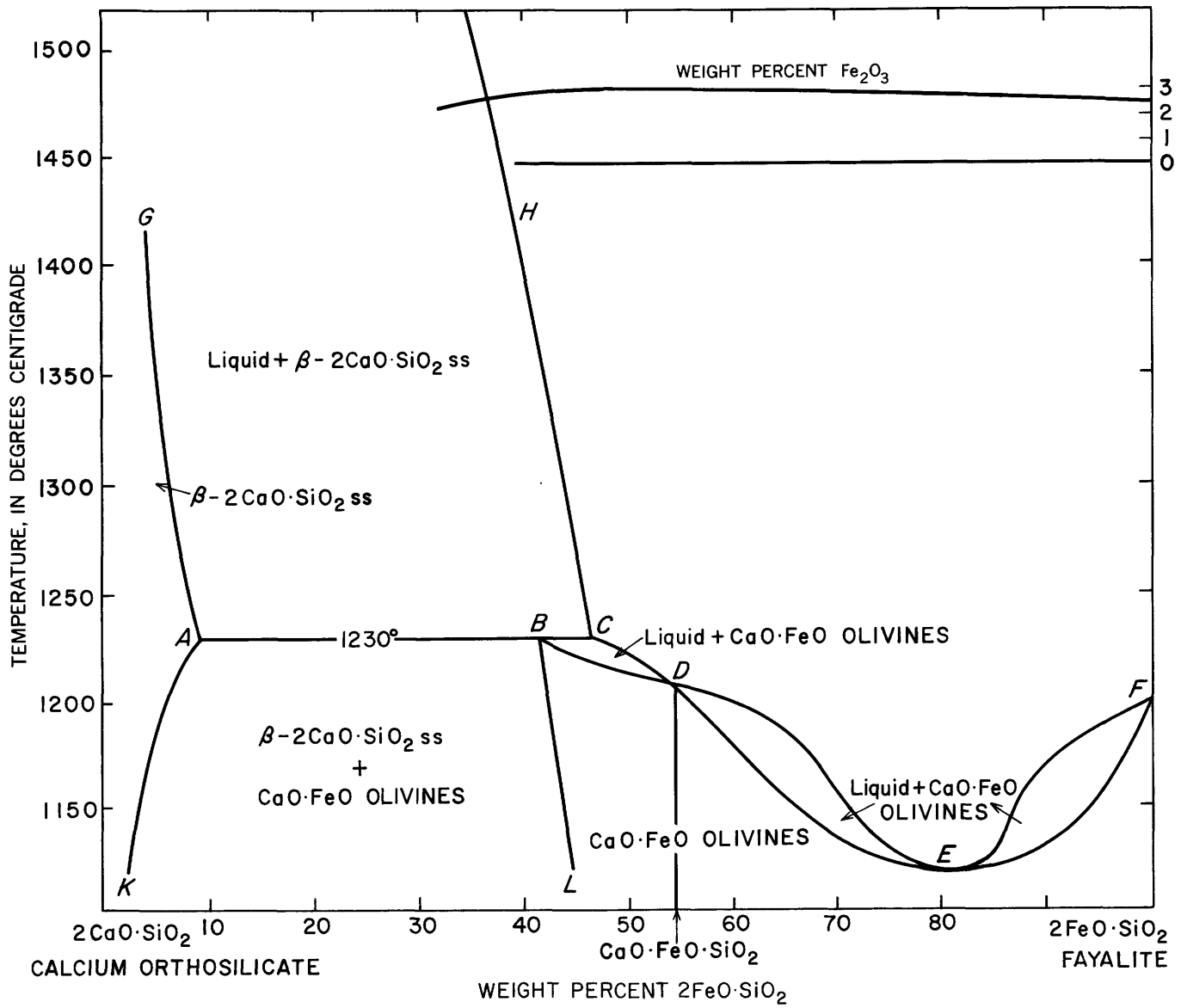

FIGURE 39.—The system $2CaO·SiO_2$ (calcium orthosilicate)-$2FeO·SiO_2$ (fayalite) expressed as a binary system by calculating all iron oxide as FeO. The actual amounts of Fe_2O_3 are shown in the upper right-hand part of the diagram. Modified from Bowen, Schairer, and Posnjak (1933). *ss*, Solid solution.

$2CaO \cdot SiO_2$ and $2FeO \cdot SiO_2$ form a 1:1 compound $CaO \cdot FeO \cdot SiO_2$ (analogous in composition to monticellite, $CaO \cdot MgO \cdot SiO_2$), which melts congruently at 1208°C. Between $CaO \cdot FeO \cdot SiO_2$ and $2FeO \cdot SiO_2$ (fayalite), there is a complete series of solid solutions with a minimum melting point at 81 percent $2FeO \cdot SiO_2$ and 1117°C (*E*, fig. 39). The solid solution series continues throughout the composition of the compound

$$CaO \cdot FeO \cdot SiO_2$$

up to point *C*. At this point, 1230°C, a liquid *C* containing 46 percent of $2FeO \cdot SiO_2$ is in equilibrium with a solid solution *B*, an olivine containing 41 percent of $2CaO \cdot SiO_2$. With mixtures richer in $2CaO \cdot SiO_2$, the olivine *B* is in equilibrium with

$$3CaO \cdot 2SiO_2$$

solid solution containing 90 percent $2CaO \cdot SiO_2$. The solid solutions of $2FeO \cdot SiO_2$ in β-$2CaO \cdot SiO_2$ along the curve *AK* decrease in $2FeO \cdot SiO_2$ content with decreasing temperature and at 1125°C contains only 2 percent; the compositions of the olivines in equilibrium are given by the line *BC*.

On cooling, the β-$2CaO \cdot SiO_2$ solid solutions invert completely or partially to α-$2CaO \cdot SiO_2$ solid solutions which have indices of refraction higher than those of pure α-$2CaO \cdot SiO_2$. This probably is caused by solid solutions of $2FeO \cdot SiO_2$ in this form also, but the limits could not be determined.

The binary system $CaO \cdot SiO_2$–$CaO \cdot FeO \cdot SiO_2$ is of simple eutectic type, with the eutectic at 1203°C, only 5°C below the melting point of $CaO \cdot FeO \cdot SiO_2$, and 80 percent of $CaO \cdot FeO \cdot SiO_2$.

The join $CaO \cdot SiO_2$–$FeO \cdot SiO_2$ is not a binary system, as shown in figure 40, because $FeO \cdot SiO_2$ does not exist as a crystalline compound.

The inversion temperature of β-$CaO \cdot SiO_2$ (wollastonite) to α-$CaO \cdot SiO_2$, (pseudowollastonite) is raised 135°C, by solid solution of $FeO \cdot SiO_2$ to point *B*, 1285°C, which contains about 9 percent $FeO \cdot SiO_2$. At 1285°C some liquid of composition *M* is formed. There are now three phases, and the temperature remains constant until the reaction β-$CaO \cdot SiO_{2ss} = \alpha$-$CaO \cdot SiO_2$ + liquid M is complete. There is no solid solution in α-$CaO \cdot SiO_2$.

When a mixture containing 40 percent $FeO \cdot SiO_2$ is cooled from a high temperature, the liquid begins to crystallize at 1308°C with separation of crystals of pure pseudowollastonite, which continues until 1285°C. At that temperature the liquid has the composition *M*, and crystals of wollastonite solid solutions of composition *B* begin to form at the expense of the pseudowollastonite. When the pseudowollastonite has entirely disappeared, further cooling occurs and the liquid changes in composition along *MZ* while the wollastonite solid solution changes in composition along *BC*. At 1160°C the last solid has reached the composition *C* and the last true liquid, now of composition *Z*, vanishes. The mass then consists entirely of a solid solution of the composition *C*.

The liquid *C* has the highest content of $FeO \cdot SiO_2$ of any liquid that behaves in this simple manner. All liquids between *C* and *Z* exhibit ternary equilibrium at some stage of their crystallization, and all between *Z* and $FeO \cdot SiO_2$ show ternary behavior at all stages of their crystallization, although some of these again become binary when all liquid has disappeared and crystallization is complete.

All liquids of composition between $CaO \cdot SiO_2$ and *B* become completely crystalline at the temperature of the horizontal *BM* and then consist of pseudowollastonite and wollastonite solid solution *B*. With further cooling, the composition of the solid solution changes along the curve *BA* at the expense of the pseudowollastonite, which eventually disappears. In a mixture with 5 percent $FeO \cdot SiO_2$, for example, pseudowollastonite disappears at 1240°C and the mass is then made up of crystals of wollastonite solid solution containing 5 percent $FeO \cdot SiO_2$.

The behavior of solid solutions that show ternary relations may be seen by reference to figure 40. A liquid of the composition of $CaO \cdot FeO \cdot 2SiO_2$ (hedenbergite) begins to crystallize at 1207°C with the separation of crystals of β-$CaO \cdot SiO_2$ (wollastonite) solid solution containing 25 percent $FeO \cdot SiO_2$. As cooling proceeds both liquid and solid solutions change in composition until at 1160°C the liquid has the composition *Z*, the solid, *C*. At this temperature tridymite begins to separate and thenceforth the composition of the phases present cannot be shown on a binary diagram. When the liquid has cooled to 1118° C both liquid and tridymite have disappeared and the mass consists entirely of a wollastonite solid solution having the composition of hedenbergite ($CaO \cdot SiO_2$ 46.8 percent, $FeO \cdot SiO_2$ 53.2 percent). A liquid of composition $CaO \cdot SiO_2$ 30 percent, $FeO \cdot SiO_2$ 70 percent begins to crystallize at 1240°C with separation of tridymite. The liquid immediately departs from metasilicate composition and cannot be shown on the binary diagram. The diagram does show, however, that at 1125°C tridymite is joined by a wollastonite solid solution, but the composition of the solid solution cannot be shown on the binary diagram. Upon further cooling, liquid and tridymite finally disappear at 1106°C and the mass is

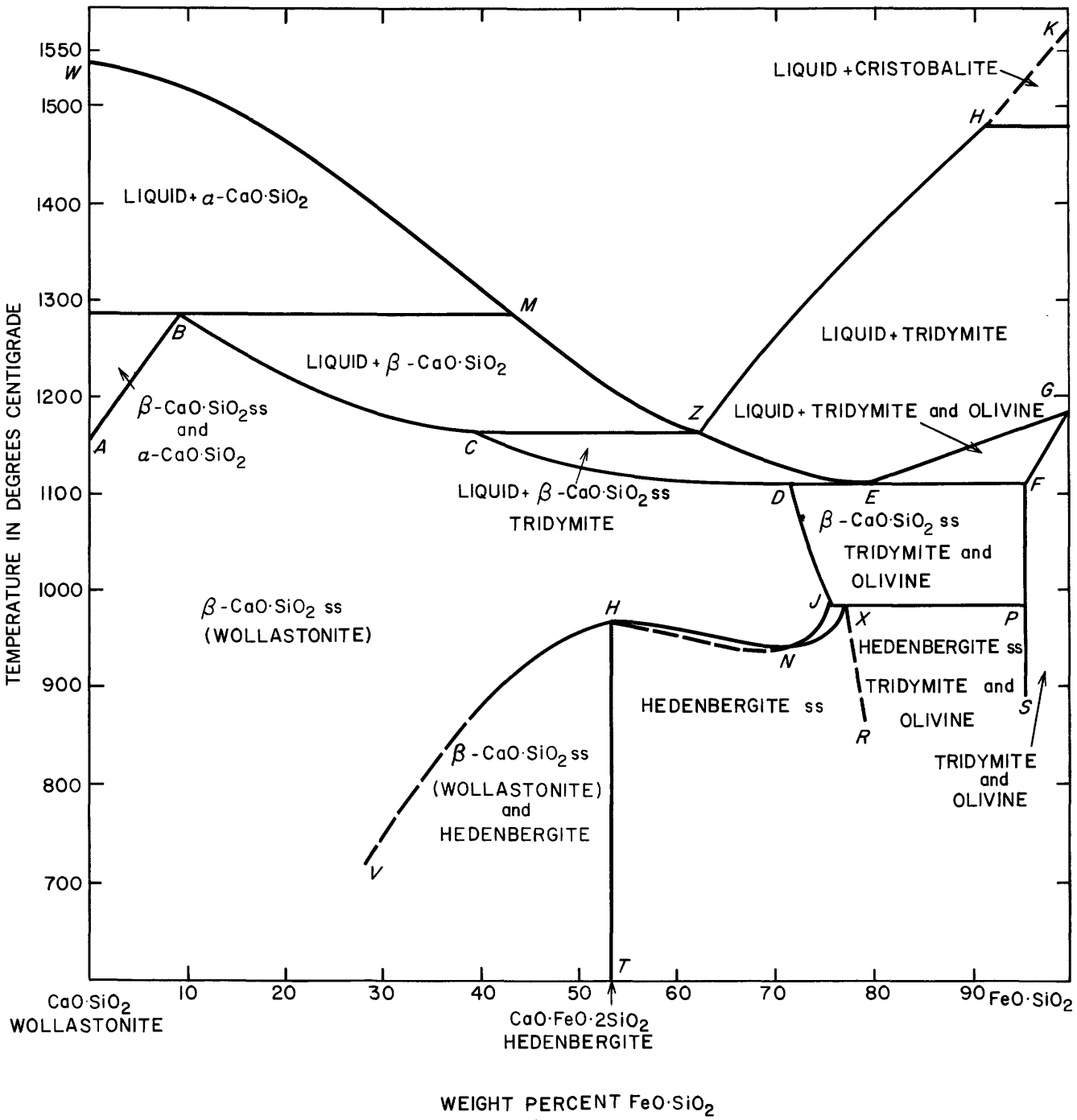

FIGURE 40.—Phase-equilibrium diagram for mixtures of $CaO \cdot SiO_2$ and $FeO \cdot SiO_2$. The heavy curves refer to binary equilibria, the light ones to ternary equilibria. These can be considered as binary and ternary only when the small amounts of ferric iron present are calculated to FeO. Modified from Bowen, Schairer, and Posnjak (1933b). *ss*, solid solution.

made up entirely of a wollastonite solid solution containing 70 percent $FeO \cdot SiO_2$.

The compound $CaO \cdot FeO \cdot 2SiO_2$ (hedenbergite), is stable at temperatures below 965°C (*H* on fig. 40). If it is heated above this temperature it changes to a stable homogeneous solid phase of the same composition. The substance is no longer a compound, but is a member, in no way unique, of the wollastonite solid-solution series. When a solid phase or mixture of solid phases is transformed in this manner into a solid solution, the equilibrium diagram can assume any of the various forms that a melting-point diagram can assume. The

higher temperature phase is a solid solution but in most respects the possible forms of the diagram are the same. Thus, the curve *VHNJ* on figure 40, with its maximum at the composition of hedenbergite, is analogous to the liquidus curve of a melting-point diagram except that the phase above it is a solid solution instead of a liquid solution. All the phase changes incident to a change of temperature and the proportions of phases present at any temperature are read from the diagram in the same manner as in the more familiar melting-point diagram.

The metasilicate and the orthosilicate solid solutions are the dominant solid phases of the ternary system and their relations to each other and to ternary liquids are the features of greatest interest in the system. The coexistence of two solid-solution series in rocks is a phenomenon of common occurrence which renders desirable a full discussion of their interrelations. They are best brought out with the aid of the series of isothermal planes of figure 41. The relations of phases of constant composition, such as tridymite, pseudowollastonite, and tricalcium disilicate, are so simple that they require no special discussion. The first isothermal plane to be described will, therefore, be 1285°C, which is the maximum temperature at which crystals of one of the solid-solution series can exist. At this temperature only one liquid, *M*, can exist in equilibrium with a β-$CaSiO_3$ (wollastonite) solid solution. The composition of the solid is *B*. The equilibrium is binary and the device is here adopted of indicating binary equilibrium by a brace. The point *M* corresponds with the point lettered *M* in figures 38 and 40, and point *B* with point *B* in figure 40. The liquids represented by points on the curves *Ma* and *Md* (except *M* itself) are in equilibrium only with α-$CaSiO_3$ (pseudowollastonite) which has the fixed composition *W*. The liquid *a* is in equilibrium with both tridymite and $CaO \cdot SiO_2$ and therefore corresponds with a point on the boundary curve *GA* of figure 38. The liquid *d* is in equilibrium with both α-$CaO \cdot SiO_2$ and $3CaO \cdot 2SiO_2$. The liquid *c* is in equilibrium with both $3CaO \cdot 2SiO_2$ and $2CaO \cdot SiO_2$ solid solution of composition *b*. As in metasilicate compositions, so in the orthosilicate compositions the binary equilibrium is indicated by a brace joining the liquid and solid in equilibrium. The point *g* therefore represents the composition of crystalline orthosilicate in equilibrium with liquid at 1285°C. All compositions in the triangle *ObL* are completely crystalline at this temperature (1285°C) and consist of two phases: one the compound $3CaO \cdot 2SiO_2$, the other a β-$2CaO \cdot SiO_2$ solid solution of a composition between *b* and *O*. The only other compositions that are completely crystalline at 1285°C are those lying in the line *WB* and those lying in the line *Og*.

Many of the characters described for various points in the figure apply to similar points in the subsequent isothermal planes and will not be again discussed. Only the new features brought out by the successive planes will, in general, be mentioned.

At the next isothermal plane, 1280°C, which is only 5°C lower, any one of the liquids lying on the curve *by* is in equilibrium with a wollastonite solid solution. There are now two liquids *b* and *y* that are in equilibrium with both α-$CaO \cdot SiO_2$ and β-$CaO \cdot SiO_2$ (wollastonite) solid solution. Moreover, the liquids *b* and *y* are in equilibrium with the same wollastonite solid solution and its composition is *z*. This follows from the fact that only one wollastonite solid solution can be in equilibrium with pseudowollastonite at any given temperature and, the temperature being 1280°C, the point *z* must represent the same composition as the point in the curve *AB* of figure 40 which lies at 1280°C.

The next isothermal plane is 1272°C, the temperature of the invariant point *A* of figure 38. There are again two liquids, *H* and *Y*, that are in equilibrium with both pseudowollastonite and a wollastonite solid solution, but here the liquid *H* is also in equilibrium with tridymite. The wollastonite solid solution has the composition *z*, which is nearly the same as *z* at 1280°C and is fixed by the same considerations. The temperature 1272°C is the minimum temperature of existence of pseudowollastonite in contact with liquids containing silica in excess of the metasilicate ratio. In liquids containing less than the metasilicate ratio, pseudowollastonite continues to much lower temperatures.

At a temperature immediately below 1272°C, the join *WH* disappears and is replaced by *zT*. All mixtures in the triangle *WzT* therefore become completely crystalline at 1272°C and consist of the three solid phases, tridymite, α-$CaO \cdot SiO_2$ (pseudowollastonite), and β-$CaO \cdot SiO_2$ (wollastonite) solid solution of composition *z*. Further cooling of this mixture of three solid phases brings about a change of composition of the wollastonite solid solution which consists of its enrichment in $CaO \cdot SiO_2$ at the expense of pseudowollastonite and which continues until the supply of pseudowollastonite is exhausted. The exact behavior is to be read from the curve *AB* of the (partially) binary figure 40, the tridymite present acting as a wholly neutral body with respect to these changes.

The next isothermal plane represents the relations at 1250°C. There is now only one liquid, *y*, which is in equilibrium with both pseudowollastonite, and a wollastonite solid solution designated by *z*. It lies much closer to *W* than it did in the isothermal planes for higher temperatures, a relation that is rendered necessary by the slope of the curve *AB* of figure 40. All

the liquids on the curve *ya* are in equilibrium with wollastonite solid solutions. The liquid *a* is also in equilibrium with tridymite and the particular wollastonite solid solution in equilibrium with it is *x*. All mixtures in the triangle *WzT* are completely crystalline at 1250°C and consist of the three solid phases, tridymite (*T*), pseudowollastonite (*W*), and wollastonite solid solution (*z*). All mixtures in the triangle *zxT* are also completely crystalline at 1250°C but they consist of only two solid phases, tridymite and a wollastonite solid solution of a composition, which may lie anywhere between *z* and *x*, the exact position depending upon the total composition.

The next isothermal plane to be described shows phase relations at 1227°C, the temperature of the invariant point *F* of figure 38, and the same point is marked *Q* in this isothermal figure. There is again a series of liquids, *ya*, each of which is in equilibrium with a wollastonite solid solution. The liquid *y* is in equilibrium with the solid solution *z* and also with pseudowollastonite. The liquid *a* is in equilibrium with the solid solution *x* and with tridymite *T*. The triangles *WzT* and *zxT* have the same qualities as the triangles so lettered in the 1250°C figure. *WzT* has become smaller and *zxT* larger. The liquid *Q* is joined with the three solid phases in equilibrium with it. These are $3CaO \cdot 2SiO_2$ (*L*), β-$2CaO \cdot SiO_2$ solid solution (*b*), and Ca-Fe olivine (*c*). The temperature 1227°C is the minimum temperature of existence of $2CaO \cdot SiO_2$ solid solutions in contact with liquid. At a temperature immediately below 1227°C, the join *bQ* disappears and its place is taken by the join *cL*.

The next isothermal plane is for 1220°C, the temperature of the invariant point *C* of figure 38. The points *a*, *y*, *x*, and *z* require no special discussion for this particular figure. The liquid *P* is joined with the three solid phases in equilibrium with it. They are pseudowollastonite (*W*), $3CaO \cdot 2SiO_2$ (*L*), and Ca-Fe olivine (*c*). The temperature 1220°C is the minimum temperature of existence of $3CaO \cdot SiO_2$ in contact with liquid. At a temperature immediately below this, the join *pL* disappears and its place is taken by the join *cW*. The triangles that represent completely crystallized material may be mentioned. In the triangle *dcL* there are two solid phases, $3CaO \cdot SiO_2$ and a Ca-Fe olivine of composition between *d* and *c*. In the triangle *dbL* there are three solid phases, β-$2CaO \cdot SiO_2$ solid solution (*b*), $3CaO \cdot 2SiO_2$ (*L*) and Ca-Fe olivine (*d*). In the triangle *LOb* there are two solid phases, $3CaO \cdot 2SiO_2$ (*L*) and a β-$CaO \cdot SiO_2$ solid solution of composition between *b* and *O*.

The next isothermal diagram is that for 1200°C. The points *a*, *y*, *z*, and *x* have their usual characters. The point *x* is now much closer to *W*, in correspondence with the fact that the wollastonite solid solution that is in equilibrium with pseudowollastonite at 1200°C has only a very small content of $FeSiO_3$. The liquid *l* is joined to the two solid phases in equilibrium with it. They are pseudowollastonite (*W*) and a Ca–Fe olivine (*n*), a point a small distance to the right of the composition of the compound $CaO \cdot FeO \cdot SiO_2$. The triangle *cnW* represents completely crystalline material in two phases, pseudowollastonite (*W*) and a Ca–Fe olivine of composition lying between *c* and *n*. The triangle *cWL* represents completely crystalline material in three phases, *W*, *L*, and *c*, the last being a Ca–Fe olivine. The triangles adjacent to these have the characters already given under the preceding isotherm. Two-phase and three-phase triangles alternate. In this figure there appears for the first time a small area representing liquid and olivine very close to fayalite.

The next isothermal diagram presents phase relations at 1193°C, the temperature of the invariant point *E* of figure 38. The two points *l* and *y* of the preceding figure have now become the single point *R*. The liquid *R* is joined with the three solid phases in equilibrium with it: pseudowollastonite (*W*), wollastonite solid solution (*z*), and Ca–Fe olivine (*n*). The temperature 1193°C is the minimum temperature of existence of pseudowollastonite in contact with liquid. At a temperature immediately below 1193°C the join *RW* disappears and is replaced by the join *nz*.

The next isothermal diagram shows phase relations at 1160°C, the temperature of the point *Z* of figure 38. The point *Z* is not an invariant point, but is merely the lower limit of the congruent melting of metasilicate solid solutions. At temperatures above 1160°C liquids on both sides of the metasilicate join are in equilibrium with wollastonite solid solutions. At temperatures below 1160°C only liquids with less silica than the metasilicate ratio are in equilibrium with wollastonite solid solutions. In the diagram for 1160°C, the points *Z* and *C* correspond with the points similarly lettered in figure 40. The point *z* represents the wollastonite solid solution in equilibrium with liquid (*m*) and with Ca–Fe olivine (*n*). It no longer represents a wollastonite solid solution in equilibrium with pseudowollastonite as it did in all previous isothermal figures. At temperatures above 1193°C the point *z* moved toward *W* with falling temperature; at temperatures below 1193°C it moves away from *W*, and at 1160°C has attained the approximate position shown. All compositions in the quadrilateral *AnzW* consist of a wollastonite solid solution of composition between *W* and *z* and a Ca-Fe olivine of composition between *A* and *n*. All compositions in the triangle *WAc* consist of pure wollastonite (*W*)

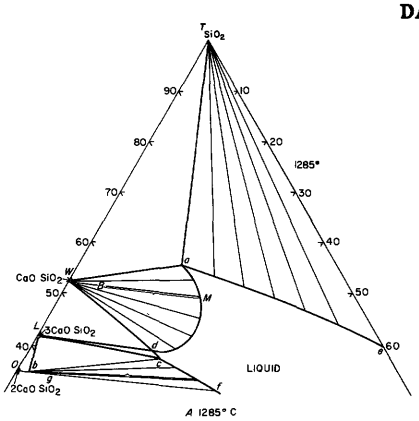

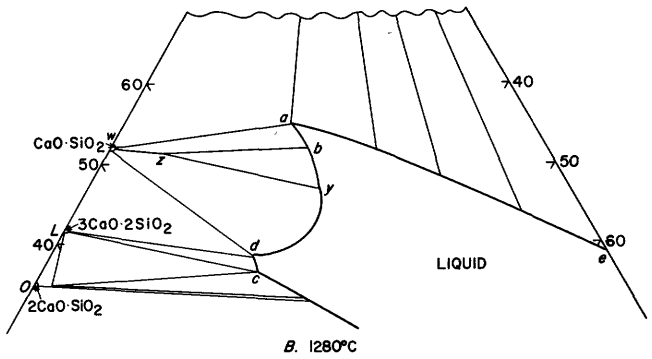

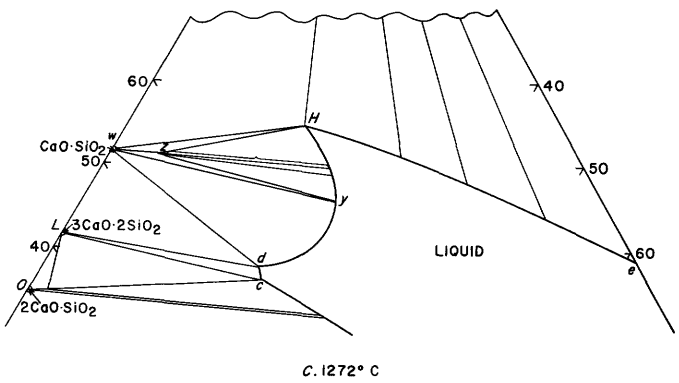

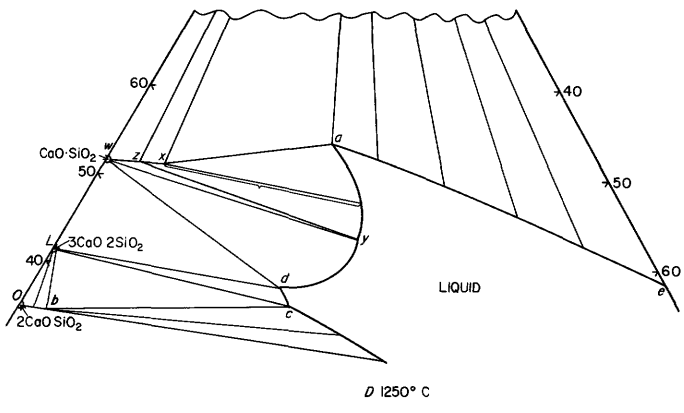

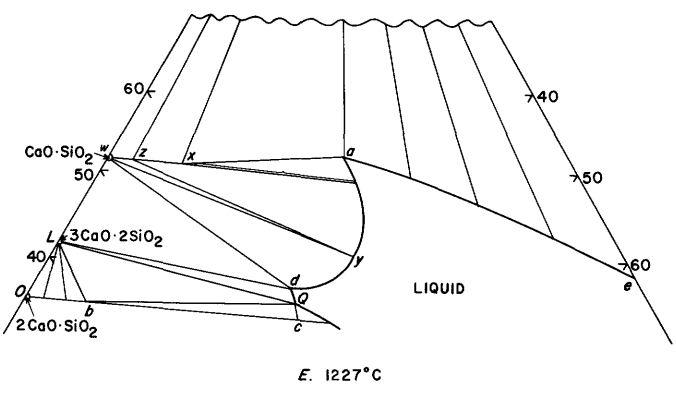

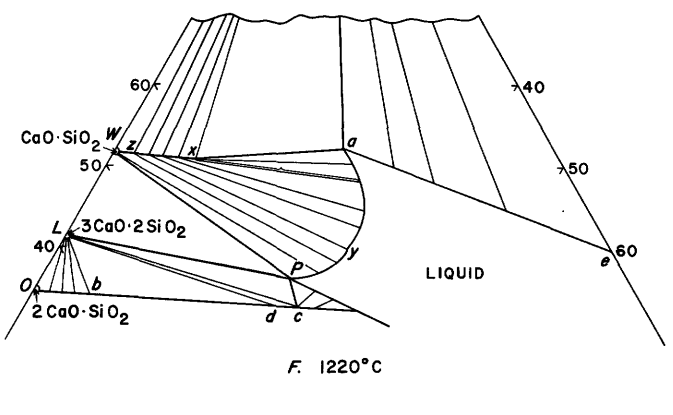

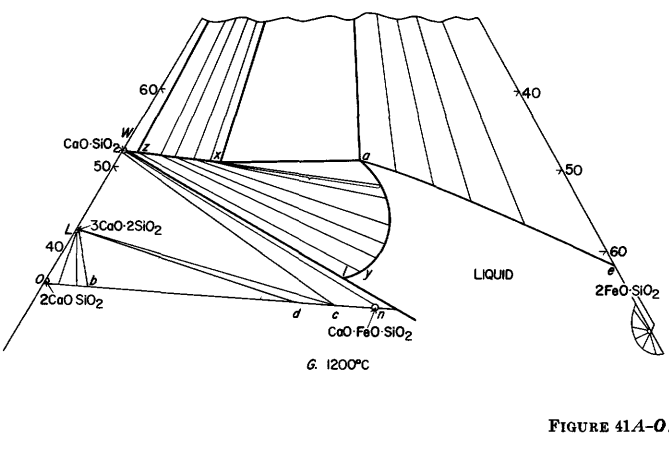

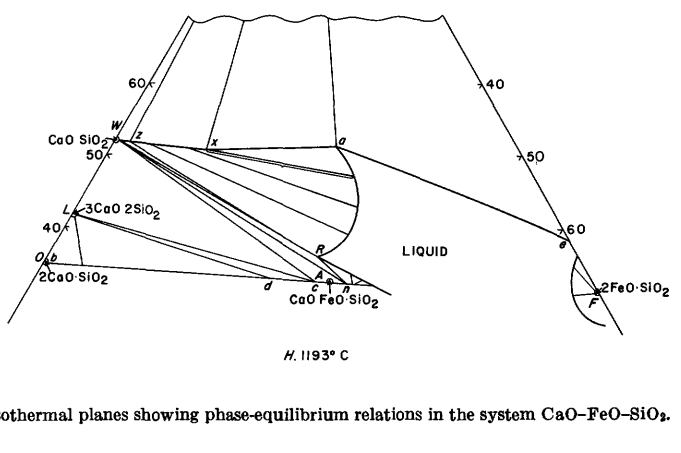

FIGURE 41*A–O*.—Isothermal planes showing phase-equilibrium relations in the system CaO–FeO–SiO_2.

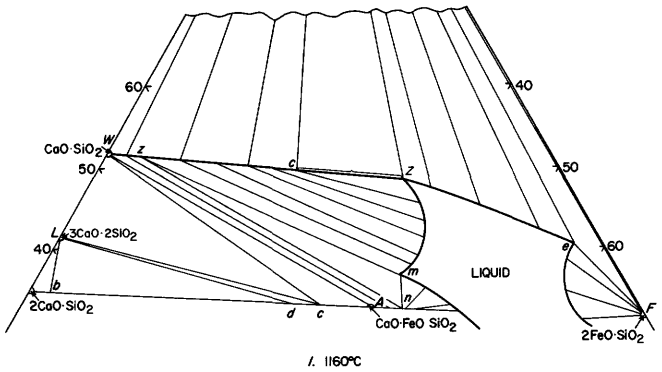

I. 1160°C

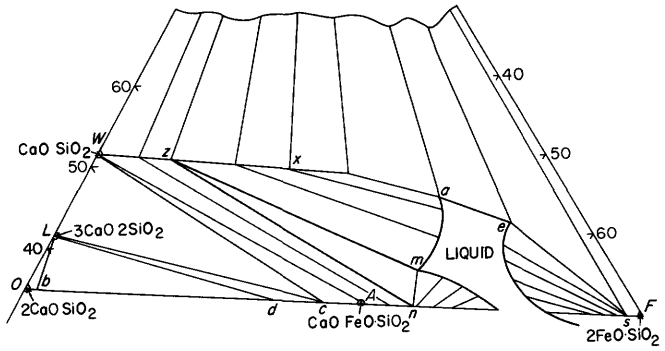

J. 1130°C

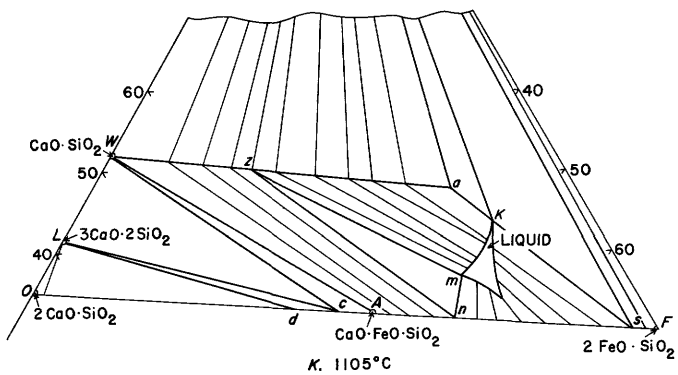

K. 1105°C

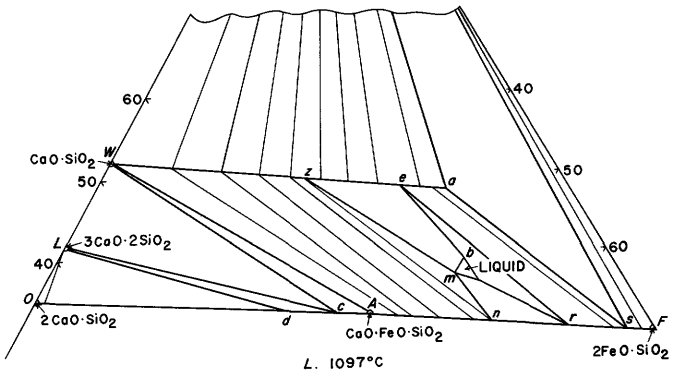

L. 1097°C

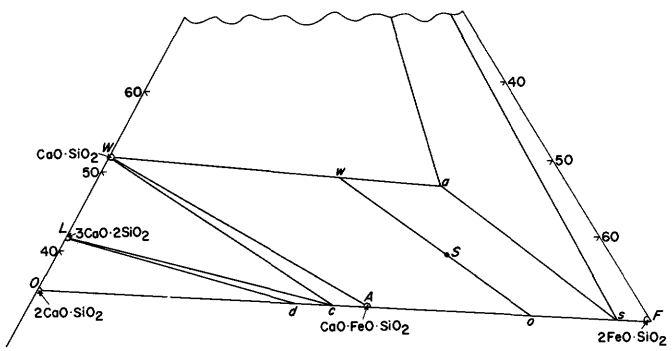

M. 1093° C

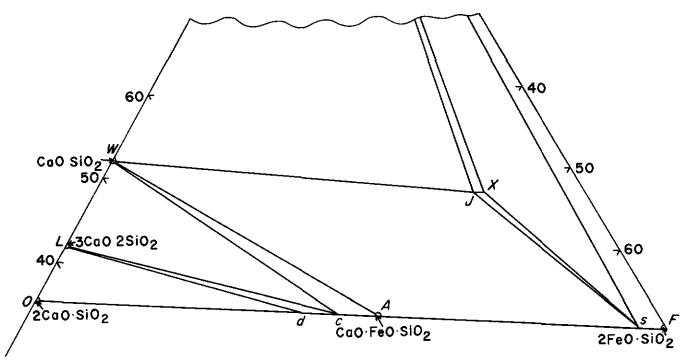

N 980° C

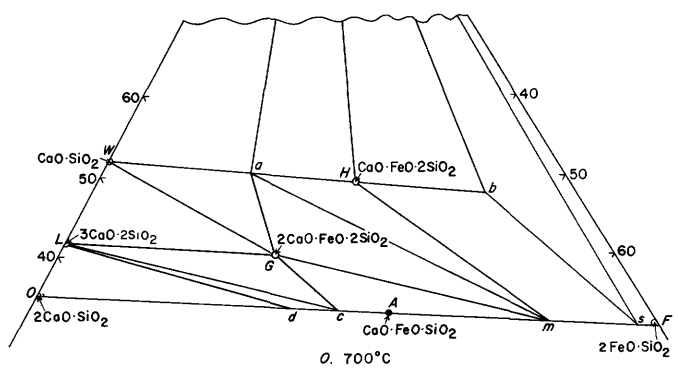

O. 700°C

Truncated SiO_2 apex = *T* in text. Modified from Bowen, Schairer, and Posnjak (1933b).

and a Ca-Fe olivine of composition between *A* and *c*. This diagram is the first of these isothermal figures on which a liquid appears that is in equilibrium with both tridymite and an olivine. It is represented by the point *e*.

The next isothermal plane shows phase relations at 1130°C, which is not a unique point but may be taken as representative of the changing equilibrium between 1160° and 1105°C. The liquids on the curve *am*, all of which have silica in less than the metasilicate ratio, are the only liquids in equilibrium with metasilicate (wollastonite) solid solutions. The triangle *sFT* represents mixtures that are completely crystalline at 1130°C and consist of tridymite and olivine of composition between *F* and *s*. A triangle having these characteristics appeared on the preceding figure but there it was too small to assign letters to it.

The next isothermal plane, 1105°C, is at the temperature of the invariant point *B* of figure 38. The liquid *K* is joined with the three solid phases in equilibrium with it, wollastonite solid solution (*a*), olivine (*s*), and tridymite (*T*). The point *K* lies nearly on a straight line joining the points *s* and *a*; in fact, experimental results do not prove conclusively that *K* does not lie in that line. If *K* lay above the join *sa*, it would be a eutectic point; if it lies below *sa*, it is a reaction point; and if it lies in the line, it is a neutral point, and tridymite is an indifferent phase and plays no part in the phase reaction. The general relations in the vicinity of *K* show that it is not a eutectic, but do not permit a decision as to whether it is a neutral point or a reaction point. In the figure it is shown slightly below the join *sa* and therefore as a reaction point, but there would be no important difference in the general relations if *K* lay in the join *sa*. The temperature 1105°C is the minimum temperature of existence of tridymite in contact with liquid. At a temperature immediately below 1105°C, the join *KT* disappears and is replaced by the join *sa*.

The next isothermal plane is for 1097°C, only 4°C above the minimum temperature of existence of liquid. The liquid *b* is in equilibrium with the wollastonite solid solution *e* and the olivine *r*, the liquid *m* with the wollastonite solid solution *z* and the olivine *n*. The quadrilateral *WznA* which appeared in higher isothermals has in this figure the companion quadrilateral *easr*, which represents mixtures that are completely crystalline and consist of a wollastonite solid solution between *e* and *a* and an olivine between *r* and *s*. The tie lines join the compositions in equilibrium. The triangle *saT* represents mixtures that are completely crystalline at 1097°C and consist of three phases, tridymite *T*, olivine *s* (96 percent $2FeO \cdot SiO_2$) and wollastonite solid solution *a* (72 percent $FeO \cdot SiO_2$).

The next isothermal plane is for 1093°C, which is the minimum temperature of existence of liquid. At this temperature only one liquid can exist and it is represented by the point *S* which corresponds with the point similarly lettered in figure 38. This liquid is in equilibrium with the two solid phases *O* (and olivine with about 80 percent $2FeO \cdot SiO_2$) and *w* (a wollastonite solid solution with 50 percent $FeO \cdot SiO_2$), and *wSo* is a straight line. Only mixtures lying in this line are partly liquid at 1093°C. All other mixtures are completely crystalline. The lines joining the solid phases in equilibrium with each other are readily pictured from the preceding figures. At a temperature immediately below 1093°C all mixtures are completely crystalline.

The next isothermal diagram represents relations at 980°C, an invariant point where four solid phases (and vapor) are in equilibrium. The four phases are wollastonite solid solution *j*, hedenbergite solid solution *X*, olivine *s*, and tridymite *T*. The points *J* and *X* correspond with the points similarly lettered in the metasilicate diagram (figure 40). Immediately above 980°C the triangle *JsT* represents the stable configuration. Immediately below 980°C *Js* and *JT* disappear and the triangle *XsT* represents the stable configuration.

The next isothermal plane shows the most probable relations at 700°C. At this temperature the compound, $2CaO \cdot FeO \cdot 2SiO_2$, is one of the phases participating in the equilibrium in mixtures of appropriate composition. The point *a* corresponds with a point at 700°C on the curve *HV* of figure 40 and the point *b* with a point at 700°C on the curve *XR* of figure 40.

The point *m* represents the composition of the olivine that is in equilibrium with hedenbergite at 700°C. Its position is not determined but is based on the assumption that this is the same olivine that is in equilibrium with hedenbergite at 965°C and therefore with a wollastonite solid solution of the same composition as hedenbergite. Even at 965°C the composition of this olivine is not determined, but again is based on the assumption that it is the same olivine that is in equilibrium with a wollastonite solid solution of the composition of hedenbergite at the still higher temperature somewhat above 1100°C, where liquid is present. The assumption is that the composition of the two phases in equilibrium at 1100°C is the same as the composition of the two phases in equilibrium at 700°C. No doubt this is not strictly true but it is probably not far from the truth.

Some of the areas of the isothermal plane at 700°C have the same significance as the similar areas in preceding planes and need not be discussed. Others may require special mention. The quadrilateral *Hbsm* includes all compositions that consist, at 700°C of two

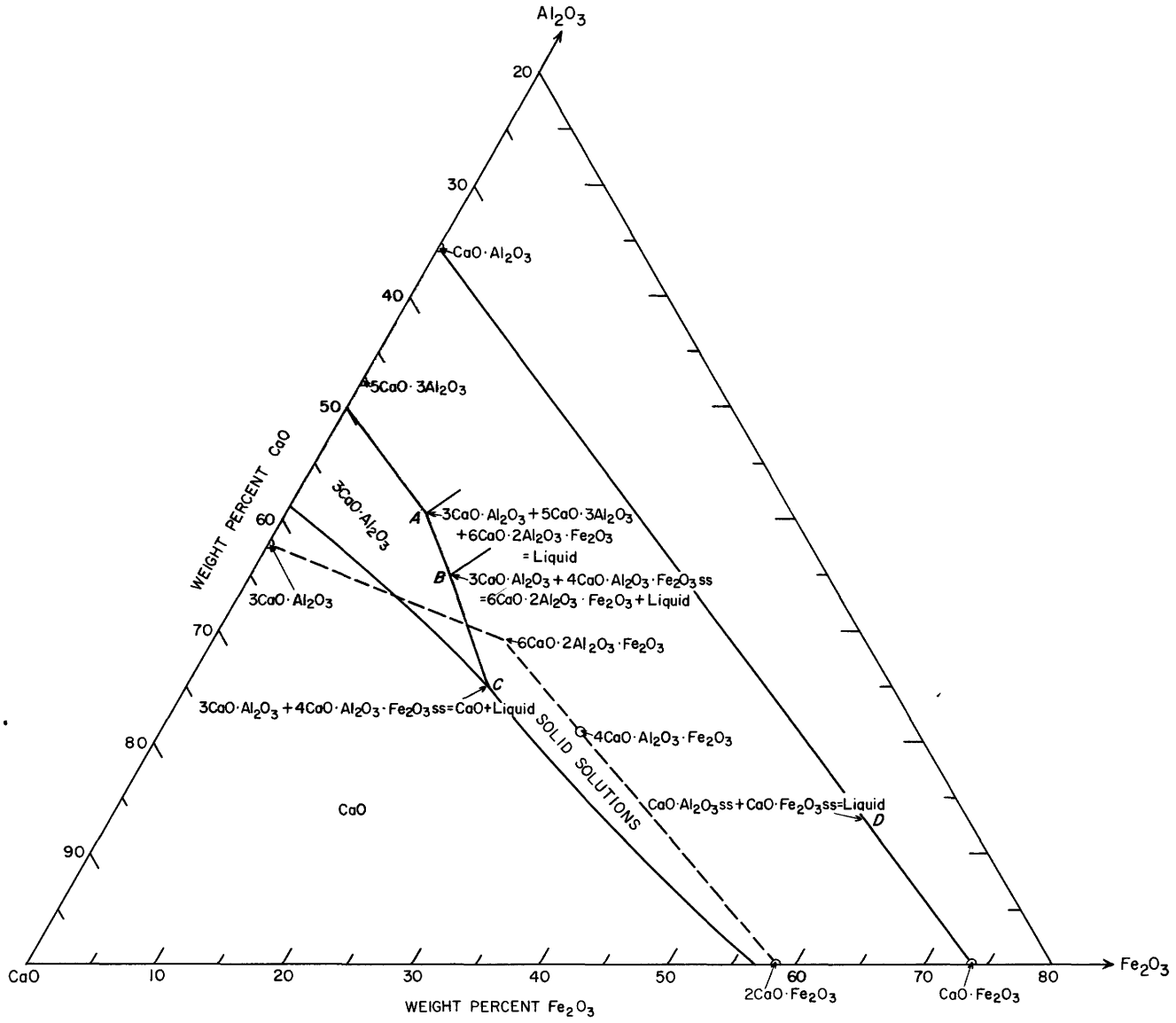

FIGURE 42.—The system CaO–Al_2O_3–Fe_2O_3. Modified from Swayze (1946). *ss*, solid solution.

phases: hedenbergite solid solution, *H* to *b*, and olivine, *m* to *s*. The triangle *Hma* includes all compositions that consist of three phases: pure hedenbergite, *H*, olivine, *m*, and wollastonite solid solution, *a*. The triangle *Gam* has the three phases, $2CaO \cdot FeO \cdot 2SiO_2$, *G*, wollastonite solid solution, *a*, and olivine, *m*. The triangle *Gcm* has the two phases, $2CaO \cdot FeO \cdot 2SiO_2$, *G*, and olivine, *c* to *m*. The triangle *GcL* has the three phases, $2CaO \cdot FeO \cdot 2SiO_2$, *G*, olivine, *c*, and $3CaO \cdot 2SiO_2$, *L*. The triangle *GLW* has the three solid phases, $2CaO \cdot FeO \cdot 2SiO_2$, $3CaO \cdot 2SiO_2$, and pure wollastonite. The triangle *GWa* has only two solid phases, $2CaO \cdot FeO \cdot 2SiO_2$, *G*, and wollastonite solid solution, *W* to *a*.

CaO–Al_2O_3–Fe_2O_3

The original study of this system, important in the cement industry, was by Hansen, Brownmiller, and Bogue (1928). McMurdie (1937) later worked on CaO–$CaO \cdot Al_2O_3$–$4CaO \cdot Fe_2O_3$, and Swayze (1946) made a further study of CaO–$5CaO \cdot 3Al_2O_3$–$2CaO \cdot Fe_2O_3$. Swayze's results which also are given in Bogue (1955), are given preference in figure 42. In the binary system $CaO \cdot Al_2O_3$–$CaO \cdot Fe_2O_3$, $CaO \cdot Al_2O_3$ takes as much as 15 percent of $CaO \cdot Fe_2O_3$ into solid solution, and $CaO \cdot Fe_2O_3$ takes as much as 19 percent of $CaO \cdot Al_2O_3$. There is a eutectic at $1205° \pm 5°C$ of composition CaO 28 percent, Al_2O_3 13 percent, Fe_2O_3 59 percent. Two ternary compounds are

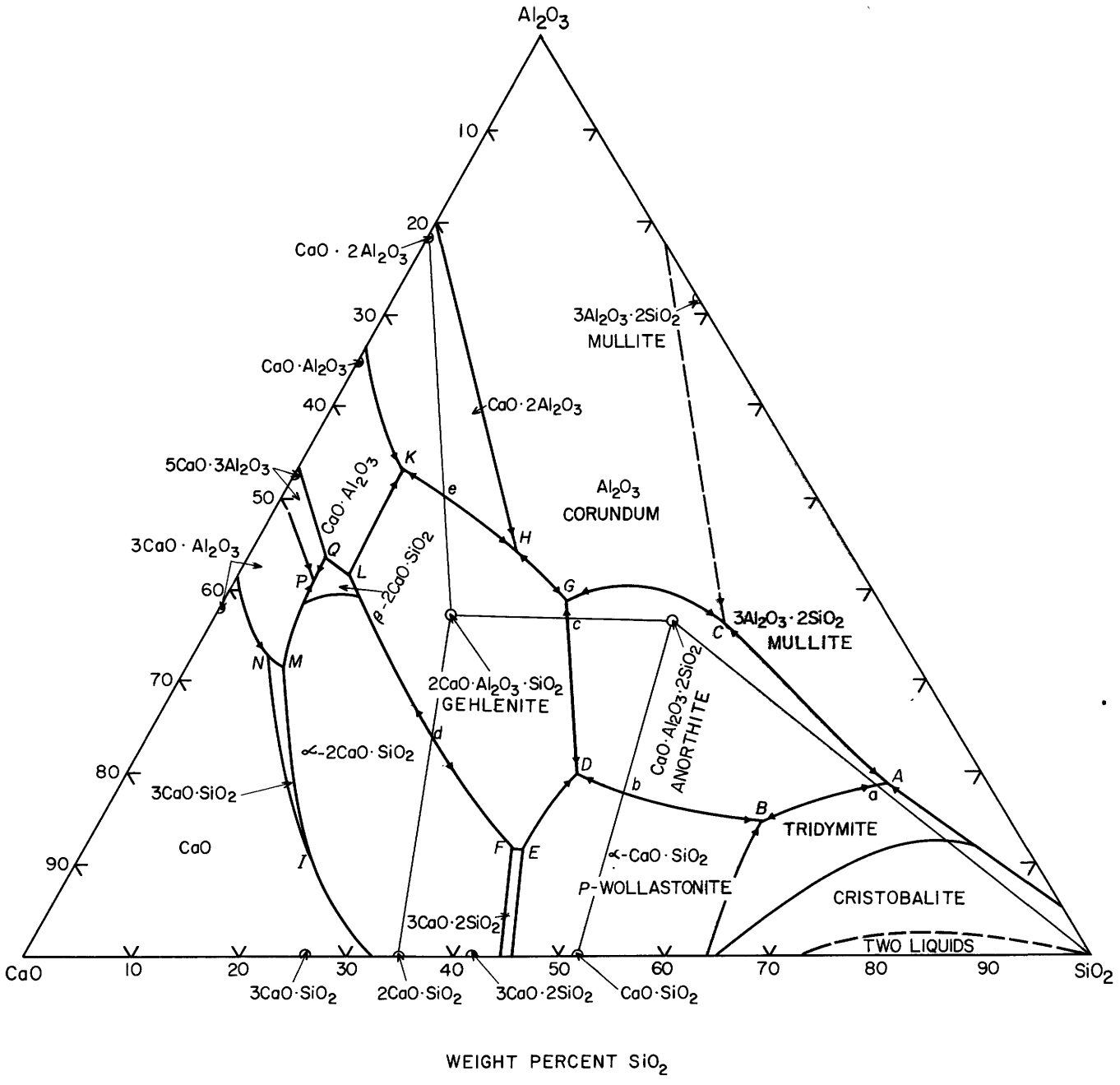

FIGURE 43.—The system CaO–Al_2O_3–SiO_2. Based on Rankin and Wright (1915), Greig (1927a), Osborn (1942), and Schairer and Bowen (1947b). The diagram has not been corrected for the incongruent melting of $3CaO \cdot SiO_2$ described by Welch and Gutt (1959), and the field of $3CaO \cdot SiO_2$ should extend to the side CaO–SiO_2 instead of terminating at *I*.

formed. The first, $4CaO \cdot Al_2O_3 \cdot Fe_2O_3$ was found by Hansen, Brownmiller, and Bogue to melt congruently at 1415°C. It forms a series of solid solutions on the line $4CaO \cdot Al_2O_3 \cdot FeO_3$ which extends on both sides of the composition $4CaO \cdot Al_2O_3 \cdot Fe_2O_3$. The second compound, $6CaO \cdot 2Al_2O_3 \cdot Fe_2O_3$, found by Swayze, in confirmation of previous observations by Yamauchi (1937*a*,*b*), melts incongruently at *B* (fig. 42) with formation of a solid solution on the join $6CaO \cdot 2Al_2O_3 \cdot Fe_2O_3$–$4CaO \cdot Al_2O_3 \cdot Fe_2O_3$ and at the temperature of complete melting, 1390°C, the residual solid phase had a molecular ratio ($Al_2O_3 : Fe_2O_3$) of 0.72:1. The region between the join $CaO \cdot Al_2O_3$–$CaO \cdot Fe_2O_3$ and the fields of $3CaO \cdot Al_2O_3$ and the region of solid solution has not been clarified.

CaO–Al_2O_3–SiO_2

Parts of this system have been studied by many investigators, chiefly because of the information it gives concerning the constitution of portland cement. This

TABLE 26.—*Invariant points in the system* $CaO–Al_2O_3–SiO_2$

Invariant point on fig. 43	Phase reactions	Temperature (° C)	Composition of liquid (percent by weight		
			CaO	Al_2O_3	SiO_2
A	$CaO·Al_2O_3·2SiO_2+SiO_2+3Al_2O_3·2SiO_2 \rightleftharpoons L$	1345	9. 8	18. 6	71. 6
a	$CaO·Al_2O_3·2SiO_2+SiO_2 \rightleftharpoons L$ (50. 5 An)	1368	10. 2	18. 5	71. 3
B	$CaO·SiO_2+SiO_2+CaO·Al_2O_3·2SiO_2 \rightleftharpoons L$	1165	23. 25	14. 75	62. 0
C	$CaO·Al_2O_3·2SiO_2+3Al_2O_3·2SiO_2 \rightleftharpoons Al_2O_3+L$	1512	15. 6	36. 5	47. 9
b	$CaO·SiO_2+CaO·Al_2O_3·2SiO_2 \rightleftharpoons L$	1307	34. 8	17. 6	47. 6
	$CaO·Al_2O_3·2SiO_2 \rightleftharpoons L$	1553	20. 16	36. 65	43. 19
D	$CaO·SiO_2+CaO·Al_2O_3·2SiO_2+2CaO·Al_2O_3·SiO_2 L+$	1265	38	20	42
E	$3CaO·2SiO_2+CaO·Al_2O_3·2SiO_2 \rightleftharpoons CaO·SiO_2+L$	1310	47. 2	11. 8	41
F	$3CaO·2SiO_2+2CaO·Al_2O_3·SiO_2 \rightleftharpoons 2CaO·SiO_2+L$	1335	48. 3	11. 8	39. 9
c	$2CaO·Al_2O_3·SiO_2+CaO·Al_2O_3·2SiO_2 \rightleftharpoons L$	1387	30. 2	36. 8	33
G	$2CaO·Al_2O_3·SiO_2+CaO·Al_2O_3·2SiO_2+Al_2O_3 \rightleftharpoons L$	1380	29. 2	39. 0	31. 8
d	$2CaO·SiO_2+2CaO·Al_2O_3·SiO_2 \rightleftharpoons L$	1545	49. 6	23. 7	26. 7
H	$2CaO·Al_2O_3·SiO_2+Al_2O_3 \rightleftharpoons CaO·2Al_2O_3+L$	1475	31. 2	44. 5	24. 3
I[1]	$3CaO·SiO_2 \rightleftharpoons CaO+2CaO·SiO_2$	1900	68. 4	9. 2	22. 4
e	$2CaO·Al_2O_3·SiO_2+CaO·2Al_2O_3 \rightleftharpoons L$	1552	35	50. 8	14. 2
L	$2CaO·SiO_2+CaO·Al_2O_3 \rightleftharpoons 2CaO·Al_2O_3·SiO_2 \rightleftharpoons L$	1380	48. 3	42	9. 7
K	$CaO·Al_2O_3+2CaO·Al_2O_3·SiO_2+CaO·2SiO_2 \rightleftharpoons L$	1505	37. 5	53. 25	9. 25
M	$2CaO·SiO_2+3CaO·Al_2O_3 \rightleftharpoons 3CaO·SiO_2+L$	1455	58. 3	33. 0	8. 7
N	$3CaO·SiO_2+3CaO·Al_2O_3 \rightleftharpoons CaO+L$	1470	59. 7	32. 8	7. 5
Q	$5CaO·3Al_2O_3+2CaO·SiO_2+CaO·Al_2O_3 \rightleftharpoons L$	1335	49. 5	43. 7	6. 8
P	$3CaO·Al_2O_3+2CaO·SiO_2+5CaO·3Al_2O_3 \rightleftharpoons L$	1335	52. 0	41. 2	6. 8

[1] The point *I* is in error since the field $3CaO·SiO_2$ extends to the side $CaO–SiO_2$.

literature has been critically reviewed by Bogue (1955) and by Lea and Desch (1956). The phase-equilibrium diagram of figure 43 is based on the work of Rankin and Wright (1915) as modified by Greig (1927a), Osborn (1942), Schairer and Bowen (1947b) and Aramaki and Roy (1959). The invariant points are summarized in table 26.

There are three ternary compounds. One of these is $2CaO·Al_2O_3·SiO_2$, corresponding to the mineral gehlenite, which melts congruently at 1590°C and crystallizes readily. The second compound,

$$CaO·Al_2O_3·2SiO_2,$$

corresponds to the mineral anorthite, the CaO-rich end member of the plagioclase feldspars, and melts congruently at 1553°C. The third ternary compound, $3CaO·Al_2O_3·SiO_2$, decomposes at 1335°C, below the liquidus surface, and hence does not have a field of stability in figure 43. It is an example of a condition which may not be uncommon; and the fact that a compound is not stable at the liquidus is not proof that it does not exist at lower temperature. Since Welch and Gutt (1959) found that $3CaO·SiO_2$ melts incongruently (see p. 18), the field of $3CaO·SiO_2$ should extend to the side $CaO–SiO_2$ instead of terminating in an invariant point *I*, which is in error.

$CaO–Fe_2O_3–SiO_2$

Burdick (1940) made a survey of this system which is of importance in the making of portland cement. No ternary compounds were found, and the fields of SiO_2, $CaO·SiO_2$, $2CaO·SiO_2$, and CaO occupy most of the phase-equilibrium diagram, with small fields of $3CaO·2SiO_2$, $3CaO·SiO_2$, and $2CaO·Fe_2O_3$. The ternary eutectic

$$3CaO·SiO_2+2CaO·SiO_2+2CaO·Fe_2O_3=L$$

is at 1414°C, and the eutectic

$$CaO+3CaO·SiO_2+2CaO·Fe_2O_3=L$$

at 1411°C. Compositions are not given, but are not far from the composition 46 percent CaO, 50 percent Fe_2O_3, 4 percent SiO_2, the only mixture studied in the field of $2CaO·FeO_3$. The study did not extend to the field of $CaO·Fe_2O_3$ or of Fe_2O_3, and the composition of the liquid at the reaction

$$3CaO·SiO_2=CaO+2CaO·SiO_2$$

was not determined.

Phillips and Muan (1959) studied this system by the quenching method in air. The results are shown in table 27 and in figure 44 which is the projection onto the plane $CaO–Fe_2O_3–SiO_2$ of the irregularly curved isobaric surface in air through the quaternary system $CaO–FeO–Fe_2O_3–SiO_2$. The composition of the liquids are within the subvolume $CaO–Fe_3O_4–Fe_2O_3–SiO_2$. The temperature along the hematite-magnetite boundary increases from 1358°C when no SiO_2 is present to 1390°C at invariant point *B* in the diagram, indicating that magnetite takes some CaO into solid solution.

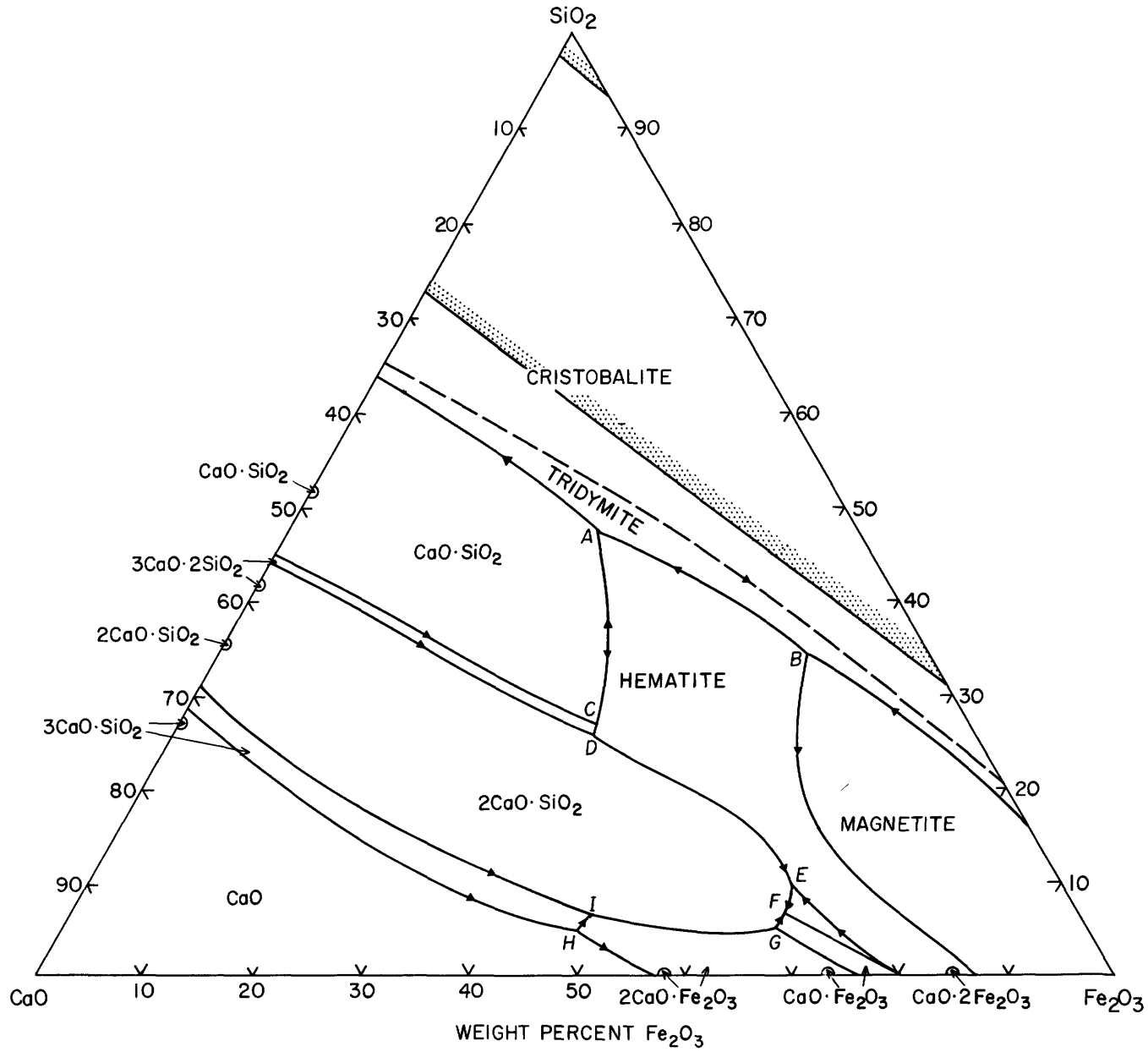

FIGURE 44.—Phase relations in the system $CaO-Fe_2O_3-SiO_2$ in air (P_{O_2}=0.21 atm). The system is not truly ternary, and this text figure represents an irregularly curved isobaric surface through the quaternary system $CaO-FeO-Fe_2O_3-SiO_2$. Heavy lines are boundary curves with arrows pointing in the direction of falling temperatures; lines with stippling on one side are approximate outlines of composition areas where two immiscible liquids form above liquidus temperature. Boundary curves and isotherms are dashed in regions where their locations are uncertain. Modified from Phillips and Muan (1959).

TABLE 27.—*Invariant points in the system* $CaO–Fe_2O_3–SiO_2$

Invariant point on fig. 44	Phase reactions	Temperature (°C)	Composition of liquid (percent by weight)		
			CaO	Fe_2O_3	SiO_2
A	$CaO·SiO_2+SiO_2+Fe_2O_3 \rightleftharpoons L$	1204	24. 0	28. 5	47. 5
B	$SiO_2+Fe_2O_3+Fe_3O_4 \rightleftharpoons L$	1390	11. 0	55. 0	34. 0
C	$3CaO·2SiO_2+CaO·SiO_2+Fe_2O_3 \rightleftharpoons L$	1214	34. 5	38. 5	27. 0
D	$3CaO·2SiO_2+Fe_2O_3 \rightleftharpoons L+2CaO·SiO_2$	1230	35. 0	39. 0	26. 0
E	$2CaO·SiO_2+CaO·2Fe_2O_3+Fe_2O_3 \rightleftharpoons L$	1216	25. 0	65. 0	10. 0
F	$2CaO·SiO_2+CaO·2Fe_2O_3 \rightleftharpoons L+CaO·Fe_2O_3$	1192	26. 5	66. 0	7. 5
G	$2CaO·SiO_2+CaO·Fe_2O_3 \rightleftharpoons L+2CaO·Fe_2O_3$	1195	29. 0	66. 0	5. 0
H	$3CaO·SiO_2+2CaO·Fe_2O_3 \rightleftharpoons L+CaO$	1412	47. 0	48. 0	5. 0
I	$3CaO·SiO_2+2CaO·SiO_2+2CaO·Fe_2O_3 \rightleftharpoons L$	1405	45. 5	48. 0	6. 5
	MAXIMUM ON BOUNDARY CURVES				
	$CaO·SiO_2+Fe_2O_3 \rightleftharpoons L$	1280	30. 5	37. 0	32. 5
	$2CaO·SiO_2+Fe_2O_3 \rightleftharpoons L$	1315	24. 5	62. 5	13. 0
	$2CaO·SiO_2+CaO·2Fe_2O_3 \rightleftharpoons L$	1242	26. 0	66. 0	8. 0

$CaO–SiO_2–TiO_2$

The latest study of this system is by DeVries, Roy, and Osborn (1955). The phase-equilibrium diagram is figure 45, and the invariant points are in table 28. The ternary compound, $CaO·SiO_2·TiO_2$, which corresponds to the mineral sphene, melts congruently at 1382°C, and forms binary systems with $CaO·SiO_2$, SiO_2, TiO_2, and $CaO·TiO_2$ (perovskite). There is a large area in which two liquid layers are formed. This sweeps from the side $CaO–SiO_2$, with cristobalite as solid phase, to the boundary curve *NN'*, where rutile becomes solid phase, and extends to the side $SiO_2–TiO_2$. The compound $3CaO·SiO_2$ has a small field of stability, *ABD*, in the ternary system, and the compounds $3CaO·2SiO_2$ and $3CaO·2TiO_2$, each of which melts incongruently, also have small stability fields.

TABLE 28.—*Invariant points in the system* $CaO–SiO_2–TiO_2$

Invariant point on fig. 45	Phase reactions	Temperature (°C)	Composition of liquid (percent by weight)		
			CaO	SiO_2	TiO_2
A	$3CaO·SiO_2+3CaO·2TiO_2 \rightleftharpoons CaO+L$	1670?	62. 0	16. 0	22. 0
B	$3CaO·SiO_2+2CaO·SiO_2+3CaO·2TiO_2 \rightleftharpoons L$	1650	61. 0	17. 5	21. 5
C	$2CaO·SiO_2+3CaO·2TiO_2 \rightleftharpoons CaO·TiO_2+L$	1670?	60. 0	18. 0	22. 0
D	$3CaO.SiO_2 \rightleftharpoons CaO+2CaO.SiO_2+L$	1900	65. 5	26. 5	8. 0
E	$3CaO.2SiO_2+CaO.TiO_2 \rightleftharpoons 2CaO.SiO_2+L$	1403	52. 3	38. 6	9. 1
F	$3CaO.2SiO_2+CaO.SiO_2+CaO.TiO_2 \rightleftharpoons L$	1398	51. 5	39. 2	9. 3
d	$CaO.SiO_2+CaO.TiO_2 \rightleftharpoons L$	1424	46. 6	39. 3	14. 1
H	$CaO·SiO_2+CaO·TiO_2·SiO_2+CaO·TiO_2 \rightleftharpoons L$	1348	36. 8	37. 0	26. 2
f	$CaO·SiO_2+CaO·TiO_2·SiO_2 \rightleftharpoons L$	1353	36. 7	39. 3	24. 0
J	$CaO·SiO_2+SiO_2+CaO·TiO_2·SiO_2 \rightleftharpoons L$	1318	33. 1	49. 4	17. 5
h	$CaO·TiO_2·SiO_2+SiO_2 \rightleftharpoons L$	1373	25. 8	32. 6	36. 6
L	$SiO_2+TiO_2+CaO·TiO_2·SiO_2 \rightleftharpoons L$	1365	22. 2	29. 0	48. 8
k	$CaO·TiO_2·SiO_2+TiO_2 \rightleftharpoons L$	1375	23. 0	24. 6	52. 4
P	$CaO·TiO_2+CaO·TiO_2·SiO_2+TiO_2 \rightleftharpoons L$	1365	24. 5	18. 0	57. 5
N	SiO_2 (cristobalite) $+TiO_2+L_1$	1535	15. 5	31. 5	53
N'	SiO_2 (cristobalite) $+TiO_2+L_2$	1535	1. 5	88. 0	10. 5

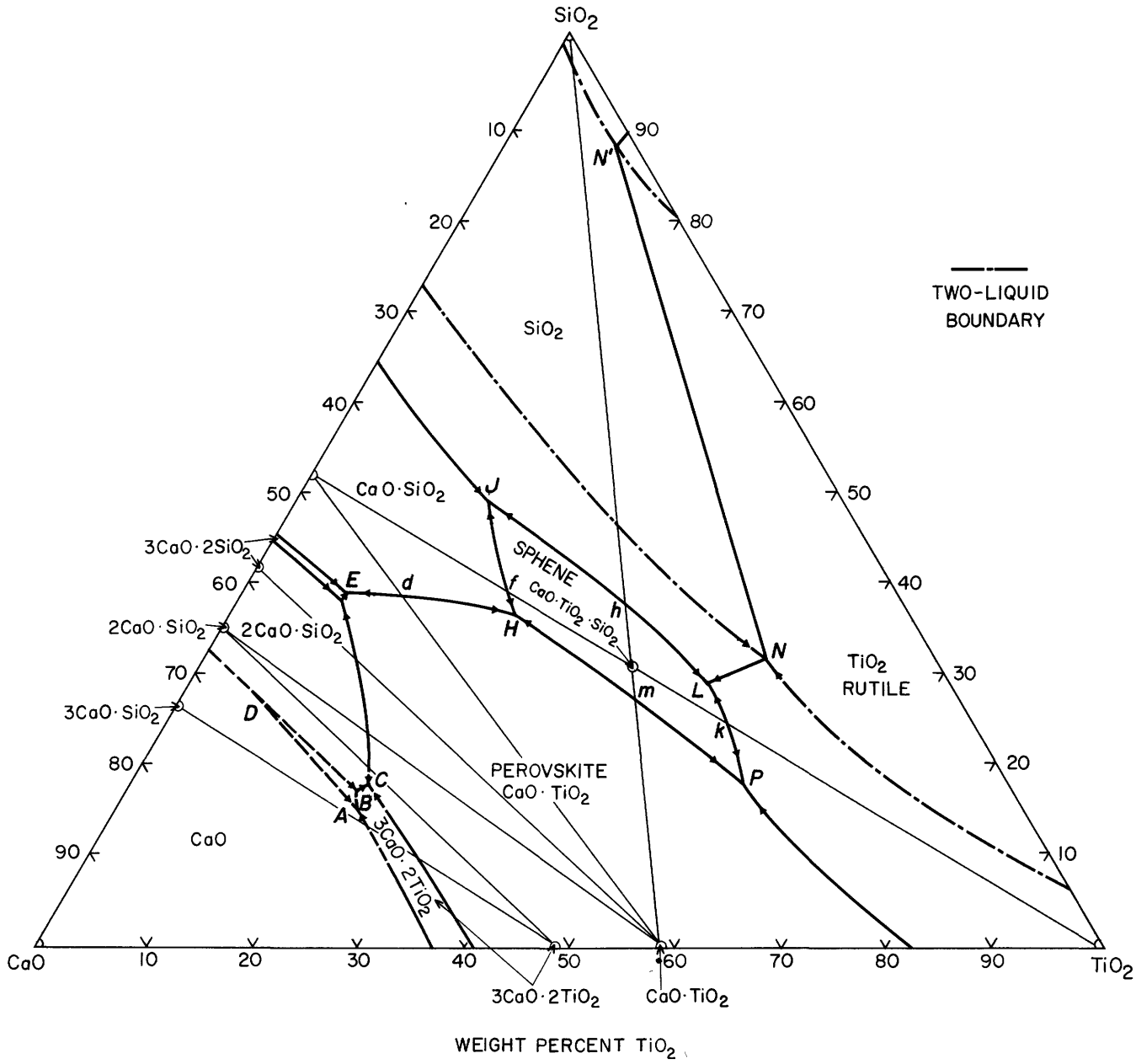

FIGURE 45.—The system CaO–SiO_2–TiO_2. Modified from DeVries, Roy, and Osborn (1955).

FeO–Fe_2O_3–Al_2O_3

The effect of temperature on the solid solution between $FeO \cdot Fe_2O_3$ (magnetite) and $FeO \cdot Al_2O_3$ (hercynite) was studied by Turnock (1959) with results shown in figure 46. The work was done by the hydrothermal method, with $P_{total} = P_{H_2O} + P_{H_2}$, using a solid buffer to control the partial pressure of oxygen. Complete solid solution exists above 858°±8°C. Below this temperature the solid solution unmixes, and the amount of unmixing increases with decreasing temperature. The reactions are sluggish, the effect of pressure on the solvus cannot be detected in the range from 1 to 4,000 atmospheres, and H_2O is not a component.

The effect of changes in the partial pressure of oxygen are oxidation and reduction reactions that change the species and bulk composition of the solid phases, as is shown by the diagram of figure 47. The tie lines connecting equilibrium assemblages in regions of two solid phases are also contour lines of the partial pressure of oxygen, with values increasing up to the hematite-corundum join.

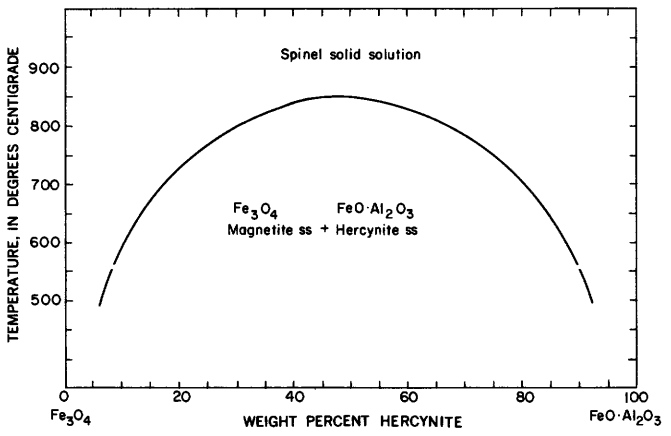

FIGURE 46.—The effect of temperature in limiting the amount of solid solution in the spinel series, Fe_3O_4 to $FeO \cdot Al_2O_3$ (hercynite). An isobaric section with a water pressure of 2,000 atm. Modified from Turnock (1959). *ss*, solid solution.

FeO–Al_2O_3–SiO_2

The system FeO–Al_2O_3–SiO_2 was studied by Schairer and Yagi (1952) by heating the final mixtures in iron crucibles in a current of nitrogen. All mixtures contained Fe_2O_3; some contained as much as 9 percent. They state that while their results properly belong in the quaternary system Fe–Fe_2O_3–Al_2O_3–SiO_2, they are more conveniently and lucidly presented by neglecting the amount of Fe_2O_3 in the liquid, and calculating the total iron as FeO. Only one ternary compound is formed, $2FeO \cdot 2Al_2O_3 \cdot 5SiO_2$, called iron cordierite in analogy with the corresponding compound in the magnesia system. The phase-equilibrium diagram (fig. 48) and table 29 show iron cordierite to melt incongruently, and to have a small narrow field, *KLMN*. The composition of the garnet almandine ($3FeO \cdot Al_2O_3 \cdot 3SiO_2$) is in the field of $FeO \cdot Al_2O_3$, and material of this composition becomes completely crystalline at the point *M*. Attempts to crystallize almandine, including hydrothermal methods, failed. Experiments with natural garnet high in almandine showed that the dissociation temperature is at least as low as 900°C and the dissociation is very sluggish. The side Al_2O_3–SiO_2 was revised by Aramaki and Roy (1959).

FeO–Fe_2O_3–SiO_2

Greig (1927b) gave an incomplete equilibrium diagram showing the extension of the region of immiscibility in the binary system FeO–SiO_2 with the addition of Fe_2O_3. The two-liquid surface was lowered from 1690° to 1665° C and the compositions of the two liquids in equilibrium with cristobalite at 1665°C were: FeO 2.38 percent, Fe_2O_3 2.05 percent, and SiO_2 95.6 percent; and FeO 31.7 percent, Fe_2O_3 36.7 percent, and SiO_2 31.6 percent. This is not an invariant point. Gurry and Darken (1950) published a tentative diagram for the equilibrium at 1600°C and 1 atm of oxygen, and at 0.2 atm CO_2. Muan (1955) studied this system with varying oxygen pressures, obtained with oxygen at 1 atm, air, or mixtures of CO_2 and H_2, and the equilibrium constants used in the calculation of oxygen pressures are given. Results are shown in figure 49. At the eutectic *A*, the phase reaction is

$$SiO_2 + 2FeO \cdot SiO_2 + Fe_3O_4 = L$$

at an oxygen partial pressure of 10^{-9} atm and 1140°C.

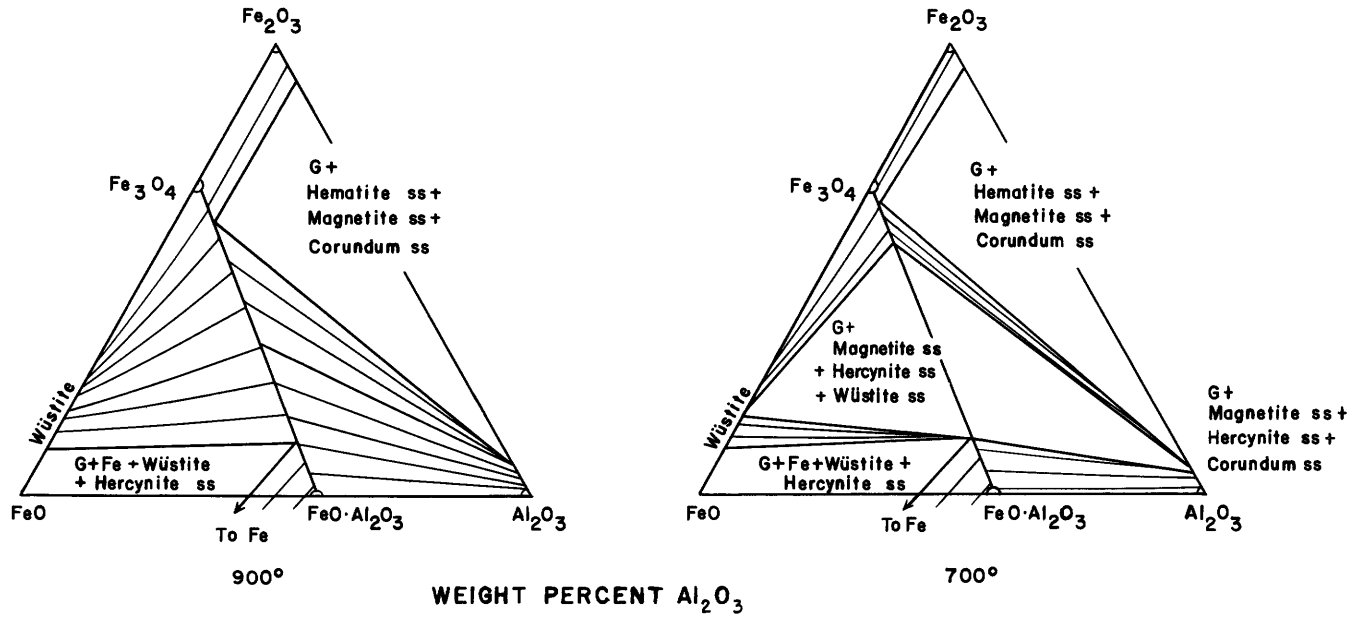

FIGURE 47.—Subsolidus relations in the system FeO–Fe_2O_3–Al_2O_3. Isothermal sections at 900° and 700° C at a total water pressure of 2,000 atm. Modified from Turnock (1959). *ss*, solid solution.

TABLE 29.—*Invariant points in the system* $FeO–Al_2O_3–SiO_2$

Invariant point on fig. 48	Phase reactions	Temperature (°C)	Composition of liquid (percent by weight)		
			FeO	Al_2O_3	SiO_2
K	$2FeO·2Al_2O_3·5SiO_2 \rightleftharpoons SiO_2 + 3Al_2O_3·2SiO_2 + L$	1210	33. 3	20	46. 7
L	$FeO·Al_2O_3 + 2FeO·2Al_2O_3·5SiO_2 \rightleftharpoons 3Al_2O_3·2SiO_2 + L$	1205	33. 9	20. 1	46. 0
N	$2FeO·SiO_2 + SiO_2 + 2FeO·2Al_2O_3·5SiO_2 \rightleftharpoons L$	1083	47. 5	12. 0	40. 5
M	$2FeO·SiO_2 + 2FeO·2Al_2O_3·5SiO_2 \rightleftharpoons FeO·Al_2O_3 + L$	1088	47. 7	12. 6	39. 7
J	$FeO·Al_2O_3 + 3Al_2O_3·2SiO_2 \rightleftharpoons Al_2O_3 + L$	1380	38. 0	27. 0	35. 0
a	$2FeO·SiO_2 + FeO·Al_2O_3 \rightleftharpoons L$	1150	67. 4	6. 3	26. 3

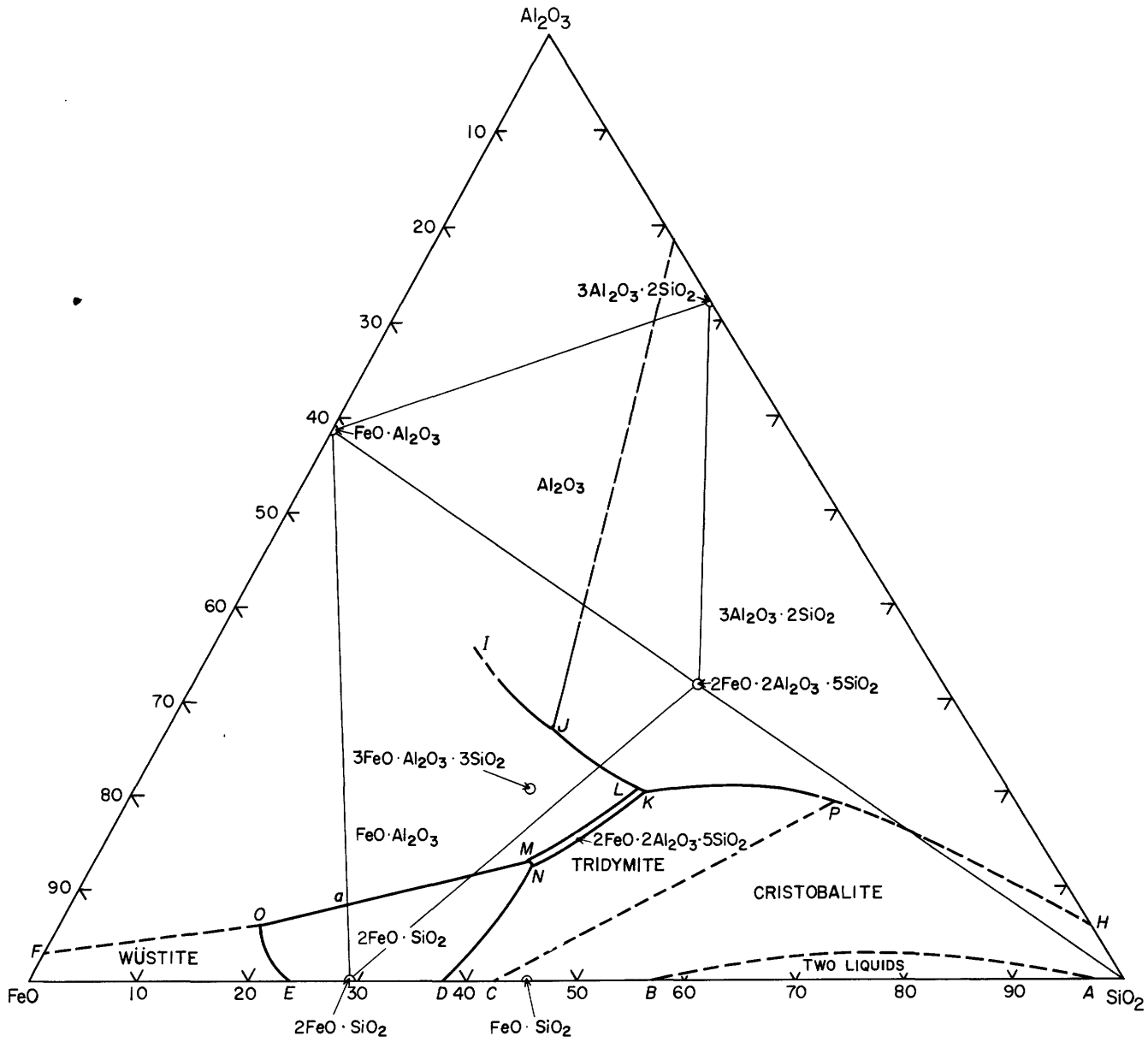

FIGURE 48.—The system $FeO–Al_2O_3–SiO_2$. Modified from Schairer and Yagi (1952).

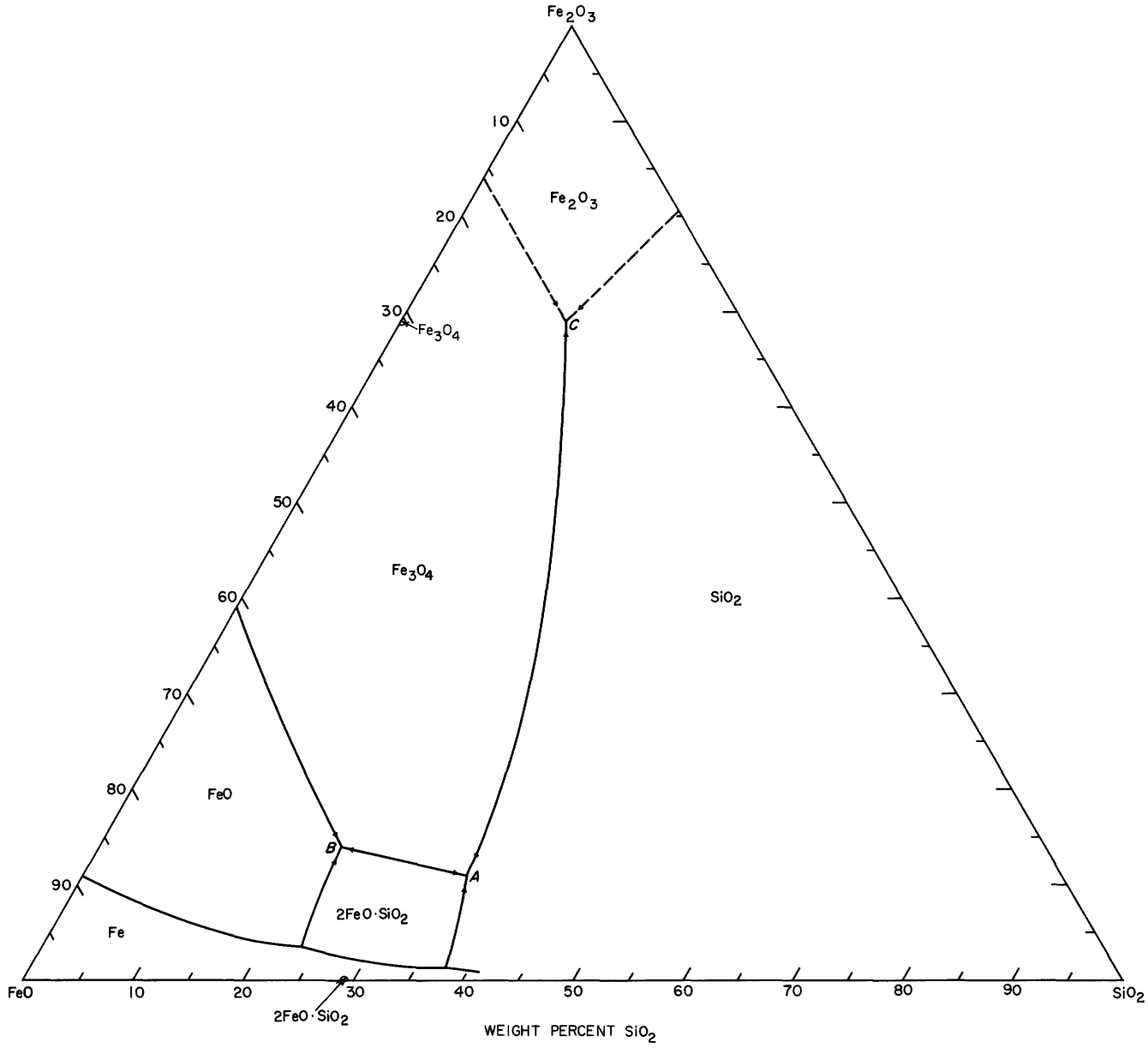

FIGURE 49.—The system FeO–Fe_2O_3–SiO_2. Modified from Muan (1955).

The liquid composition is: FeO 54 percent, Fe_2O_3 11 percent, and SiO_2 35 percent. At the eutectic B the phase reaction is $Fe_3O_4+2FeO\cdot SiO_2+FeO=L$ at $P_{O_2}=10^{-9.9}$ atm, 1150°C. The FeO phase, a wüstite solid solution, contains 35 percent Fe_2O_3 and the liquid contains FeO 64 percent, Fe_2O_3 14 percent, and SiO_2 22 percent. A third eutectic C, $Fe_3O_4+Fe_2O_3+SiO_2=L$, was inferred to be located at an oxygen pressure of slightly more than 1 atm and 1455°C, FeO 16 percent, Fe_2O_3 69 percent, and SiO_2 15 percent.

Al_2O_3–SiO_2–TiO_2

Agamawi and White (1952) studied a part of the system Al_2O_3–SiO_2–TiO_2 by a survey determining cone fusion points, followed by quenching studies. The resulting diagram is figure 50. The field of cristobalite is adjacent to that of mullite, the compound $Al_2O_3\cdot TiO_2$ and TiO_2 (rutile). The point R, at 1480°C is a reaction point, $SiO_2+Al_2O_3\cdot TiO_2=3Al_2O_3\cdot 2SiO_2+L$, with the liquid composition 8.2 percent Al_2O_3, 79.4 percent SiO_2, and 12.4 percent TiO_2. Point E at 1470°C

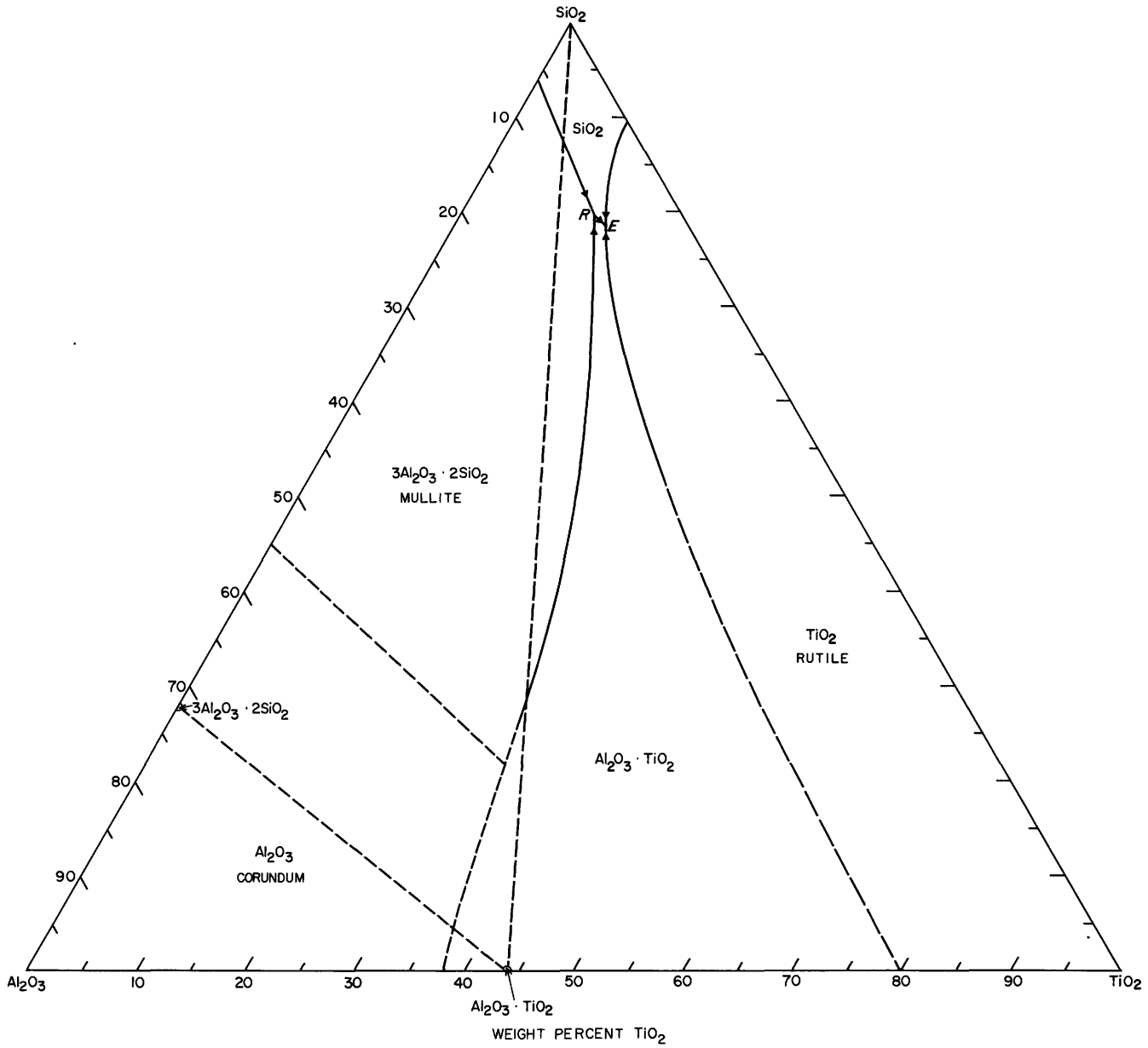

FIGURE 50.—The system Al_2O_3-SiO_2-TiO_2. Modified from Agamawi and White (1952).

is a eutectic, $SiO_2+Al_2O_3 \cdot TiO_2+TiO_2=L$, with the liquid composition Al_2O_3 7.5 percent, SiO_2 79.0 percent and TiO_2 13.5 percent. The melting point of $Al_2O_3 \cdot TiO_2$ was not determined nor was the boundary between the fields of mullite and corundum. The join SiO_2–$Al_2O_3 \cdot TiO_2$ is not binary, since it crosses the field of mullite.

Galakhov (1958) confirmed the congruent melting of $Al_2O_3 \cdot TiO_2$.

QUATERNARY SYSTEMS

Systems containing four components are usually represented by a regular tetrahedron, with each apex representing one component. Such a tetrahedron is composed of four or more primary phase volumes, each of which represents the compositions of all liquids which can coexist in equilibrium with a given solid phase. The boundaries between the volumes are surfaces representing the coexistence of two solid phases with liquid, and the meeting of four surfaces gives rise to a quaternary invariant point at which a liquid coexists with four solid phases. When the composition of the liquid at an invariant point lies within the tetrahedron formed by the compositions of the four solid phases, the invariant point is a quaternary eutectic; when the liquid is outside of that tetrahedron, the invariant point

is a reaction point. A special case is that of a phase inversion where a solid phase undergoes a polymorphous change without a change in composition. From a quaternary invariant point at constant pressure proceed four curves representing the change with temperature of a univariant equilibrium between a liquid and three solid phases.

Four-component systems usually are studied by means of sections through the tetrahedron produced by planes cutting the tetrahedron into triangles. Morey (1930d) has discussed the calculation of mixtures lying in a plane determined by any three compositions in the four-component system. The intersection of a plane with a primary phase volume gives rise to an area in the triangle; the boundary surfaces between phase volumes give rise to traces of the boundary curves; and the univariant equilibrium between a liquid and three solid phases give rise to piercing points in the triangle. When the components of the plane have been so chosen that the composition of all phases in the triangle can be represented by positive amounts of these components, the piercing point becomes a eutectic and is a point of maximum temperature on the curve representing the change of composition with temperature of the univariant reaction in question. Such a section is a ternary system.

Details of the method of working out a quaternary system and of the interpretation of the planes through a tetrahedron and their relationship to each other are exemplified by the discussion of the system K_2O–MgO–Al_2O_3–SiO_2.

Na_2O–K_2O–Al_2O_3–SiO_2

The representation of this system is a tetrahedron is figure 51, in which is shown the plane

$$Na_2O \cdot Al_2O_3 – K_2O \cdot Al_2O_3 – SiO_2$$

which includes most of the known compounds. The compositions of the dehydrated micas, paragonite and muscovite, which do not lie in this plane, are shown by crosses. The position of the system $Na_2O \cdot Al_2O_3 \cdot 2SiO_2$ (carnegieite, nepheline)–$K_2O \cdot Al_2O_3 \cdot 2SiO_2$ (kaliophilite)–SiO_2, published by Schairer (1950), is indicated. This diagram is reproduced as figure 52. The join

$$Na_2O \cdot Al_2O_3 \cdot 2SiO_2 – K_2O \cdot Al_2O_3 \cdot 2SiO_2$$

was studied by Bowen (1917). The composition

$$Na_2O \cdot Al_2O_3 \cdot 2SiO_2$$

crystallizes as carnegieite, and takes into solid solution excess of both $K_2O \cdot Al_2O_3 \cdot 2SiO_2$ and $Na_2O \cdot Al_2O_3 \cdot 6SiO_2$, giving rise to a field of solid solutions which are terminated on the albite side by formation of a nepheline solid solution at 1280°C, on the $K_2O \cdot Al_2O_3 \cdot 2SiO_2$ side by formation of a Na-K nepheline solid solution at 1404°C. The inversion temperature of nepheline to carnegieite is raised by solid solution from 1250°C in the pure compound to the intersection of the field of the Na-K nepheline with that of the field of the carnegieite solid solution. The field of the Na-K nephelines is terminated on the K_2O side by a field of orthorhombic Na-K solid solutions. The complicated relationships in the solid solutions in this binary system, both at and below the liquidus, have been discussed by Smith and Tuttle (1957).

The alkali feldspars,

$$Na_2O \cdot Al_2O_3 \cdot 6SiO_2 – K_2O \cdot Al_2O_3 \cdot 6SiO_2,$$

form a complete series of solid solutions, and this join is only in part binary, owing to the formation of leucite from 0 to 51 percent of $Na_2O \cdot Al_2O_3 \cdot 6SiO_2$. At this point the temperature is 1078°C. There is a minimum on the melting and freezing curves of these feldspars at 1063°C and 35 percent $K_2O \cdot Al_2O_3 \cdot 6SiO_2$. Each of these ternary fields will have phase spaces in the quaternary system, but these regions have not been studied. The eutectic $K_2O \cdot Al_2O_3 \cdot 4SiO_2$ + a Na-K nepheline + a Na-K feldspar = L is at 1020°C and about 48 percent $Na_2O \cdot Al_2O_3 \cdot 6SiO_2$, 20 percent $K_2O \cdot Al_2O_3 \cdot 6SiO_2$, and 32 percent SiO_2.

The complex interrelationship among the alkali feldspars is yet to be explained. Tuttle and Bowen (1950) showed that there are two distinct modifications of $Na_2O \cdot Al_2O_3 \cdot 6SiO_2$, which they described as high-temperature and low-temperature albite. X-ray studies of albite (MacKenzie, 1957) crystallized in the presence of water at 450° to 1000°C, and at pressures ranging from 14,000 to 88,000 psi suggested that at each temperature there is a stable crystalline form of $Na_2O \cdot Al_2O_3 \cdot 6SiO_2$ which is intermediate between high-temperature albite, stable only above 1000°C, and low-temperature albite, stable only below about 450°C. Bowen and Tuttle (1950) used bombs under a water pressure of 1000 to 2000 atm and found that solid solutions of the two feldspars unmixed at temperatures below the liquidus, and they determined the equilibrium curve for this unmixing. Smith and MacKenzie (1958) revised the equilibrium curve and discussed the crystallization history of some natural feldspars.

Na_2O–MgO–CaO–SiO_2

Morey (1930b) studied the effect of MgO on the liquidus relationships of a glass of the mole composition 1.15 $Na_2O \cdot 0 \cdot 0.84CaO \cdot 6SiO_2$, or 14.86 percent Na_2O, 9.83 percent CaO, 75.2 percent SiO_2, liquidus 1085°C, primary phase tridymite. When 2.4 percent MgO was

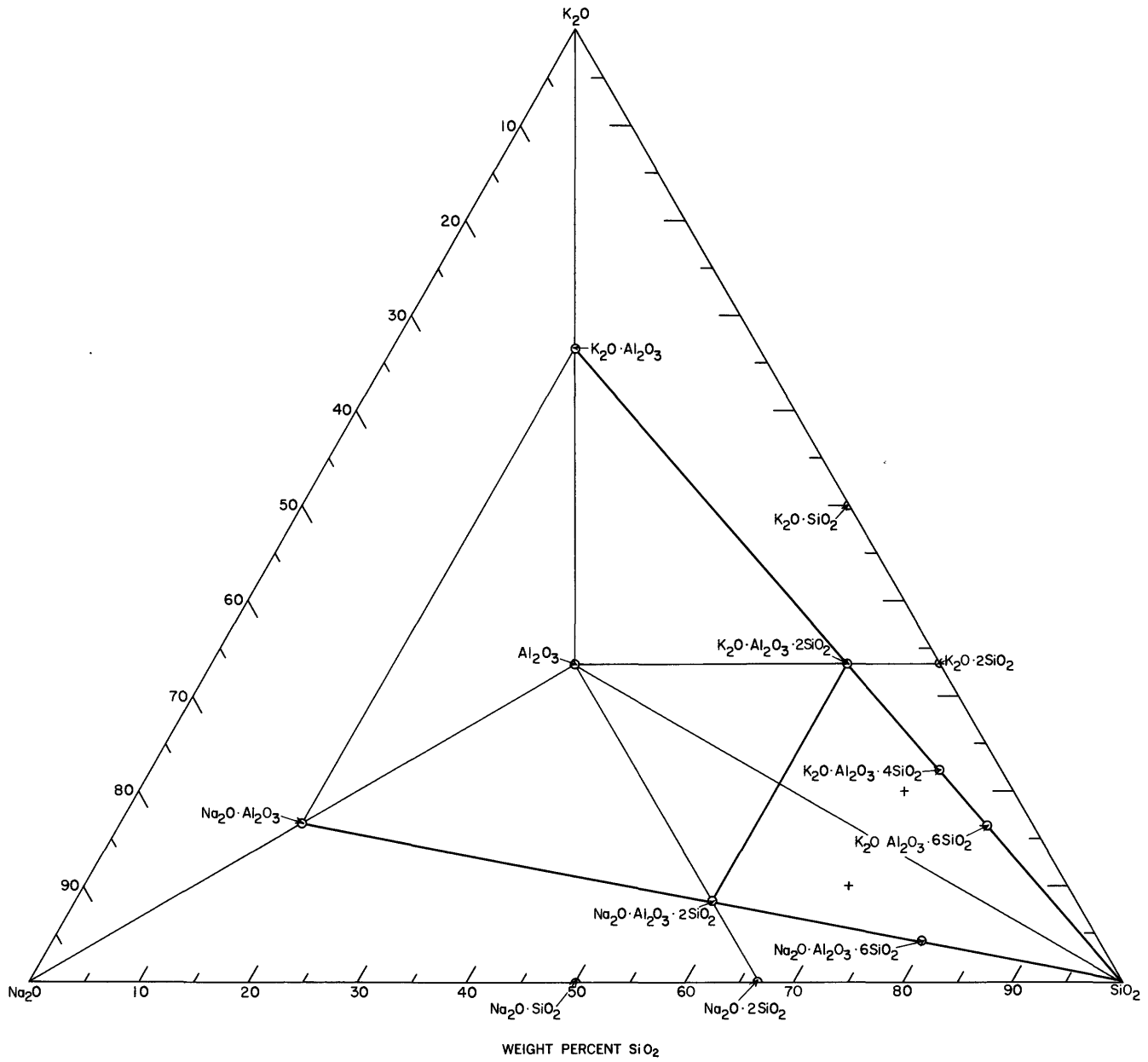

FIGURE 51.—Projection of the tetrahedron Na_2O–K_2O–Al_2O_3–SiO_2 on base Na_2O–K_2O–SiO_2 showing the position of the plane $Na_2O \cdot Al_2O_3$–$K_2O \cdot Al_2O_3$–SiO_2.

added, the melting point was lowered to 895°C with tridymite as primary phase. On further addition of MgO the glass passes into a narrow region of $Na_2O \cdot 3CaO \cdot 6SiO_2$ (devitrite) with a slight rise in temperature, after which the mixture passes into the region of $CaO \cdot MgO \cdot 2SiO_2$ (diopside) with rapid rise in liquidus temperature to 1218°C, at a glass composition of Na_2O 12.4, MgO 16.7, CaO 8.2, SiO_2 62.7. In contrast, when CaO was replaced by MgO, mole per mole, the mixture remained in the tridymite field with much smaller lowering of the melting point. When MgO was completely replaced by CaO, giving a glass of the composition Na_2O 16.1, CaO 7.1, SiO_2 76.8, the liquidus was 1013°C. When a mixture of the composition (Na_2O, MgO, CaO, $3SiO_2$) was crystallized, it gave a mixture of 50 percent $CaO \cdot MgO \cdot 2SiO_2$, some $2MgO \cdot SiO_2$, and an unknown compound, hence this composition is not a stable compound at the liquidus.

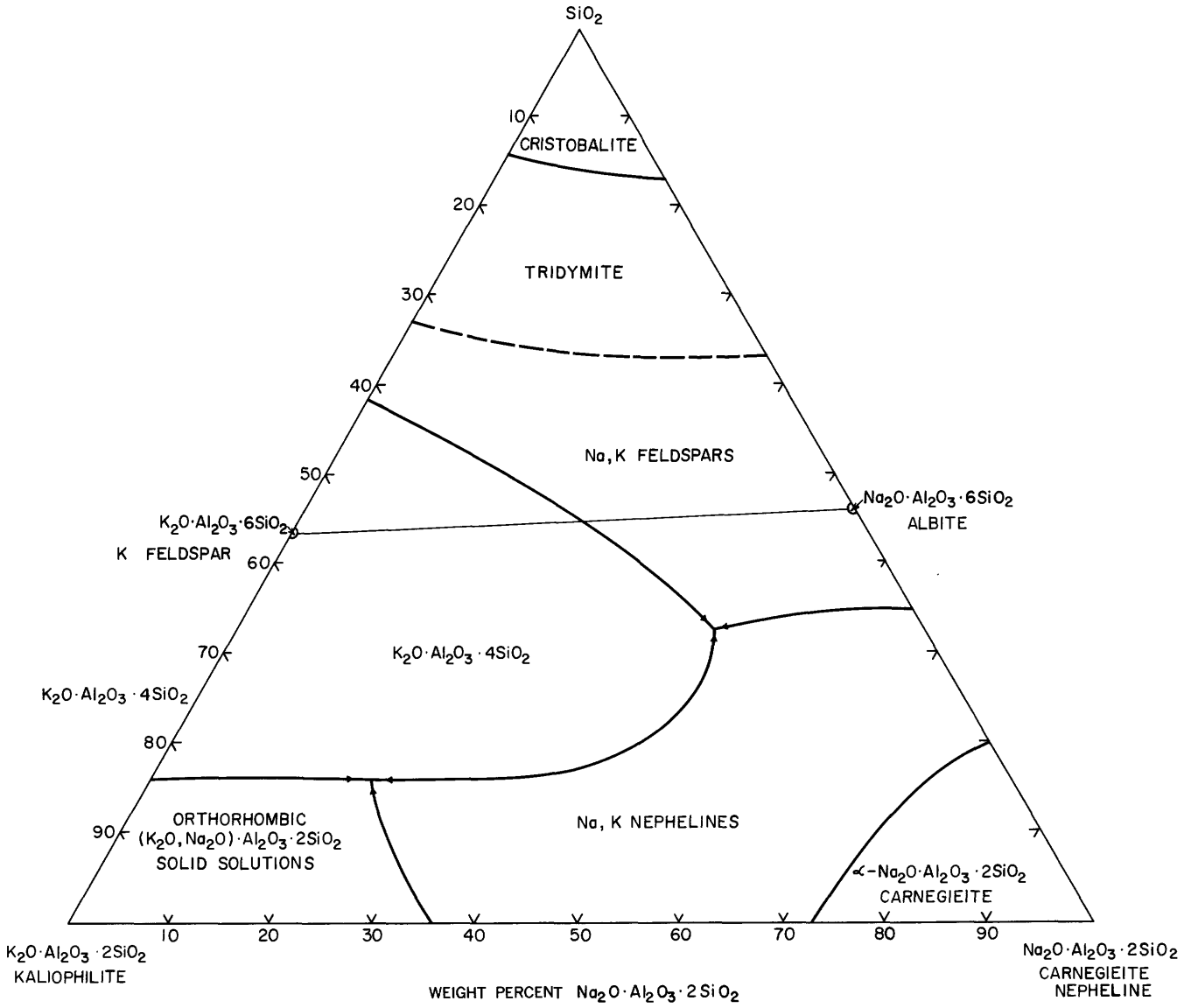

FIGURE 52.—The system $Na_2O \cdot Al_2O_3 \cdot 2SiO_2$ (carnegieite, nepheline)–$K_2O \cdot Al_2O_3 \cdot 2SiO_2$ (kaliophilite)–SiO_2. Modified from Schairer (1950).

Na_2O–MgO–Al_2O_3–SiO_2

A study of the system Na_2O–MgO–Al_2O_3–SiO_2 was begun by Schairer (1957b), who studied three planes through the tetrahedron representing this system. One of these planes (fig. 53) is the system $Na_2O \cdot Al_2O_3 \cdot 6SiO_2$ (albite) –$2MgO \cdot 2Al_2O_3 \cdot 5SiO_2$ (cordierite) –SiO_2. This plane cuts the phase volumes of $3Al_2O_3 \cdot 2SiO_2$ (mullite), cordierite, $MgO_2 \cdot Al_2O_3$ (spinel), albite, tridymite, and cristobalite. Three lines of univariant equilibrium pierce this plane at the points *C*, *G*, and *I*, respectively. Point *I* is a ternary eutectic at which the solid phases are albite, cordierite, and tridymite, and hence is a point of maximum temperature on the 4-component univariant curve along which these phases coexist with liquid. Mixtures near the binary eutectic *F*, between cordierite and albite, are viscous and require several weeks to reach equilibrium. The side albite-cordierite is not a binary system, since the field of spinel cuts across it, and cordierite melts incongruently with formation of mullite.

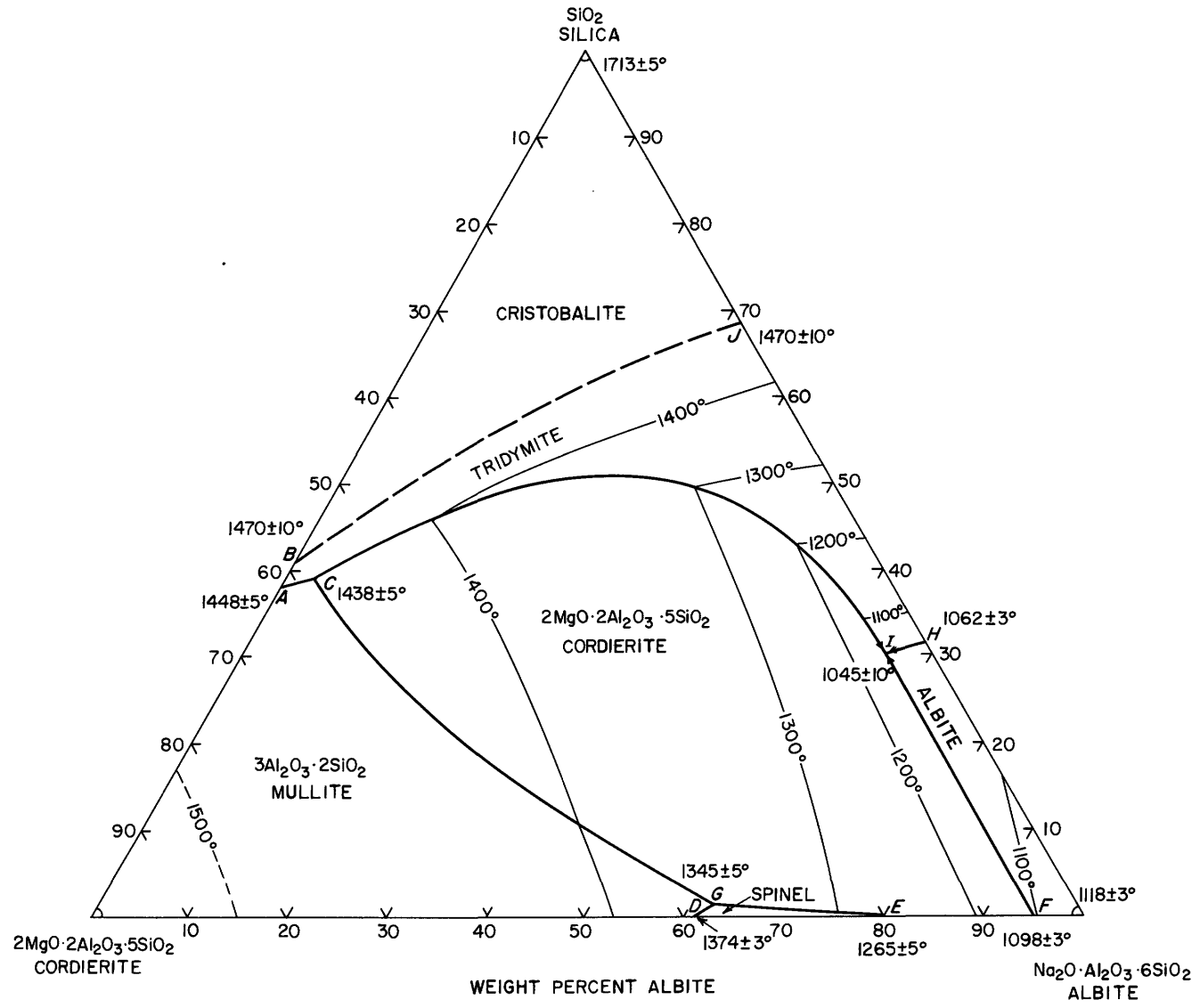

FIGURE 53.—The system $Na_2O \cdot Al_2O_3 \cdot 6SiO_2$ (albite)–$2MgO \cdot 2Al_2O_3 \cdot 5SiO_2$ (cordierite)–SiO_2. This is part of the plane $Na_2O \cdot Al_2O_3$–$MgO \cdot Al_2O_3$–SiO_2 through the tetrahedron Na_2O–MgO–Al_2O_3–SiO_2. Modified from Schairer (1957b).

Figure 54 is the system $Na_2O \cdot Al_2O_3 \cdot 6SiO_2$ (albite)–$2MgO \cdot SiO_2$ (forsterite)–$2MgO \cdot 2Al_2O_3 \cdot 5SiO_2$ (cordierite) and is represented by part of a plane passing through the tetrahedron, and cutting the phase volume of forsterite, spinel, mullite, albite, and twice through the cordierite volume. *N*, *O*, and *P* are piercing points of univariant equilibria, and *P* is a ternary eutectic at which the solid phases are albite+forsterite+cordierite. The side forsterite-albite is a binary system, but neither of the other sides is binary because of the incongruent melting of cordierite.

Figure 55 is the system $Na_2O \cdot Al_2O_3 \cdot 6SiO_2$ (albite)–$MgO \cdot SiO_2$ (enstatite)–$2MgO \cdot 2Al_2O_3 \cdot 5SiO_2$ (cordierite), and it also is part of a plane through the tetrahedron. This plane cuts the phase volumes of $2MgO \cdot SiO_2$ (forsterite), $MgO \cdot SiO_3$ (protoenstatite), albite, cordierite, spinel, and mullite, and there are three piercing points of univariant equilibria, at *U*, *V*, and *W*. None of the sides of this triangle is a binary system. Schairer and Yoder (1959) studied the system $Na_2O \cdot Al_2O_3 \cdot 2SiO_2$ (carnegieite, nepheline)–$MgO \cdot Al_2O_3$ (spinel)–SiO_2, with results shown in figure

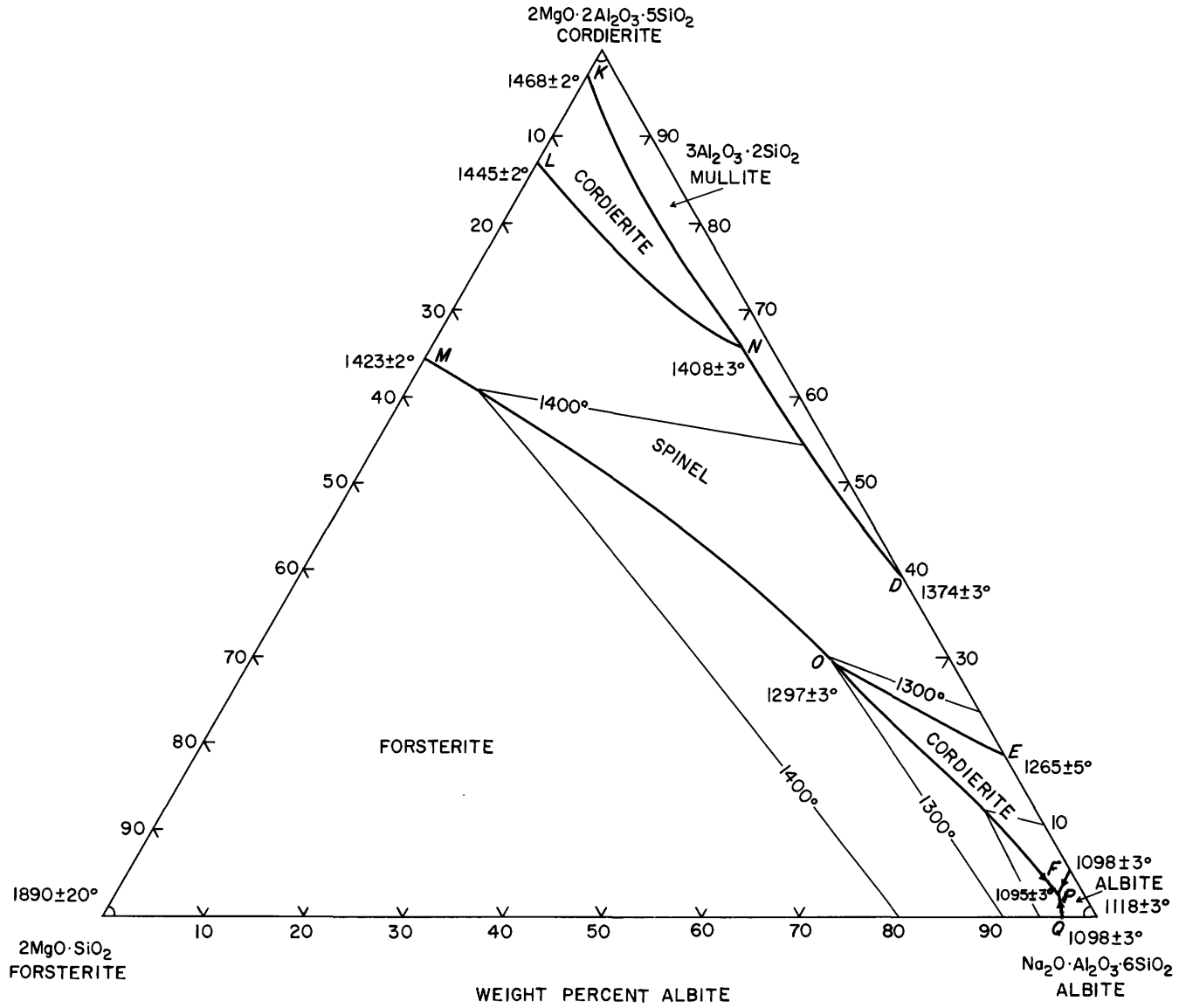

FIGURE 54.—The system $Na_2O \cdot Al_2O_3 \cdot 6SiO_2$ (albite)–$2MgO \cdot SiO_2$ (forsterite)–$2MgO \cdot 2Al_2O_3 \cdot 5SiO_2$ (cordierite). This is part of a plane through the tetrahedron Na_2O–MgO–Al_2O_3–SiO_2. Modified from Schairer (1957b).

56. This plane through the tetrahedron cuts the phase volumes of carnegieite and nepheline, which are the high- and low-temperature forms of $Na_2O \cdot Al_2O_3 2SiO_2$, of spinel, mullite, cordierite, albite, and the two forms of silica, tridymite and cristobalite. There are six piercing points of univariant equilibrium, C, G, I, K, L, and O, temperatures of which are shown in a tabular insert in the figure. The side $MgO \cdot Al_2O_3$–SiO_2 is not a binary system because of the appearance of a field of mullite.

All compositions in the triangle nepheline-spinel-albite become completely crystalline at the ternary eutectic L; those in the triangle albite-spinel-cordierite become completely crystalline at the ternary reaction point K; those in the triangle albite-cordierite-silica become completely crystalline at I. Since L, K, and I are near the side nepheline-silica, residual liquids from crystallization are poor in spinel or corundum or both and rich in albite or nepheline or both. Compositions on the silica side of the line albite-spinel which are in

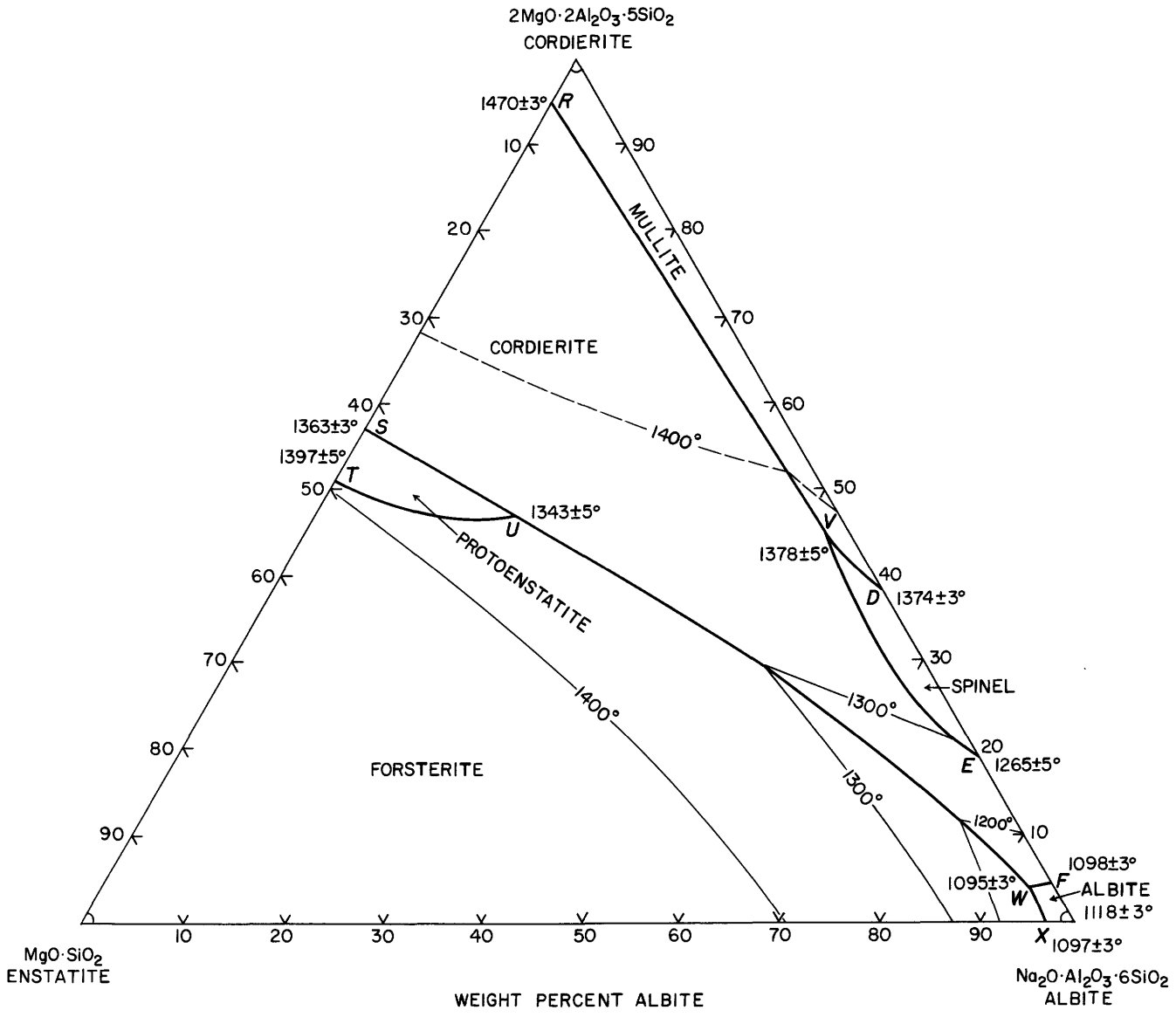

FIGURE 55.—The system $Na_2O \cdot Al_2O_3 \cdot 6SiO_2$ (albite)–$MgO \cdot SiO_2$ (enstatite)–$2MgO \cdot 2Al_2O_3 \cdot 5SiO_2$ (cordierite). This is part of a plane through the tetrahedron Na_2O–MgO–Al_2O_3–SiO_2. Modified from Schairer (1957b).

the triangle albite-spinel-cordierite have a residual liquid at *K*, which lies on the nepheline side of albite-spinel. If the residual liquid were separated from early-formed crystals, it would give a nepheline-bearing product of crystallization.

Schairer and Yoder (1960a) have published a preliminary diagram of the system $Na_2O \cdot Al_2O_3 \cdot 6SiO_2$ (albite)–$2MgO \cdot SiO_2$ (forsterite)–SiO_2 (fig. 57). Heavy lines are the boundary curves between the several solid and liquid phases. The tieline albite-enstatite divides the system into two parts. All compositions in the triangle albite-forsterite-enstatite become completely crystalline at the temperature of the point *H* (1098°±10°C). Those in the triangle albite-enstatite-silica become completely crystalline only at the temperature of the eutectic *I*, which has not been determined.

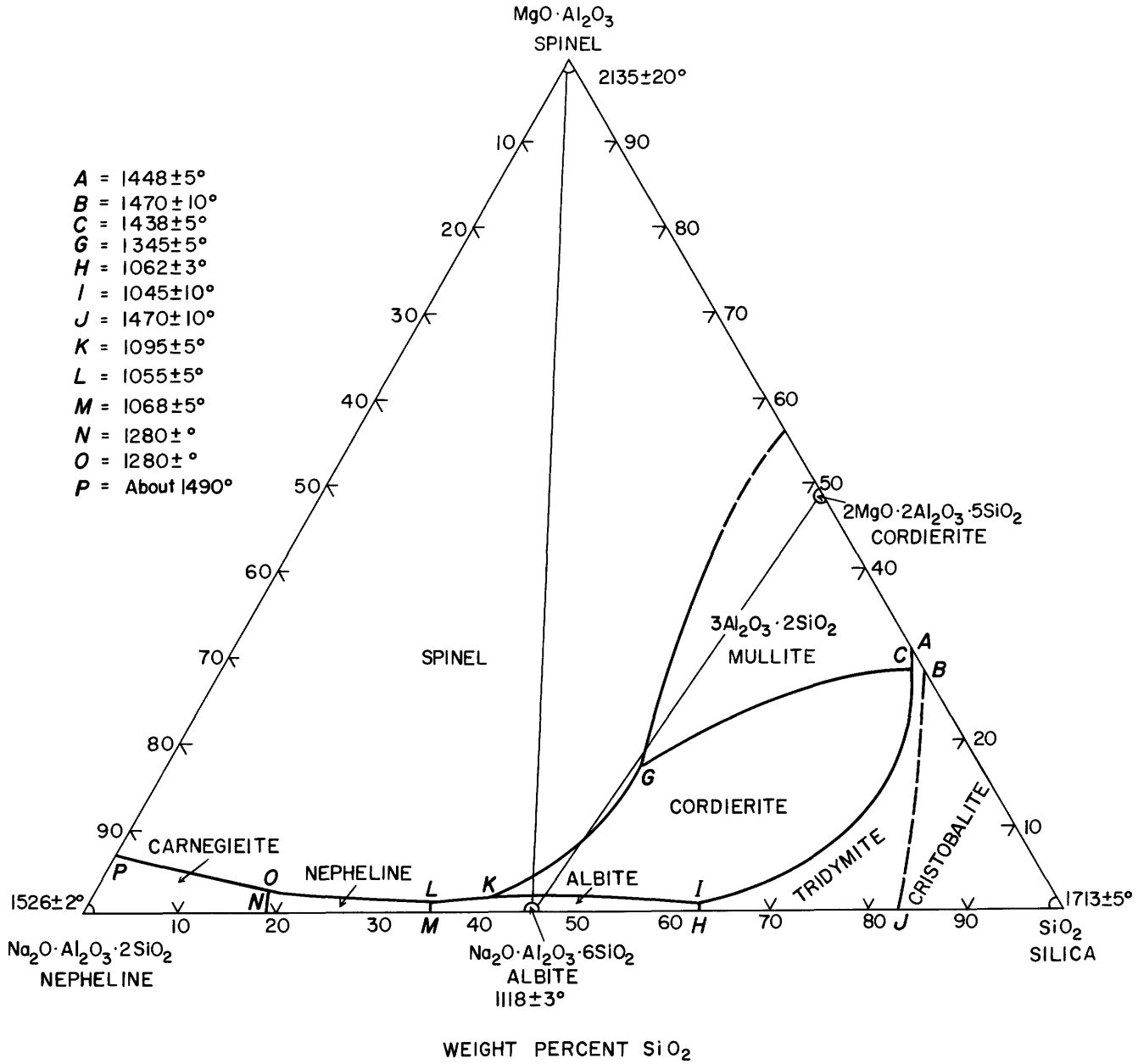

FIGURE 56.—The system Na_2O-Al_2O_3-$2SiO_2$ (carnegieite nepheline)-MgO-Al_2O_3 (spinel)-SiO_2. This is part of a plane through the tetrahedron Na_2O-MgO-Al_2O_3-SiO_2 Modified from Schairer and Yoder (1958).

Na_2O–CaO–Al_2O_3–Fe_2O_3

Planes through the system Na_2O–CaO–Al_2O_3–Fe_2O_3, which are indicated in figure 58, were studied by Eubank and Bogue (1948). One plane, the pseudoternary system CaO–the arbitrary composition (Na_2O,$3Al_2O_3$)–$4CaO \cdot Al_2O_3 \cdot Fe_2O_3$ is shown as an equilateral triangle in figure 59. No invariant points appear in this plane, but rather piercing points of univariant equilibrium in

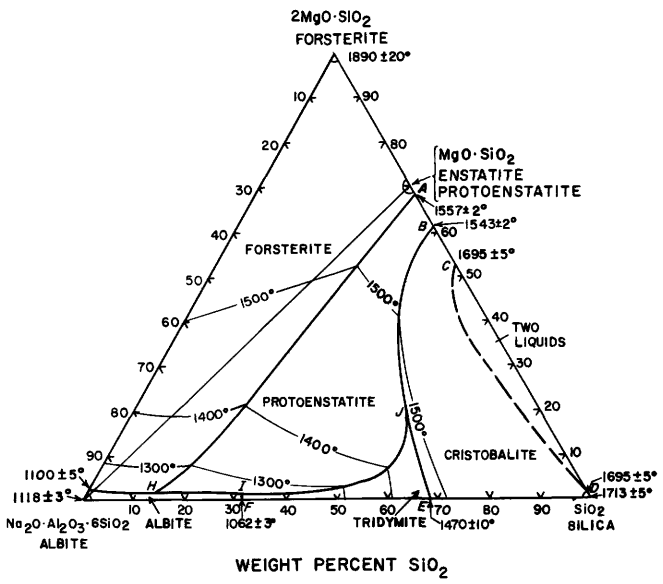

FIGURE 57.—Preliminary diagram of the system $Na_2O·Al_2O_3·6SiO_2$ (albite)–$2MgO·SiO_2$ (forsterite)–SiO_2. Modified from Schairer and Yoder (1960a).

the quaternary system. Point L, at 1390°±10°C is the piercing point of the univariant equilibrium

$$CaO+4CaO·Al_2O_3·Fe_2O_3+Na_2O·8CaO·2Al_2O_3=L.$$

The composition of the liquid is 2.3 percent Na_2O, 48.4 percent CaO, 26.8 percent Al_2O_3, and 22.3 percent Fe_2O_3; or 17 percent CaO, 67 percent $4CaO·Al_2O_3·Fe_2O_3$ and 16 percent $(Na_2O,3Al_2O_3)$. The composition of the compound $Na_2O·8CaO·3Al_2O_3$ is not in this plane. The solid phases at point H, 1399°±5°C are $4CaO·Al_2O_3·Fe_2O_3ss$, $5CaO·3Al_2O_3$, and $Na_2O·8CaO·3Al_2O_3$. The composition is 4.7 percent Na_2O, 44 percent CaO, 34.2 percent Al_2O_3, and 17.1 percent Fe_2O_3; or 20 percent CaO, 52 percent $4CaO·Al_2O_3·Fe_2O_3$ and 28 percent $(Na_2O,3Al_2O_3)$. At point K the solid phases are $Na_2O·8CaO·3Al_2O_3+5CaO·3Al_2O_3+2Na_2O·3CaO·5Al_2O_3$, the composition of which is not in the plane. The temperature is 1410°±10°C, the composition 7.8 percent Na_2O, 48.2 percent CaO, 32.8 percent Al_2O_3, and 7.2 percent Fe_2O_3; or 32 percent CaO, 22 percent $4CaO·Al_2O_3·Fe_2O_3$, and 46 percent $(Na_2O,3Al_2O_3)$.

There is a small field of Al_2O_3 extending over the composition $(Na_2O, 3Al_2O_3)$. In the plane CaO–$(Al_2O_3·Fe_2O_3)$–Al_2O_3 there is a region of $3CaO·Al_2O_3$, which has been replaced in the plane

$$CaO–(Na_2O·3Al_2O_3)–4CaO·Al_2O_3·Fe_2O_3$$

by the region of $Na_2O·8CaO·3Al_2O_3$, so between these planes will be an invariant point. To locate this point, a series of planes were explored by adding increasing amounts of Na_2O to the ternary system CaO–$5CaO·3Al_2O_3$–$2CaO·Fe_2O_3$ shown in figure 58. The planes containing 2 and 4 percent Na_2O did not show $Na_2O·8CaO·3Al_2O_3$ as primary phase, but planes containing 6, 5, and 4.5 percent Na_2O did cut its primary-phase region, the section of which at 6 percent was narrow and elliptical, extending from about 3 to 22 percent $2CaO·Fe_2O_3$. At the invariant point the Na_2O content is taken as about 4.2 percent.

Na_2O–CaO–Al_2O_3–SiO_2

The first study of the system Na_2O–CaO–Al_2O_3–SiO_2 was the classic one by Day and Allen (1905) of the plagioclase feldspars, which was the first paper published by the Geophysical Laboratory of the Carnegie Institution of Washington. This work, started in the laboratories of the U.S. Geological Survey, led to the establishment of the Geophysical Laboratory and demonstrated that exact physiochemical methods could be applied to the study of problems in geology. The paper by Day and Allen was followed by the work of Bowen (1913) who applied the newly developed quenching method. Figure 60 is by Bowen, modified by some unpublished results by J. F. Schairer. The position of the line $CaO·Al_2O_3·2SiO_2$–$Na_2O·Al_2O_3·6SiO_2$ is indicated by a broken line in figure 61.

This system, of fundamental importance in geochemistry, is a classic example of a complete solid-solution series showing neither a maximum nor a minimum. When, for example, a molten mixture of 60 percent of albite and 40 percent anorthite is cooled, at about 1420°C, crystals of plagioclase feldspar separate of composition given by the point on the lower or solidus curve at 1420°C, approximately 25 percent albite and 75 percent anorthite. On further cooling, the composition of the liquid follows the upper or liquidus curve, and the composition of the solid follows the solidus curve. At about 1200°C the mixture solidifies completely to a solid solution of composition 60 percent albite and 40 percent anorthite.

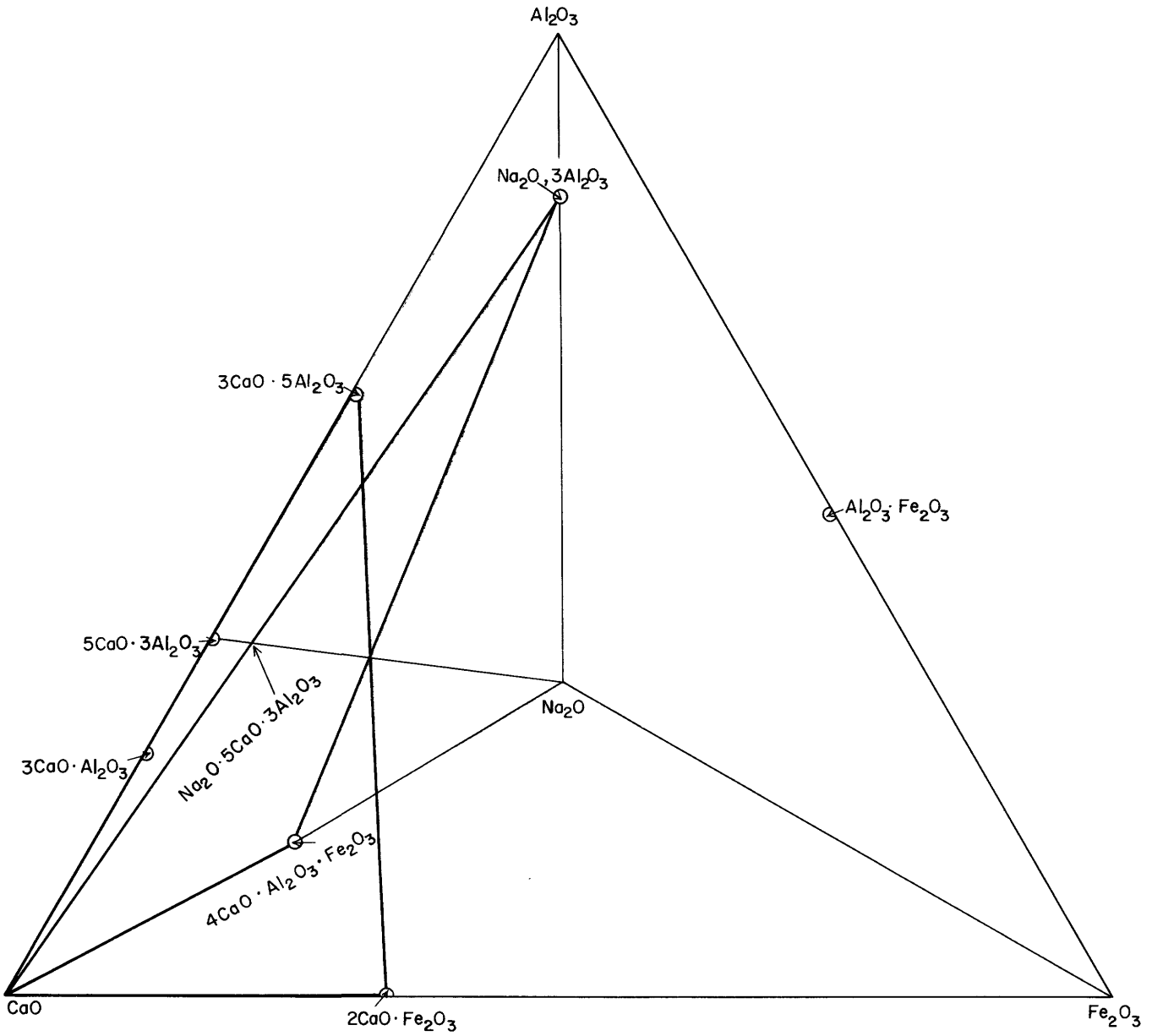

FIGURE 58.—The system Na_2O–CaO–Al_2O_3–Fe_2O_3, showing the position of planes which have been studied.

The pioneering work of Day and Allen and Bowen was followed much later by several studies which have given a comprehensive knowledge of the phase equilibrium relationships in this system. Figure 61 indicates the relation of each of these studies to the system as a whole.

Foster (1942) studied the system

$Na_2O \cdot Al_2O_3 \cdot 2SiO_2$–$CaO \cdot SiO_2$–$Na_2O \cdot Al_2O_3 \cdot 6SiO_2$

with results indicated in figure 62. This is a plane through the tetrahedron of figure 61, and shares a side, $CaO \cdot SiO_2$–$Na_2O \cdot Al_2O_3 \cdot 2SiO_2$, with the two following systems. The side $CaO \cdot SiO_2$–$Na_2O \cdot Al_2O_3 \cdot 2SiO_2$ is a binary system, with a eutectic at 1164°±2°C, 59 percent $Na_2O \cdot Al_2O_3 \cdot 2SiO_2$ (7.0 percent Na_2O, 20.2 percent CaO, 11.5 percent Al_2O_3, and 61.3 percent SiO_2). The nepheline-carnegieite inversion is raised 13°C by between 5 and 10 mol percent solid solution in nepheline,

695-382 O - 64 - 7

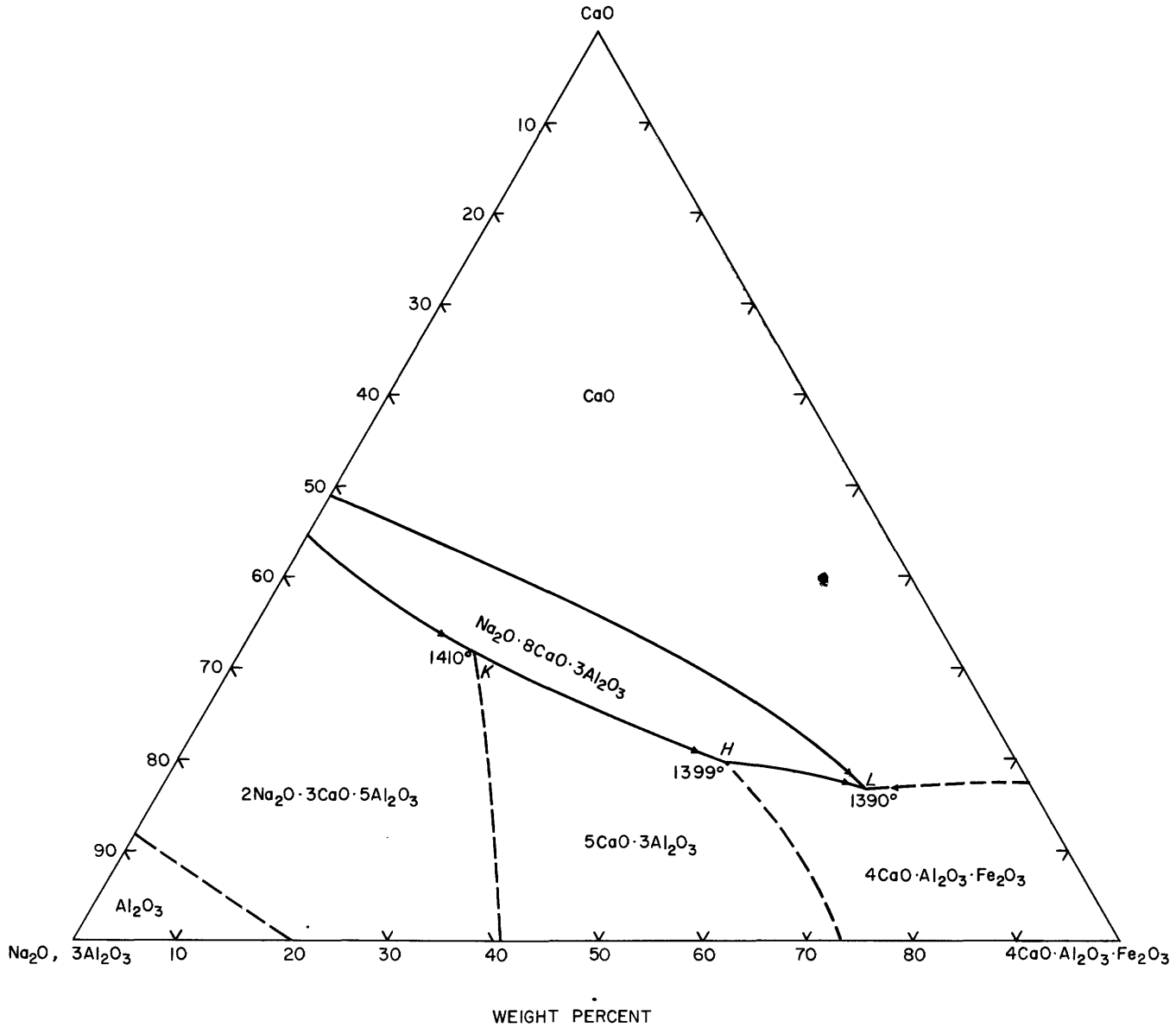

FIGURE 59.—The pseudoternary system CaO–the composition $Na_2O,3Al_2O_3$–the compound $4CaO \cdot Al_2O_3 \cdot Fe_2O_3$. Based on Eubank and Bogue (1948).

practically none in carnegieite. The join $CaO \cdot SiO_2$–$Na_2O \cdot Al_2O_3 \cdot 6SiO_2$ is not binary. Pseudowollastonite crystallizes out with lowering liquidus temperatures until at 1125°C and about 89 percent albite a plagioclase feldspar of undetermined composition separates. The boundary between the fields of α- and β-$CaO \cdot SiO_2$ (pseudowollastonite and wollastonite) is the line of constant temperature 1125°C, since there is no solid solution. The fields of α- and β-$Na_2O \cdot Al_2O_3 \cdot 2SiO_2$ are separated by an inversion line, but solid solution in nepheline raises the inversion to 1267°C in the binary system $Na_2O \cdot Al_2O_3 2SiO_2$–$CaO \cdot SiO_2$, and 1280°C in $Na_2O \cdot Al_2O_3 \cdot 2SiO_2$–$Na_2O \cdot Al_2O_3 \cdot 6SiO_2$. The composition $Na_2O \cdot Al_2O_3 \cdot 6SiO_2$ is surrounded by an almost flat field of plagioclase feldspar, and the points at which these fields of wollastonite, plagioclase, and nepheline

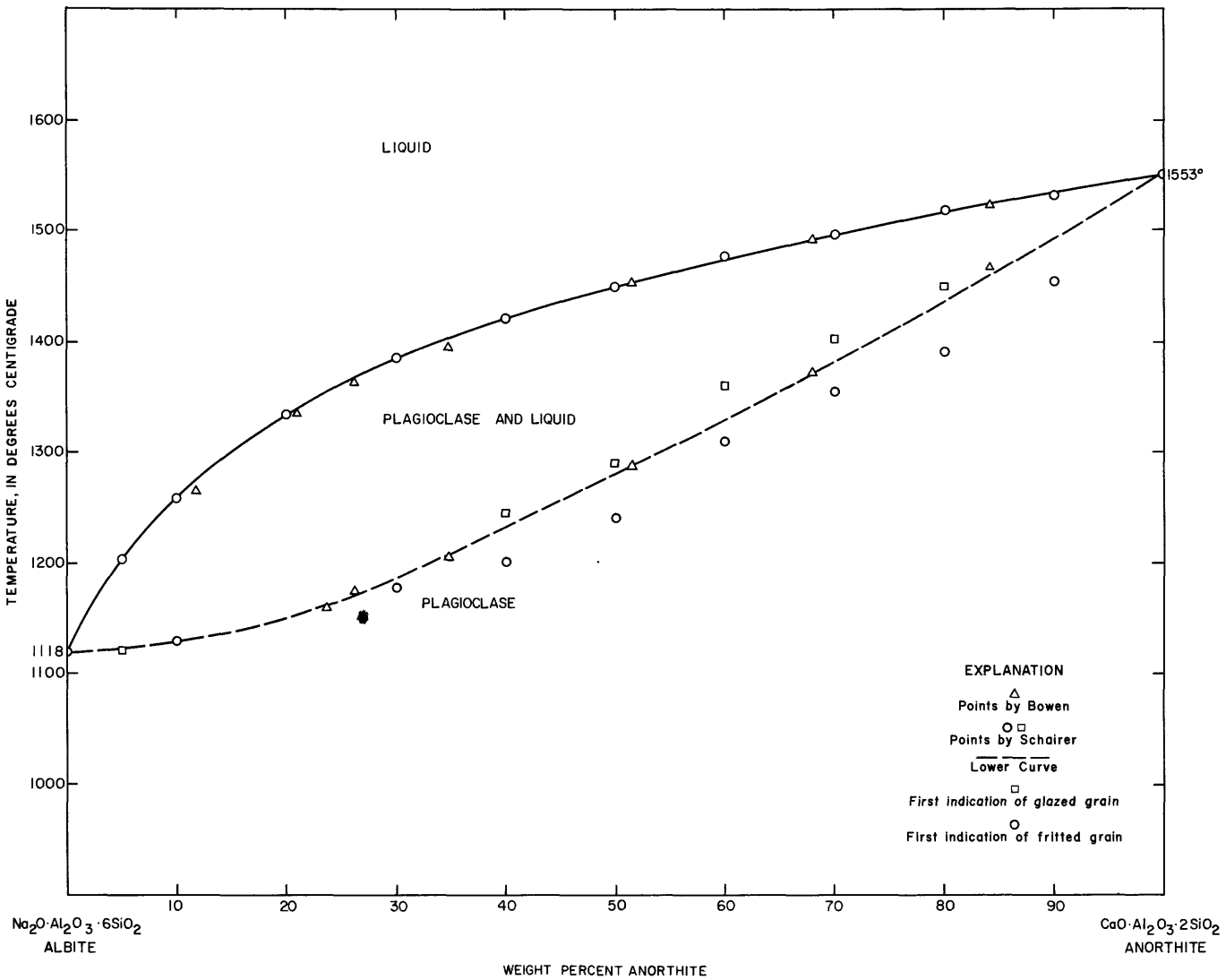

FIGURE 60.—The system $Na_2O \cdot Al_2O_3 \cdot 6SiO_2$ (albite)–$CaO \cdot Al_2O_3 \cdot 2SiO_2$ (anorthite). Based on Bowen (1913) with additional points by J. F. Schairer (written communication, 1960).

solid solutions meet is not an invariant point, but the piercing point in this plane of the invariant equilibrium containing these three solids and a liquid.

A second plane through this quaternary system is $NaO \cdot Al_2O_3 \cdot 2SiO_2$–$CaO \cdot SiO_2$–$CaO \cdot Al_2O_3 \cdot 2SiO_2$ (fig. 63) studied by Gummer (1943). This shares a side, $Na_2O \cdot Al_2O_3 \cdot 2SiO_2$–$CaO \cdot SiO_2$, with the preceding and following diagrams. The primary phase fields occuring in the plane are: (1) $CaO \cdot SiO_2$, as α-$CaO \cdot SiO_2$ (pseudowollastonite); (2) plagioclase feldspar, largely anorthite ($CaO \cdot Al_2O_3 \cdot 2SiO_2$), but containing some $Na_2O \cdot Al_2O_3 \cdot 6SiO_2$ in solid solution; (3) the two forms of $Na_2O \cdot Al_2O_3 \cdot 2SiO_2$ (carnegieite and a nepheline solid solution) with the inversion temperature ranging from 1267° to 1352° C; (4) a field indicated as β-alumina, resulting from a decomposition reaction which makes this section no longer ternary; and (5) a field indicated as $2CaO \cdot Al_2O_3 \cdot SiO_2$ (gehlenite), which has a primary phase field in the boundary system $CaO \cdot Al_2O_3$–SiO_2. There is a maximum on the boundary curve between the

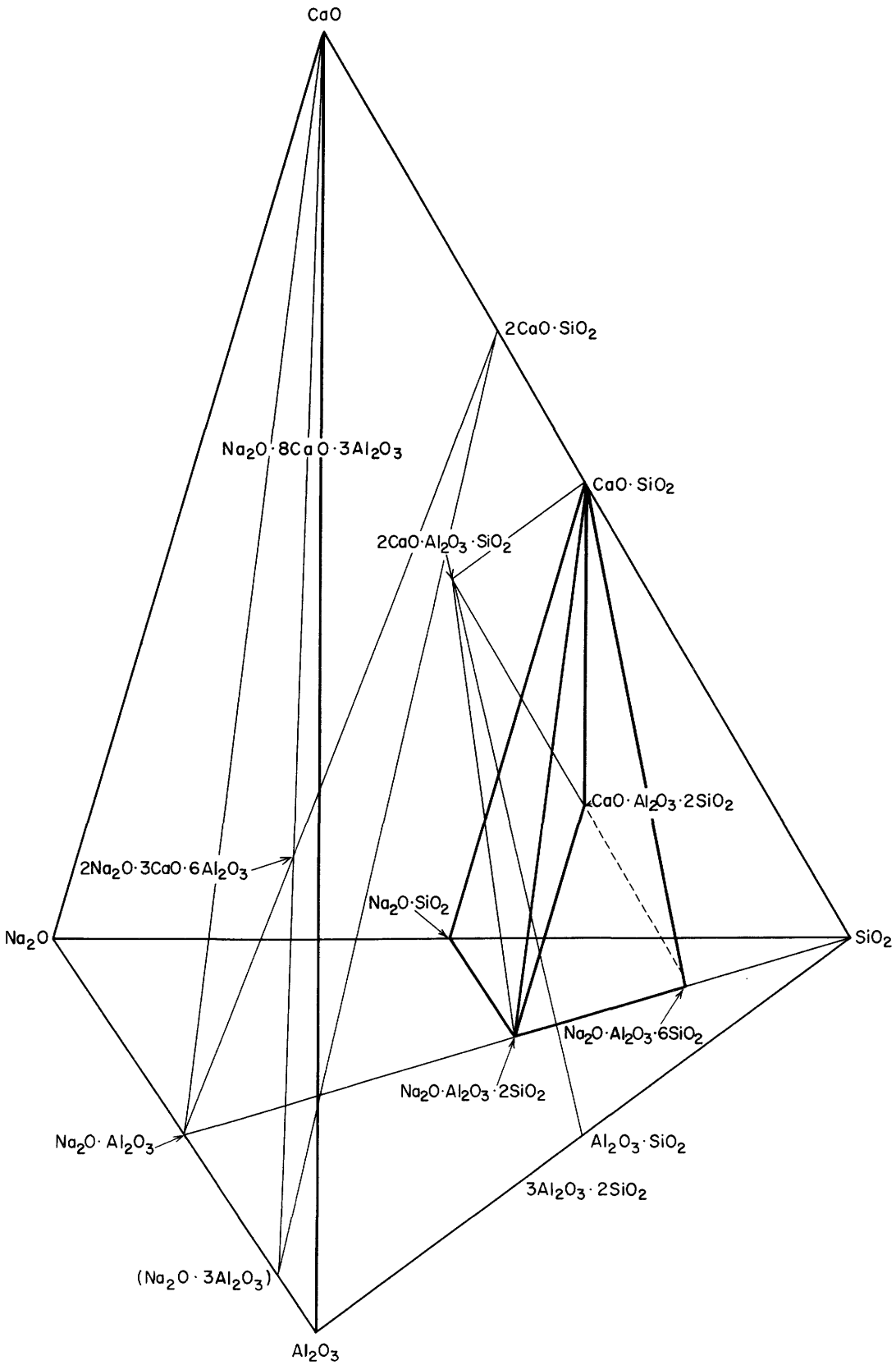

FIGURE 61.—The tetrahedron representing the system Na_2O–CaO–Al_2O_3–SiO_2 showing the numerous planes which have been studied.

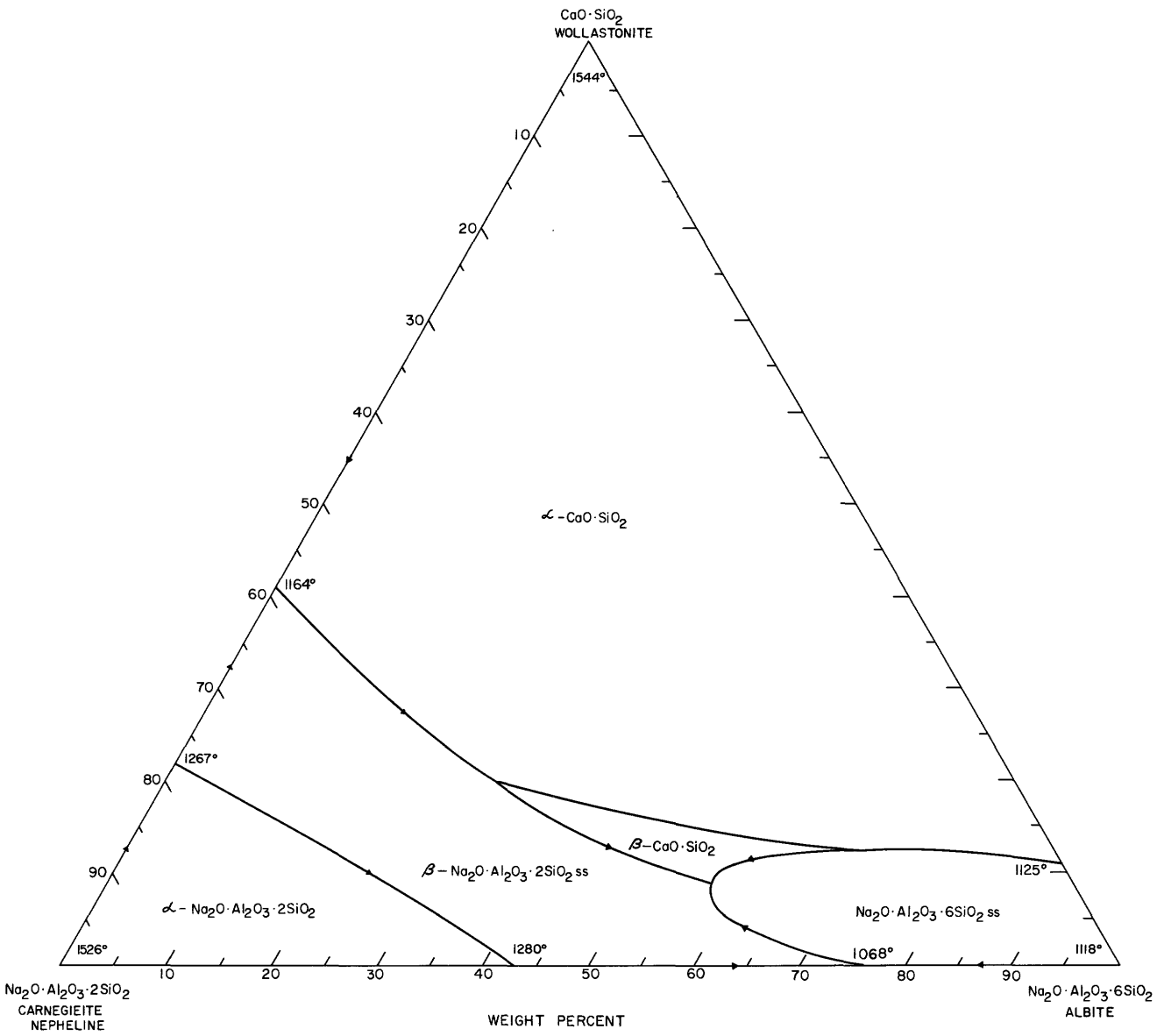

FIGURE 62.—The plane $Na_2O \cdot Al_2O_3 \cdot 2SiO_2$ (carnegieite, nepheline)–$CaO \cdot SiO_2$ (wollastonite)–$Na_2O \cdot Al_2O_3 \cdot 6SiO_2$ (albite) through the tetrahedron Na_2O–CaO–Al_2O_3–SiO_2. Modified from Foster (1942). *ss* solid solution.

the fields of pseudowollastonite and nepheline solid solutions. Since there is no solid solution in the $CaO \cdot SiO_2$, the composition of the nepheline solid solution in equilibrium with pseudowollastonite at this point of maximum temperature must be on the line passing through $CaO \cdot SiO_2$ and this point.

A third section, $Na_2O \cdot SiO_2$–$CaO \cdot SiO_2$–$Na_2O \cdot Al_2O_3 \cdot 2SiO_2$ (fig. 64), through the tetrahedron Na_2O–CaO–Al_2O_3–SiO_2 studied by Spivak (1944), shares the side $Na_2O \cdot Al_2O_3 \cdot 2SiO_2$–$CaO \cdot SiO_2$ with the two preceding sections, and the side $Na_2O \cdot SiO_2$–$CaO \cdot SiO_2$ was worked out by Morey and Bowen (1925). No new compounds are formed and the system is ternary except that the compositions of some of the nepheline solid solutions require the inclusion of $CaO \cdot Al_2O_3 \cdot 2SiO_2$, which is outside of this section. The field of $CaO \cdot SiO_2$ is entirely pseudowollastonite, and is bounded by the fields of $Na_2O \cdot 2CaO_2 \cdot 3SiO_2$ and nepheline solid solutions. The ternary eutectic, E_1, $Na_2O \cdot 2CaO \cdot 3SiO_2 + CaO \cdot SiO_2$ + nepheline solid solutions containing 8 percent $CaO \cdot Al_2O_3 \cdot 2SiO_2 = L$

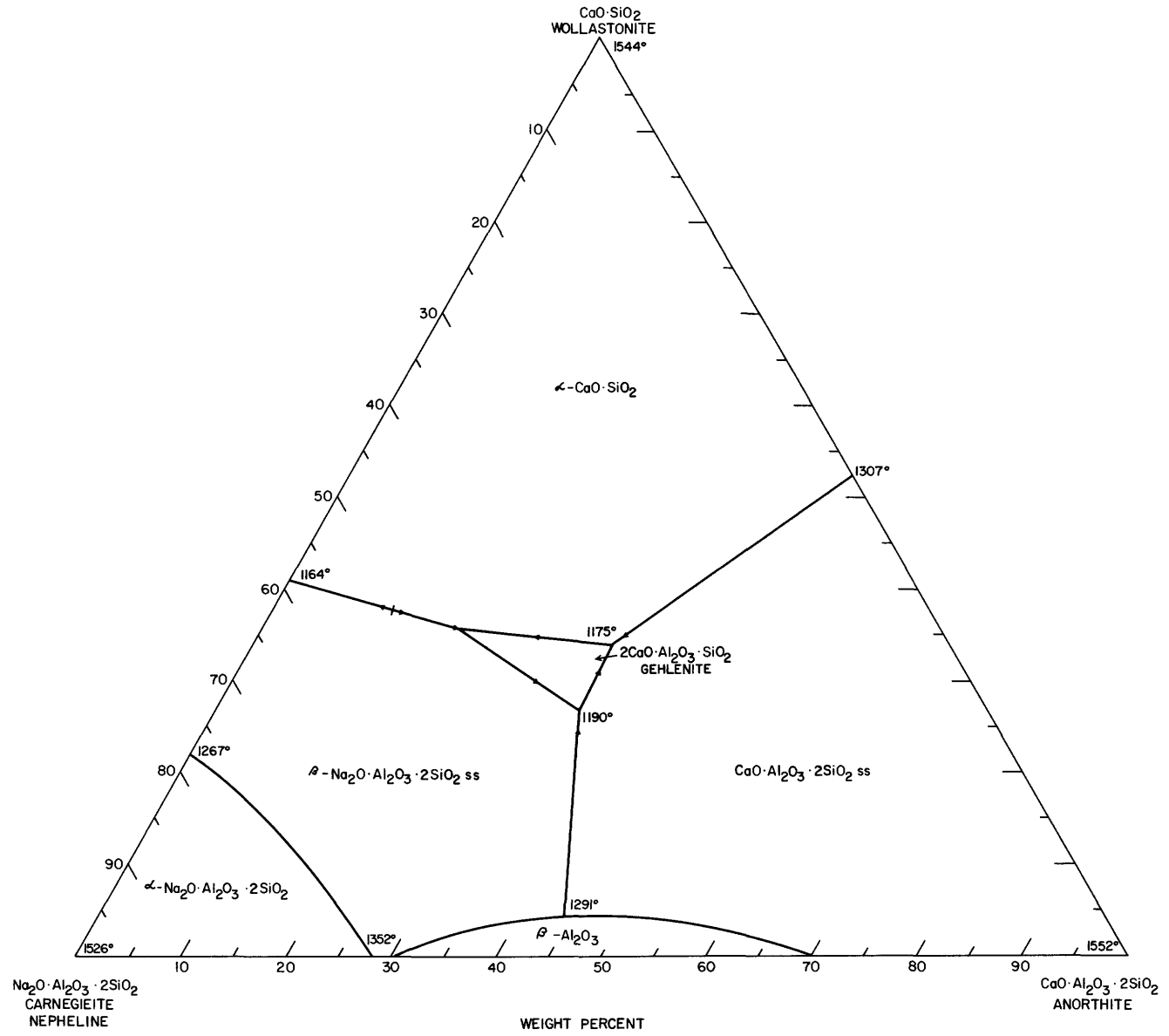

FIGURE 63.—The plane $Na_2O{\cdot}Al_2O_3{\cdot}2SiO_2$ (carnegieite, nepheline)–$CaO{\cdot}SiO_2$ (wollastonite)–$CaO{\cdot}Al_2O_3{\cdot}2SiO_2$ (anorthite) through the tetrahedron Na_2O–CaO–Al_2O_3–SiO_2. Modified from Gummer (1943). *ss* solid solution.

is at 1120°±3°C, 13.6 percent $Na_2O{\cdot}SiO_2$, 39.4 percent $CaO{\cdot}SiO_2$, and 47.0 percent $Na_2O{\cdot}Al_2O_3{\cdot}2SiO_2$. The field of $Na_2O{\cdot}2CaO{\cdot}3SiO_2$ occupies a large part of the phase triangle, and spreads over the composition of $2Na_2O{\cdot}CaO{\cdot}3SiO_2$. At point *R*, 985°±8°C, the reaction is $2Na_2O{\cdot}CaO{\cdot}3SiO_2$+nepheline solid solution containing 5 percent $CaO{\cdot}Al_2O_3{\cdot}2SiO_2$= $Na_2O{\cdot}2CaO{\cdot}3SiO_2+L$ and the liquid is 47.8 percent $Na_2O{\cdot}SiO_2$, 8.8 percent $CaO{\cdot}SiO_2$, and 42.5 percent $Na_2O{\cdot}Al_2O_3{\cdot}2SiO_2$. The join $Na_2O{\cdot}2CaO{\cdot}3SiO_2$–$Na_2O{\cdot}Al_2O_3{\cdot}2SiO_2$ is not a binary system because of solid solution, and the maximum on the boundary curve at 1128°C is not on the join but at 35.5 percent $CaO{\cdot}SiO_2$. The narrow field of the incongruently melting $2Na_2O \cdot CaO \cdot 3SiO_2$ falls to a eutectic, E_2, $Na_2O{\cdot}SiO_2+2Na_2O{\cdot}CaO{\cdot}SiO_2$+ nepheline solid solution containing approximately 1 percent $CaO{\cdot}Al_2O_3{\cdot}2SiO_2=L$, at 892°±2°C, 51.8 percent

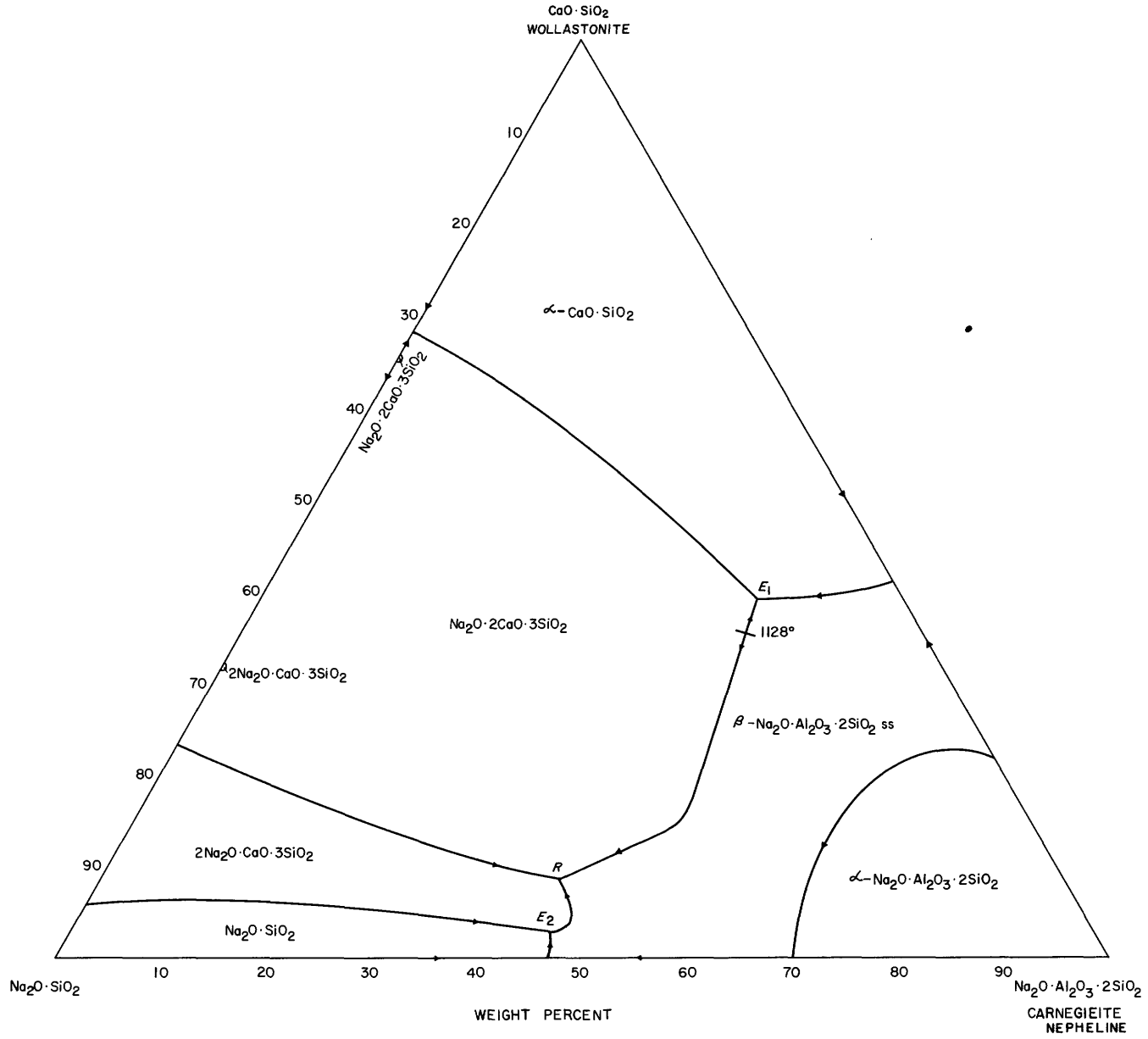

FIGURE 64.—The plane $Na_2O·SiO_2$–$CaO·SiO_2$ (wollastonite)–$Na_2O·Al_2O_3·2SiO_2$ (carnegieite, nepheline) through the tetrahedron Na_2O–CaO–Al_2O_3–SiO_2. Modified from Spivak (1944). *ss* solid solution.

$Na_2O·SiO_2$, 2.8 percent $CaO·SiO_2$, and 45.4 percent $Na_2O·Al_2O_3·2SiO_2$. The temperature of the inversion of nepheline to carnegieite is lowered in the system $Na_2O·SiO_2$–$Na_2O·Al_2O_3·2SiO_2$ because of the solid solution in carnegieite, and in the system $CaO·SiO_2$–Na_2O–$Al_2O_3·2SiO_2$ it is raised by solid solution in nepheline.

The join $Na_2O·Al_2O_3·2SiO_2$ (carnegieite, nepheline)–$2CaO·Al_2O_3·SiO_2$ (gehlenite) was studied by Smalley (1947) and the plane $Na_2O·Al_2O_3·2SiO_2$ (carnegieite, nepheline)–$CaO·SiO_2$ (wollastonite)–$2CaO·Al_2O_3·SiO_2$ (gehlenite) by Juan (1950). This plane is not a ternary system because both carnegieite and nepheline form solid solutions of composition out-

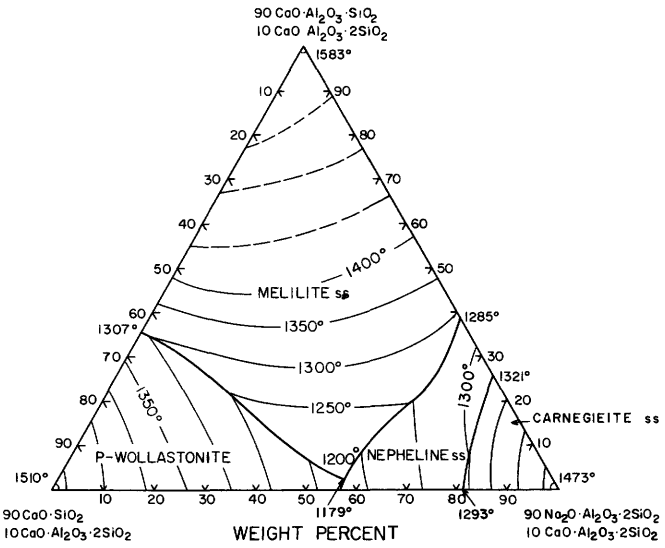

FIGURE 65.—The plane obtained by adding 10 percent $CaO \cdot Al_2O_3 \cdot 2SiO_2$ to the plane $Na_2O \cdot Al_2O_3 \cdot 2SiO_2$–$CaO \cdot SiO_2$–$2CaO \cdot Al_2O_3 \cdot SiO_2$ through the tetrahedron Na_2O–CaO–Al_2O_3–SiO_2. Modified from Yoder (1952b). *ss*, solid solution.

side of this plane, and the phase spreading out from $2CaO \cdot Al_2O_3 \cdot SiO_2$ is not gehlenite but a melilite solid solution. The piercing point of the univariant equilibrium α–$CaO \cdot SiO_2$ (pseudowollastonite) + nepheline solid solutions + melilite solid solutions + liquid is at 1174°C and the composition of the liquid is approximately 54 percent $Na_2O \cdot Al_2O_3 \cdot 2SiO_2$, 37 percent $CaO \cdot SiO_2$, 9 percent $2CaO \cdot Al_2O_3 \cdot SiO_2$. There is a maximum temperature on the trace of the boundary between the phase volume of $CaO \cdot SiO_2$ and nepheline solid solutions at 1182°C and about 6 percent of $2CaO \cdot Al_2O_3 \cdot SiO_2$.

A similar maximum was found by Gummer (1943) in his study of the plane

$$CaO \cdot SiO_2\text{–}Na_2O \cdot Al_2O_3 \cdot 2SiO_2\text{–}CaO \cdot Al_2O_3 \cdot 2SiO_2.$$

Yoder (1952b) added 10 percent $CaO \cdot Al_2O_3 \cdot 2SiO_2$ to this plane,

$$Na_2O \cdot Al_2O_3 \cdot 2SiO_2\text{–}CaO \cdot SiO_2\text{–}2CaO \cdot Al_2O_3 \cdot SiO_2,$$

and located the piercing point of the equilibrium α–$CaO \cdot SiO_2$ (pseudowollastonite) + nepheline solid solution + melilite solid solution + liquid at 1173°C. His results are shown in figure 65, in which are shown the boundaries of the fields of pseudowollastonite, melilite solid solutions, nepheline solid solutions, and carnegieite solid solutions. The temperature maximum on the trace of the pseudowollastonite-nepheline solid solution boundary found by Juan and by Gummer has disappeared on the addition of 10 percent of $CaO \cdot Al_2O_3 \cdot 2SiO_2$.

Goldsmith (1947) studied the plane

$$CaO \cdot Al_2O_3 \cdot 2SiO_2\text{–}2CaO \cdot Al_2O_3 \cdot SiO_2\text{–}Na_2O \cdot Al_2O_3 \cdot 2SiO_2.$$

The phase-equilibrium diagram (fig. 66) is not ternary. The plane cuts the primary-phase volumes of a calcic plagioclase feldspar extending from $CaO \cdot Al_2O_3 \cdot 2SiO_2$, of a melilite solid solution extending from $2CaO \cdot Al_2O_3 \cdot SiO_2$, and of carnegieite and nepheline solid solutions extending from $Na_2O \cdot Al_2O_3 \cdot 2SiO_2$. There is a slight maximum on the trace of the boundary surface between melilite and nepheline solid solutions, and the piercing point of the univariant-equilibrium plagioclase feldspar (melilite), nepheline solid solutions, and liquid is at 1266°C, 39.5 percent $CaO \cdot Al_2O_3 \cdot 2SiO_2$, 27.5 percent $2CaO \cdot Al_2O_3 \cdot SiO_2$, and 33 percent $Na_2O \cdot Al_2O_3 \cdot 2SiO_2$. There is another piercing point, at which the phases are plagioclase feldspar, a nepheline solid solution, and β-Al_2O_3. Goldsmith also located the piercing point of the univariant-equilibrium plagioclase feldspar + melilite solid solution + nepheline solid solution + liquid in the plane obtained by adding 10 percent $CaO \cdot SiO_2$ to the plane

$$CaO \cdot Al_2O_3 \cdot 2SiO_2\text{–}2CaO \cdot Al_2O_3 \cdot SiO_2\text{–}Na_2O \cdot Al_2O_3 \cdot 2SiO_2.$$

The temperature is 1248°C and the composition of the liquid is 35.7 percent $CaO \cdot Al_2O_3 \cdot 2SiO_2$, 17.8 percent $2CaO \cdot Al_2O_3 \cdot SiO_2$, 36.5 percent $Na_2O \cdot Al_2O_3 \cdot 2SiO_2$, and 10 percent $CaO \cdot SiO_2$.

Schairer (1957a) published a preliminary diagram of the section

$$Na_2O \cdot Al_2O_3 \cdot 2SiO_2\text{–}CaO \cdot Al_2O_3 \cdot 2SiO_2\text{–}SiO_2$$

(fig. 67). This is not a ternary system because of the occurrence of a field of alumina in the diagram. The section is dominated by the large field of plagioclase feldspar.

Morey (1930c) replaced CaO by Al_2O_3, mole for mole, in a glass of the composition 1.15 Na_2O, 0.84 CaO, $6SiO_2$ and found that the liquidus fell from 1075°C with tridymite as solid phase, to 990°C, where $Na_2O \cdot 3CaO \cdot 6SiO_2$ (devitrite) became a solid phase, after which it rose to a maximum of about 1030°C with about 8 percent Al_2O_3, then fell to about 1000°C at 12 percent Al_2O_3, when $CaO \cdot SiO_2$ became a solid phase, after which temperatures rose uniformly until at about 1060°C, 17 percent Al_2O_3, when $Na_2O \cdot Al_2O_3 \cdot 6SiO_2$ became a solid phase. When Al_2O_2 was added to the

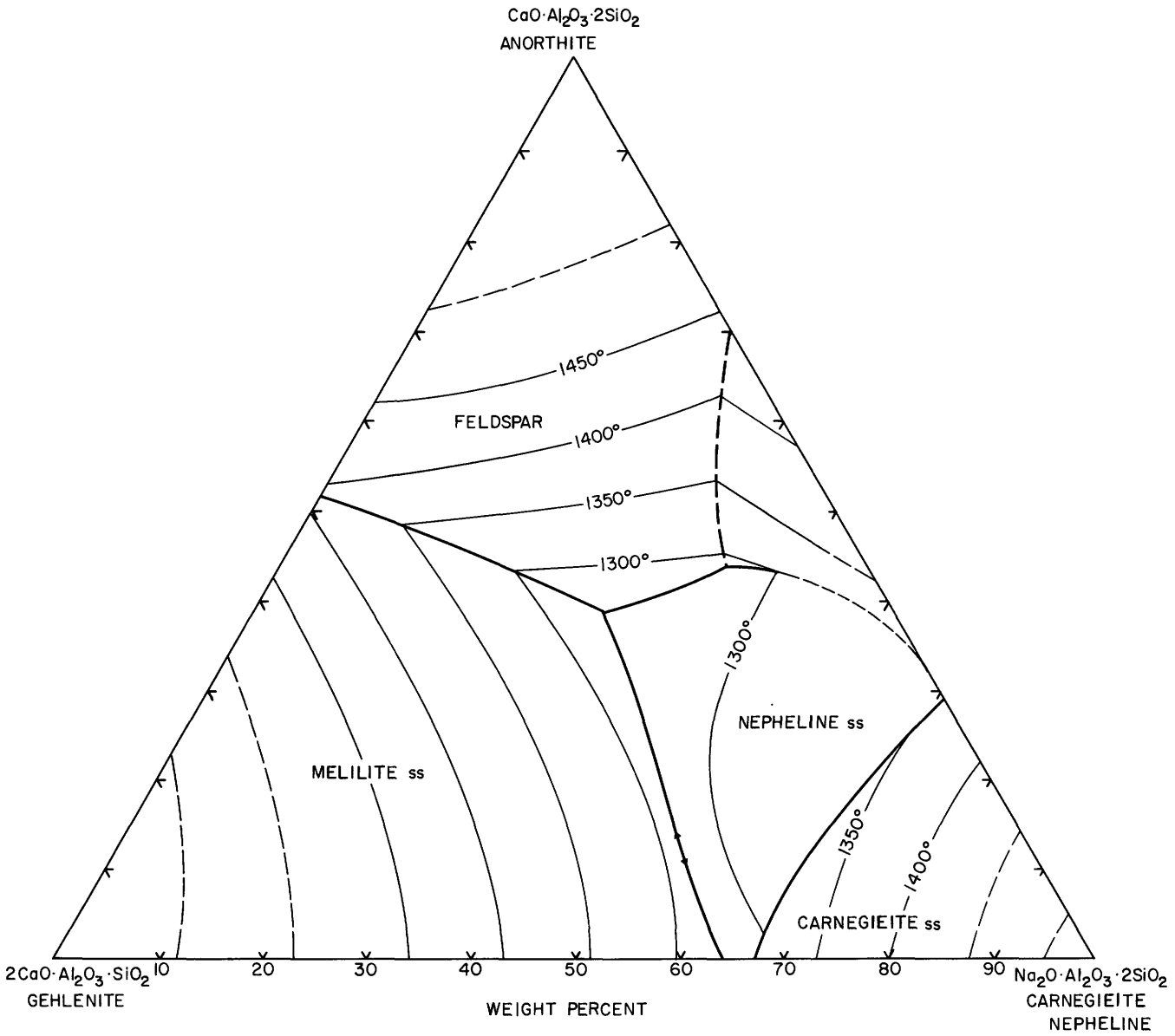

FIGURE 66.—The plane $CaO \cdot Al_2O_3 \cdot 2SiO_2$ (anorthite)–$2CaO \cdot Al_2O_3 \cdot SiO_2$ (gehlenite)–$Na_2O \cdot Al_2O_3 \cdot 2SiO_2$ (carnegieite, nepheline) through the tetrahedron Na_2O–CaO–Al_2O_3–SiO_2. Modified from Goldsmith (1947). *ss*, solid solution.

above glass, a narrow field of devitrite was met, followed by a field of CaO–SiO_2. The final mixture of this series had the composition 13 percent Na_2O, 10.0 percent CaO, 9.1 percent Al_2O_3, 67.9 percent SiO_2, liquidus 1156°C with $CaO \cdot SiO_2$ as primary phase.

Greene and Bogue (1946) studied two planes high in CaO. One was the plane

$$CaO\text{–}2CaO \cdot SiO_2\text{–}(Na_2O + 6Al_2O_3),$$

and in it appear the compounds $Na_2O \cdot 8CaO \cdot 3Al_2O_3$ and $2Na_2O \cdot 3CaO \cdot 5Al_2O_3$. The field of

$$Na_2O \cdot 8CaO \cdot 3Al_2O_3$$

is very narrow, and the univariant reaction point $2CaO \cdot SiO_2$, $3CaO \cdot Al_2O_3$, $5CaO \cdot 3Al_2O_3$, $Na_2O \cdot 8CaO \cdot 3Al_2O_3$, and liquid is slightly outside the plane of this diagram, at 3.5 percent Na_2O, 50.2 percent CaO, 37.6 percent Al_2O_3, 8.7 percent SiO_2; 1365°±10°C. The phase $2Na_2O \cdot 3CaO \cdot 5Al_2O_3$ is probably a member of a solid-solution series, which occupies a larger area in the section $CaO\text{–}2CaO \cdot SiO_2\text{–}(Na_2O + 3Al_2O_3)$.

From results in this section it is estimated that the liquid at the univariant point CaO, $3CaO \cdot SiO_2$, $Na_2O \cdot 8CaO \cdot 3SiO_2$ has the composition 50 percent Na_2O, 54.1 percent CaO, 28.6 percent Al_2O_3, 12.3 percent SiO_2, at 1445°±10°C. Another reaction point out-

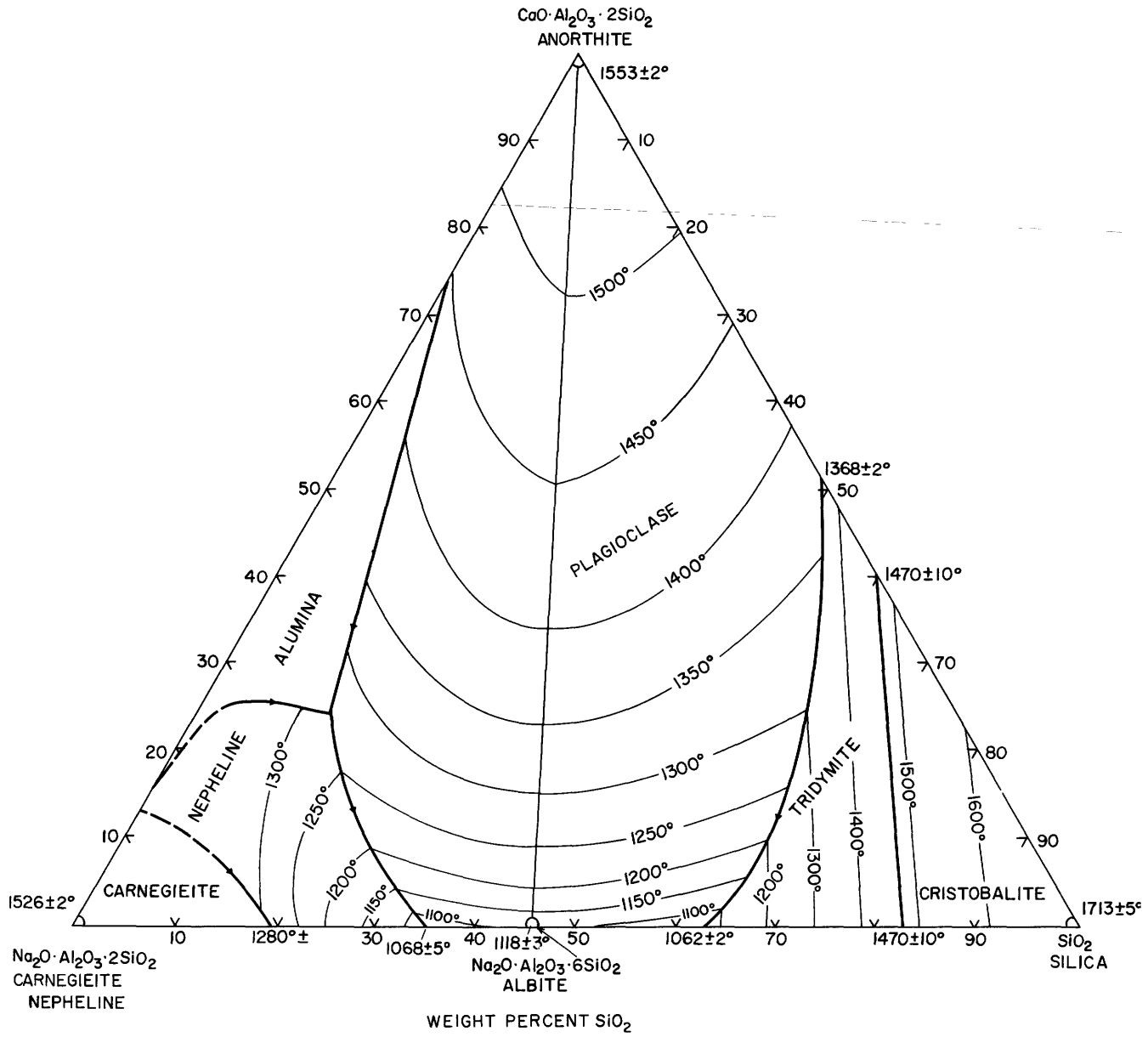

FIGURE 67.—The plane $Na_2O \cdot Al_2O_3 \cdot 2SiO_2$ (carnegieite, nepheline)–$CaO \cdot Al_2O_3 \cdot 2SiO_2$ (anorthite)–SiO_2 through the tetrahedron Na_2O–CaO–Al_2O_3–SiO_2. Modified from preliminary diagram by Schairer (1957a).

side this plane is at 1440°±10°C and the solid phases are $2CaO \cdot SiO_2$, $3CaO \cdot SiO_2$, $3CaO \cdot Al_2O_3$ and $Na_2O \cdot 8CaO \cdot 3Al_2O_3$, and the liquid, 3.5 percent Na_2O, 55.2 percent CaO, 31 percent Al_2O_3, 10.3 percent SiO_2. Another plane studied was CaO–$2CaO \cdot SiO_2$–$Na_2O \cdot Al_2O_3$. $Na_2O \cdot Al_2O_3$–$2CaO \cdot SiO_2$ is a binary system with a eutectic at 1405°±10° C, and 61 percent $2CaO \cdot SiO_2$, or 14.7 percent Na_2O, 39.7 percent CaO, 24.3 percent Al_2O_3, 21.3 percent SiO_2. This section is essentially ternary, with the exception of a small amount of solid solution in $2CaO \cdot SiO_2$ and probably in $Na_2O \cdot Al_2O_3$. The ternary eutectic $CaO + 2CaO \cdot SiO_2 + Na_2O \cdot Al_2O_3 = L$ is at 1355°±10°C and the liquid composition is 28 percent $Na_2O \cdot Al_2O_3$, 16 percent CaO, 56 percent $2CaO \cdot SiO_2$, or 11 percent Na_2O, 52 percent CaO, 17 percent Al_2O_3, 20 percent SiO_2. This part of the quaternary system contains much solid solution and is difficult to work with because of the volatilization of Na_2O at the high temperature necessary to melt the mixtures.

Na_2O–CaO–Fe_2O_3–SiO_2

Eubank and Bogue (1948) explored a plane in this system, obtained by adding 5 percent Na_2O to the system CaO–$2CaO \cdot SiO_2$–$CaO \cdot Fe_2O_3$. No ternary compounds were found. Compositions near the $2CaO \cdot SiO_2$–$CaO \cdot Fe_2O_3$ join near $2CaO \cdot SiO_2$ were very refractory and showed little liquid at 1550° C. As the composition contained increasing amounts of $2CaO \cdot Fe_2O_3$, the amount of liquid increased, and a mix containing 31.5 percent CaO was completely liquid at 1320°C. No $3CaO \cdot SiO_2$ was found.

Na_2O–FeO–Al_2O_3–SiO_2

Bowen and Schairer (1936, 1938) studied the system $Na_2O \cdot Al_2O_3 \cdot 2SiO_2$–$FeO \cdot SiO_2$–$SiO_2$, which is part of the plane $Na_2O \cdot Al_2O_3 \cdot 2SiO_2$–FeO–$SiO_2$ through the tetrahedron Na_2O–FeO–Al_2O_3–SiO_2, and this is a part of the larger plane $Na_2O \cdot Al_2O_3 + FeO + SiO_2$. The relations in the ternary section $Na_2O \cdot Al_2O_3 \cdot 2SiO_2$–FeO–$SiO_2$ are shown in figure 68, which is only in part ternary because of the apperance of a field of $FeO \cdot Al_2O_3$ (hercynite). Moreover, the melts always contained some Fe_2O_3, in amount determined by analysis, but the amount is small and the presentation of the results is greatly facilitated by calculating all the iron as FeO. The largest field in the diagram of figure 68 is that of $2FeO \cdot SiO_2$ (fayalite), which forms a binary system with $Na_2O \cdot Al_2O_3 \cdot 6SiO_2$ (albite), with a eutectic at 1050°C and 84 percent albite. The ternary eutectic

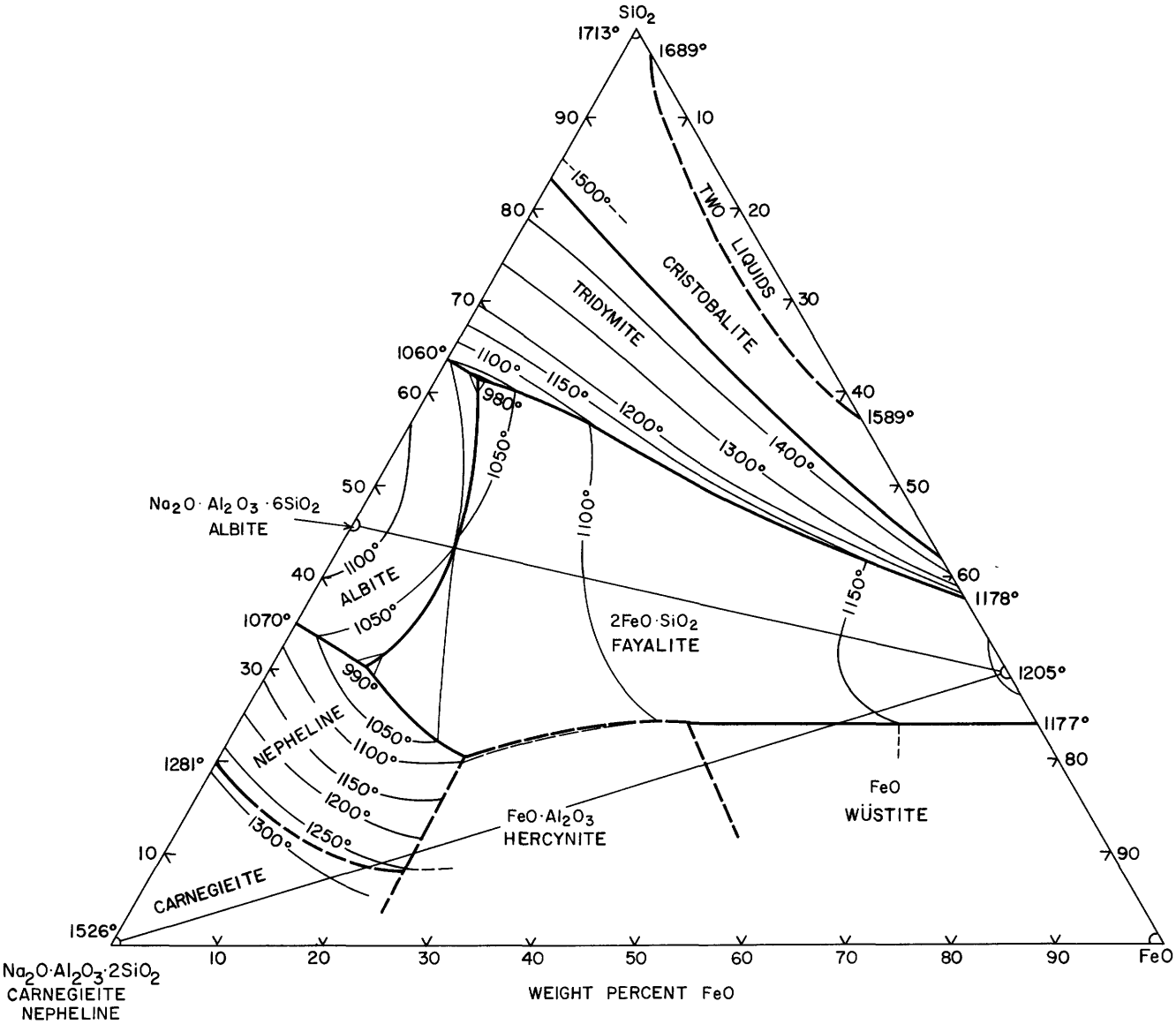

FIGURE 68.—The plane $Na_2O \cdot Al_2O_3 \cdot 2SiO_2$ (carnegieite, nepheline)–FeO–SiO_2 through the tetrahedron Na_2O–FeO–Al_2O_3–SiO_2. Modified from Bowen and Schairer (1938).

$Na_2O \cdot Al_2O_3 \cdot 6SiO_2 + SiO_2 + 2FeO \cdot SiO_2 = L$ is at 34 percent $Na_2O \cdot Al_2O_3 \cdot 2SiO_2$, 4.5 percent FeO, 61.5 percent SiO_2, and 980°C, and the eutectic

$$Na_2O \cdot Al_2O_3 \cdot 2SiO_2 + Na_2O \cdot Al_2O_3 \cdot 6SiO_2 + 2FeO \cdot SiO_2 = L$$

at 60.5 percent $Na_2O \cdot Al_2O_3 \cdot 2SiO_2$, 9.0 percent FeO, 30.5 percent SiO_2, and 990°C. The point in this diagram at which the fields of nepheline, fayalite, and hercynite meet, which is a piercing point for the univariant equilibrium in the quaternary system, is at about 56.5 percent $Na_2O \cdot Al_2O_3 \cdot 2SiO_2$, 23 percent FeO, 20.5 percent SiO_2, and 1090°C. The join $Na_2O \cdot Al_2O_3 \cdot 2SiO_2$–$2FeO \cdot SiO_2$ is not binary because of the crystallization of hercynite and wüstite.

K_2O–MgO–Al_2O_3–SiO_2

Schairer (1954) studied the phase-equilibrium relations in four planes in the tetrahedron representing the system (fig. 69), and in a later paper, Schairer (1955) gave results of the study of two additional planes.

The plane $2MgO \cdot SiO_2$ (forsterite)–$K_2O \cdot Al_2O_3 \cdot 4SiO_2$ (leucite)–SiO_2 through the tetrahedron K_2O–MgO–Al_2O_3–SiO_2 is shown in figure 70. This is a ternary system, since the composition of all

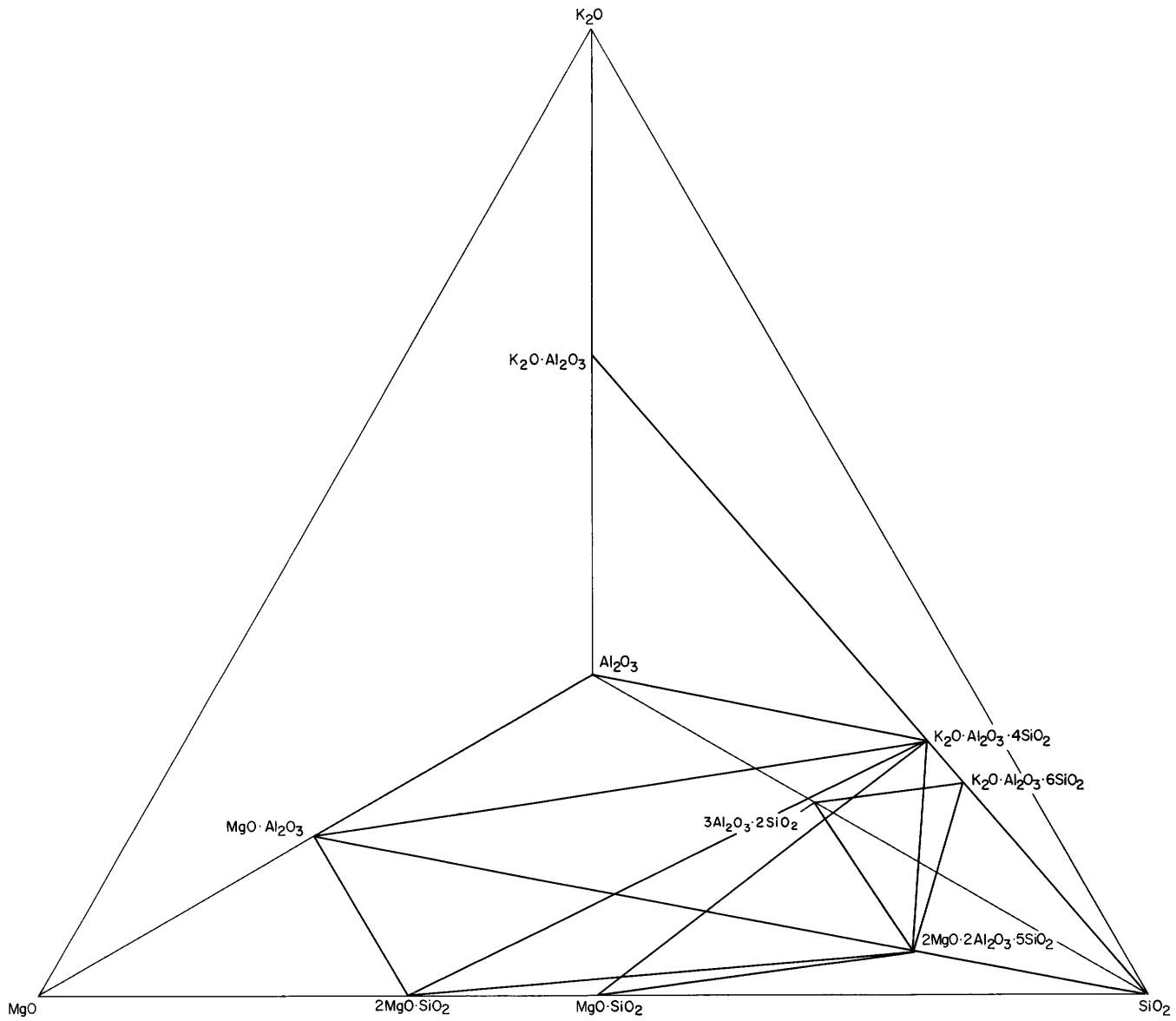

FIGURE 69.—Diagrammatic representation of the tetrahedron K_2O–MgO–Al_2O_3–SiO_2, showing planes through it which have been studied.

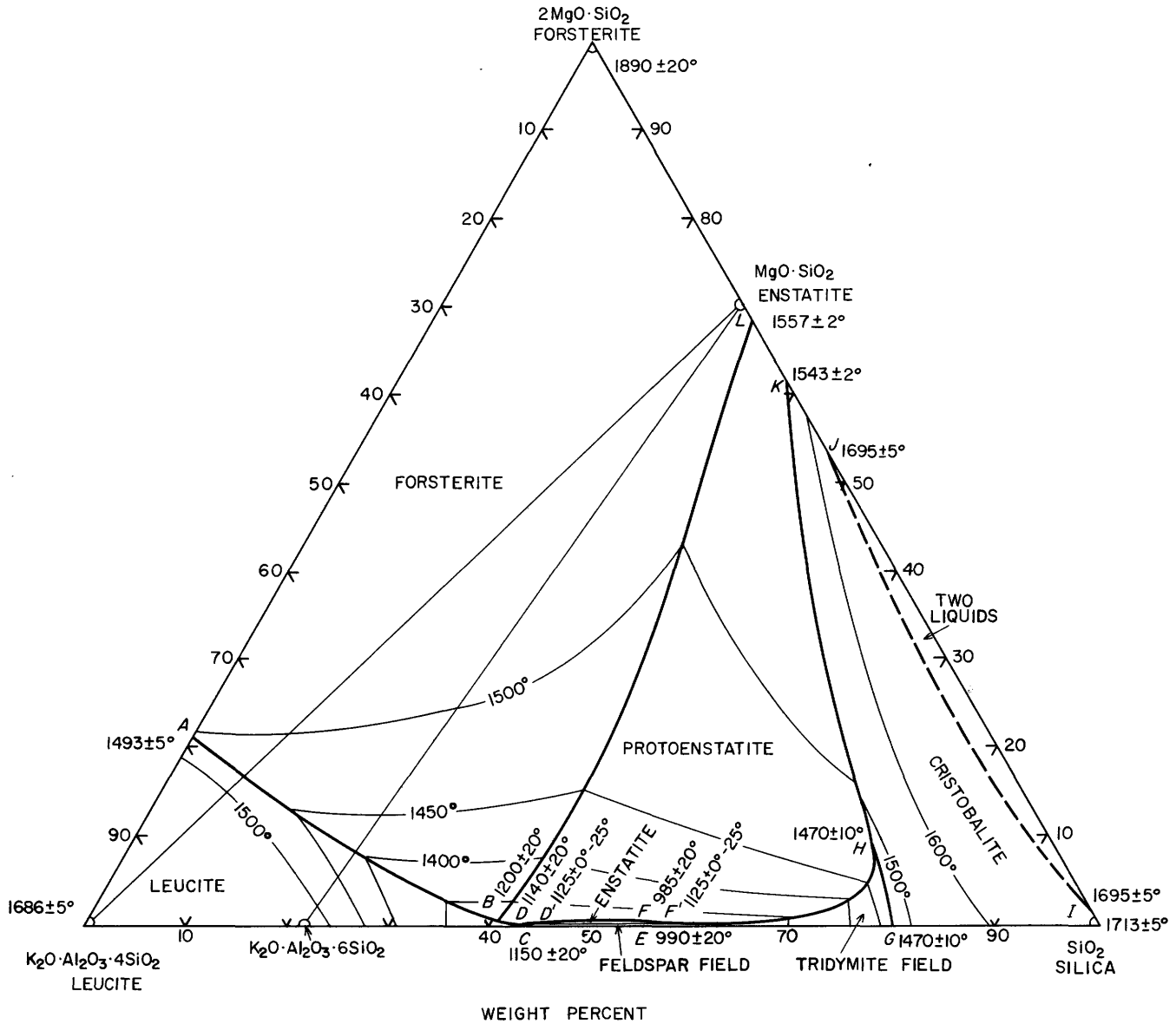

FIGURE 70.—The plane $K_2O \cdot Al_2O_3 \cdot 4SiO_2$ (leucite)-$2MgO \cdot SiO_2$ (forsterite)-SiO_2 through the tetrahedron K_2O–MgO–Al_2O_3–SiO_2. Modified from Schairer (1954).

the phases which appear in crystallization may be expressed in terms of positive amounts of the components and hence any of the quaternary univariant curves which pierce it will have a point of maximum temperature in this plane. Accordingly, this plane is a barrier which no quaternary liquid can cross during crystallization. Seven primary phase volumes are cut by this plane: leucite, forsterite, the two forms of $MgO \cdot SiO_2$ (protoenstatite and enstatite), potassium feldspar ($K_2O \cdot Al_2O_3 \cdot 6SiO_2$), tridymite, cristobalite, and a region of two immiscible liquids. The fields of potassium feldspar and enstatite in figure 70 are narrow. Two compositions studied which were near these fields but contained only 1 percent $MgO \cdot SiO_2$ were in the field of protoenstatite, with liquidus temperatures around 1200°C. The points *C* and *D* must be very close together both in temperature and composition, as must also points *E* and *F*. The heavy lines of fig. 70 are not only the traces of boundary curves between primary phase volumes in the tetrahedron representing the four-component system, but since this is a ternary system they also are boundary curves. The points of intersection of these boundary curves, data for which are given in table 30, are univariant points in this ternary system and also piercing points for univariant curves in the quaternary system.

The relation of the invariant points and boundary curves in the ternary system to the quaternary system are shown in (fig. 71).

The three points B, D, and F (fig. 70) not only lie, respectively, on three invariant lines, but each is a maximum of temperature on one of these curved lines because the plane leucite-forsterite-silica is a composition plane for the crystalline phases along each of these three lines. A composition plane in a quaternary system is the equivalent of a tieline in a ternary system, and has at its apices the composition of the three crystalline phases which may coexist in equilibrium with liquid. Such a composition plane, when and if this plane (or sometimes this plane extended) cuts the quaternary in-

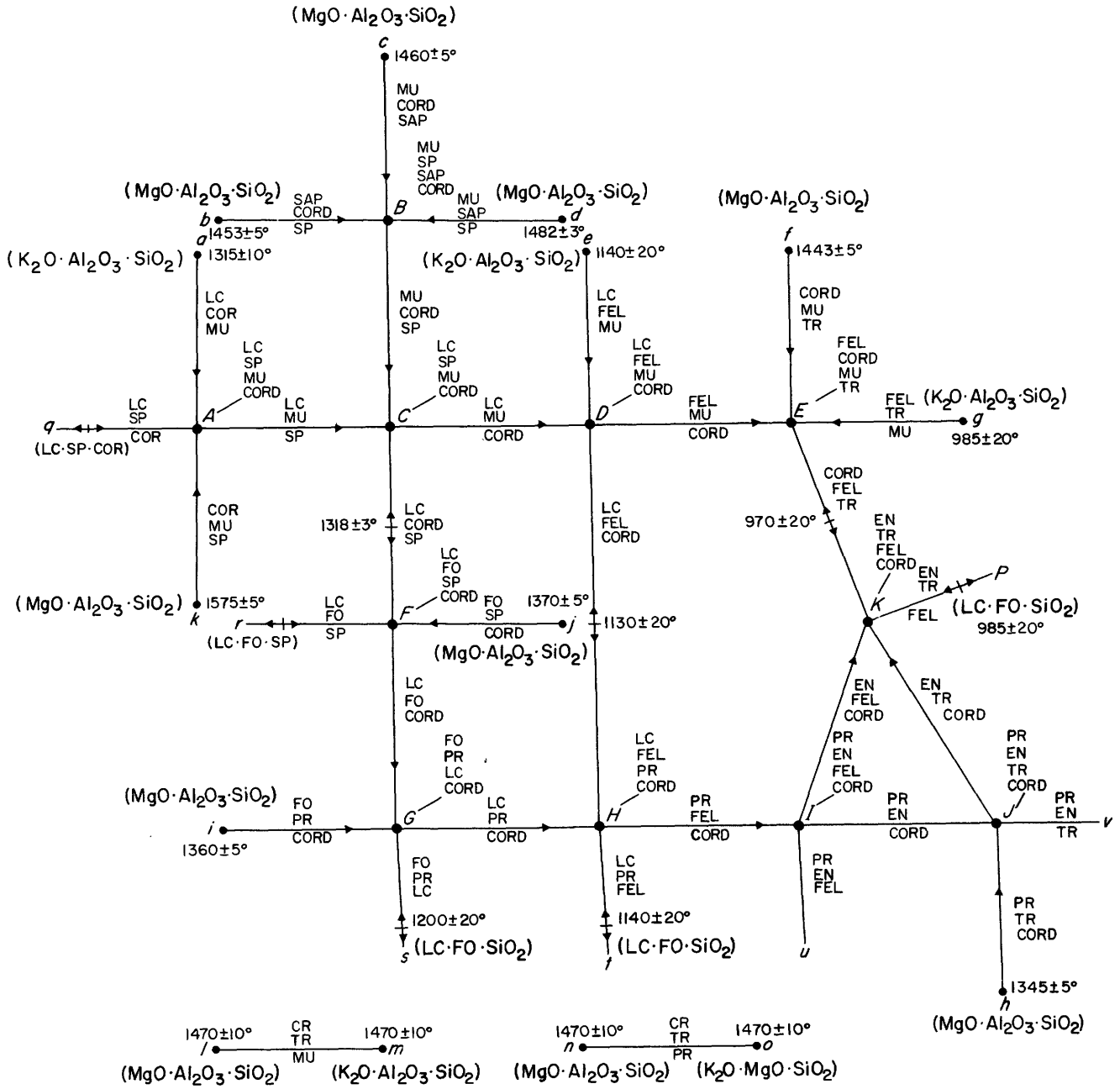

FIGURE 71.—The system K_2O–MgO–Al_2O_3–SiO_2. Diagram showing univariant lines and their relation to ternary invariant points (small black dots and lowercase letters *a* through *o*) in limiting systems and to quaternary invariant points (large black dots and capital letters). These lines and points do not lie in a plane. Only their relations to one another are shown in this diagram, which is not intended to show their angular or spatial relations. The lengths of the lines and the position of a temperature maximum on a line are arbitrary and without significance. Arrows indicate the direction of falling temperatures. Abbreviations for crystalline solid phases along the lines and at the points: *LC*=leucite, *COR*=corundum, *MU*=mullite, *SP*=spinel, *CORD*=cordierite, *SAP*=sapphirine, *FEL*=potassium feldspar, *TR*=tridymite, *CR*=cristobalite, *FO*=forsterite, *PR*=protoenstatite, *EN*=enstatite. Reprinted from Schairer (1954).

variant line along which these three crystalline phases coexist with liquid, defines a temperature maximum on the curved invariant line where it cuts it.

The phase assemblages along each of the six invariant lines (curved lines within the tetrahedron, K_2O–MgO–Al_2O_3–SiO_2) which pierce the plane leucite–forsterite–silica are as follows:

1. Leucite + forsterite + protoenstatite + liquid. Point *B* (fig. 70) lies on this line and is a temperature maximum on it. This line is *sG* of figure 71 and *B* of figure 70 is the maximum shown on *sG*.
2. Leucite + protoenstatite + potassium feldspar + liquid. Point *D* (fig. 70) lies on this line and is a temperature maximum on the line *tH* (fig. 71).
3. Enstatite + potassium feldspar + tridymite + liquid. Point *F* lies on this line and is the point of maximum temperature of *pK* of figure 71.
4. Protoenstatite + enstatite + potassium feldspar + liquid. *D'* of figure 70 lies on this line, which is *uI* of figure 71.
5. Protoenstatite + enstatite + tridymite + liquid. *F'* (fig. 70) lies on this line, which is *vJ* of figure 71.
6. Protoenstatite + cristobalite + tridymite + liquid. Point *H* (fig. 70) lies on this line, which is *no* of figure 71, and joins the points *H* of figure 36 and *K* of figure 28.

With the exception of protoenstatite + cristobalite + tridymite + liquid, which ends at two ternary invariant points in different faces of the tetrahedron, each of these invariant lines connects two quaternary invariant points. Four invariant lines meet at each quaternary invariant point (fig. 71). The points *B*, *D*, and *F* as temperature maxima on their respective invariant lines are significant because they locate three maxima of temperature, below which the temperature of each of the three pairs of quaternary invariant point must lie. The positions of *B*, *D*, and *F* in the plane and the position of this plane leucite-forsterite-silica in the tetrahedron set some limits to the possible locations six quaternary invariant points.

TABLE 30.—Significant points in the system K_2O–MgO–Al_2O_3–SiO_2

[Locations of significant points in the five joins on univariant lines of figure 71. Based on Schairer, 1954]

Letter (significant point)	Figure on which point is shown	Temperature (°C)	Three solid phases	Line (fig. 71) on which letter point lies
B	70	1200±20	Leucite+forsterite+protoenstatite [1]	*sG*
D	70	1140±20	Leucite + feldspar + protoenstatite	*tH*
D'	70	1125+0, −25	Feldspar + protoenstatite + enstatite [1]	*uI*
F'	70	1125+0, −25	Tridymite + protoenstatite + enstatite [1]	*vJ*
F	70	985±20	Feldspar + tridymite + enstatite [1]	*pK*
H	70	1470±10	Cristobalite + tridymite + protoenstatite	*no*
M	72	1445±5	Leucite + forsterite + spinel	*rF*
P	72	1450±5	Cordierite + sapphirine + spinel	*bB*
P'	72	1458±5	Cordierite + mullite + sapphirine	*dB*
P''	72	1460±5	Mullite + sapphirine + spinel	*cB*
V	73	1435±5	Mullite + cordierite + tridymite	*fE*
W	73	1440±3	Cordierite + mullite + spinel	*BC*
X	73	1318±3	Leucite + cordierite + spinel [1]	*CF*
Y	73	1130±20	Cordierite + leucite + feldspar [1]	*DH*
Z	73	970±20	Cordierite + feldspar + tridymite [1]	*EK*
B'	74	1405±5	Leucite + forsterite + spinel	*rF*
C'	74	1370±5	Forsterite + cordierite + spinel	*jF*
F'	74	1358±5	Forsterite + protoenstatite + cordierite	*iG*
H'	74	1455±5	Mullite + sapphirine + cordierite	*cB*
H''	74	1458±5	Spinel + mullite + sapphirine	*dB*
H'''	74	1450±5	Cordierite + sapphirine + spinel	*bB*
K'	75	1478±3	Corundum + mullite + spinel	*kA*
M'	75	1370±3	Leucite + corundum + spinel	*qA*

[1] Following are the compositions of the liquids at their ternary invariant points within the quaternary system, in weight percent:

Letter point	Leucite	Forsterite	Cordierite	SiO_2
B	58.8	0.8		40.4
D	57.7	.2		42.1
D'	57.8	.2		42.0
F	45.5	.2		54.3
F'	44.8	.2		55.0
X	62.0		16.0	22.0
Y	55.0		2.5	42.5
Z	44.5		2.0	53.5

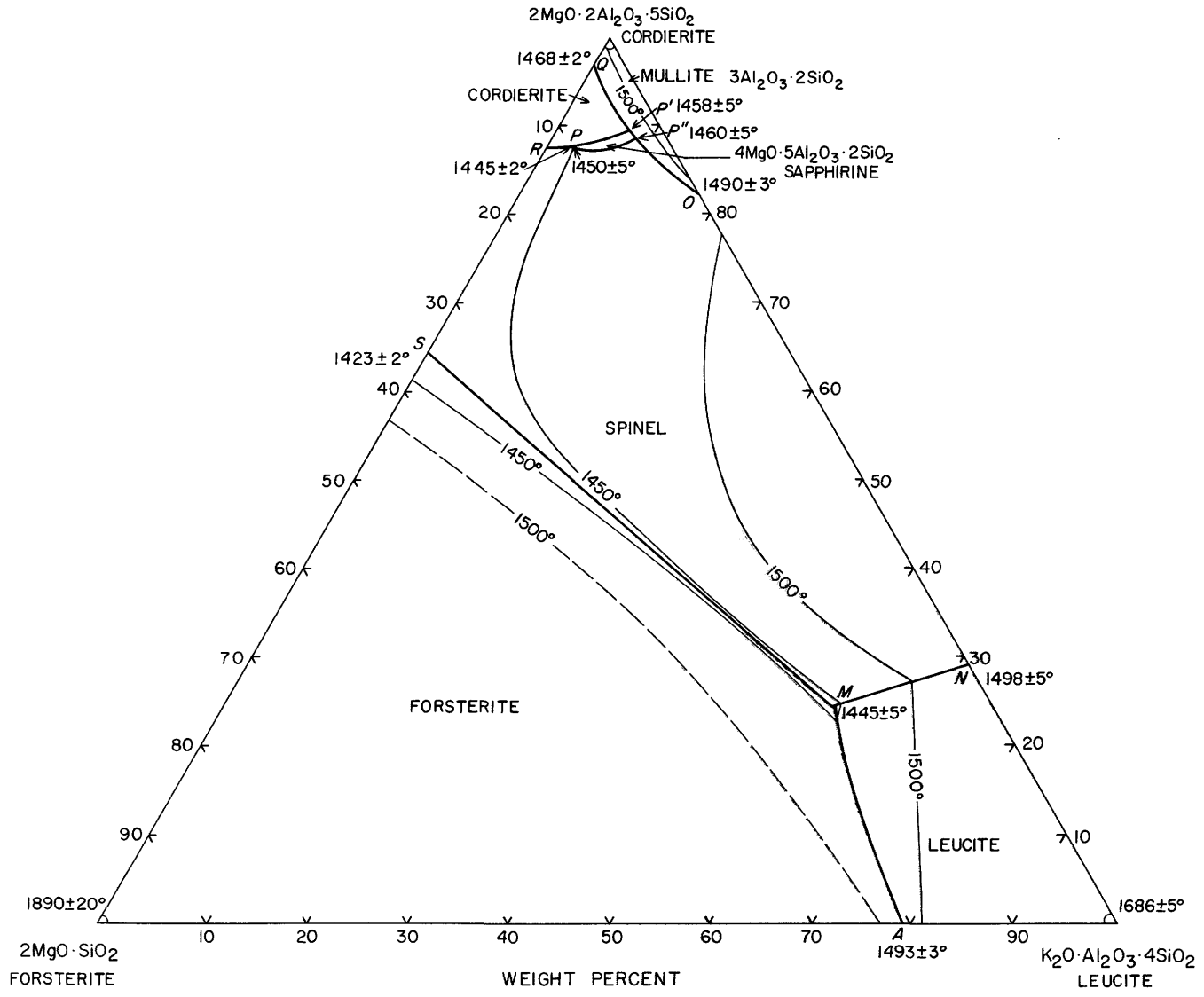

FIGURE 72.—The plane $K_2O \cdot Al_2O_3 \cdot 4SiO_2$ (leucite)-$2MgO \cdot SiO_2$ (forsterite)-$2MgO \cdot 2Al_2O_3 \cdot 5SiO_2$ (cordierite) through the tetrahedron K_2O-MgO-Al_2O_3-SiO_2. Modified from Schairer (1954).

The plane $K_2O \cdot Al_2O_3 \cdot 4SiO_2$ (leucite)–$2MgO \cdot SiO_2$ (forsterite)–$2MgO \cdot 2Al_2O_3 \cdot 5SiO_2$ (cordierite) through the tetrahedron K_2O–MgO–Al_2O_3–SiO_2 is shown in figure 72. It shows the side

$$2MgO \cdot SiO_2\text{–}K_2O \cdot Al_2O_3 \cdot 4SiO_2$$

in common with figures 70 and 77. This plane cuts the primary phase volumes of forsterite, leucite, spinel, cordierite, mullite, and $4MgO \cdot 5Al_2O_3 \cdot 2SiO_2$ (sapphirine). This is not a ternary system, since cordierite melts incongruently to mullite, and there are fields of spinel and sapphirine, the compositions of which are not in this plane.

The nine curves *AM*, *NM*, *SM*, *RP*, *OP''*, *PP'*, *PP''*, *P'P''*, and *QP'* of figure 72 are traces of curved surfaces, along which two adjacent phase volumes meet in the plane forsterite-cordierite-leucite. The points *M*, *P'*, *P''*, and *P* are piercing points in the plane of four univariant lines in the tetrahedron and each of these points is a point on one of the four univariant lines in the plane. Along each of these curved univariant lines three crystalline phases are in equilibrium with liquidus of compositions in the plane forsterite-cordierite-leucite. The phase assemblages on each of the four univariant lines which pierce this plane are:

1. Fosterite+leucite+spinel+liquid. Point *M* (fig. 72) is on this line, and the plane enstatite-cordierite-leucite cuts this line at *B'* of figure 74. This is the line *rF* of figure 71.
2. Spinel+mullite+sapphirine+liquid. *P''* (fig. 72)

lies on this line, and the plane enstatite-cordierite-leucite cuts it at *H''* (fig. 74). This line is *dB* of figure 71.

3. Mullite+cordierite+sapphirine+liquid. *P'* (fig. 72) is on this line and the plane enstatite-cordierite-leucite cuts it at *H'* (fig. 74). This line is *cB* of figure 71.
4. Cordierite+sapphirine+spinel+liquid. Point *P* (fig. 72) is on this line, and the plane enstatite-cordierite-leucite cuts it at H''' (fig. 74). This line is dB of figure 71.

The plane $K_2O \cdot Al_2O_3 \cdot 4SiO_2$ (leucite)–$2MgO \cdot 2Al_2O_3 \cdot 5SiO_2$ (cordierite)–SiO_2, which is part of the larger plane $K_2O \cdot Al_2O_3 \cdot 4SiO_2$–$MgO \cdot Al_2O_3$–$SiO_2$ through the tetrahedron K_2O–MgO–Al_2O_3–SiO_2, is shown in figure 73. It also is not a ternary system since neither mullite nor spinel is in this plane. It shares the side cordierite-leucite with figure 74.

The point *U* in the side line cordierite-silica is the point where the tieline cordierite-silica in the limiting ternary system MgO–Al_2O_3–SiO_2 cuts *QP*, the boundary curve between the fields of mullite and tridymite (fig. 36). The 11 heavy curves, or heavy dashed curves where the data are insufficient to locate them accurately, are traces of curved surfaces along which two adjacent primary phase volumes meet in the tetrahedron K_2O–MgO–Al_2O_3–SiO_2. The points *V*, *W*, *X*, *Y*, and *Z* are piercing points in the plane cordierite-leucite-silica of five univariant lines within the tetrahedron. At three of the five piercing points the compositions of

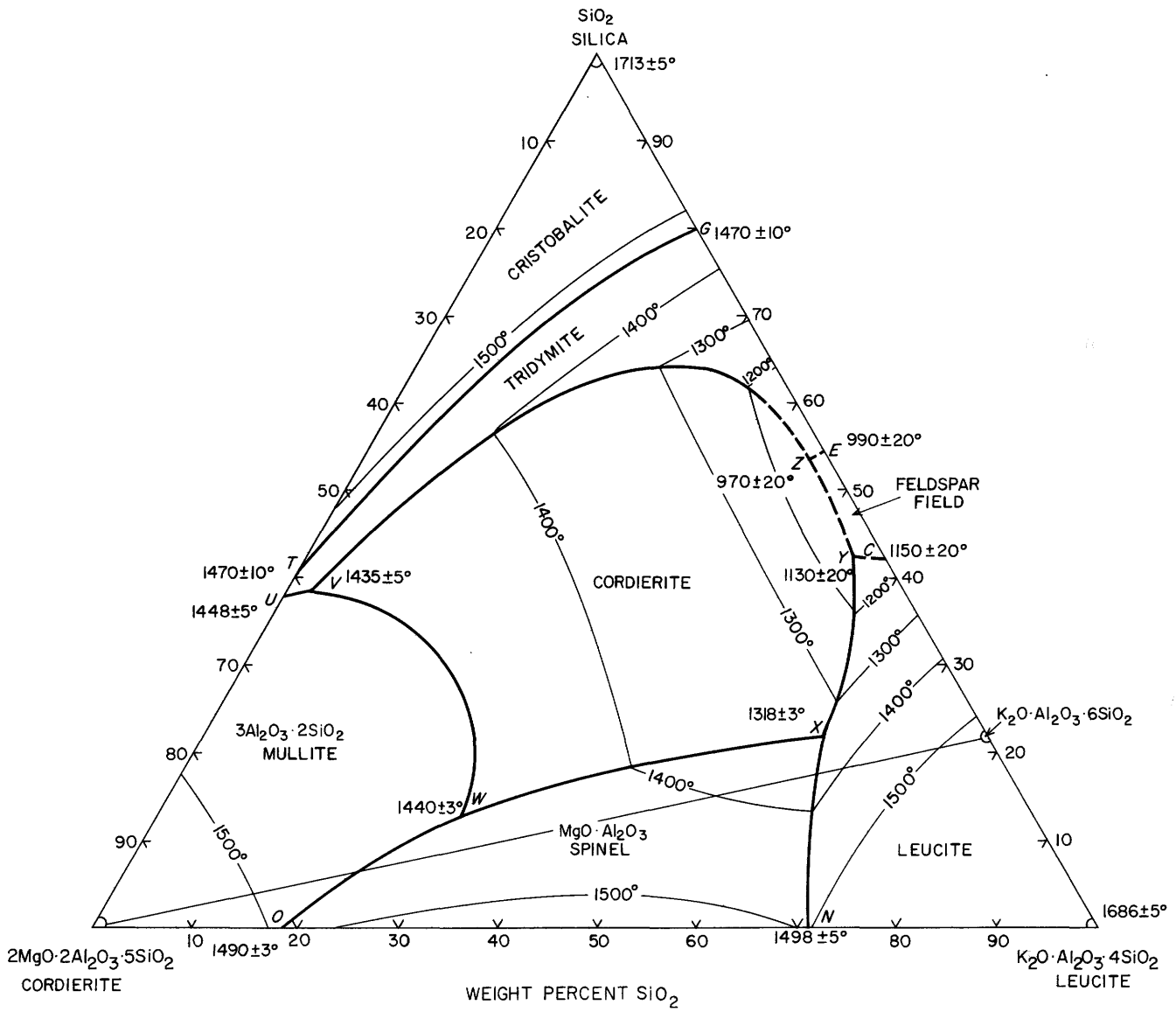

FIGURE 73.—The plane $K_2O \cdot Al_2O_3 \cdot 4SiO_2$ (leucite)–$2MgO \cdot 2Al_2O_3 \cdot 5SiO_2$ (cordierite)–SiO_2 through the tetrahedron K_2O–MgO–Al_2O_3–SiO_2. Modified from Schairer (1954).

695-382 O - 64 - 8

all the phases in equilibrium lie in the plane of the diagram or in this plane produced (cordierite-leucite-silica is a part of the larger plane spinel-silica-leucite). Thus, Y (fig. 73) is the piercing point of the univariant line leucite+potassium feldspar+cordierite+liquid, and since the composition plane leucite-potassium feldspar-cordierite lies in this plane, Y is a temperature maximum on this univariant line. Similarly, Z (fig. 73) is the piercing point of cordierite+potassium feldspar+tridymite+liquid and a temperature maximum on this invariant line. Similarly, X (fig. 73) is the piercing point of the univariant line leucite+cordierite+spinel+liquid, and since cordierite-silica-leucite is a portion of the larger plane spinel-silica-leucite, the point X is a temperature maximum on this univariant line.

The phase assemblages along each of the five univariant lines which pierce the plane cordierite-leucite-silica are as follows:

1. Mullite + cordierite + tridymite + liquid. Point V (fig. 73) lies on this line, which is fE of figure 71. The point P of figure 36 is one terminus of this line.
2. Mullite + cordierite + spinel + liquid. Point W lies on this line, which is BC of figure 71.
3. Cordierite + spinel + leucite + liquid. Point X lies on this line and is the temperature maximum on it. This line is CF of figure 71 and point X is the maximum on CF.
4. Leucite + potassium feldspar + cordierite + liquid. Point Y is on this line and is a point of maximum temperature. This line is DH of figure 71, and Y is the maximum shown on it.
5. Cordierite + potassium feldspar + tridymite + liquid. Point Z of figure 73 is on this line and is a temperature maximum both on it and on line EK of figure 71.

The plane $K_2O \cdot Al_2O_3 \cdot 4SiO_2$ (leucite)–$MgO \cdot SiO_2$ (enstatite)–$2MgO \cdot 2Al_2O_3 \cdot 5SiO_2$ (cordierite) through the tetrahedron K_2O–MgO–Al_2O_3–SiO_2 is shown in figure 74. It shares the side $K_2O \cdot Al_2O_3 \cdot 4SiO_2$–$2MgO \cdot 2Al_2O_3 \cdot 5SiO_2$ with figure 73. The section cuts the seven primary phase volumes of the three components and of $2MgO \cdot SiO_2$ (forsterite), $4MgO \cdot 5Al_2O_3 \cdot 2SiO_2$ (sapphirine), mullite, and spinel, but, since the compositions of these last four phases cannot be represented by the components chosen, it is not a ternary system. Because of the incongruent melting of $MgO \cdot SiO_2$ (enstatite), it does not appear on the phase-equilibrium diagram, but the field of forsterite extends over the metasilicate composition and sweeps over the field until it meets the field of leucite. The side leucite-cordierite is not binary due to the formation first of spinel, then of mullite, and because of the incongruent melting of cordierite. The heavy curves are traces of curved surfaces along which two adjacent primary phase volumes meet in the tetrahedron, in the plane $MgO \cdot SiO_2$–cordierite-leucite. The points B', C', F', H''', H'', and H' are piercing points of six univariant lines within the tetrahedron. Along each of these curved univariant lines, three crystalline phases are in equilibrium with liquids whose compositions lie on this curved line. The phase assemblages along each of these six lines are as follows:

1. Leucite+forsterite+spinel+liquid. Point B' is on this line and the plane forsterite-cordierite-leucite cuts it at M (fig. 72). This line is rF in figure 71.
2. Forsterite+spinel+cordierite+liquid. Point C' lies on this line, which is jF of figure 71.
3. Forsterite+protoenstatite+cordierite+liquid. Point F' (fig. 74) is on this line, and U (fig. 36) is one terminus. This line is iG of figure 71.
4. Spinel+mullite+sapphirine+liquid. Point H'' lies on this line, and the plane forsterite-cordierite-leucite cuts it at P'' of figure 72. It is dB of figure 71.
5. Mullite+cordierite+sapphirine+liquid. H' is on this line, and the plane forsterite-cordierite-leucite cuts it at P' of figure 72. This line is eB of figure 71.
6. Cordierite+sapphrine+spinel+liquid. Point H''' lies on this line and the plane forsterite-cordierite-leucite cuts it at P of figure 72. It is bB of figure 71.

The plane $2MgO \cdot 2Al_2O_3 \cdot 5SiO_2$ (cordierite)–$3Al_2O_3 \cdot 2SiO_2$ (mullite)–$K_2O \cdot Al_2O_3 \cdot 6SiO_2$ (potassium feldspar) through the tetrahedron K_2O–MgO–Al_2O_3–SiO_2 shown in figure 75, cuts the primary phase volumes of mullite, corundum, spinel, and leucite. This again is not a ternary system, since each of the components melts incongruently.

The point I' lies at the intersection of the tieline cordierite-mullite and the boundary curve JM of figure 36. The side line cordierite-mullite lies in the plane cordierite-leucite-silica (fig. 73). The five heavy curves are traces of curved surfaces along which two adjacent primary phase volumes meet within the tetrahedron in the plane cordierite-mullite-potassium feldspar. The point K' and M' are piercing points of two

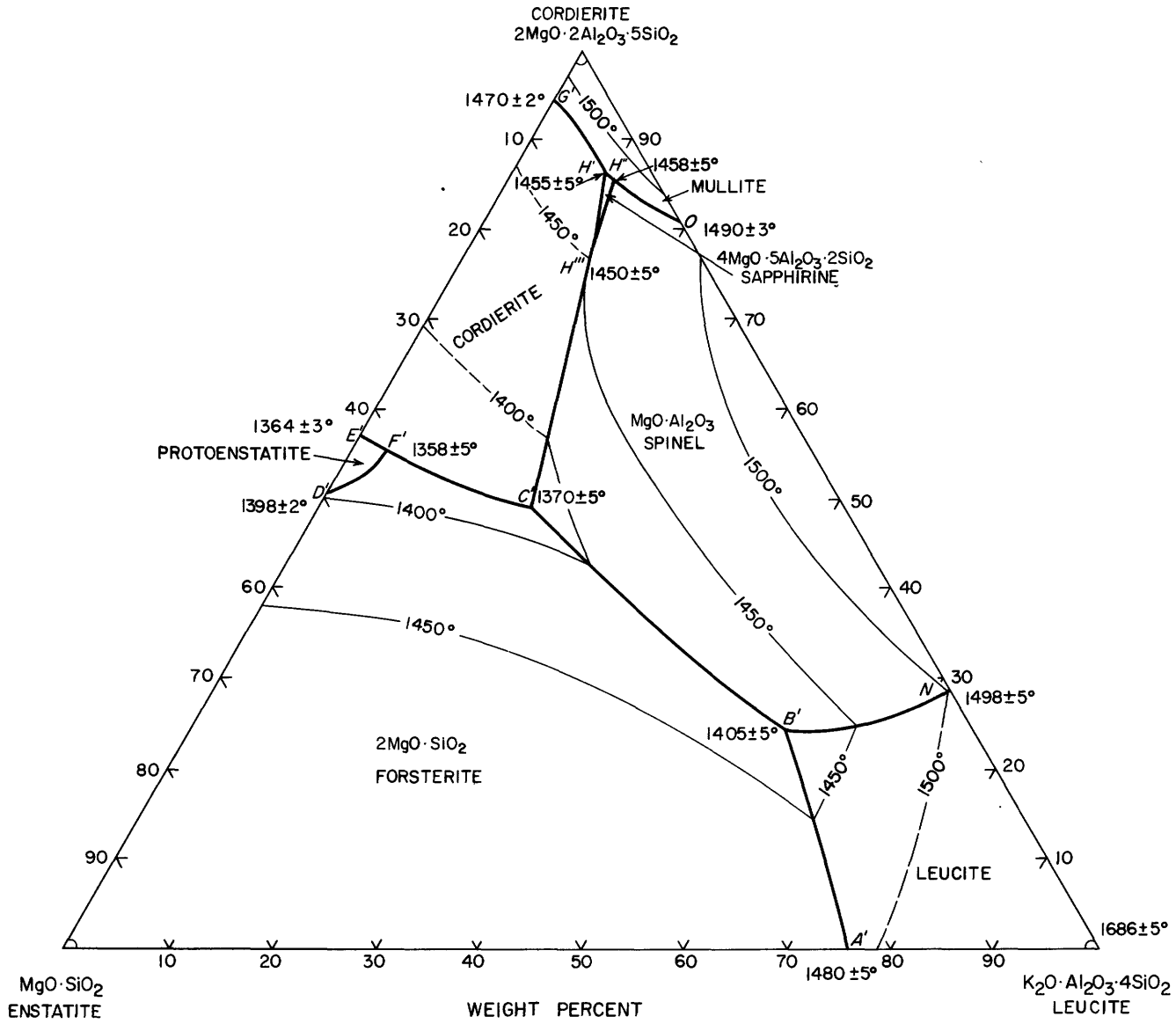

FIGURE 74.—The plane $K_2O \cdot Al_2O_3 \cdot 4SiO_2$ (leucite)-$MgO \cdot SiO_2$ (enstatite)-$2MgO \cdot 2Al_2O_3 \cdot 5SiO_2$ (cordierite) through the tetrahedron K_2O–MgO–Al_2O_3–SiO_2. Modified from Schairer (1954).

univariant lines within the tetrahedron. The phase assemblages along each of these two lines are as follows:

1. Corundum+mullite+spinel+liquid. Point K' is on this line, and point M (fig. 36) is one terminus. This line is kA of figure 71.
2. Leucite+corundum+spinel+liquid. Point M' is on this line, which is qA of figure 71.

The plane $K_2O \cdot Al_2O_3 \cdot 4SiO_2$ (leucite)–$MgO \cdot Al_2O_3$ (spinel)–Al_2O_3 (corundum) (fig. 76) is a ternary system and the maximum temperature of the univariant equilibrium leucite-corundum-spinel (line qA, fig. 71) is a ternary eutectic in this plane. The ternary eutectic (point D of fig. 76) is at 1543°±5°C and 88 percent leucite, 1.5 percent Al_2O_3, 10.5 percent $MgO \cdot Al_2O_3$. The binary eutectic spinel+leucite=L is at 1553°±5°C and 88.5 percent leucite (point A).

The plane $K_2O \cdot Al_2O_3 \cdot 4SiO_2$ (leucite)–$2MgO \cdot SiO_2$ (forsterite)–$MgO \cdot Al_2O_3$ (spinel) (fig. 77) also is a ternary system, and the maximum temperature of the univariant equilibrium leucite+forsterite+spinel=L (line rF of fig. 71) is the eutectic G of figure 77 at 1473°±5°C, 74.0 percent leucite, 18.5 percent forsterite, 7.5 percent spinel.

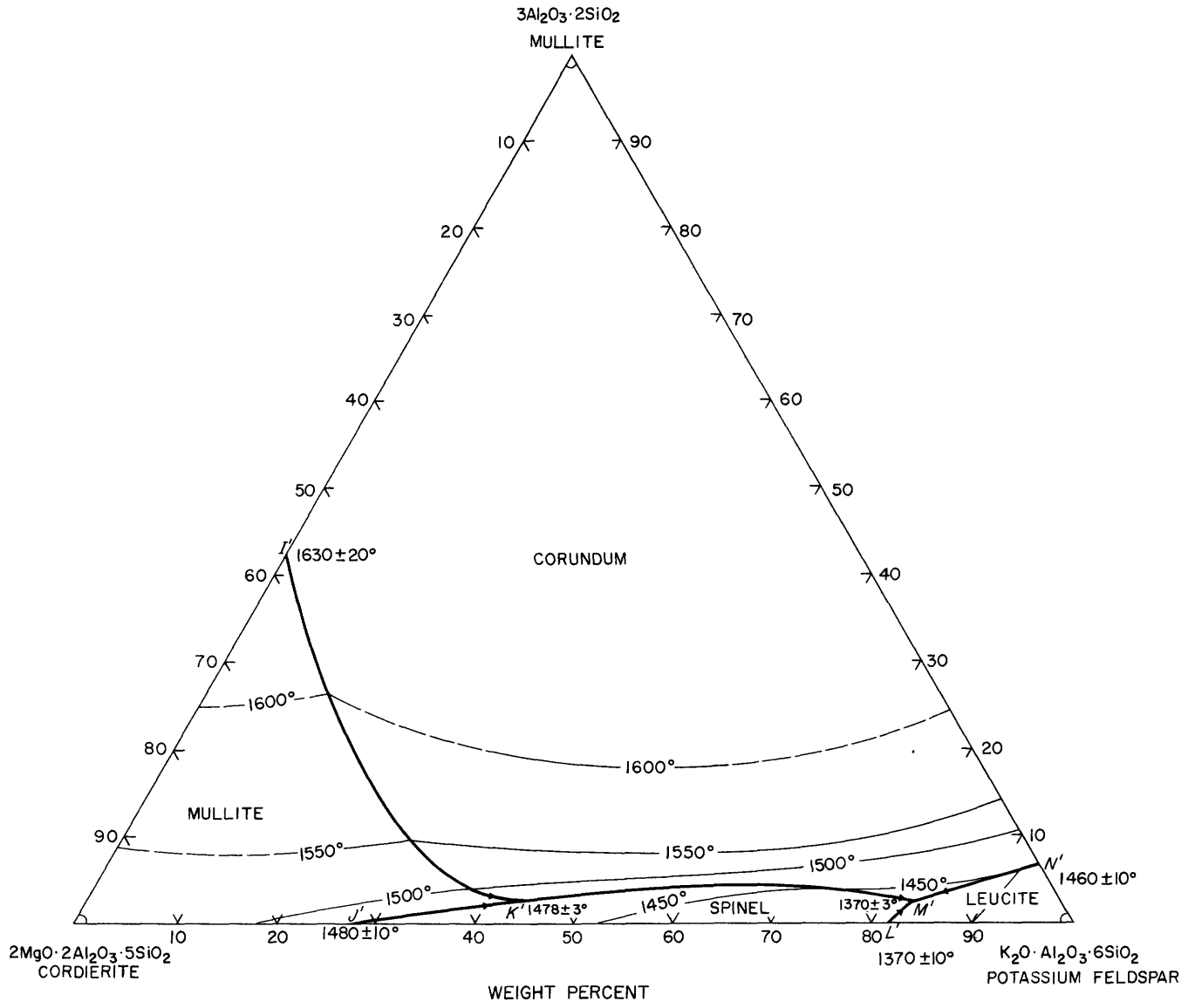

FIGURE 75.—The plane $2MgO \cdot 2Al_2O_3 \cdot 5SiO_2$ (cordierite)–$3Al_2O_3 \cdot 2SiO_2$ (mullite)–$K_2O \cdot Al_2O_3 \cdot 6SiO_2$ (potassium feldspar) through the tetrahedron K_2O–MgO–Al_2O_3–SiO_2. Modified from Schairer (1954).

Figure 71 gives in diagrammatic form the interrelations of the significant points in the quaternary system, and table 30 lists these points, their location and temperature, the coexisting solid phases, and in some cases the composition of the liquid. From the information obtained in studying the above planes, it was deduced that the liquid at the reaction point A must be in the volume feldspar-cordierite-mullite–SiO_2, not far from the ternary invariant point a in the ternary system K_2O–Al_2O_3–SiO_2, at which the solid phases are leucite, corundum, and mullite. The liquid composition at A is 13.9 percent K_2O, 18.5 percent Al_2O_3, 67.6 percent SiO_2 and the temperature is approximately 1300°C. The reaction point B must be near point H''' of figure 74 in composition, and at 1445°±5°C. Reaction point C must be in the volume feldspar-cordierite-mullite-silicate, at approximately 1290°C. Reaction point D must be near in composition to the invariant point N in the ternary system K_2O–Al_2O_3–SiO_2 (point e of figure 71) and near point Y of figure 73, and at 1120°±20°C. Point E is a eutectic, hence must be within the tetrahedron feldspar-cordierite-mullite–SiO_2. It must be near point M in the system K_2O–Al_2O_3–SiO_2 (g of fig. 71) and near Z of figure 73, and at 960°±20°C. Reaction point F is in the volume leucite–$MgO \cdot SiO_2$–cordierite–SiO_2, not far in composition from X of figure 73, and not far from 1318°C, the temperature maximum on the line CF. Reaction point G is near B of figures 73 in both composition and temperature, 1200°C. Reaction point H must be near in temperature and composition

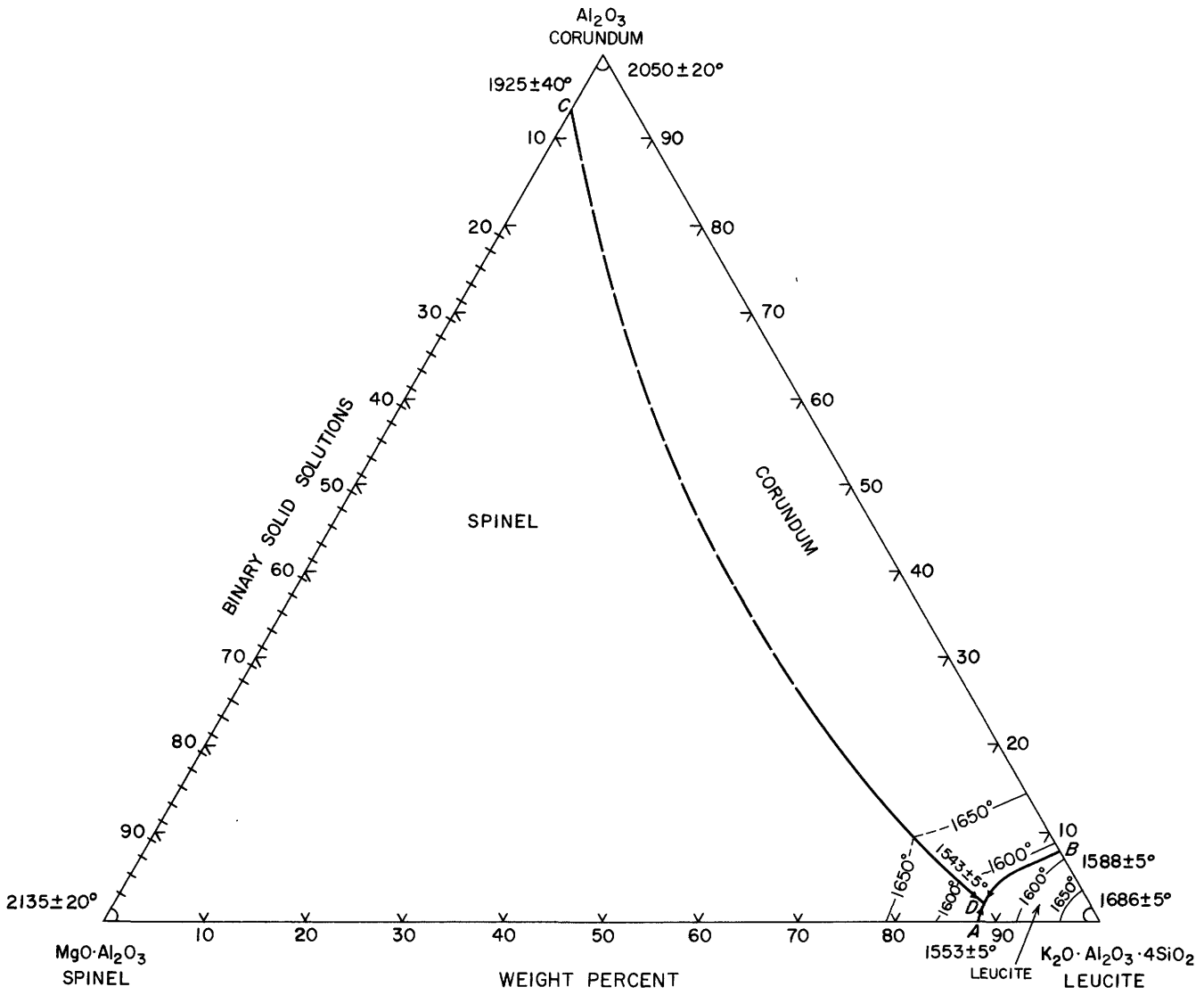

FIGURE 76.—The plane $K_2O·Al_2O_3·4SiO_2$ (leucite)–$MgO·Al_2O_3$ (spinel)–Al_2O_3 (corundum) through the tetrahedron K_2O–MgO–Al_2O_3–SiO_2. Modified from Schairer (1955).

to both *D* of figure 70 and *Y* of figure 73. Points *I* and *J* are inversion points of enstatite and protoenstatite in the quaternary system, and unless there is some solid solution the temperature is 1125°C. The composition of points *I* and *J* are near to each other and to point *H* of figure 71. Point *K* is a quaternary eutectic, at 960°±20°C, and in composition it is near to *Z* of figure 73 and to *F* of figure 70.

K_2O–CaO–Al_2O_3–SiO_2

Schairer and Bowen (1947b) studied the ternary system $K_2O·Al_2O_3·4SiO_2$ (leucite)–$CaO·Al_2O_3·2SiO_2$ (anorthite)–SiO_2 (figure 78). This is that part richer in SiO_2 than the join leucite-anorthite of the plane $K_2O·Al_2O_3$–$CaO·Al_2O_3$–SiO_2 through the tetrahedron representing the quaternary system. The side leucite-anorthite is a simple binary system with a eutectic at 45 percent anorthite and 1413°±5°C. Because of the incongruent melting of $K_2O·Al_2O_3·6SiO_2$ (potassium feldspar), the join potassium feldspar–anorthite is not a binary system. Anorthite is the primary phase from its melting point down to the point *S*, at 1348°C, 78 percent $K_2O·Al_2O_3·6SiO_2$, 22 percent $CaO·Al_2O_3·2SiO_2$. The field of anorthite occupies the largest area in the ternary diagram, extending down to the reaction point *R*; $K_2O·Al_2O_3·6SiO_2 + CaO·Al_2O_3·2SiO_2 = K_2O·Al_2O_3·4SiO_2 + L$ at 1040°±20°C, and to the eutectic *V*; $K_2O·Al_2O_3·6SiO_2 + CaO·Al_2O_3·2SiO_2 + SiO_2 = L$ at 950°±20°C. Melts near the curve *RV* are so exceedingly viscous that the composition relations have not been accurately determined, but the anorthite content is less than 5 percent.

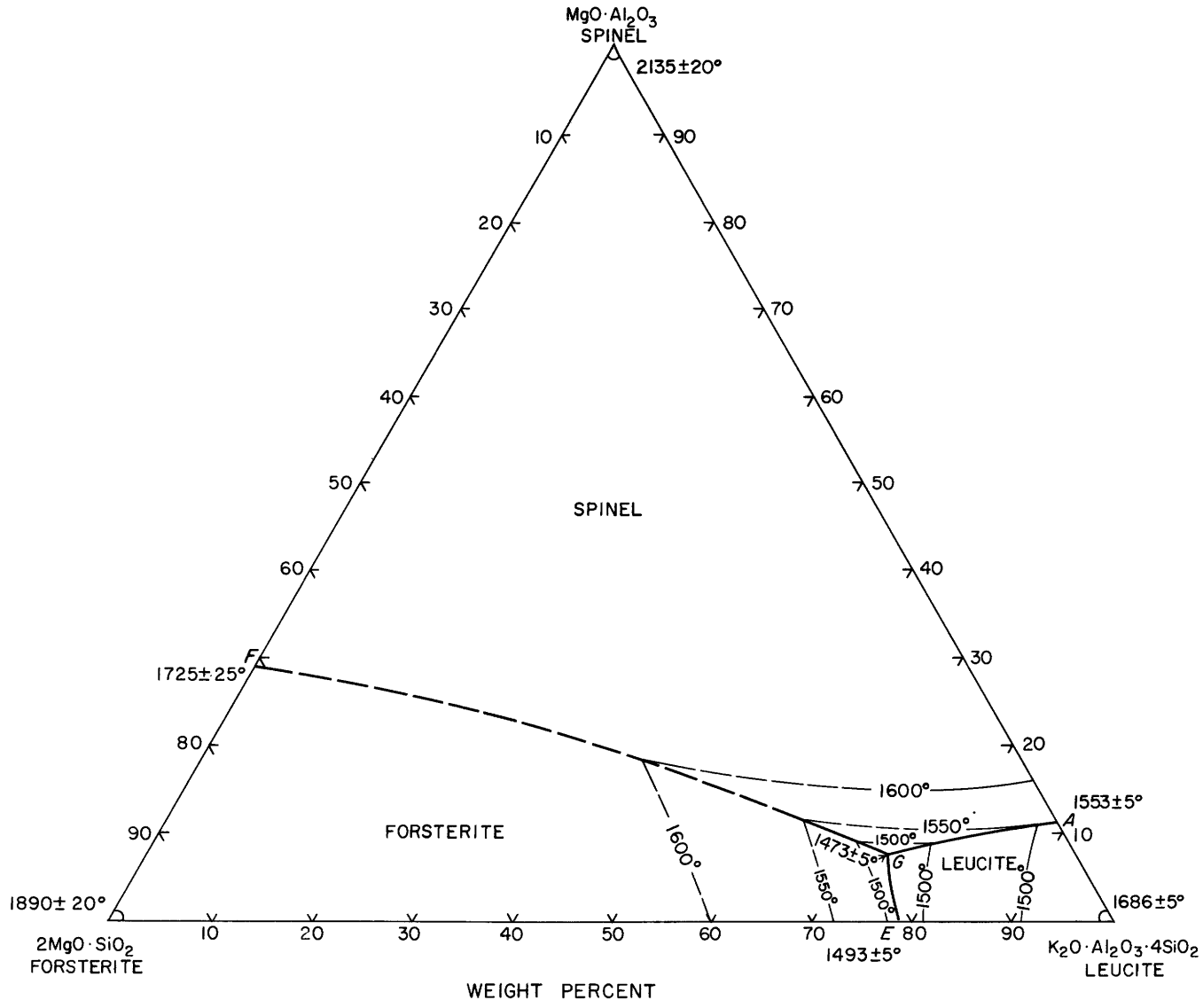

FIGURE 77.—The plane $K_2O \cdot Al_2O_3 \cdot 4SiO_2$ (leucite)–$2MgO \cdot SiO_2$ (forsterite)–$MgO \cdot Al_2O_3$ (spinel) through the tetrahedron K_2O–MgO–Al_2O_3–SiO_2. Modified from Schairer (1955).

K_2O–FeO–Al_2O_3–SiO_2,

Roedder (1951b) published a preliminary study of the section $K_2O \cdot Al_2O_3 \cdot 4SiO_2$ (leucite)–$2FeO \cdot SiO_2$ (fayalite)–SiO_2, which is part of the plane $K_2O \cdot Al_2O_3$–$FeO \cdot SiO_2$–SiO_2, with results shown in figure 79. This section of the plane cuts the phase volumes of leucite, fayalite, cristobalite, tridymite, and two-phase regions in which two immiscible liquids are formed within the quaternary system. The line AA' gives the compositions of two immiscible liquids, in equilibrium with each other and with fayalite and tridymite, and the points AA', are conjugate piercing points for the univariant equilibrium $L_1 + L_2 +$ tridymite + fayalite. In later publications Roedder (1953a,b) describes this immiscibility volume as roughly ellipsoidal, flattened parallel to and approximately astride the 1:1 $K_2O \cdot Al_2O_3$ mole-ratio plane, with its longest axis subparallel to the FeO–SiO_2 edge. The compositional limits are roughly 8 to 52 percent FeO and 5 to 16 percent of the sum of K_2O plus Al_2O_3. The closest portion of the immiscibility volume to either of the limiting ternary systems K_2O–FeO–SiO_2 or FeO–Al_2O_3–SiO_2 contains about 2 percent of the fourth component in each case. The divariant equilibrium surface between the phase volumes of fayalite and tridymite cuts through this immiscibility volume. No quaternary compounds have been

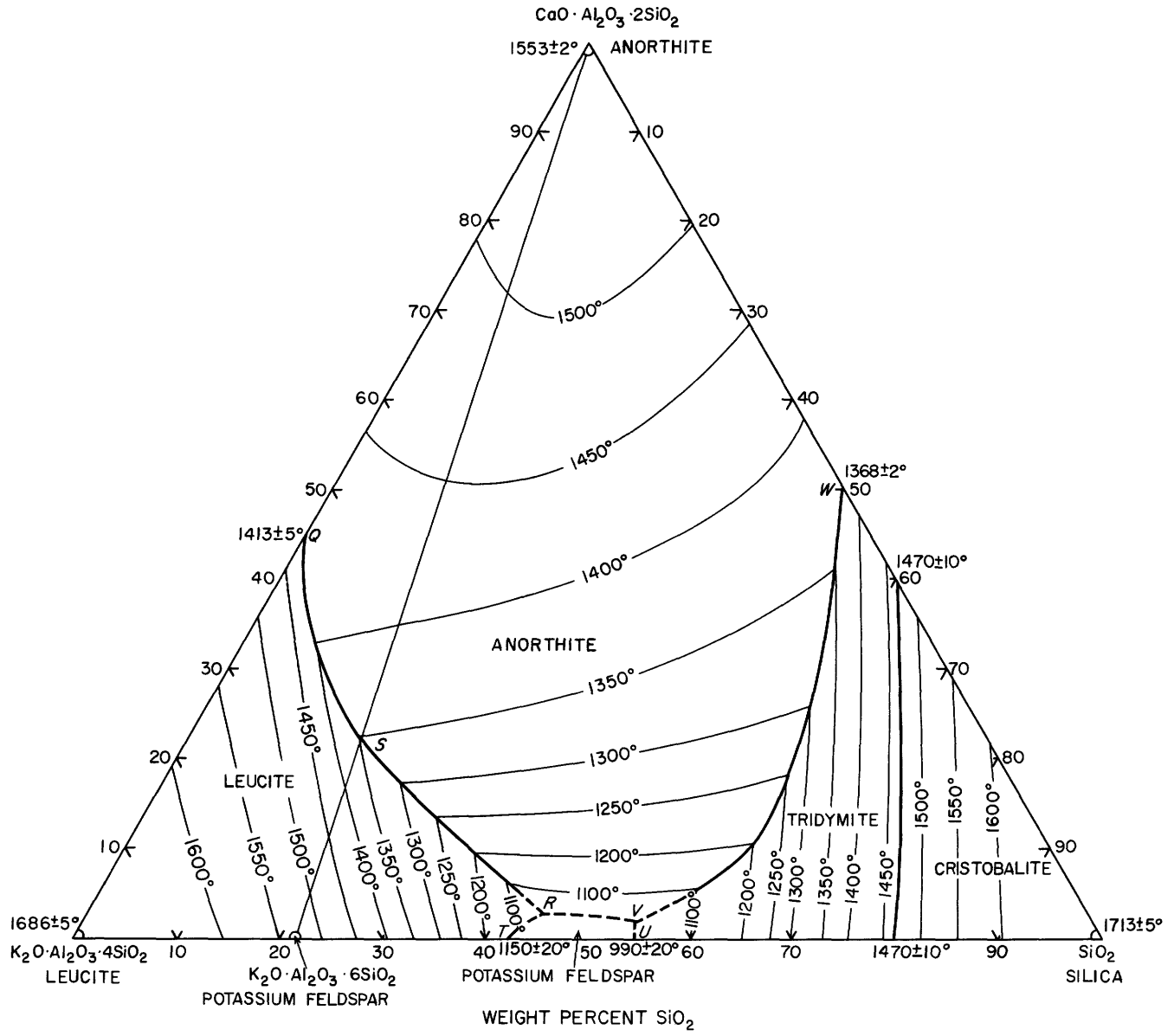

FIGURE 78.—The system K_2O·Al_2O_3·$4SiO_2$ (leucite)–CaO·Al_2O_3·$2SiO_2$ (anorthite)–SiO_2, a part of a plane through the tetrahedron K_2O–CaO–Al_2O_3–SiO_2. Modified from Schairer and Bowen (1947b).

found, but evidence points toward at least partial solid solutions between

$$K_2O \cdot Al_2O_3 \cdot 2SiO_2 \text{ and } K_2O \cdot FeO \cdot 3SiO_2$$

and between

$$K_2O \cdot Al_2O_3 \cdot 4SiO_2 \text{ and } K_2O \cdot FeO \cdot 5SiO_2.$$

MgO–CaO–FeO–SiO_2

Schairer and Osborn (1950) studied the system $CaO \cdot SiO_2$ (wollastonite)–$CaO \cdot MgO \cdot SiO_2$ (monticellite)–FeO (fig. 80), which is part of the plane passing through $CaO \cdot SiO_2$, MgO, and FeO in the tetrahedron MgO–CaO–FeO–SiO_2. Monticellite melts incongruently with formation of MgO, and the area monticellite– FeO–*H*–*C*–*D* is a section cut by the plane through the phase volume of the magnesiowüstite solid solutions. In this triangle there is a section *EBCD* through the phase volume of $3CaO \cdot MgO \cdot 2SiO_2$ (merwinite), the composition of which is outside this plane. The area *BCHGA* is a trace of the phase volume of olivine solid solutions intermediate between monticellite and its iron analog $CaO \cdot FeO \cdot 2SiO_2$. There is also a section through the phase volume of melilite solid solutions

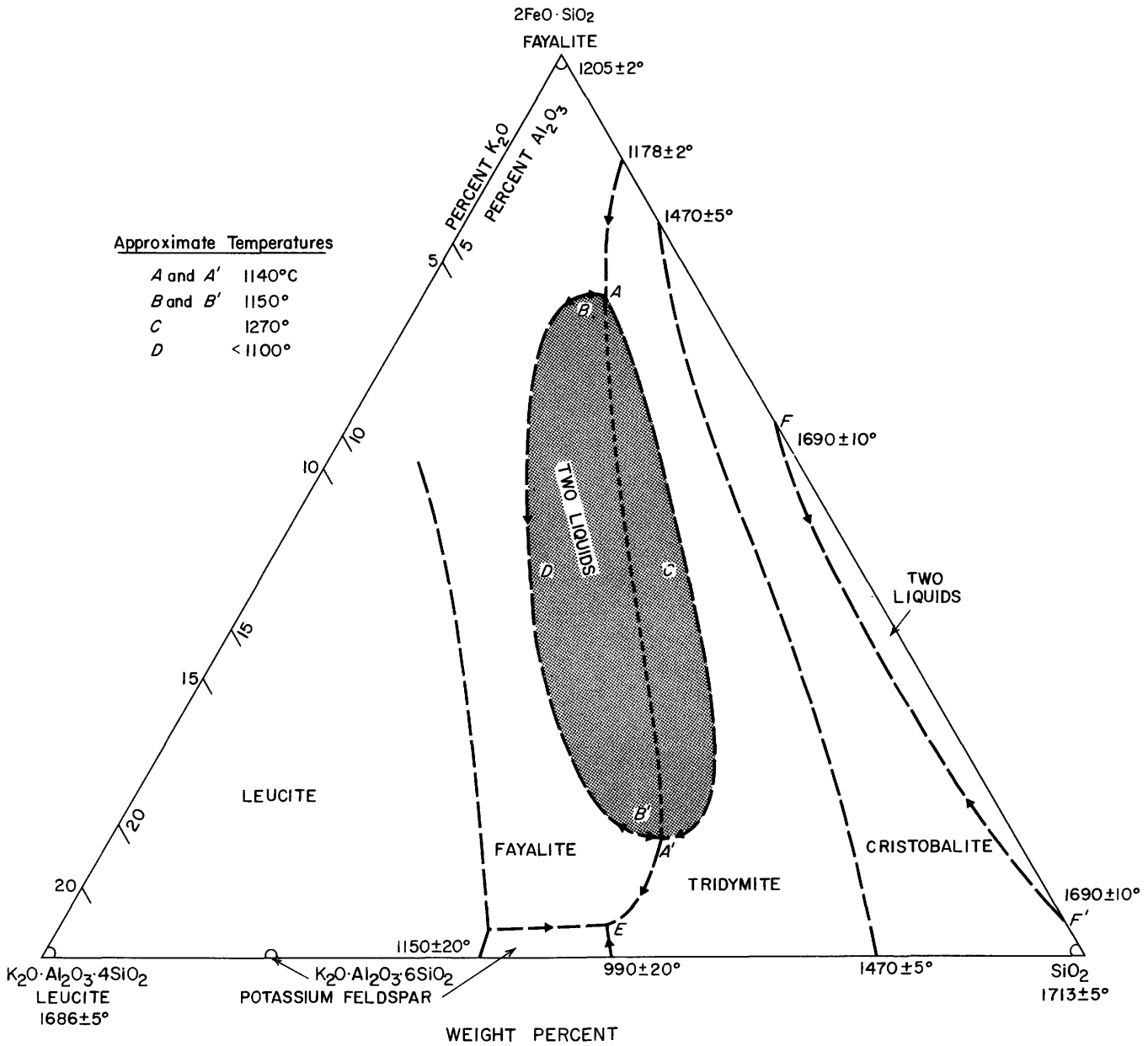

FIGURE 79.—A preliminary study of the section $K_2O \cdot Al_2O_3 \cdot 4SiO_2$ (leucite)–$2FeO \cdot SiO_2$ (fayalite)–SiO_2, which is part of the plane $K_2O \cdot Al_2O_3$–$2FeO \cdot SiO_2$–SiO_2 through the tetrahedron K_2O-FeO–Al_2O_3–SiO_2. Modified from Roedder (1951b).

intermediate between akermanite and iron-akermanite, area *FEBA*. The join akermanite–Fe akermanite may be considered as binary up to its intersection with the curve *FAG*, the trace of the boundary curve between the phase volumes of α–$CaO \cdot SiO_2$ (pseudowollastonite) and melilite. Beyond this point pseudowollastonite is formed, which does not form solid solutions containing either MgO or FeO. When mixtures in this region are cooled below the inversion temperature, the β–$CaO \cdot SiO_2$ (wollastonite) formed contains some solid solution, and at subsolidus temperatures on this join the phases are β–$CaO \cdot SiO_2$, melilite, and olivine.

MgO–CaO–Al_2O_3–Fe_2O_3

Hansen and Brownmiller (1928) and Insley and McMurdie (1938) found the system

$$MgO–4CaO \cdot Al_2O_3 \cdot Fe_2O_3$$

to be binary with a eutectic at 1347°±3°C, at 6.5 percent MgO, 93.5 percent $4CaO \cdot Al_2O_3 \cdot Fe_2O_3$. No indication of solid solution was found.

MgO–CaO–Al_2O_3–SiO_2

Many planes through the tetrahedron representing the system MgO–CaO–Al_2O_3–SiO_2 have been studied.

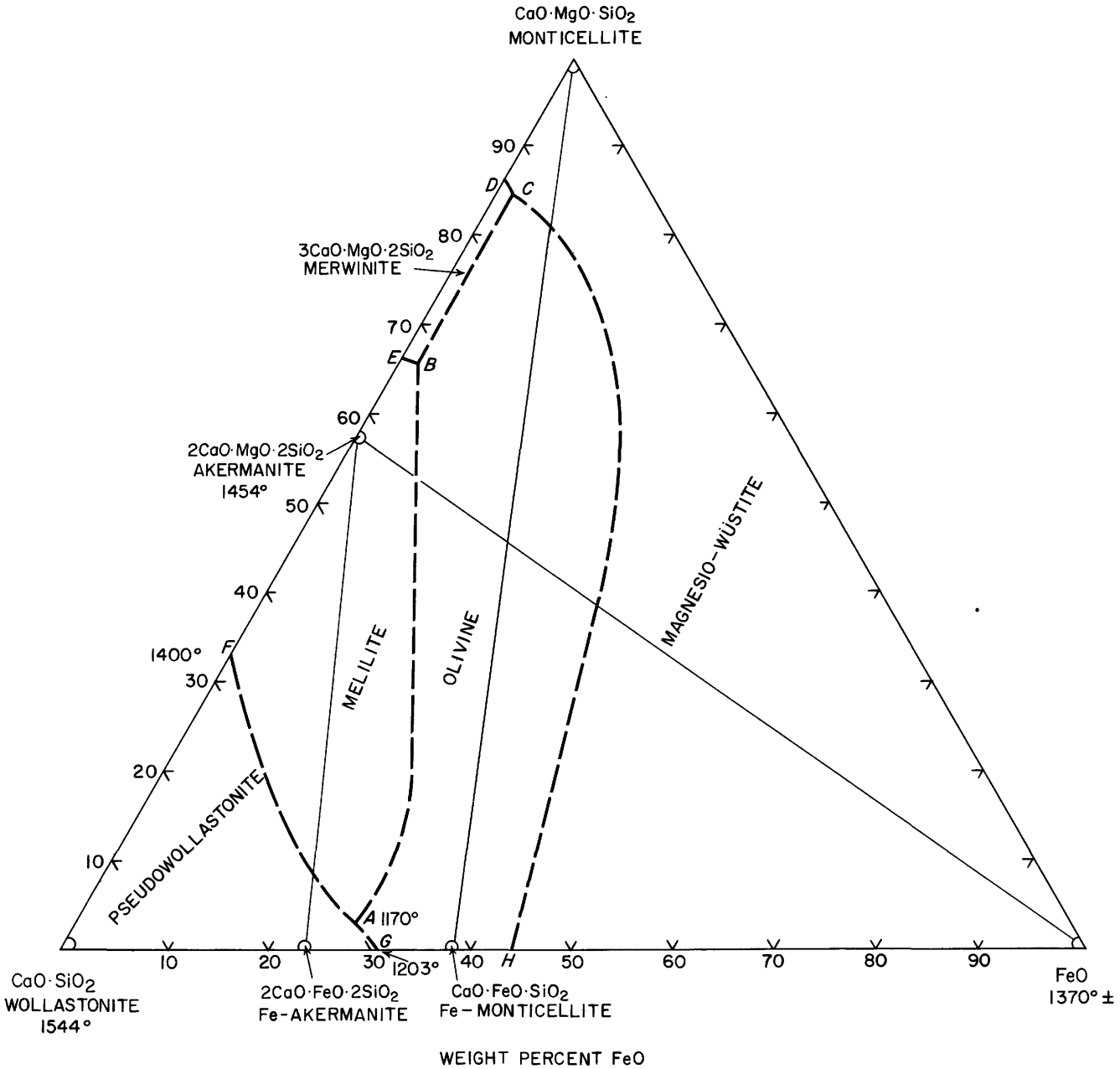

FIGURE 80.—Phase-equilibrium diagram of the area $CaO \cdot SiO_2$ (wollastonite)–$CaO \cdot MgO \cdot SiO_2$ (monticellite)–FeO, a part of the plane $CaO \cdot SiO_2$–MgO–FeO, through the tetrahedron MgO–CaO–FeO–SiO_2. Modified from Schairer and Osborn (1950).

No quaternary compounds are formed, and each of the planes is a triangular section, having its corners at an apex, or a side, or in one of the limiting triangles. The various compounds are shown in figure 81 in which the base of the tetrahedron is the system MgO–CaO–SiO_2, and two of the sides, CaO–Al_2O_3–SiO_2 and MgO–Al_2O_3–SiO_2, are laid out flat. The side MgO–CaO–Al_2O_3 is omitted because none of the compounds used as components lie in it.

Prince (1951) found that the join $2CaO \cdot SiO_2$–$MgO \cdot Al_2O_3$ is a binary system, with a eutectic at 1418°C, 65.6 percent $2CaO \cdot SiO_2$, 34.5 percent MgO. Al_2O_3, or 9.8 percent MgO, 24.7 percent Al_2O_3, 65.5 percent $2CaO \cdot SiO_2$. This line divides the plane MgO–Al_2O_3–$2CaO \cdot SiO_2$ (fig. 82) into two ternary systems. The piercing point T of the equilibrium

$$MgO + MgO \cdot Al_2O_3 + 2CaO \cdot SiO_2 + \text{liquid},$$

at 1417°C, 10.4 percent MgO, 23.9 percent Al_2O_3, 65.7

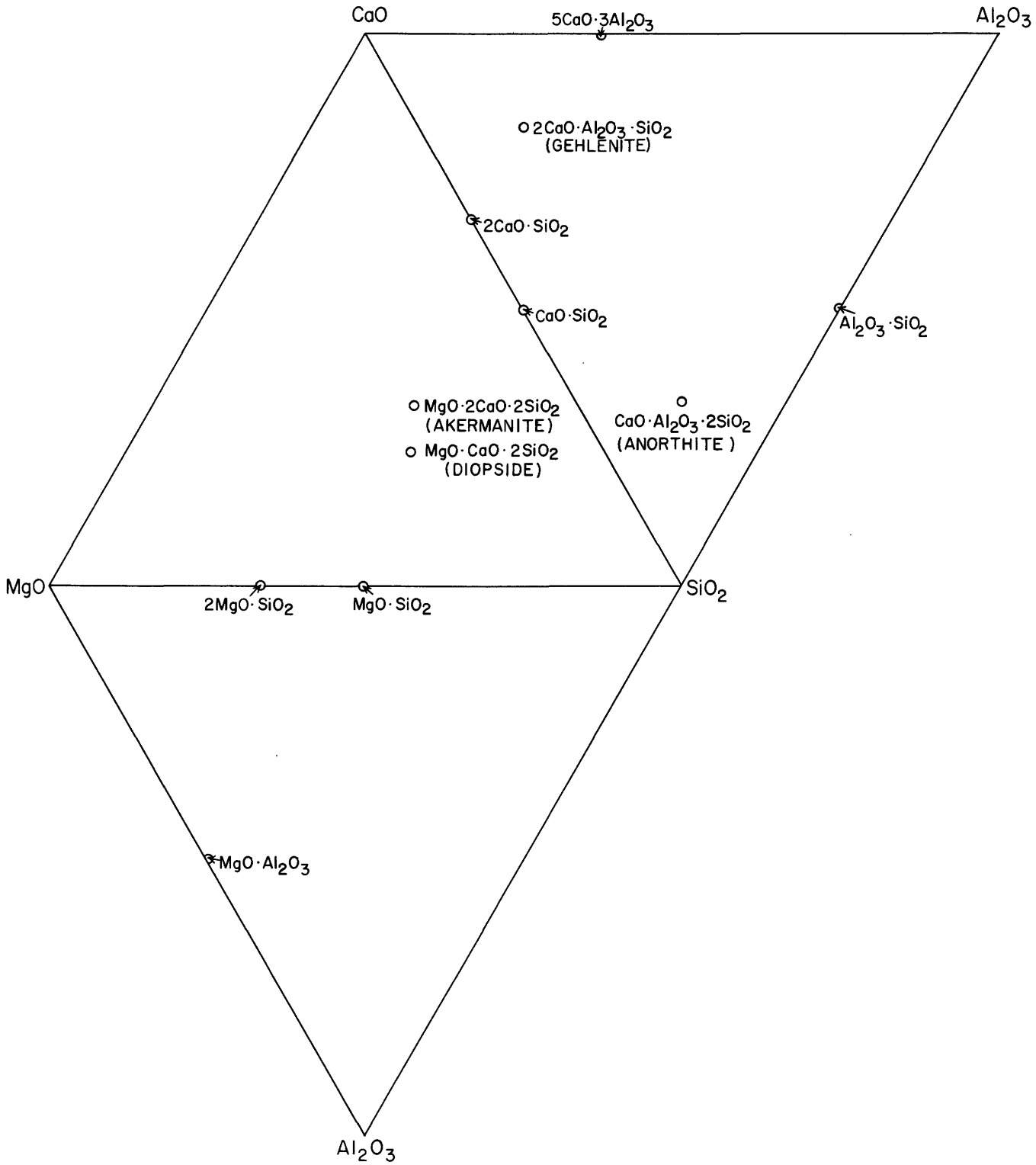

FIGURE 81.—The tetrahedron MgO–CaO–Al_2O_3–SiO_2, represented by the base MgO–CaO–SiO_2, and two of the triangular sides, CaO–Al_2O_3–SiO_2 and MgO–Al_2O_3–SiO_2, which terminate at the Al_2O_3-apex, laid out flat.

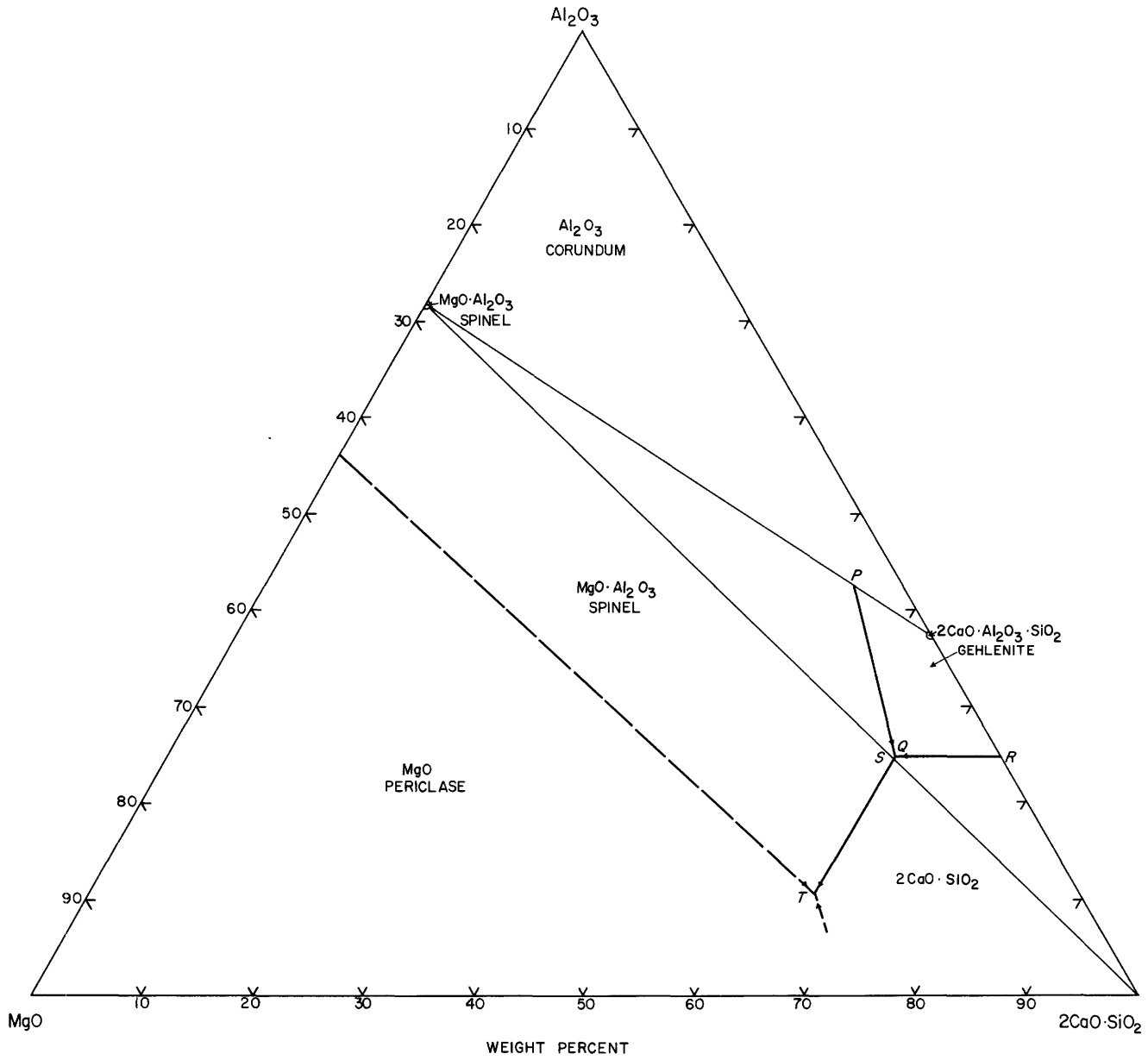

FIGURE 82.—The plane MgO–Al_2O_3–$2CaO \cdot SiO_2$ through the tetrahedron MgO–CaO–Al_2O_3–SiO_2. Modified from Prince (1951).

percent $2CaO \cdot SiO_2$ is a eutectic, as is also the piercing point Q of the equilibrium $MgO \cdot Al_2O_3 + 2CaO \cdot Al_2O_3 \cdot SiO_2$ (gehlenite) + $2CaO \cdot SiO_2$ + liquid, at 1414°C, 9.3 percent MgO, 24.8 percent Al_2O_3, 65.9 percent $2CaO \cdot SiO_2$. Point R is the eutectic between $2CaO \cdot SiO_2$ and $2CaO \cdot Al_2O_3 \cdot SiO_2$, at 1545°C, 24.9 percent Al_2O_3, 75.1 percent $2CaO \cdot SiO_2$. Point P is a binary eutectic between $MgO \cdot Al_2O_3$ and $2CaO \cdot Al_2O_3 \cdot SiO_2$, at 1527°C, 4.4 percent MgO, 42.5 percent Al_2O_3, 53.1 percent $2CaO \cdot SiO_2$.

The system MgO–Al_2O_3–$CaO \cdot Al_2O_3 \cdot 2SiO_2$ (anorthite), figure 83, was studied by DeVries and Osborn (1957). The sides Al_2O_3–anorthite and MgO–Al_2O_3 are binary systems previously considered, but the side MgO–anorthite is not binary because it intersects the phase volume of $MgO \cdot Al_2O_3$ (spinel). The join anorthite-spinel is not binary because it cuts the phase volume of corundum. The field of anorthite in this section is bounded by the trace of the boundary anorthite–Al_2O_3 on which the temperature falls from 1551°C in the binary system to 1485°C at the piercing point in

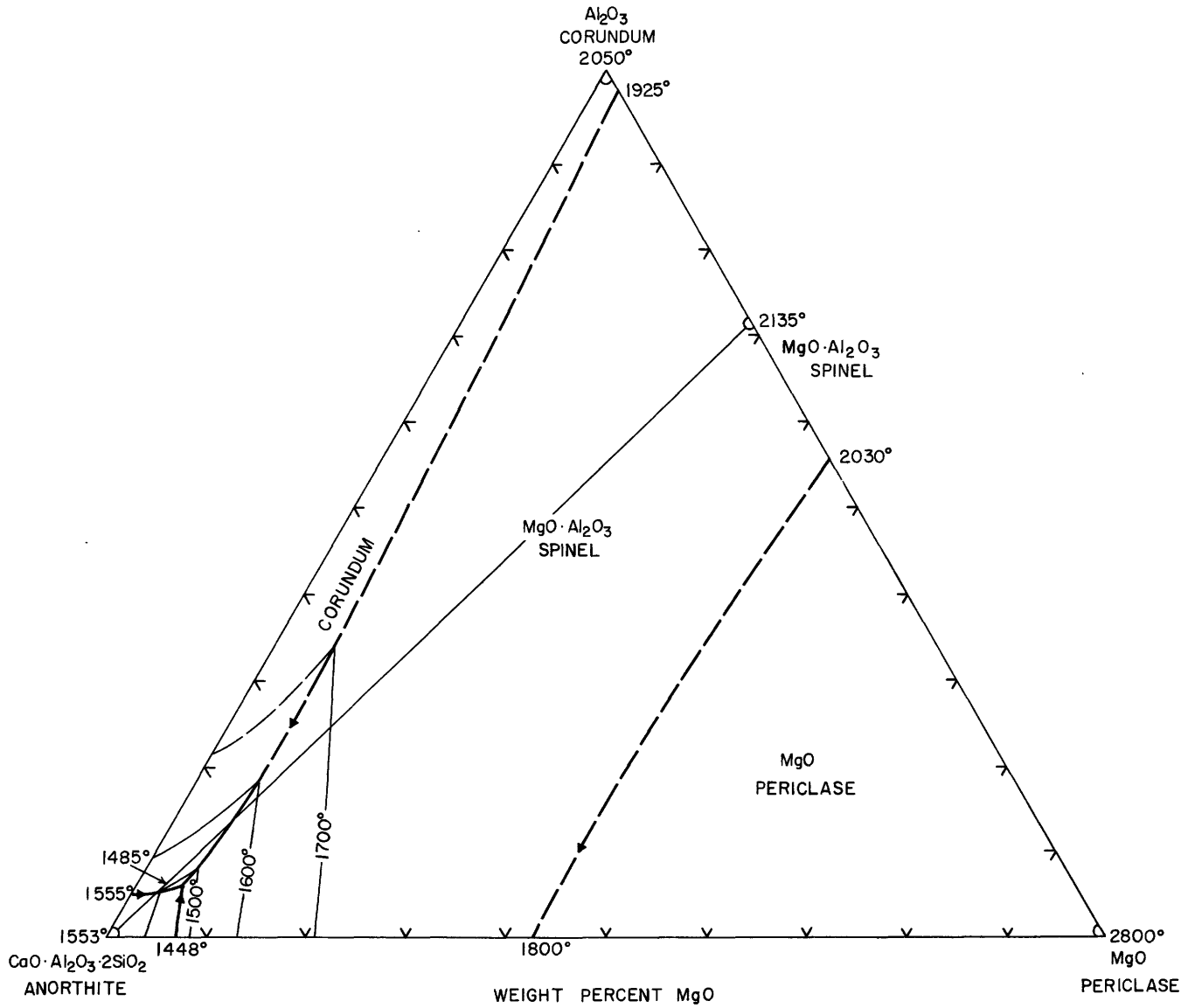

FIGURE 83.—The plane MgO (periclase)–Al_2O_3 (corundum)–$CaO \cdot Al_2O_3 \cdot 2SiO_2$ (anorthite) through the tetrahedron MgO–CaO–Al_2O_3–SiO_2. Modified from DeVries and Osborn (1957).

this section of the equilibrium anorthite-corundum-spinel-liquid. The trace of the boundary between $CaO \cdot Al_2O_3 \cdot 2SiO_2$ and $MgO \cdot Al_2O_3$ then falls to its intersection with the join MgO–anorthite, at 1448°C. This section thus cuts the primary phase volumes of anorthite, corundum, spinel, and periclase.

The plane MgO (periclase)–$2MgO \cdot SiO_2$ (forsterite)–$CaO \cdot Al_2O_3 \cdot 2SiO_2$ (anorthite) (fig. 84), studied byDeVries and Osborn (1957), cuts the phase volumes of MgO (periclase), forsterite, spinel, and anorthite, and since the composition of spinel does not lie in this plane, the system is not ternary. The piercing point of the univariant equilibrium periclase+forsterite+spinel+liquid is at 1610°C, but the exact composition was not determined.

The system $MgO \cdot SiO_2$ (enstatite)–$CaO \cdot Al_2O_3 \cdot 2SiO_2$ (anorthite)–$CaO \cdot MgO \cdot 2SiO_2$ (diopside) was studied by Hytönen and Schairer (1960) and the results are shown in the preliminary diagram figure 85. Heavy curves are traces of boundary surfaces between the primary-phase volumes of the several solid phases that appear on the liquidus surface. The subliquidus crystallization is complex and the details have not been worked out. Three polymorphic modifications of $MgO \cdot SiO_2$ (protoenstatite, clinoenstatite, and ortho-

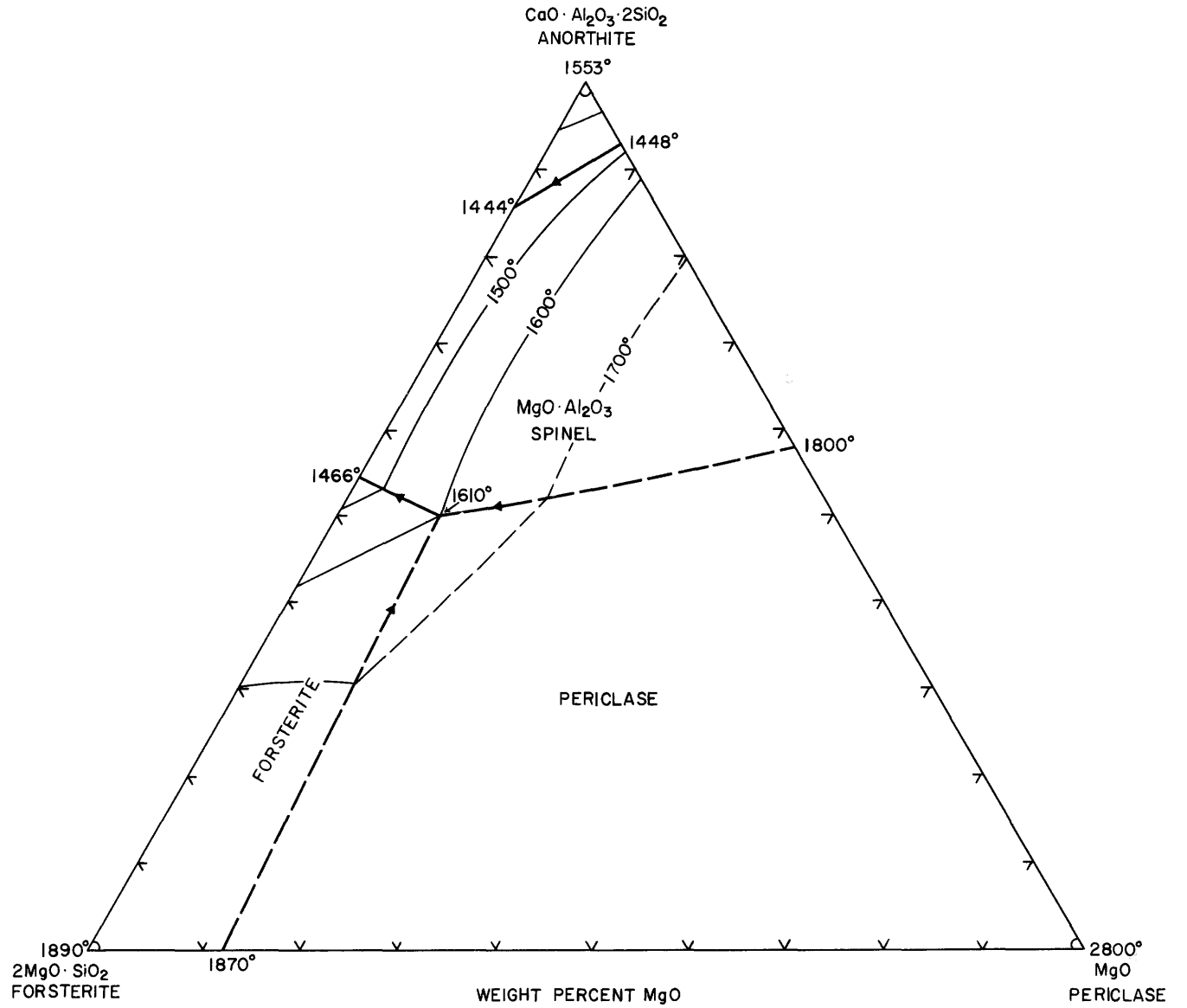

FIGURE 84.—The plane MgO (periclase)-2MgO·SiO$_2$ (forsterite)-CaO·Al$_2$O$_3$·2SiO$_2$ (anorthite) through the tetrahedron MgO–CaO–Al$_2$O$_3$–SiO$_2$. Modified from DeVries and Osborn (1957).

enstatite), each as solid solutions, appear at various temperatures during crystallization or as quenching products. Small amounts of free silica (present as metastable cristobalite) were observed in some of the compositions rich in diopside at and below solidus temperatures.

The plane, MgO–2CaO·SiO$_2$–5CaO·3Al$_2$O$_3$, was studied by Hansen (1928) with special reference to the constitution of portland cement. The plane cuts the primary-phase volume of MgO, which occupies most of the section of 2CaO·SiO$_2$ and of 5CaO·3Al$_2$O$_3$. The piercing point of the equilibrium

$$MgO + 2CaO \cdot SiO_2 + 5CaO \cdot 3Al_2O_3 + \text{liquid}$$

is a eutectic, at 1315°±5°C, 5 percent MgO, 12 percent 2CaO·SiO$_2$, 76 percent 5CaO·3Al$_2$O$_3$.

The plane CaO·Al$_2$O$_3$·2SiO$_2$ (anorthite)–MgO·Al$_2$O$_3$ (spinel)–2MgO·SiO$_2$ (forsterite) (fig. 86), studied by DeVries and Osborn (1957), is not a ternary system. In addition to the phase volumes of the components, it intersects the phase volume of corundum, and on the side anorthite-forsterite there is a region in which spinel is the primary phase, and the composition of the liquid in equilibrium with spinel, anorthite, and forsterite lies outside of this triangle at 1420°C. The piercing point of the equilibrium anorthite+corundum+spinel+liquid is at 1480°C.

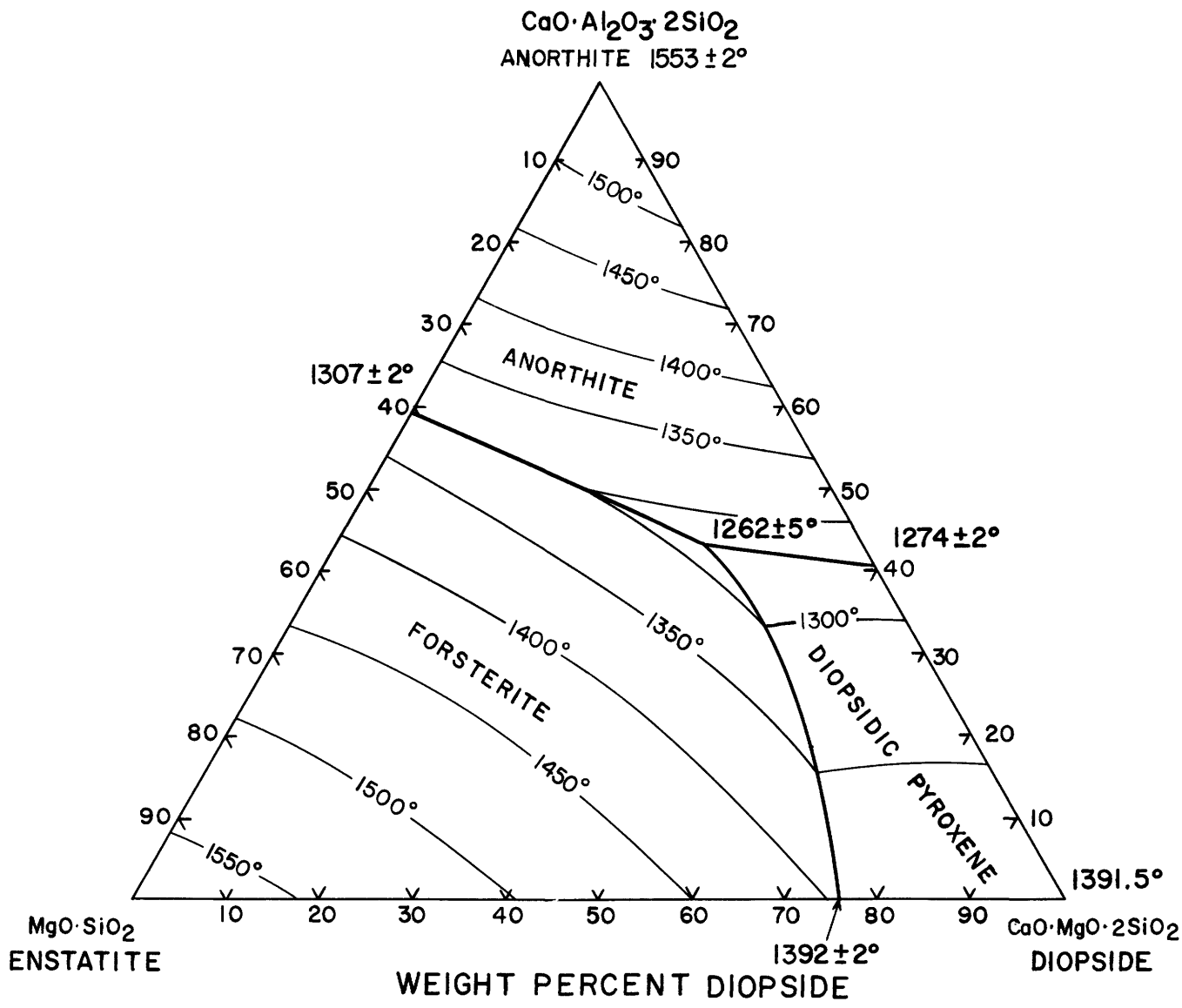

FIGURE 85.—Phase-equilibrium diagram for the plane $MgO \cdot SiO_2$ (enstatite)–$CaO \cdot Al_2O_3 \cdot 2SiO_2$ (anorthite)–$CaO \cdot MgO \cdot 2SiO_2$ (diopside). Modified from Hytönen and Schairer (1960).

The plane, $2CaO \cdot Al_2O_3 \cdot SiO_2$ (gehlenite)–Al_2O_3 corundum)–$MgO \cdot Al_2O_3$ (spinel), represented by figure 87, was studied by DeVries and Osborn (1957). The field of spinel, $MgO \cdot Al_2O_3$, occupies the largest part of this diagram, but the plane also cuts the primary-phase volumes of $2CaO \cdot Al_2O_3 \cdot SiO_2$, Al_2O_3, $CaO \cdot 2Al_2O_3$, and $CaO \cdot 6Al_2O_3$, and since the compositions of the two calcium aluminates are not in this triangle, the section is not a ternary system. There are three piercing points: $2CaO \cdot Al_2O_3 \cdot SiO_2 + CaO \cdot 2Al_2O_3 +$ spinel + liquid, at 1515°C; $CaO \cdot 2Al_2O_3 + CaO \cdot 6Al_2O_3 +$ spinel + liquid, at 1640°C; and $CaO \cdot 6Al_2O_3 +$ spinel, at 1775°C.

The plane $2CaO \cdot Al_2O_3 \cdot SiO_2$ (gehlenite)–$CaO \cdot Al_2O_3 \cdot 2SiO_2$ (anorthite)–$MgO \cdot Al_2O_3$ (spinel) shown in figure 88, was studied by DeVries and Osborn (1957). It cuts the primary phase volume of spinel, gehlenite, anorthite, corundum, and also of $CaO \cdot 6Al_2O_3$, a composition outside of the component triangle. Liquids in equilibrium with anorthite, gehlenite, and spinel are represented by points outside this triangle.

The plane $2MgO \cdot SiO_2$ (forsterite)–$CaO \cdot MgO \cdot 2SiO_2$ (diopside)–$CaO \cdot Al_2O_3 \cdot 2SiO_2$ (anorthite) through the tetrahedron was studied by Osborn and Tait (1952)

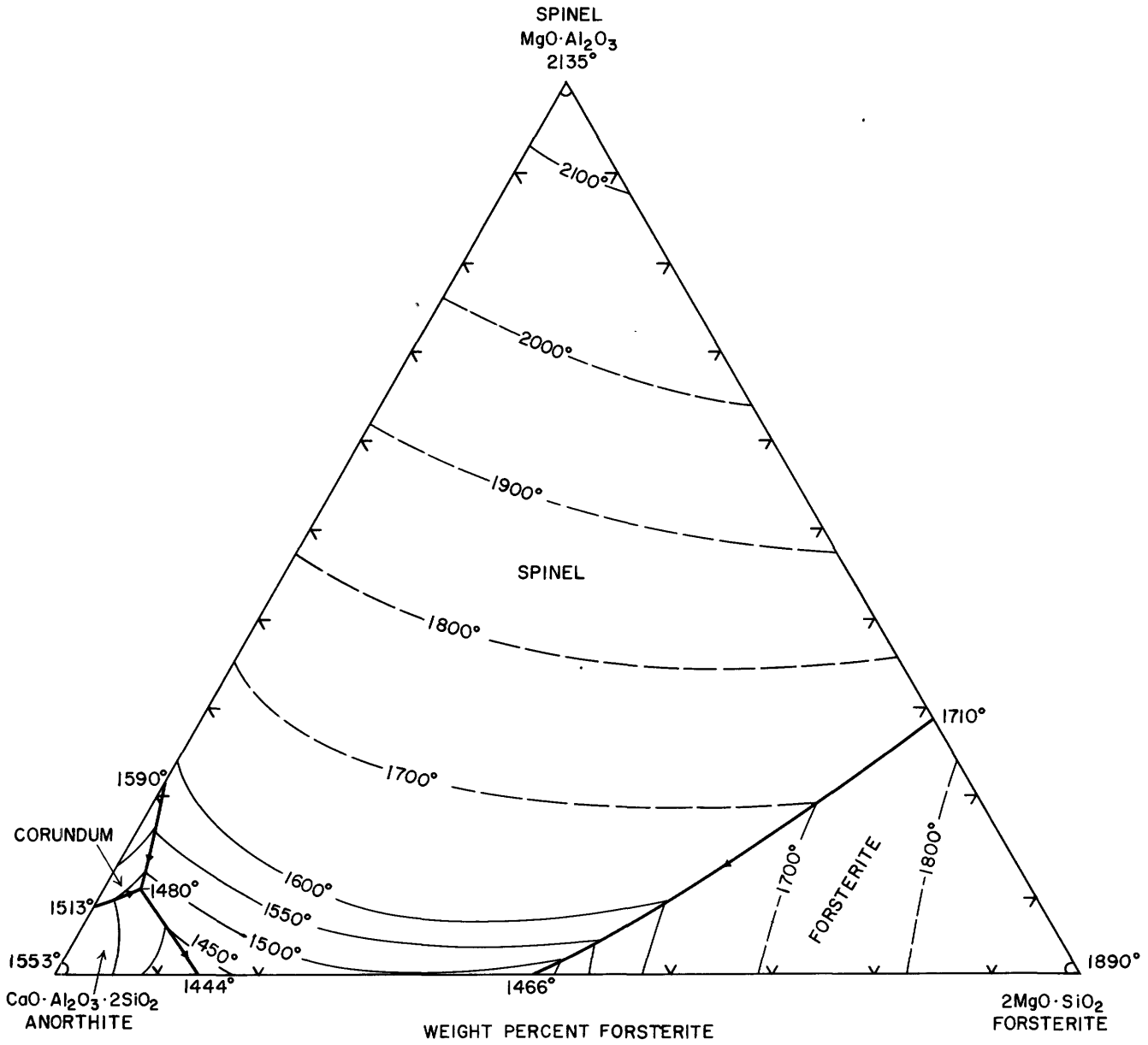

FIGURE 86.—The plane $MgO \cdot Al_2O_3$ (spinel)–$2MgO \cdot SiO_2$ (forsterite)–$CaO \cdot Al_2O_3 \cdot 2SiO_2$ (anorthite) through the tetrahedron MgO–CaO–Al_2O_3–SiO_2. Modified from DeVries and Osborn (1957).

and their phase-equilibrium diagram is figure 89. It is not a ternary system because it cuts the phase volume of spinel, and because the diopside contains some Al_2O_3. Point D, at 1317° ±5°C is the piercing point of the equilibrium $CaO \cdot Al_2O_3 \cdot 2SiO_2 + MgO \cdot Al_2O_3 + 2MgO \cdot SiO_2$ + liquid. The minimum temperature of the system is at point E, 1270° ±5°C, at the composition 7.5 percent $2MgO \cdot SiO_2$, 49 percent $MgO \cdot CaO \cdot 2SiO_2$, 43.5 percent $CaO \cdot Al_2O_3 \cdot 2SiO_2$. It is the piercing point of the equilibrium $2MgO \cdot SiO_2 + CaO \cdot MgO \cdot 2SiO_2$ solid solution + $CaO \cdot Al_2O_3 \cdot 2SiO_2$ + liquid, and would be eutectic were it not for the small amount of solid solution in the diopside.

The section $2MgO \cdot SiO_2$ (forsterite)–$CaO \cdot Al_2O_3 \cdot 2SiO_2$ (anorthite)–SiO_2 through the tetrahedron CaO–MgO–Al_2O_3–SiO_2 was the first plane to be studied (Andersen, 1915). It is not a ternary system, for the plane cuts the phase volume of $MgO \cdot Al_2O_3$ (spinel) on the side $2MgO \cdot SiO_2$–

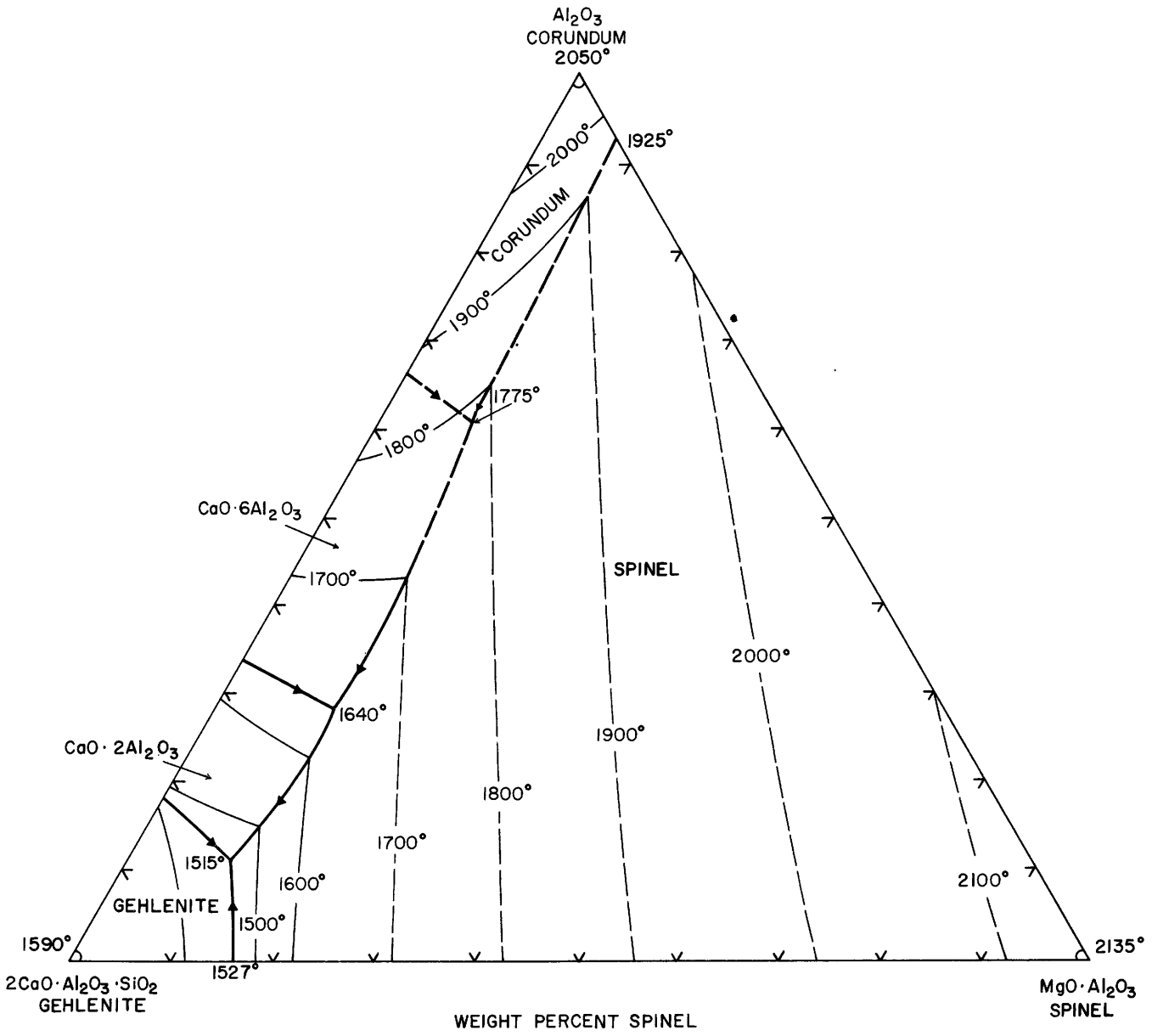

FIGURE 87.—The plane $2CaO \cdot Al_2O_3 \cdot SiO_2$ (gehlenite)–Al_2O_3 (corundum)–$MgO \cdot Al_2O_3$ (spinel), through the tetrahedron MgO–CaO–Al_2O_3–SiO_2. Modified from DeVries and Osborn (1957).

$CaO \cdot Al_2O_3 \cdot 2SiO_2$. In figure 90 the traces of the boundaries between the various phase volumes are shown, with their intersections at the piercing points. *K* is the piercing point for the univariant equilibrium $2MgO \cdot SiO_2 + MgO \cdot Al_2O_3 + CaO \cdot Al_2O_3 \cdot 2SiO_2$ + liquid, at 1320°C, and the liquid has the composition 61 percent $CaO \cdot Al_2O_3 \cdot 2SiO_2$, 29.5 percent $2MgO \cdot SiO_2$, 9.5 percent SiO_2. Point *M* corresponds to the equilibrium $MgO \cdot SiO_2 + 2MgO \cdot SiO_2 + CaO \cdot Al_2O_3 \cdot 2SiO$ + liquid, at 1260°C, 25.5 percent $2MgO \cdot SiO_2$, 55 percent $CaO \cdot Al_2O_3 \cdot 2SiO_2$ 19.5 percent SiO_2. Piercing point *N* is a eutectic, since the liquid lies within the triangle determined by the solid phases $MgO \cdot SiO_2$, $CaO \cdot Al_2O_3 \cdot 2SiO_2$, and SiO_2. The temperature is 1222°C, the composition 16.4 percent $2MgO \cdot SiO_2$, 50.6 percent $CaO \cdot Al_2O_3 \cdot 2SiO_2$, 33.0 percent SiO_2. The

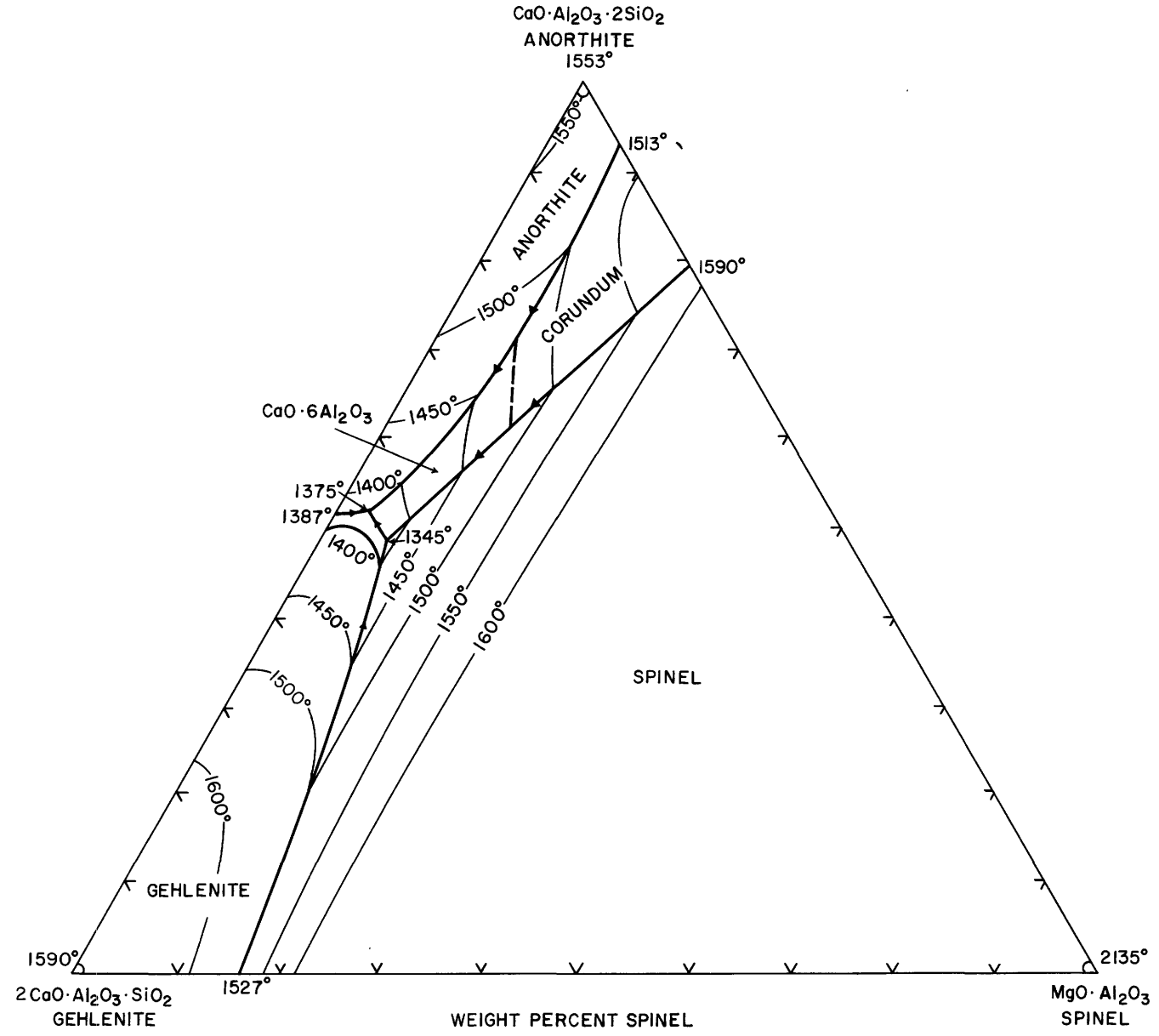

FIGURE 88.—The plane $2CaO \cdot Al_2O_3 \cdot SiO_2$ (gehlenite)–$CaO \cdot Al_2O_3 \cdot 2SiO_2$ (anorthite)–$MgO \cdot Al_2O_3$ (spinel) through the tetrahedron MgO–CaO–Al_2O_3–SiO_2. Modified from DeVries and Osborn (1957).

plane also cuts a section through the region of two immiscible liquid layers, but the location of the boundary has not been determined.

The plane $MgO \cdot SiO_2$–$CaO \cdot SiO_2$–Al_2O_3 through the tetrahedron was studied by Segnit (1956) with results shown in figure 91. The section is not a ternary system, and it cuts the primary-phase volumes of corundum, spinel, enstatite solid solutions, pyroxene solid solutions, wollastonite solid solutions, pseudowollastonite, melilite, and anorthite.

The section $CaO \cdot SiO_2$ (wollastonite)–$CaO \cdot MgO \cdot 2SiO_2$ (diopside)–$CaO \cdot Al_2O_3 \cdot 2SiO_2$ (anorthite) (fig. 92), studied by Osborn (1942), is part of a plane through the tetrahedron passing through the points $MgO \cdot SiO_2$, $CaO \cdot SiO_2$, and $Al_2O_3 \cdot SiO_2$. It is not a ternary system

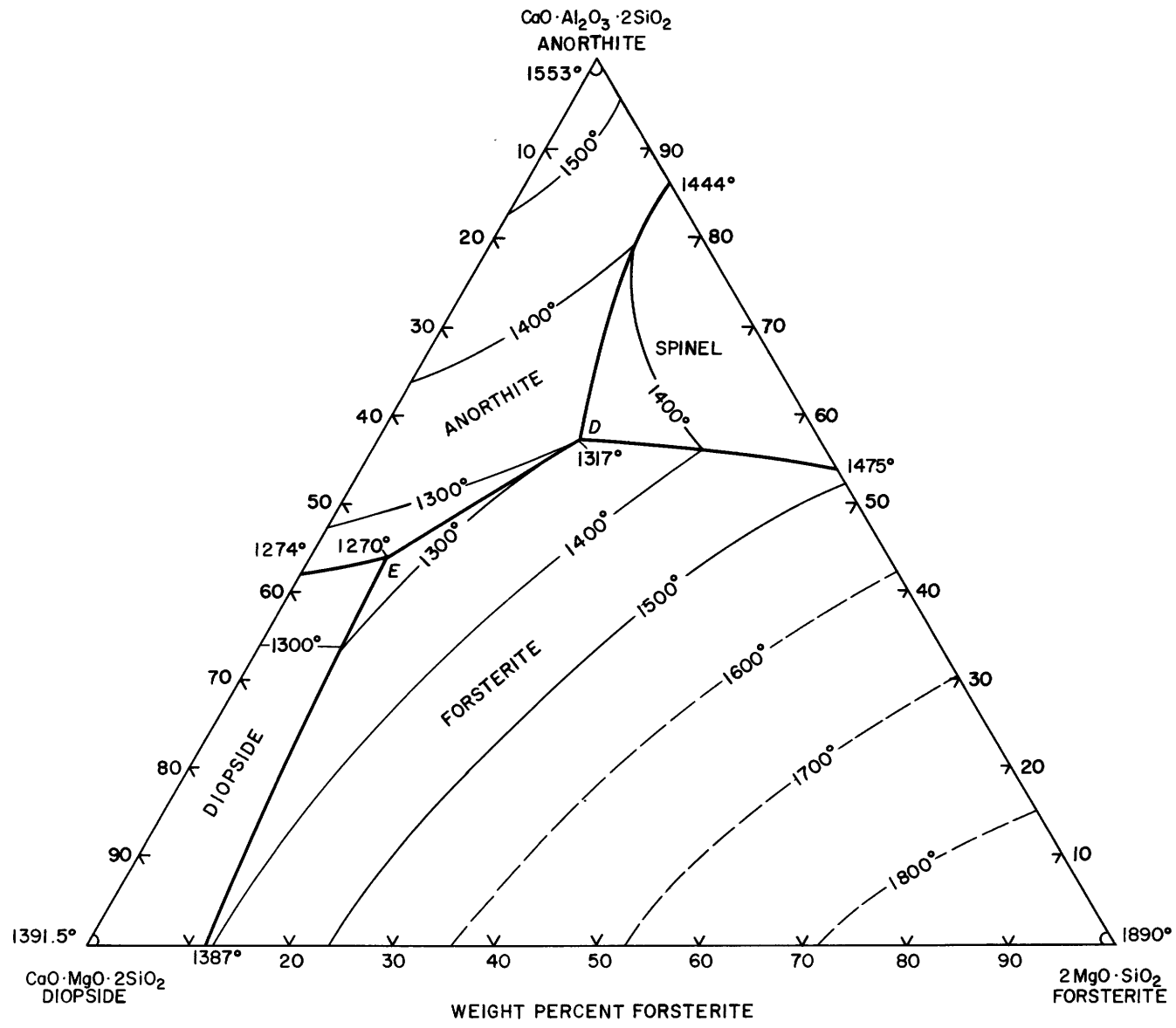

FIGURE 89.—The plane $2MgO \cdot SiO_2$ (forsterite)–$CaO \cdot MgO \cdot 2SiO_2$ (diopside)–$CaO \cdot Al_2O_3 \cdot 2SiO_2$ (anorthite) through the tetrahedron MgO–CaO–Al_2O_3–SiO_2. Modified from Osborn and Tait (1952).

because the diopside ($CaO \cdot MgO \cdot 2SiO_2$) contains a small amount of Al_2O_3. The boundary between the phase volumes of α-$CaO \cdot SiO_2$ (pseudowollastonite) and β-$CaO \cdot SiO_2$ (wollastonite) solid solutions is the curve ZR, and is not a line of constant temperature because of solid solution in β-$CaO \cdot SiO_2$. The piercing-point R of the equilibrium between α-$CaO \cdot SiO_2$ and β-$CaO \cdot SiO_2$ solid solutions, anorthite, and liquid is at 1245°±3°C, 36 percent $CaO \cdot SiO_2$, 25.5 percent $CaO \cdot MgO \cdot 2SiO_2$, 38.5 percent $CaO \cdot Al_2O_3 \cdot 2SiO_2$, and the wollastonite solid solution contains 91 percent $CaO \cdot SiO_2$, 9 percent $CaO \cdot MgO \cdot 2SiO_2$. The phases at the piercing point E, at 1236°±3°C, are the wollastonite solid solution containing 89 percent $CaO \cdot SiO_2$ and 11 percent $CaO \cdot MgO \cdot 2SiO_2$; diopside; anorthite; and the liquid of the composition 32 percent $CaO \cdot SiO_2$, 30 percent $CaO \cdot MgO \cdot 2SiO_2$, and 38 percent $CaO \cdot Al_2O_3 \cdot 2SiO_2$.

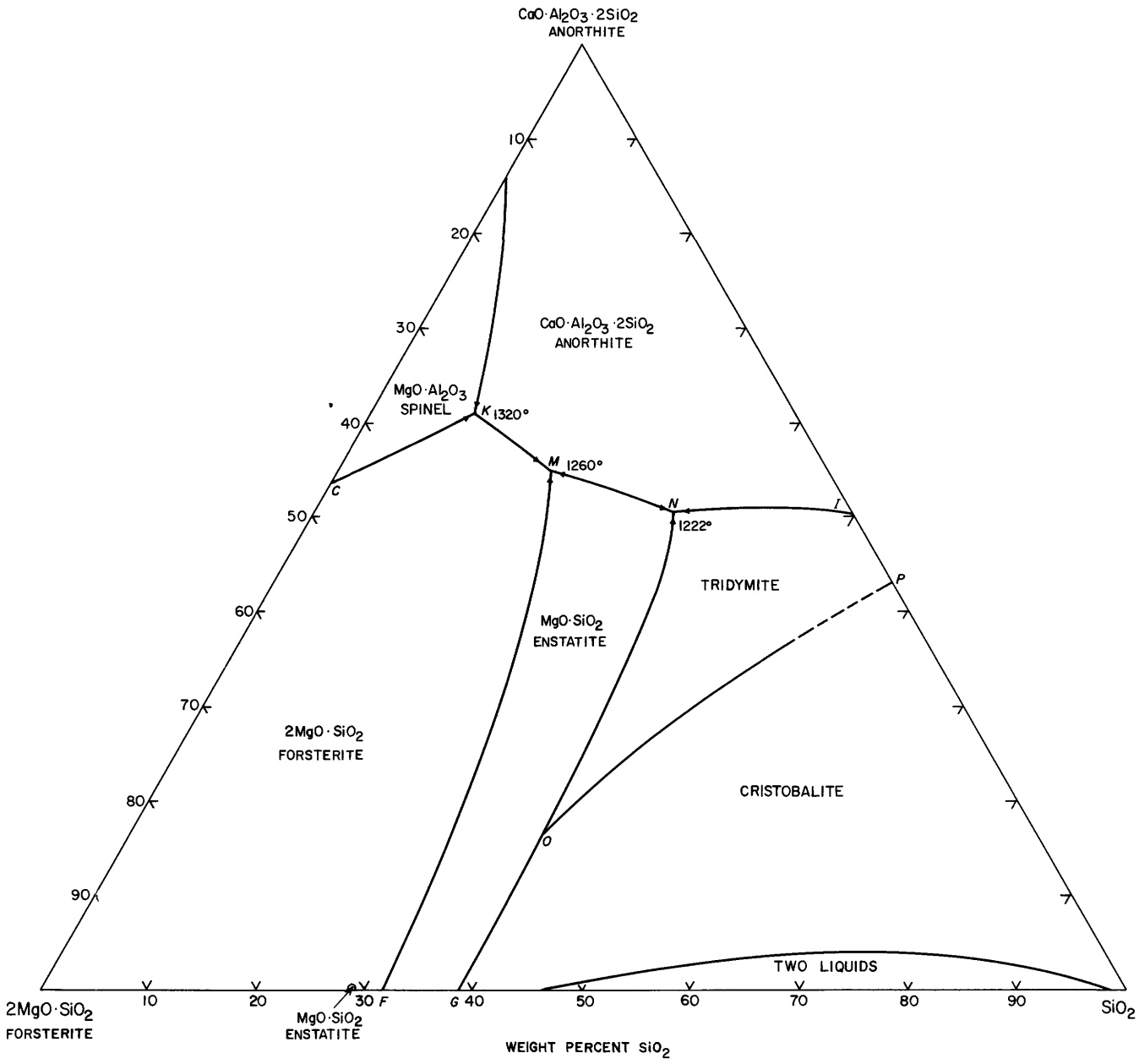

FIGURE 90.—The plane $2MgO \cdot SiO_2$ (forsterite)–$CaO \cdot Al_2O_3 \cdot 2SiO_2$ (anorthite)–SiO_2 through the tetrahedron MgO–CaO–Al_2O_3–SiO_2. Modified from Andersen (1915).

The system $CaO \cdot SiO_2$ (wollastonite)–$2CaO \cdot Al_2O_3 \cdot SiO_2$ (gehlenite)–$2CaO \cdot MgO \cdot 2SiO_2$ (akermanite) is part of the plane

$$MgO–CaO \cdot SiO_2–CaO \cdot Al_2O_3$$

through the tetrahedron MgO–CaO–Al_2O_3–SiO_2 (fig. 81). It was studied by Osborn and Schairer (1941) and their phase-equilibrium diagram is figure 93. The side akermanite-gehlenite is a solid-solution series with a minimum at 1390°C, 73 percent akermanite; the side $CaO \cdot SiO_2$–gehlenite has a eutectic at 1318°C, 36.7 percent gehlenite; the side $CaO \cdot SiO_2$–akermanite a eutectic at 1400°C and 53 percent akermanite. There are but two fields, one of α–$CaO \cdot SiO_2$ (pseudowollastonite) in

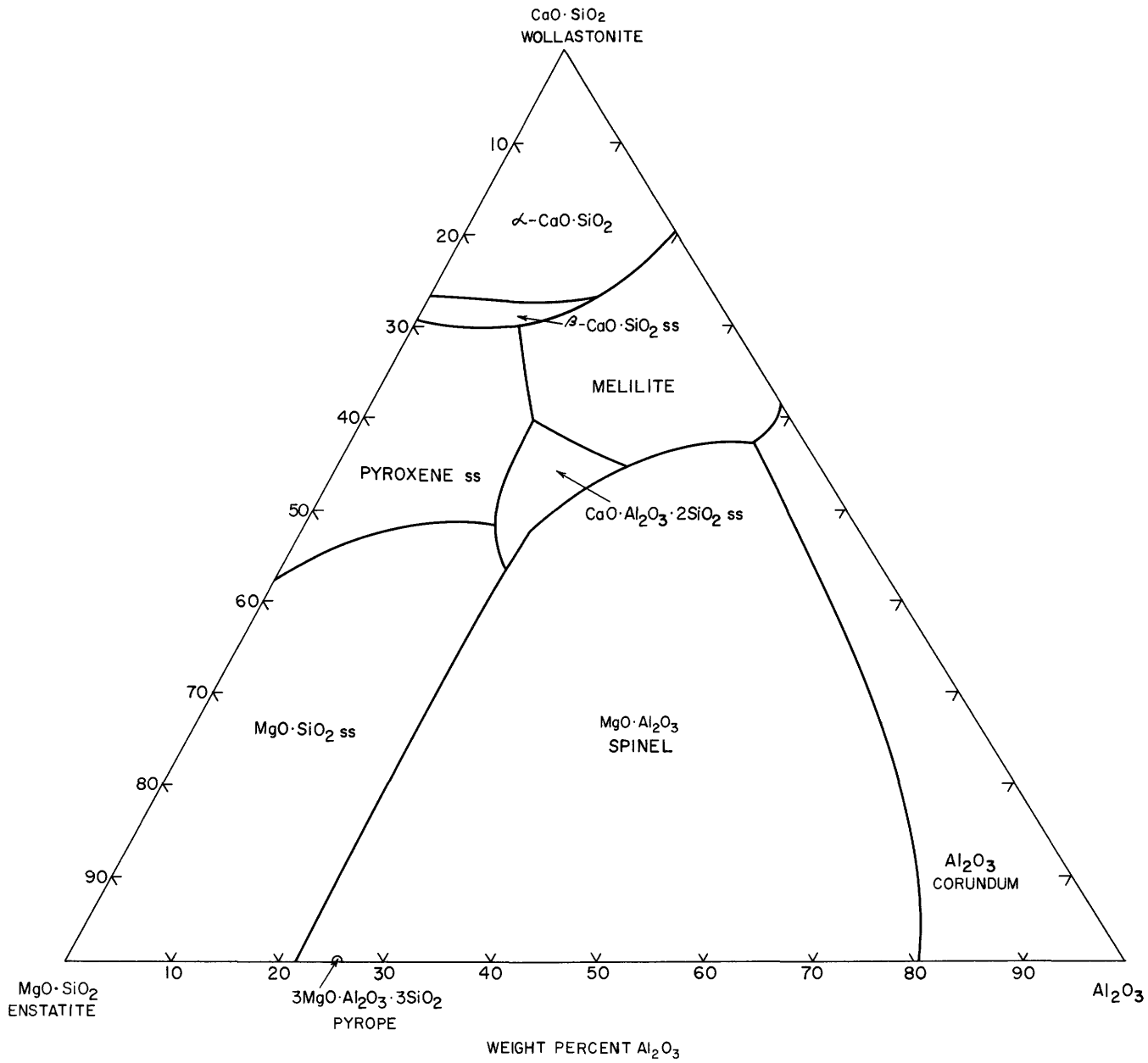

FIGURE 91.—The plane $MgO{\cdot}SiO_2$ (enstatite)–$CaO{\cdot}SiO_2$ (wollastonite)–Al_2O_3 through the tetrahedron MgO–CaO–Al_2O_3–SiO_2. Modified from Segnit (1956). *ss*, Solid solution.

which there is no solid solution, and a complete series of solid solutions between gehlenite and akermanite. The minimum along the boundary between these two fields is at 1302°C and 51.1 percent $CaO{\cdot}SiO_2$, 20±2 percent $2CaO{\cdot}MgO{\cdot}2SiO_2$, 29±1 percent $2CaO{\cdot}Al_2O_3{\cdot}SiO_2$.

DeWys and Foster (1956) found that $CaO{\cdot}Al_2O_3{\cdot}2SiO_2$ (anorthite)–$2CaO{\cdot}MgO{\cdot}2SiO_2$ (akermanite) form a binary system, with a eutectic at 1234°C and 54 percent akermanite. DeWys and Foster (1958) found the system $CaO{\cdot}MgO{\cdot}2SiO_2$ (diopside)–$CaO{\cdot}Al_2O_3{\cdot}2SiO_2$ (anorthite)–$2CaO{\cdot}MgO{\cdot}2SiO_2$

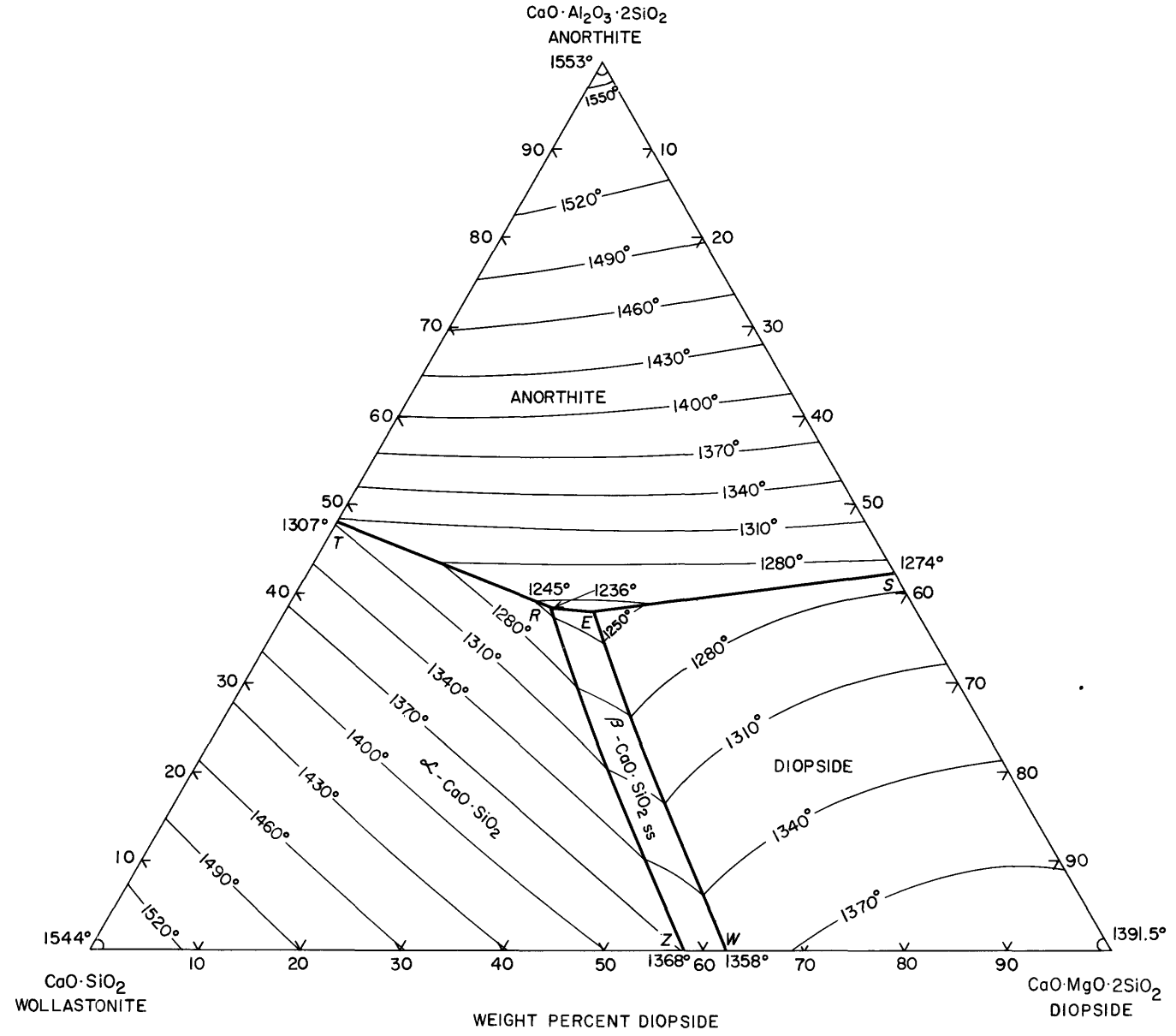

FIGURE 92.—The section $CaO \cdot SiO_2$ (wollastonite)–$CaO \cdot MgO \cdot 2SiO_2$ (diopside)–$CaO \cdot Al_2O_3 \cdot 2SiO_2$ (anorthite), part of a plane through the tetrahedron MgO–CaO–Al_2O_3–SiO_2. Modified from Osborn (1942). *ss*, Solid solution.

(akermanite) to have a ternary eutectic at 1226°C, 9 percent diopside, 44 percent anorthite, 47 percent akermanite.

Prince (1954) studied the plane through the tetrahedron MgO–CaO–Al_2O_3–SiO_2 parallel to the side CaO–Al_2O_3–SiO_2 and containing 10 percent of MgO. Figure 94 and table 31 give his results. The plane cuts the primary phase volumes of MgO (periclase), CaO, $3CaO \cdot SiO_2$, $2CaO \cdot SiO_2$, $3CaO \cdot MgO \cdot 2SiO_2$ (merwinite), $2CaO \cdot Al_2O_3 \cdot SiO_2$–$2CaO \cdot MgO \cdot 2SiO_2$ solid solution (melilite), α–$CaO \cdot SiO_2$ (pseudowollastonite), β–$CaO \cdot SiO_2$ (wollastonite), $CaO \cdot MgO \cdot 2SiO_2$ (diopside) solid solutions, $CaO \cdot Al_2O_3 \cdot 2SiO_2$ (anorthite), $MgO \cdot Al_2O_3$ (spinel), Al_2O_3, $3Al_2O_3 \cdot 2SiO_2$ (mull-

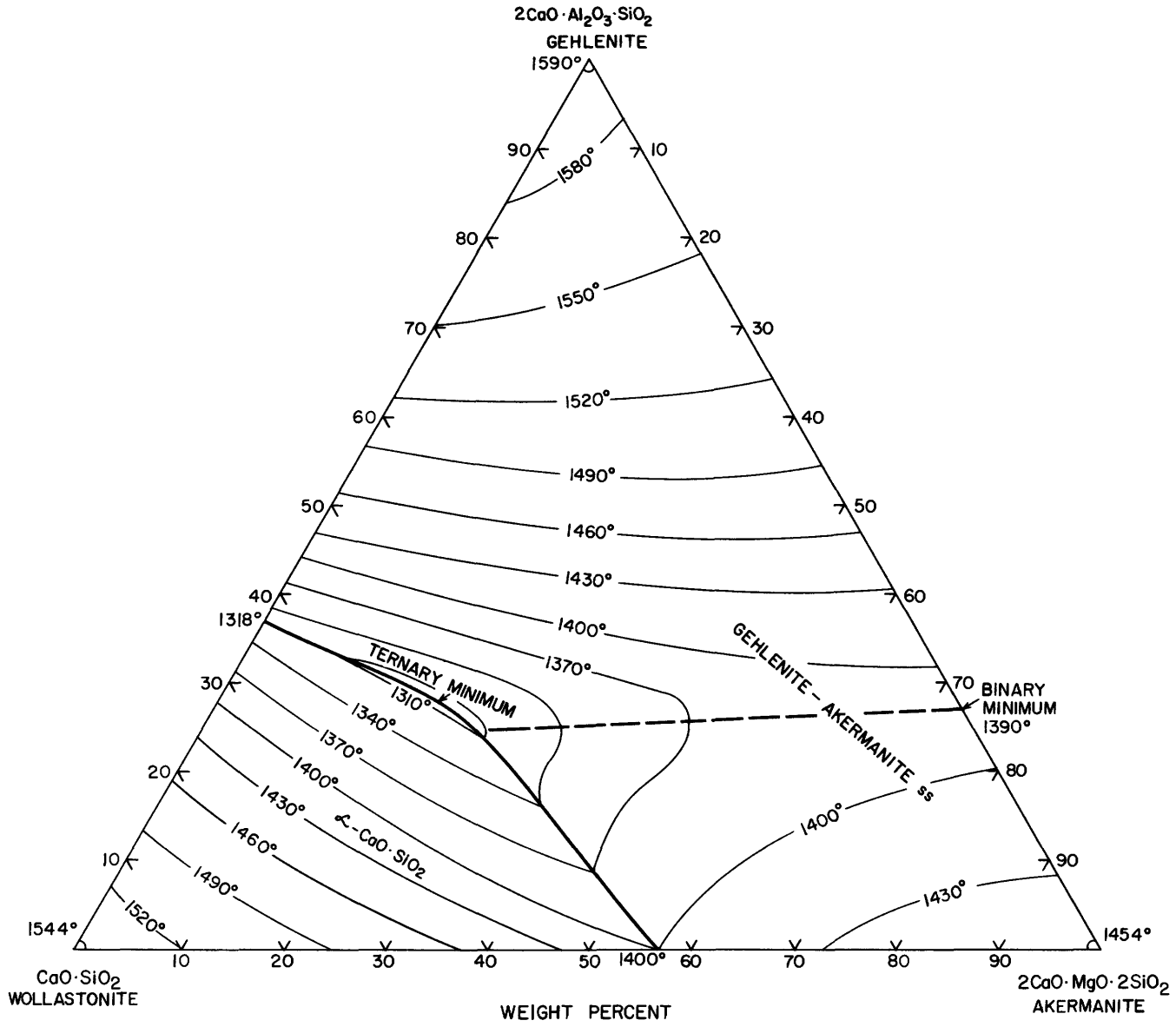

FIGURE 93.—The section $CaO \cdot SiO_2$ (wollastonite)–$2CaO \cdot Al_2O_3 \cdot SiO_2$ (gehlenite)–$2CaO \cdot MgO \cdot 2SiO_2$ (akermanite) of the plane $MgO \cdot CaO \cdot Al_2O_3$–$CaO \cdot SiO_2$ through the tetrahedron MgO–CaO–Al_2O_3–SiO_2. Modified from Osborn and Schairer (1941). *ss*, Solid solution.

ite), $2MgO \cdot 2Al_2O_3 \cdot 5SiO_2$ (cordierite), tridymite, cristobalite, and a volume of immiscibility. The heavy lines outlining the traces of the intersection of this plane with the boundaries between these phase volumes intersect at 11 lettered points in figure 94, which are the piercing points of the various univariant equilibria.

The join $3CaO \cdot Al_2O_3 \cdot 3SiO_2$ (grossularite)–$3MgO \cdot Al_2O_3 \cdot 3SiO_2$ (pyrope) is always quaternary, since each of the end members melts incongruently. Chinner and Schairer (1959, 1960) determined the subsolidus assemblages and temperatures of crystallization shown in figure 95. By combining these data with that of previous investigations in this system, they were able to deduce the relationship of the quaternary invariant points and univariant lines in the silica-rich portions of this system. Compositions lying between grossularite and approximately $Gro_{78}Py_{22}$ are represented in the subsolidus region by the assemblage pseudowollastonite + pyroxene + melilite + anorthite, which melts at 1235°C. Between about $Gro_{78}Py_{22}$ and $Gro_{45}Py_{55}$ the subsolidus assemblage pyroxene + melilite + anorthite + forsterite melts at 1225°C. The proportion of pyroxene is very small and cannot always be identified either optically or by means of X-rays. At 1238°C these compositions pass through a quaternary reaction point at which the phases are liquid + melilite + anorthite + forsterite + spinel. In a very narrow range of compositions between $Gro_{45}Py_{55}$

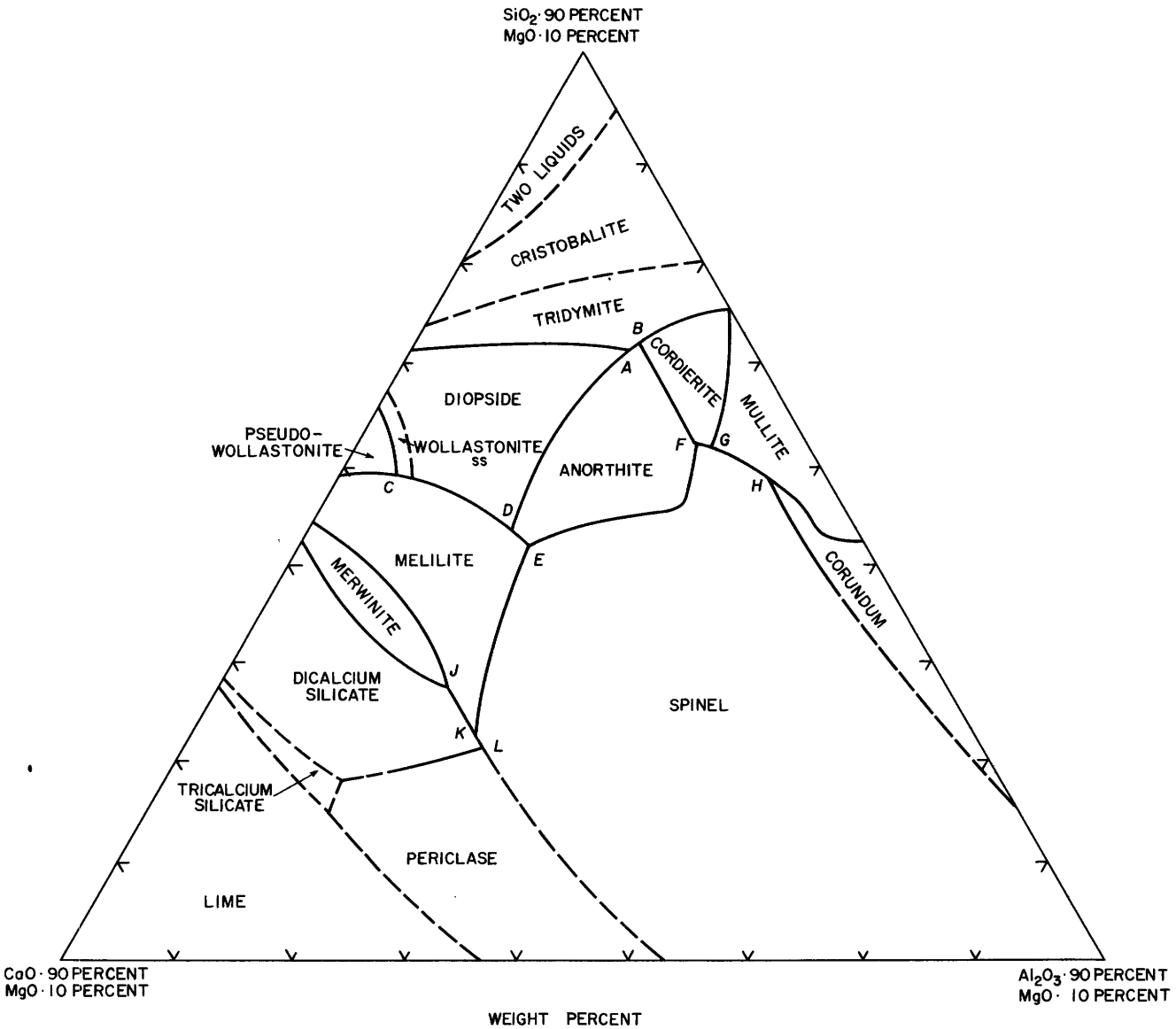

FIGURE 94.—The plane through the tetrahedron MgO–CaO–Al_2O_3–SiO_2 parallel to the side CaO·Al_2O_3–SiO_2 and containing 10 percent MgO. Modified from Prince (1954). *ss*, Solid solution.

TABLE 31.—*Temperatures and compositions of piercing points in the 10 percent* MgO *plane*

Point on fig. 94	Temperature (±5°C)	Crystalline phases	Composition of liquid (weight percent)			
			MgO	CaO	Al_2O_3	SiO_2
A	1230	Tridymite, diopside, anorthite	10	10	18	62
B	1245	Tridymite, cordierite, anorthite	10	8.5	18.5	63
C	1330	Melilite, pseudowollastonite, wollastonite *ss*	10	35.5	4.5	50
D	1235	Melilite, diopside, anorthite	10	29	17	44
E	1250	Melilite, anorthite, spinel	10	29	19	42
F	1345	Anorthite, cordierite, spinel	10	9	28	53
G	1370	Cordierite, mullite, spinel	10	8	30	52
H	1485	Mullite, corundum, spinel	10	4.5	37	48.5
J	1425	2CaO·SiO_2, merwinite, melilite	10	43	19.5	27.5
K	1410	2CaO·SiO_2, melilite, spinel	10	43	23.5	23.5
L	1410	Periclase, 2CaO·SiO_2, spinel	10	43	25.5	21.5

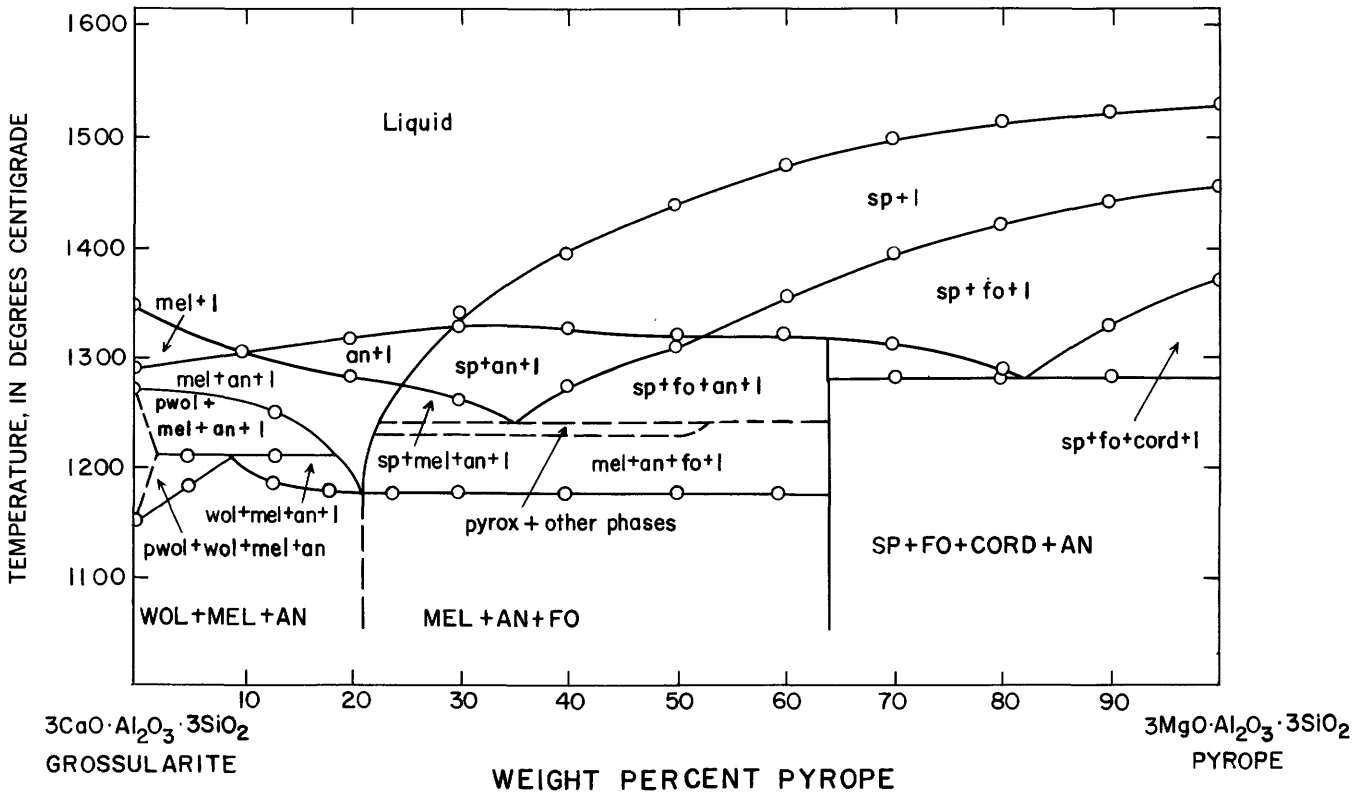

FIGURE 95.—The join $3CaO \cdot Al_2O_3 \cdot 3SiO_2$ (grossularite)–$3MgO \cdot Al_2O_3 \cdot 3SiO_2$ (pyrope). Modified from Chinner and Schairer (1960).

and $Gro_{36}Py_{64}$, the subsolidus assemblage melilite + anorthite + forsterite + spinel melts at the temperature of this reaction point. Between Gro_{36} and pyrope the assemblage anorthite + forsterite + spinel + cordierite melts at 1280°C.

$MgO–FeO–Fe_2O_3–SiO_2$

In the study of the system $MgO–FeO–Fe_2O_3–SiO_2$ by Muan and Osborn (1956), the partial pressure of oxygen was held constant at 1 atm—obtained by passing commercial tank oxygen through the special quenching furnace—at 0.21 atm, by using air, and at smaller partial pressures—obtained by using mixtures of carbon dioxide and hydrogen in the ratios of 40:1, 24:1, and 19:1. The system is not truly quaternary because of the formation of metallic iron. For the purpose of simple illustration the phase relation can be represented as projections of irregularly curved surfaces in the tetrahedron onto triangular diagrams with $FeO \cdot Fe_2O_3$ as one component. The most complete data were obtained in an air atmosphere, under which conditions the mixtures fall reasonably close to the plane $MgO–FeO \cdot Fe_2O_3–SiO_2$. The phase-equilibrium diagram in air is figure 96. The primary phase volumes met are those of the magnesiowüstite, magnesioferrite (magnesioferrites are solid solutions of $MgO \cdot Fe_2O_3$ with magnetite), olivine, pyroxene solid solutions; tridymite; cristobalite; and a region of two immiscible liquid layers; and where three of these phase volumes meet is a piercing point of univariant equilibrium. The primary phase volumes shift with changing partial pressure of oxygen, from an inferred condition at a sufficiently high pressure of oxygen to keep essentially all the iron in the ferric condition over to the reducing condition of melts that are in contact with metallic iron (fig. 97).

$CaO–FeO–Al_2O_3–SiO_2$

Schairer (1942) published the results of quenching experiments on five planes in this quaternary system. Because of the presence of FeO as a component, meltings were made in iron crucibles in an atmosphere of

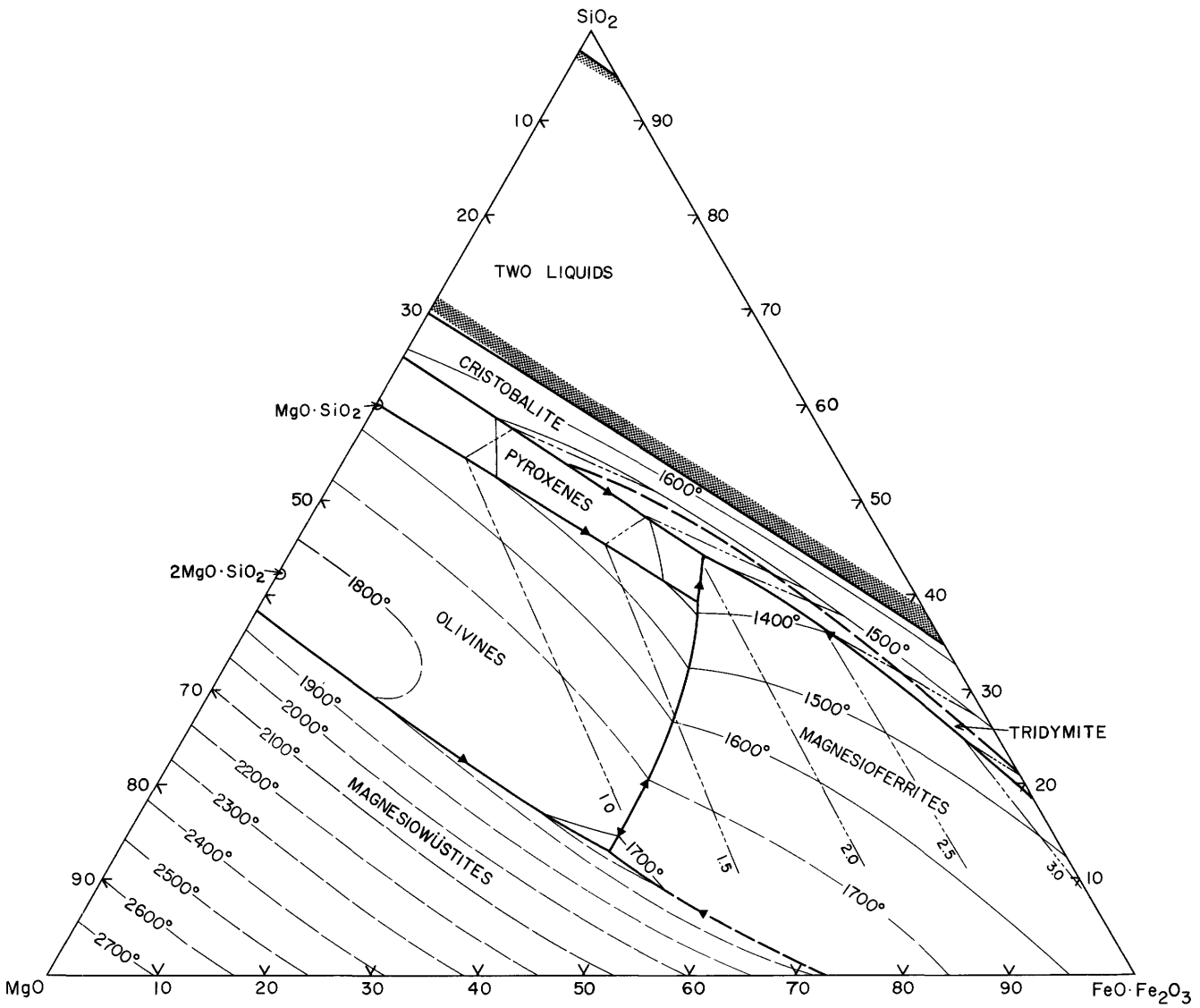

FIGURE 96.—Phase-equilibrium relations in air of the system MgO–FeO–Fe_2O_3–SiO_2 represented as projected on the plane MgO–SiO_2–FeO·Fe_2O_3. Points of approximately the same Fe_2O_3/FeO ratio lie on the light dash-triple dot curves; lines with stippling on one side indicate the limits of the region of two liquid layers. Modified from Muan and Osborn (1956).

purified nitrogen, thus keeping the content of ferric iron to the minimum imposed by the equilibrium conditions. All melts were analyzed for ferrous and ferric iron. In general, the amount of Fe_2O_3 was small, and the results are presented with all the iron calculated to FeO, instead of the quinary system including both FeO and Fe_2O_3 as components. The amount of Fe_2O_3 ranged from nearly zero in liquids that contained little iron to 11.56 percent at the Fe-apex of the tetrahedron. The planes studied are shown in figure 98, each of which cuts several primary phase volumes within the tetrahedron. Where the plane cuts the curved boundary surface between the primary phase volumes it results in a curved line which is not a boundary curve, as in a ternary system, but the traces of the bounding surface in the plane.

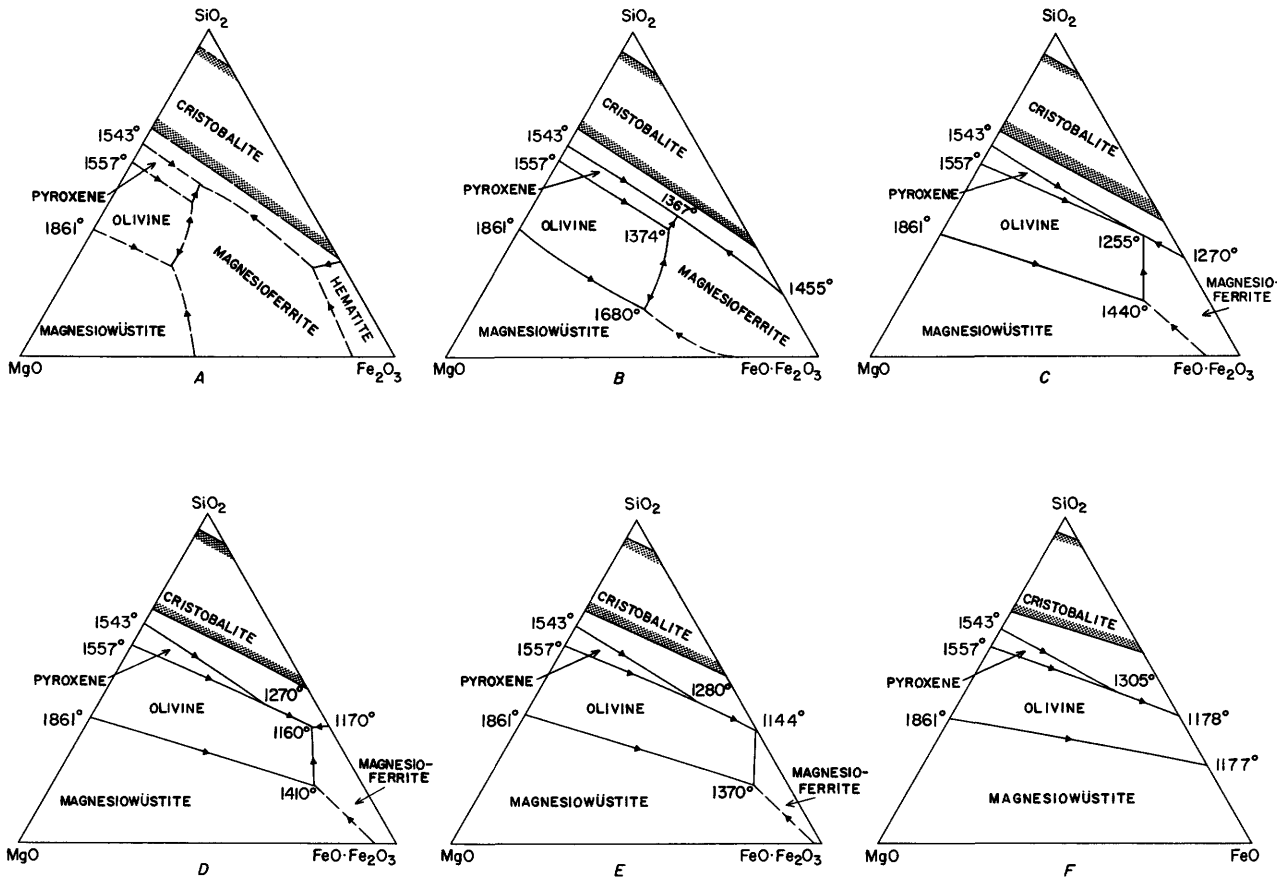

FIGURE 97.—Diagrams to show changes in phase-equilibrium relations in the system MgO–FeO–Fe_2O_3–SiO_2 with change in oxygen pressure. Diagram (*A*) shows the inferred relations at sufficiently high oxygen pressure to keep essentially all the iron in the ferric state; (*B*) the phase relations in air; (*C*), (*D*), and (*E*) at constant CO_2:H_2 ratios of 40:1, 24:1, and 19:1 respectively; (*F*) extreme reducing conditions of melts in contact with metallic iron. Modified from Muan and Osborn (1956).

The traces of the intersection of the plane SiO_2–$CaO \cdot Al_2O_3 \cdot 2SiO_3$(anorthite)–FeO with the curved contacts of two primary phase volumes, determined by Schairer (1942), are shown in figure 99. The points of intersection of these lines are not ternary invariant points but are piercing points of lines within the tetrahedron representing univariant equilibrium between three solid phases and liquid. Point *J*, 1070°±4°C, is the point at which the liquid of the reaction $CaO \cdot Al_2O_3 \cdot 2SiO_2$(anorthite) + $2FeO \cdot SiO_2$(fayalite) + $SiO_2 = L$ lies in this plane, and the composition of the liquid is 28 percent An, 39.4 percent FeO, 32.5 percent SiO_2. Each of these solid phases is in this plane. At point *I*, 1108°C, one of the phases, $FeO \cdot Al_2O_3$ (hercynite), lies outside of this plane; the univariant reaction is

$$CaO \cdot Al_2O_3 \cdot 2SiO_2 + 2FeO \cdot SiO_2 = FeO \cdot Al_2O_3 + L$$

and the composition of the liquid is 27.7 percent An, 50.3 percent FeO, 22.0 percent SiO_2. At the piercing point *F*, at 1120°±4°C, the phase reaction is

$$2FeO \cdot SiO_2 + FeO \cdot Al_2O_3 + FeO = L$$

and the composition of the liquid is approximately 14 percent An, 77 percent FeO, 9 percent SiO_2.

Figure 100 gives in diagrammatic form the relations among the various invariant lines, ternary univariant points (small letters), and quaternary univariant points. Schairer discussed in detail the location of the probable phase volume within these quaternary invariant points and their temperature relationships. On several of the univariant lines appear temperature maxima—for example, at the composition plane anorthite–tridymite–fayalite on the line *EC*. The maxima on *EC* and *FI* separate the five invariant points *H*, *G*, *D*, *E*, and *F* from the rest of the quaternary invariant points. Table 31 gives the locations of significant points on the several lines of figure 100.

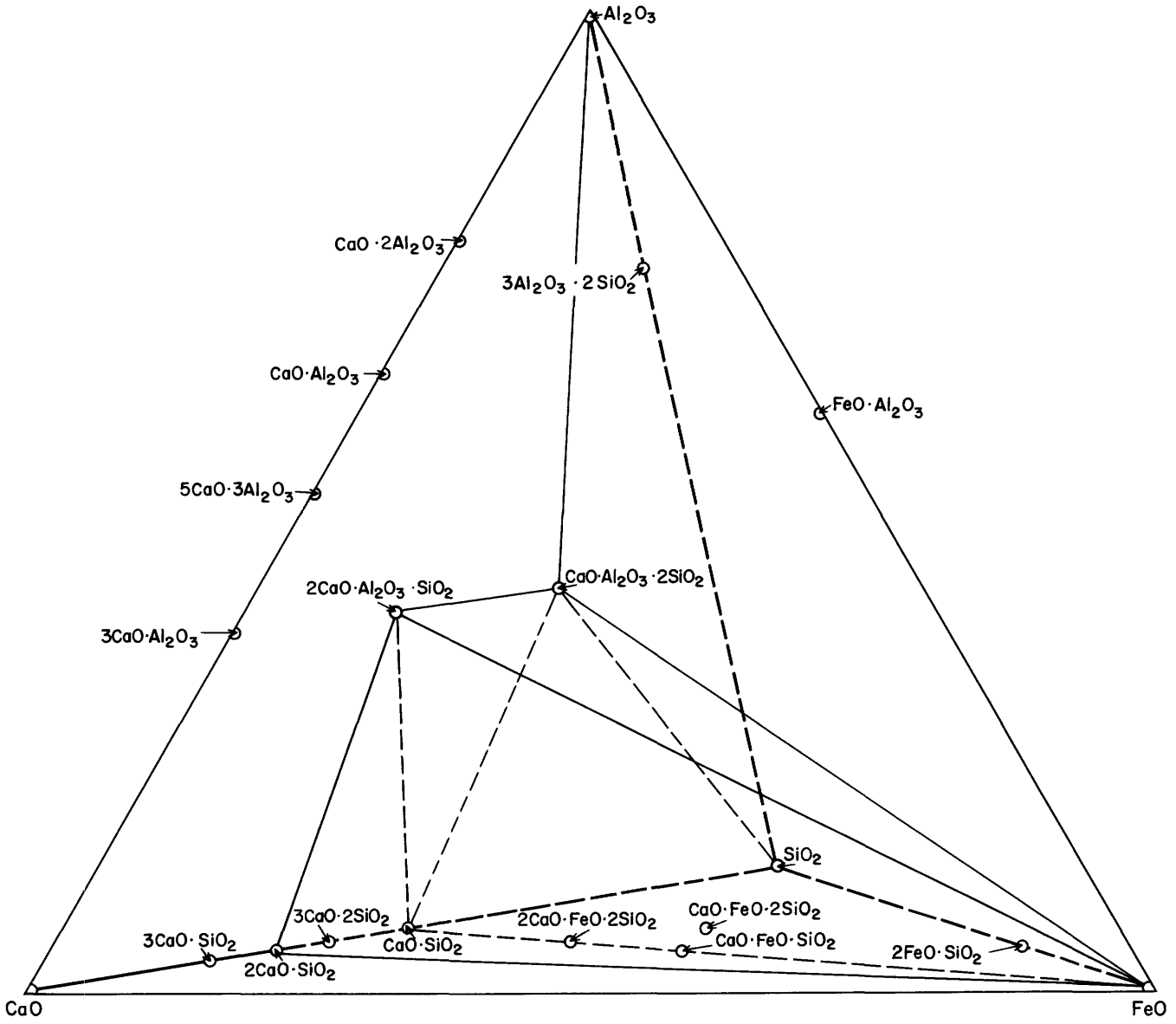

FIGURE 98.—The tetrahedron CaO–FeO–Al_2O_3–SiO_2, showing the position of the several planes on which phase-equilibrium studies have been made. Modified from Muan and Osborn (1951).

A second plane, $CaO \cdot Al_2O_3 \cdot 2SiO_2$ (anorthite)–Al_2O_3–FeO, is almost entirely taken up by intersections with the primary phase volumes of Al_2O_3 and $FeO \cdot Al_2O_3$. There is a small region of FeO, not exactly located, and one of anorthite. The piercing point, N, of the univariant reaction anorthite + hercynite $= Al_2O_3 + L$ is at 1393°±4°C, and the liquid has the composition 74.5 percent An, 4.5 percent Al_2O_3, 11.0 percent FeO. This point is a maximum on the univariant curve AK of figure 100, because it lies in the plane anorthite–Al_2O_3–FeO.

A third plane passes through $CaO \cdot SiO_2$–$CaO \cdot Al_2O_3 \cdot 2SiO_2$–FeO and the traces of the boundary curves are in figure 101. The primary-phase volumes cut by this plane are: anorthite; hercynite, whose composition is outside of this plane; wüstite (FeO); meli-

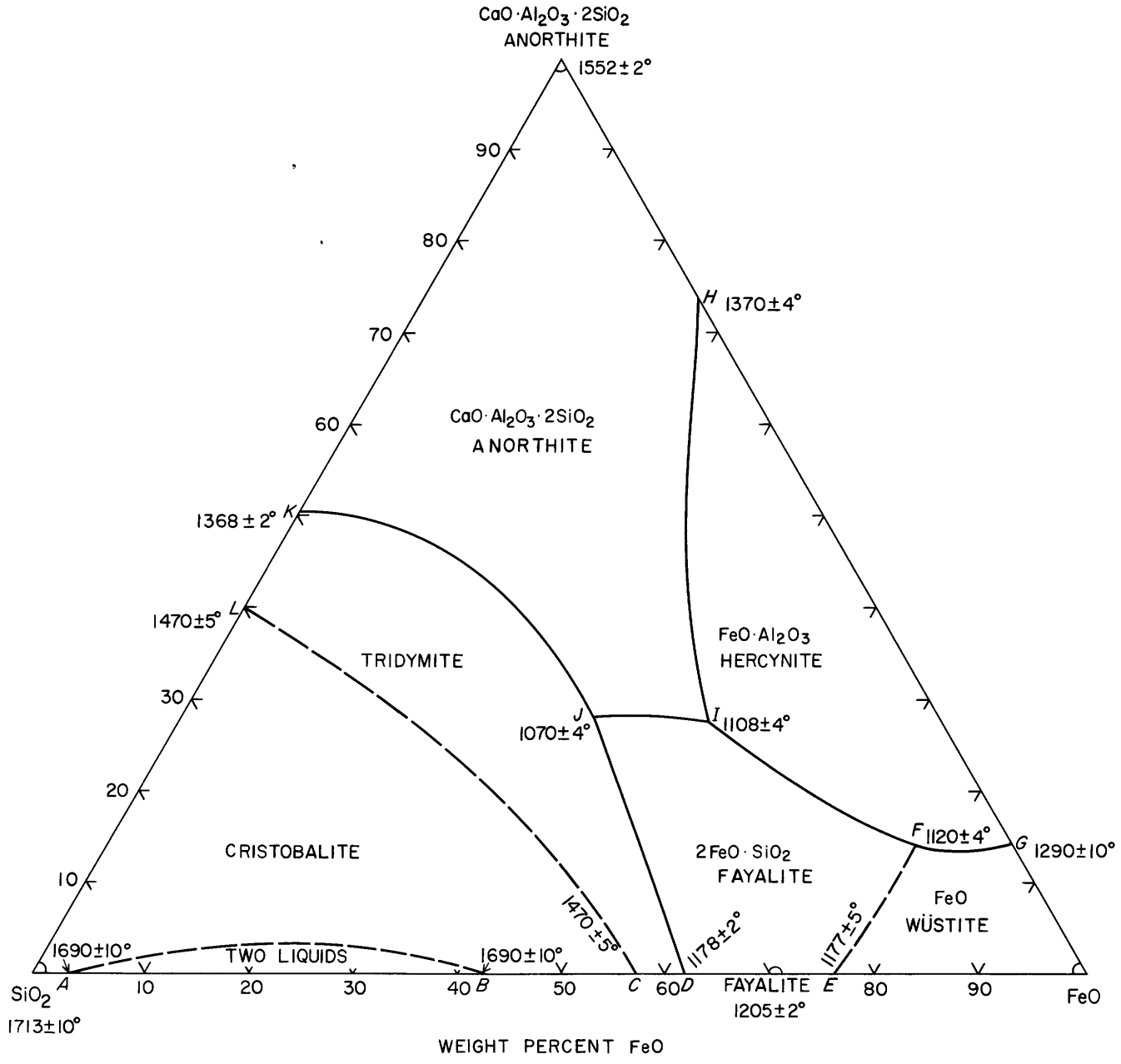

FIGURE 99.—The plane SiO_2–$CaO·Al_2O_3·2SiO_2$ (anorthite)–FeO through the tetrahedron CaO–FeO–Al_2O_3–SiO_2. Modified from Schairer (1942).

lite, a phase outside this plane which consists of a solid solution of an unknown amount of iron-akermanite ($2CaO·FeO·2SiO_2$) in $2CaO·Al_2O_3·SiO_2$ (gehlenite); olivine; probably solid solutions of $CaO·FeO·SiO_2$ and $2FeO·SiO_2$; α-$CaO·SiO_2$; and β-$CaO·SiO_2$ solid solutions. Piercing point R', at 1186°±5°C, is the intersection of this plane with the univariant equilibrium α-$CaO·SiO_2$, β-$CaO·SiO_2$ solid solutions, anorthite, and liquid of composition 47 percent $CaO·SiO_2$, 35.5 percent $CaO·Al_2O_3·2SiO_2$, 17.5 percent FeO. Point R, 1125°±5°C, is that of the equilibrium: β-$CaO·SiO_2$ solid solutions, anorthite, melilite, and liquid of composition 46.2 percent $CaO·SiO_2$, 30.6 percent An, 23.2 percent FeO. Point V', 1188°±5°C, is the piercing point of the equilibrium α-$CaO·SiO_2$, β-$CaO·SiO_2$ solid solutions, olivine solid solutions, and liquid of composition 64 percent $CaO·SiO_2$, 6 percent An, 30 percent FeO. This equilibrium terminates at the invariant point

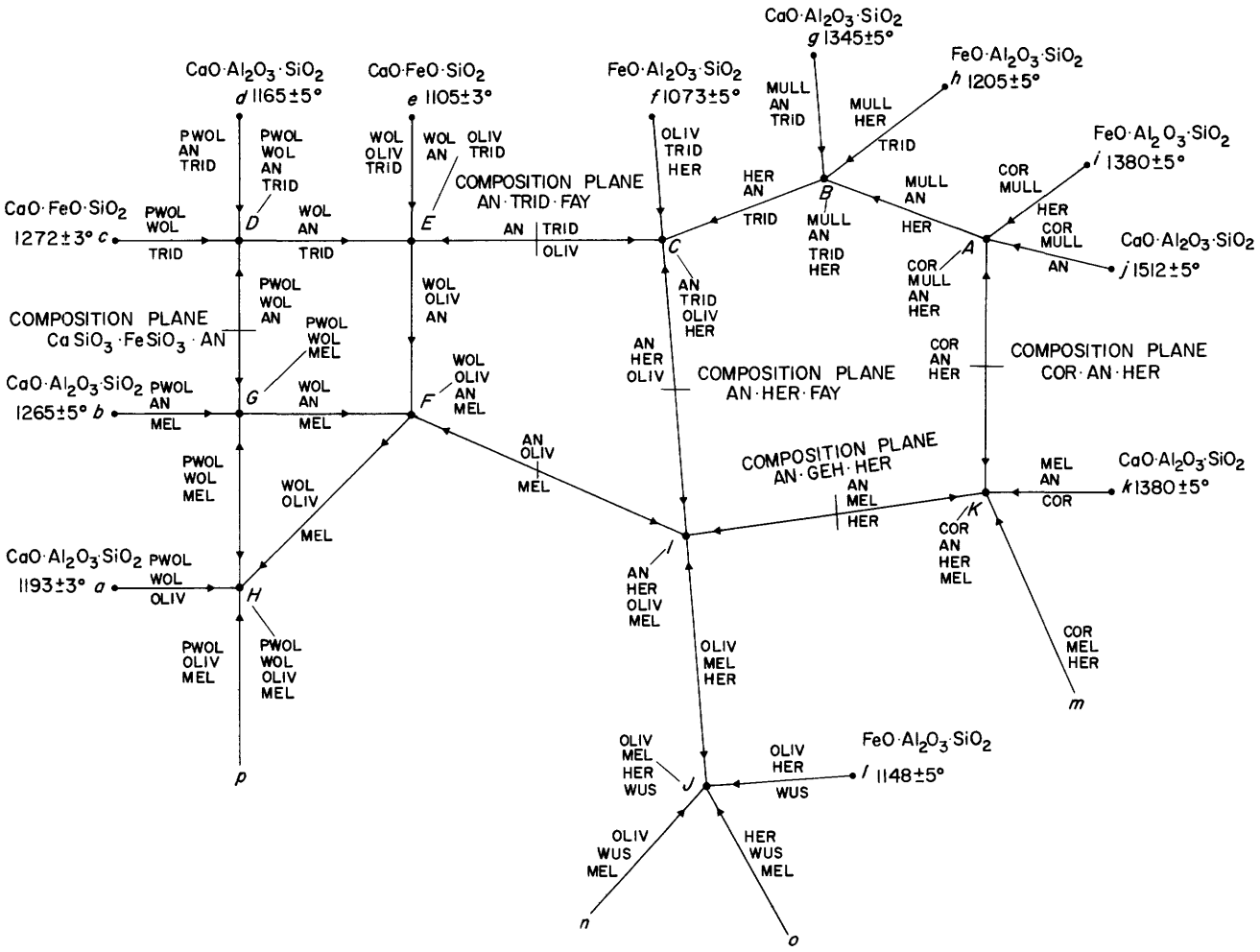

FIGURE 100.—Diagram showing relations between univariant lines, ternary invariant points in the limiting systems (small letters), and quaternary invariant points (capital letters). These lines and points do not lie in a plane. Only their relations to one another are shown in this diagram which is not intended to depict their spatial or angular relations. The lengths of the univariant lines of this figure are arbitrary and without significance. Abbreviations for solid phases along the lines and at the points: *AN* anorthite; *COR*, corundum; *FAY*, fayalite; *GEH*, gehlenite; *HER*, hercynite; *MEL*, melilite; *MULL*, mullite; *OLIV*, olivine; *PWOL*, pseudowollastonite; *TRID*, tridymite; *WOL*, wollastonite; and *WUS*, wüstite. Reprinted from Schairer (1942).

TABLE 32.—*Significant points in the system* $CaO–FeO–Al_2O_3–SiO_2$

[Locations of significant points in the five joins on univariant lines of figure 100]

Letter (significant point)	Figure on which point is shown	Temperature (°C)	Three solid phases	Line (fig. 100) on which letter point lies
F	99	1120±4	Olivine + hercynite + wüstite	*lJ*
I	99	1108±4	Anorthite + hercynite + olivine	*CI*
J	99	1070±4	Anorthite + tridymite + olivine	*EC*
R'	101	1186±5	Pseudowollastonite + wollastonite + anorthite	*DG*
R	101	1125±5	Wollastonite + anorthite + melilite	*GF*
S	101	1130±5	Anorthite + melilite + hercynite	*IK*
T	101	1188±5	Olivine + melilite + hercynite	*IJ*
U	101	1118±5	Olivine + hercynite + wüstite	*lJ*
V'	101	1188±5	Pseudowollastonite + wollastonite + olivine	*aH*
V	101	1145±5	Wollastonite + olivine + melilite	*HF*
Z	102	1320±5	Anorthite + gehlenite + hercynite	*IK*
A	102	1263±10	Hercynite + wüstite + gehlenite	*oJ*
D	103	1178±4	Pseudowollastonite + olivine + melilite	*pH*
E	103	1180±5	Olivine + wüstite + melilite	*nJ*
N[1]	----------	1393±4	Corundum + anorthite + hercynite	*AK*

[1] Point *N* refers to the plane $CaO.Al_2O_3.2SiO_2–Al_2O_3–FeO$

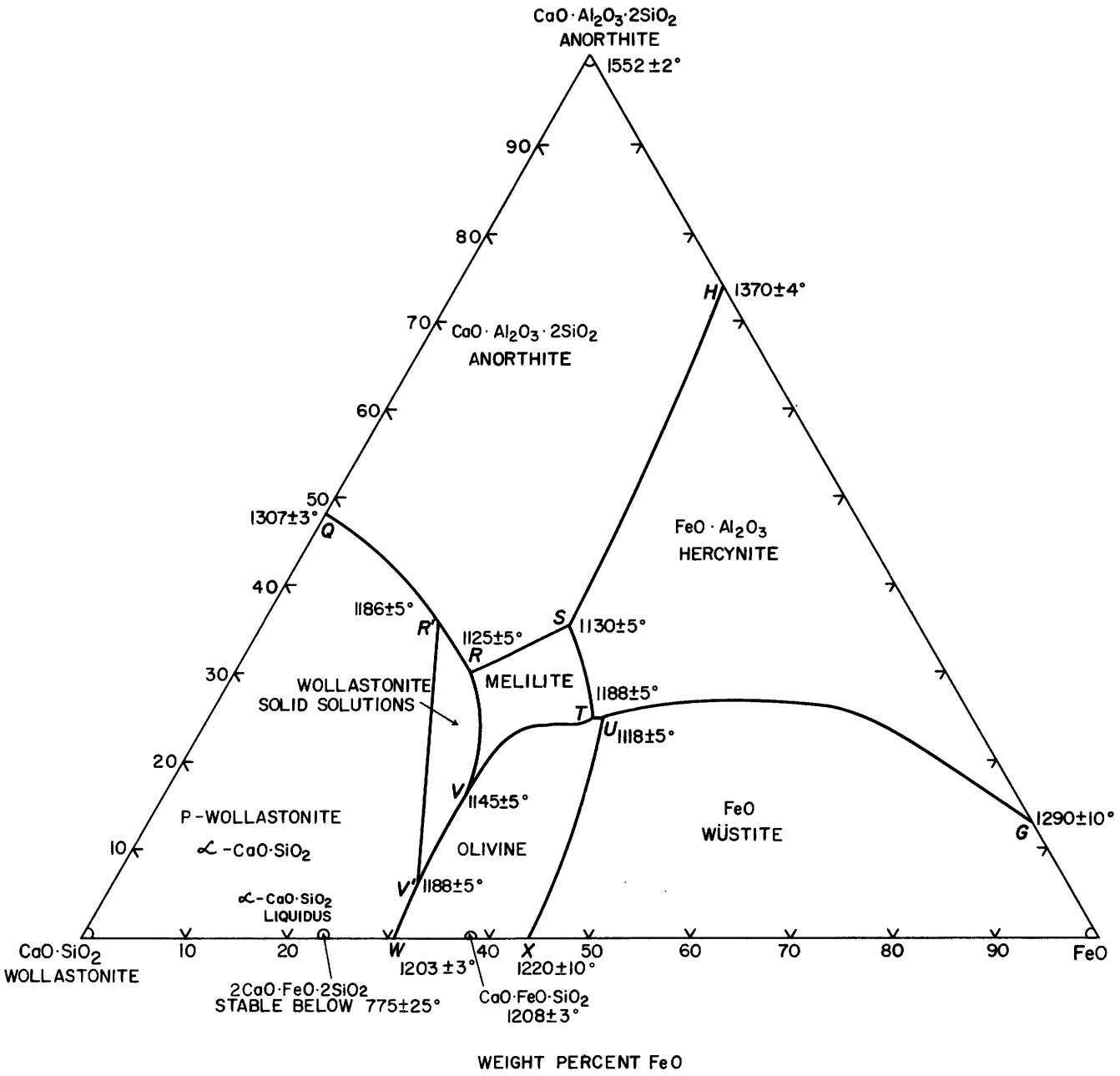

FIGURE 101.—The plane $CaO \cdot SiO_2$ (wollastonite)–$CaO \cdot Al_2O_3 \cdot 2SiO_2$ (anorthite)–FeO through the tetrahedron CaO–FeO–Al_2O_3–SiO_2. Modified from Schairer (1942).

SiO_2 + β-$CaO \cdot SiO_2$ solid solutions + olivine solid solutions = L in the limiting ternary system CaO–FeO–SiO_2. Point V, 1145°±5°C, is the piercing point for the equilibrium β-$CaO \cdot SiO_2$ solid solutions, olivine solid solutions, melilite, and liquid of composition 54 percent $CaO \cdot SiO_2$, 16.5 percent anorthite, 29.5 percent FeO. Point S, 1130°±5°C, is the piercing point for the equilibrium anorthite, $FeO \cdot Al_2O_3$, melilite, and liquid of composition 34.3 percent $CaO \cdot SiO_2$, 35.5 percent anorthite, 30.2 percent FeO. Point T 1118°±5°C, is the

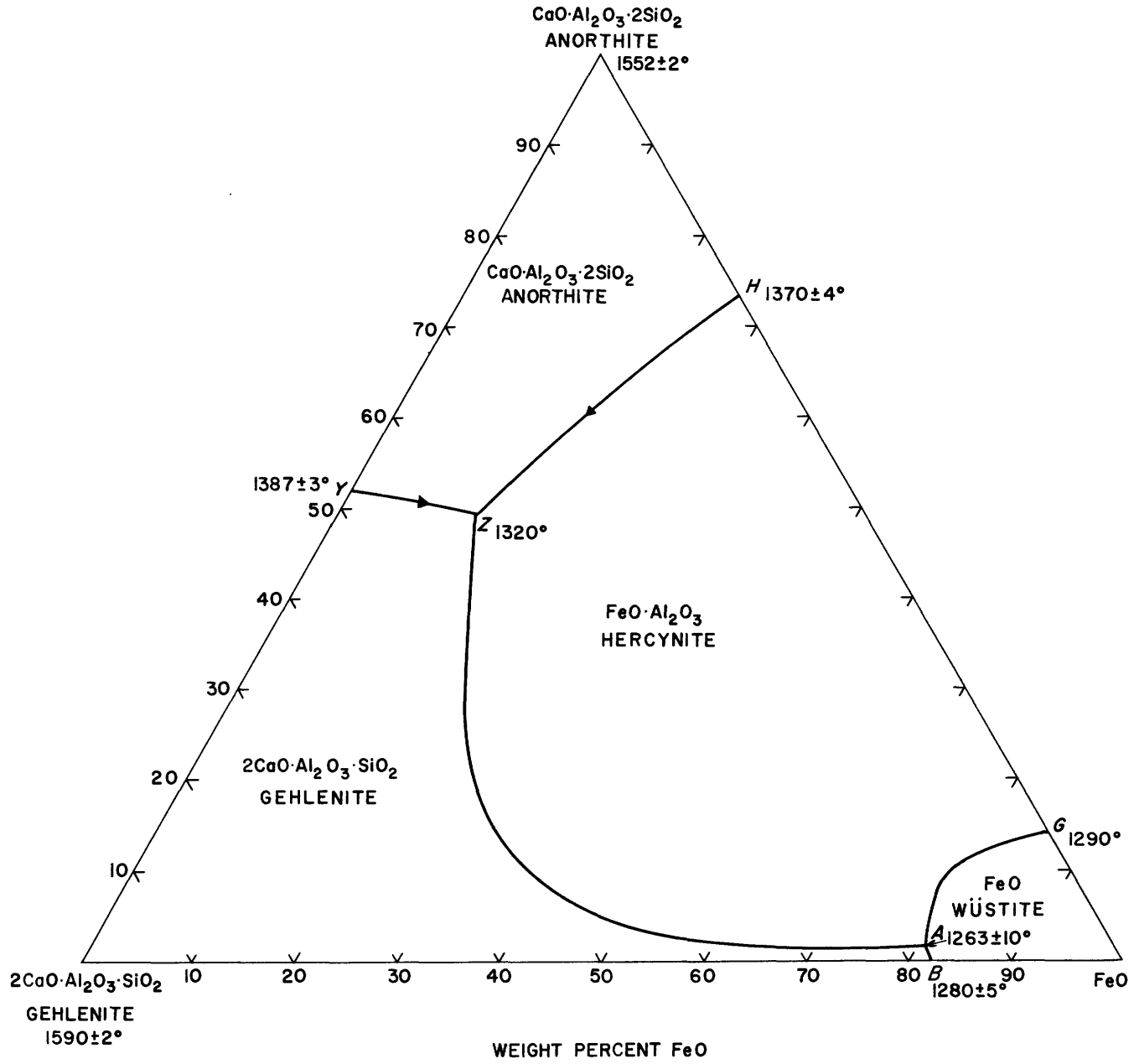

FIGURE 102.—The plane $2CaO \cdot Al_2O_3 \cdot SiO_2$ (gehlenite)–$CaO \cdot Al_2O_3 \cdot 2SiO_2$ (anorthite)–FeO through the tetrahedron CaO–FeO–Al_2O_3–SiO_2. Modified from Schairer (1942).

piercing point for $FeO \cdot Al_2O_3$, olivine solid solution, melilite, and liquid of composition 37 percent $CaO \cdot SiO_2$, 25 percent anorthite, 38 percent FeO. Point *U*, 1118°±5°C, is the piercing point for the equilibrium olivine solid solutions, $FeO \cdot Al_2O_3$, FeO, and liquid of composition 36 percent $CaO \cdot SiO_2$, 25 percent anorthite, 39 percent FeO.

A fourth plane is shown in figure 102, with components $2CaO \cdot Al_2O_3 \cdot SiO_2$ (gehlenite), $CaO \cdot Al_2O_3 \cdot 2SiO_2$ (anorthite), and FeO. The primary phase volumes cut are those of FeO (wüstite), $FeO \cdot Al_2O_3$ (hercynite), anorthite, and gehlenite, and the crystals formed in the gehlenite area may be melilite—solid solutions of $2CaO \cdot Al_2O_3 \cdot SiO_2$ and $2CaO \cdot FeO \cdot SiO_2$ (iron-aker-

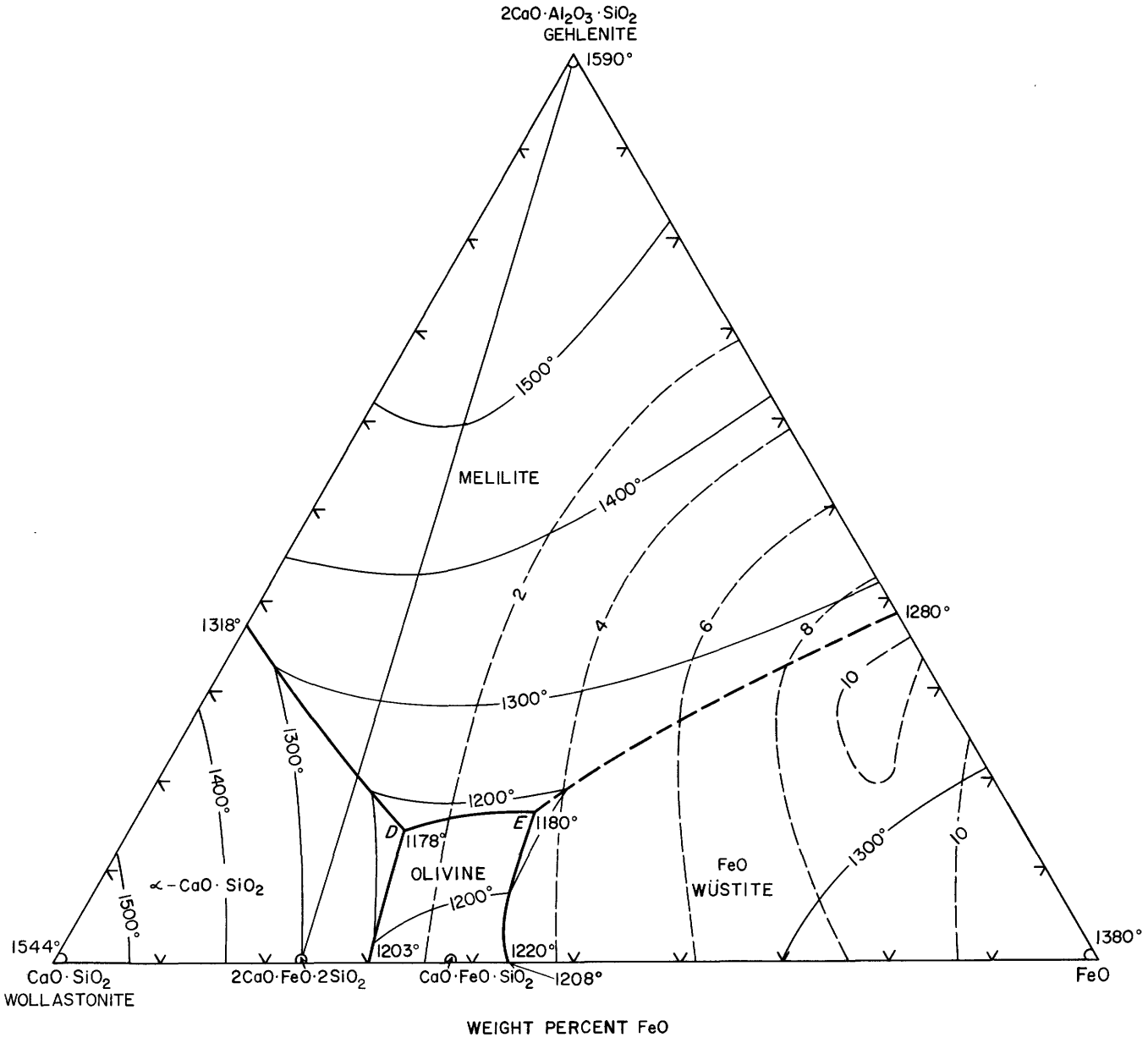

FIGURE 103.—The plane $CaO \cdot SiO_2$ (wollastonite)–$2CaO \cdot Al_2O_3 \cdot SiO_2$ (gehlenite)–FeO through the tetrahedron CaO–FeO–Al_2O_3–SiO_2. Modified from Muan and Osborn (1951).

manite). At the piercing point A, 1263°±5°C, the phases are gehlenite solid solutions, $FeO \cdot Al_2O_3$, FeO, and liquid of the approximate composition 17.8 percent gehlenite, 1.4 percent anorthite, 80.8 percent FeO. At Z, 1320°±5°C, the reacting phases are gehlenite solid solution, anorthite, $FeO \cdot Al_2O_3$, and liquid of composition 37.3 percent gehlenite, 49.6 percent anorthite, 13.1 percent FeO.

A fifth plane, $CaO \cdot SiO_2$–$2CaO \cdot Al_2O_3 \cdot SiO_2$–FeO, was studied by Schairer (1942) and revised by Muan and Osborn (1951). The revised diagram is figure 103. The primary phase volumes intersected are α-$CaO \cdot SiO_2$, melilite solid solutions, olivine solid solutions, and wüstite. At the piercing point of the equilibrium α-$CaO \cdot SiO_2$ + melilite solid solution + olivine solid solution + liquid, point D, the temperature is 1178°±4°C, the liquid composition 59.8 percent $CaO \cdot SiO_2$, 13.4 percent $2CaO \cdot Al_2O_3 \cdot SiO_2$, 26.8 percent FeO. At the piercing point of the equilibrium olivine solid solution + melilite solid solution + wüstite + liquid, point E, the temperature is 1180°±5°C, the liquid composition 46.1 percent $CaO \cdot SiO_2$, 15.7 percent $2CaO \cdot Al_2O_3 \cdot SiO_2$, 38.2 percent FeO. Muan and Osborn redetermined the binary (negelecting Fe_2O_3)

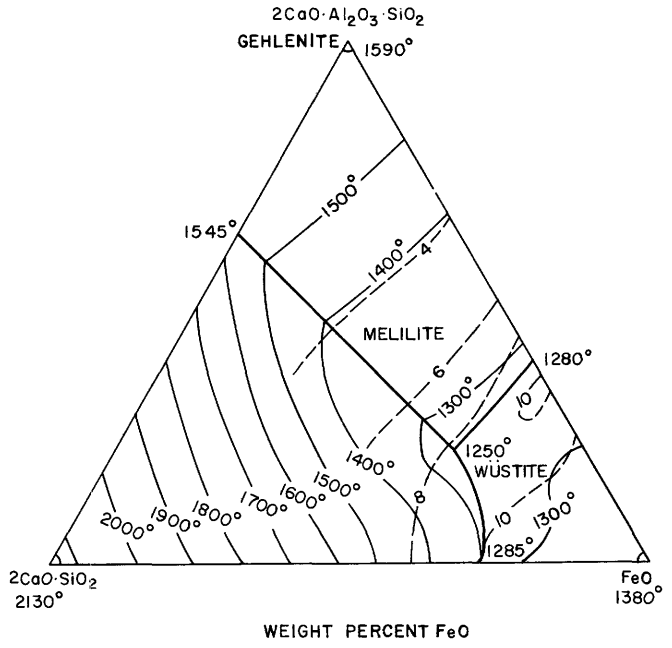

FIGURE 104.—The plane $2CaO \cdot SiO_2$–$2CaO \cdot Al_2O_3 \cdot SiO_2$ (gehlenite)–FeO through the tetrahedron CaO–FeO–Al_2O_3–SiO_2. Modified from Muan and Osborn (1951).

system $2CaO \cdot Al_2O_3 \cdot SiO_2$–FeO, and found the eutectic to be at 1280°C, 62 percent FeO, and they relocated the position of the trace of the boundary between wüstite and melilite.

Muan and Osborn (1951) studied this quaternary system in an interior tetrahedron whose base is the triangle $2CaO \cdot SiO_2$–$2CaO \cdot Al_2O_3 \cdot SiO_2$–$CaO \cdot SiO_2$ in the system CaO–Al_2O_3–SiO_2, and whose apex is FeO. The plane $2CaO \cdot SiO_2$–$2CaO \cdot Al_2O_3 \cdot SiO_2$ (gehlenite)–FeO is shown in figure 104. The primary phase volumes cut are $2CaO \cdot SiO_2$, $2CaO \cdot Al_2O_3 \cdot SiO_2$ solid solution (melilite), and wüstite. At 1250°C, where the boundaries of these phase spaces meet, is the piercing point of the equilibrium of these phase with a liquid of composition 21.3 percent $2CaO \cdot SiO_2$, 21.3 percent $2CaO \cdot Al_2O_3 \cdot SiO_2$, and 57.4 percent FeO. The "FeO" component at this point is actually 48.9 percent FeO, 8.5 percent Fe_2O_3. In this interior tetrahedron appears a narrow primary phase volume of $3CaO \cdot 2SiO_2$ (fig. 98). There are 3 invariant points in this interior tetrahedron. One of these is at 1195°±10°C, and the phases are $2CaO \cdot SiO_2$, olivine solid solution, melilite solid solution, wüstite, and liquid of composition 7 percent $2CaO \cdot SiO_2$, 41 percent $CaO \cdot SiO_2$, 17 percent $2CaO \cdot Al_2O_3 \cdot SiO_2$, or 32 percent CaO, 35 percent FeO, 6 percent Al_2O_3, 27 percent SiO_2. This invariant point is connected with the piercing point mentioned above in the plane $2CaO \cdot SiO_2$–$2CaO \cdot Al_2O_3 \cdot SiO_2$–FeO. A second invariant point is at 1200°±10°C, and the phases are $2CaO \cdot SiO_2$, $3CaO \cdot 2SiO_2$, olivine, melilite, and liquid of composition 10 percent $2CaO \cdot SiO_2$, 51 percent $CaO \cdot SiO_2$, 17 percent $2CaO \cdot Al_2O_3 \cdot SiO_2$, or 37.5 percent CaO, 25 percent FeO, 5.5 percent Al_2O_3, 33 percent SiO_2. At a third invariant point, 1175°±5°C, the phases are $3CaO \cdot 2SiO_2$, $CaO \cdot SiO_2$, olivine, melilite, and liquid of composition 5 percent $2CaO \cdot SiO_2$, 61 percent $CaO \cdot SiO_2$, 12 percent $CaO \cdot Al_2O_3 \cdot SiO_2$, 22 percent FeO, or 37.5 percent CaO, 22 percent FeO, 4.5 percent Al_2O_3, 36 percent SiO_2. This is connected with the line pH of figure 100 by the equilibrium α-$CaO \cdot SiO_2$+olivine+melilite+L.

CaO–Al_2O_3–Fe_2O_3–SiO_2

The system CaO–Al_2O_3–Fe_2O_3–SiO_2, which is of importance in the portland cement industry, has been studied by Lea and Parker (1934) and by Swayze (1946) and a full discussion is given by Rait (1949) and by Bogue (1955). The region of most interest in cement technology is included in the tetrahedron with apex at CaO, with the base

$2CaO \cdot SiO_2$–$4CaO \cdot Al_2O_3 \cdot Fe_2O_3$–$5CaO \cdot 3Al_2O_3$

shown in figure 105. One side of this tetrahedron CaO–$2CaO \cdot SiO_2$–$5CaO \cdot 3Al_2O_3$ was determined by Rankin and Wright (1915) in their study of the system CaO–Al_2O_3–SiO_2; the side

CaO–$5CaO \cdot 3Al_2O_3$–$4CaO \cdot Al_2O_3 \cdot Fe_2O_3$

by Hansen, Brownmiller, and Bogue (1928) and is included in figure 43. The side

CaO–$2CaO \cdot SiO_2$–$4CaO \cdot Al_2O_3 \cdot Fe_2O_3$

was worked out by Lea and Parker. The system CaO–$4CaO \cdot Al_2O_3 \cdot Fe_2O_3$ is binary, with a eutectic at 1350°±10°C and 49.6 percent CaO, 17.1 percent Al_2O_3, 26.8 percent Fe_2O_3, 6.5 percent SiO_2. There is a narrow field of $3CaO \cdot SiO_2$, terminating at the ternary eutectic, CaO+$3CaO \cdot SiO_2$+$4CaO \cdot Al_2O_3 \cdot Fe_2O_3$=$L$, at 1347°±5°C, and the composition of the liquid is 52.8 percent CaO, 16.2 percent Al_2O_3, 25.4 percent Fe_2O_3, 5.6 percent SiO_2. There is also a reaction point,

$3CaO \cdot SiO_2$+$4CaO \cdot Al_2O_3 \cdot Fe_2O_3$=$2CaO \cdot SiO_2$+$L$,

at 1348°±5°C, and the composition of the liquid is 52.4 percent CaO, 16.3 percent Al_2O_3, 25.5 percent Fe_2O_3, 5.8 percent SiO_2. The invariant point

CaO+$3CaO \cdot SiO_2$+$2CaO \cdot SiO_2$+L

was not located, but it is on the CaO-side of the join $3CaO \cdot SiO_2$–$4CaO \cdot Al_2O_3 \cdot Fe_2O_3$.

The base of this inside tetrahedron,

$2CaO \cdot SiO_2$–$4CaO \cdot Al_2O_3 \cdot Fe_2O_3$–$5CaO \cdot 3Al_2O_3$,

was studied by Lea and Parker. There is a ternary eutectic at 1280°±5°C, with a liquid of composition 50.0 percent CaO, 34.5 percent Al_2O_3, 9.9 percent Fe_2O_3, 5.6 percent SiO_2. The quaternary system was

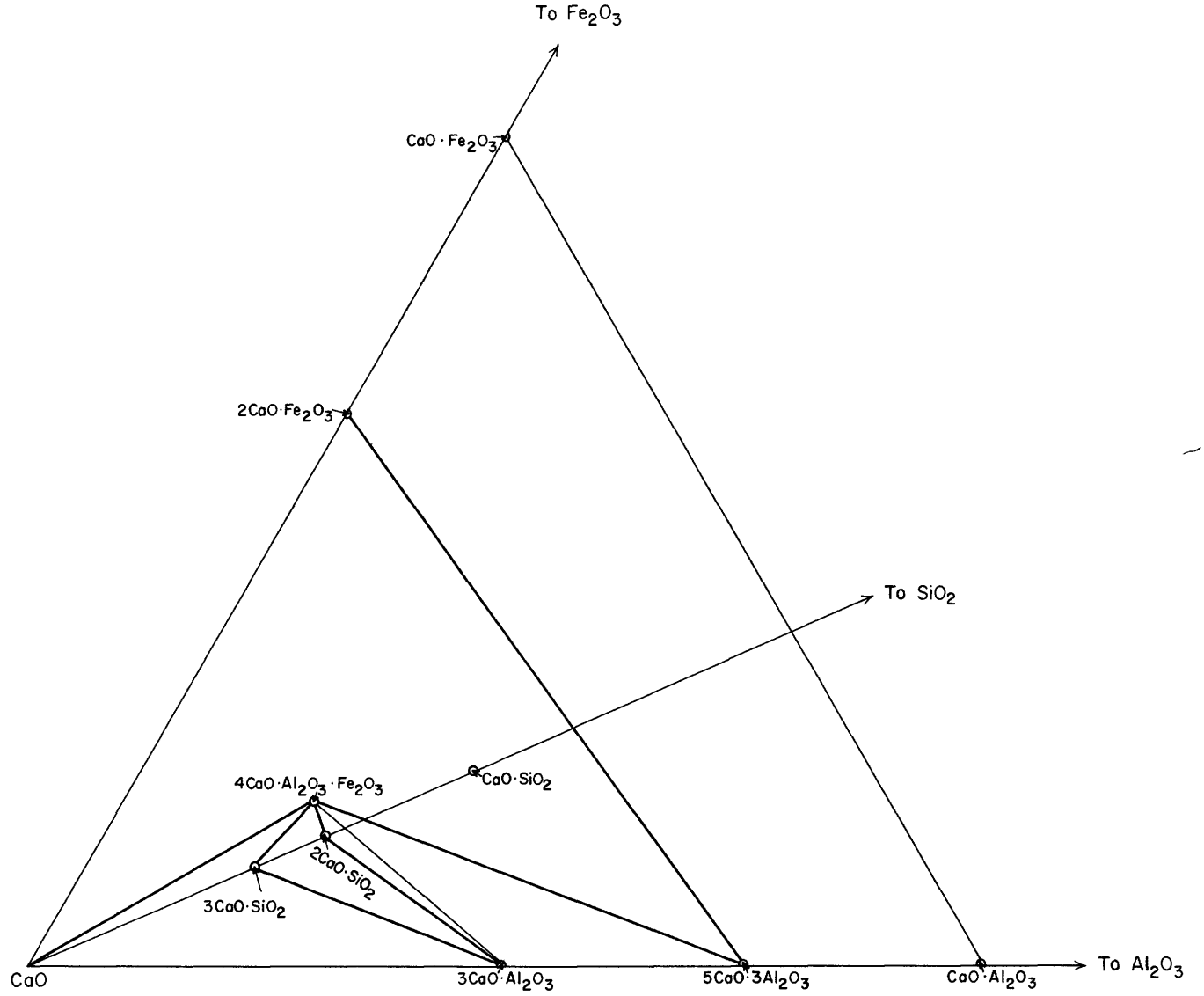

FIGURE 105.—Diagrammatic representation of part of the tetrahedron CaO–Al_2O_3–Fe_2O_3–SiO_2 showing the regions studied.

studied by means of planes through the tetrahedron containing 2, 5, 10, and 20 percent Fe_2O_3, respectively. In considering the crystallization relations the quaternary system is divided into three sections. One of these is the smaller tetrahedron

CaO–$3CaO \cdot SiO_2$–$4CaO \cdot Al_2O_3 \cdot Fe_2O_3$–$3CaO \cdot Al_2O_3$,

and these phases form a quaternary eutectic at 1341°C, 55 percent CaO, 22.7 percent Al_2O_3, 16.5 percent Al_2O_3, 5.8 percent SiO_2. Within the wedge-shaped tetrahedron $3CaO \cdot SiO_2$–$2CaO \cdot SiO_2$–$4CaO \cdot Al_2O_3 \cdot Fe_2O_3$–$3CaO \cdot Al_2O_3$, crystallization leads to an invariant point at 1338° ± 3°C, at which the liquid composition is 54.8 percent CaO, 22.7 percent Al_2O_3, 16.5 percent Fe_2O_3, 6.0 percent SiO_2. The third tetrahedron is $2CaO \cdot SiO_2$–$4CaO \cdot Al_2O_3 \cdot Fe_2O_3$–$5CaO \cdot 3Al_2O_3$–$3CaO \cdot Al_2O_3$, and the invariant point is at 1280° ± 5°C, 50 percent CaO, 34.4 percent Al_2O_3, 10 percent Fe_2O_3, 5.6 percent SiO_2. Swayze (1946) extended the study to $2CaO \cdot Fe_2O_3$, that is, to the tetrahedral section

CaO–$2CaO \cdot SiO_2$–$2CaO \cdot Fe_2O_3$–$5CaO \cdot 3Al_2O_3$,

and located the position of two invariant points. One of these, at which the solid phases are CaO, $3CaO \cdot SiO_2$, $3CaO \cdot SiO_2$, $3CaO \cdot Al_2O_3$, and the solid solution $6CaO \cdot xAl_2O_3 \cdot yFe_2O_3$, is at 1342°C, and the liquid has the composition 53.9 percent CaO, 21.2 percent Al_2O_3, 19.1 percent Fe_2O_3, 5.8 percent SiO_2. At the other, solid phases are $3CaO \cdot SiO_2$, $2CaO \cdot SiO_2$, $3CaO \cdot Al_2O_3$, and the solid solution

$6CaO \cdot xAl_2O_3 \cdot yFe_2O_3$;

the liquid has the composition 53.5 percent CaO, 22.3 percent Al_2O_3, 18.2 percent Fe_2O_3, 6.0 percent SiO_2, and the temperature is 1338°C.

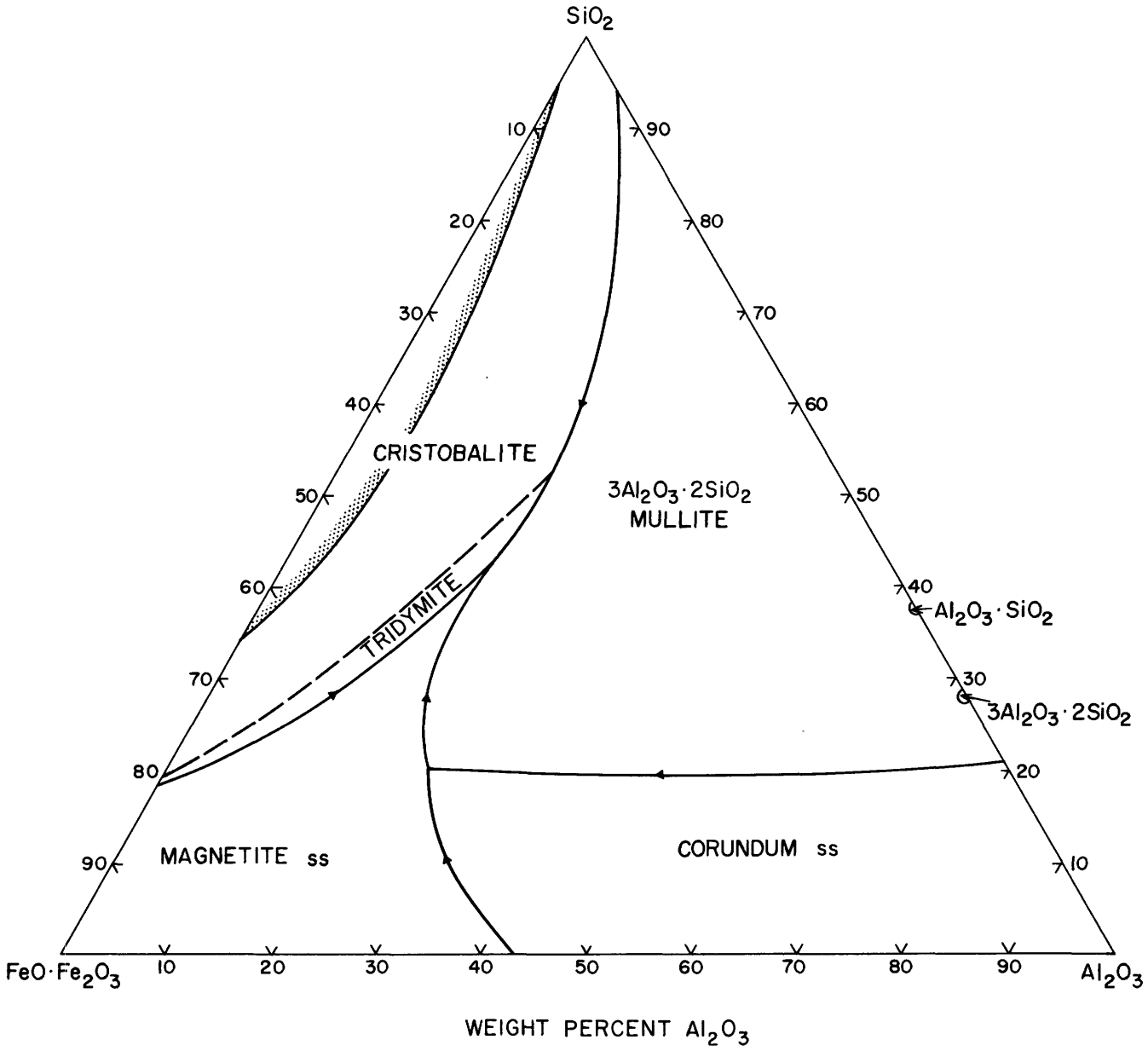

FIGURE 106.—The system iron oxide–Al_2O_3–SiO_2 in air. Modified from Muan (1957a). *ss* Solid solution.

CaO–Al_2O_3–SiO_2–TiO_2

Iwase and Nisioka (1936) studied the ternary system $CaO \cdot SiO_2$–$CaO \cdot Al_2O_3 \cdot 2SiO_2$ (anorthite)–$CaO \cdot SiO_2 \cdot TiO_2$ and found a eutectic at 1240°C, 37.5 percent $CaO \cdot SiO_2$, 37.5 percent $CaO \cdot Al_2O_3 \cdot 2SiO_2$, 25 percent $CaO \cdot SiO_2 \cdot TiO_2$, with these compounds as solid phases. Nisioka (1935) found a single eutectic relationship between $CaO \cdot Al_2O_3 \cdot 2SiO_2$ and $CaO \cdot TiO_2$.

FeO–Al_2O_3–Fe_2O_3–SiO_2

Greig (1927b), following his study of liquid immiscibility in the system FeO–Fe_2O_3–SiO_2, studied the effect of addition of Al_2O_3, and expressed his results by the intersection of the curved surface of two immiscible liquids with planes at 1, 2, 3, 4, 5, and 6 percent Al_2O_3. Between 2 and 3 percent of Al_2O_3 sufficed to make the liquids miscible.

Muan (1957a) studied the system

$$FeO\text{–}Fe_2O_3\text{–}Al_2O_3\text{–}SiO_2$$

by the quenching method in air ($P_{O_2}=0.21$). The results in air are shown in figure 106. The crystalline phases existing in equilibrium with a liquid are: tridymite and cristobalite; a spinel, which is a solid solu-

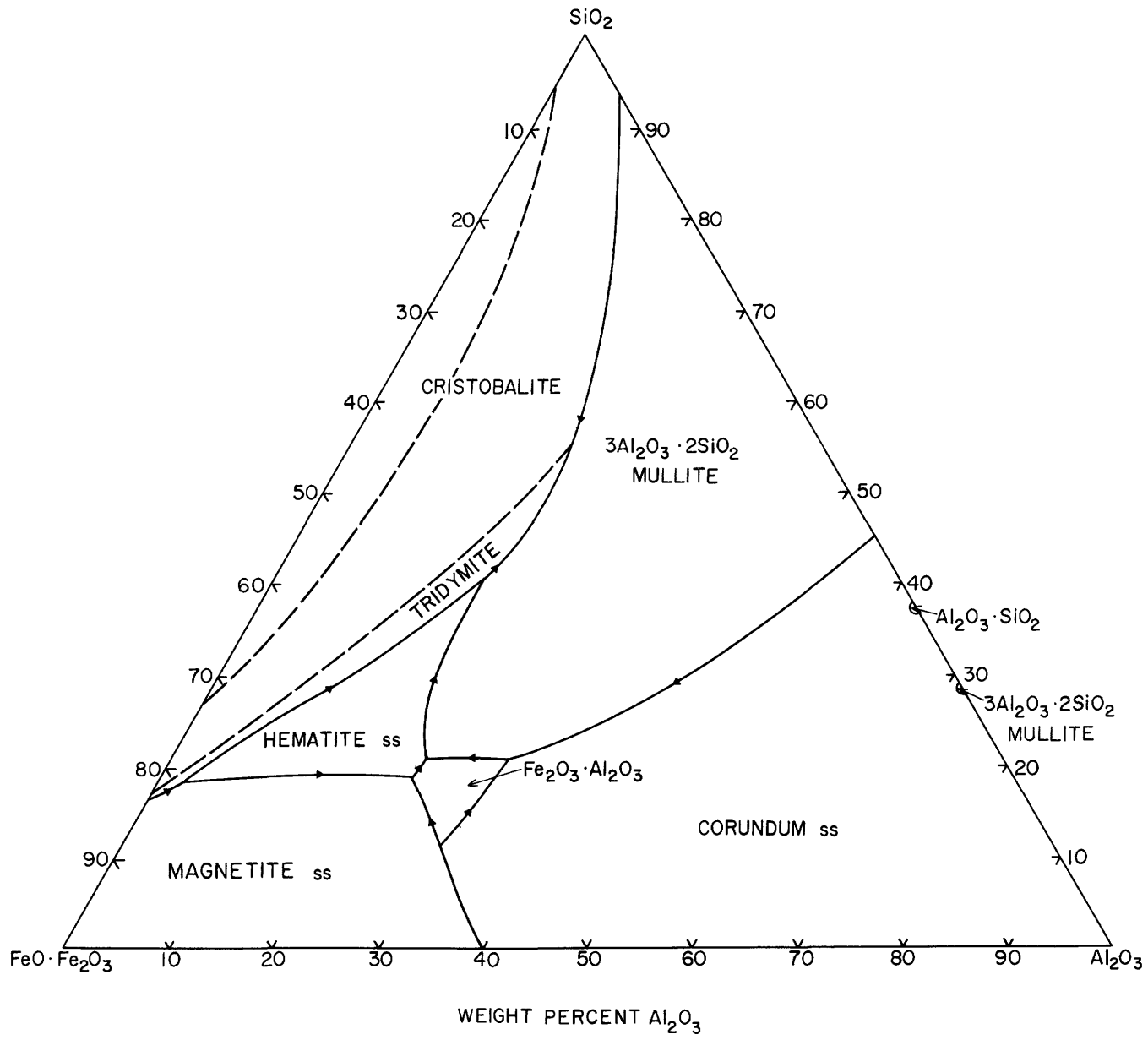

FIGURE 107.—The system iron oxide–Al_2O_3–SiO_2 at 1 atm oxygen pressure. Modified from Muan (1957b). *ss* Solid solution.

tion between $FeO \cdot Fe_2O_3$ (magnetite) and $FeO \cdot Al_2O_3$ (hercynite) with some excess Al_2O_3 and(or) Fe_2O_3 in solid solution; $3Al_2O_3 \cdot 2SiO_2$ (mullite) containing some Fe_2O_3; corundum with some Fe_2O_3 in solid solution; two immiscible liquid layers, which become miscible with more than 6 percent Al_2O_3. There are two quaternary piercing points: at 1460°C and 0.21 atm O_2 the phases are liquid of composition 17 percent FeO, 38 percent Fe_2O_3, 25 percent Al_2O_3, and 20 percent SiO_2, cristobalite; tridymite; mullite solid solution; spinel solid solution; and corundum solid solution. At 1380°C and 0.21 atm O_2 the phases are liquid of composition 17 percent FeO, 38 percent Fe_2O_3, 25 percent Al_2O_3, and 20 percent SiO_2. The liquid immiscibility gap in the system iron oxide–SiO_2 is removed by the addition of 6 percent Al_2O_3.

In another paper, Muan (1957b) worked chiefly at $P_{O_2}=1$ atm but also made runs at pressures ranging from 0.9 atm to $10^{-12.5}$ atm. The results at 1 atm are shown in figure 107. The crystalline phases are the same as in air, with variations in the limits of solid solution; and $Fe_2O_3 \cdot Al_2O_3$ with some variation in the Fe_2O_3/Al_2O_3 ratio. The tabulation below shows the six quaternary piercing points found at $P_{O_2}=1$ atm.

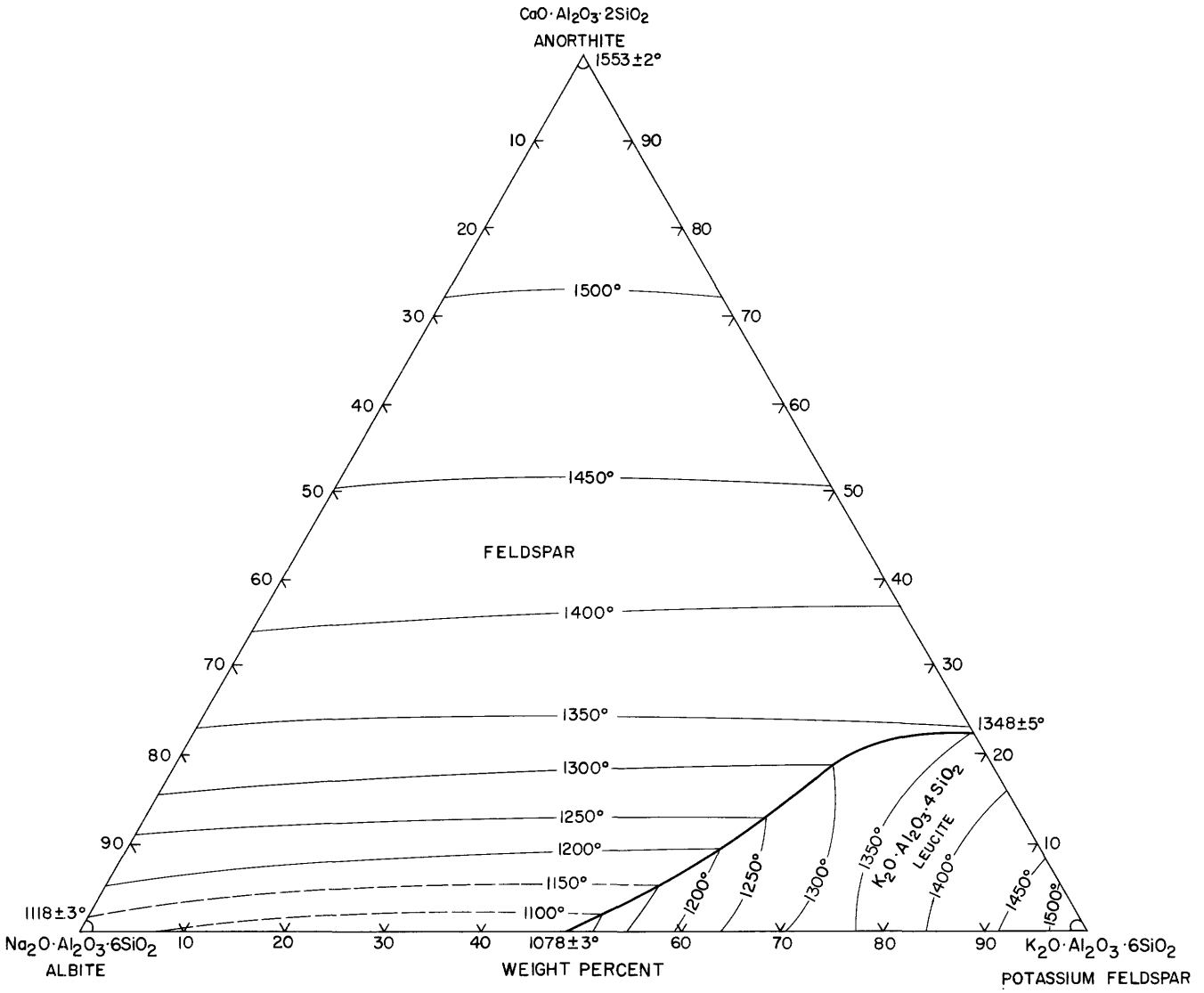

FIGURE 108.—Crystallization of mixtures of three feldspars. This triangular diagram is a section through the tetrahedron $Na_2O·Al_2O_3·6SiO_2$–$K_2O·Al_2O_3·6SiO_2$–$CaO·Al_2O_3·2SiO_2$–SiO_2. Modified from Franco and Schairer (1951).

Quaternary piercing points at $P_{O_2}=1$ atm

Temperature (°C)	Reaction phase	Composition of liquid (percent by weight)			
		FeO	Fe_2O_3	Al_2O_3	SiO_2
1390	Tridymite, mullite *ss*, hematite *ss*	13	27	20	40
1452	Tridymite, hematite *ss*, spinel *ss*	15	65	2	18
1440	Mullite *ss*, hematite *ss*, hercynite *ss*	15	40	29	21
1445	Hematite *ss*, hercynite *ss*, spinel *ss*	16	41	24	19
1470	Mullite *ss*, hercynite *ss*, corundum *ss*	15	39	32	21
1495	Hercynite *ss*, spinel *ss*, corundum *ss*	15	43	31	11

QUINARY SYSTEMS

Systems containing five components may formally be considered as represented by a pentahedroid or pentatope, the analog in four-dimensional space of a tetrahedron in three-dimensional space. The pentatope *ABCDE* may be considered as resulting from the fusing together in four-dimensional space of the two tetrahedra *ABCD* and *ABCE*, each of which has the same base, *ABC*, and *D* and *E* remain on the same side of the plane *ABC*. Morey (1930d) discussed the calculation of mixtures in a tetrahedral section of a pentatope, and of the triangular intersection of two tetrahedra. The few quinary systems which have been worked on have been composed of three stable compounds; they could therefore be represented by triangular diagrams.

Na_2O–K_2O–CaO–Al_2O_3–SiO_2

The study by Franco and Schairer (1951) of liquidus temperature in mixtures of the potassium, sodium, and calcium feldspars was an exploration of a part of this quinary system. Their results are shown in the triangular diagram of figure 108, which is not a ternary sys-

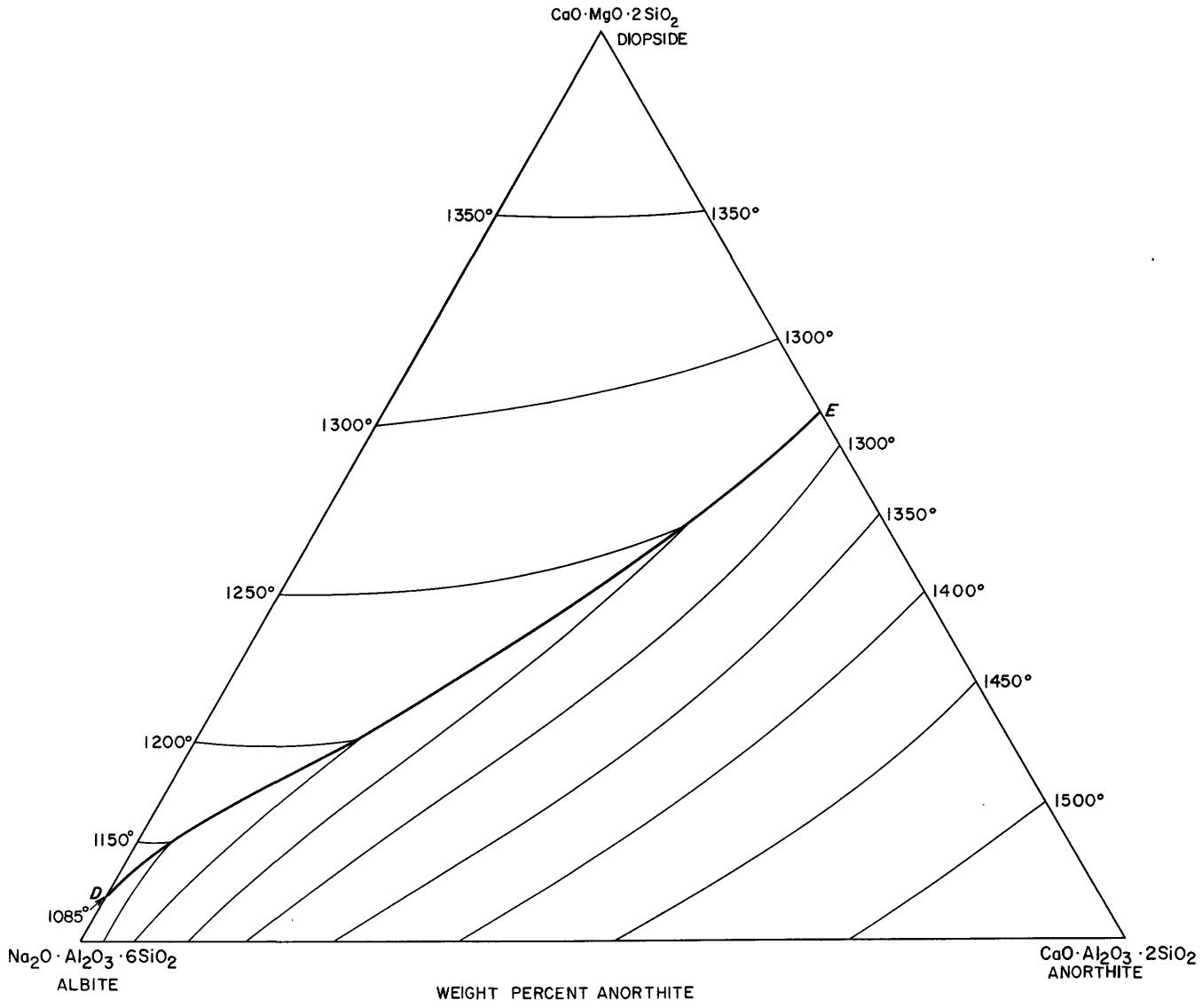

FIGURE 109.—Crystallization of mixtures of $Na_2O \cdot Al_2O_3 \cdot 6SiO_2$ (albite)–$CaO \cdot MgO \cdot 2SiO_2$ (diopside)–$CaO \cdot Al_2O_3 \cdot 2SiO_2$ (anorthite). Modified from Bowen (1915).

tem. The feldspars which separate over most of the diagram presumably can be represented in terms of the three components, but since $K_2O \cdot Al_2O_3 \cdot 6SiO_2$ melts incongruently there is an area in which $K_2O \cdot Al_2O_3 \cdot 4SiO_2$ (leucite) is the primary phase; hence, the more siliceous liquid formed is outside the component triangle. The melting relations probably could be represented by a plane through the tetrahedron $Na_2O \cdot Al_2O_3 \cdot 6SiO_2$–$K_2O \cdot Al_2O_3 \cdot 6SiO_2$–$CaO \cdot Al_2O_3 \cdot 2SiO_2$–$SiO_2$.

Na_2O–MgO–CaO–Al_2O_3–SiO_2

Bowen (1915) studied the system $Na_2O \cdot Al_2O_3 \cdot 6SiO_2$ (albite)–$CaO \cdot MgO \cdot 2SiO_2$ (diopside)–$CaO \cdot Al_2O_3 \cdot 2SiO_2$ (anorthite), which is part of the quinary system Na_2O–MgO–CaO–Al_2O_3–SiO_2. The results are shown in figure 109. The triangular diagram is divided into two parts by the curve *DE*. On one side is a field of diopside, on the other a field of plagioclase feldspars, solid solutions of albite and anorthite. The curve *DE* rises from the albite-diopside eutectic, D, near 1085°C and 97 percent albite, to the anorthite-diopside eutectic *E*, at 1270°C and 42 percent anothite. The side $Na_2O \cdot Al_2O_3 \cdot 2SiO_2$–$CaO \cdot MgO \cdot 2SiO_2$ is not binary because of the field of forsterite, $2MgO \cdot SiO_2$.

In the discussion of this system Bowen gave a clear example of the methods for the determination of 3-phase boundaries. In figure 110, in which *DFE* is the

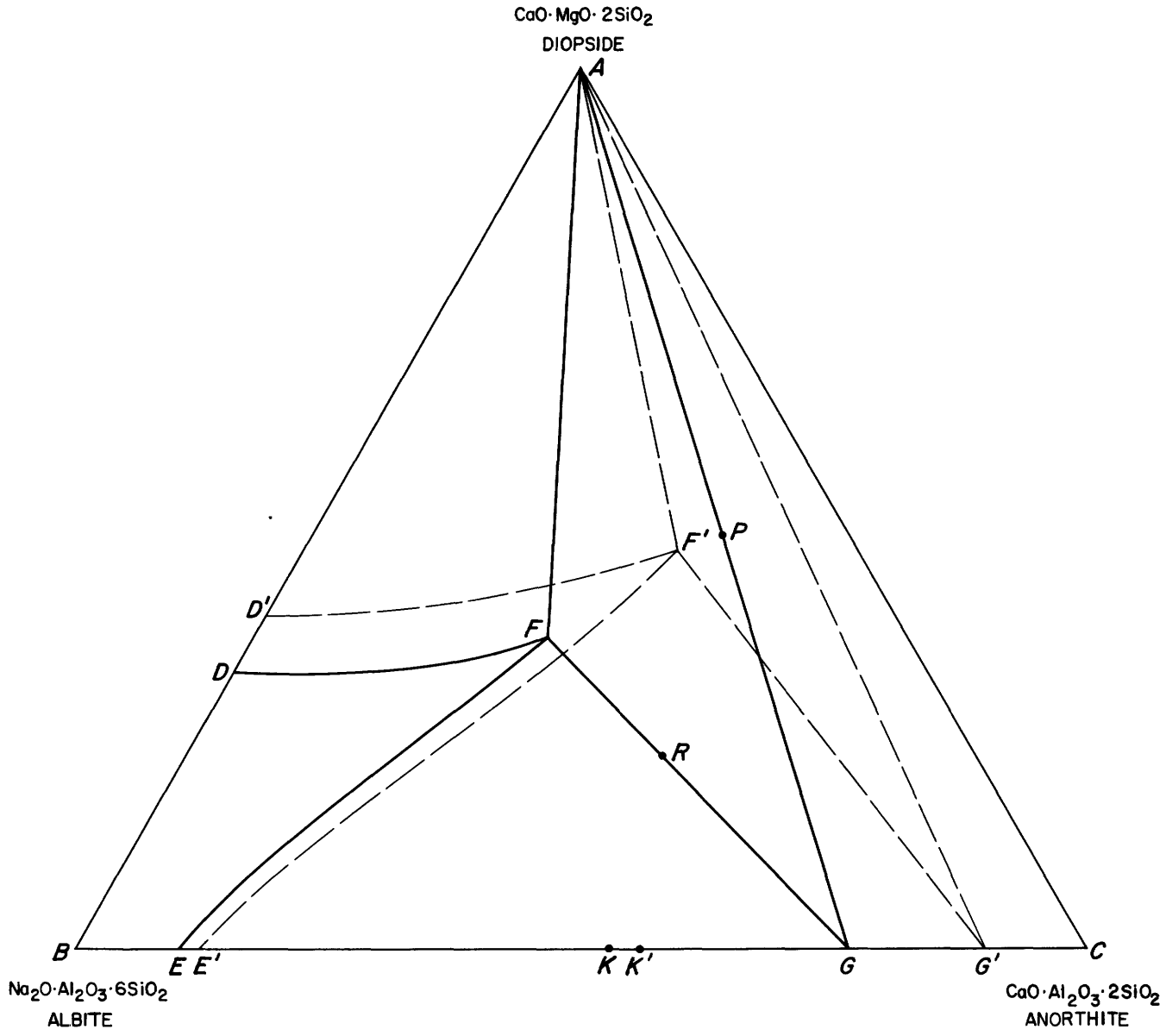

FIGURE 110.—Phase relations at 1230°C (solid lines) and 1250°C (broken lines) in the system $Na_2O \cdot Al_2O_3 \cdot 6SiO_2$ (albite)–$CaO \cdot MgO \cdot 2SiO_2$ (diopside)–$CaO \cdot Al_2O_3 \cdot 2SiO_2$ (anorthite). Modified from Bowen (1915).

isotherm at 1230°C, the phases present in the various areas are:

Area *DFEB*, all liquid
Area *EFG*, liquid E–F and plagioclase *K–G*
Area *ADF*, liquid *D–F* and diopside
Area *AFG*, liquid *F*, plagioclase *G*, and diopside
Area *AGC*, plagioclase *G–C* and diopside

This line *FG* which bounds the field *AFG* is called a 3-phase boundary (Bowen, 1915). *AF* and *AG* likewise bound the 3-phase field, but they are merely lines radiating from *A*, their position being completely determined by the points *F* and *G*. To predict the phases present at 1230°C in a given mixture it is necessary to know the position of the line *FG*, the 3-phase boundary for that temperature, or at 1250°C, on line *F'G'* and so on for other temperatures.

The determinations of the 3-phase boundaries can be accomplished in a number of ways, the principles of which are discussed with reference to figure 110. For a given position of the isotherm *DFE*—that is, a known temperature—it is only necessary to note that *G* represents the composition of the plagioclase which is in equilibrium with both liquid and diopside. If a mixture which gives all three phases is held at the desired

temperature, and the composition of the plagioclase is determined by optical methods, then the point G is determined and the figure for that temperature can be drawn. This may be called a composition method since it depends on the composition of the mix-crystal.

The 3-phase boundaries may be located by starting with a mixture of known composition and determining the temperature at which the 3-phase area is entered either from above or below. Any point on the line AG, such as P, lies on the border of the 3-phase area for 1230°C, and at this temperature, as at all lower temperatures it consists entirely of diopside and plagioclase, but if the temperature is raised a little the point enters the 3-phase area for this higher temperature (note that the point P lies well within the 3-phase area for 1250°C, $AF'G'$) — that is, liquid is added to the phases already present. A 3-phase boundary, then, can be located by determining the temperature of beginning of melting for any mixture. Thus if any mixture of diopside with plagioclase of composition G is taken and the temperature of beginning of melting determined it will be found at 1230°C. If the isotherm for 1230°C as previously determined is drawn, then the join FG is the 3-phase boundary for 1230°C.

The 3-phase boundary may also be determined by entering the 3-phase region from a higher temperature. The point R lies within the field of liquid and plagioclase, $E'F'G'$, at 1250°C, and is in the border of the 3-phase area at 1230°C, and if the temperature is lowered a little it enters the 3-phase area for this lower temperature, and liquid and plagioclase are joined by diopside. By determining the temperature (approached from above) at which the liquid and plagioclase are joined by diopside, the 3-phase boundary passing through the composition of the mixture can be determined. Thus, if the mixture R is taken it is found that diopside just appears at 1230°C, and if the isotherm of 1230°C, DEF, is drawn, FR joined and produced to G, then FG is the 3-phase boundary.

Determination of the crystallization paths can be quantitatively described when the 3-phase boundaries are known. Thus in figure 111 the mixture F (Ab_1An_1[5] 50 percent, diopside 50 percent) begins to crystallize at 1275°C, diopside separating and the liquid changing composition along the straight line AFG toward G. At 1235°C when the liquid has the composition G, plagioclase of composition H (Ab_1An_4) begins to crystallize; the point H is determined by the 3-phase boundary, GH, through G. As the temperature is lowered the composition of the liquid follows the boundary curve DE toward M. At 1218°C when the liquid has the composition K, plagioclase has changed in composition from H (Ab_1An_4) to L (Ab_1An_2). Finally at 1200°C the liquid is used up, the last minute quantity having the composition M, the plagioclase has the composition Z (Ab_1An_1) the intersection of the line AF with the side albite-anorthite. The composition X (Ab_2An_1 60 percent—diopside 40 percent) begins to crystallize at 1252°C with the separation of diopside, meets the curve DE at 1218°C at K with separation of plagioclase of composition L (Ab_1An_2), and solidifies completely at 1176°C to a mixture of diopside and plagioclase of composition T (Ab_2An_1).

For all mixtures in the diopside field, the change of composition of the liquid is represented by a straight line until the boundary curve DE is reached. For mixtures in the plagioclase field the liquid follows a curved course in reaching the boundary curve. In order to find the composition of liquid in equilibrium with solid it is necessary to determine the index of refraction of the quenched glass. This fixes its position on a series of curves of equal index of refraction called isofracts. The composition of the glass must also be on the isotherm of the temperature at which the liquid was held. It must, therefore, be at the point of intersection of the isofract and the isotherm.

The crystallization paths of two mixtures in the plagioclase field are shown on figure 112. The mixture (Ab_1An_1 85 percent–diopside 15 percent) (D, fig. 112) begins to crystallize at 1375°C with separation of plagioclase of composition Ab_1An_4. As the temperature falls the plagioclase increases in amount and changes in composition until at 1300°C the liquid has the composition P and plagioclase the composition Ab_1An_3. When the temperature has fallen to 1261°C diopside begins to crystallize and the liquid has the composition M, the plagioclase the composition S (Ab_1An_2), and SM is the 3-phase boundary through D. With further lowering of temperature the liquid follows the boundary, with simultaneous crystallization of diopside and plagioclase, until at 1200°C the mixture solidifies completely. The plagioclase has the composition F (Ab_1An_1), on the line ADF, and FH is a 3-phase boundary.

In the liquid E ($Ab_{18}An_{82}$ 90 percent–diopside 10 percent), crystallization begins at 1480°C with separation of Ab_5An_{95}, and the composition of the liquid follows the curve ERN. At 1245°C diopside begins to crystallize. The composition of the plagioclase is T ($Ab_{15}An_{85}$), and NT is the 3-phase boundary. The mixture freezes completely at 1237°C, the composition of the liquid is O, the feldspar ($Ab_{18}An_{82}$).

The crystallization curves, DPM and ERN apply to the liquids D and E, respectively, and to no other

[5] This means that the composition of the plagioclase is 1 part albite, 1 part anorthite.

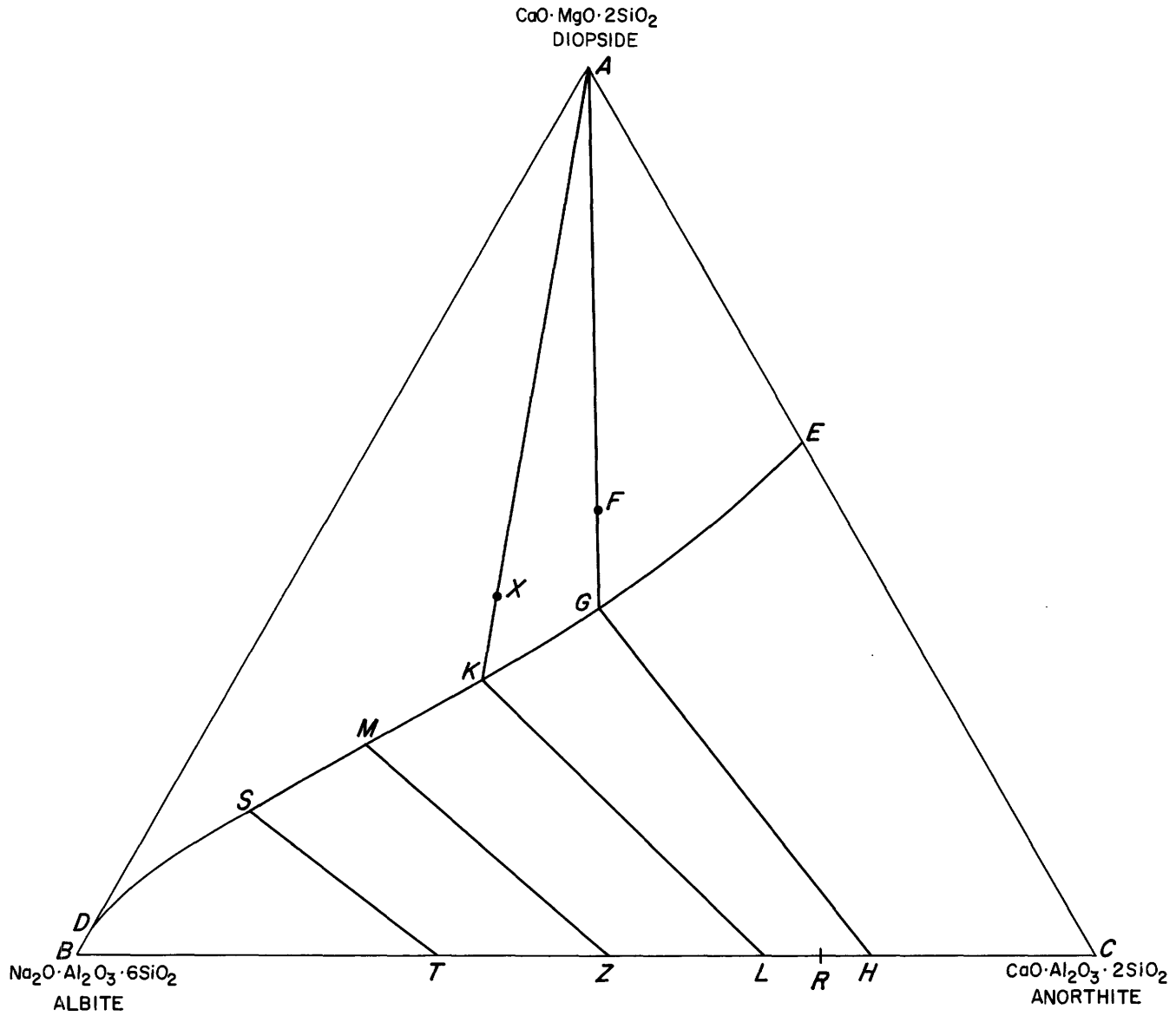

FIGURE 111.—Crystallization paths of mixtures in the diopside field in the system $Na_2O·Al_2O_3·6SiO_2$ (albite)–$CaO·MgO·2SiO_2$ (diopside)–$CaO·Al_2O_3·2SiO_2$ (anorthite). Modified from Bowen (1915).

liquids. Thus, the crystallization curve of the liquid *P* is not the curve *PM* but the new curve *PL*, that is, a liquid of composition *P* free from crystals follows the curve *PL*. Only when the liquid *P* contains the crystals formed during the change from *D* to *P* does the further course of the liquid coincide with *PM*. Moreover, the liquid *P* when originally free from crystals becomes completely crystalline on cooling, not at 1200°C (*H*) as before, but at a lower temperature.

Several sections through the quaternary system $Na_2O·Al_2O_3·2SiO_2$ (nepheline)–$2MgO·SiO_2$ (forsterite)–$CaO·MgO·2SiO_2$ (diopside)–SiO_2 have been studied (fig. 113). This quaternary system is a part of the quinary system Na_2O–MgO–CaO–Al_2O_3–SiO_2. Schairer (1957a) published the phase-equilibrium diagram of the system nepheline-diopside-silica (fig 114).

Schairer and Morimoto (1958) studied the system $Na_2O·Al_2O_3·6SiO_2$ (albite)-$2MgO·SiO_2$ (forsterite)-$CaO·MgO·2SiO_2$ (diopside), and found an initial falling of the liquidus temperature toward the point where sodium-rich plagioclase and diopside coexist with liquid at the side line albite-diopside, which is not binary. The diopside crystals may contain some Al_2O_3. The relation of this system to the quaternary system nepheline-forsterite-diopside-silica is shown in figure 113, and the phase-equilibrium diagram is figure 115. Schairer and Morimoto (1959) extended this work by a study of the plane albite-protoenstatite-diopside.

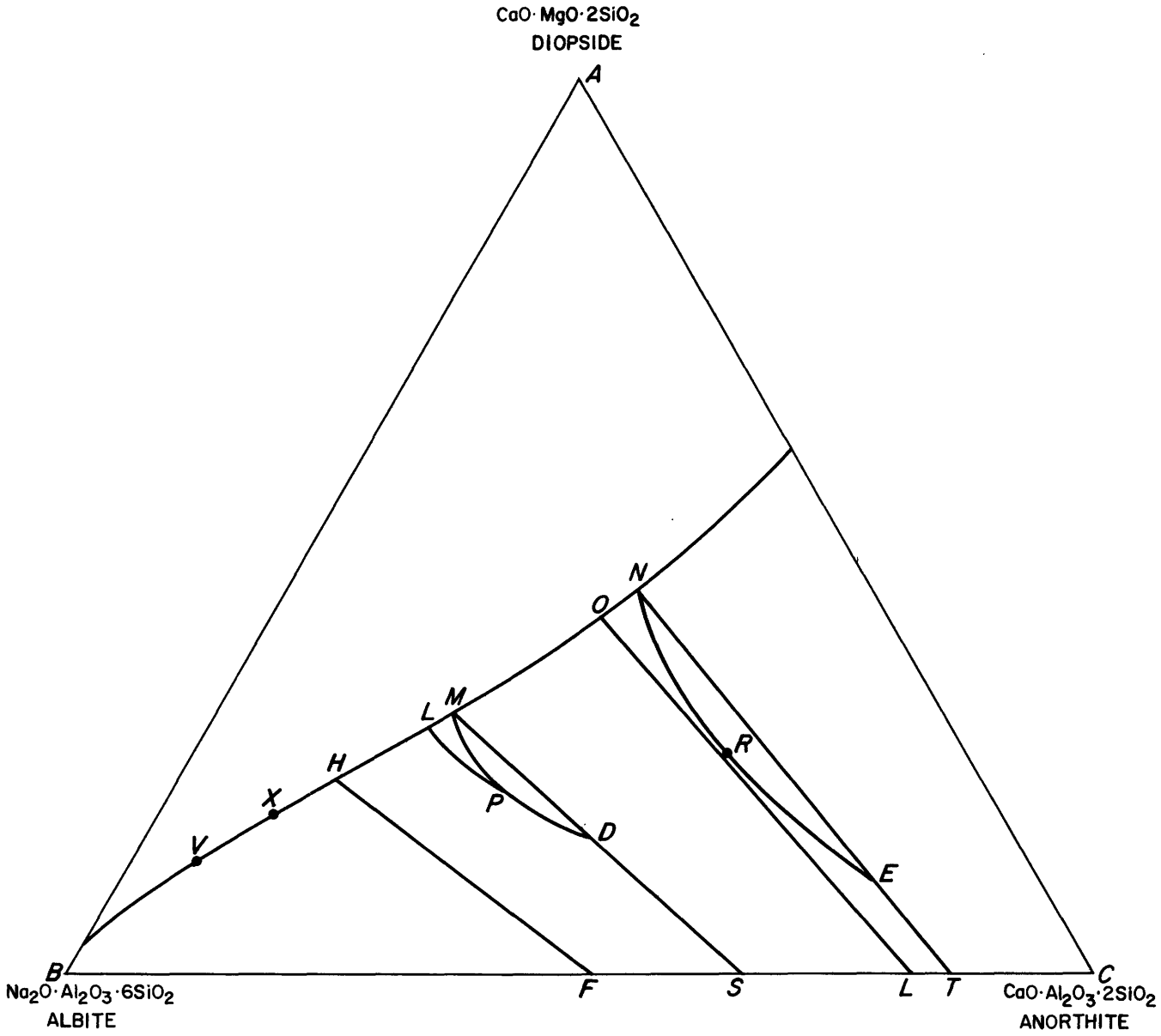

FIGURE 112.—Crystallization paths of mixtures in the plagioclase field in the system $Na_2O \cdot Al_2O_3 \cdot 6SiO_2$ (albite)–$CaO \cdot MgO \cdot 2SiO_2$ (diopside)–$CaO \cdot Al_2O_3 \cdot 2SiO_2$ (anorthite). Modified from Bowen (1915).

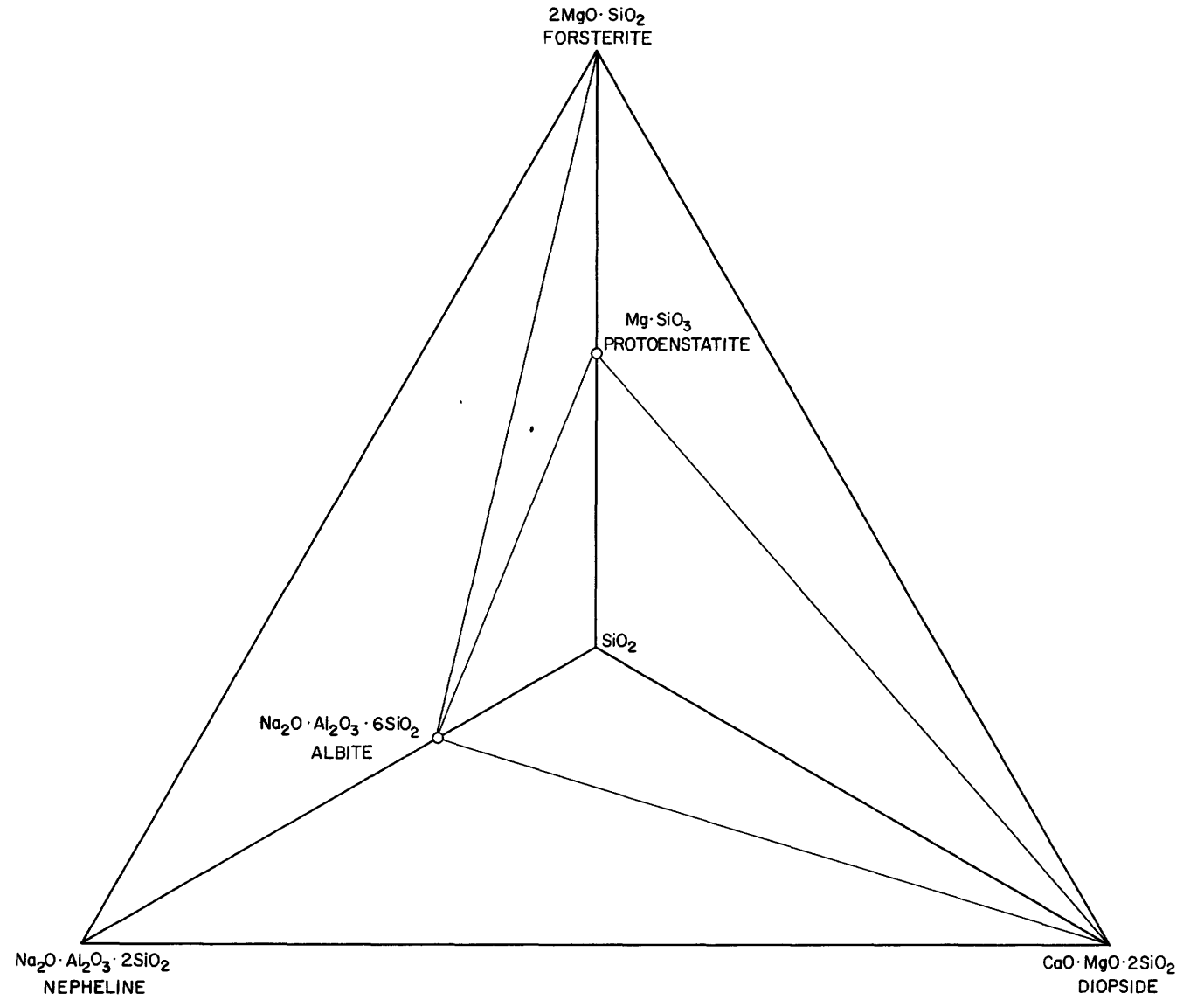

FIGURE 113.—The quaternary system $Na_2O \cdot Al_2O_3 \cdot 2SiO_2$ (nepheline)–$2MgO \cdot SiO_2$ (forsterite)–$CaO \cdot MgO \cdot 2SiO_2$ (diopside)–SiO_2, showing the ternary sections which have been studied.

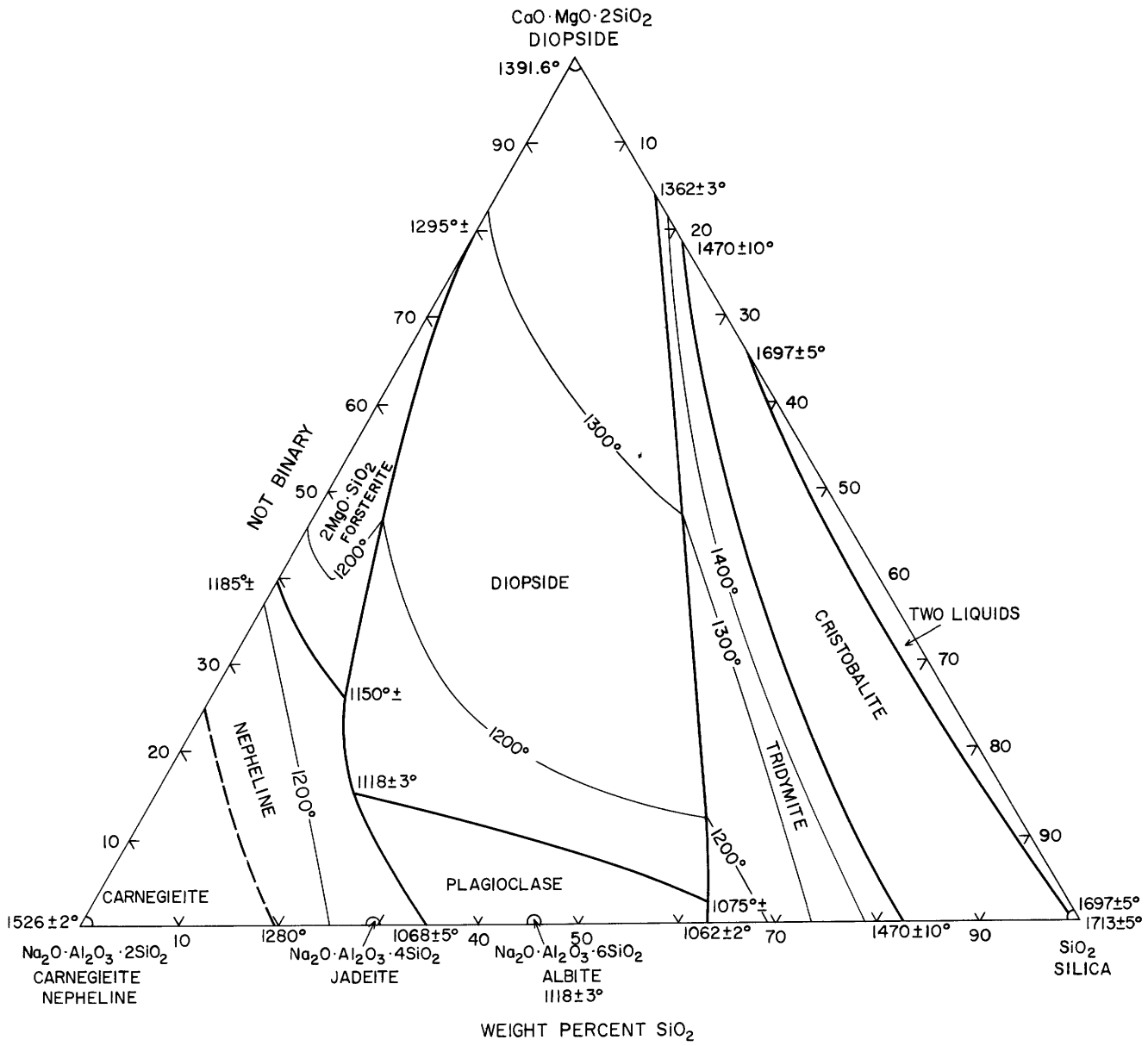

FIGURE 114.—The ternary system $Na_2O \cdot Al_2O_3 \cdot 2SiO_2$ (nepheline)–$CaO \cdot MgO \cdot 2SiO_2$ (diopside)–SiO_2. Modified from Schairer (1957a).

The relation of this plane to the system nepheline-forsterite-diopside-silica is indicated by a plane in figure 113 and the phase-equilibrium diagram is figure 116. Since forsterite, the composition of which does not lie in this plane, is a primary phase, the liquid also cannot lie in this plane, the composition range enstatite-albite-diopside is not a ternary system, and the crystallization sequence on cooling is not simple.

Schairer and Yoder (1960b) have published a preliminary diagram for the system $2MgO \cdot SiO_2$ (forsterite)–$Na_2O \cdot Al_2O_3 \cdot 2SiO_2$ (nepheline)–$CaO \cdot MgO \cdot 2SiO_2$ (diopside) (fig. 117). The primary phases forsterite, spinel, carnegieite solid solutions, nepheline solid solutions, and diopsidic pyroxenes appear on the liquidus surface. During crystallization the spinel disappears by reaction with liquid at 1245°±5°C. Melilites, which probably contain some sodium, in addition to akermanite and gehlenite, appear at subliquidus temperatures as crystalline solid phases.

K_2O–MgO–CaO–Al_2O_3–SiO_2

The system $K_2O \cdot Al_2O_3 \cdot 4SiO_2$ (leucite)–$CaO \cdot MgO \cdot 2SiO_2$ (diopside), studied by Bowen and Schairer (1929a), and the system $K_2O \cdot Al_2O_3 \cdot 4SiO_2$–

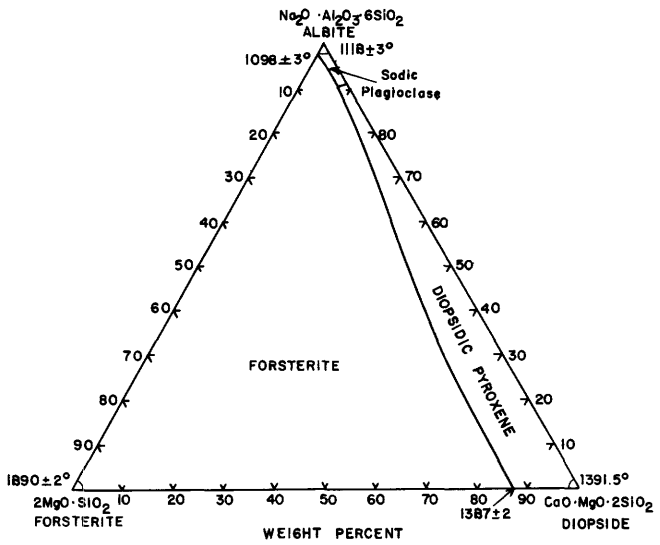

FIGURE 115.—The ternary system $Na_2O \cdot Al_2O_3 \cdot 6SiO_2$ (albite)–$2MgO \cdot SiO_2$ (forsterite)–$CaO \cdot MgO \cdot 2SiO_2$ (diopside). Modified from Schairer and Morimoto (1958).

$CaO \cdot MgO \cdot 2SiO_2$–$SiO_2$, studied by Schairer and Bowen (1938), represent portions of the five-component system K_2O–MgO–CaO–Al_2O_3–SiO_2. Leucite and diopside form a binary system, with a eutectic at 1300°±2°C, and 61.5 percent diopside. The ternary system is shown in figure 118. The field of diopside drops down so close (to less than 2 percent diopside) to the leucite-silica side, that the field of potassium feldspar in the ternary system is very small, and the compositions in this low-temperature region are so very viscous as to be impossible or almost impossible to crystallize. The ternary reaction point $K_2O \cdot Al_2O_3 \cdot 2SiO_2 + K_2O \cdot Al_2O_3 \cdot 6SiO_2 +$ liquid is below 1100°C; the eutectic $K_2O \cdot Al_2O_3 \cdot 6SiO_2 +$ $MgO \cdot CaO \cdot 2SiO_2$ + tridymite=L is below 900°C. These liquids contain little diopside, but their composition could not be precisely determined.

MgO–CaO–Al_2O_3–Fe_2O_3–SiO_2

Swayze (1946) studied the effect of adding 5 percent of MgO to the quaternary system

CaO–$2CaO \cdot SiO_2$–$5CaO \cdot 3Al_2O_3$–$2CaO \cdot Fe_2O_3$.

The invariant point at which the solid phases are CaO, $3CaO \cdot SiO_2$, $3CaO \cdot Al_2O_3$, and the solid solution $6CaO \cdot xAl_2O_3 \cdot yFe_2O_3$ at 1342°C is lowered to 1305°C, and the composition of the liquid changed to: 5 percent MgO, 50.9 percent CaO, 22.7 percent Al_2O_3, 15.8 percent Fe_2O_3, 5.6 percent SiO_2. At the other invariant point, at which the solid phases are $3CaO \cdot SiO_2$, $2CaO \cdot SiO_2$, $3CaO \cdot Al_2O_3$, and the solid solution $6CaO \cdot xAl_2O_3 \cdot yFe_2O_3$, at 1338°C, the temperature is lowered to 1301°C, and the liquid changed to 5 percent MgO, 50.5 percent CaO 23.9 percent Al_2O_3, 14.7 percent Fe_2O_3, 5.9 percent SiO_2. The addition of MgO raised the Al_2O_3 content at each invariant point, and diminished the Fe_2O_3 and CaO content more than the corresponding amount, thus lengthening the field of the iron-containing solid solution.

Na_2O–CaO–Al_2O_3–SiO_2–TiO_2

Prince (1943) studied the system $Na_2O \cdot Al_2O_3 \cdot 6SiO_2$ (albite)–$CaO \cdot Al_2O_3 \cdot 2SiO_2$ (anorthite)–$CaO \cdot SiO_2 \cdot TiO_2$ (sphene), with results shown in figure 119. The side albite-sphene is not a binary system, because the feldspar separating is not pure albite but a plagioclase containing some CaO. On the side anorthite-sphene there is a binary eutectic at 1301°C, 37 percent anorthite (point E, fig. 119). The triangular diagram shows a large area of plagioclase feldspars, bounded by the line EF, and there are no invariant points.

PETROGENY'S RESIDUA SYSTEM

Bowen (1937) called the system

$Na_2O \cdot Al_2O_3 \cdot 2SiO_2$–$K_2O \cdot Al_2O_3 \cdot 2SiO_2$–$SiO_2$

"petrogeny's residua system." He showed that the association of alkalic lavas of the region of the Great Rift Valley in Africa has those chemical characters of residual liquids that one is led to expect from the experimental studies of a number of relatively simple systems combining one of the early-crystallizing minerals in rocks with late-crystallizing alumino-silicates. The relations of these simple systems to petrogeny's residua system are shown in figure 120, reprinted from Schairer and Bowen (1956). Petrographic evidence indicates that an olivine, a solid solution of $2MgO \cdot SiO_2$ (forsterite) and $2FeO \cdot SiO_2$ (fayalite), is one of the earliest minerals to crystallize from rocks. One of the next minerals to crystallize is a pyroxene, and $CaO \cdot MgO \cdot SiO_2$ (diopside) is a simple pyroxene. Another early mineral to crystallize is a plagioclase feldspar rich in $CaO \cdot Al_2O_3 \cdot 2SiO_2$ (anorthite). By combining the four early-crystallizing minerals—forsterite, fayalite, diopside, and pyroxene—with the potassium and the sodium aluminosilicates, we get a series of eight simple systems. In the system leucite-foresterite-silica (fig. 70), the lowest melting liquid is the ternary eutectic between potassium feldspar, tridymite, and enstatite, which is nearly coincident in temperature and composition with the binary eutectic be-

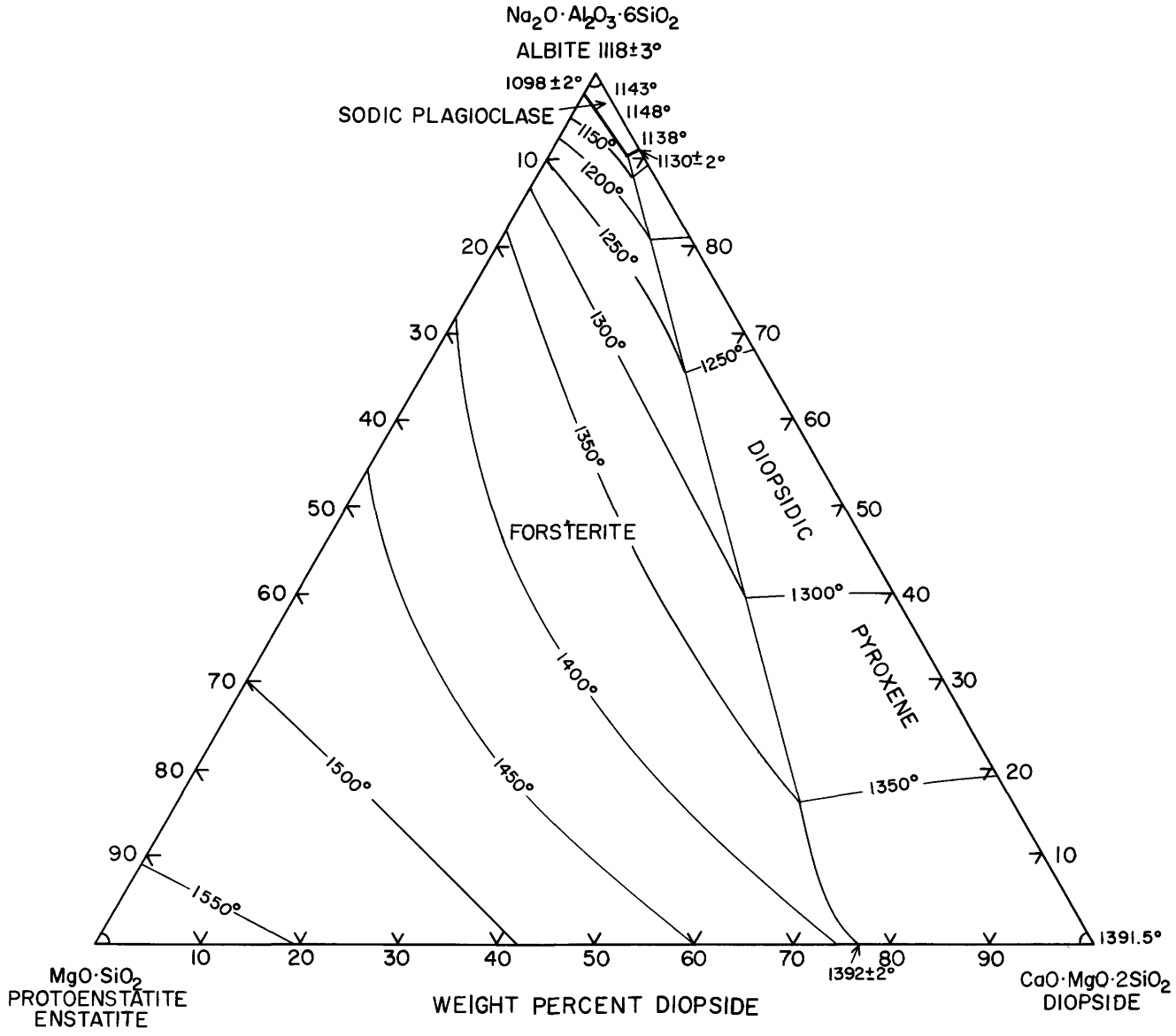

FIGURE 116.—The system $MgO \cdot SiO_2$ (protoenstatite)–$Na_2O \cdot Al_2O_3 \cdot 6SiO_2$ (albite)–$CaO \cdot MgO \cdot 2SiO_2$ (diopside). Modified from Schairer and Morimoto (1959).

tween potassium feldspar and tridymite. The system leucite-fayalite-silica (fig. 79) shows a similar low-melting liquid, as do also the systems leucite-diopside-silica (fig. 118) and leucite-anorthite-silica (fig. 78). In each case the lowest melting mixture is rich in aluminosilicates and lies close in temperature and composition to the binary eutectic between potassium feldspar and tridymite. The same general relationship is

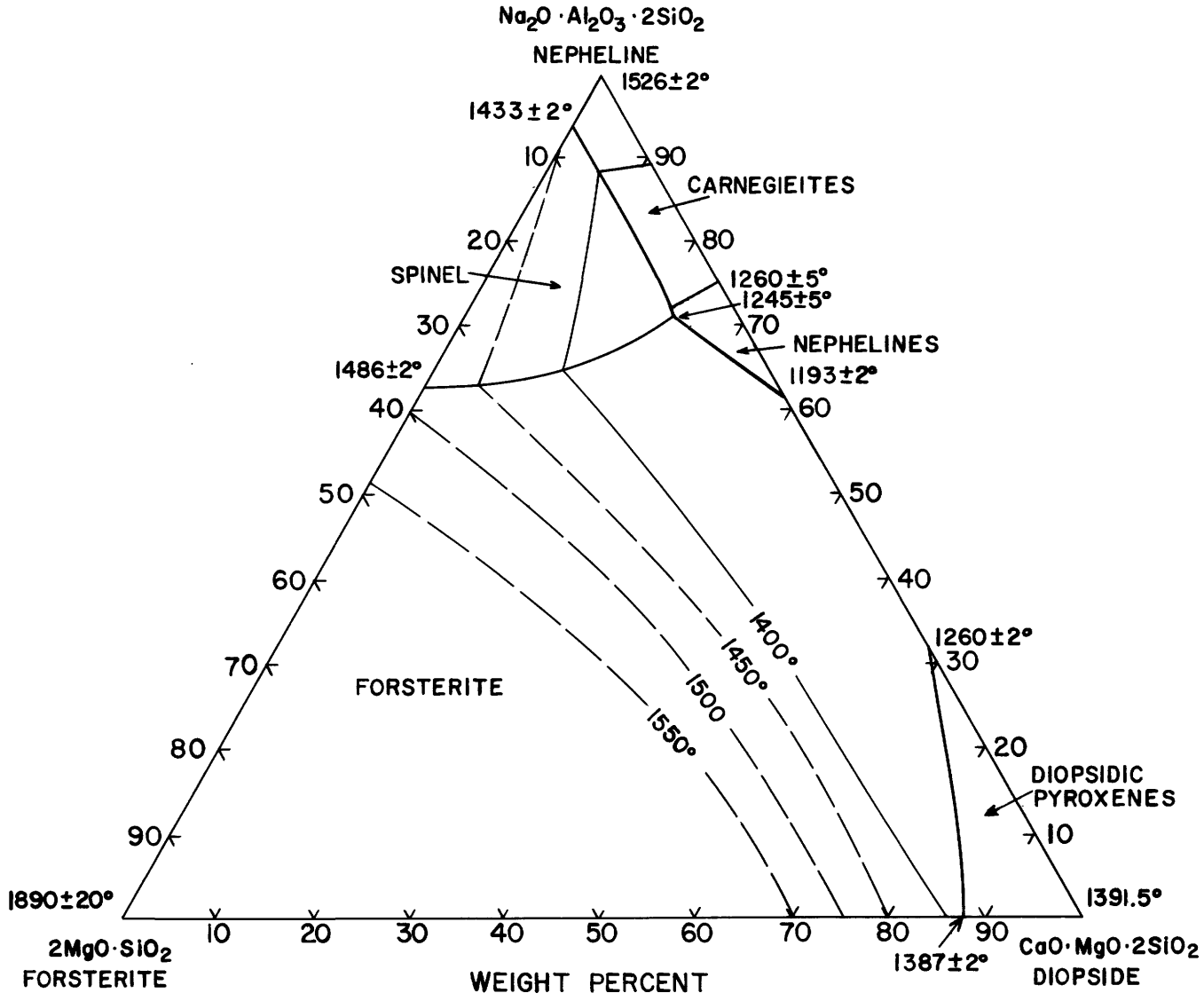

FIGURE 117.—The system $2MgO \cdot SiO_2$ (forsterite)–$Na_2O \cdot Al_2O_3 \cdot 2SiO_2$ (nepheline)–$CaO \cdot MgO \cdot 2SiO_2$ (diopside). Modified from Schairer and Yoder (1960b).

true in the simple systems with nepheline and silica, as will be seen by inspection of figures 67, 68, and 114. All these simple systems yield residual liquids from crystallization which are rich in aluminosilicates, and crystallization even of complex mixtures leads to the low-temperature trough in petrogeny's residua system. All these experimental systems lead to the conclusion that a granitic liquid is the goal toward which crystallization proceeds, and Bowen's discussion indicates that similarly a granitic liquid is the goal in magmatic processes.

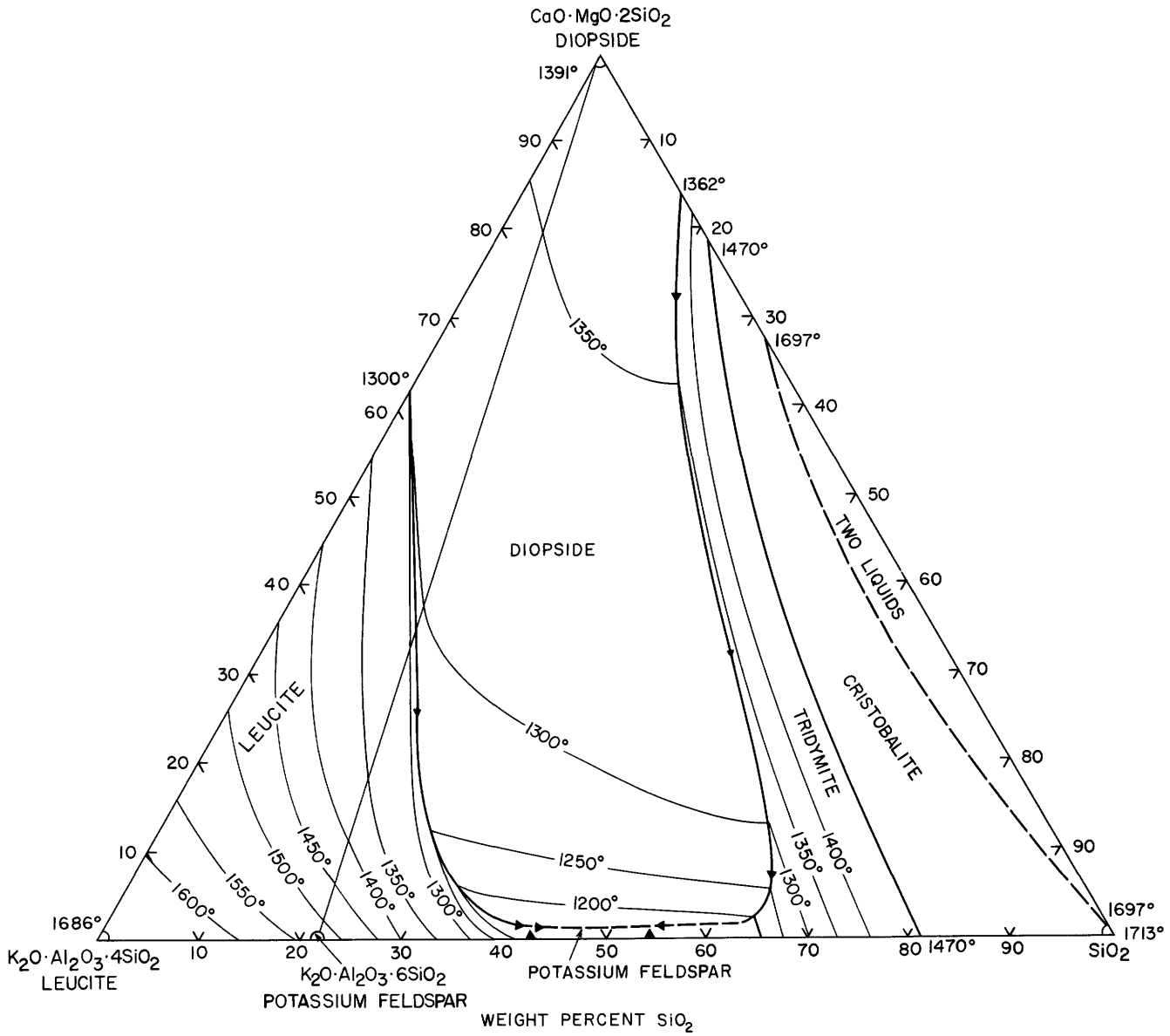

FIGURE 118.—The ternary system $K_2O \cdot Al_2O_3 \cdot 4SiO_2$ (leucite)–$CaO \cdot MgO \cdot 2SiO_2$ (diopside)–SiO_2. Modified from Schairer and Bowen (1938).

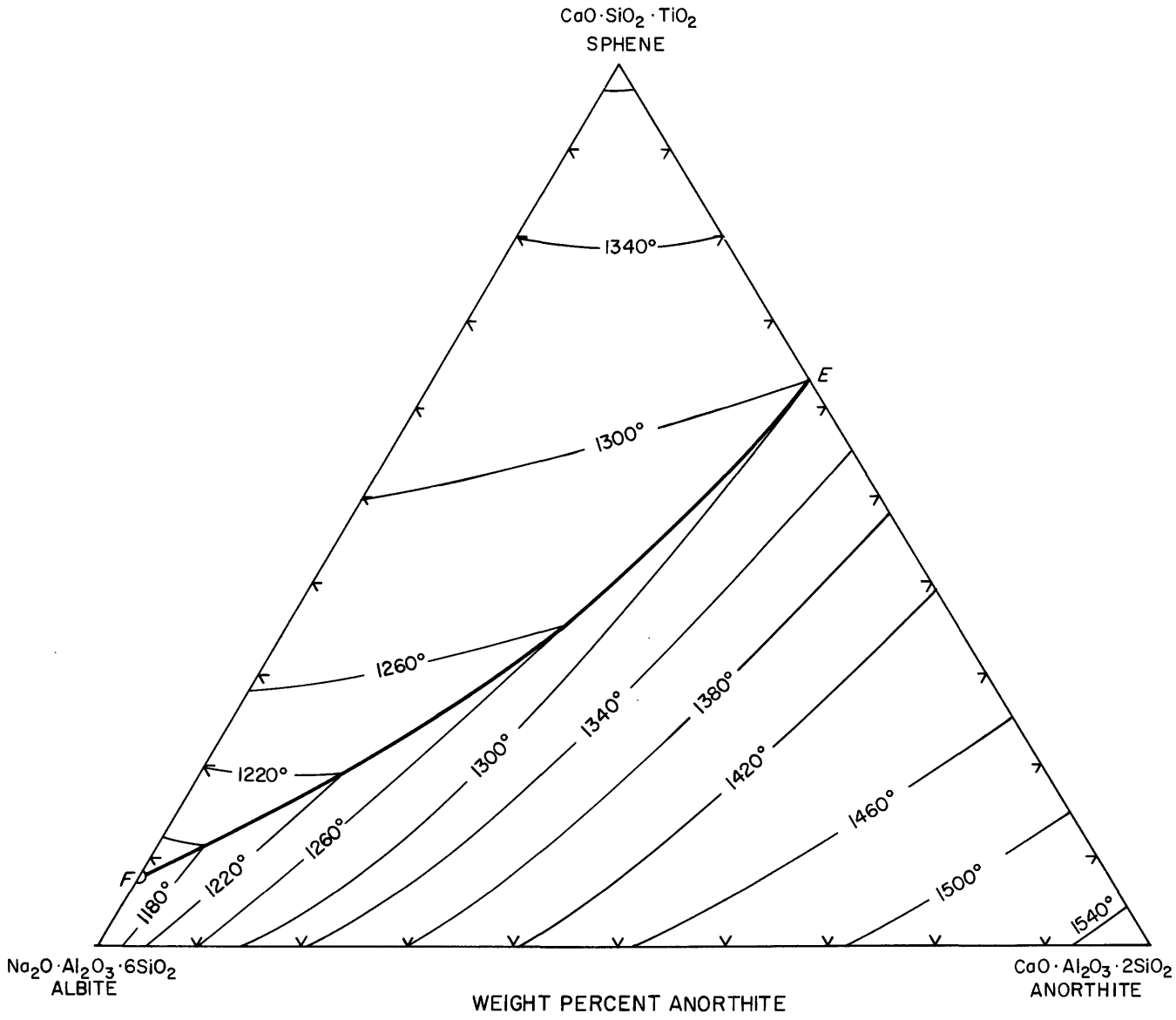

FIGURE 119.—The triangular section $Na_2O \cdot Al_2O_3 \cdot 6SiO_2$ (albite)–$CaO \cdot Al_2O_3 \cdot 2SiO_2$ (anorthite)–$CaO \cdot SiO_2 \cdot TiO_2$ (sphene) showing isotherms. Modified from Prince (1943).

695-382 O - 64 - 11

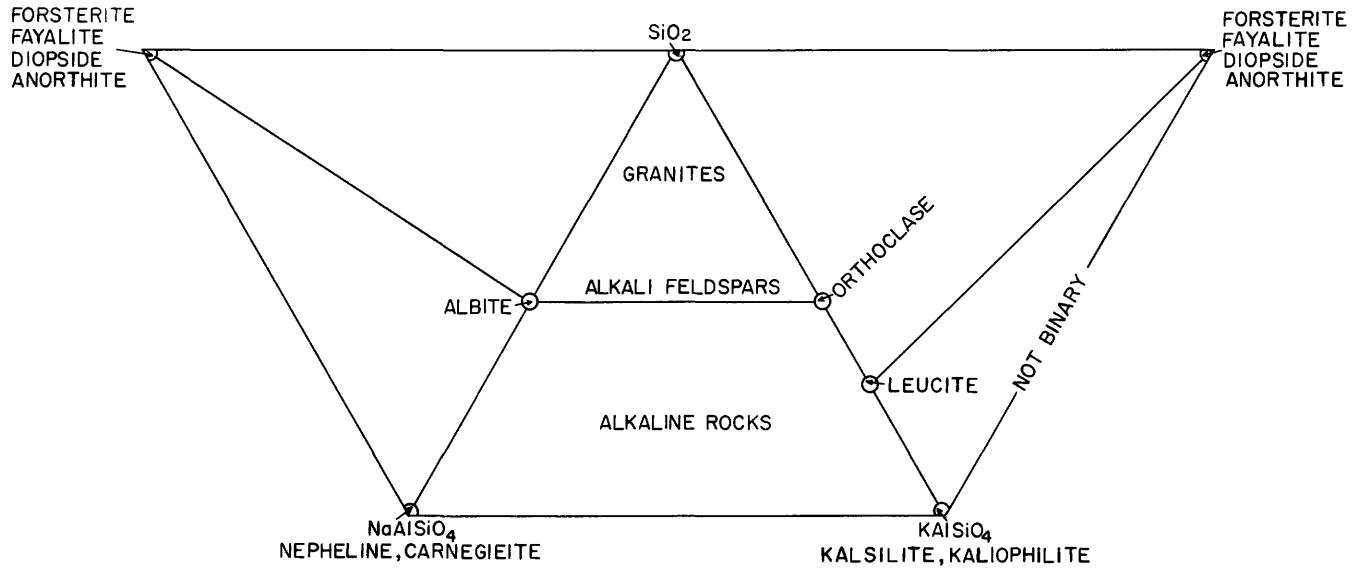

FIGURE 120.—Petrogeny's residua system. Reprinted from Schairer and Bowen (1956).

REFERENCES

Adams, L. H., 1953, A note on the stability of jadeite: Am. Jour. Sci., v. 251, p. 299–308.

Agamawi, Y. M., and White, J., 1952, The system Al_2O_3–TiO_2–SiO_2: British Ceramic Soc. Trans., v. 51, p. 293–325.

Allen, E. T., and White, W. P., 1909, Diopside and its relation to calcium and magnesium metasilicates: Am. Jour. Sci., 4th ser., v. 27, p. 1–47.

Andersen, Olaf, 1915, The system anorthite–forsterite–silica: Am. Jour. Sci., 4th ser., v. 39, p. 407–454.

———1919, The volatilization of lead oxide from lead silicate melts: Am. Ceramic Soc. Jour., v. 2, p. 784–789.

Aramaki, Shigeo, and Roy Rustum, 1959, Revision of equilibrium diagram for the system Al_2O_3–SiO_2: Nature, v. 184, p. 631–632.

Aruja, E., 1959, The unit cell of pentacalciumtrialuminate, $5CaO \cdot 3Al_2O_3$: Acta Cryst., v. 10, p. 337–341.

Atlas, Leon, 1952, The polymorphism of $MgSiO_3$: Jour. Geology, v. 60, p. 125–147.

Bakhuis Roozeboom, H. W. 1901–13, Die heterogenen Gleichgewichte von Standpunkte der Phasenlehre: v. 1—Systeme aus einer Komponente, 1901; v. 2—Systeme aus zwei Komponenten, 1904; v. 3—Die ternären Gleichgewichte, by F. A. H. Schreinmakers, pt. 1, Systeme mit nur einer Flussigkeit ohne Mischkristalle und ohne Dampf, 1911; pt. 2, Systeme mit zwei und mehr Flussigkeiten und ohne Dampf, 1913: Braunschweig, F. Vieweg und Sohn.

Bates, Frederick, and Phelps, F. P., 1927, A new base point on the thermometric scale and the $\alpha \rightleftharpoons \beta$ inversion of quartz: U.S. Natl. Bur. Standards, No. 557, Sci. Papers v. 22, p. 315–327.

Beevers, C. A., and Ross, M. A. S., 1937, The crystal structure of "Beta-alumina," $Na_2O \cdot 11Al_2O_3$: Zeitschr. Kristallographie, v. 97, p. 59–66.

Bernal, J. D., 1936, Geophysical discussion: Observatory, v. 59, 268 p.

Birch, Francis, and LeComte, Paul, 1960, Temperature-pressure plane for albite composition: Am. Jour. Sci., v. 258, p. 209–217.

Bogue, R. H., 1955, The chemistry of Portland cement: New York, Reinhold Publishing Co., 572 p.

Botvinkin, O. K., and Popova, T. A., 1937, The melting diagram of the system Na_2SiO_3–Mg_2SiO_4–SiO_2: 2d Conf. Experimental Mineralogy, Petrog., Moscow 1936, p. 87–93. Pub. by Akad. Nauk SSSR, Geol. Gruppa i Petrograf. Inst. Imeni F. Yu. Levinson-Lessing (in Russian).

Bowen, N. L., 1912, The binary system $Na_2Al_2Si_2O_8$ (nepheline, carnegiete)–$CaAl_2Si_2O_8$ (anorthite): Am. Jour. Sci., 4th ser., v. 33, p. 551–573.

———1913, Melting phenomenon of plagioclase feldspar: Am. Jour. Sci., 4th ser., v. 35, p. 577–599.

———1914, The ternary system: diopside–forsterite–silica: Am. Jour. Sci., 4th ser., v. 38, p. 207–264.

———1915, The crystallization of haplobasaltic, halplodioritic, and related magmas: Am. Jour. Sci., 4th ser., v. 40, p. 161–185.

———1917, The sodium-potassium nephelites: Am. Jour. Sci., 4th ser., v. 43, p. 115–132.

———1922, The reaction principle in petrogenesis: Jour. Geology, v. 30, p. 177–198.

——— 1937, Recent high-temperature research on silicates and its significance in igneous geology: Am. Jour. Sci., 5th ser., v. 33, p. 1–21.

——— 1956, The evolution of the igneous rocks, with a new introduction by J. F. Schairer: New York, Dover Publications, 332 p.

Bowen, N. L., and Anderson, Olaf, 1914, The binary system MgO–SiO_2: Am. Jour. Sci., 4th ser., v. 37, p. 487–500.

Bowen, N. L., and Greig, J. W., 1924, The system Al_2O_3–SiO_2: Am. Ceramic Soc. Jour., v. 7, p. 238–254.

——— 1925, The crystalline modifications of $NaAlSiO_4$: Am. Jour. Sci., 5th ser., v. 10, p. 204–212.

Bowen, N. L., and Schairer, J. F., 1929a; The system: Leucite–diopside: Am. Jour. Sci., v. 18, p. 301–312.

——— 1929b, The fusion relations of acmite: Am. Jour. Sci., v. 18, p. 365–374.

——— 1932, The system FeO–SiO_2: Am. Jour. Sci., v. 24, p. 177–213.

Bowen, N. L., and Schairer, J. F., 1935, The system MgO–FeO–SiO_2: Am. Jour. Sci., v. 29, p. 151–217.

——— 1936, The system, albite-fayalite: U.S. Natl. Acad. Sci. Proc., v. 22, p. 345–350.

——— 1938, Crystallization equilibrium in nepheline-albite-silica mixtures with fayalite: Jour. Geology, v. 46, p. 397–411.

Bowen, N. L., Schairer, J. F., and Posnjak, E., 1933a, The system, Ca_2SiO_4–Fe_2SiO_4: Am. Jour. Sci., 5th ser., v. 25, p. 273–297.

——— 1933b, The system, CaO–FeO–SiO_2: Am. Jour. Sci., 5th ser., v. 26, p. 193–284.

Bowen, N. L., Schairer, J. F., and Willems, W. V., 1930, The ternary system, Na_2SiO_3–Fe_2O_3–SiO_2: Am. Jour. Sci., 5th ser., v. 20, p. 405–455.

Bowen, N. L., and Tuttle, O. F., 1950, The system $NaAlSi_3O_8$–$KAlSi_3O_8$: Jour. Geology, v. 58, p. 489–511.

Boyd, F. R., Jr., and England, J. L., 1956, Phase equilibria at high pressures, *in* P. H. Abelson, Ann. Rept. Director Geophysical Laboratory: Carnegie Inst. Washington Year Book 55, p. 154–157.

——— 1958, Melting of diopside under high pressure, *in* P. H. Abelson, Ann. Rept. Director Geophysical Laboratory: Carnegie Inst. Washington Year Book 57, p. 173.

——— 1959, Pyrope, *in* P. H. Abelson, Ann. Rept. Director Geophysical Laboratory: Carnegie Inst. Washington Year Book 58, p. 83–87.

——— 1960, Minerals of the mantle, *in* P. H. Abelson, Ann. Rept. Director Geophysical Laboratory: Carnegie Inst. Washington Year Book 59, p. 47–52.

——— 1961a, Melting of enstatite, *in* P. H. Abelson, Ann. Rept. Director Geophysical Laboratory: Carnegie Inst. Washington Year Book 60, p. 115–117.

——— 1961b, Melting of silicates at high pressure, *in* P. H. Abelson, Ann. Rept. Director Geophysical Laboratory: Carnegie Inst. Washington Year Book, 60, p. 118–119.

Bozorth, R. M., 1927, Structure of a protection coating of iron oxide: Am. Chem. Soc. Jour., v. 49, p. 969–976.

Bragg, W. L., Gottfried, C., and West, J., 1931, The structure of β-alumina: Zeitschr. Kristallographie, v. 77, p. 255–274.

Bredig, M. A., 1945, High-temperature crystal chemistry of A_mBX_m compounds with particular reference to calcium orthosilicate: Jour. Phys. Chemistry, v. 49, p. 537–553.

——— 1950, Polymorphism of calcium orthosilicate: Am. Ceramic Soc. Jour., v. 33, p. 188–192.

Brewer, Leo, and Margrave, John, 1955, The vapor pressures of lithium and sodium oxides: Jour. Phys. Chemistry, v. 59, p. 421.

Bridgman, P. W., 1939, The high-pressure behavior of miscellaneous minerals: Am. Jour. Sci., v. 237, p. 7–18.

Brownmiller, L. T., 1935, A study of the system lime-potash-alumina: Am. Jour. Sci., 5th ser., v. 29, p. 260–277.

Brownmiller, L. T., and Bogue, R. H., 1932, The system CaO–Na_2O–Al_2O_3: U.S. Natl. Bur. Standards Jour. Research, v. 8, p. 289–307.

Budnikov, P. P., Tresvyatskii, S.G., and Kushnakovskii, V. I., 1953, The refinement in the Al_2O_3–SiO_2 phase diagram: Akad. Nauk SSSR Doklady, v. 93, p. 281–283 (in Russian).

Budnikov, P. P., and Mateev, M. A.,1956, Synthesis of crystalline $Na_2O \cdot 3SiO_2$ and its properties: Akad. Nauk SSSR Doklady, v. 107, p. 547–550 (in Russian).

Bunting, E. N., 1931, Phase equilibrium in the system Cr_2O_3–Al_2O_3: U.S. Natl. Bur. Standards Jour. Research, v. 6, p. 947.

——— 1933, Phase equilibria in the system TiO_2, TiO_2–SiO_2, and TiO_2–Al_2O_3: U.S. Natl. Bur. Standards Jour. Research, v. 11, p. 719–725.

Burdick, M. D., 1940, Studies in the system lime-ferric oxide-silica: U.S. Natl. Bur. Standards Jour. Research, v. 25, p. 475–488.

Büssem, W. and Eitel, A., 1936, Die Struktur des Pentacalciumtrialuminats: Zeitschr. Kristallographie, v. 95, p. 175–188.

Carter, P. J., and Ibrahim, M., 1952, The ternary system Na_2O–FeO–SiO_2: Soc. Glass Technology Jour., v. 36, p. 142–163.

Chao, E. C. T., Fahey, J. J., and Littler, Janet, 1961, Coesite from Wabar, near Al Hadida, Arabia: Science, v. 133, no. 3456, p. 882–883.

Chao, E. C. T., Fahey, J. J., Littler, Janet, and Milton, D. J., 1962, Stishovite, SiO_2, a very high pressure new mineral from Meteor Crater, Arizona: Jour. Geophys. Research, v. 67, p. 419–421.

Chao, E. C. T., Shoemaker, E. M., and Madsen, B. M., 1960, The first natural occurrence of coesite from Meteor Crater, Arizona: Science, v. 132, p. 220.

Chinner, G. A., and Schairer, J. F., 1959, The join grossularite-pyrope at atmospheric pressure, *in* P. H. Abelson, Ann. Rept. Director Geophysical Laboratory: Carnegie Inst. Washington Year Book, 58, p. 107–109.

——— 1960, The join grossularite–pyrope at atmospheric pressure and its bearing on the system CaO–MgO–Al_2O_3–SiO_2, *in* P. H. Abelson, Ann. Rept. Director Geophysical Laboratory: Carnegie Inst. Washingon Year Book 59, p. 72–76.

Clark, S. P., Jr., 1960, Kyanite-sillimanite equilibrium, *in* P. H. Abelson, Ann. Rept. Director Geophysical Laboratory: Carnegie Inst. Washington Year Book 59, p. 52–54.

Clark, S. P., Jr., Robertson, E. C., and Birch, Francis, 1957, Experimental determination of kyanite-sillimanite equilibrium relations at high temperatures and pressures: Am. Jour. Sci., v. 255, p. 628–648.

Clarke, F. W., and Washington, H. S., 1922, The average chemical composition of igneous rocks: U.S. Natl. Acad. Sci. Proc., v. 8, p. 108–115.

Coes, L., Jr., 1953, A new dense crystalline silica: Science, v. 118, p. 131–132.

Cohen, A. J., 1959, Origin of Libyan desert silica glass: Nature, v. 183, p. 1548–1549.

Coughanour, L. W., and DeProsse, V. A., 1953, Phase equilibria in the system MgO–TiO_2: U.S. Natl. Bur. Standards Jour. Research, v. 51, p. 87–91.

Coughanour, L. W., Roth, R. S., and DeProsse, V. A., 1954, Phase-equilibrium relations in the system lime-titania and zirconia-titania: U.S. Natl. Bur. Standards Jour. Research, v. 52, p. 37–43.

Coughanour, L. W., Roth, R. S., Marzullo, D., and Sennett, F. E., 1955, Solid-state reactions and dielectric properties in the system magnesia-lime-tin oxide-titania: U.S. Natl. Bur. Standards Jour. Research, v. 54, p. 149–162.

Coughlin, J. P., 1954, Contribution to the data of theoretical metallurgy: XII, Heats and free energies of formation of inorganic oxides: U.S. Bur. Mines Bull. 542, 80 p.

D'Ans, J., and Loeffler, J., 1930, Untersuchung im System Na_2O–SiO_2–ZrO_2: Zeitschr. anorg. allg. Chemie, v. 191, p. 1–35.

Darken, L. S., and Gurry, R. W., 1945, The system iron-oxygen: I, the wüstite field and related equilibria: Am. Chem. Soc. Jour., v. 67, p. 1398–1412.

——— 1946, The system iron-oxygen: II, Equilibrium and thermodynamics of liquid oxide and other phases: Am. Chem. Soc. Jour., v. 68, p. 798–816.

——— 1953, Physical chemistry of metals: New York, McGraw-Hill Book Co., 535 p.

Day, A. L., and Allen, E. T., 1905, The isomorphism and thermal properties of the feldspars: Carnegie Inst. Washington, Pub. 31, 95 p.

Day, A. L., and Shepherd, E. S., 1906, The lime-silica series of minerals: Am. Chem. Soc. Jour., v. 28, p. 1089–1114.

Day, A. L., Shepherd, E. S., and Wright F. E., 1906, The lime-silica series of minerals: Am. Jour. Sci., 4th ser., v. 22, p. 265–302.

Day, A. L., Sosman, R. B., and Hostetter, J. C., 1914, The determination of mineral and rock densities at high temperatures: Am. Jour. Sci., 4th ser., v. 37, p. 1–39.

DeVries, R. C., and Osborn, E. F., 1957, Phase equilibria in the high-alumina part of the system CaO–MgO–Al_2O_3–SiO_2: Am. Ceramic Soc. Jour., v. 40, p. 6–15.

DeVries, R. C., Roy, Rustum, and Osborn, E. F., 1954a, The system TiO_2-SiO_2: British Ceramic Soc. Trans., v. 53, p. 525–540.

——— 1954b, Phase equilibria in the system CaO–TiO_2: Jour. Phys. Chemistry, v. 58, p. 1069–1073.

——— 1955, Phase equilibria in the system CaO–TiO_2–SiO_2: Am. Ceramic Soc. Jour., v. 38, p. 158–171.

DeWys, E. C., and Foster, W. R., 1956, The binary system anorthite ($CaAl_2Si_2O_8$)–akermanite ($Ca_2MgSi_2O_7$): Am. Ceramic Soc. Jour., v. 39, p. 372–376.

——— 1958, The system diopside-anorthite-akermanite: Mineralog. Mag., v. 31, p. 736–743.

Edwards, J. D., and Tosterud, M., 1933, The oxides and hydrates of alumina: Jour. Phys. Chemistry, v. 37, p. 483–488.

Ervin, Guy, Jr., 1952, Structural interpretation of the diaspore-corundum-boehmite-γ-Al_2O_3 transitions: Acta Cryst. v. 5, p. 103–108.

Eubank, W. R., and Bogue, R. H., 1948, Preliminary study on portions of the systems Na_2O–CaO–Al_2O_3–Fe_2O_3 and Na_2O–CaO–Fe_2O_3–SiO_2: U.S. Natl. Bur. Standards Jour. Research, v. 40, p. 225–234.

Eugster, H. P., Reduction and oxidation in metamorphism, *in* P. H. Abelson, ed., Researches in geochemistry: New York, John Wiley & Sons, p. 397–426.

Faust, G. T., 1936, The fusion relations of iron orthoclase, with a discussion of the evidence for the existence of an iron-orthoclase molecule in feldspars: Am. Mineralogist, v. 21, p. 735–763.

Faust, G. T., and Peck, A. B., 1938, Refractive indices of some glasses in the ternary system K_2O–$4SiO_2$–Fe_2O_3–SiO_2: Am. Ceramic Soc. Jour., v. 21, p. 322-324.

Fenner, C. N., 1913, The stability relations of the silica minerals: Am. Jour. Sci., 4th ser., v. 36, p. 331–384.

Ferguson, J. B., and Merwin, H. E., 1918, The melting points of cristobalite and tridymite: Am. Jour. Sci., 4th ser., v. 46, p. 417–426.

——— 1919a, The ternary system CaO–MgO–SiO_2: Am. Jour. Sci., 4th ser., v. 48, p. 81–123.

——— 1919b, Wollastonite and related solid solutions in the ternary system lime-magnesia-silica: Am. Jour. Sci., 4th ser., v. 48, p. 165–189.

Filonenko, N. E., and Lavrov, I. V., 1953, The melting of mullite: Akad. Nauk SSSR Doklady, v. 89, p. 141–142 (in Russian).

Findlay, Alexander, 1951, The phase rule and its applications, 9th ed., revised by A. N. Campbell and N. O. Smith: New York, Dover Publications, 494 p.

Flörke, O. W., 1955, Strukturanomalien beim Tridymit und Kristobalit: Deutsche Keram. Gesell. Ber., v. 37, p. 369–381.

Foster, W. R., 1942, The system $NaAl_3SiO_8$–$CaSiO_3$–$NaAlSiO_4$: Jour. Geology, v. 50, p. 152–173.

——— 1950, Synthetic sapphirine and its stability relations in the system MgO–Al_2O_3–SiO_2: Jour. Geology, v. 58, p. 135–151.

——— 1951, High temperature X-ray diffraction study of the polymorphism of $MgSiO_3$: Am. Ceramic Soc. Jour., v. 34, p. 255–259.

Franco, R. R., and Schairer, J. F., 1951, Liquidus temperatures in mixtures of the feldspars of soda, potash, and lime: Jour. Geology, v. 59, p. 259–267.

Galakhov, F. Ya., 1958, Alumina regiona for ternary aluminosilicate systems: III, The system TiO_2–Al_2O_3–SiO_2: Akad. Nauk SSSR, Izv. Otdel. Khim. Nauk, p. 529–534 (in Russian).

Geller, R. F., and Yavorsky, P. J. 1945, Melting point of alpha-alumina: U.S. Natl. Bur. Standards Jour. Research, v. 34, p. 395–401.

Gibbs, J. W., 1906, On the equilibrium of heterogeneous substances: The Scientific papers of J. Willard Gibbs, v. 1, p. 85–349, New Haven, Conn., Yale Univ. Press.

Gibson, R. E. 1928a, The influence of pressure on the high-low inversion of quartz: Jour. Phys. Chemistry, v. 32, p. 1197–1205.

——— 1928b, A note on the high-low inversions of quartz and the heat capacity of low quartz at 573°C.: Jour. Phys. Chemistry, v. 32, p. 1206–1210.

Goldsmith, J. R., 1947, The system $CaAl_2Si_2O_8$–$Ca_2Al_2SiO_7$–$NaAlSiO_4$: Jour. Geology, v. 55, p. 381–404.

——— 1948, The compound $CaO \cdot 2Al_2O_3$: Jour. Geology, v. 56, p. 80–81.

Goranson, R. W., and Kracek, F. C., 1932, An experimental investigation of the phase relations of $K_2Si_4O_9$ under pressure: Jour. Phys. Chemistry, v. 36, p. 913–926.

Greene, K. T., and Bogue, R. H., 1946, Phase equilibrium relations in a portion of the system Na_2O–CaO–Al_2O_3–SiO_2: U.S. Natl. Bur. Standards Jour. Research, v. 36, p. 185–207.

Greig, J. W., 1926, Formation of mullite from kyanite, andalusite, and sillimanite: Am. Jour. Sci. 5th ser., v. 11, p. 1–26.

———1927a, Immiscibility in silicate melts: Am. Jour. Sci., 5th ser., v. 13, p. 1–44.

———1927b, On liquid immiscibility in the system FeO–Fe_2O_3–Al_2O_3–SiO_2: Am. Jour. Sci., 5th ser., v. 14, p. 473–484.

——— 1932, The existence of the high-temperature form of cristobalite at room temperatures and the crystallinity of opal: Am. Chem. Soc. Jour., v. 54, p. 2846–2849.

Greig, J. W., and Barth, T. F. W., 1938, The system, $Na_2O \cdot Al_2O_3 \cdot 2SiO_2$ (nephelite, carnegieite)–$Na_2O \cdot Al_2O_3 \cdot 6SiO_2$ (albite): Am. Jour. Sci., v. 35A, p. 93–112.

Greig, J. W., Posnjak, E., Merwin, H. E., and Sosman, R. B., 1935, Equilibrium relationships of Fe_3O_4, Fe_2O_3, and oxygen: Am. Jour. Sci., v. 30, p. 239–316.

Grieve, J., and White, J., 1939, The system FeO–TiO_2: Royal Tech. Coll. (Glasgow) Jour., v. 4, p. 441–448.

Griggs, D. T., and Kennedy, G. C. 1956, A simple apparatus for high pressures and temperatures: Am. Jour. Sci., v. 254, p. 722–735.

Gummer, W. K., 1943, The system $CaSiO_3$–$CaAl_2Si_2O_8$–$NaAlSiO_4$: Jour. Geology, v. 51, p. 503–530.

Gurry, R. W., and Darken, L. S., 1950, The composition of CaO–FeO–Fe_2O_3 and MnO–FeO–Fe_2O_3 melts at several oxygen pressures in the vicinity of 1600°C.: Am. Chem. Soc. Jour., v. 72, p. 3906–3910.

Hansen, W. C., 1928, Phase equilibria in the system $2CaO \cdot SiO_2$–MgO–$5CaO \cdot 3Al_2O_3$: Am. Chem. Soc. Jour., v. 50, p. 2155–2160.

Hansen, W. C., and Brownmiller, L. T., 1928, Equilibrium studies on alumina and ferric oxide, and on combinations of these with magnesia and calcium oxide: Am. Jour. Sci., 5th ser., v. 15, p. 225–242.

Hansen, W. C., Brownmiller, L. T., and Bogue, R. H., 1928, Studies on the system calcium oxide-alumina-ferric oxide: Am. Chem. Soc. Jour., v. 50, p. 396–406.

Hay, R., and White, J., 1940, Slag systems: W. Scotland Iron and Steel Inst. Jour., v. 47, p. 87–92.

Hill, V. G., and Roy, Rustum, 1958a, Silica structure studies: VI, Tridymites: British Ceramic Soc. Trans., v. 57, p. 496–510.

——— 1958b, Silica structures: V. The variable inversion in cristobalite: Am. Ceramic Soc. Jour., v. 41, p. 532–537.

Hytönen, Kai, and Schairer, J. F., 1960, The system enstatite-anorthite-diopside, *in* P. H. Abelson, Ann. Rept. Director Geophysical Laboratory Carnegie Inst. Washington Year Book 59, p. 71–72.

Insley, H., and McMurdie, H. E., 1938, Minor constituents of Portland cement clinker: U.S. Natl. Bur. Standards Jour. Research, v. 20, p. 173–184.

Iwase, K., and Nisioka, U., 1936, The equilibrium diagram of the ternary system CaO–$Al_2O_3 \cdot 2SiO_2$–$CaO \cdot SiO_2$: Tohoku Imp. Univ. Sci. Repts., 1st ser., K. Hondra Anniv. Vol., p. 44–451.

Juan, V. C., 1950, The system $CaSiO_3$–$Ca_2Al_2SiO_7$–$NaAlSiO_4$: Jour. Geology, v. 58, 1–15.

Kammermeyer, K., and Peck, A. B., 1933, High temperature preparation and the optical properties of sodium aluminate: Am. Ceramic Soc. Jour., v. 16, p. 363–366.

Kanolt, C. W., 1914, Melting points of some refractory oxides: U.S. Natl. Bur. Standards Bull., v. 10, p. 295–313.

Karkhanavala, M. D., and Hummel, F. A., 1953, The polymorphism of cordierite: Am. Ceramic Soc. Jour., v. 36, p. 389–392.

Keat, P. P., 1954, A new crystalline silica: Science, v. 120, p. 328–330.

Keith, M. L., and Schairer, J. F., 1952, The stability field of sapphirine in the system MgO–Al_2O_3–SiO_2: Jour. Geology, v. 60, p. 181–186.

Keith, M. L., and Tuttle, O. F., 1952, Significance of variation in the high-low inversion of quartz: Am. Jour. Sci., Bowen Volume, p. 203–280.

Kennedy, G. C., Wasserburg, G. J., Heard, H. C., and Newton, R. C., 1962, The upper three-phase region of the system SiO_2–H_2O: Am. Jour. Sci., v. 260, p. 501–521.

Korzhinskii, D. S. 1959, Physicochemical basis of the analysis of the paragenesis of minerals: Consultants Bureau, New York.

Kracek, F. C., 1930, The system sodium oxide–silica: Jour. Phys. Chemistry, v. 34, p. 1583–1589.

——— 1932, The ternary system K_2SiO_3–Na_2SiO_3–SiO_2: Jour. Phys. Chemistry, v. 36, p. 2529–2542.

Kracek, F. C., 1939, Phase-equilibrium relations in the system Na_2SiO_3–Li_2SiO_3–SiO_2: Am. Chem. Soc. Jour., v. 61, p. 2863–2877.

Kracek, F. C., Bowen, N. L., and Morey, G. W., 1929, The system potassium metasilicate–silica: Jour. Phys. Chemistry, v. 33, p. 1857–1879.

——— 1939, Equilibrium relations and factors influencing their determination in the system K_2SiO_3–SiO_2: Jour. Phys. Chemistry, v. 41, p. 1183–1193.

Kracek, F. C., Neuvonen, K. J., and Burley, G., 1951, A thermodynamic study of the stability of jadeite: Washington Acad. Sci. Jour., v. 41, p. 378–383.

Larsen, E. S., Jr., and Foshag, W. F., 1921, Merwinite, a new calcium magnesium orthosilicate from Crestmore, Calif.: Am. Mineralogist, v. 6, p. 143–148.

Lea, F. M., and Desch, C. H., 1956, The chemistry of cement and concrete, 2d ed.: London, Edward Arnold and Co., 690 p.

Lea, F. M., and Parker, T. W., 1934, Investigations on a portion of the quaternary system CaO–Al_2O_3–SiO_2–Fe_2O_3: The quaternary system CaO–$2CaO \cdot SiO_2$–$5CaO \cdot 3Al_2O_3$–$4CaO \cdot Al_2O_3 \cdot Fe_2O_3$: Royal Soc. London Trans., v. 234, p. 1–42.

Levin, E. M., McMurdie, H. F., and Hall, F. P., 1956, Phase diagrams for ceramists: Columbus, Ohio, Am. Ceramic Soc., 286 p.

Levine, I., and Ott, Emil, 1932, The crystallinity of opals, and the existence of high-temperature cristobalite at room temperature: Am. Chem. Soc. Jour., v. 54, p. 828–829.

MacChesney, J. B., and Muan, A., 1959, Studies in the system iron-oxide-titanium oxide: Am. Mineralogist, v. 44, p. 926–945.

McConnell, J. D. C., and McKie, Duncan, 1960, The kinetics of the ordering process in triclinic $NaAlSi_3O_8$: Mineralog. Mag., v. 32, p. 436–454.

MacDonald, G. J. F., 1956, Quartz-coesite stability relations at high temperatures and pressures: Am. Jour. Sci., v. 254, p. 713–721.

M'Intosh, A. B., Rait, J. R., and Hay, R., 1937, The binary system FeO–Al_2O_3: Royal Tech. Coll. (Glasgow) Jour., v. 4, p. 72–76.

MacKenzie, W. S., 1957. The crystalline modifications of $NaAlSi_3O_8$: Am. Jour. Sci., v. 255, p. 481–516.

McMurdie, Howard, 1937, Studies on a portion of the system: CaO–Al_2O_3–Fe_2O_3: U.S. Natl. Bur. Standards Jour. Research, v. 18, p. 475–484.

Manuilova, N. S., 1937, Crystalline phases in the system Na_2O–MgO–SiO_2: 2d Conf. Experimental Mineralogy, Petrog., Moscow 1936, p. 96–101, Pub. by Akad Nauk SSSR, Geol. Gruppa i Petrograf Inst. Imeni F. Yu Levinson-Lessing (in Russian).

Matignon, C., 1923, Action des temperatures elevees sur quelques substances refractaires: Acad. Sci. (Paris) Comptes rendus, v. 177, p. 1270–1273.

Miyashiro, A., and Iiyama, T., 1954, Mineral indialite, polymorphic with cordierite: Japan Acad. Proc., v. 30, p. 746–751.

Morey, G. W., 1914, New crystalline silicates of potassium and sodium, their preparation and general properties: Am. Chem. Soc. Jour., v. 36, p. 215–230.

——— 1923, A comparison of the heating-curve and quenching methods of melting-point determinations: Washington Acad. Sci. Jour., v. 13, p. 326–329.

——— 1930a, The devitrification of soda-lime-silica glasses: Am. Ceramic Soc. Jour., v. 13, p. 683–713.

Morey, G. W., 1930b, The effect of magnesia on the devitrification of a soda-lime-silica glass: Am. Ceramic Soc. Jour., v. 13, p. 714–717.

——— 1930c, The effect of alumina on the devitrification of a soda-lime-silica glass: Am. Ceramic Soc. Jour., v. 13, p. 718–724.

——— 1930d, Analytical methods in phase-rule problems: Jour. Phys. Chemistry, v. 34, p. 1745–1750.

——— 1936, The phase rule and heterogeneous equilibrium. A commentary on the scientific writing of J. Willard Gibbs: New Haven, Conn., Yale Univ. Press, p. 233–293.

Morey, G. W., and Bowen, N. L., 1922, The melting of potash feldspar: Am. Jour. Sci., 5th ser., v. 4, p. 1–21.

——— 1924, The binary system sodium metasilicate-silica: Jour. Phys. Chemistry, v. 28, p. 1167–1179.

——— 1925, The ternary system sodium metasilicate-calcium metasilicate-silica: Soc. Glass Tech. Trans., v. 9, p. 262–264.

——— 1931, Devitrite: Glass Indus., v. 12, p. 133.

Morey, G. W., and Fenner, C. N., 1917, Ternary system H_2O–K_2SiO_3–SiO_2: Am. Chem. Soc. Jour., v. 39, p. 1173–1229.

Morey, G. W., and Ingerson, Earl, 1937, The pneumatolytic and hydrothermal alteration and synthesis of silicates: Econ. Geology, supp. to v. 32, no. 5, p. 607–761.

——— 1941, Solubility of solids in "gases" or "vapors" [abs.]: Geol. Soc. America Bull., v. 52, p. 1924.

Morey, G. W., Kracek, F. C., and Bowen, N. L., 1930, The ternary system K_2O–CaO–SiO_2: Soc. Glass Tech. Trans., v. 14, p. 149–187.

——— 1931, The ternary system K_2O–CaO–SiO_2: a correction: Soc. Glass Tech. Trans., v. 15, p. 57–58.

Morey, G. W., Kracek, F. C., and England, J. L., 1953, Polymorphism of sodium disilicate, $Na_2Si_2O_5$; *in* G. W. Morey, Ann. Rept. Director of Geophysical Laboratory: Carnegie Inst. Washington Year Book 52, p. 58–59.

Mosesman, M. A., and Pitzer, K. S., 1941, Thermodynamic properties of the crystalline forms of silica: Am. Chem. Soc. Jour., v. 63, p. 2348–2356.

Muan, Arnulf, 1955, Phase equilibria in the system FeO–Fe_2O_3–SiO_2: Am. Inst. Metals Trans., v. 203, p. 965–976.

——— 1957a, Phase equilibria at liquidus temperatures in the system iron oxide–Al_2O_3–SiO_2 in air atmosphere: Am. Ceramic Jour., v. 40, p. 121–133.

——— 1957b, Phase-equilibria relationships in the system, FeO–Fe_2O_3–Al_2O_3–SiO_2: Am. Ceramic Soc. Jour., v. 40, p. 420–431.

——— 1958a, Phase equilibria at high temperatures in oxide systems involving changes in oxidation states: Am. Jour. Sci., v. 256, p. 171–207.

——— 1958b, On the stability of the phase $Fe_2O_3 \cdot Al_2O_3$: Am. Jour. Sci., v. 256, p. 413–422.

Muan, Arnulf, and Gee, C. L., 1956, Phase equilibrium studies in the system iron oxide–Al_2O_3 in air and 1 atm. O_2 pressure: Am. Ceramic Soc. Jour., v. 39, p. 207–214.

Muan, Arnulf, and Osborn, E. F., 1951, Phase relations in the system $2CaO \cdot SiO_2$–$CaO \cdot SiO_2$–$2CaO \cdot Al_2O_3$–SiO_2–FeO: Am. Iron and Steel Inst., Year Book, p. 325–361.

——— 1956, Phase equilibria at liquidus temperatures in the system MgO–FeO–Fe_2O_3–SiO_2: Am. Ceramic Soc. Jour., v. 39, p. 121–140.

Niggli, P., 1913, The phenomena of equilibrium between silica and the alkali carbonates: Am. Chem. Soc. Jour., v. 35, p. 1693–1727.

Nisioka, U., 1935, The equilibrium diagram of the system $CaO \cdot Al_2O_3 \cdot 2SiO_2$–$CaO \cdot TiO_2$: Tohoku Imperial Univ. Sci. Repts., v. 24, p. 708–717.

Nurse, R. W., 1962, Phase equilibria and constitution of portland cement clinker, *in* Chemistry of Cement, Proc. 4th Internat. Symposium, Washington, 1960: [U.S.] Natl. Bur. Standards Mon. 43, v. 1, sess. 2, paper 21, p. 9–37.

Osborn, E. F., 1942, The system $CaSiO_3$–diopside–anorthite: Am. Jour. Sci., v. 240, p. 751–788.

——— 1943, The compound merwinite ($3CaO \cdot MgO \cdot 2SiO_2$) and its stability relations in the system $CaO \cdot MgO$–SiO_2: Am. Ceramic Soc. Jour., v. 26, p. 321–332.

Osborn, E. F., and Schairer, J. F., 1941, The ternary system pseudowollastonite-akermanite-gehlenite: Am. Jour. Sci., v. 239, p. 715–763.

Osborn, E. F., and Tait, D. B., 1952, The system diopside-forsterite-anorthite: Am. Jour. Sci., Bowen Volume, pt. 2, p. 413–433.

Ostrovskii, I. A., 1956, Study of mineral formation in some silicate melts under pressure of water vapor and hydrogen: Inst. Geol. Rudnykh Mestorozhdennii, Petrog. i. Geochemii, Trudy, p. 3–199. [Russian.]

Pablo-Galan, L. E. de, and Foster, W. R., 1959, Investigations of the role of beta-alumina in the system, Na_2O–Al_2O_3–SiO_2: Am. Ceramic Soc. Jour., v. 42, p. 491–498.

Paladino, A. E., 1960, Phase equilibrium in the ferrite region of the system FeO–MgO–SiO_2: Am. Ceramic Soc. Jour., v. 43, p. 183–191.

Pecora, W. T., 1960, Coesite craters and space geology: Geotimes, v. 5, no. 2, p. 16–19, 32.

Phemister, James, Nurse, R. W., and Bannister, F. A., 1942, Merwinite as an artificial mineral: Mineralog. Mag. v. 26, p. 225–230.

Phillips, B., and Muan, Arnulf, 1958, Phase equilibria in the system CaO–iron oxide in air and in 1 atm. O_2 pressure: Am. Ceramic Soc. Jour., v. 41, p. 445–454.

——— 1959, Phase equilibria in the system CaO–iron oxide–SiO_2 in air: Am. Ceramic Soc. Jour., v. 42, p. 413–423.

Prince, A. T., 1943, The system albite-anorthite-sphene: Jour. Geology, v. 51, p. 1–16.

——— 1951, Phase relations in a portion of the system MgO–Al_2O_3–$2CaO \cdot SiO_2$: Am. Ceramic Soc. Jour., v. 34, p. 44–51.

——— 1954, Liquidus relationships on 10 percent MgO plane of the system lime-magnesia-alumina-silica: Am. Ceramic Soc. Jour., v. 37, p. 402–408.

Rait, J. R., 1949, Basic refractories—their chemistry in relation to their performance: Iron and Steel, v. 22, p. 189, 289, 493, 623.

Ralston, O. C., 1929, Iron oxide reduction equilibria: a critique from the standpoint of the phase rule and thermodynamics: U.S. Bur. Mines Bull. 296, 326 p.

Rankin, G. A., and Merwin, H. W., 1916, The ternary system CaO–Al_2O_3–MgO: Am. Chem. Soc. Jour., v. 38, p. 568–588.

——— 1918, The ternary system MgO–Al_2O_3–SiO_2 Am. Jour. Sci., 4th ser., v. 45, p. 301–325.

Rankin, G. A., and Wright, F. E., 1915, The ternary system CaO–Al_2O_3–SiO_2: Am. Jour. Sci., 4th ser., v. 39, p. 1–79.

Ricci, J. E., 1951, The phase rule and heterogeneous equilibrium: Princeton, N.J., D. Van Nostrand Co., 505 p.

Ricker, R. W., and Osborn, E. F., 1954, Additional phase-equilibrium data of the system CaO–MgO–SiO_2: Am. Ceramic Soc. Jour., v. 37, p. 133–139.

Ridgeway, R. R., Klein, A. A., and O'Leary, W. V., 1936, Preparation and properties of so-called "beta-alumina": Electrochem. Soc. Trans., v. 70, p. 71–87.

Ringwood, A. E., 1958, The constitution of the mantle: II, Further data on the olivine-spinel transition: Geochem. et Cosmochim. Acta, v. 15, p. 18–29.

Roberts, H. S., and Merwin, H. E., 1931, The system MgO–FeO–Fe_2O_3 in air at one atmosphere: Am. Jour. Sci., v. 21, p. 145–157.

Robertson, E. C., Birch, Francis, and MacDonald, G. J. F., 1955, Fields of stability of jadeite, kyanite, and pyrope [abs.]: Geol. Soc. America Bull., v. 66, p. 1608.

Roedder, E. W., 1951a, The system K_2O–MgO–SiO_2: Am. Jour. Sci., v. 249, p. 89–130, 224–248.

——— 1951b, Low-temperature liquid immiscibility in the system K_2O–FeO–Al_2O_3–SiO_2: Am. Mineralogist, v. 36, p. 282–286.

——— 1952, A reconnaissance of liquidus relations in the system $K_2O \cdot 2SiO_2$–FeO–SiO_2: Am. Jour. Sci., Bowen Volume, p. 435–456.

——— 1953a, Liquid immiscibility in the system K_2O–FeO–Al_2O_3–SiO_2 [abs.]: Geol. Soc. America Bull., v. 64, p. 1466.

——— 1953b, High silica portion of the system K_2O–FeO–Al_2O_3–SiO_2 [abs.]: Geol. Soc. America Bull., v. 64, p. 1554.

——— 1959, Silicate melt systems, *in* Ahrens, L. H., and others, eds., Physics and chemistry of the earth, v. 3, p. 224–297, London, Pergamon Press, 464 p.

Rooksby, H. P., and Rooymans, C. J. M., 1961, The formation and structure of delta-alumina: Clay Minerals Bull., v. 4, p. 234–238.

Roth, R. S., 1958, Revision of the phase-equilibrium diagram of the binary system calcia–titania, showing the compound $Ca_4Ti_3O_{10}$: U.S. Natl. Bur. Standards Jour. Research, v. 61, p. 437–440.

Roy, D. M., 1954, Hydrothermal synthesis of andalusite: Am. Mineralogist, v. 39, p. 140–143.

Roy, D. M., and Roy, Rustum, 1955, Synthesis and stability of minerals in the system: MgO–Al_2O_3–SiO_2–H_2O: Am. Mineralogist, v. 40, p. 147–178.

Roy, Rustum, 1959, Silica O, a new common form of silica: Zeitschr. Kristallographie, v. 111, p. 185–189.

Ruff, O., and Schmidt, P., 1921, Die Dampfdrucke der Oxyde des Siliciums, Aluminums, Calciums, und Magnesiums: Zeitschr. anorg. allg. Chemie, v. 117, p. 172–190.

Saalfeld, H., 1958, Dehydration of gibbsite: Clay Minerals Bull., v. 3, p. 249–257.

Schairer, J. F., 1942, The system CaO–FeO–Al_2O_3–SiO_2: I, Results of quenching experiments on five joins: Am. Ceramic Soc. Jour., v. 25, p. 241–274.

——— 1950, The alkali-feldspar join in the system $NaAlSiO_4$–$KAlSiO_4$–SiO_2: Jour. Geology, v. 58, p. 512–517.

——— 1954, The system K_2O–MgO–Al_2O_3–SiO_2: I, Results of quenching experiments on four joins in the tetrahedron cordierite-forsterite-leucite-silica and on the join cordierite-mullite-potash feldspar: Am. Ceramic Soc. Jour., v. 37, p. 501–533.

——— 1955, The ternary systems leucite-corundum-spinel and leucite- forsterite-spinel: Am. Ceramic Soc. Jour., v. 38, p 153–158.

——— 1957a, Melting relations of the common rock-forming oxides: Am. Ceramic Soc. Jour., v. 49, p. 215–235.

Schairer, J. F., 1957b, The crystallization of rock-forming minerals from magmas and the nature of the residual liquid; *in* P. H. Abelson, Ann. Rept. Director Geophysical Laboratory: Carnegie Inst. Washington Year Book 56, p. 217–222.

Schairer, J. F., and Bowen, N. L., 1935, Preliminary report on equilibrium relations between feldspathoids, alkali-feldspars and silica: Am. Geophys. Union Trans., 16th Ann. mtg., p. 323–328.

——— 1938, The system, leucite-diopside-silica: Am. Jour. Sci., v. 35A, p. 289–309.

——— 1942, The binary system $CaSiO_3$–diopside and the relations between $CaSiO_3$ and akermanite: Am. Jour. Sci., v. 240, p. 725–742.

——— 1947a, Melting relations in the systems Na_2O–Al_2O_3–SiO_2 and K_2O–Al_2O_3–SiO_2: Am. Jour. Sci., v. 245, p. 193–204.

——— 1947b, The system anorthite-leucite-silica: Soc. Geol. Finland Bull., v. 20, p. 67–87.

——— 1955, The system K_2O–Al_2O_3–SiO_2: Am. Jour. Sci., v. 253, p. 681–746.

——— 1956, The system Na_2O–Al_2O_3–SiO_2: Am. Jour. Sci., v. 254, p. 129–195.

Schairer, J. F., and Morimoto, N., 1958, Systems with rock-forming olivines, pyroxenes, and feldspars: *in* P. H. Abelson, Ann. Rept. Director Geophysical Laboratory: Carnegie Inst. Washington Year Book 57, p. 212–213.

——— 1959, The system forsterite-diopside-silica-albite, *in* P. H. Abelson, Ann. Rept. Director Geophysical Labortory: Carnegie Inst. Washington Year Book 58, p. 113–118.

Schairer, J. F., and Osborn, E. F., 1950, The system CaO–MgO–FeO–SiO_2: 1, Preliminary data on the join $CaSiO_3$–MgO–SiO_2: Am. Cermanic Soc. Jour., v. 33, p. 160–167.

Schairer, J. F., and Yagi, K., 1952, The system FeO–Al_2O_3–SiO_2: Am. Jour. Sci., Bowen Volume, p. 471–512.

Schairer, J. F., and Yoder, H. S., Jr., 1958, The quaternary system Na_2O–MgO–Al_2O_3–SiO_2, *in* P. H. Abelson, Ann. Rept. Director Geophysical Laboratory: Carnegie Inst. Washington Year Book 57, p. 210–212.

——— 1960a, The system albite-forsterite-silica, *in* P. H. Abelson, Ann. Rept. Director Geophysical Laboratory: Carnegie Inst. Washington Year Book 59, p. 69–70.

——— 1960b, The system forsterite-nepheline-diopside, *in* P. H. Abelson, Ann. Rept. Director Geophysical Laboratory: Carnegie Inst. Washington Year Book 59, p. 70–71.

Schairer, J. F., Yoder, H. S., Jr., and Keene, A. G., 1953, The system Na_2O–MgO–SiO_2, *in* P. H. Abelson, Ann. Rept. Director Geophysical Laboratory: Carnegie Inst. Washington Year Book 52, p. 62–64.

——— 1954, The systems Na_2O–MgO–SiO_2, and Na_2O–FeO–SiO_2, *in* P. H. Abelson, Ann. Rept. Director Geophysical Laboratory: Carnegie Inst. Washington Year Book 53, p. 123–125.

Schreyer, W., and Schairer, J. F., 1959, Anhydrous cordierites and the system MgO–Al_2O_3–SiO_2, *in* P. H. Abelson, Ann. Rept. Director Geophysical Laboratory: Carnegie Inst. Washington Year Book 58, p. 98–100.

——— 1960, Metastable quartz solid solutions in the system: MgO–Al_2O_3–SiO_2, *in* P. H. Abelson, Ann. Rept. Director Geophysical Laboratory: Carnegie Inst. Washington Year Book 59, p. 97–98.

Schroder, A., 1928, Beitrage zur Kentnis des Feinbaus des Brookits und des physikalischen Verhalten sowie der Zustandsänderung der drei naturalichen Titandioxyde: Zeitschr. Kristallographie, v. 67, p. 485–542.

Segnit, E. R., 1953, Further data on the system Na_2O–CaO–SiO_2; Am. Jour. Sci., v. 251, p. 586–601.

——— 1956, The section $CaSiO_3$–$MgSiO_3$–Al_2O_3: Mineralog. Mag., v. 31, p. 255–264.

Shepherd, E. S., Rankin, G. A., and Wright, F. E., 1909, The binary systems of alumina with silica, lime, and magnesia: Am. Jour. Sci., 4th ser., v. 28, p. 293–333.

Shropshire, Joseph, Keat, P. P., and Vaughan, P. A., 1959, The crystal structure of keatite, a new form of silica: Zeitschr. Kristallographie, v. 112, p. 409–413.

Smalley, R. G., 1947, The system $NaAlSiO_4$–$Ca_2Al_2SiO_7$: Jour. Geology, v. 55, p. 27–37.

Smith, J. V., and MacKenzie, W. S., 1958, The alkali feldspars: IV, The cooling history of high-temperature soda-rich feldspars: Am. Mineralogist, v. 43, p. 872–889.

Smith, J. V., and Tuttle, O. F., 1957, The nepheline-kalsilite system: 1, X-ray data for the crystalline phases: Am. Jour. Sci. v. 25, p. 282–305.

Smits. A. and Endell, K., 1919, Eine Notiz zu der Abhandlung des Systems SiO_2: Zeitschr. anorg. allg. Chemie, v. 106, p. 143–148.

Sosman, R. B., 1927, The properties of silica: New York, Chemical Catalog Co., 856 p.

——— 1952, Temperature scales and silicate research: Am. Jour. Sci., Bowen Volume, p. 517–528.

——— 1954, New high-pressure phases of silica: Science, v. 119, p. 738–739.

Sosman, R. B., Hostetter, J. C., and Merwin, H. E., 1915, The dissociation of calcium carbonate below 500°C: Washington Acad. Sci. Jour., v. 5, p. 563–569.

Sosman, R. B., and Merwin, H. E., 1916, Preliminary report on the system lime-ferric oxide: Washington Acad. Sci. Jour., v. 6, p. 532–537.

Spivak, J., 1944, The system $NaAlSiO_4$–$CaSiO_3$–Na_2SiO_3: Jour. Geology, v. 52, p. 24–52.

Stewart, D. B., 1960, Silicate phase equilibria, *in* Encyclopedia of Science and technology, v. 12: New York, McGraw-Hill Book Co., p. 312–317.

Stishov, S. M., and Popova, S. V., 1961, A new dense modification of silica: Geokhimiya, no. 10, p. 837–839. [Russian.]

Swayze, M. F., 1946, A report of studies of: 1, The ternary system CaO–C_5H_3–C_2F; 2, The quaternary system CaO–C_5A_3–C_2F–C_2S; 3, The quaternary system as modified by 5 percent magnesia. Pt. 1: Am. Jour. Sci., v. 244, p. 1–31.

Taylor, W. C., 1941, The system $2CaO \cdot SiO_2$–$K_2O \cdot SiO_2$ and other phase-equilibrium studies involving potash: U.S. Natl. Bur. Standards Jour. Research, v. 27, p. 311–323.

Tilley, C. E., 1933, The ternary system, Na_2SiO_3–$Na_2Si_2O_5$–$NaAlSiO_4$: Mineralog. petrog. Mitt., v. 43, p. 406–421.

Tilley, C. E., and Vincent, H. C. G., 1948, The occurence of an orthorhombic high-temperature form of Ca_2SO_4 (bredigite) in the Scawt Hill contact zone and as a constituent of slags: Mineralog. Mag., v. 28, p. 255–271.

Tornebohm, A. E., 1897, Die Petrographie des Portlandzements: Tonindustrie-Zeitung, v. 21, p. 1148–1151, 1157–1159.

Toropov, N. A., and Arakelyan, O. I., 1950, New calcium and sodium orthosilicates: Akad. Nauk SSSR Doklady, v. 72, p. 365–368 (in Russian).

Toropov, N. A. and Galakhov, F. Ya., 1951, The mullite problem: Akad. Nauk SSSR Doklady, v. 78, p. 299–302 (in Russian).

Tromel, G., Obst., K. H., Konopicky, K., Baver, H., and Patzek, I., 1957, Untersuchungen im System SiO_2–Al_2O_3: Deutsche keram. Gesell. Ber., v. 34, p. 397–402.

Turnock, A. C., 1959, Spinels, *in* P. H. Abelson, Ann. Rept. Director Geophysical Laboratory. Carnegie Inst. Washington Year Book 58, p. 134–137.

Tuttle, O. F., and Bowen, N. L., 1950, High temperature albite and contiguous feldspars: Jour. Geology, v. 58, p. 572–583.

——— 1958, Origin of granite in the light of experimental studies in the system $NaAlSi_3O_8$–$KAlSi_3O_8$–SiO_2–H_2O: Geol. Soc. America Mem. 74, 153 p.

Tuttle, O. F., and Smith, J. V., 1953, The system $KAlSiO_4$–$NaAlSiO_4$, *in* P. H. Abelson, Ann. Rept. Director Geophysical Laboratory: Carnegie Inst. Washington Year Book 52, p. 118.

——— 1958, The nepheline–kalsilite system: II, Phase relations: Am. Jour. Sci., v. 256, p. 571–589.

Wartenberg, H. von, and Prophet, E., 1932, Schmelzpunktdiagramme hochstfeuerfester Oxyde, V: Zeitschr. anorg. allg. Chemie, v. 207, p. 373–379.

Wartenberg, H. von, and Reusch, H. J., 1932, Schmelzpunktdiagramme hochstfeuerfester Oxyde, IV: Zeitschr. anorg. allg. Chemie, v. 207, p. 1–20.

Wartenberg, H. von, Reusch, H. J., and Saran, E. 1937, Schmelzpunktdiagramme höchstfeuerfester Oxyde, VII: Zeitschr. anorg. allg. Chemie, v. 230, p. 257–276.

Washburn, E. W., and Bunting, E. N., 1934, Note on phase equilibria in the system Na_2O–TiO_2: U.S. Natl. Bur. Standards Jour. Research, v. 12, p. 239.

Weiss, Alarich, and Weiss, Armin, 1954, Siliziumchalkogenide VI. Zur Kentniss der faserigen Siliziumdioxyd-modification: Zeitschr. anorg. allg. Chemie, v. 276, p. 95–112.

Welch, J. H., and Gutt, W., 1959, Tricalcium silicate and its stability within the system CaO–SiO_2: Am. Ceramic Soc. Jour., v. 42, p. 11–15.

Wyckoff, W. G., and Morey, G. W., 1926, X-ray diffraction measurements on compounds in the system soda-lime-silica: Am. Jour. Sci., v. 12, p. 419–440.

Yamauchi, Ti., 1937a, Celite system $3CaO \cdot Al_2O_3$–$2CaO \cdot Fe_2O_3$: Japan Ceramic Assoc. Jour., v. 45, p. 433.

———1937b, Celite. IV. The system $5CaO \cdot Al_2O_3$–$2CaO \cdot Fe_2O_3$: Japan Ceramic Assoc. Jour., v. 45, p. 614–631.

Yoder, H. S., Jr., 1950, High-low quartz inversion up to 10,000 bars: Am. Geophys. Union Trans., v. 31, p. 827–835.

——— 1952a, Change of melting point of diopside with pressure: Jour. Geology, v. 60, p. 364–374.

——— 1952b, The 10 percent $CaAl_2Si_2O_8$ plane in the system $CaSiO_3$–Ca_2AlSiO–$NaAlSiO_4$–$CaAl_2Si_2O_8$: Jour. Geology, v. 60, p. 586–593.

——— 1952c, The MgO–Al_2O_3–SiO_2–H_2O system and related metamorphic facies: Am. Jour. Sci., Bowen Volume, p. 569–627.

Yoder, H. S., and Weir, C. E., 1951, Change of free energy with pressure of the reaction nepheline+albite=2 jadeite: Am. Jour. Sci., v. 249, p. 683–694.

Zernike, J., 1955, Chemical phase theory: Deventer, Netherlands, Kluwer's Publishing Co., 493 p.

INDEX